Higher Sugar Analogs and Carbohydrate-Derived Molecular Diversity

Dissertation
der Mathematisch-Naturwissenschaftlichen Fakultät
der Eberhard Karls Universität Tübingen
zur Erlangung des Grades eines
Doktors der Naturwissenschaften
(Dr. rer. nat.)

vorgelegt von
Daniel Borowski
aus Wangen im Allgäu

Tübingen
2019

Gedruckt mit Genehmigung der Mathematisch-Naturwissenschaftlichen Fakultät der Eberhard Karls Universität Tübingen.

Tag der mündlichen Qualifikation:	08.11.2019
Dekan:	Prof. Dr. Wolfgang Rosenstiel
1. Berichterstatter:	Prof. Dr. Thomas Ziegler
2. Berichterstatter:	Prof. Dr. Martin E. Maier

Teilergebnisse dieser Arbeit sind bereits in den Ergebnissen der Bachelorarbeiten von R. M. Oechsner, C. Jeuck und C. Reik enthalten. Diese wurden während der Anfertigung der vorliegenden Dissertation theoretisch und präparativ betreut. An entsprechender Stelle ist dies durch Verweise kenntlich gemacht.

Ergebnisse dieser Arbeit wurden bereits umfassend in Fachzeitschriften publiziert. Die entsprechenden Publikationen sind der beiligenden Publikationsliste zu entnehmen.

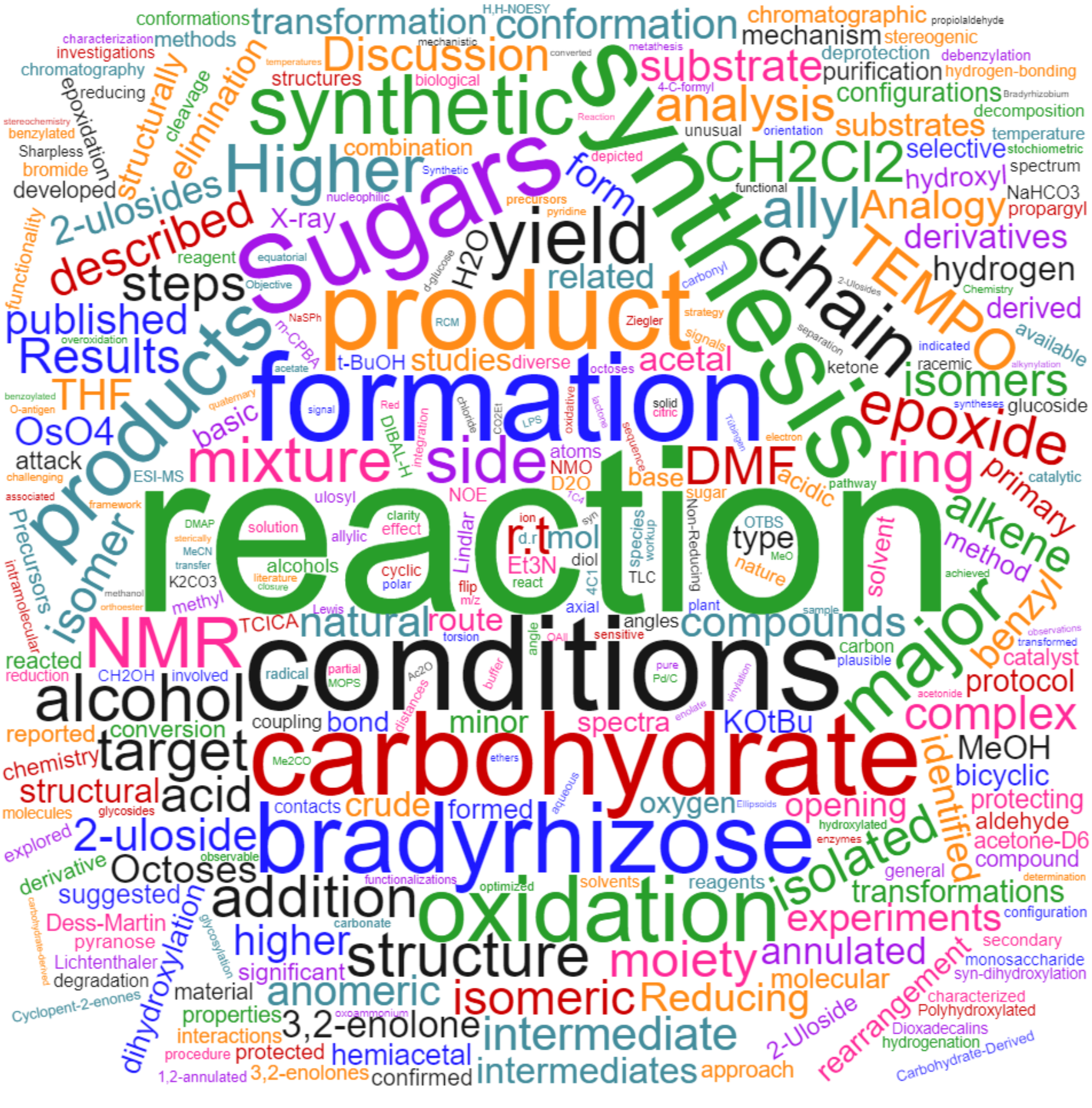
reaction
conditions
carbohydrate
formation
bradyrhizose
synthesis
product
Sugars
oxidation
products
synthetic
Higher
NMR
alcohol
yield
chain
TEMPO
epoxide
mixture
side
major
DMF
ring
target
addition
structure
isolated
alkene
CH2Cl2
analysis
substrate
Discussion
transformation
conformation
isomers
allyl
described
steps
published
Results
2-ulosides
2-uloside
OsO4
THF
isomer
acid
Octoses
compounds
natural
route
complex
protocol
benzyl
r.t
mol
Et3N
isomeric
intermediate
intermediates
3,2-enolone
anomeric
higher
moiety
Reducing
annulated
experiments
transformations
identified
MeOH
bicyclic
opening
crude
formed
oxygen
spectra
minor
bond
KOtBu
acetal
studies
related
form
Analogy
derivatives
hydrogen
derived
primary
method
mechanism
purification
configurations
substrates
selective
hydroxyl
chromatographic
stereogenic
deprotection
debenzylation
hydrogen-bonding
decomposition
temperature
spectrum
NaHCO3
propargyl
glucoside
racemic
ketone
available
catalytic
indicated
structural
chemistry
reported
conversion
reacted
reduction
coupling
radical
CH2OH
involved
TCICA
Precursors
intramolecular
basic
attack
ESI-MS
X-ray
H2O
elimination
structurally
cleavage
epoxidation
reducing
Sharpless
bromide
developed
benzylated
functionality
chromatography
methods
conformations
investigations
characterization
structures
biological
combination
precursors
nucleophilic
equatorial
Objective
reagent
t-BuOH
diverse
Ziegler
RCM
NaSPh
m-CPBA
DIBAL-H
Red
citric
LPS
NMO
D2O
NOE
uloysl
atoms
base
sugar
acidic
Non-Reducing
type
diol
TLC
OTBS
solvent
nature
alcohols
solution
effect
clarity
allylic
cyclic
polar
react
Lindlar
K2CO3
methyl
DMAP
MeCN
transfer
literature
closure
methanol
orthoester
Lewis
axial
plant
angles
m/z
flip
ion
d.r
species
workup
4C1
solid
sensitive
angle
partial
MOPS
Ac2O
buffer
distances
enolate
vinylation
Pd/C
carbon
plausible
catalyst
acetonide
sample
observations
transformed
achieved
MeO
pathway
electron
syntheses
Tubingen
alkynylation
separation
2-Ulosides
Chemistry
strategy
signals
carbonyl
octoses
lactone
oxidative
sequence
integration
chloride
CO2Et
signal
acetate
quaternary
overoxidation
benzoylated
O-antigen
challenging
associated
framework
d-glucose
functional
H,H-NOESY
mechanistic
converted
metathesis
4-C-formyl
Reaction
depicted
Synthetic
unusual
orientation
stochiometric
Bradyrhizobium
propiolaldehyde
temperatures
stereochemistry
sterically
observable
Me2CO
ethers
aqueous
contacts
molecules
glycosides
explored
derivative
suggested
Dess-Martin
pyranose
Lichtenthaler
carbohydrate-derived
degradation
Cyclopent-2-enones
dihydroxylation
glycosylation
material
properties
interactions
procedure
1,2-annulated
3,2-enolones
protected
hemiacetal
confirmed
approach
molecular
oxoammonium
functionalizations
optimized
solvents
carbonate
significant
reagents
general
Ellipsoids
hydroxylated
enzymes
aldehyde
acetone-D6
compound
protecting
determination
configuration
secondary
monosaccharide
syn-dihydroxylation
characterized
Polyhydroxylated
Dioxadecalins
hydrogenation
Carbohydrate-Derived
2-Uloside
rearrangement
pure
OAll
torsion
1C4
syn
NaHCO3

Für Deike.

Danksagungen

Meinem Doktorvater Herrn Prof. Dr. Thomas Ziegler bin ich zu allergrößtem Dank verpflichtet. Er gab mir die Möglichkeit, ein interessantes Thema in wissenschaftlicher Freiheit zu bearbeiten, unterstützte mich mit vielen anregenden Diskussionen, ermöglichte den Besuch zahlreicher Konferenzen, und förderte eine großartige Atmosphäre im Arbeitskreis. Seine Unterstützung der Sohena GmbH in allen Bereichen war überaus hilfreich, und keineswegs selbstverständlich.

Herrn Dr. Gregor Lemanski danke ich für die Unterstützung bei der Korrektur zahlreicher Manuskripte, wertvolle Unterstützung in chemischen und organisatorischen Fragen, sowie für seine Expertise bezüglich der Deutschen Eishockey-Liga. Für das Korrekturlesen dieser Arbeit bin ich ihm sehr dankbar.

Mit Felix Bächle durfte ich unzählige Stunden während des Chemiestudiums und anschließend im Labor, im Rahmen der Doktorarbeit und im Rahmen von Sohena, verbringen. Es war eine wunderschöne und humorvolle Zeit, an Freitagen häufig geprägt von schlechter Musik. Ich hoffe wir dürfen uns einmal wieder eine Laborzeile teilen.

Herrn Prof. Dr. Martin E. Maier möchte ich für seine Tätigkeit als zweiter Berichterstatter danken.

Herrn Prof. Dr. K.-P. Zeller danke ich für einige hilfreiche mechanistische Überlegungen.

Herrn Dr. Jochen Neumaier möchte ich für sein Engagement beim Aufbau des HPLC-Labors und für die IT-Betreuung danken. Ebenso unterstützte er mich mit wertvollen Ratschlägen bei NMR-Problemen.

Herrn Dr. Daniel Schmollinger danke ich für die Einführung in den AK Ziegler und in Sohena, und für unschätzbare Unterstützung während der letzten Jahre.

Herrn Dr. Melchior Menzel danke ich für eine schöne Zeit in einer gemeinsamen Laborbox, und für die Überlassung des Projekts der formylverzweigten Octosen.

Herr Dr. Jochen Kraft und Herr Dr. Markus Nörrlinger als ehemalige Seniordoktoranden unterstützten mich mit unzähligen Ratschlägen zu Beginn meiner Arbeit. Dafür bin ich Ihnen sehr dankbar.

Herrn Tobias Zweiböhmer danke ich für das Last-minute-Korrekturlesen.

Allen ehemaligen und aktuellen Kollegen und Freunden im AK Ziegler danke ich für eine wunderbare Zeit und viel Unterstützung. Dazu zählen insbesondere die Folgenden: Dr. Daniel Schmollinger, Dr. Göran Crucius, Dr. Melchior Menzel, Dr. Jochen Kraft, Dr. Markus Nörrlinger, Thomas Kutter, Per André Franz, Marius Bayer, Tobias Zweiböhmer, Thomas Klein, Alexander Klaiber, Michael Imrich, Axel Daikeler, Jurij Kessler, Felix Preusch, Dennis Köhn, Laura Srzan, Vincent Mehrmann.

Frau Petra Krüger danke ich für das Messen zahlreicher Elementaranalysen.

Herrn Dr. Markus Kramer, Herrn Paul Schuler, Frau Priska Kolb und Herrn Dominik Brzecki danke ich für die Betreuung der NMR-Spektrometer und für zahlreiche Messungen an den Hochfeldgeräten.

Frau Dr. Dorothee Wistuba, Herrn Dr. Peter Haiss und Frau Claudia Kruse danke ich für das Messen zahlreicher Massenspektren.

Frau Dr. Cäcilia Maichle-Mössmer, Herrn Dr. Hartmut Schubert und Frau Dr. Eva Jürgens danke ich für die Kristallstrukturanalysen.

Allen Bachelorstudenten und Praktikanten die zu dieser Arbeit beigetragen haben möchte ich danken, insbesondere: Andreas Paul, Jurij Kessler, Wiebke Grahneis, Regina M. Oechsner, Christian Reik, Carsten Jeuck und Patricia Hafner.

Frau Annette Berroth und Herrn Ali Öztürk danke ich für die Hilfe in vielen formalen Fragen.

Für die Möglichkeit viele unschätzbare Erfahrungen bei Sohena zu sammeln, möchte ich mich bei Frau Dr. Heike Sowinski, Herrn Dr. Ulrich Heber und Herrn Dr. Daniel Schmollinger bedanken. Weiterer Dank gilt den ehemaligen Kollegen Ali Öztürk, Dr. Jochen Kraft und Dr. Anna-Theresa Schmidt. Dem aktuellen Sohena-Team Alexander Klaiber und Tobias Zweiböhmer, sowie Jurij Kessler und Felix Preusch danke ich für den unermüdlichen Einsatz.

Allen Mitarbeiterinnen und Mitarbeitern des Chemischen Zentralinstituts danke ich für ihren Einsatz, der mich in meiner Arbeit sehr unterstützte.

Herrn Prof. Biao Yu danke ich für ein interessantes Gespräch auf dem 18. European Carbohydrate Symposium in Moskau, in welchem er anregte, die Synthese der formylverzweigten Octosen im Kontext des Naturstoffs Bradyrhizose weiter zu untersuchen.

Der CO-ADD Initiative danke ich für die Durchführung der antimikrobiellen Screenings.

Sven Hafner möchte ich für viele unterhaltsame Stunden während des Chemiestudiums, sowie für unschätzbare Hilfe in der Latex-Textverarbeitung danken.

Leonard Pollak danke ich für Ratschläge in technischen Fragen, sowie für eine wunderbare Zeit in der WG.

Dem Tübinger Freundeskreis möchte ich für viele schöne Jahre danken, insbesondere: Alex und Sarah, André, David und Madlen, Elisabeth und Christian, Eva und Tobi, Felix und Caren, Marli und Mo, und Therry.

Für viel Verständnis, Unterstützung und unvergessliche Wochenenden: Vielen Dank Basti, Bode, Michi, Niki und Tobi.

Ich bedanke mich bei meinen Brüdern Simon und Michael, sowie bei Karin. Weiterhin danke ich Lilo und Claus.

Besonderer Dank gilt meinen Eltern Gerlinde und Dieter, die mich während meines Studiums stets unterstützt haben, und ohne deren Hilfe diese Arbeit nicht möglich gewesen wäre.

CV of the Author

Daniel Borowski

Vor dem Kreuzberg 26
72070 Tübingen
Germany

Date of birth: April 16, 1987
Place of birth: Wangen im Allgäu, Germany

Work Experience

Since 10.2016	*Business Executive*, Sohena GmbH, Tübingen
11.2013–12.2018	*Doctorate position*, Institute of Organic Chemistry, University of Tübingen
10.2013–10.2016	*Synthesis chemist*, Sohena GmbH, Tübingen
04.2013–09.2013	*Student assistant*, Institute of Organic Chemistry, University of Tübingen
02.2010–10.2012	*Student assistant*, Institute of Physical and Theoretical Chemistry, University of Tübingen
09.2006–05.2007	*Community service*, Oberschwabenklinik, Wangen im Allgäu

Education

Since 11.2013	*Doctorate*, Institute of Organic Chemistry, University of Tübingen
09.2007–09.2013	*Diploma in Chemistry*, University of Tübingen
06.2006	*Abitur*, Rupert-Neß-Gymnasium, Wangen im Allgäu

List of Publications

An updated list of publications can be obtained from the following ORCID iD:

`https://orcid.org/0000-0002-9884-8987`

Peer-Reviewed Journal Articles

The results described in this thesis were, in part, published in the following peer-reviewed journal articles:

- **Synthetic Adventures with 2-*C*-Branched Carbohydrates: 4-*C*-Formyl Branched Octoses with Structural Analogy to Bradyrhizose.**

  D. Borowski, C. Maichle-Mössmer and T. Ziegler,
  Eur. J. Org. Chem. **2019**, 2653-2670.

- **Carbohydrate-Derived 3,2-Enolones in the Base-Catalyzed Rearrangement to Highly Functionalized *C*4-Quaternary 4-Hydroxy-2-cyclopentenones.**

  D. Borowski, R. M. Oechsner, E. Jürgens and T. Ziegler,
  Eur. J. Org. Chem. **2017**, 4490-4499.

- **1,2-Annulated Sugars: Synthesis of Polyhydroxylated 2,10-Dioxadecalins with β-*manno* Configuration.**

  D. Borowski, T. Zweiböhmer and T. Ziegler,
  Eur. J. Org. Chem. **2016**, 5248-5256.

- **2-*C*-Alkynyl and 2-*C*-*cis*-Alkenyl β-Mannosides with Acetal Protected γ-Aldehyde Functionality via 2-Uloside Alkynylation and Lindlar Hydrogenation.**

  D. Borowski, M. Menzel and T. Ziegler,
  Molbank **2016**, *2016*, M916.

Conference Talks

- **2-*keto*-Glucosides: Substrates for Unexpected Rearrangements and Building Blocks for the Synthesis of Higher Carbohydrate Analogs.**

  (Initial German title: 2-*keto*-Glucoside: Substrate für unerwartete Umlagerungen und Bausteine für die Synthese höherer Kohlenhydrat-Analoga.)

  D. Borowski at 21. TOCUS (Day of Organic Chemistry),
  University of Stuttgart, Germany, October 13, **2017**.

Poster Presentations

The following posters were presented at international conferences:

- **Synthetic 4-*C*-Formyl Branched Octoses with Structural Analogy to Bradyrhizose.**

  D. Borowski and T. Ziegler,
  29th International Carbohydrate Symposium,
  Lisbon, Portugal, July 15-19, **2018**.

- **Carbohydrate-Derived 3,2-Enolones in the Rearrangement to Highly Functionalized *C*4-Quaternary 4-Hydroxy-2-cyclopentenones.**

  D. Borowski and T. Ziegler,
  20th European Symposium on Organic Chemistry,
  Cologne, Germany, July 2-6, **2017**.

- **Annulated Sugars: 2-Ulosides in the Synthesis of Reducing and Non-Reducing Dioxadecalins.**

  D. Borowski and T. Ziegler,
  15th Belgian Organic Synthesis Symposium,
  Antwerp, Belgium, July 10-15, **2016**.

- **Synthesis and Characterization of New Bicyclic Carbon-Branched Carbohydrate Derivatives.**

  D. Borowski, M. Menzel and T. Ziegler,
  18th European Carbohydrate Symposium,
  Moscow, Russia, August 2-6, **2015**.

Other Publications

Publications without connection to this thesis:

- **Faster Response Times of Rare-Earth Oxycarbonate Based CO_2 Sensors and Another Readout Strategy for Real-World Applications.**

  A. Haensch, D. Borowski, N. Barsan, D. Koziej, M. Niederberger, U. Weimar,
  Procedia Engineering **2011**, *25*, 1429-1432.

Kurzzusammenfassung (deutsch)

Anfängliche Synthesestudien zeigten, dass Dess-Martin-Oxidation eine geeignete Methode für die Synthese der empfindlichen neuen Allyl-3,4,6-tri-*O*-benzyl-β-D-*arabino*-hexopyranosid-2-ulose darstellt. In gleicher Weise konnten die entsprechenden bekannten 3,4,6-benzylgeschützten β-Benzyl- und β-Methyl-2-*keto*-glucoside (2-Uloside) aus den entsprechenden 2-OH-ungeschützten Glucosiden erhalten werden. Ausgehend von dem entsprechenden Allyl-2-ulosid wurde zunächst die Synthese von 1,2-anellierten Kohlenhydraten mit *trans*-Decalin-artiger Struktur (polyhydroxylierte 2,10-Dioxadecaline) verfolgt. Das 2-*keto*-Substrat wurde durch Vinylierung des Ketons, gefolgt von Ringschlussmetathese, *syn*-/*anti*-Dihydroxylierung und globaler Entschützung in die 1,2-Pyran-anellierten Zielmoleküle überführt, die eine neue Klasse von bicyclischen Kohlenhydraten mit β-*manno*-Konfiguration darstellen. Die Strukturaufklärung der außerordentlich polaren anellierten Zucker erfolgte mittels NMR-Spektroskopie in D_2O. Ein weiterer Strukturbeweis konnte für die entsprechende *syn*-konfigurierte Zielverbindung durch Röntgenstrukturanalyse gewonnen werden, welche Einblicke in ein dichtes Netzwerk an Wasserstoffbrückenbindungen lieferte. Für strukturell verwandte 1,2-anellierte Zucker konnte gezeigt werden, dass diese Kohlenhydratmimetika darstellen, und als Inhibitoren von natürlichen Glycosidaseenzymen wirken können. Ausgehend vom entsprechenden β-Benzyl-2-*keto*-glucosid lieferte die Umsetzung mit lithiierten Alkinspezies (Propargylaldehydacetale oder Propargylalkoholderivate) 2-*C*-alkinylverzweigte Mannoside. Durch partielle Hydrierung der Alkinfunktion, gefolgt von *syn*-/*anti*-Dihydroxylierung, konnten 1,2,3-trihydroxyprop-1-yl-verzweigte Mannoside mit variabler Konfiguration der Seitenkette erhalten werden. Diese trihydroxypropyl-verzweigten Intermediate wurden durch selektive Oxidation der primären Alkoholfunktion in 2-Spirofuranose-Pyranosen umgesetzt, welche eine bisher unbekannte Klasse von Kohlenhydrat-Hybridmolekülen darstellen. Die selektive Oxidation erfolgte unter Verwendung eines neuen Oxidationsprotokolls mit der bekannten Kombination TEMPO/Trichlorisocyanursäure in einem optimierten Puffer-/Lösungsmittelsystem. Globale Debenzylierung der Spirofuranose-Intermediate lieferte 4-*C*-formylverzweigte Octosen mit variabler Konfiguration der *C*-2/3 Stereozentren in Form von komplexen Isomerengemischen aus entsprechenden cyclischen Halbacetalformen. Detaillierte NMR-Studien in D_2O identifizierten die vorliegenden Hauptisomere als anellierte 1,5-Pyranose-9,7-pyranosen bzw. spiro-1,4-Furanose-9,7-pyranosen, und damit als Bis(Halbacetal)-Isomere. Die entsprechenden 9,7-Pyranose-1,9-pyranoseformen (Acetal-Halbacetal-Isomere), strukturell verwandt mit dem Naturstoff Bradyrhizose, konnten nicht als Hauptisomere der komplexen höheren Zucker gefunden werden. In einem abschließenden Projekt wurden die drei benzylgeschützten 2-*keto*-Glucoside (β-Allyl/Benzyl/Methyl-2-uloside) durch Eliminierung von Benzylalkohol unter basischen Bedingungen in die 3,6-Di-*O*-benzyl-4-desoxy-β-D-*glycero*-hex-3-enopyranosid-2-ulosen (3,2-Enolone) überführt. Diese 3,4-ungesättigten 2-*keto*-Glucoside gehen mit basischen Reagenzien (Kalium-*tert*-butanolat) in DMF eine Umlagerung in racemische 2-Benzyloxy-4-benzyloxymethyl-4-hydroxy-5-alkoxycyclopent-2-enone ein. Mechanistische Erklärungen für diese neue Reaktion wurden ausgearbeitet, und diskutiert im Kontext von bekannten Umlagerungen, welche zu den regioisomeren 5-hydroxy-substituierten Cyclopent-2-enonen führen.

Abstract

Initial synthetic studies identified Dess-Martin oxidation to be the method of choice for the formation of the unknown, sensitive allyl 3,4,6-tri-*O*-benzyl-β-D-*arabino*-hexopyranoside-2-ulose. In a similar manner, the respective known 3,4,6-*O*-benzylated β-benzyl and β-methyl 2-*keto*-glycosides (2-ulosides) could be obtained from the corresponding 2-OH-unprotected glucosides. In a project directed towards the synthesis of 1,2-annulated carbohydrates with a *trans*-decalin structure (polyhydroxylated 2,10-dioxadecalins), the respective allyl 2-uloside underwent vinylation of the 2-ketone, followed by ring-closing metathesis. Stereoselective *syn*- or *anti*-dihydroxylation and debenzylation afforded the wanted 1,2-pyran-annulated target structures as a new class of bicyclic carbohydrate derivatives with the previously undescribed β-*manno*-configuration. Structural characterizations of the highly polar annulated sugars included NMR analysis in D_2O. Furthermore, X-ray crystallography confirmed the structure of the respective *syn*-isomer, and provided insight into a dense network of hydrogen-bonding interactions. Structurally related published 1,2-annulated sugars have been reported to be carbohydrate mimetics acting as inhibitors for natural glycosidase enzymes. Following a related synthetic route, the corresponding benzyl 2-uloside was treated with alkynyllithium species, either derived from propiolaldehyde acetals or from propargyl alcohol derivatives, to afford the 2-*C*-alkynylated mannosides. A sequence comprising partial hydrogenation of the alkyne, followed by *syn*- or *anti*-dihydroxylation, afforded 1,2,3-trihydroxyprop-1-yl-branched mannosides with diverse stereochemical configurations of the hydroxylated side chain. These trihydroxypropyl-branched intermediates were converted into 2-spirofuranose-pyranoses, reducing carbohydrate hybrid molecules with previously undescribed structure, *via* selective primary alcohol oxidation. For this transformation, a new oxidation protocol utilizing the known combination TEMPO/trichloroisocyanuric acid in combination with an optimized solvent/buffer system was developed. Global debenzylation of the spirofuranose intermediates yielded 4-*C*-formyl octoses with diverse configurations of the *C*-2/3 stereogenic centers as complex mixtures of cyclic hemiacetal isomers. Detailed structural NMR studies in D_2O identified the major isomers to be the annulated 1,5-pyranose-9-7-pyranose forms, or the 1,4-furanose-9,7-pyranose spiro-forms, and thus, isomeric forms with two hemiacetal functionalities. The corresponding 9,7-pyranose-1,9-pyranose isomeric forms (acetal-hemiacetal forms), structurally related to the natural product bradyrhizose, were not identified to be major constituents of these complex higher sugars. In a concluding project, all three benzylated 2-*keto*-glucosides (β-allyl/benzyl/methyl 2-ulosides) were transformed into the corresponding 3,6-di-*O*-benzyl-4-deoxy-β-D-*glycero*-hex-3-enopyranoside-2-uloses (3,2-enolones) by base-induced elimination of benzyl alcohol. Reactivity studies revealed that these 3,4-unsaturated 2-*keto*-glucosides undergo a rearrangement into racemic 2-benzyloxy-4-benzyloxymethyl-4-hydroxy-5-alkoxycyclopent-2-enones in the presence of basic reagents (potassium *tert*-butoxide) in DMF. Mechanistic considerations for this previously undescribed rearrangement were established, and discussed in the context of related published transformations, which were reported to give the regioisomeric 5-hydroxy-substituted cyclopent-2-enones.

Contents

CV of the Author xi

List of Publications xii

Kurzzusammenfassung (deutsch) xiv

Abstract xv

1. Introduction 1

2. Synthesis of 2-Uloside Precursors 7
- 2.1. Introduction to the Chemistry of 2-Ulosides 7
  - 2.1.1. Synthesis of Protected 2-Ulosides 10
  - 2.1.2. From 2-Ulosides to Unsaturated Heterocycles 13
- 2.2. Objective of this Chapter 17
- 2.3. Results and Discussion 17
- 2.4. Summary of this Chapter 24

3. Non-Reducing Higher Sugars: Polyhydroxylated Dioxadecalins 27
- 3.1. Introduction to Carbohydrate-Derived Decalin Structures 27
  - 3.1.1. Natural Carbohydrate-Derived Decalins 29
  - 3.1.2. Synthetic Carbohydrate-Derived Decalins 31
- 3.2. Objective of this Chapter 37
- 3.3. Results and Discussion 38
  - 3.3.1. Preliminary Synthetic Studies 39
  - 3.3.2. Optimized Synthetic Route 43
  - 3.3.3. Characterization of the Target Compounds 48
- 3.4. Summary of this Chapter 55

4. Reducing Higher Sugars: Octoses with Analogy to Bradyrhizose 57
- 4.1. Introduction to Nitroxyl Radical-Based Alcohol Oxidations 57
- 4.2. Introduction to Higher Sugars 61
- 4.3. Introduction to Bradyrhizose: An Unusual Higher Monosaccharide 68
- 4.4. Objective of this Chapter 79
- 4.5. Results and Discussion 82
  - 4.5.1. Preliminary Synthetic Studies 82
  - 4.5.2. Synthesis of the *syn*-Isomers 92
  - 4.5.3. Synthesis of the *anti*-Isomers 113
  - 4.5.4. Characterization of the Target Compounds 129
- 4.6. Summary of this Chapter 137

5. Cyclopent-2-enones from 2-Uloside Precursors 143
5.1. Introduction to Carbohydrate-Derived 3,2-Enolones and 3,2-Enones . . 143
5.2. Objective of this Chapter 149
5.3. Results and Discussion 149
5.3.1. Synthesis of 3,2-Enolone Substrates 150
5.3.2. Base-induced Rearrangement: Formation of Cyclopent-2-enones 151
5.3.3. Mechanistic Considerations 159
5.3.4. Antimicrobial Activity Screenings 174
5.4. Summary of this Chapter 175

6. Experimental Part 177
6.1. Instruments and Techniques 177
6.2. General Methods 179
6.3. Reagents and Materials 180
6.3.1. Key Reagents, Prepared Reagents and Purified Reagents 180
6.4. Numbering, Nomenclature and Fischer Projections 181
6.5. Synthetic Procedures 184

7. Summary of Results 253

List of Abbreviations and Symbols 261

List of Compounds 267

Appendix A. X-Ray Crystallography 271

Appendix B. HPLC Chromatograms 295

Appendix C. Antimicrobial Screenings 299

Appendix D. Selected 2D NMR Spectra 303

Appendix E. NMR Spectra 313

References 393

1. Introduction

D-Glucose **A** **(Scheme 1.1)**, the most abundant monosaccharide on earth, is produced in the photosynthesis of green plants, and is incorporated into structural polysaccharides like cellulose **B** or chitin. In that regard, carbohydrates constitute the major fraction of the biomass on earth.[1] Apart from these structural stability purposes, bioavailable saccharides like D-glucose **A**, or polysaccharides like starch or glycogen, are crucial in terms of energy supply. As either direct or indirect substrates for the glycolysis metabolic pathway they play the key role in the carbohydrate catabolism, and the formation of energy-rich ATP for the intracellular energy transfer in biological systems.[2] Two numbers can be given to properly demonstrate the importance of carbohydrates in this macroscopic context: cellulose **B** is produced in the photosynthesis in annual amounts of ca. $1.5 \cdot 10^{12}$ tons, and is therefore the most prevalent source of renewable organic feedstock.[3] In a similar period of one year, the total industrial starch production from crops like corn, rice or wheat is roughly $4.9 \cdot 10^{7}$ tons.[4]

On a rather microscopic picture, carbohydrates have gained attention in what is now referred to as the field of *glycobiology*. Carbohydrates themselves are not directly encoded for by the genome. However, carbohydrate-processing enzymes like *glycosyltransferases* and *glycosidases* are encoded, and a combination of these enzymes results in individual glycosylation patterns of biomolecules in living organisms.[5] As a prominent example, all cell surfaces are coated by a dense layer (the *glycocalyx*) of structurally diverse glycans bound by proteins (*glycoproteins*) or lipids (*glycolipids*).[6] In this individually different, heterogeneous functionalization of the cell surface, carbohydrates operate as anchor points for biological processes of high importance, for example cell-cell recognition and cell signaling, or host-pathogen interactions and the host immune response in the case of infections.[5, 6] In such recognition events, proteins (*lectins*) with carbohydrate recognition domains are reversibly mediating interactions with high specificity for certain glycosylation patterns. The ensemble of biological processes relying on such carbohydrate recognition events is still subject to scientific investigation and far beyond the scope of this introduction.[7] The glycosylated moieties addressed by lectins are diverse and dependent on the individual protein. Apart from conventional sugar residues like D-galactose **C** or N-acetyl-D-glucosamine **D**, more sophisticated,

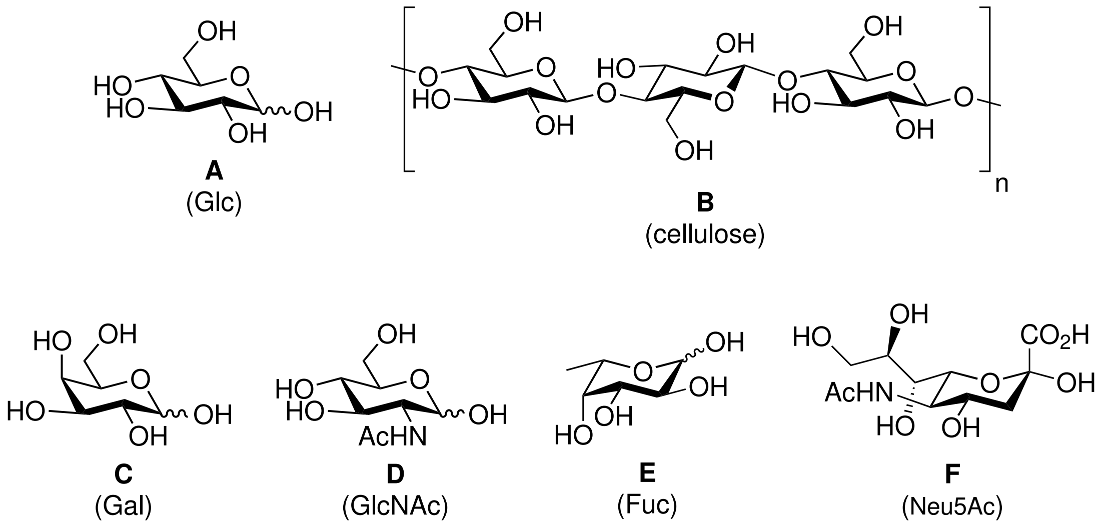

Scheme 1.1 Top: abundant saccharides D-glucose **A** and cellulose **B**. Bottom: carbohydrates frequently found in lectin binding motifs: D-galactose **C**, *N*-acetyl-D-glucosamine **D**, L-fucose **E** and α-sialic acid **F**.

macroscopically rare monosaccharides like L-fucose **E** or derivatives of α-sialic acid **F** are found in the saccharidic ligands of biomolecules targeted by lectins.[6]

In terms of structurally peculiar carbohydrates, however, a certain environment is unchallenged: incorporated into the outer membrane of Gram-negative bacteria, a carbohydrate-rich component termed the *lipopolysaccharides* (LPS, **Fig. 1.1**), a dense protective layer, is the residence of unique sugars found nowhere else in nature.[8, 9] Bacterial LPS usually feature three distinct regions **(Scheme 1.2)**. The *lipid A* region consists of a glucosamine disaccharide $(GlcN)_2$, functionalized with anionic phosphate groups, which is anchored to the outer membrane of the bacterium by acylation with fatty acid residues. The *core region* is attached to this glucosamine dimer *via* glycosidic linkages. Here, higher sugars (heptoses and octoses) like 3-deoxy-α-D-*manno*-oct-2-ulosonic acid (or keto-deoxyoctulosonate, Kdo) **G** and L-*glycero*-D-*manno*-heptose (LDmanHep) **H** form an oligosaccharide.[10] Further glycosides are incorporated into this core oligosaccharide, but their number and nature is highly dependent on the individual bacterium and strain.[9] The core oligosaccharide is further functionalized with an outer repetitive glycan (either branched or linear), which is referred to as the *O-polysaccharide* (or *O-antigen*). This saccharide is structurally the most variable region of the LPS, and a number of relevant biological interactions between the bacterium and a potential host (e.g. evasion or triggering of immune responses) are dependent on this saccharide region.[8] O-saccharides usually possess highly immunogenic properties and are capable of provoking strong antibody responses. Although the chain length and monosaccharide constituents of the repeating unit of O-polysaccharides vary widely,

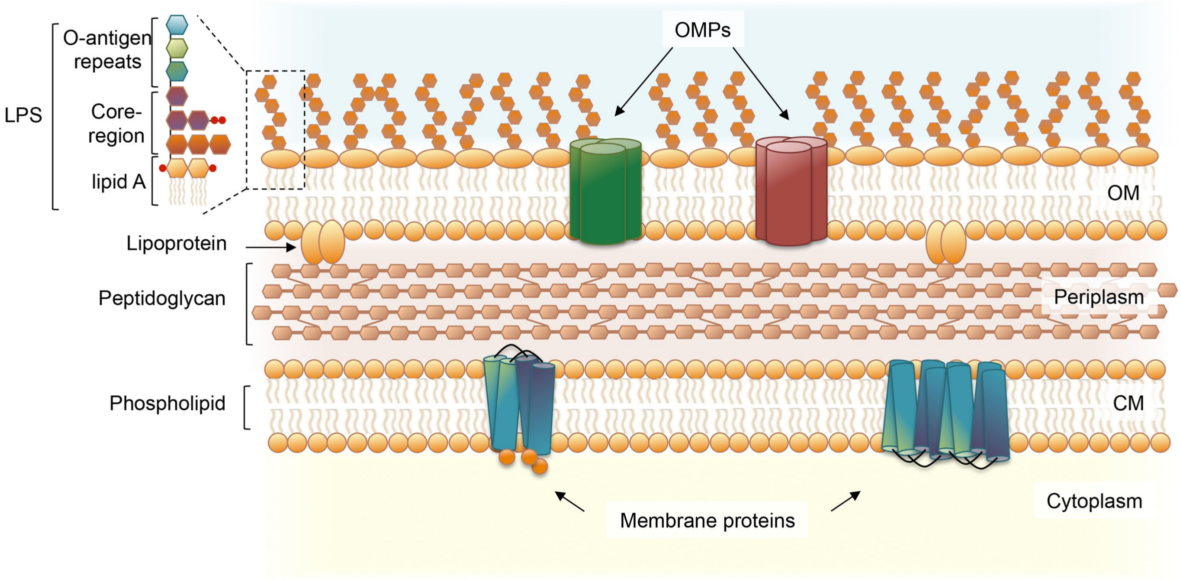
LPS
O-antigen repeats
Core-region
lipid A
OMPs
OM
Lipoprotein
Peptidoglycan
Periplasm
Phospholipid
CM
Membrane proteins
Cytoplasm

Figure 1.1 Membrane region of Gram-negative bacteria including the outer membrane (OM) and the cytoplasmic membrane (CM). Top left: Lipopolysaccharide (LPS) with lipid A, core region and O-antigen. OMPs = outer membrane proteins. Figure gratefully reprinted with permission from Oxford University Press.[9]

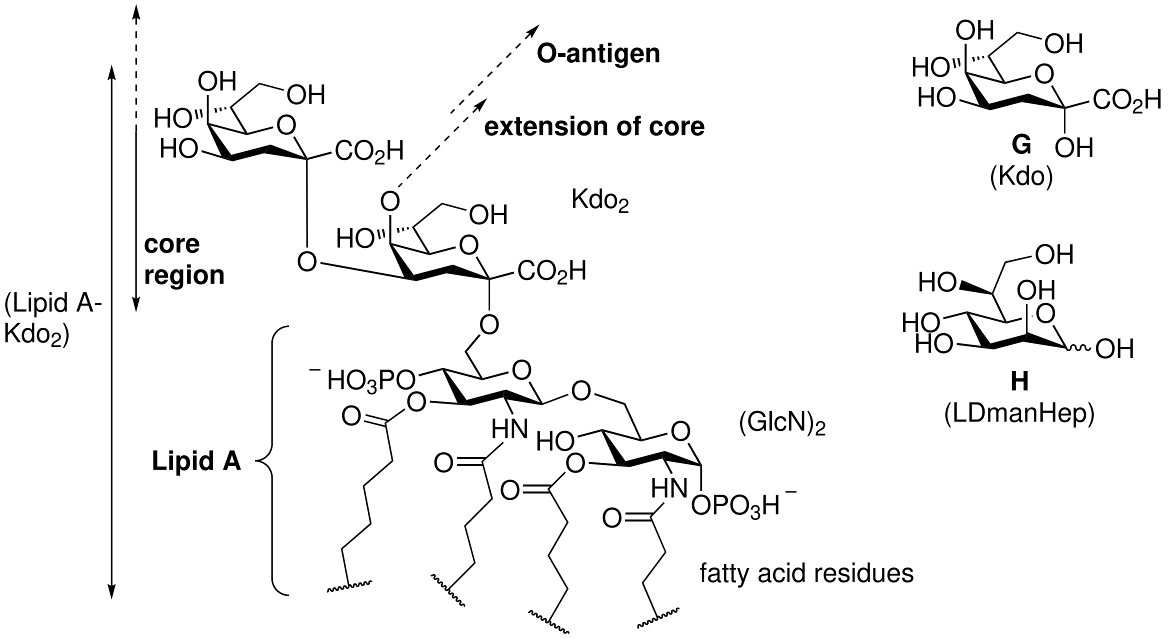
O-antigen
extension of core
Kdo2
core region
(Lipid A-Kdo2)
Lipid A
(GlcN)2
fatty acid residues
G
(Kdo)
H
(LDmanHep)

Scheme 1.2 Typical chemical structure of the Lipid A region and beginning of the core region of bacterial LPS.[6, 9]

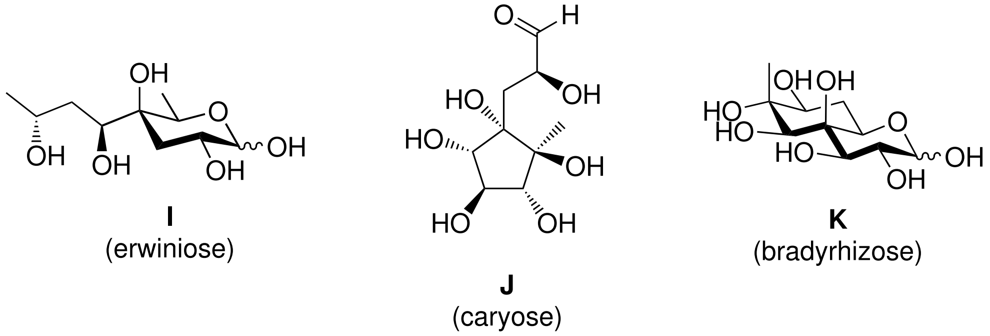

Scheme 1.3 Higher sugars isolated from bacterial LPS, including erwiniose **I**[11], caryose **J**[12] and bradyrhizose **K**[13].

this region was found to contain rare sugars such as *keto*-sugars or branched sugars.[8] In addition, structurally unique higher sugars have been extracted from bacterial O-saccharide regions **(Scheme 1.3)**. In this regard, the interesting structures of the 4-*C*-branched erwiniose **I**[11], the carbocyclic formylalkyl-branched caryose **J**[12], and the galactoside-annulated inositol (carbasugar) bradyrhizose **K**[13] serve as appropriate examples.

Naturally, due to the peculiar structures and high biological relevance frequently associated with it, such higher sugars have been attractive targets for synthetic carbohydrate chemistry. For instance, in the first total synthesis of bradyrhizose **K** as published in 2015 by Yu, Molinaro and Coworkers, 26 synthetic steps were required to transform a simple glucal precursor into the challenging carbohydrate target **K**.[14] In this regard, the chemical synthesis of complex higher sugars can be seen as a subdomain of the field of natural product synthesis. Apart from this, simple carbohydrates are popular starting materials for the synthesis of non-carbohydrate natural products, too. Focussing on such carbohydrate-based total synthesis strategies, a landmark review article was published by Nicolaou and Mitchell in 2001.[15] As a result of such extensive synthetic endeavors, synthetically useful transformations of easily accessible carbohydrate precursors for the generation of advanced molecular complexity are developed by the carbohydrate chemistry community with great efforts, and can still be seen as a key research objective in this area.

In this context, the present thesis reports on synthetic endeavors towards three individual carbohydrate target structures **T-3,4,5**, each of them featuring structural analogies to naturally occurring unusual saccharides, or contributing to the molecular diversity accessible from simpler carbohydrate-derived building blocks **(Scheme 1.4)**. The developed synthetic approaches are covered in individual chapters of this thesis **(Chapters 3–5)**, and can be regarded as independent synthesis projects. In each chapter, a strong emphasis is put on the basic reactivities of the traversed carbohydrate intermediates in order to extend the collection of reliable transformations of sugar building blocks. Furthermore, detailed structural characterizations of the advanced carbohydrate products are described with a focus on the highly complex carbohydrate stereochemistry.

As a connection between these individual projects, retrosynthetic considerations identified 2-*keto*-sugars **T-2** as common carbohydrate precursors for the following approaches towards the advanced carbohydrate derivatives. The synthesis of such *keto*-sugar precursors **T-2**, partially known and partially novel, is covered in **Chapter 2**.

Chapter 3 reports on the synthesis of non-reducing (non-hemiacetal) 1,2-annulated sugars **T-3** with a hydroxylated *trans*-decalin type annulated framework. Due to the *C*-2 carbonyl functionality, the common precursors **T-2** serve as suitable substrates for the introduction of a *C*-2 side chain *via* classic carbonyl addition reactions. These products can subsequently be transformed into the desired 1,2-annulated carbohydrate derivatives **T-3**. Structurally related synthetic molecules have attracted interest as carbohydrate mimetics, for example in relation with natural glycosidase enzymes. Therefore, structural investigations into such annulated carbohydrates and new synthetic strategies towards such structures are of interest.

In a related synthetic sequence described in **Chapter 4**, the corresponding reducing (free hemiacetal) derivatives **T-4** of such 1,2-annulated sugars were targeted. This class of compounds (4-*C*-formyl branched octoses in the open-chain forms) features structural analogies to the naturally occurring annulated hemiacetal bradyrhizose **K (Scheme 1.3)**. With a focus on stereo- and chemoselective oxidation reactions of the introduced side chain, detailed synthetic studies towards this type of molecules are described, and can be seen as an addition to the chemistry of higher-carbon sugars. Furthermore, the complex hemiacetal equilibria of the target compounds **T-4** are analyzed, and compared to the isomeric forms found for the natural bradyrhizose **K**.

Finally, in **Chapter 5**, new reactivity of the 2-*keto*-sugar precursors **T-2** in a cascade reaction, affording racemic 4-hydroxycyclopent-2-enones **T-5**, is presented. Mechanistic experiments are reported and a plausible mechanism is given, and compared to related transformations described in the literature.

Each of the individual chapters is preceded by an introduction to the target compounds of interest, and relevant published work is summarized where appropriate.

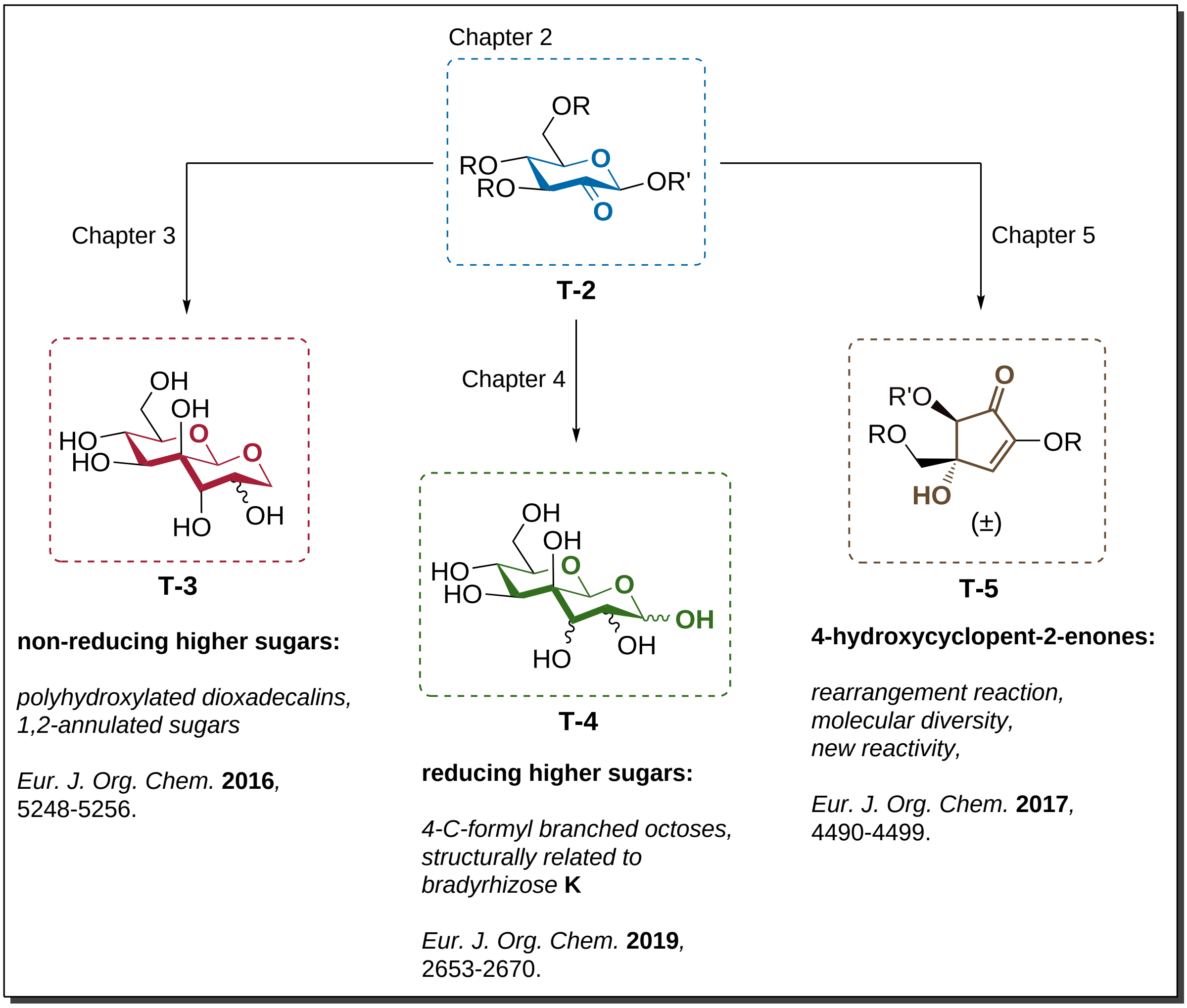
Chapter 2
OR
RO
RO
O
O
OR'
T-2
Chapter 3
Chapter 4
Chapter 5
OH
OH
HO
HO
O
O
HO
OH
T-3
OH
OH
HO
HO
O
O
OH
HO
OH
T-4
R'O
O
RO
OR
HO
(±)
T-5

non-reducing higher sugars:

polyhydroxylated dioxadecalins, 1,2-annulated sugars

Eur. J. Org. Chem. **2016**, 5248-5256.

reducing higher sugars:

4-C-formyl branched octoses, structurally related to bradyrhizose **K**

Eur. J. Org. Chem. **2019**, 2653-2670.

4-hydroxycyclopent-2-enones:

rearrangement reaction, molecular diversity, new reactivity,

Eur. J. Org. Chem. **2017**, 4490-4499.

Scheme 1.4 Schematic representation of the synthetic projects covered in this thesis. R/R' = protecting groups. For clarity, the reducing higher sugars **T-4** of **Chapter 4** are depicted in the (9*S*)-9,7-pyranose-1,9-pyranose isomeric form.

2. Synthesis of 2-Uloside Precursors

As key intermediates for the synthesis of higher sugars, and for the generation of carbohydrate-derived molecular diversity as delineated in the following chapters, suitably protected 2-*keto*-sugars of the general structure **T-2** (**Scheme 1.4** on page 6) were required. After an introduction to the chemistry of this class of carbohydrate compounds, synthetic studies towards known an unknown 2-*keto*-sugars are described in this chapter.

2.1. Introduction to the Chemistry of 2-Ulosides

The oxidation of a secondary hydroxyl group in an aldose results in a *keto*-sugar which can be referred to as a ketoaldose or as an aldosulose[16], an important member within the diverse class of carbohydrate oxidation products.[17] The corresponding glycosides of such dicarbonyl sugars are termed aldosulosides, frequently referred to as ulosides in a simplified manner. Formal oxidation of the *C*-2 in D-glucose **A** gives the 2-ulose D-glucosone **L** (GlcOS, **Scheme 2.1, a**), which can be regarded as the prototype example of an aldos-2-ulose carbohydrate. Together with other dicarbonyl saccharides, **L** is formed in the Maillard reaction, the reaction of reducing carbohydrates with amino compounds like proteins, during the processing of food as well as under physiological conditions.[18, 19] In such processes, **L** is tentatively formed *via* oxidation of the Amadori product (an 1-amino-1-deoxyketose). However, the exact formation of **L** is still not fully understood, and a protein-free mechanism involving direct autocatalytic oxidation of the 1,2-enediol derived from D-glucose is also discussed.[20] Due to the biological importance of such sugar 1,2-dicarbonyls, the chemical synthesis of pure **L**, or derivatives of it, has attracted early interests.[21, 22] Apart from this, other naturally occurring substances are known to incorporate a 2-uloside (2-*keto*-sugar) moiety. For example, highly bioactive steroidal glycosides belonging to the cardenolide glycosides (a subgroup of the cardiac glycosides) were found to contain an annulated 2-uloside fragment. The affinosides, isolated from seeds of the plant *Anodendron affine*, belong to this family, and the structure **M** of affinoside A **(Scheme 2.1, b)** shows a 4,6-dideoxy-2-uloside moiety annulated to the steroidal backbone via a fused 1,4-dioxane.[23] The general

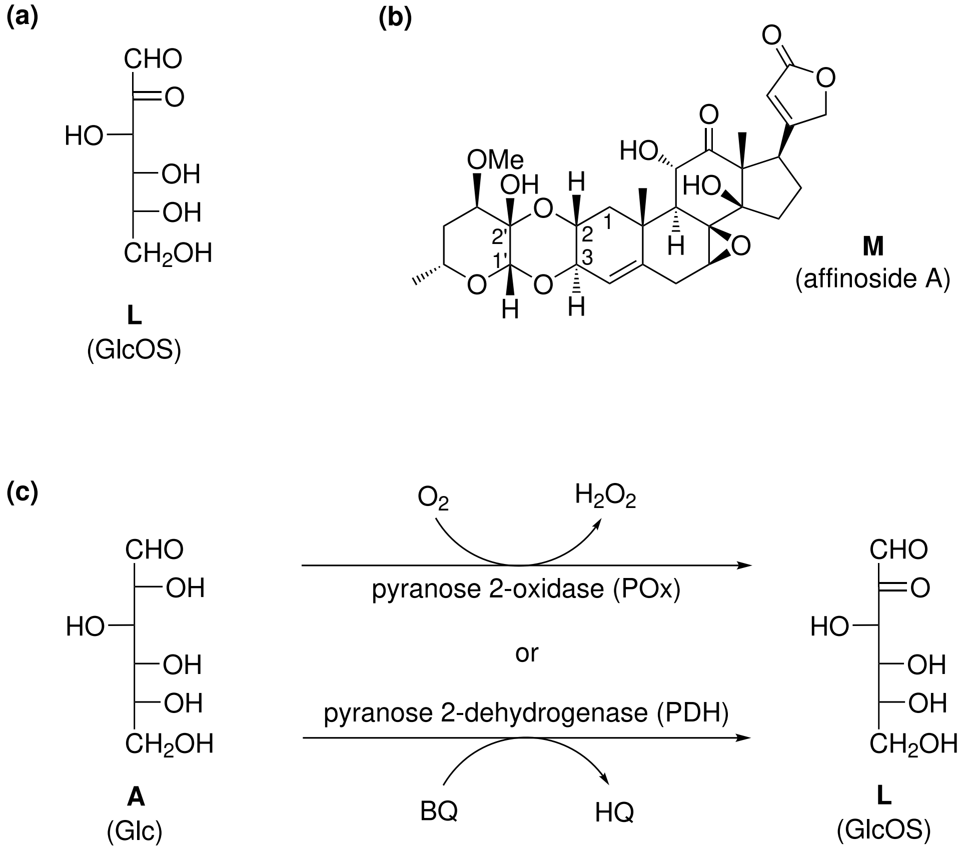
(a)
CHO
O
HO
OH
OH
CH2OH
L
(GlcOS)
(b)
OMe
OH
H
HO
O
HO
2'
1'
2
3
1
H
H
H
M
(affinoside A)
(c)
CHO
OH
HO
OH
OH
CH2OH
A
(Glc)
O2
H2O2
pyranose 2-oxidase (POx)
or
pyranose 2-dehydrogenase (PDH)
BQ
HQ
CHO
O
HO
OH
OH
CH2OH
L
(GlcOS)

Scheme 2.1 **(a)** Structure of D-glucosone **L**. **(b)** Structure **M** of the cardenolide glycoside affinoside A.[23] **(c)** Enzymatic transformations of D-glucose **A** to D-glucosone **L**. BQ = benzoquinone. HQ = hydroquinone.[24–29]

question how *keto*-sugars might be formed biosynthetically has been addressed. For example, certain enzymes, mostly from fungi resident on wood decay, have been found to catalyze the oxidation of aldoses to aldos-2-uloses **(Scheme 2.1, c)**. In most cases, these types of enzymes are rather unspecific, and several saccharides can be substrates for one individual enzyme. Pyranose 2-oxidase (POx, EC 1.1.3.10) is an intracellular, tetrameric flavoenzyme capable of oxidizing D-glucose **A** to D-glucosone **L** using oxygen as an electron acceptor. Notably, this enzyme class is able to transform other saccharide substrates with similar configurations and pyranose conformations (D-xylose, L-sorbose or D-glucono-1,5-lactone) to the oxidized products. Hydrogen peroxide is formed as the byproduct, and can potentially be used as a substrate for peroxidases involved in the degradation of lignocellulose (ligninolysis).[24–26] In contrast, pyranose 2-dehydrogenase (PDH, EC 1.1.99.29) is an extracellular, monomeric flavoenzyme. Since this enzyme class is not able to use molecular oxygen, other electron acceptors like the system benzoquinone/hydroquinone (BQ/HQ) must be employed. A wide range of substrates including reducing and non-reducing monosaccharides and oligosaccharides of different

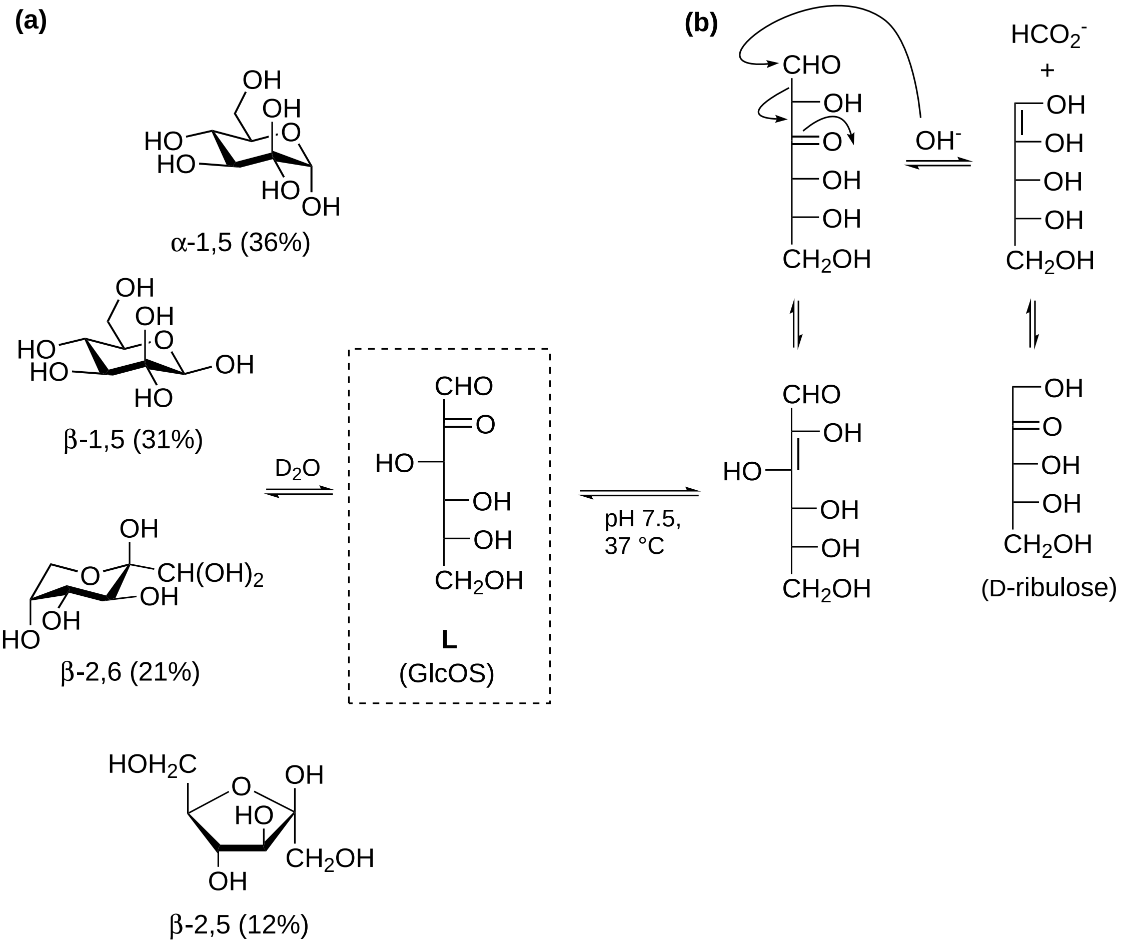

Scheme 2.2 **(a)** Cyclic forms of D-glucosone **L** in D_2O at 27 °C.[30] **(b)** Major degradation pathway of D-glucosone **L** in aqueous phosphate buffer.[20]

anomeric configurations can be transformed. Although D-glucose **A** is intermediately converted to D-glucosone **L** by the PDH enzyme, the corresponding 3-*keto* derivative is also formed, and upon prolonged reaction time oxidation to the 2,3-*diketo* product is observed.[27–29]

Aldos-2-uloses, although structurally simple molecules, exhibit an interesting chemistry that can pose challenges towards synthesis, isolation and purification. As compared to conventional sugars, the second carbonyl group can participate in additional hemiacetal ring closures. Furthermore, 1,2-dicarbonyl systems of carbohydrates are prone to the formation of hydrates, and these factors result in often complex mixtures of unprotected 2-uloses in solution. Köpper and Freimund analyzed the cyclic forms of D-glucosone **L** in aqueous solution by NMR spectroscopy **(Scheme 2.2, a)**.[30] Accordingly, the equilibrium was found to contain the hydrated forms of the α-1,5-pyranose (36%) and the β-1,5-pyranose (31%), along with the hydrates of the β-2,6-pyranose (21%) and the β-2,5-furanose (12%). Since **L**, as part of the glucose degradation process, is degraded under physiological conditions or *ex vivo* in near-neutral solution, Zhang and Serianni utilized NMR spectroscopy, in combination with isotope labeling of **L**, to track the initial steps of its degradation in phosphate-buffered solution **(Scheme 2.2, b)**.[20] The major degradation pathway, determining the fate of 90% of **L**, was found to proceed *via* formation of the 2,3-enediol, tautomerization to the 1,3-dicarbonyl, and hydroxide-induced cleavage of the 1,3-dicarbonyl, giving D-ribulose and formate as the byproduct. These studies further revealed that 10% of **L** undergo a phosphate-catalyzed skeletal rearrangement, albeit, the formed product is D-ribulose, too. Noteworthy, in other studies, base-induced rearrangements of the corresponding methyl glycosides of **L** into the 3-*keto* derivatives have been observed, and Liu and Tsuda disclosed the rearrangements of 2-ulosides to the 3-ulosides to progress *via* a hydride shift mechanism.[31]

In this regard, the chemistry of D-glucosone **L** as introduced here serves as a representative example for the general chemistry of 2-ulosides, which is characterized by reactions like carbonyl hydration, tautomerization/enediol formation, and elimination/dehydration. Several of these reactions can also be observed for protected 2-uloside carbohydrates, a topic which will briefly be discussed in **Section 2.1.1**.

2.1.1. Synthesis of Protected 2-Ulosides

The synthesis of protected 2-ulosides, for example as building blocks in carbohydrate chemistry, can be achieved by subjecting suitable carbohydrate precursors to oxidation, furnishing the 2-*keto* functionality. Obviously, a possible strategy would involve oxidation of the free secondary C-2-OH group to the corresponding ketone, and this frequently applied method has been summarized in an early review.[32] In this context, initial work was done by Theander and Coworkers, who treated partially unprotected glycosides with chromium trioxide to obtain mixtures of isomeric ulosides.[33, 34] Later, many common alcohol oxidation methods proved to be reliable **(Scheme 2.3)**. For example, Hughes utilized the combination DMSO/acetic anhydride for the oxidation of 1,6-anhydrogalactopyranose **N** to the 2-uloside **O**, which was found to be prone to hydration, forming the hydrate **P** while standing open overnight.[35] Other DMSO-based methods have been applied, too. For instance, Nakamura and Shiozaki used the classic Swern oxidation protocol for the synthesis of the allyl α-2-uloside **R**, which was needed as a synthetic intermediate in the total synthesis of the antifungal natural product sphingofungin E.[36] Recently, Priebe and Coworkers treated benzylidene acetal **S** with Dess-Martin periodinane (DMP) to obtain 2-uloside **T**, which was next subjected to the *gluco*-selective reduction with $NaBD_4$ to give access to 2-deuterated glucosides.[37]

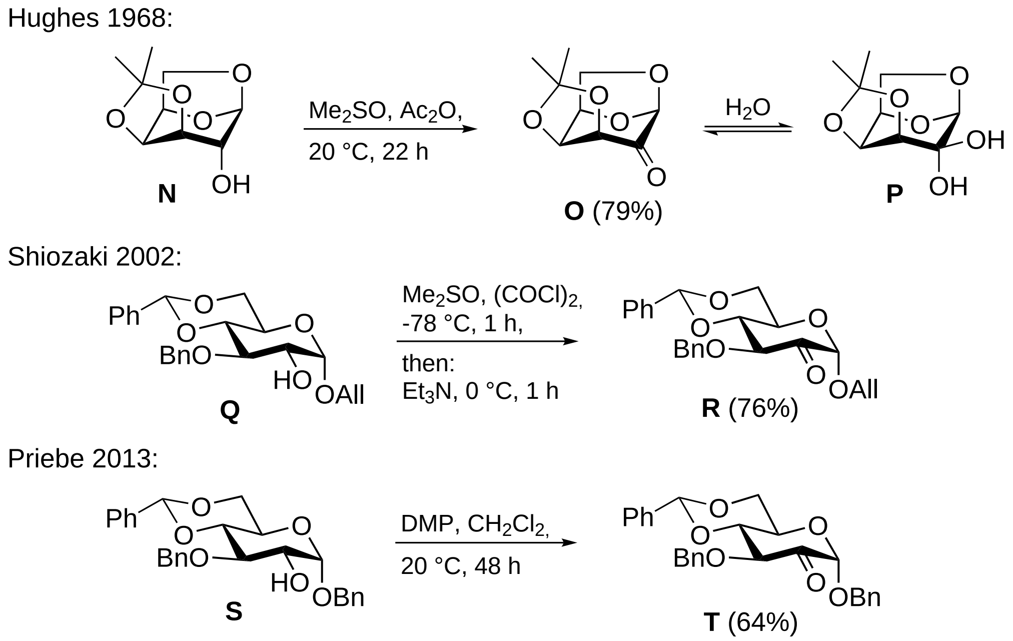

Scheme 2.3 Formation of 2-ulosides **O**[35], **R**[36] and **T**[37] *via* oxidation of the *C*-2-OH of different carbohydrate precursors.

Apart from *O*-2-unprotected glycosides, 2-oxyglycal derivatives have been found to be suitable substrates for the oxidative formation of 2-ulosides **(Scheme 2.4)**, and the majority of the work in this area, as well as the chemistry of related compounds, was done by Lichtenthaler and Coworkers. Accordingly, 2-benzoyloxyglucal **U** was found to undergo *syn*-addition of bromine to the vicinal dibromides **V** and **W**, which could be hydrolyzed with transposition of the benzoyloxy group in the presence of silver carbonate to the 2-ulosides **X** and **Y**.[38] Furthermore, when similar 2-acyloxyglycals like **Z** are treated with hydroxylamine hydrochloride **(Scheme 2.5)**, upon cleavage of the intermediary oxime with acetaldehyde in acidic solution, 1,5-anhydrouloses like **AA** (the 1-deoxy derivatives) can be obtained.[39, 40] The proanomeric center in **AA** was found to be susceptible to radical reactions, and photobromination gave anomeric α-ulosyl bromides like **AB**.[41] As an alternative to the radical photobromination, electrophilic bromination with NBS[42], in combination with a low molecular alcohol as a sacrificial nucleophile, can furnish the same ulosyl bromide products, and this method was also applicable for the transformation of the corresponding benzyl protected derivative **AC** to ulosyl bromide **AD**.[43] Subsequently, the glycosylation chemistry of both benzoylated **AB** and benzylated **AD** was explored by the Lichtenthaler group in detail. Standard Koenigs-Knorr[45] conditions (alcohol, silver carbonate in CH_2Cl_2) were identified to be applicable to these ulosyl bromide donors **(Scheme 2.5, bottom)**. The electron-withdrawing 2-*oxo*-substituent is believed to facilitate S_N2-type displacement

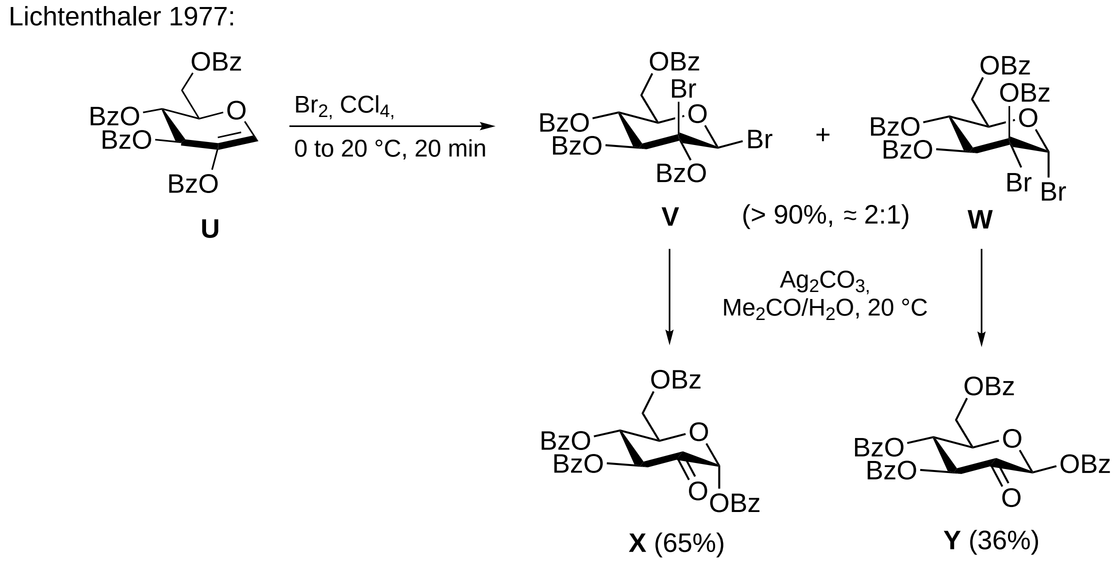
Lichtenthaler 1977:
U
Br_2, CCl_4,
0 to 20 °C, 20 min
V
W
(> 90%, ≈ 2:1)
Ag_2CO_3,
Me_2CO/H_2O, 20 °C
X (65%)
Y (36%)

Scheme 2.4 Bromination of oxyglucal **U**, and hydrolysis of the addition products to the 2-ulosides **X** and **Y**.[38]

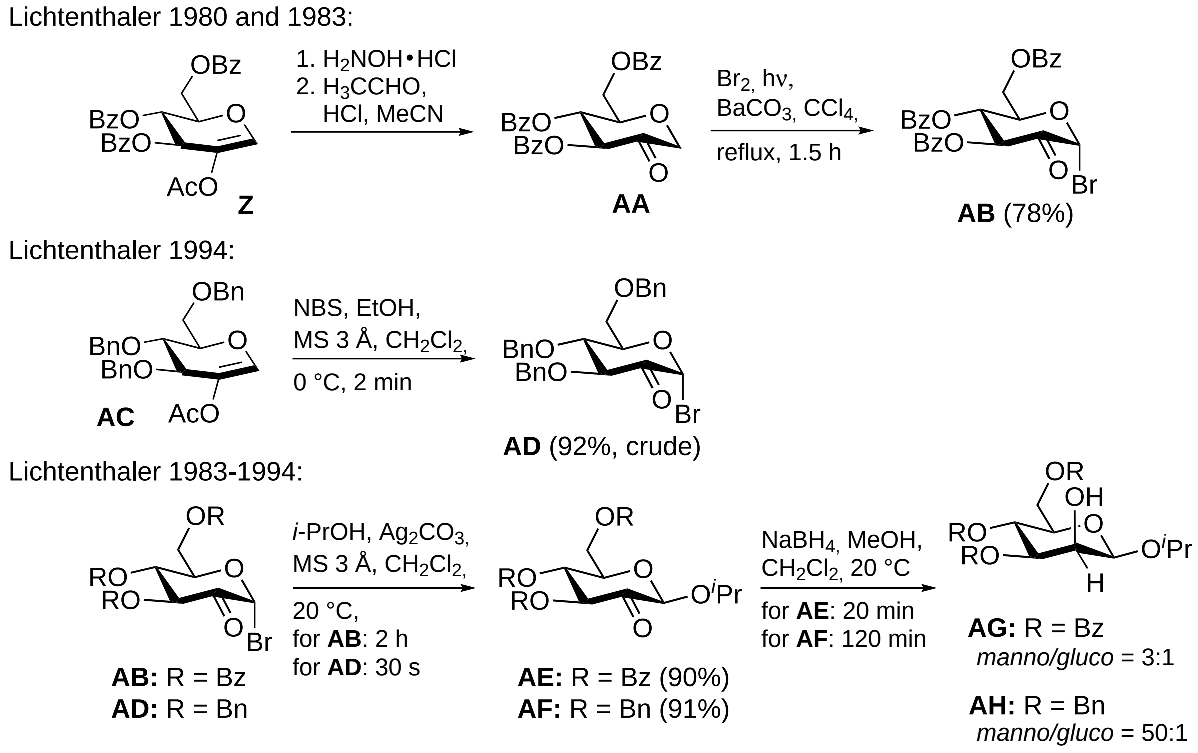
Lichtenthaler 1980 and 1983:
Z
1. $H_2NOH{\bullet}HCl$
2. H_3CCHO, HCl, MeCN
AA
Br_2, hν, $BaCO_3$, CCl_4,
reflux, 1.5 h
AB (78%)
Lichtenthaler 1994:
AC
NBS, EtOH, MS 3 Å, CH_2Cl_2,
0 °C, 2 min
AD (92%, crude)
Lichtenthaler 1983-1994:
i-PrOH, Ag_2CO_3, MS 3 Å, CH_2Cl_2,
20 °C, for AB: 2 h, for AD: 30 s
AB: R = Bz
AD: R = Bn
AE: R = Bz (90%)
AF: R = Bn (91%)
$NaBH_4$, MeOH, CH_2Cl_2, 20 °C
for AE: 20 min
for AF: 120 min
AG: R = Bz
manno/gluco = 3:1
AH: R = Bn
manno/gluco = 50:1

Scheme 2.5 Reactions involving the formation of ulosyl bromides **AB**[41] and **AD**[42, 43], β-selective glycosylations giving **AE/AF**, and *manno*-selective hydride reduction to **AG/AH**.[44]

of the bromide under heterogeneous conditions, resulting in a high β-selectivity of the glycosylation reaction when condensing **AB/AD** with alcohols in the presence of insoluble silver carbonate. Such glycosylations have evolved to be established methods for the preparation of 2-ulosides of type **AE/AF**. Furthermore, the hydride reductions of β-2-ulosides, e.g. with $NaBH_4$, proceed with high equatorial selectivity and give the corresponding mannoside products **AG/AH**. Since the preparation of 1,2-*cis*-glycosides like β-mannosides is usually challenging[46, 47], this combination of β-selective ulosyl bromide glycosylation, followed by *manno*-selective hydride reduction, has found application in the synthesis of β-mannosides.[44]

Apart from enabling the described stereoselective halogenation and glycosylation reactions at the anomeric position, the 2-*keto* functionality of 2-ulosides results in an activation of position 3. As a consequence, deprotonation of the *H*-3, followed by elimination reactions, are side reactions frequently encountered in transformations of 2-ulosides. This type of chemistry, including subsequent degradation reactions of the primary elimination products, can be regarded as a transition from carbohydrate chemistry to the chemistry of unsaturated heterocycles. Since the results covered in **Chapter 5** of this thesis are related to this field, some basic reactions of 2-ulosides towards unsaturated downstream products will be introduced in **Section 2.1.2**.

2.1.2. From 2-Ulosides to Unsaturated Heterocycles

In early experiments involving the oxidative formation of 2-ulosides from the corresponding 2-*O*-unprotected glycosides, Lichtenthaler and Heidel observed that glucoside **AI (Scheme 2.6)**, upon oxidation with DMSO/acetic anhydride to the intermediate 2-uloside **AJ**, undergoes direct elimination of acetic acid to form an unsaturated product of lower molecular weight, which was identified to be the 3-enol-2-ketone (or, simplified: 3,2-enolone[48]) **AK**.[49] Putatively, this transformation would involve deprotonation of the *H*-3 to form an enol species **AJ-a**, which could undergo 1,4-elimination of acetic acid. Subsequently, such elimination reactions were found to be common for transformations involving 2-ulosides, either as substrates or as products, under a variety of conditions. For example, Rayner and Coworkers synthesized the acetylated 2-uloside **AM** *via* oxidation of **AL** with RuO_4. Thermal treatment (175 °C) upon gas chromatography of **AM** gave a second component in the collected product, which could be characterized as the 3,2-enolone **AN**.[50] In a comparable manner with *in situ* generated RuO_4, Lundt and Pedersen prepared benzoylated 2-uloside **AP**. Upon subjecting **AP** to weakly basic conditions at elevated temperatures ($NaHCO_3$ in wet benzene at 80 °C), 3,2-enolone **AQ** could be isolated as the major product.[51] The nature of the 4-*O*-protecting group

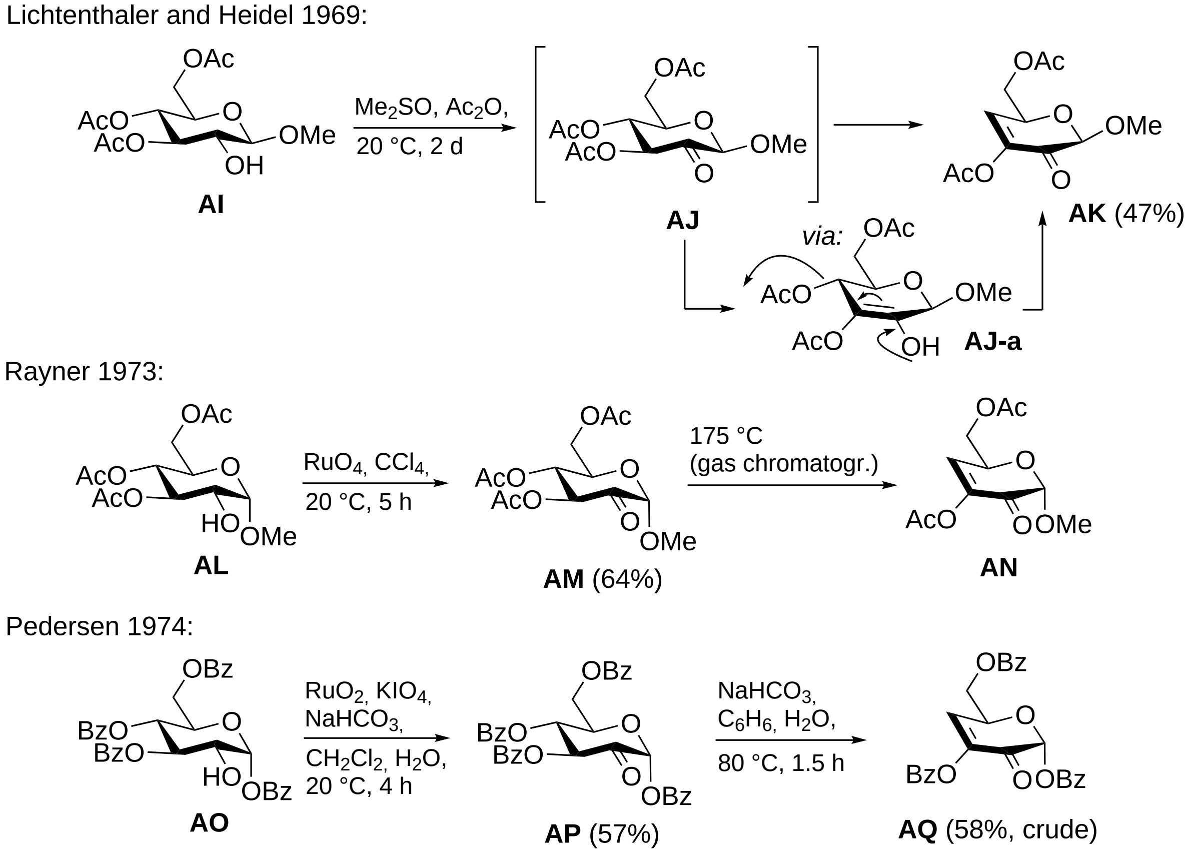
Lichtenthaler and Heidel 1969:
OAc
AcO
AcO
O
OMe
OH
AI
Me2SO, Ac2O,
20 °C, 2 d
AJ
AK (47%)
via:
OH
AJ-a
Rayner 1973:
AL
RuO4, CCl4,
20 °C, 5 h
HO
AM (64%)
175 °C
(gas chromatogr.)
AN
Pedersen 1974:
OBz
BzO
AO
RuO2, KIO4,
NaHCO3,
CH2Cl2, H2O,
20 °C, 4 h
AP (57%)
NaHCO3,
C6H6, H2O,
80 °C, 1.5 h
AQ (58%, crude)

Scheme 2.6 Synthetic sequences involving the elimination of 2-uloside intermediates to the corresponding 3,2-enolones **AK**[49], **AN**[50] and **AQ**[51].

can be expected to have an influence on the enolone formation from 2-ulosides, and indeed, the majority of examples described in the literature feature ester-protected 2-ulosides with the corresponding carboxylate as a suitable leaving group. Examples involving other protecting groups like 4,6-*O*-benzylidene acetals[52] or benzyl ethers[53] do exist, however, in these cases stronger basic reagents in polar solvents (e.g. Wittig reagents in DMSO, or K_2CO_3 in MeOH) are required for the elimination step.

An interesting cascade of advanced degradation reactions of 3,2-enolone intermediates was initially observed by Lichtenthaler and Heidel[49], and later expanded onto variably protected 3,2-enolones.[51, 54] Accordingly, when 3,2-enolone intermediates like **AK** are subjected to harsh acidic conditions, for example neat trifluoroacetic acid (**Scheme 2.7, top**), a second equivalent of carboxylic acid is lost, and achiral acylated derivatives of kojic acid like acetylkojic acid **AR** (a γ-pyrone system) are formed.[49] In a similar transformation, but under basic conditions, dibenzoylkojic acid **AS** can be obtained upon heating of benzoylated 3,2-enolone **AQ** in pyridine at 60 °C.[51] Because of the interesting biological activities of kojic acid itself, which can be used as a whitening agent due to its tyrosinase inhibiting properties[55], such transformations of 3,2-enolones to kojic acid derivatives have been explored in detail. Lichtenthaler and Coworkers proposed a mechanism involving the initial formation of a vinylogous enol/enolate *via* *H*-5 deprotonation **(Scheme 2.7, bottom)**.[54] Subsequent acyl group migration and expulsion of the anomeric substituent could give the kojic acid derivative **AS**. Notably, the nature of the anomeric substituent can have an influence: whereas 1-*O*-acylated (R = acyl) enolones with a suitable leaving group at position 1 undergo a fast reaction to the respective kojic acid derivatives, the corresponding methyl derivatives (R = Me) are rather insensitive towards acids, tentatively because expulsion of the

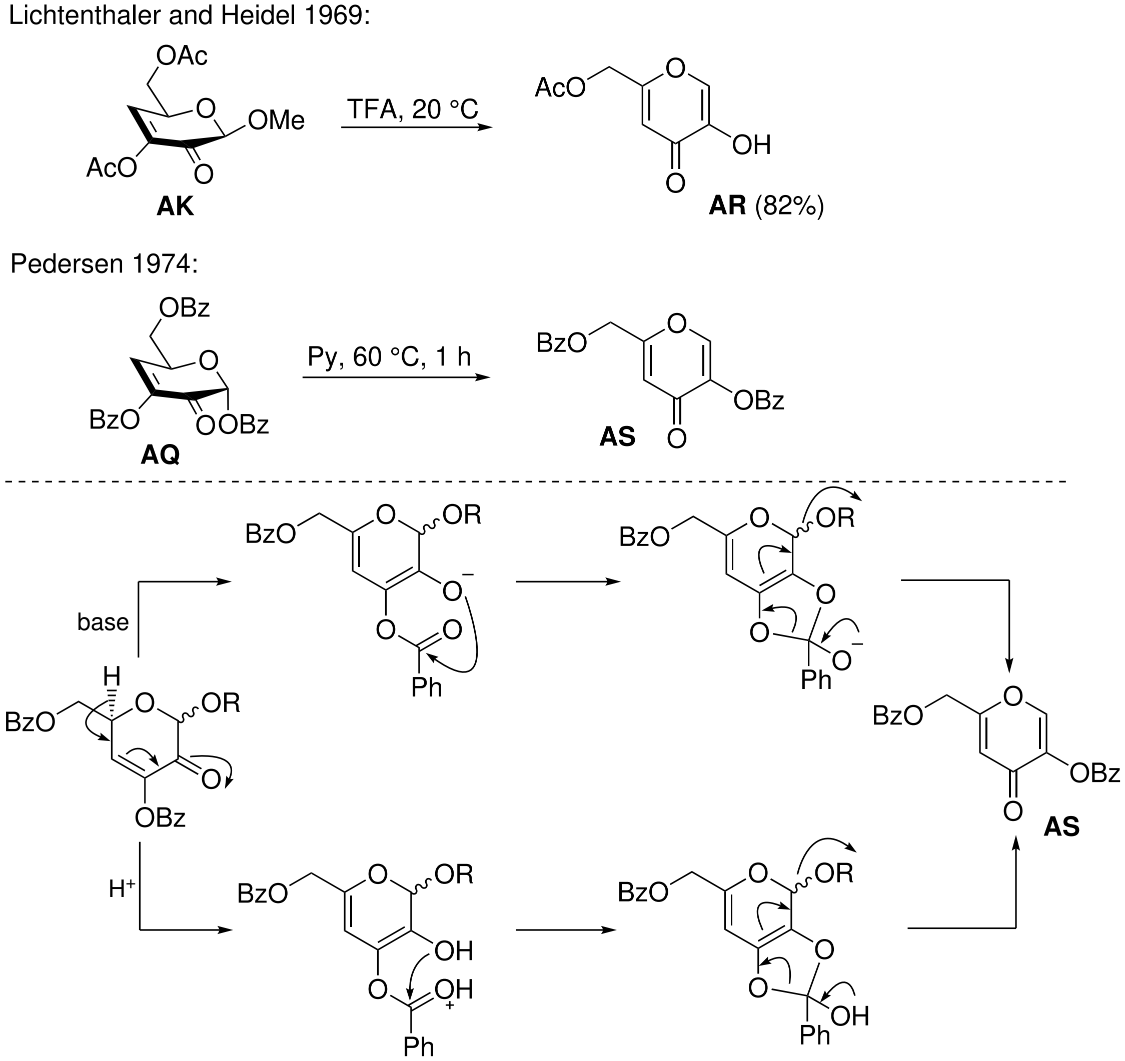
Lichtenthaler and Heidel 1969:
OAc
O
OMe
AcO
O
AK
TFA, 20 °C
AcO
O
OH
O
AR (82%)
Pedersen 1974:
OBz
O
BzO
OOBz
AQ
Py, 60 °C, 1 h
BzO
O
OBz
AS
O
base
H
BzO
O
OR
O
OBz
BzO
O
OR
O−
O
O
Ph
BzO
O
OR
O
O
O−
Ph
BzO
O
OBz
O
AS
H+
BzO
O
OR
OH
O
OH+
Ph
BzO
O
OR
O
O
OH
Ph

Scheme 2.7 Top: formations of kojic acid derivatives **AR**[49] and **AS**[51] from 3,2-enolone substrates under acidic or basic conditions. Bottom: proposed mechanism for the formation of kojic acid derivatives, exemplified for dibenzoylkojic acid **AS**. R = methyl, acyl.[54]

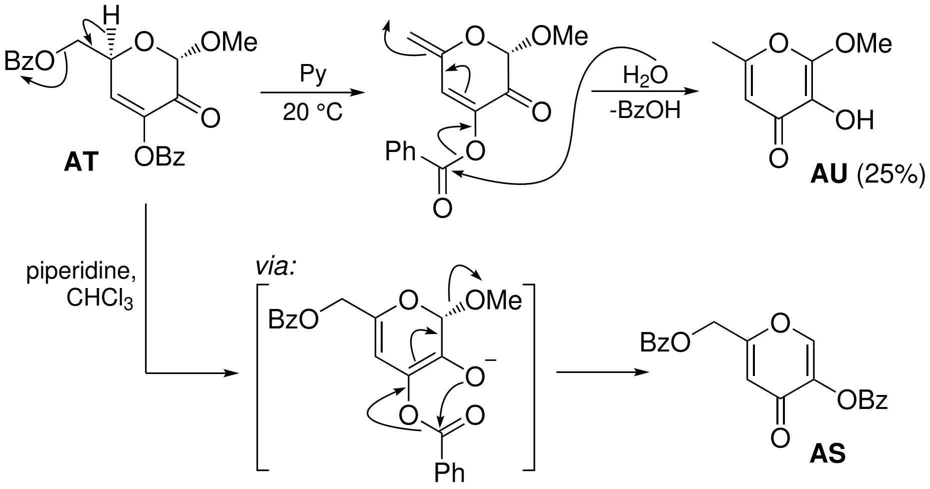

Scheme 2.8 Base-induced transformations of 3,2-enolone **AT** into methoxy-allomaltol **AU** or dibenzoylkojic acid **AS**.[54, 56]

anomeric substituent is disfavored.[54] Remarkably, the exact progression of this type of degradation reactions seems to be dependent on the individual conditions, and some 1-*O*-alkyl 3,2-enolones like **AT**, in combination with pyridine as the base, undergo 5,6-elimination to the *exo*-methylene intermediate rather than vinylogous enolization **(Scheme 2.8)**.[54, 56] In this case, after hydrolysis, other γ-pyrone products like methoxy-allomaltol **AU** can be obtained, together with multiple other, unidentified products. Interestingly, when piperidine is used as the base, the pathway towards dibenzoylkojic acid **AS** is favored again, demonstrating that this kind of degradation and rearrangement chemistry of unsaturated sugars is diverse.

In this context, it should be noted that in very early work in 1936, K. Maurer examined reactions of acylated 2-ulosides (acetylated and benzoylated derivatives of glucosone **L**). Upon treatment of these 2-*keto*-sugars with NaOAc/Ac_2O or pyridine/Ac_2O, Maurer made the early observation that kojic acid derivatives are formed.[21, 57] However, the mechanistic picture of these reaction cascades (e.g. the formation of 3,2-enolones as the initial elimination products) was not yet fully understood, and required the deliberate synthesis of 3,2-enolones from available sugar intermediates as achieved by Lichtenthaler and others.

2.2. Objective of this Chapter

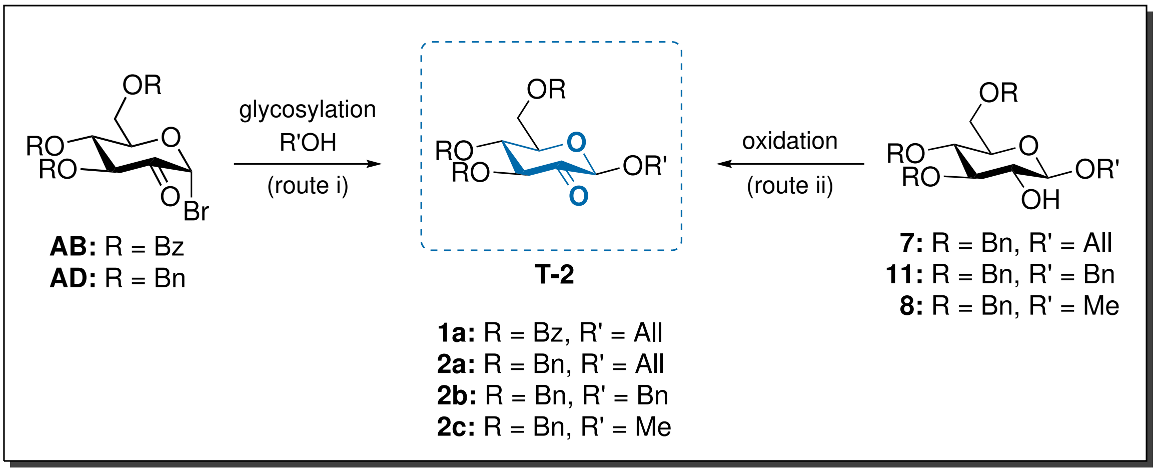

Scheme 2.9 Schematic representation of the synthetic routes described in this chapter towards target 2-ulosides **T-2**.

The synthesis of β-2-uloside precursors of type **T-2** with diverse anomeric substituents R', the synthetic key precursors towards the target compounds **T-3,4,5**, is covered in this chapter **(Scheme 2.9)**. First, early efforts for the synthesis of allyl β-2-ulosides **1a** and **2a** from Lichtenthaler's ulosyl bromides **AB** and **AD** (route i) are discussed. Subsequently, the formation of allyl uloside **2a**, benzyl uloside **2b** and methyl uloside **2c** *via* oxidation of the *C*-2-OH (route ii) is described. The majority of compounds traversed in route ii are known. However, since most reactions were carried out with variations from the published procedures, these syntheses are included in the Experimental Part **(Chapter 6)** to ensure reproducibility of the experiments.

2.3. Results and Discussion

In initial synthetic studies, Lichtenthaler's ulosyl bromide donors **AB** and **AD**, accessible from D-glucose in 4–5 steps, were anticipated to be suitable starting materials for the synthesis of the unknown allyl β-2-ulosides **1a** and **2a (Scheme 2.10)**. For that purpose, benzoylated ulosyl bromide **AB** was condensed with allyl alcohol under Koenigs-Knorr[45] conditions (Ag_2CO_3 and molecular sieves in CH_2Cl_2) according to the reported protocol.[42] After 3 h, TLC confirmed the formation of a single product, however, upon workup and chromatographic purification (SiO_2), only traces of the wanted allyl uloside **1a**, together with 3,2-enolone **3a** as the major product (31%), could be isolated. Accordingly, acylated 2-ulosides have frequently been observed to undergo elimination to

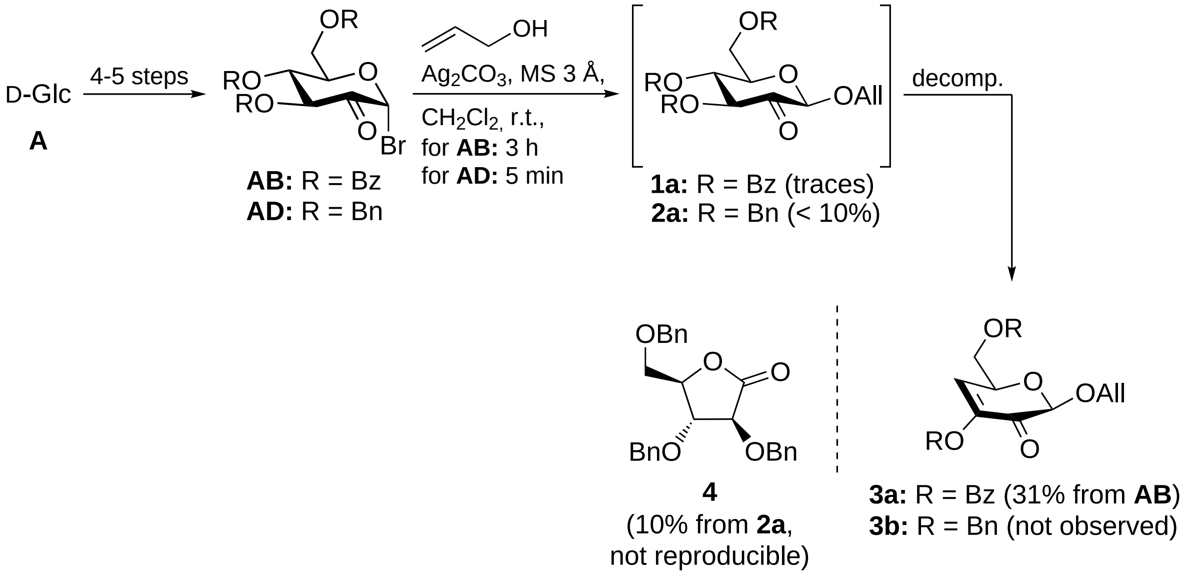

Scheme 2.10 Initial Koenigs-Knorr glycosylations of ulosyl bromides **AB** and **AD** in the formation of allyl 2-ulosides **1a** and **2a**, and the derived decomposition products **3a,b** and **4**.

the 3,2-enolone products (comp. **Section 2.1.2**) under a variety of conditions, including silica-induced elimination upon chromatography.[58] Consequently, benzyl-protected allyl 2-uloside **2a** was anticipated to be more resistant towards elimination/3,2-enolone formation, and therefore benzylated ulosyl donor **AD** was reacted with allyl alcohol under standard conditions.[43] After a short reaction time of 5 min TLC indicated the formation of a complex mixture. After workup and chromatography (SiO_2) of the crude oil, **2a** was obtained in a severely impure manner in decent yields ($< 63\%$), albeit, repeated chromatography resulted in significant loss of material, and only $< 10\%$ of **2a** could be isolated in pure form. Notably, upon chromatography of **2a**, the corresponding 3,2-enolone **3b** was not found. Surprisingly, from the great number of endeavors to isolate pure **2a** in a satisfactory yield, benzylated D-arabino-1,4-lactone **4** was isolated in low yield (10%) upon chromatographic purification, and spectral properties were in full accordance with published data.[59, 60] Albeit, all attempts to reproduce the formation of **4** from **2a**, tentatively proceeding *via* expulsion of the anomeric carbon, remained unsuccessful, and therefore effects of contamination of reagents, solvents or glassware, respectively, must be taken into account. Nevertheless, low yields in the isolation of **2a** without isolation of the 3,2-enolone **3b**, together with the enigmatic and unreproducible formation of **4**, indicated that Lichtenthaler's ulosyl bromides **AB**/**AD** in combination with Koenigs-Knorr conditions were unsuitable for sensitive allyl ulosides of type **1a** or

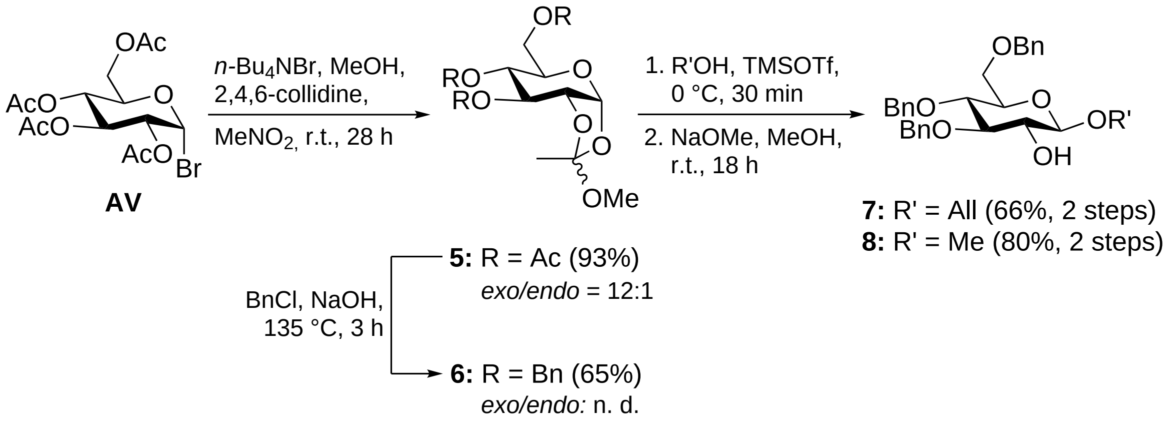

Scheme 2.11 Synthesis of allyl glucoside **7** and methyl glucoside **8** *via* methyl orthoesters **5** and **6** employing protocols published by Draghetti *et al.*[61] and Nepogodiev *et al.*[62].

2a. Therefore, access to **2a** by oxidation of the *C*-2-OH of a corresponding protected allyl glucoside substrate was explored as an alternative (route ii).

A well-known strategy for the synthesis of *O*-2-unprotected β-glucosides, the required substrates for the oxidative formation of 2-ulosides of type **2**, utilizes carbohydrate 1,2-orthoesters as intermediates. This class of compounds was explored in detail for their applicability in carbohydrate chemistry by Kochetkov and Coworkers.[63] Such carbohydrate 1,2-orthoesters are amenable to Lewis acid-promoted 1,2-*trans*-selective glycosylation, followed by selective deacetylation of the *C*-2-OAc to furnish the *O*-2-unprotected glucosides.[64] In line with this, Draghetti *et al.* described the synthesis of 3,4,6-tri-*O*-benzylated allyl β-D-glucoside **7** *via* the formation of the intermediate methyl orthoester.[61] Based on these published results, a similar synthetic route with minor variations was utilized in the present work **(Scheme 2.11)**. The synthesis started with the carbohydrate precursor tetra-*O*-acetylglucopyranosyl bromide **AV**, which was subjected to Lemieux's tetra-*n*-butylammonium bromide-promoted *in situ* anomerization[65] in the presence of methanol and 2,4,6-collidine as a base to afford acetylated methyl orthoester **5** as an *exo*/endo-mixture. A protocol using nitromethane as the solvent, instead of neat collidine as proposed by Draghetti, was published by Nepogodiev *et al.* for the corresponding benzyl orthoester **9**, and was found to facilitate the workup procedure since smaller amounts of high-boiling collidine had to be removed.[62] Subsequently, heating of **5** in benzyl chloride in the presence of NaOH gave benzylated **6** in a one-pot deacetylation/benzylation reaction, which was also utilized by Nepogodiev *et al.*[62] Although orthoester **6** was putatively received as an isomeric *exo*/endo mixture similar to **5**, determination of the isomeric ratio by NMR integration was not feasible. Reaction of **6** in anhydrous allyl alcohol as the solvent in the presence

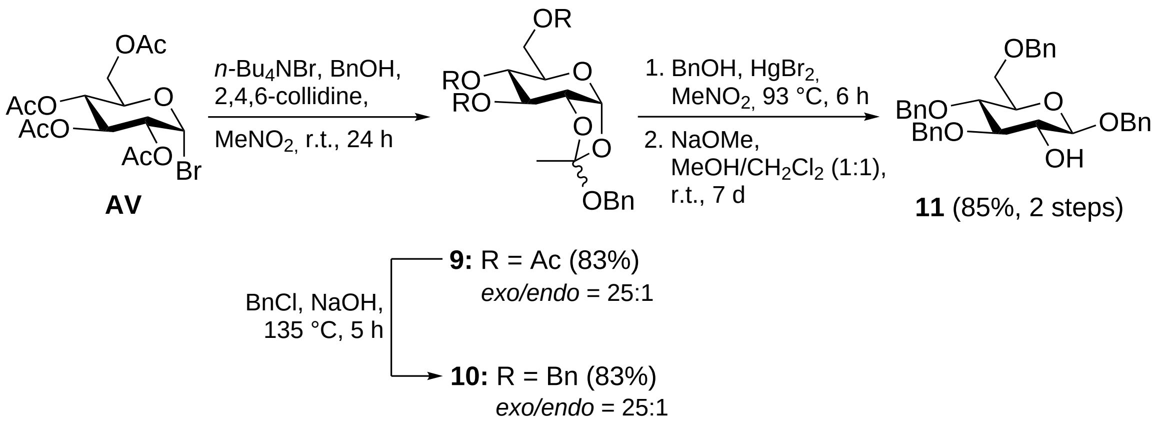

Scheme 2.12 Synthesis of benzyl glucoside **11** *via* benzyl orthoesters **9** and **10** employing a protocol published by Nepogodiev *et al.*[62]

of catalytic amounts of TMSOTf initiated the Lewis acid-mediated orthoester cleavage and gave a mixture of the *O*-2-acetylated allyl glucoside, together with deacetylated **7** as reported by Draghetti *et al.*[61] The crude mixture was finally deacetylated under Zemplén's[66] conditions to provide allyl β-glucoside **7** as a substrate for oxidative formation of the corresponding 2-uloside **2a**. In a completely analogous manner from orthoester **6**, methyl glucoside **8** could be obtained **(Scheme 2.11)**, which was previously synthesized by Mayato *et al.*[67] The corresponding benzyl glucoside **11** was prepared by the route described by Nepogodiev *et al.*[62] After analogous formation of acetylated benzyl orthoester **9** **(Scheme 2.12)** and deacetylation/benzylation, benzylated orthoester **10** was available. $HgBr_2$-mediated orthoester cleavage in nitromethane, a method from early orthoester chemistry[63], was found to be superior as compared to other methods, and gave the 2-*O*-acetylated glucoside conveniently on a 30 g scale. Zemplén deacetylation of the crude material, in a mixture of methanol and dichloromethane due to low solubility in methanol, gave benzyl glucoside **11**.[62]

With the *O*-2-unprotected substrates in hand, glucosides **7**, **8** and **11** were subjected to oxidation reactions for the synthesis of 2-ulosides of type **2**. Dess-Martin oxidation[68] as a mild method was used before for the synthesis of sensitive 2-ulosides.[37] Thus, both benzyl glucoside **11** and methyl glucoside **8** were reacted with Dess-Martin periodinane **(Scheme 2.13)**, and gave the corresponding 2-ulosides **2b** and **2c** in excellent yields after chromatography (96% each). Although both **2b**[37] and **2c**[69] were prepared before *via* other synthetic routes, the here described syntheses were evaluated to be beneficial due to the clean and highly convenient Dess-Martin oxidation. Surprisingly, **2a** was found to be more susceptible towards the unwanted acid-mediated formation of 3,2-enolone **3b** under the conditions of the Dess-Martin oxidation. Hence, $NaHCO_3$ was

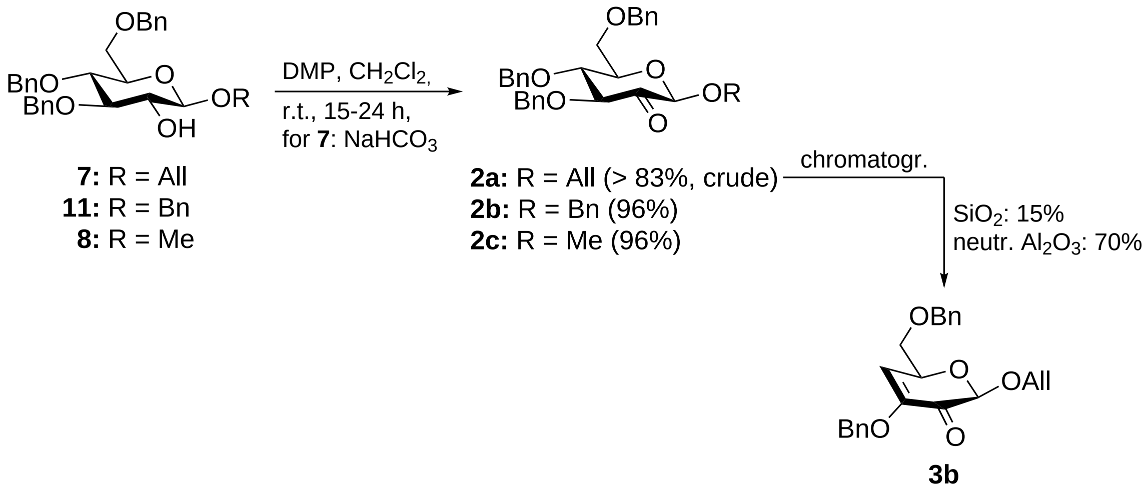

Scheme 2.13 Dess-Martin oxidations towards 2-ulosides **2a,b,c**, and decomposition of **2a** upon chromatography, giving 3,2-enolone **3b**.

added to the Dess-Martin oxidation as a buffer in the transformation of **7**. Conventional silica gel chromatography, as applied to crude **2b/2c**, resulted in severe loss of material in the case of **2a**, and the elimination product **3b** could be isolated in significant amounts (15%). Chromatography on neutral Al_2O_3 provided **3b** as the major product (70%). Noteworthy, the wanted allyl uloside **2a** was previously synthesized by Bundle and Coworkers, albeit, the compound was not characterized, and transformed into the corresponding mannoside *via* hydride reduction without further purification.[70] While acylated 2-ulosides are frequently reported to undergo elimination and 3,2-enolone formation upon workup or purification, similar observations for benzylated 2-ulosides seem to be rather scarce. In contrast, problems concerning the purification of other benzylated 2-ulosides were attributed to the formation of ketone hydrates by Danishefsky.[46] Particularly, structurally related allyl 2-ulosides like *C*-glycosidic **BU**[71] (**Scheme 3.6** on page 35) or benzylidene acetal **R**[36] (**Scheme 2.3** on page 11) could be isolated in pure form. Therefore, the here described property of **2a** to undergo elimination upon purification can be regarded as uncommon, but somewhat in agreement with the aforementioned problems in the synthesis of **2a** *via* glycosylation chemistry from **AD**. All other attempts for the purification of **2a**, either by recrystallization or by solvent extractions of the crude material, remained unsuccessful, and therefore crude **2a** as obtained from the buffered Dess-Martin oxidation was subjected to the following transformations without further purification.

Both the known benzyl glucoside **11** as well as the known derived 2-uloside **2b** were isolated in the form of highly crystalline material. Since crystal structures of sensitive *keto*-sugars are rare, X-ray crystallography was applied to single crystals obtained from

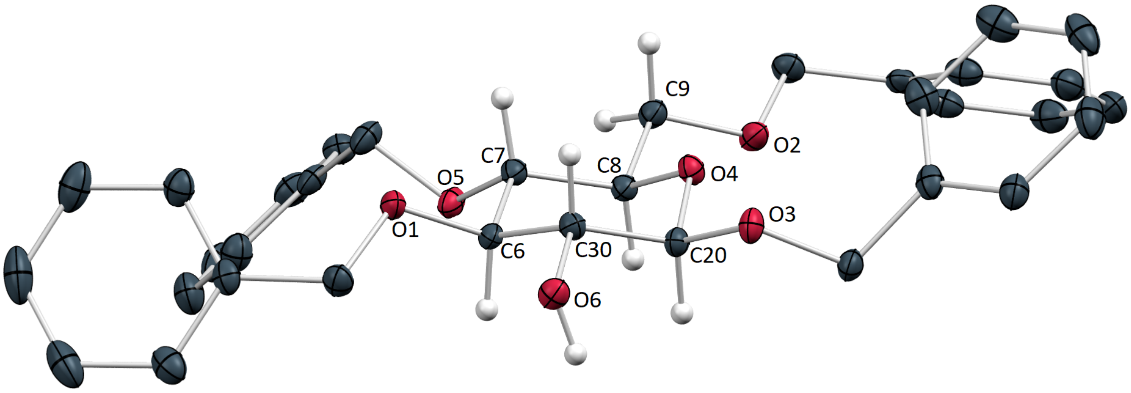

Figure 2.1 X-ray structure of glucoside **11**. Hydrogen atoms of the benzyl ethers are omitted for clarity. Ellipsoids are drawn at the 50% probability level. Red = oxygen, gray = carbon, white = hydrogen. Significant distances and torsion angles: C30-O6 1.424 Å, O6-C30-C20-O3 −60.2°, O6-C30-C6-O1 65.4°.

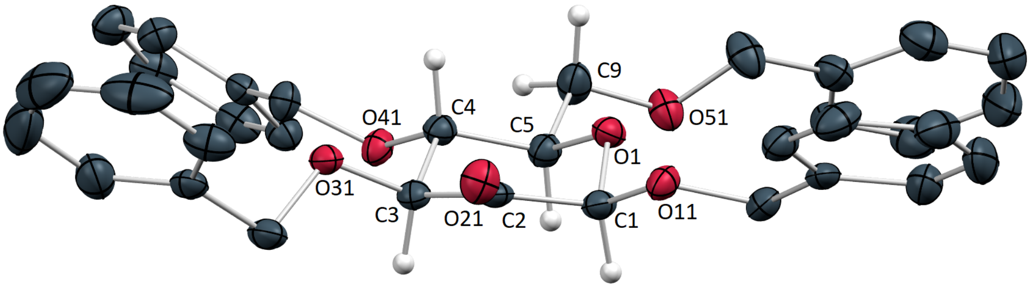

Figure 2.2 X-ray structure of 2-uloside **2b**. Hydrogen atoms of the benzyl ethers and a disorder involving the O51 benzyl group are omitted for clarity. Ellipsoids are drawn at the 50% probability level. Red = oxygen, gray = carbon, white = hydrogen. Significant distances and torsion angles: C2-O21 1.204 Å, O21-C2-C1-O11 −8.5°, O21-C2-C3-O31 11.8°.

11 and **2b** to provide insight into potential changes of the ring conformation upon introduction of the ketone functional group. Benzyl glucoside **11** crystallized in the orthorhombic space group $P2_12_12_1$ with $Z = 4$ **(Fig. 2.1)**. As expected, **11** occupied the $^4C_1$ conformation. The O-C-C-O torsion angles involving the C-2-OH were close to the expected value of 60° for bis(equatorial) orientations (O6-C30-C20-O3 −60.2°, O6-C30-C6-O1 65.4°).

Benzyl 2-uloside **2b (Fig. 2.2)** crystallized in the monoclinic space group $P2_1$ with $Z = 2$, and the bond length of the C-2-ketone moiety (C2-O21 1.204 Å) was found to be as anticipated and comparable to other *keto*-sugars.[72] An analysis of the torsion angles around the ketone (O21-C2-C1-O11 −8.5°, O21-C2-C3-O31 11.8°) revealed a considerably planarized geometry as compared to **11**. Nevertheless, **2b** exhibited a distorted $^4C_1$ conformation, and similar observations were made for 3-*keto*-pyranosides, which were also found to exhibit a distorted $^4C_1$ conformation in the solid state.[72]

2.4. Summary of this Chapter

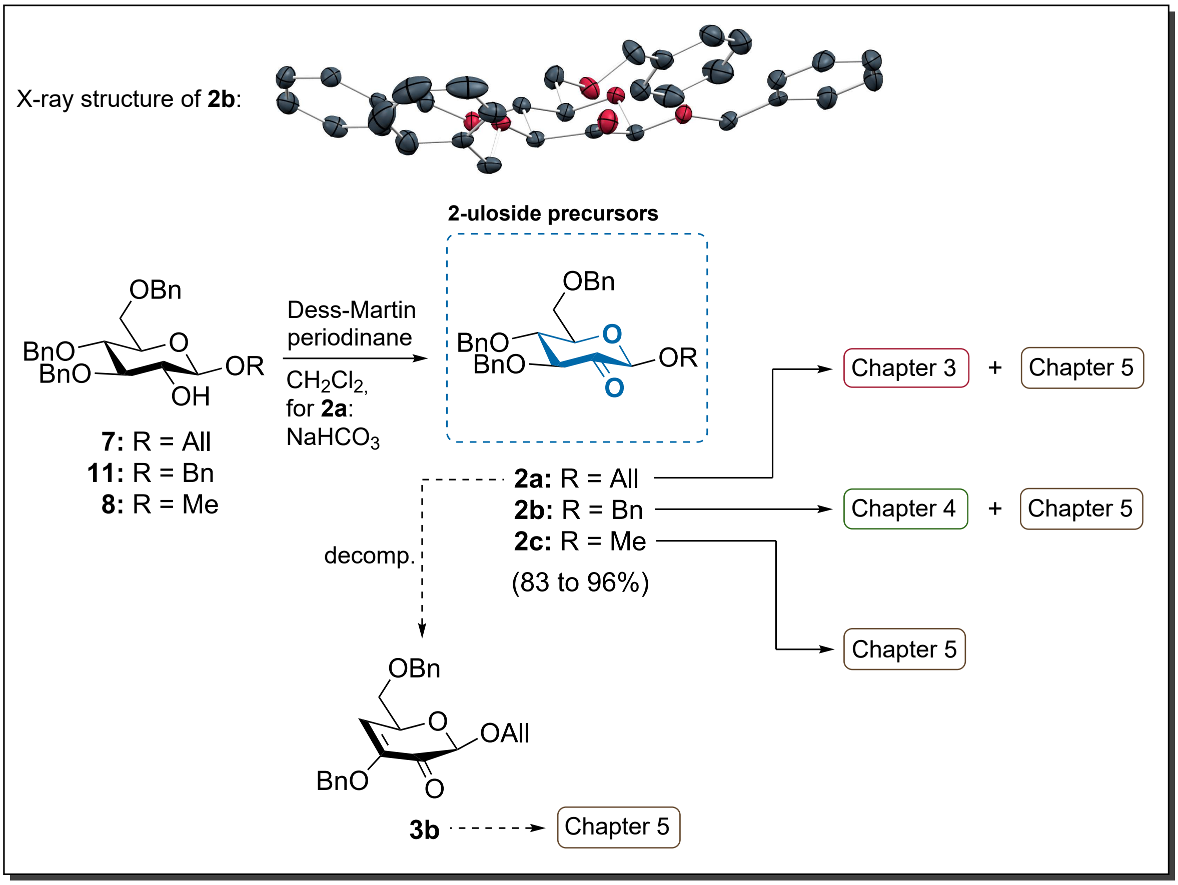
X-ray structure of **2b**:
2-uloside precursors
OBn
BnO
BnO
O
OR
OH
7: R = All
11: R = Bn
8: R = Me
Dess-Martin periodinane
CH_2Cl_2,
for **2a**:
$NaHCO_3$
2a: R = All
2b: R = Bn
2c: R = Me
(83 to 96%)
decomp.
Chapter 3
+
Chapter 5
Chapter 4
+
Chapter 5
Chapter 5
OAll
3b
Chapter 5

Scheme 2.14 Schematic summary of this chapter. Oxidative formations of 2-uloside precursors **2a,b,c**, and 3,2-enolone decomposition product **3b**. Cross-references to the following chapters are given to show the destinations of the obtained products.

Dess-Martin oxidation, a method previously utilized for the synthesis of other *keto*-sugars, was found to transform the 3,4,6-tri-*O*-benzylated glucosides **11** and **8** into the wanted known 2-ulosides **2b** and **2c** in a clean and convenient manner **(Scheme 2.14)**. In contrast, the previously unknown allyl 2-uloside **2a**, derived from known glucoside **7**, was found to be surprisingly prone to the elimination of benzyl alcohol, and formation of the 3,2-enolone **3b** occurred upon unbuffered Dess-Martin oxidation or upon chromatographic purification. The elusive allyl 2-uloside **2a** could be obtained in pure form for characterization purposes, however, only in mediocre yield. For this reason, the application of crude material of **2a** was evaluated to be the method of choice for following transformations involving the sensitive *keto*-sugar. In previously reported similar elimination reactions of benzyl-protected *keto*-sugars, basic reagents in combination with highly polar solvents were required to invoke the elimination of benzyl alcohol. In this regard, the observed unusual property of **2a** is an addition to the chemistry of 2-ulosides and derived carbohydrate 3,2-enolones, and might be of use for other syntheses employing 2-ulosides as carbohydrate building blocks. X-ray single crystal analyses of the known benzyl glucoside **11** and the derived known 2-uloside **2b** provided insight into structural features of 2-*keto*-sugars, and proved that **2b** exhibited a distorted $^4C_1$ conformation in the solid state.

Having established a convenient method to obtain 2-ulosides **2b,c** in pure form, and the sensitive allyl derivative **2a** in crude form, the application of these *keto*-sugars as carbohydrate building blocks in the syntheses of target compounds **T-3,4,5** was feasible.

3. Non-Reducing Higher Sugars: Polyhydroxylated Dioxadecalins

Based on the investigations regarding the synthesis of 2-*keto*-sugars as described in **Chapter 2**, application of these valuable precursors as building blocks for the synthesis of complex carbohydrates was feasible. In this regard, allyl 2-uloside **2a** (**Scheme 2.14** on page 24) was envisioned to be a suitable precursor for the synthesis of 1,2-annulated sugars of type **T-3** (**Scheme 1.4** on page 6), since the 2-ketone as well as the anomeric allyl residue should potentially be amenable to straightforward functionalizations. The results obtained in this context are covered after a general introduction to annulated carbohydrates with a decalin-type structure.

3.1. Introduction to Carbohydrate-Derived Decalin Structures

An interesting class of compounds, arising from the formal annulation of a parent carbohydrate precursor with a second six-membered ring, can be referred to as carbohydrate-derived decalins due to their potential structural similarity with the decalin (decahydronaphthalene or bicyclo[4.4.0]decane) framework. Interesting stereochemical properties arise from the introduction of such an annulation, and the diversity of products can be accounted for by the following general considerations: 1,2-annulation of a generic pyranose with a second six-membered ring **(Scheme 3.1, a)** results in the formation of a bicyclic product, which may further be functionalized by substituents at the positions of the ring fusion (R, R'), by the incorporation of heteroatoms X at any position in the second ring, and by further functionalizations Y of the annulated ring. As shown for a simple annulated product without functionalizations of the second ring (Y = H), the chair-chair ring fusion can occur in four different modes **(Scheme 3.1, b)** and is defined by the anomeric configuration (α or β) and by its relative configuration to the connection at position 2 (*cis* or *trans*). Both 1,2-*cis*-fused isomers α-*cis* and β-*cis* each give rise to a set of two different isomers (1-axial-2-equatorial or 1-equatorial-2-

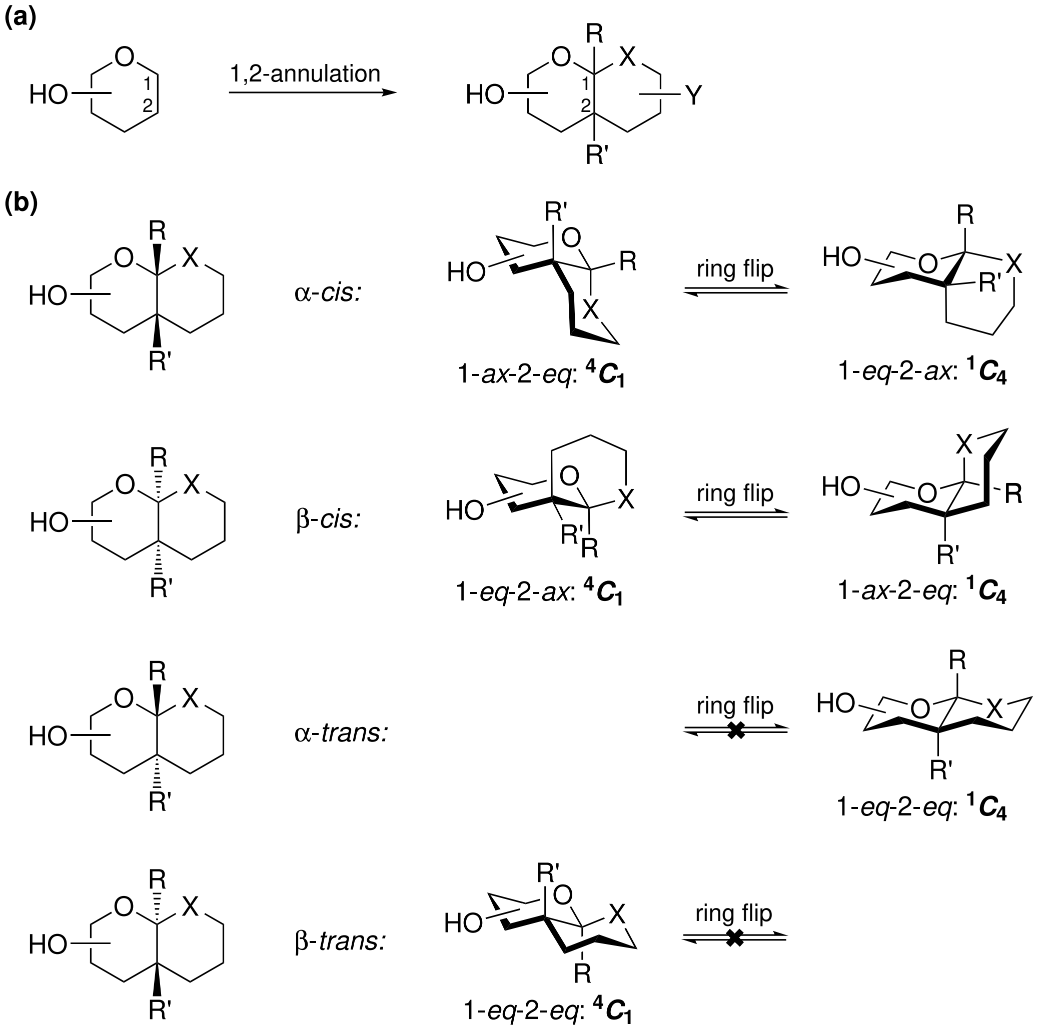
(a)
HO
O
1
2
1,2-annulation
R
O
X
Y
R'
(b)
α-cis:
1-ax-2-eq: $^4C_1$
ring flip
1-eq-2-ax: $^1C_4$
β-cis:
1-eq-2-ax: $^4C_1$
ring flip
1-ax-2-eq: $^1C_4$
α-trans:
ring flip
1-eq-2-eq: $^1C_4$
β-trans:
1-eq-2-eq: $^4C_1$
ring flip

Scheme 3.1 **(a)** 1,2-Annulation of a generic pyranose with a six-membered ring. **(b)** Stereochemical considerations for the obtained 1,2-annulated products. X = CH_2 or heteroatom. R, R', Y = H, OH or organic residue.

axial), one exhibiting a $^4C_1$ conformation and the other a $^1C_4$ conformation, which are interconvertible *via* ring flip (analogous to the ring flip in *cis*-decalin between two enantiomeric isomers). The corresponding 1,2-*trans*-fused isomers α-*trans* and β-*trans* both only exist in the 1,2-diequatorial isomer. For α-*trans*, the bicyclic compound exhibits a $^1C_4$ conformation, and for β-*trans* a $^4C_1$ conformation. In analogy to the situation in *trans*-decalin, ring flip from these *trans*-isomers is not possible, since it would result in an unfavorable *trans*-diaxial fusion not feasible for annulated six-membered rings. These considerations demonstrate the interesting stereochemical properties imposed on a simple monosaccharide upon annulation with a second saturated six-membered ring. As a result, such annulated sugars (or sugar derivatives like carbasugars or iminosugars) exhibiting diverse patterns of annulations and functionalizations have been popular targets for synthetic carbohydrate chemistry, and several reviews have been published, particularly for the synthesis of 1,2-annulated carbohydrates.[73–75]

The following sections give a brief summary of such annulated carbohydrates with different positions of annulation and functionalizations of the non-carbohydrate ring, and with a focus on annulations of a six-membered ring and, consequently, oxadecalin-type structures. In this regard, examples are given for molecules from either natural or synthetic origin. However, several types of natural products with annulated frameworks bear resemblance to the carbohydrate-derived decalin structures discussed here, but are not subject to this introduction. Among these, the polycyclic ladder polyethers of the marine polyketides, and the fused oxasqualenoid natural products of the marine terpenoids, feature highly annulated decalin-type frameworks, but their low degree of hydroxylation and non-carbohydrate based biosynthesis (polyketide or terpene biosynthesis) preclude a discussion here.[76] Furthermore, natural products with aromatic annulated rings, like the flavonoids, shall not be discussed.

3.1.1. Natural Carbohydrate-Derived Decalins

Annulated sugars forming a decalinic structural unit have been identified in a number of structurally peculiar natural products, many of them with interesting biological activities. For example, the aminocyclitol antibiotic spectinomycin **AW (Scheme 3.2, a)**, isolated from the bacterium *Streptomyces spectabilis*, is a used drug for the treatment of gonorrhea in patients allergic to penicillin. It features a 2,3-diulose moiety (4,4a in the spectinomycin numbering), which is annulated to the aminocyclitol ring *via* a 1,2-*cis*-annulated 1,4-dioxane ring in an overall *cis-cisoid-trans* fashion.[77] Similar *cis-cisoid-trans* dioxane linkages of *keto*-sugars were identified in unusual steroidal natural products, including the affinosides like **M** (**Scheme 2.1** on page 8).[23] Other structurally related steroids like gomphoside **AZ (Scheme 3.2, b)** have been found, and have been synthesized by the Lichtenthaler group by employing the ulosyl donor approach (comp. **Section 2.1.1**) starting with unsaturated ulosyl chloride **AX** and the 2,3-diol **AY**.[78] A structurally unique class of natural products incorporating a carbohydrate-derived decalin framework are the herbicidins, complex nucleoside undecose antibiotics like herbicidin C (**BA** in **Scheme 3.3, a**) with a hydroxylated *trans*-dioxadecalin moiety. **BA** itself, isolated from bacteria of the genus *Streptomyces*, possesses some interesting biological properties. It is, for example, a growth inhibitor of another bacterium (*Xanthomonas oryzae*) that causes leaf blight infection in rice. Notably, the complex annulated sugar structure in **BA**, together with the *N*-glycosidic nucleoside moiety, have been attractive challenges for total syntheses, and a selection of former synthetic routes

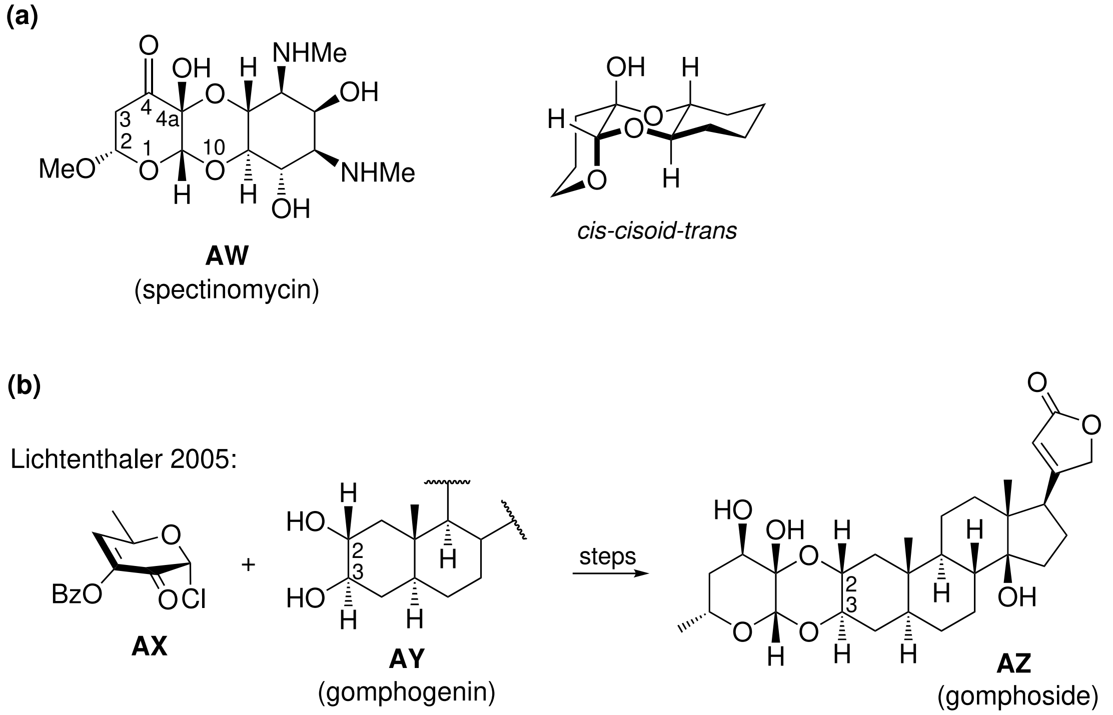

Scheme 3.2 (**a**) Structure of the aminocyclitol antibiotic spectinomycin **AW** and representation of the *cis-cisoid-trans* relationship with omitted substituents.[77] (**b**) Structure **AZ** of the steroid gomphoside and Lichtenthaler's synthetic approach from ulosyl chloride **AX** and gomphogenin **AY**.[78]

together with a modern synthetic approach is given in a recent publication by Trauner and Coworkers.[79] Additionally, some norlignan glucosides isolated from the plant *Curculigo sinensis* contain unusual annulated glycoside residues, among these sinenside A (**BB** in **Scheme 3.3, b**). Together with other co-isolated glucosides, **BB** displayed a strong radical scavenging activity comparable to that of ascorbic acid. The unusual structure of **BB** shows a 1,2-*trans*-annulated β-glucoside fused to a 1,4-dioxane, forming a trioxadecalin. A second annulation to a tetrahydropyran ring completes the tricyclic skeleton. Recently, Vadhadiya and Ramana described a total synthesis for **BB** based on glucose-1,2-orthoester glycosylation chemistry.[80] Another peculiar representative of a naturally occurring annulated sugar is bradyrhizose (**K** in **Scheme 1.3** on page 4), which can be described as an inositol (or: carbasugar) annulated to a reducing galactose moiety. The oxadecalin **K** was isolated as a monosaccharide constituent of the lipopolysaccharides of certain nitrogen-fixing Gram-negative soil bacteria, and is believed to play a role in the initiation of symbiosis with their corresponding host plant (for a detailed discussion, see **Chapter 4.3**).[13]

The examples given here, although not a comprehensive collection, illustrate the unusual ways in which simple monosaccharides are incorporated into complex natural

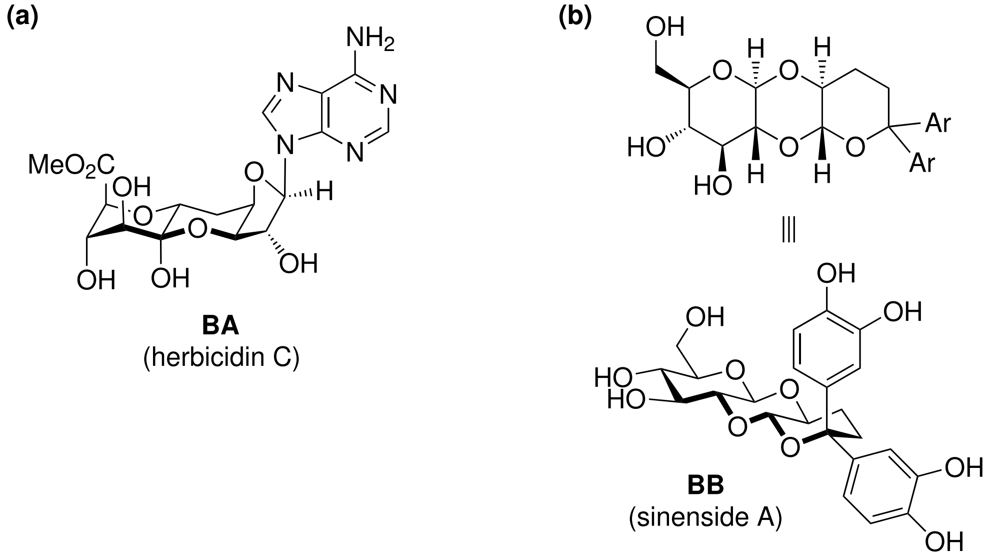

BA
(herbicidin C)

BB
(sinenside A)

Scheme 3.3 **(a)** Structure **BA** of herbicidin C.[79] **(b)** Structure **BB** of sinenside A.[80]

products through diverse ring annulations. In addition to such carbohydrate-derived decalinic structures of natural origin, similar designed frameworks have been synthesized, for example with the goal of creating molecular diversity from readily available carbohydrates. In this regard, some examples will be given in the upcoming section.

3.1.2. Synthetic Carbohydrate-Derived Decalins

Annulated sugars comprise a diverse stereochemistry (comp. **Scheme 3.1**) in combination with a potentially very high density of (often hydroxylated) stereogenic centers. Annulation of a pyranose furthermore produces a conformationally restricted carbohydrate derivative, and this reduced conformational flexibility is particularly distinct in 1,2-*trans*-annulated systems where ring flip isomerism of the bicyclic system is not possible. Since further functionalizations of such conformationally locked bicyclic systems could be expected to be feasible with a high level of stereocontrol, carbohydrate-derived decalin systems have been employed as chiral building blocks for the elaboration of complex molecules.

For instance, Fraser-Reid and Coworkers developed the concept of pyranosidic homologation during their efforts to establish stereoselective syntheses for the complex ansa chains of the ansamycin antibiotics.[81, 82] Stereoselective formation of a polycyclic annulated carbohydrate scaffold, incorporating the stereoinformation of the future ansa chain, was envisioned to be favorable due to the conformational bias of such annulated systems, and the resulting feasibility of highly stereoselective reactions and the facilitated characterization of the bicyclic products. With this objective, Fraser-Reid

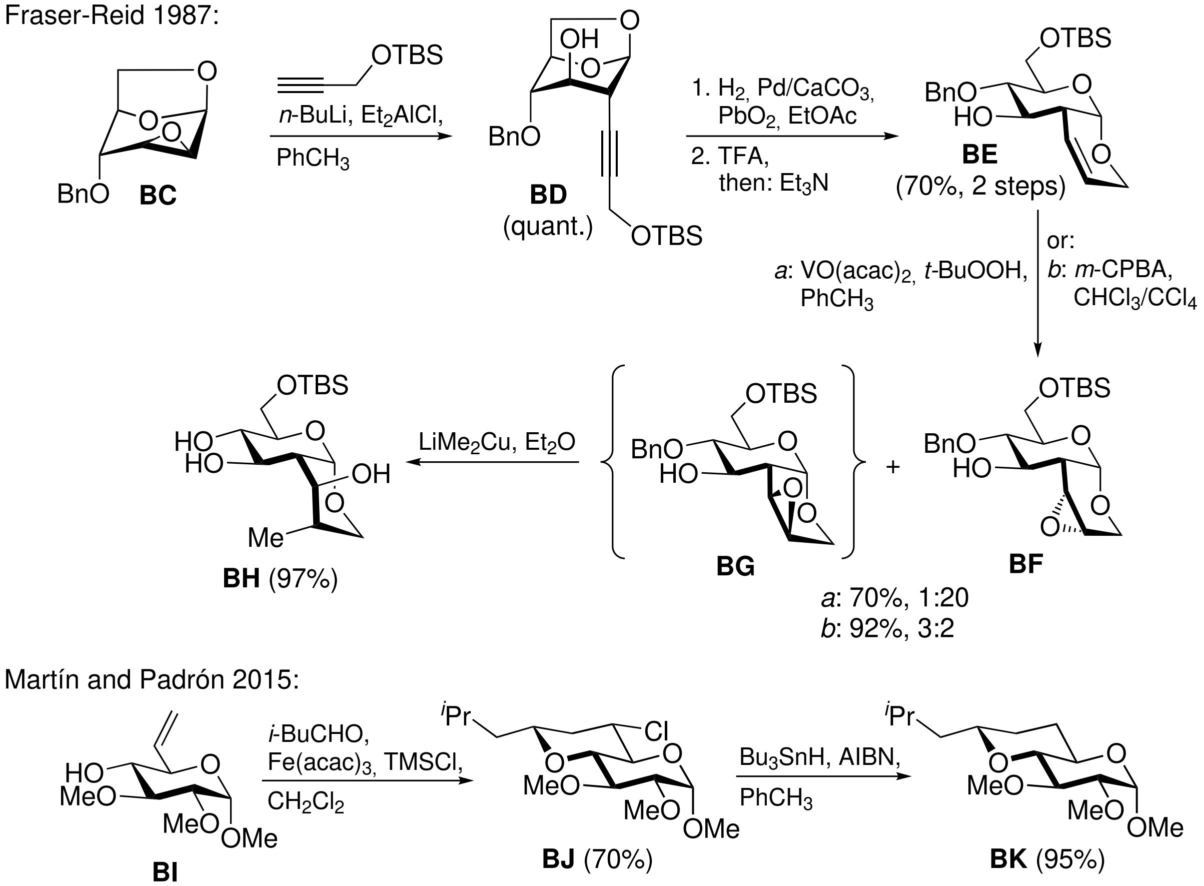
Fraser-Reid 1987:
BnO BC
OTBS
n-BuLi, Et2AlCl,
PhCH3
OH
BnO
BD
(quant.)
OTBS
1. H2, Pd/CaCO3, PbO2, EtOAc
2. TFA, then: Et3N
OTBS
BnO
HO
BE
(70%, 2 steps)
or:
a: VO(acac)2, t-BuOOH, PhCH3
b: m-CPBA, CHCl3/CCl4
OTBS
HO
HO
OH
Me
BH (97%)
LiMe2Cu, Et2O
OTBS
BnO
HO
BG
+
OTBS
BnO
HO
BF
a: 70%, 1:20
b: 92%, 3:2
Martín and Padrón 2015:
HO
MeO
MeO
OMe
BI
i-BuCHO, Fe(acac)3, TMSCl,
CH2Cl2
iPr
Cl
MeO
MeO
OMe
BJ (70%)
Bu3SnH, AIBN,
PhCH3
iPr
MeO
MeO
OMe
BK (95%)

Scheme 3.4 Top: Fraser-Reid's approach to carbohydrate-derived dioxadecalin **BH**.[81, 82] Bottom: diversity-oriented approach towards dioxadecalin **BK**.[83]

and Coworkers subjected epoxide **BC (Scheme 3.4, top)** to epoxide opening with an *in situ* formed alkinylalane, followed by Lindlar hydrogenation. Treatment with TFA induced intramolecular glycosylation/silyl migration upon opening of the 1,6-anhydro bridge, giving bicyclic alkene **BE**. Epoxidation with VO(acac)$_2$/t-BuOOH gave epoxide **BF** as the major product due to the directing effect of the C-3-OH, whereas epoxidation with m-CPBA gave epoxide **BG** as the major isomer. *trans*-Diaxial epoxide opening of **BG** with LiMe$_2$Cu gave the expected 1,2-*cis*-fused dioxadecalin **BH** as an advanced synthetic intermediate for the subsequent installation of further stereogenic centers. Apart from such target-oriented strategies, with the goal of generating bicyclic molecular complexity from simpler carbohydrates, Martín, Padrón and Coworkers used homoallylic alcohol **BI (Scheme 3.4, bottom)** for the Fe(III)-catalyzed Prins reaction with different aldehydes to generate *trans*-dioxadecalinic products like **BJ** with complete stereocontrol of the formed stereogenic centers.[83] The chloride, resulting from trapping

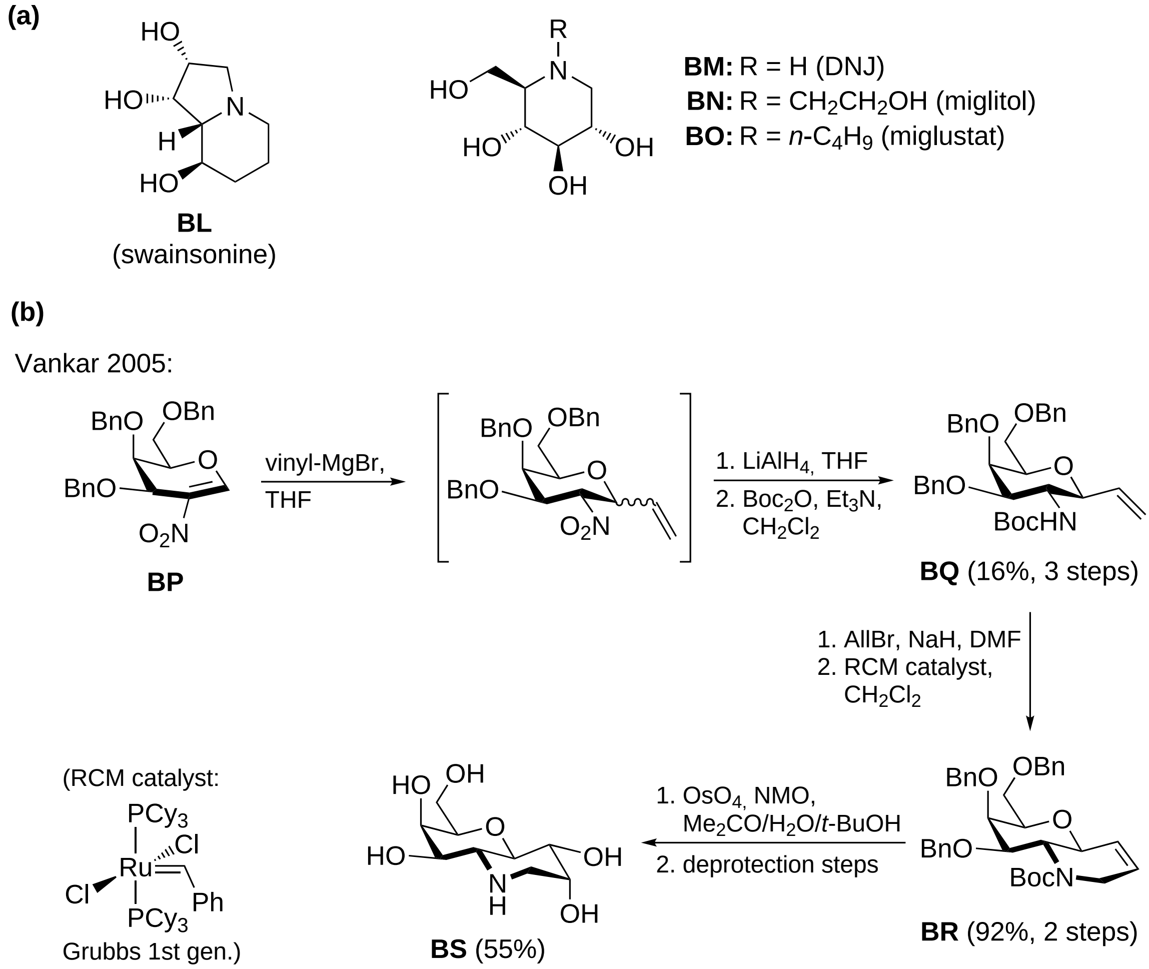
(a)
BL
(swainsonine)
BM: R = H (DNJ)
BN: R = CH2CH2OH (miglitol)
BO: R = n-C4H9 (miglustat)
(b)
Vankar 2005:
BP
vinyl-MgBr,
THF
1. LiAlH4, THF
2. Boc2O, Et3N, CH2Cl2
BQ (16%, 3 steps)
1. AllBr, NaH, DMF
2. RCM catalyst, CH2Cl2
BR (92%, 2 steps)
1. OsO4, NMO, Me2CO/H2O/t-BuOH
2. deprotection steps
BS (55%)
(RCM catalyst:
Grubbs 1st gen.)

Scheme 3.5 **(a)** Structures of swainsonine **BL** and 1-deoxynojirimycin **BM** and the derived marketed drugs miglitol **BN** and miglustat **BO**.[84] **(b)** Vankar's synthesis of galactose-annulated iminosugar **BS**.[85]

of the intermediate carbenium ion with TMSCl, could then be dehalogenated with Bu_3SnH/AIBN.

A frequently addressed area of research arises from the following lines of thought: the carbohydrate-processing enzymes, glycosidases (or glycoside hydrolases, GHs) and glycosyltransferases (GTs), are involved in a plethora of highly relevant biological processes, and malfunctions of these enzymes are associated with severe diseases like diabetes, HIV/AIDS, cancer and lysosomal storage disorders.[86–88] Hence, inhibitors of these enzymes are potential biological tools with possible applications as drugs. Several iminosugars like the naturally occurring swainsonine **BL** **(Scheme 3.5, a)** and 1-deoxynojirimycin **BM** (DNJ) possess glycosidase inhibiting properties. 1-Deoxynojirimycin **BM** itself is an α-glucosidase inhibitor, and its derivatives miglitol **BN** (against type II diabetes) and miglustat **BO** (against type I Gaucher's disease and

Niemann-Pick type C disease) are marketed drugs derived from the natural product.[84] Understandably, due to their closely carbohydrate-related structures, such iminosugars are believed to be mimetics for the carbohydrate substrates of enzymes, or for the transition state traversed in the enzymatic reaction. However, early iminosugar drugs like **BN** or **BO** suffer from low specificity for the target enzyme and, consequently, considerable clinical side-effects.[84] Among the diverse strategies for the structural improvement of glycosidase or glycosyltransferase inhibitors concerning their applicability as therapeutics, novel annulated iminosugar compounds have attracted interest.[89] Alteration of the chemical structure by annulation is, in this regard, expected to provide conformationally rigid bicyclic molecules with improved enzymatic specificity and higher resistance towards enzymatic degradation of the inhibitor, respectively. Along these lines, considerable effort has been invested in the synthesis of novel annulated carbohydrate mimetics like iminosugars, but also annulated carbasugars or conventional sugars, as inhibitors for clinically relevant glycosidases and glycosyltransferases. For instance, Vankar and Coworkers **(Scheme 3.5, b)** introduced a synthesis for D-galactose-annulated iminosugar hybrid molecules.[85] 2-Nitrogalactal **BP** underwent anomeric vinylation with vinylmagnesium bromide, and subsequent reduction of the nitro group and Boc-protection of the amine gave 1-deoxy-1-*C*-vinyl-β-D-galactosamine **BQ** together with other stereoisomeric products. Allylation of the amine, followed by ring-closing metathesis with the Grubbs 1st generation catalyst[90], gave bicyclic alkene **BR**. Osmium-based *syn*-dihydroxylation occurred from the α-side, and after deprotection steps annulated **BS** could be isolated. The *trans*-decalin type structure with $^4C_1$ conformation of the galactose moiety was confirmed by X-ray structural analysis of the *N*-Boc-protected pentaacetate of **BS**. Glycosidase inhibition studies revealed that **BS** is a moderate inhibitor of α-glucosidase (rice yeast) and β-galactosidase (bovine liver), and other stereoisomers of **BS** were found to be inhibitors of other glycosidases. Similarly, numerous other approaches towards annulated iminosugar scaffolds as potential glycosidase inhibitors have been published.[89, 91–94]

Apart from iminosugars, Vankar and Coworkers designed several other bicyclic carbohydrate analogs, such as *C*-glycosidically inositol-annulated carbohydrates **BX** and **BZ (Scheme 3.6)**.[95] Starting from benzylated 1,2-anhydro-D-glucose **BT**, β-selective anomeric allylation, followed by oxidation of the *C*-2-OH, gave *C*-glycosidic 2-ulose **BU**. Allylation of the ketone with equatorial selectivity and ring-closing metathesis provided alkene precursor **BV** for the *syn*-dihydroxylation, which gave a separable 4:1 mixture of major **BW** *via* addition from the α-side, and minor **BY**. Hydrogenolytic debenzylation gave mannose-annulated carbasugars **BX** and **BZ**, respectively. The minor isomer **BZ** was identified to be a moderate inhibitor of β-galactosidase (bovine).

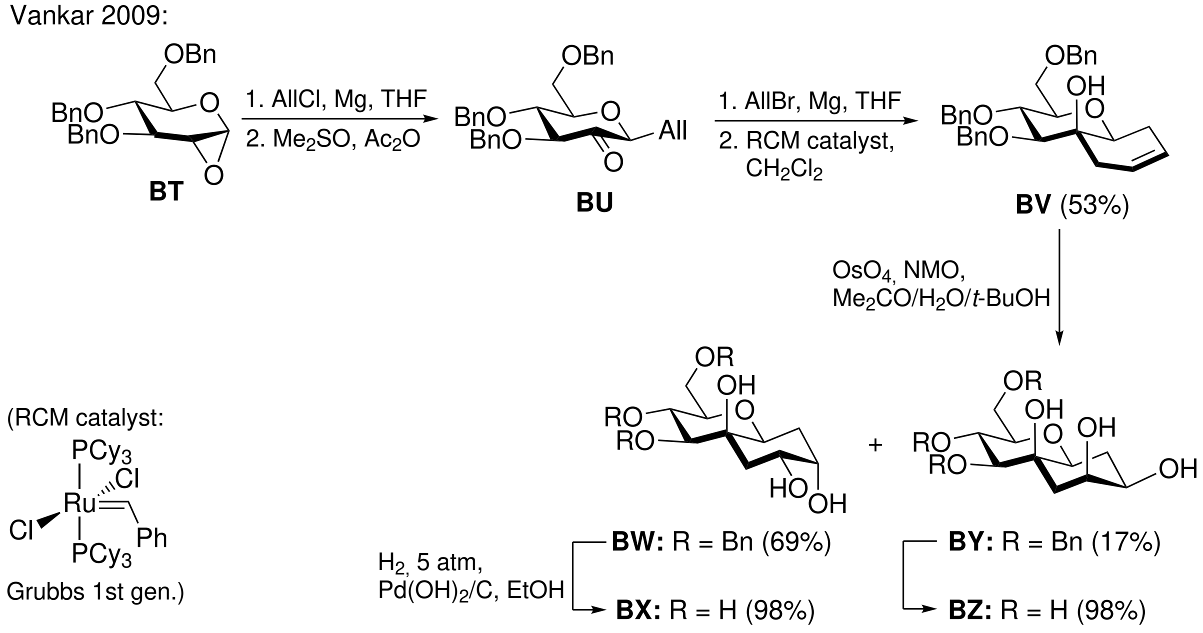
Vankar 2009:
OBn
BnO
BnO
O
O
BT
1. AllCl, Mg, THF
2. Me2SO, Ac2O
BU
All
1. AllBr, Mg, THF
2. RCM catalyst, CH2Cl2
BV (53%)
OH
OsO4, NMO, Me2CO/H2O/t-BuOH
OR
RO
HO
OH
+
BW: R = Bn (69%)
BX: R = H (98%)
BY: R = Bn (17%)
BZ: R = H (98%)
H2, 5 atm, Pd(OH)2/C, EtOH
(RCM catalyst:
PCy3
Cl
Ru
Ph
Grubbs 1st gen.)

Scheme 3.6 Vankar's synthesis of carbohydrate-derived oxadecalins **BX** and **BZ** *via* allylation/ring-closing metathesis and dihydroxylation.[95]

In a related project, the Vankar group synthesized pyran-annulated *O*-glycosides *via* a comparable route **(Scheme 3.7)**.[93] 2-Acetoxyglucal **CA** was reacted with allyl alcohol in the presence of $BF_3{\cdot}Et_2O$ in a Ferrier reaction[96] followed by enone formation. After *gluco*-selective vinylation of the ketone and silyl-protection of the deprotected primary *C*-6-OH, ring-closing metathesis with the Grubbs 2nd generation catalyst[97] gave 1,2-*trans*-annulated bicyclic diene **CD**. Dihydroxylation of both alkene functionalities occurred from the β-face and gave, after subsequent deprotection steps, dioxadecalin **CF** with *galacto*-configuration of the parent pyranose moiety. Notably, due to the β-*trans* nature of the annulation, **CF** must be assumed to adopt a $^1C_4$ conformation of the galactose ring, although the authors did not comment on this detail. In glycosidase inhibition studies with **CF** and a collection of structurally related compounds, **CF** was found to be a remarkably selective inhibitor of β-galactosidase (bovine liver). This approach provided structurally interesting *O*-glycosidically fused carbohydrate-decalin-structures. However, a disadvantage of this strategy can be seen in the following circumstances: both the *C*-3 and *C*-4 stereogenic centers of the substrate **CA** are lost in the Ferrier reaction/elimination step. As a consequence, four hydroxylated stereogenic centers have to be established in the dihydroxylation step (**CD** to **CE**). This can be regarded as a restriction of the stereochemical variety of products potentially accessible with this synthetic approach. Concludingly, a synthetic strategy with complete conservation of the carbohydrate stereochemical information at the non-fusion positions would be

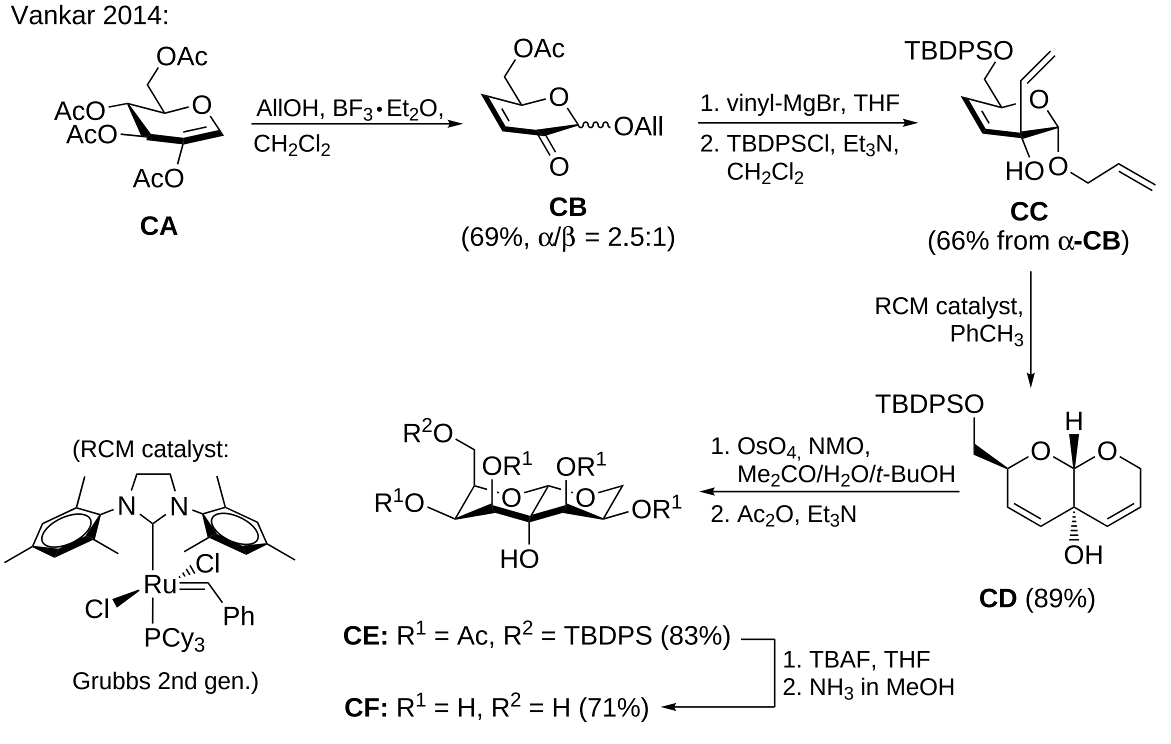
Vankar 2014:
OAc
AcO
AcO
O
AcO
CA
AllOH, BF3•Et2O,
CH2Cl2
OAc
O
OAll
O
CB
(69%, α/β = 2.5:1)
1. vinyl-MgBr, THF
2. TBDPSCl, Et3N, CH2Cl2
TBDPSO
O
HO
O
CC
(66% from α-CB)
RCM catalyst,
PhCH3
TBDPSO
H
O
O
OH
CD (89%)
1. OsO4, NMO, Me2CO/H2O/t-BuOH
2. Ac2O, Et3N
R2O
OR1
OR1
R1O
O
O
OR1
HO
CE: R1 = Ac, R2 = TBDPS (83%)
CF: R1 = H, R2 = H (71%)
1. TBAF, THF
2. NH3 in MeOH
(RCM catalyst:
N
N
Cl
Ru
Cl
Ph
PCy3
Grubbs 2nd gen.)

Scheme 3.7 Synthesis of annulated $^{1}C_4$-system **CF** *via* vinylation/ring-closing metathesis and dihydroxylation as published by Vankar and Coworkers.[93]

desirable. In this regard, the development of a synthetic approach towards structurally related annulated sugars is discussed in the upcoming section.

3.2. Objective of this Chapter

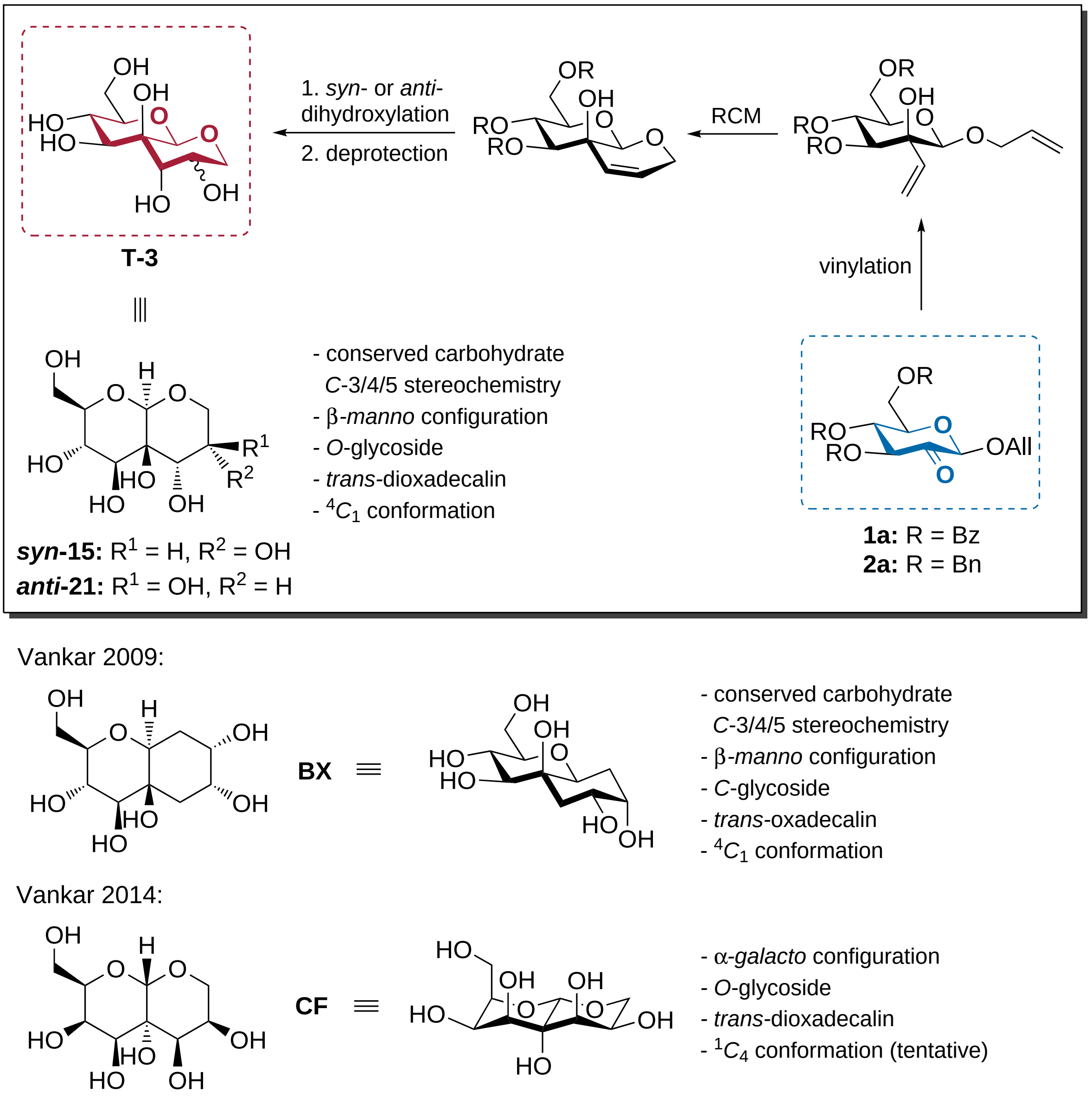
T-3
1. syn- or anti-dihydroxylation
2. deprotection
RCM
vinylation
syn-15: R1 = H, R2 = OH
anti-21: R1 = OH, R2 = H
- conserved carbohydrate C-3/4/5 stereochemistry
- β-manno configuration
- O-glycoside
- trans-dioxadecalin
- 4C1 conformation
1a: R = Bz
2a: R = Bn
OAll
Vankar 2009:
BX ≡
- conserved carbohydrate C-3/4/5 stereochemistry
- β-manno configuration
- C-glycoside
- trans-oxadecalin
- 4C1 conformation
Vankar 2014:
CF ≡
- α-galacto configuration
- O-glycoside
- trans-dioxadecalin
- 1C4 conformation (tentative)

Scheme 3.8 Top: schematic representation of the synthetic routes described in this chapter for 1,2-annulated target compounds **T-3**. Bottom: structurally related published oxadecalin **BX**[95] and dioxadecalin **CF**[93].

In light of the aforementioned efforts in the synthesis of either natural or of designed carbohydrate-derived products with an annulated decalin-type structure, allyl 2-ulosides **1a** or **2a** were assumed to be ideal precursors for the synthesis of new 1,2-annulated carbohydrates. Specifically, the given synthetic strategy followed from a retrosynthetic analysis, and based on the assumption that both the carbonyl functional group and the allyl residue in **1a**/**2a** were amenable to straightforward further functionalizations

(Scheme 3.8, top). Thus, vinylation of the ketone moiety could give a diene intermediate as a suitable substrate for ring-closing metathesis, which would provide a bicyclic alkene as an annulated intermediate. Subsequently, *syn*- or *anti*-selective dihydroxylation of the bicyclic alkene, followed by global deprotection, were anticipated to furnish dioxadecalins of type **T-3** with variable configurations of the side chain diol moiety.

Analogous synthetic routes with a ring-closing metathesis/dihydroxylation approach were frequently utilized by the Vankar group for the synthesis of 1,2-annulated sugars like **BX**[95] or **CF**[93] **(Scheme 3.8, bottom)**, both with the objective of synthesizing new carbohydrate mimetics as glycosidase inhibitors. The target compounds **T-3** can, from a heterocyclic point of view, be described as 2,10-dioxadecalins (or: pyranopyrans), or as 1,2-pyran-annulated β-mannosides focussing on the carbohydrate moiety. Due to the β-*trans* nature of the annulation, both *syn*- and *anti*-isomers of **T-3** (***syn*-15** and ***anti*-21**) can be anticipated to exist in a *trans*-decalin-type structure with $^4C_1$ conformation of the parent β-mannose. In this context, compounds **T-3** can be regarded as hybrid molecules between Vankar's inositol-annulated (*C*-glycosidic) β-mannoside **BX** in $^4C_1$ conformation, and pyran-annulated (*O*-glycosidic) α-galactoside **CF**, which can be expected to adopt a $^1C_4$ conformation. Notably, although a large number of bicyclic carbohydrate analogs have been prepared to date (comp. **Section 3.1.2**), an approach towards *O*-glycosidic β-mannosides of the type **T-3** has not been developed. As an additional feature, the described synthetic route involving 2-*keto*-sugars would proceed with complete conservation of the configurations of the carbohydrate *C*-3,4,5 stereogenic centers, thereby offering potential for a diversification of this synthesis with respect to the starting *keto*-sugar. Given the fact that mannosides are widely present in biologically highly relevant molecular patterns, and considering the synthetic challenge generally associated with 1,2-*cis*-glycosides, the development of a synthesis of target compounds **T-3** would be desirable.[46, 47, 98] Apart from this, a detailed structural characterization of the deprotected target compounds would be of interest, especially from the perspective that similar highly hydroxylated, and thus, highly polar carbohydrate mimetics are frequently characterized as their protected (e.g. peracetylated) derivatives for reasons of convenience.

3.3. Results and Discussion

Taking into account the challenges encountered in the isolation of allyl β-2-ulosides **1a** and **2a** from the corresponding ulosyl bromides **AB** and **AD** (**Scheme 2.10** on page 18), a preliminary synthetic route towards target structures **T-3** was developed based on the following considerations: whereas benzylated **AD** gave a complex mixture upon reaction with allyl alcohol under Koenigs-Knorr conditions, benzoylated **AB** reacted with allyl alcohol in a clean manner to give a single product **1a**. Albeit, isolation and purification of **1a** was not feasible due to the formation of 3,2-enolone **3a** upon chromatographic purification. As a result, in initial experiments towards **T-3**, the application of crude **1a** as received from the Koenigs-Knorr glycosylation of **AB** was explored. A discussion of these early investigations is given in **Section 3.3.1**.

3.3.1. Preliminary Synthetic Studies

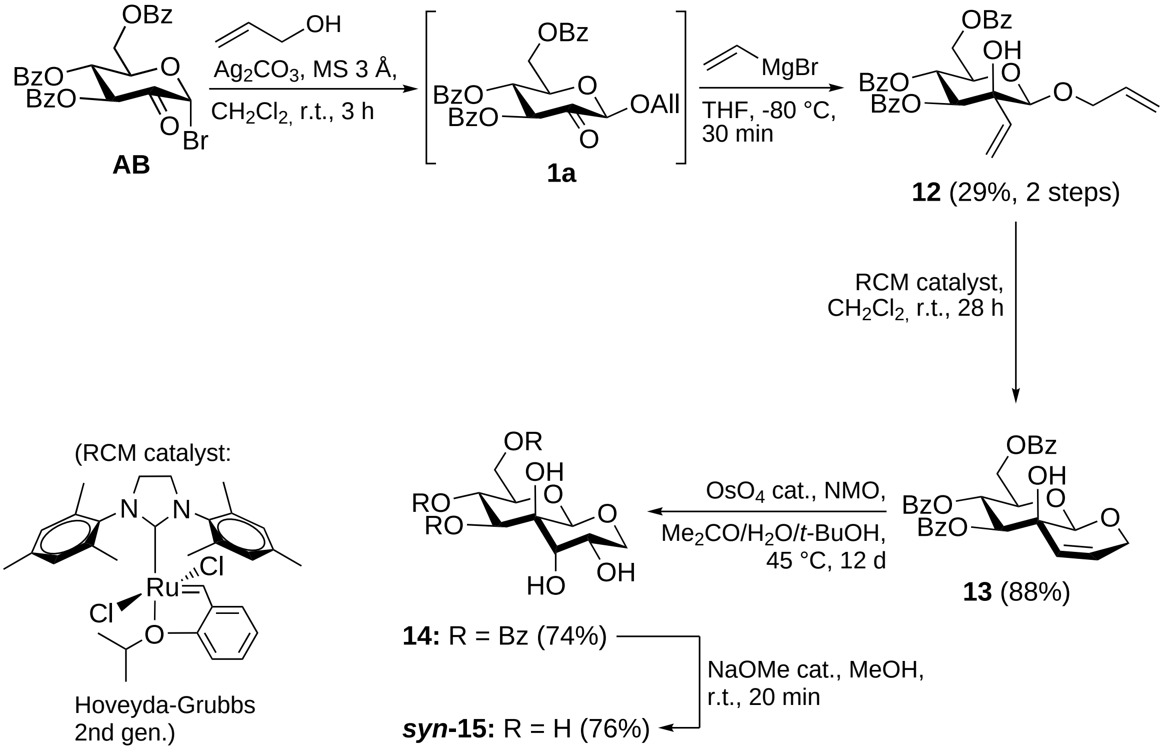
OBz
BzO
BzO
O
O
Br
AB
OH
Ag2CO3, MS 3 Å,
CH2Cl2, r.t., 3 h
OBz
BzO
BzO
O
OAll
O
1a
MgBr
THF, -80 °C,
30 min
OBz
OH
BzO
BzO
O
O
12 (29%, 2 steps)
RCM catalyst,
CH2Cl2, r.t., 28 h
(RCM catalyst:
N
N
Ru
Cl
Cl
O
Hoveyda-Grubbs
2nd gen.)
OR
OH
RO
RO
O
O
HO
OH
OsO4 cat., NMO,
Me2CO/H2O/t-BuOH,
45 °C, 12 d
OBz
OH
BzO
BzO
O
O
13 (88%)
14: R = Bz (74%)
NaOMe cat., MeOH,
r.t., 20 min
syn-15: R = H (76%)

Scheme 3.9 Preliminary synthetic studies towards ***syn*-15** from ulosyl bromide **AB**.

In initial experiments, Lichtenthaler's benzoylated ulosyl bromide **AB**[42] was condensed with allyl alcohol in the presence of Ag_2CO_3 and molecular sieves in CH_2Cl_2 according to the standard procedure **(Scheme 3.9)**. After removal of the insoluble components and evaporation of the volatile parts, crude **1a** was treated with vinylmagnesium bromide at −80 °C in THF. Due to the more electrophilic nature of the ketone functionality, a selective addition to the ketone in the presence of the benzoyl groups was anticipated. In this way, the desired 2-*C*-vinylated product **12** could be isolated in mediocre yield

(29%). The low yield and sluggish nature of the formation of **12** must be attributed to the unwanted formation of 3,2-enolone **3a** (**Scheme 2.10** on page 18), observed as a side product with high chromatographic mobility in TLC control under the conditions of the Grignard reaction. Since **3a** could not be isolated from the reaction in significant amounts, it most likely reacts with further available vinylmagnesium bromide to derived decomposition products. In addition, upon prolonged reaction time, an increased number of decomposition products with low chromatographic mobility suggested at least partial reaction of the benzoyl groups under these conditions. Nevertheless, diolefin **12** could be characterized by its NMR-spectroscopic properties to be a single isomer with β-*manno*-configuration. The β-configuration of the anomeric center was evident from the direct coupling constant $^1J_{\mathrm{C1,H1}} = 160.8\,\mathrm{Hz}$ **(Fig. 3.1, a)** measured in an undecoupled ^{13}C NMR experiment, which was significant for a β-glycoside (ca. 160 Hz) and smaller than would be expected for an α-anomer (ca. 170 Hz).[99, 100] Likewise, the anomeric β-configuration of **12** could additionally be confirmed by the H,H-NOESY spectrum **(Fig. 3.1, b)**, which showed NOE contacts between the carbohydrate *H*-1, *H*-3 and *H*-5 as expected for the spatial proximity associated with a 1,3,5-triaxial relationship. In a similar manner, if not stated otherwise, the configurations of the following other 2-*C*-branched saccharides could be determined from comparable spectral properties. Notably, the vinylation proceeded with complete stereoselectivity for the equatorial attack, giving product **12** with *manno*-configuration. This finding is in accordance with detailed studies on nucleophilic addition reactions at structurally related 2-ulosides by Ley and Coworkers.[101] In general, α-2-ulosides react *via* axial attack, giving products of α-*gluco*-configuration, whereas β-2-ulosides usually react *via* equatorial attack, giving the corresponding β-*manno*-products as observed. In the following reaction, diene **12** was subjected to ring-closing metathesis[90] with the Hoveyda-Grubbs catalyst of the second generation[102, 103], which proceeded smoothly and provided bicyclic alkene **13** in 88% yield. Dihydroxylation of alkene **13** under Standard Upjohn conditions[104] was found to progress reluctantly, and a slightly elevated temperature (45 °C) and prolonged reaction time (12 d) was required. In this manner, bicyclic diol **14** was furnished *via* addition from the α-face and opposite to that of the axial *C*-2-OH. Spectroscopically, the stereochemistry of the dihydroxylation reaction was evident from the ^{1}H NMR spectrum, which displayed vicinal coupling constants of the side chain methylene *C*-9a,b as expected for one axial-equatorial ($^3J_{8,9\mathrm{a}} = 5.8\,\mathrm{Hz}$) and one axial-axial ($^3J_{8,9\mathrm{b}} = 10.9\,\mathrm{Hz}$) relationship. Similarly, comprehensive examinations by Kishi and Coworkers on the osmoylation of allylic alcohols have confirmed the general preference for the addition from the *anti*-face with respect to the preexisting hydroxyl group.[105, 106] This finding is sometimes referred to as “Kishi’s empirical rule“. Finally,

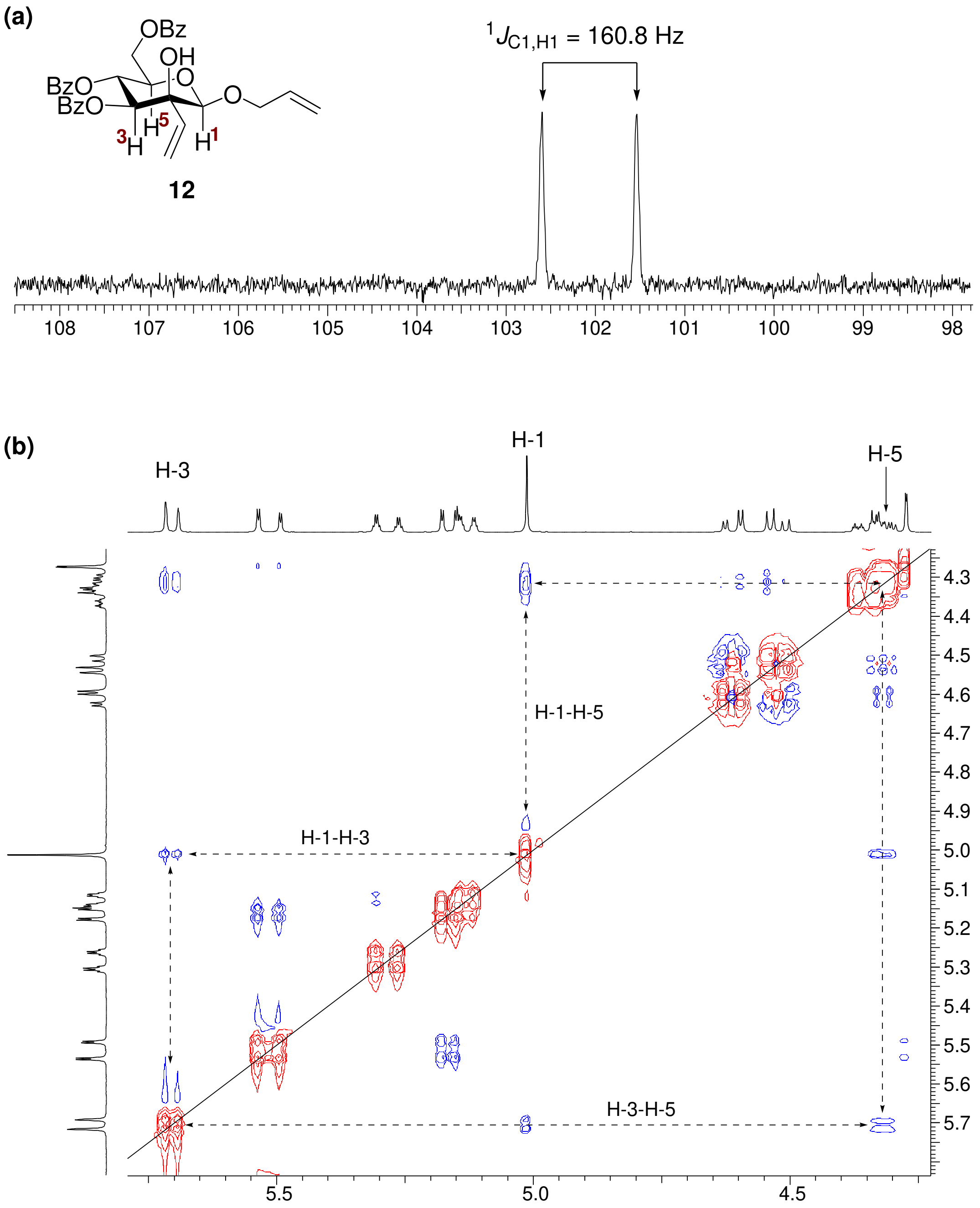

Figure 3.1 **(a)** Anomeric region of the undecoupled ^{13}C NMR spectrum of diolefin **12** at 150.9 MHz in acetone-D_6 with assignment of the $^1J_{\mathrm{C1,H1}}$ coupling constant. **(b)** Section of the H,H-NOESY spectrum of **12** at 400.2 MHz in acetone-D_6. Significant signals are labeled, and dashed arrows indicate NOE contacts between the axial H-1, H-3 and H-5. The shown spectrum is symmetrized.

debenzoylation of tribenzoate **14** under Zemplén's[66] conditions gave target compound ***syn*-15**. The highly polar hexol was found to be insoluble in organic solvents like DMSO or methanol, but in water. Therefore, in these early experiments, the purification of crude ***syn*-15** was realized by washing of the solid with mixtures of organic solvents to obtain pure ***syn*-15** with a manageable loss of product in 76% yield.

Based on these promising initial results, the low-yield vinylation of crude 2-uloside **1a** for the formation of **12** was evaluated to be a substantial disadvantage. For that reason, a screening for suitable reagents and conditions for the vinylation of **1a** was performed **(Table 3.1)**. Starting from the initial procedure (entry 1), which gave **12** in 29% yield over 2 steps from **AB** by using commercial vinylmagnesium bromide in THF, a comparable experiment was conducted with vinylmagnesium bromide freshly prepared from vinyl bromide and magnesium (entry 2).[107] Notably, in some cases, serious improvements are reported for the prepared reagent over commercial material.[108] Nevertheless, the reaction proceeded sluggishly, and gave **12** in a 26% two-step yield and thus comparable to the commercial reagent. Solvating ether additives like bis(2-methoxyethyl) ether (diglyme) are known to increase the nucleophilicity of Grignard reagents, and Song and Coworkers found that additional catalytic quaternary ammonium salts lead to an increase of the addition reaction over enolization/reduction side reactions.[109] Albeit, in the transformation of **1a**, in the presence of diglyme (entry 3) or diglyme/catalytic n-Bu_4NCl (entry 4), no improved results could be observed. Subsequently, metal additives for Grignard reactions were explored. Nakamura and Coworkers could show that challenging substrates like enolizable ketones or α,β-unsaturated ketones give better results in Grignard reactions upon addition of equimolar amounts of anhydrous $CeCl_3$, and the method has been shown to be compatible with vinylmagnesium bromide.[110] In the reaction of **1a** (entry 5), however, no improvements could be detected, and **12** was formed in comparably low yield (25%). In a similar method for the Lewis acid activation of Grignard reagents, Knochel and Coworkers reported the THF-soluble complex $LaCl_3 \cdot 2LiCl$ as a suitable activator in stoichiometric or catalytic amounts.[111] Nevertheless, application of this protocol to the transformation of **1a** (entry 6) in combination with vinylmagnesium chloride as the Grignard species did not lead to better results, and **12** was formed in an unsatisfactory yield (25%).

Concludingly, although the formation of diene **12** from benzoylated ulosyl bromide **AB** was thoroughly examined, no adequate method could be found. Under all tested conditions, the formation of **12** proceeded sluggishly and in mediocre yields below 30%. For this reason, in advanced synthetic studies, another approach was examined. Benzylated allyl 2-uloside **2a**, although not accessible *via* Koenigs-Knorr glycosylation of ulosyl bromide **AD**, was formed in the Dess-Martin oxidation of 2-*O*-unprotected allyl

Table 3.1 Reaction screening for the formation of diene **12** from crude **1a**.

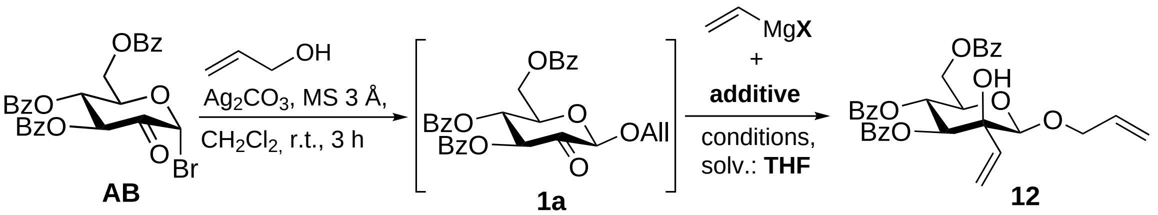

#	X	additive[a]	T, t	yield **12**[b]	Ref.
1[c]	Br	—	−80 °C, 30 min	29%	—
2	Br[d]	—	−80 °C, 90 min	26%	[107, 108]
3	Br	diglyme	−80 °C, 2 h	22%	[109]
4	Br	diglyme, *n*-Bu_4NCl	−80 °C, 2 h	27%	[109]
5	Br	$CeCl_3$	−80 °C, 24 h	25%	[110]
6	Cl	$LaCl_3 \cdot 2LiCl$[e]	−80 °C, 24 h	25%	[111]

[a] Equivalents according to the given reference.
[b] Chromatographically isolated yield over 2 steps from **AB**.
[c] Experimental procedure given in **Chapter 6**.
[d] Grignard reagent freshly prepared from vinylbromide/Mg.
[e] According to the stoichiometric protocol: 1.1 equiv. $LaCl_3$, 2.2 equiv. LiCl.

glucoside **7** in a clean and reliable manner (**Scheme 2.13** on page 21). Chromatographic purification of **2a** resulted in elimination of benzyl alcohol and formation of 3,2-enolone **3b**, together with diminished amounts of impure **2a**. Consequently, crude **2a**, as obtained from the Dess-Martin oxidation, was anticipated to be a suitable substrate for the following vinylation.

3.3.2. Optimized Synthetic Route

Accordingly, an optimized synthetic route was conceived to involve Dess-Martin oxidation of allyl glucoside **7**, giving allyl 2-uloside **2a** as reported in **Chapter 2**, followed by vinylation of the crude material to furnish the 2-*C*-vinyl-branched product. Two aspects of this approach were expected to be favorable as compared to the synthesis involving benzoylated 2-uloside **1a**. Dess-Martin oxidation of **7** was found to provide ketone **2a** in high yield and in a very clean reaction, as opposed to the somewhat unclean Koenigs-Knorr glycosylation of **AB**, which can, in addition to that, potentially form minor amounts of the undesired α-anomeric product. Moreover, comparing the quality of the leaving group at the *O*-4-position, the benzoylated derivative **1a** was assumed to

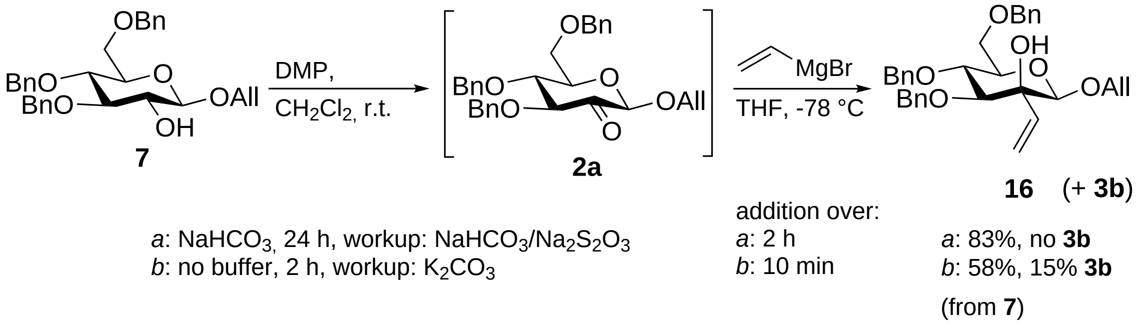

Scheme 3.10 Optimized (method *a*) and unoptimized (method *b*) synthesis of diene **16** *via* Dess-Martin oxidation/Grignard addition.

have a higher tendency for elimination and formation of the unwanted 3,2-enolone as compared to benzylated **2a**, featuring the poor benzyl oxide leaving group.

Hence, as described in **Chapter 2**, allyl glucoside **7** was treated with Dess-Martin periodinane in the presence of NaHCO$_3$ as a buffer to give allyl 2-uloside **2a (Scheme 3.10)**. Treatment of crude **2a** with vinylmagnesium bromide, which was slowly added to the reaction mixture over 2 h, provided 2-*C*-vinyl-branched **16** in an excellent 83% two-step yield and without observable formation of the unwanted elimination product **3b** (**Scheme 3.10**, method *a*). The presence of the buffer NaHCO$_3$ in the Dess-Martin oxidation, a non-basic workup (NaHCO$_3$/Na$_2$S$_2$O$_3$), and subsequent slow addition (over 2 h) of the Grignard reagent were all found to be beneficial for the overall yield of **16**. Opposed to this, in an earlier unoptimized procedure (method *b*), a sequence of unbuffered Dess-Martin oxidation, followed by basic workup (K$_2$CO$_3$) and rapid addition of the Grignard reagent (over 10 min), provided **16** in lower yield (58%), together with 15% of 3,2-enolone **3b**. By employing the optimized synthetic sequence, **16** was conveniently available on gram scale, and thus a promising intermediate.

Ring-closing metathesis of **16** with the Hoveyda-Grubbs catalyst of the second generation[102, 103] gave, similar to the unoptimized reactions involving benzoyl-protected derivatives, bicyclic benzylated alkene **17** (**Scheme 3.11** on page 46). Annulated **17** was isolated in an excellent yield (94%), and from *n*-hexane/ethyl acetate, single crystals suitable for X-ray structural analysis could be obtained. **17** crystallized in the monoclinic space group $P2_1$ with $Z = 2$, and the molecular structure **(Fig. 3.2, a)** confirmed the anticipated $^4C_1$ conformation of the mannoside moiety. The annulated dihydropyran ring could be determined to exist in a distorted envelope (E) type conformation with the side chain (C6,C7,C8 in the crystal structure numbering), the carbohydrate *O*-1 (O6) and the carbohydrate *C*-2 (C2) in a quasi-planar arrangement, and the carbohydrate *C*-1 (C1) below the plane **(Fig. 3.2, b)**. Only a very slight out-of-plane distortion of

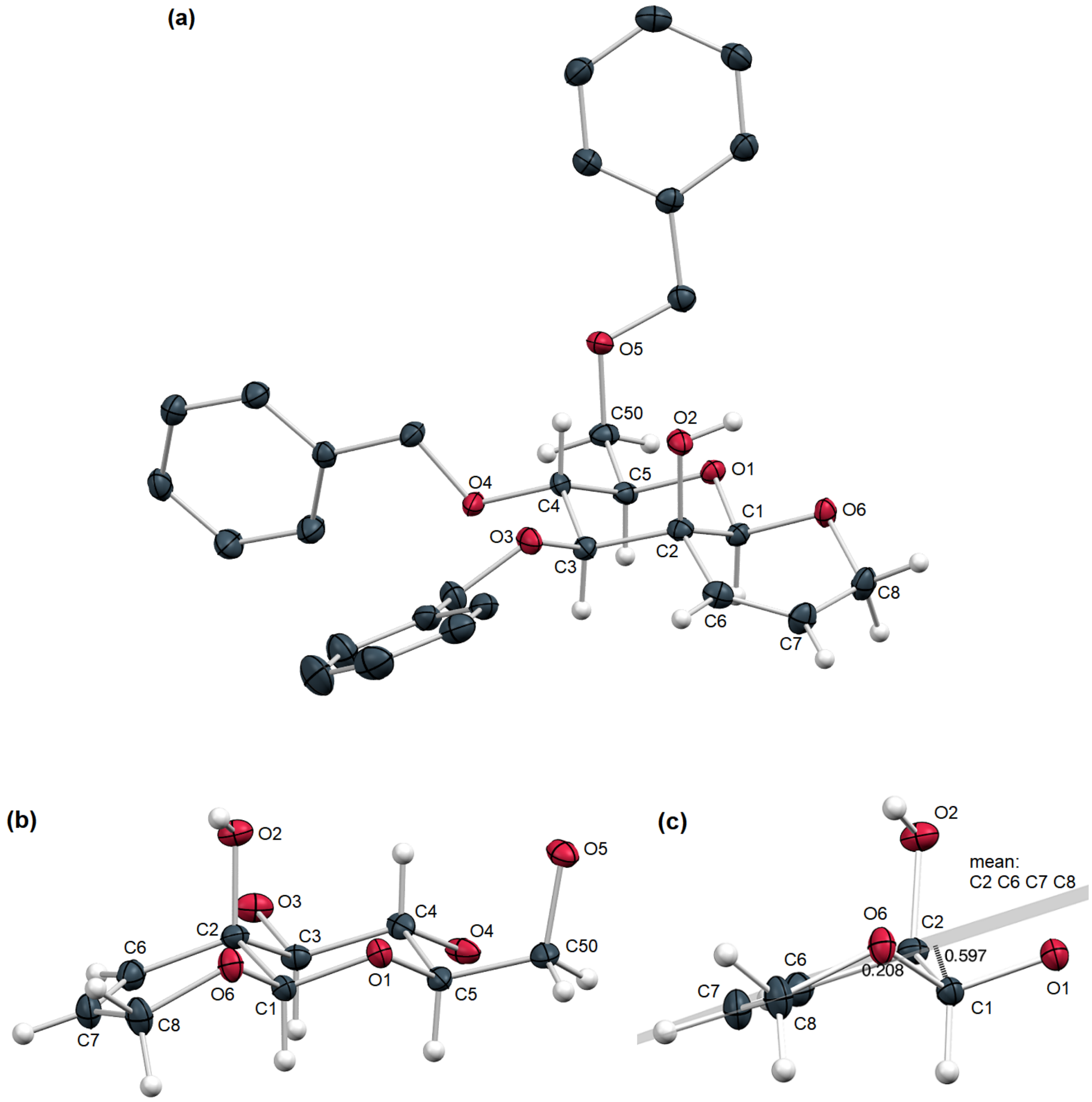
(a)
O5
C50
O2
O1
O4
C4
C5
C1
O6
O3
C3
C2
C8
C6
C7
(b)
O2
O5
O3
C4
O4
C6
C2
C3
C50
O6
O1
C5
C1
C7
C8
(c)
O2
mean:
C2 C6 C7 C8
O6
C2
C6
0.597
0.208
C7
O1
C8
C1

Figure 3.2 **(a)** X-ray structure of bicyclic alkene **17**. Hydrogen atoms of the benzyl ethers are omitted for clarity. Ellipsoids are drawn at the 50% probability level. Red = oxygen, gray = carbon, white = hydrogen. **(b)** Molecular structure of **17** (benzyl ethers not shown) for clarification of the chair and envelope-like ring conformations. **(c)** Calculated plane through atoms C2,C6,C7,C8 and distances to the plane: O6 0.208 Å, C1 0.597 Å.

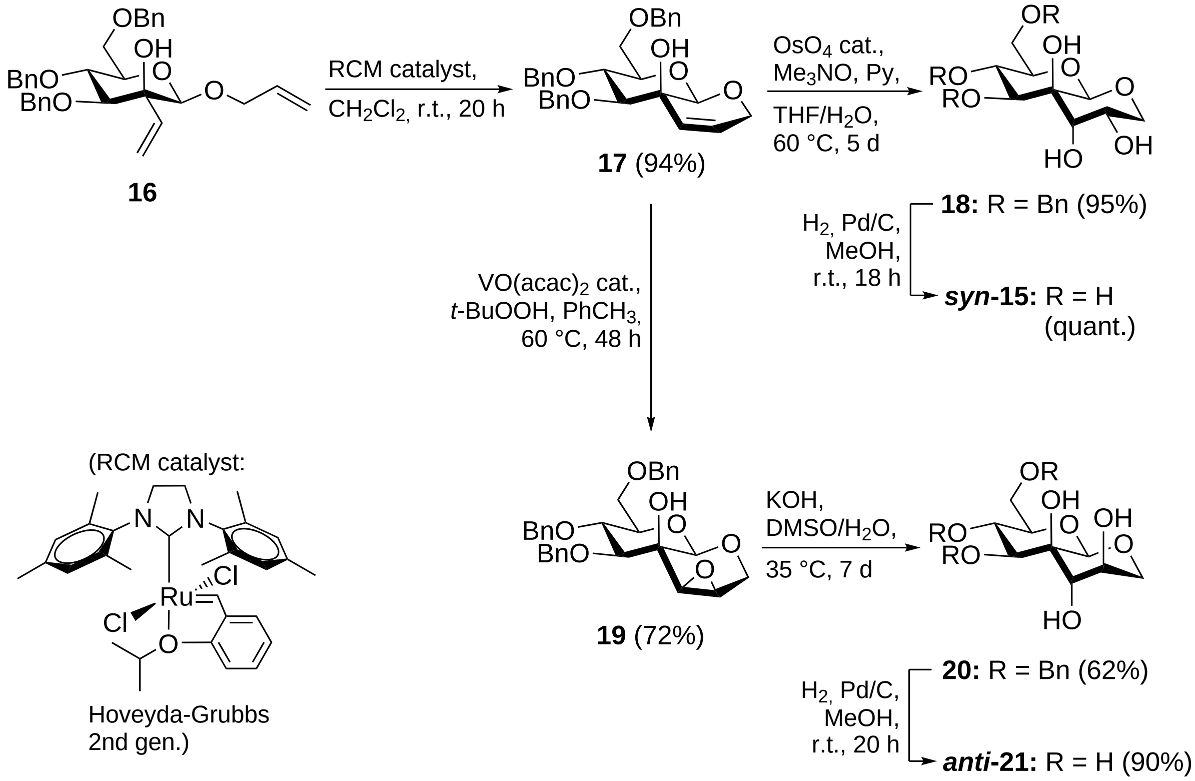
16
RCM catalyst,
CH2Cl2, r.t., 20 h
17 (94%)
OsO4 cat.,
Me3NO, Py,
THF/H2O,
60 °C, 5 d
H2, Pd/C,
MeOH,
r.t., 18 h
18: R = Bn (95%)
syn-15: R = H
(quant.)
VO(acac)2 cat.,
t-BuOOH, PhCH3,
60 °C, 48 h
(RCM catalyst:
Hoveyda-Grubbs
2nd gen.)
19 (72%)
KOH,
DMSO/H2O,
35 °C, 7 d
H2, Pd/C,
MeOH,
r.t., 20 h
20: R = Bn (62%)
anti-21: R = H (90%)

Scheme 3.11 Optimized syntheses of annulated target compounds ***syn*-15** and ***anti*-21** *via* bicyclic alkene **17**.

O6 indicative of a weak tendency to a half-chair (H) conformation could be observed. In accordance, to a plane calculated through C2,C6,C7,C8, a considerably smaller distance of O6 (0.208 Å) than the out-of-plane C1 (0.597 Å) illustrated these relationships **(Fig. 3.2, c)**. Usually, monocyclic dihydropyrans occupy a half-chair conformation[112], and envelope conformations of six-membered rings are only observed in highly rigid systems like carbohydrate-derived α,β-unsaturated carbonyls (enuloses).[113] Thus, in the case of **17**, the realization of an envelope-like conformation must be attributed to a rigidifying effect caused by the annulated mannose moiety. Accordingly, in structurally comparable fused molecules, similar partial planarizations of a dihydropyran moiety towards an envelope-like conformation are observable.[114]

Subsequently, *syn*- and *anti*-selective dihydroxylations of bicyclic alkene **17** were explored **(Scheme 3.11)**. *syn*-Dihydroxylation of **17** under standard Upjohn conditions[104] (cat. OsO_4, NMO in acetone/*t*-BuOH/water) proceeded reluctantly similar to the reaction of benzoylated **13**. Therefore, alternative protocols were tested. Among the multitude of osmium-based dihydroxylation protocols with diverse co-oxidants and additives, DeCamp and Mills published a protocol using Me_3NO as the stoichiometric oxidant and pyridine as an additive for the large-scale dihydroxylation of a hindered

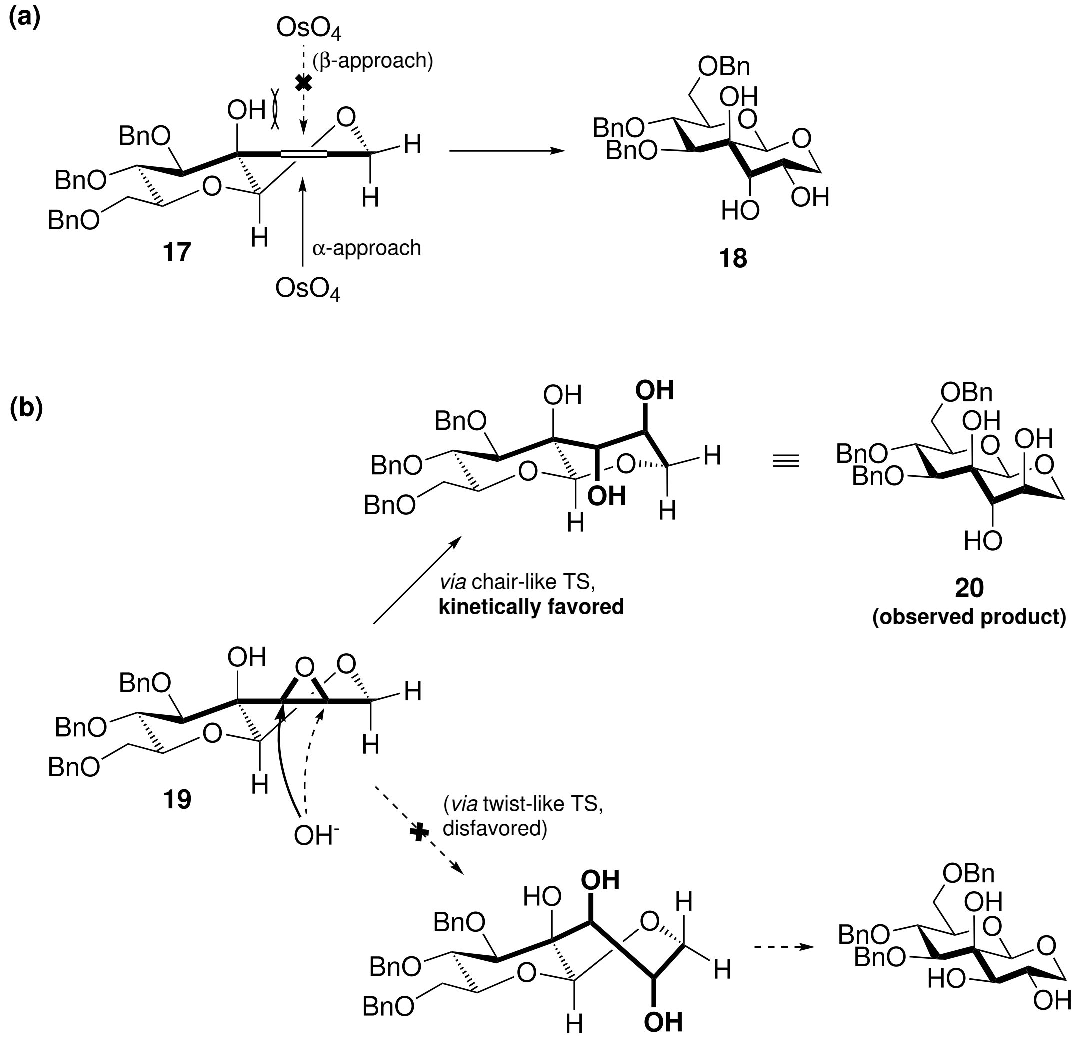
(a)
OsO4
(β-approach)
OH
BnO
BnO
BnO
O
O
H
H
H
17
α-approach
OsO4
OBn
OH
BnO
BnO
O
O
HO
OH
18
(b)
OH
OH
BnO
BnO
BnO
O
O
OH
H
H
H
≡
OBn
OH
O
OH
O
BnO
BnO
HO
20
(observed product)
via chair-like TS,
kinetically favored
OH
O
O
BnO
BnO
BnO
O
H
H
H
19
OH-
(via twist-like TS,
disfavored)
HO
OH
H
O
BnO
BnO
BnO
O
H
H
OH
OBn
OH
O
O
BnO
BnO
HO
OH

Scheme 3.12 (**a**) Favored approach of OsO_4 in the *syn*-dihydroxylation of **17**, giving triol **18**. (**b**) Fürst-Plattner considerations for the kinetically favored *trans*-diaxial epoxide opening of **19**, resulting in the formation of **20**.

trisubstituted alkene.[115] Under these conditions, alkene **17** could be transformed into triol **18** in 95% yield in a reasonable reaction time of 5 d. The attack from the α-face of the alkene opposite to the axial *C*-2-OH[105, 106] can be rationalized by using an annulated half-chair model (**Scheme 3.12, a**) that is frequently utilized in this regard.[116, 117] The model clearly demonstrates the unfavorable interactions with the axial hydroxyl group in a potential approach of OsO_4 from the β-side. Finally, hydrogenolytic debenzylation of **18** gave, after an optimized purification involving RP-C18 chromatography, the highly polar hexol ***syn*-15** in quantitative yield, and thus in 74% yield over 5 steps from the known allyl glucoside **7** (10 steps in total from D-glucose). Spectroscopic data obtained for ***syn*-15** fully corresponded to those obtained for material as received from the debenzoylation of **14**.

In order to get access to the corresponding side chain *anti*-diol isomer, a sequence of epoxidation and nucleophilic epoxide opening was explored. The initially tested reactions for the epoxidation of **17** involved common epoxidizing agents like *m*-CPBA (unbuffered or buffered with $NaHCO_3$), peroxyacetic acid[118], trifluoroperoxyacetic acid[119, 120] and DMDO[121]. Albeit, surprisingly, all tested methods failed to give satisfactory results in the transformation of **17**. Transition metal-catalyzed epoxidations are known to be particularly useful for the site-selective epoxidation of allylic alcohols[122, 123], and therefore this type of epoxidation reactions was tested next. Barriault and Deon reported on the vanadium-catalyzed directed epoxidation[122, 124] of a *trans*-fused bicyclic alkene with a tertiary allylic alcohol, and thus, structurally closely related to **17**.[125] Application of comparable conditions including catalytic $VO(acac)_2$ and stoichiometric *t*-BuOOH in toluene at 60 °C (**Scheme 3.11** on page 46) gave epoxide **19** *via* epoxidation from the β-face and in a *syn*-fashion with respect to the tertiary hydroxyl as expected. It should be noted, that the yield of the epoxidation reaction was found to be heavily dependent on the individual batch of the substrate **17**. A possible explanation might involve residual ruthenium impurities in **17** from the preceding ring-closing metathesis step that could have an adverse effect on the metal-catalyzed epoxidation. In a protocol published by Liu and Coworkers, polar vinyl ethers were applied to ruthenium carbene residues, forming stable Fischer carbene complexes and thereby facilitating chromatographic separation of the catalyst residues.[126] Consequently, according to the published protocol, di(ethylene glycol) vinyl ether was added to crude **17** prior to chromatographic purification. Using substrate **17** pretreated in this way gave epoxide **19** in reproducibly good yield (72%). Subsequently, treatment of **19** with KOH in DMSO/water gave, after a prolonged reaction time (7 d) *anti*-diol **20**. The epoxide opening occurred as expected with preference for the diaxial product, and thus, in conformity with Fürst-Plattner[127] considerations of stereoelectronic circumstances in the annulated half-chair model **(Scheme 3.12, b)**. Finally, deprotection of **20** *via* hydrogenolytic debenzylation provided the second target compound ***anti*-21** in a total yield of 31% over 6 steps from the known allyl glucoside **7** (11 steps in total from D-glucose). The highly polar target compound ***anti*-21** displayed high solubility in water and, as opposed to ***syn*-15**, in methanol, too.

3.3.3. Characterization of the Target Compounds

Both ***syn*-15** and ***anti*-21** were amenable to NMR-spectroscopic characterization in D_2O. A comparison of the ^1H NMR spectra **(Fig. 3.3)** of both compounds revealed similar low-field and high-field boundary signals. The anomeric H-1 signals were detected

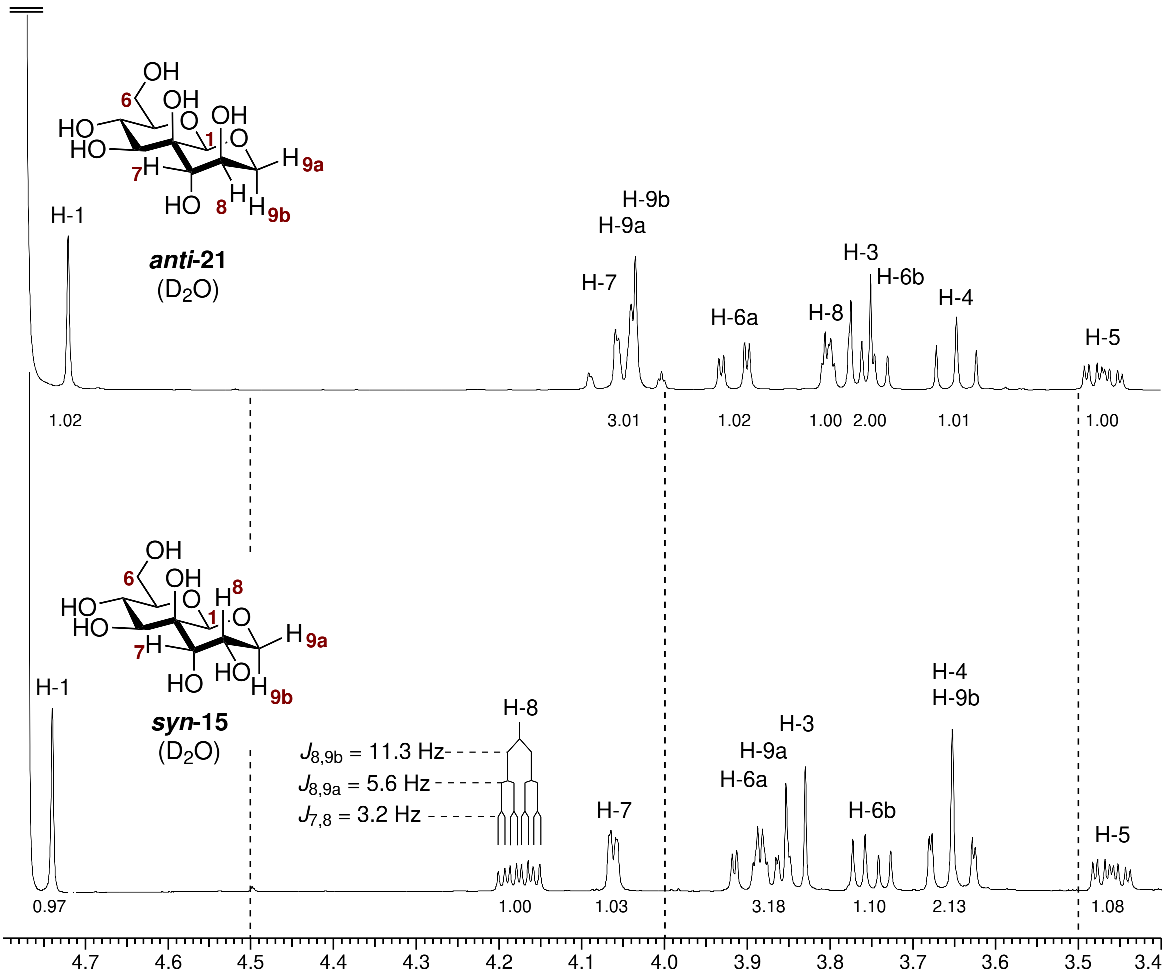

Figure 3.3 ^{1}H NMR spectra of target compounds ***syn*-15** and ***anti*-21** in the range 3.4–4.8 ppm in D_2O at 400.2 MHz. The shown spectra are unprocessed.

as singlets in proximity to the solvent residual signal at ca. 4.7 ppm (***syn*-15**: 4.74 ppm, ***anti*-21**: 4.72 ppm), and the carbohydrate *H*-5 gave rise to resolved ddd's at ca. 3.5 ppm (3.46, 3.47 ppm). The remaining signals were, in a typical manner for deprotected saccharides[128], found in a narrow region between 3.6 ppm and 4.2 ppm. In the case of ***syn*-15**, the coupling constants for the side chain *H*-8 allowed for the determination of the configurations of the diol stereogenic centers. *H*-8 gave rise to a resolved ddd with coupling constants as expected for one *trans*-diaxial ($J_{8,9b} = 11.3$ Hz) and two axial-equatorial ($J_{8,9a} = 5.6$, $J_{7,8} = 3.2$ Hz) relationships, thus giving clear evidence for the depicted stereochemistry. For ***anti*-21**, the side chain signals of *H*-7 and *H*-9a/b were observed as a heavily obscured multiplet. Likewise, *H*-8 exhibited a weakly resolved signal. Albeit, the visible absence of a large *trans*-diaxial splitting (> 7 Hz[128]) suggested the equatorial orientation of *H*-8. The H,H-NOESY spectrum of ***anti*-21** was inconclusive, and did not allow for the determination of significant contacts. However,

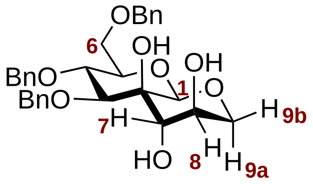
OBn
6
OH
OH
BnO
BnO
O
1
O
H9b
7H
HO
8
H
H9a

20
(acetone-D_6)

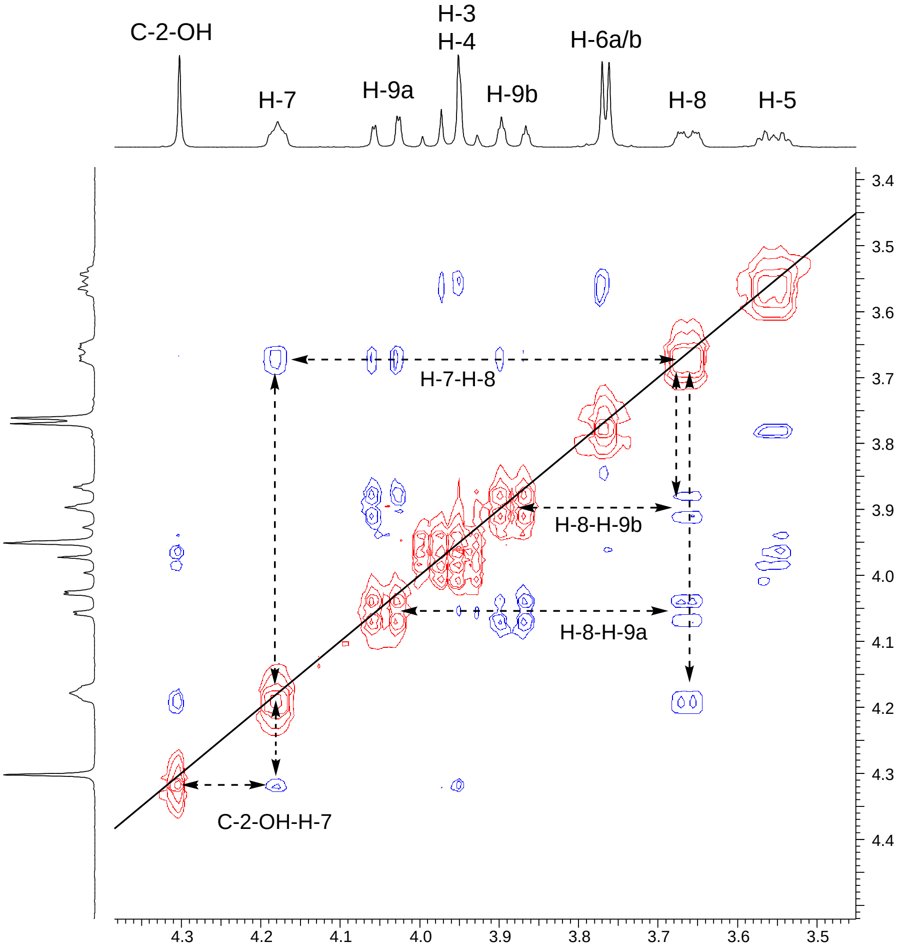

Figure 3.4 Section of the H,H-NOESY spectrum of **20** at 400.2 MHz in acetone-D_6. Dashed arrows were added manually to indicate significant NOE contacts. The shown spectrum is symmetrized.

for precursor **20**, the H,H-NOESY spectrum **(Fig. 3.4)** displayed an NOE contact between the axial C-2-OH, which was visible in acetone-D_6, and the side chain H-7, thereby giving evidence for the *trans*-diaxial diol orientation of **20**, and indirectly, of the derived ***anti*-21**.

Due to its only weak solubility in methanol, target compound ***syn*-15** could be recrystallized from a mixture of methanol and water. Fortunately, in this way, colorless plates were obtained of a quality suitable for X-ray structural analysis. The highly hydroxylated ***syn*-15** was found to crystallize in the monoclinic space group $P2_1$ with $Z = 4$, and with two molecules in the asymmetric unit. The molecular structure **(Fig. 3.5)** of ***syn*-15** clearly confirmed the preference for a *trans*-decalin-like structure with both the parent β-mannoside moiety as well as the annulated 1-deoxypyranose ring in a $^4C_1$ conformation. An analysis of the bond lengths (for selected bond lengths and angles, see **Table A.4** on page 278) revealed endocyclic carbon-carbon bond lengths in the range 1.524–1.535 Å and a shorter exocyclic bond length (C5-C6 1.507 Å). The exocyclic carbon-oxygen bond lengths were found to be in the range 1.421–1.438 Å. In contrast, the endocyclic carbon-oxygen bonds could be separated into two groups: the distances around the anomeric C1 were shorter than the exocyclic distances (C1-O1 1.405, C1-O1' 1.411 Å), whereas the remaining two C-O bonds were longer than the exocyclic C-O bonds (C5-O1 1.455, C1'-O1' 1.446 Å). The majority of the endocyclic bond angles were found to be in an anticipated range slightly above the ideal tetrahedron angle (109.7–111.1°). However, the bond angles around the fusion positions at C1 and C2 deviated from this: the endocyclic O-C-O angle around the anomeric C1 was considerably narrower (O1-C1-O1' 104.2°), and the angle involving the C2 position was slightly wider (C3-C2-C3' 113.7°), both indicating a subtle distortion of the decalinic system.

As highly hydroxylated molecules, carbohydrate structures possess a great number of functional groups (hydroxyl groups) that can act both as a hydrogen bond donor, and as an acceptor. In this regard, solid-state structures of carbohydrates differ from multiple other biomolecules like proteins, in which the donor/acceptor roles are clearly separated (e.g. N-H donors and C=O acceptors). This fact, together with the high biological relevance of carbohydrates in general, have prompted a great number of detailed solid-state examinations of carbohydrate structures with regard to hydrogen-bonding interactions, either by neutron diffraction or, more frequently, by X-ray crystallography.[129] Typically, the majority of hydrogen-bonding interactions found in carbohydrates can be regarded as moderately strong interactions, characterized by O···O distances (donor oxygen to acceptor oxygen) in the range 2.5–3.2 Å and O-H···O angles above 130°. An aspect which is frequently observed in carbohydrate

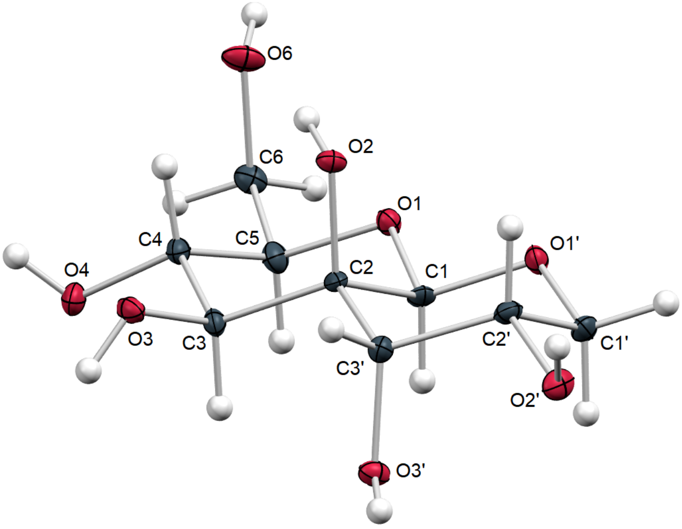

Figure 3.5 Molecular structure of ***syn*-15**. A second molecule in the asymmetric unit is omitted. Ellipsoids are drawn at the 50% probability level. Red = oxygen, gray = carbon, white = hydrogen. For a selection of bond lengths, angles and torsion angles, see **Table A.4** on page 278.

solid-state structures, and which has attracted detailed examinations, is a high fraction of bifurcated (or multifurcated) hydrogen bonds. The term bifurcated is traditionally used to describe a hydrogen-bonding interaction, in which one donor (O-H) interacts with two acceptors (O, O') simultaneously (type: O···H(-O)···O').[130] Another type of multicentered hydrogen-bonding is characterized by one acceptor binding two donors simultaneously (type: H···O···H'), and this type of interaction is sometimes termed three-centered. Albeit, some confusion regarding this terminology exists in the literature, and one term or the other is sometimes used to describe both types of interactions. In extensive neutron diffraction studies on pyranoses and pyranosides, a high fraction of 25% of all hydrogen-bonding interactions was evaluated to be bifurcated (type: O···H(-O)···O').[131] As a possible explanation, it was reasoned that the ring oxygen present in carbohydrates could only participate as a hydrogen bond acceptor (as opposed to the hydroxyl groups), resulting in an overproportional number of acceptors, and therefore in a competitive energetic contribution of bifurcated hydrogen-bonding interactions.[131, 132]

An analysis of the hydrogen-bonding interactions within the crystal lattice of ***syn*-15** was performed with the following frequently applied criteria: inter-atomic distances between the acceptor oxygen atoms and the donor hydrogen atoms were required to

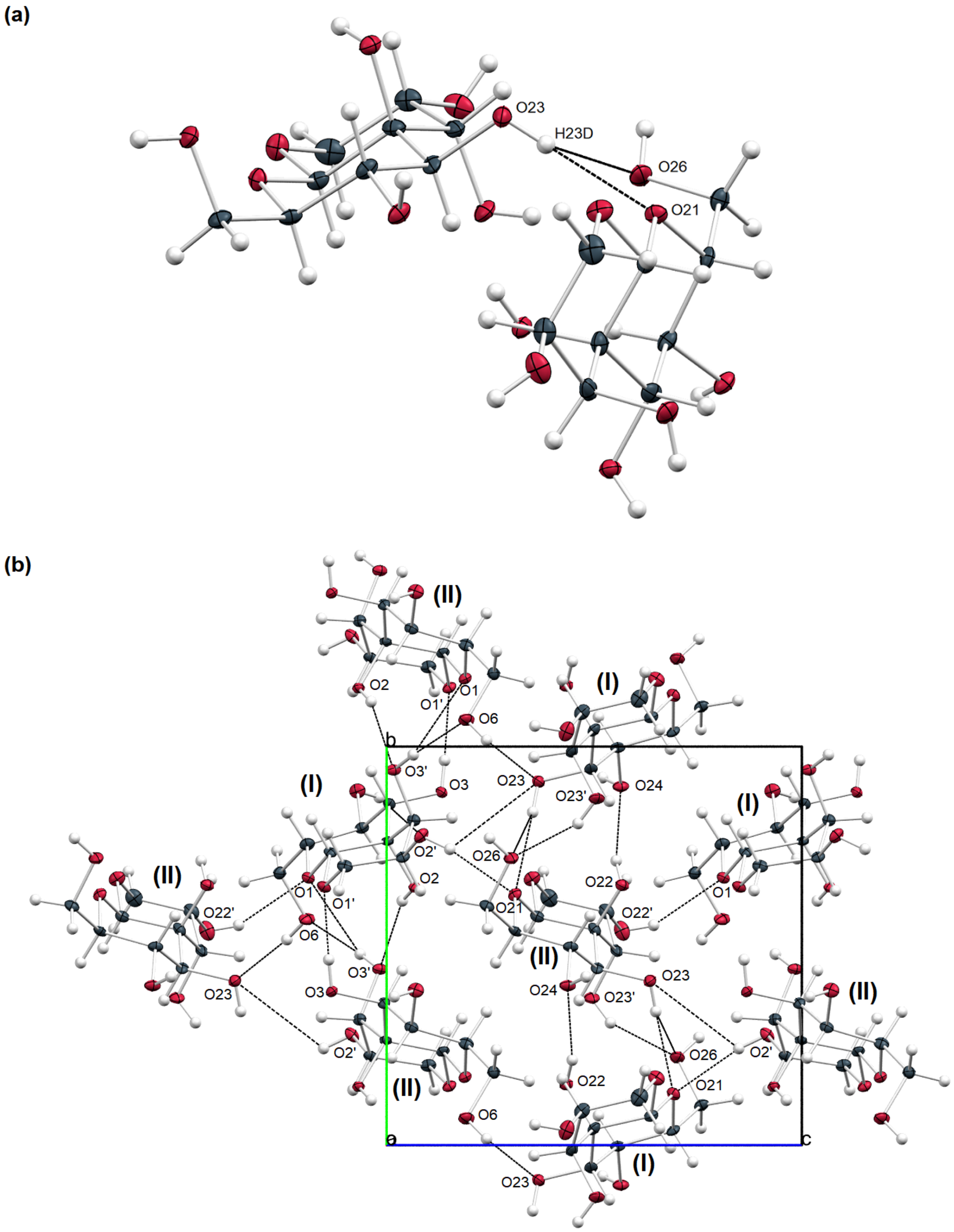
(a)
O23
H23D
O26
O21
(b)
(II)
O2
O1'
O1
O6
(I)
b
O3'
O3
O23
O23'
O24
(I)
(I)
(II)
O2'
O26
O22
O22'
O2
O1
O1'
O21
O22'
O1
O6
(II)
O3'
O3
O23
O24
O23'
O23
(II)
O26
O2'
O2'
(II)
O22
O21
O6
a
c
(I)
O23

Figure 3.6 **(a)** Bifurcated hydrogen-bonding interaction in ***syn*-15**. Significant distances and angles: major component: O23···O21 3.006 Å, H23D···O21 2.238 Å, O23-H23D···O21 152.1°; minor component: O23···O26 3.119 Å, H23D···O26 2.455 Å, O23-H23D···O26 136.5°. Remaining angle: O21···H23D···O26 70.8°. **(b)** Molecular packing and hydrogen-bonding interactions of ***syn*-15** along the crystallographic *a*-axis. The two crystallographically independent molecules are labeled **(I)** and **(II)**. Ellipsoids are drawn at the 50% probability level. Red = oxygen, gray = carbon, white = hydrogen.

be below 3.0 Å (distance criterion: $d_{O \cdots H} < 3.0$ Å), and the hydrogen bonding angle above 90° (angle criterion: $\theta_{O-H \cdots O} > 90°$).[130, 133] Since the treatment of hydrogen atoms in the X-ray structural analysis included constraints to ideal geometries (O-H 0.84 Å, C-O-H 109.5°), all further discussions of hydrogen bond distances can, as an alternative, be on the basis of O···O distances, which is also a parameter commonly used to describe hydrogen bond distances in X-ray structures. Under the criteria mentioned above, the crystal lattice of ***syn*-15** revealed a prototype bifurcated hydrogen-bonding interaction involving the O23-H23D hydroxyl group **(Fig. 3.6, a)**. As is usually the case for bifurcated hydrogen bonds[130, 133], in the observed interaction a major component with a shorter contact and an angle closer to a linear bonding can be observed (O23···O21 3.006 Å, H23D···O21 2.238 Å, O23-H23D···O21 152.1°), together with a minor component with longer distance and narrower angle (O23···O26 3.119 Å, H23D···O26 2.455 Å, O23-H23D···O26 136.5°). Another criterion for a bifurcated hydrogen bond is the requirement, that the hydrogen atom should be in close proximity to a plane spanned by the surrounding three oxygen atoms.[133] For a quantification, the sum of angles around the hydrogen atom, which is 360° in the ideal case and below 360° in the case of pyramidal distortion, can be calculated. In the given example, a sum of angles of 359.4° around H23D expresses an almost ideally planar arrangement. An expansion of the hydrogen-bonding analysis for ***syn*-15** revealed a dense network of hydrogen bonds in the crystal lattice **(Fig. 3.6, b)**. Among the multiple hydrogen-bonding interactions (for a summary of identified hydrogen bonds, see **Table A.5** on page 279), O···O distances were found to vary in the range between 2.73 Å (O1'-O3 and O6-O23) and 3.40 Å (O23-O2'). Both the hydroxyl groups and the acetal ring oxygen atoms were found to participate as hydrogen bond acceptors. The general tendency, that shorter hydrogen-bonding interactions usually feature an angle closer to linearity[130], was also observed for the structure of ***syn*-15**. This can be expressed by the following calculated average angle values: for $d_{O \cdots O'} < 3.0$ Å: $\bar{\theta}_{O-H \cdots O'} = 161.6°$, and for $d_{O \cdots O'} > 3.0$ Å: $\bar{\theta}_{O-H \cdots O'} = 127.6°$. Of the identified hydrogen bonds, at least 6 out of 13 interactions have to be evaluated as truly bifurcated (type: O···H(-O)···O') in nature, and several other interactions (classified as two-centered) could be identified to be part of a H···O···H' type bonding. However, it should be noted that a solely X-ray crystallography-based analysis of hydrogen-bonding interactions should be evaluated as prone to errors, for example with regards to the determination of detailed geometric parameters of specific interactions. In particular, the identification of a contact to be of a structure-determining nature, and not just a consequence of geometric circumstances, can be commonly regarded as questionable.

3.4. Summary of this Chapter

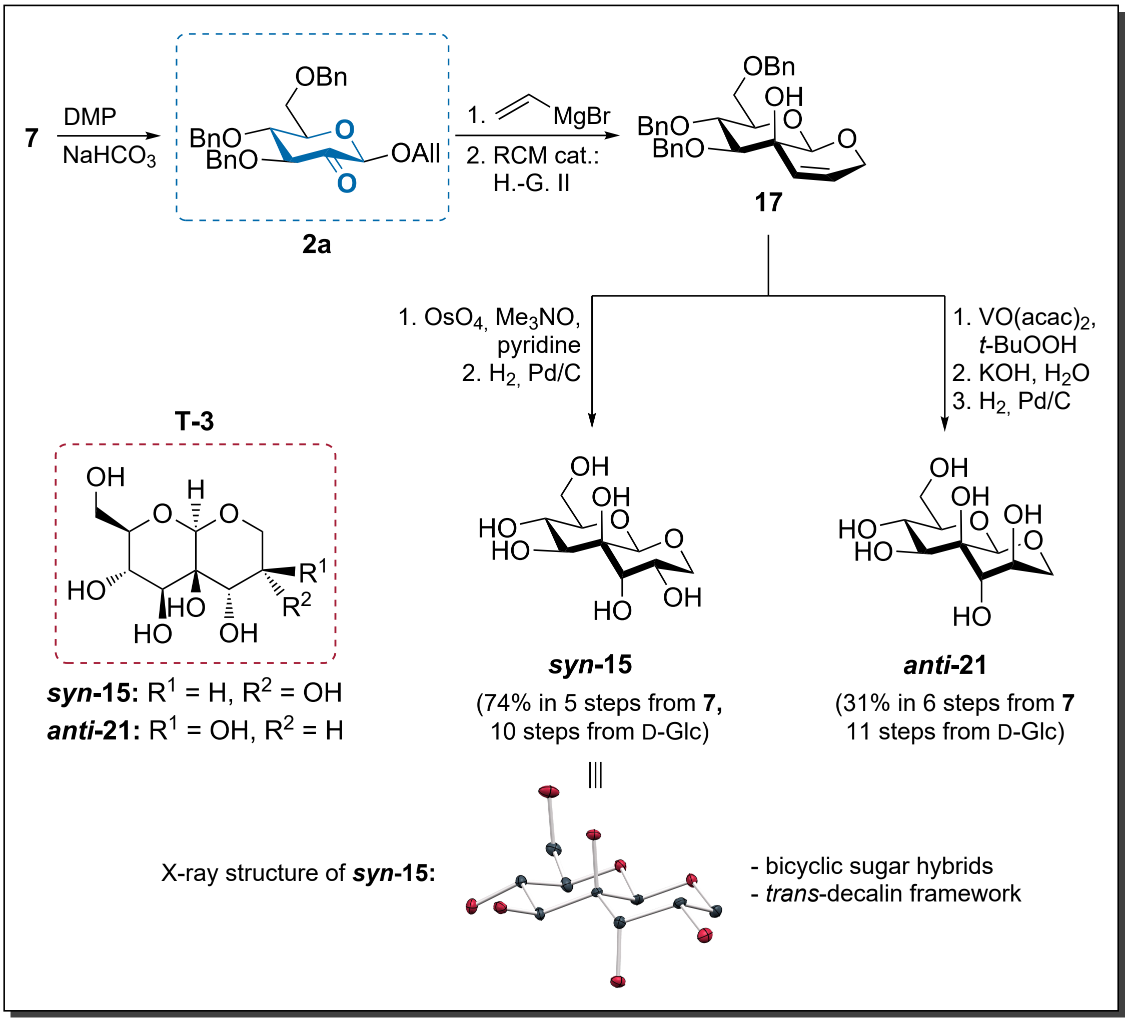
7
DMP
NaHCO$_3$
2a
1. MgBr
2. RCM cat.: H.-G. II
17
1. OsO$_4$, Me$_3$NO, pyridine
2. H$_2$, Pd/C
1. VO(acac)$_2$, *t*-BuOOH
2. KOH, H$_2$O
3. H$_2$, Pd/C
T-3
***syn*-15**: R^1 = H, R^2 = OH
***anti*-21**: R^1 = OH, R^2 = H
***syn*-15**
(74% in 5 steps from **7**, 10 steps from D-Glc)
***anti*-21**
(31% in 6 steps from **7** 11 steps from D-Glc)
X-ray structure of ***syn*-15**:
- bicyclic sugar hybrids
- *trans*-decalin framework

Scheme 3.13 Schematic summary of this chapter. Synthesis of 1,2-annulated target carbohydrates **T-3**, represented by ***syn*-15** and ***anti*-21**, as derived from bicyclic alkene **17**.

Detailed synthetic examinations provided an optimized protocol for the formation of the elusive allyl 2-uloside **2a** by Dess-Martin oxidation, followed by *C*-2 vinylation of crude **2a** under optimized conditions **(Scheme 3.13)**. The obtained 2-*C*-vinyl branched allyl mannoside was transformed into bicyclic alkene **17** as a key intermediate *via* ring-closing metathesis. Stereoselective *syn*- or *anti*-selective dihydroxylations of the side chain enabled, after debenzylation, the formation of the annulated target compounds ***syn*-15** and ***anti*-21** in 10–11 steps from D-glucose, respectively. As a major advantage, and as opposed to several other approaches, this synthetic route to *O*-glycosidically 1,2-annulated carbohydrates proceeded with conservation of the configurations of the

C-3,4,5 stereogenic centers of the parent carbohydrate. Both highly hydroxylated target compounds could be structurally characterized by multiple methods, including detailed NMR studies in aqueous solution (D_2O). In these spectroscopic experiments, the *syn*- and *anti*-configurations of the side chain diols could be derived. Most notably, X-ray structural analysis of ***syn*-15** confirmed the anticipated *trans*-decalin type molecular framework, and allowed for the characterization of a dense network of hydrogen-bonding interactions in the crystal lattice. Structurally comparable 1,2-annulated sugar motifs are found in natural products, or in synthetic molecules with interesting biological properties, for example as glycomimetic inhibitors for glycosidase enzymes. However, similar *O*-glycosidically 1,2-annulated sugars with the synthetically challenging β-*manno* configuration have not been prepared previously. Therefore, the described synthetic strategy utilizing allyl 2-ulosides for the synthesis of such annulated carbohydrate analogs is a valuable preparative contribution. In this context, the given discussion of synthetic challenges encountered in reactions involving allyl 2-uloside **2a** could potentially facilitate the application of other sensitive *keto*-sugars as versatile carbohydrate building blocks.

In following studies beyond the scope of this thesis, an evaluation of the obtained target compounds ***syn*-15** and ***anti*-21** with respect to potential glycosidase-inhibiting properties would be of interest. Furthermore, the developed synthetic strategy could be utilized to obtain structurally related stereoisomers of **T-3** with axially-oriented substituents at the parent carbohydrate, e.g. by employing 2-*keto*-glycosides of the *altro*-, *ido*- or *talo*-configuration.

4. Reducing Higher Sugars: Octoses with Analogy to Bradyrhizose

A second project pursued in the course of this thesis based on the application of benzyl 2-uloside **2b**[37] (**Scheme 2.14** on page 24) as a synthetic intermediate. The 2-*keto*-sugar was anticipated to be a suitable substrate for functionalizations of the *C*-2, and thus, for the generation of structurally diverse 2-*C*-branched carbohydrates in a manner comparable to the vinylation of the allyl derivative **2a** as captured in **Chapter 3**. After several synthetic transformations starting from **2b**, formyl-branched higher sugars (octoses) **T-4** were expected to be accessible. These target compounds can potentially occupy bicyclic hemiacetal isomeric forms with structural analogies to the unique natural monosaccharide bradyrhizose **K** (**Scheme 1.3** on page 4). In this context, detailed synthetic studies towards the target higher sugars **T-4** are described, followed by an examination of isomeric hemiacetal forms. Thus, the identified isomeric forms of reducing sugars **T-4** can be compared to the isomeric distribution found for the natural monosaccharide **K**.

First, an introduction to nitroxyl radical-mediated methods for the oxidation of alcohols is provided, since this type of transformation is relevant to the results discussed here. Following this, a general introduction to the chemistry of higher sugars is given, with a focus on published synthetic approaches for structurally interesting target molecules. Subsequently, relevant published work regarding the natural product bradyrhizose **K** is summarized.

4.1. Introduction to Nitroxyl Radical-Based Alcohol Oxidations

Persistent nitroxyl radicals, the most prevalent being 2,2,6,6-tetramethylpiperidin-*N*-oxyl (TEMPO), are a class of organic compounds amenable to a sophisticated redox chemistry (**Scheme 4.1**). TEMPO, itself a commercially available, red crystalline solid, can undergo formal single electron oxidation to the derived oxoammonium ion

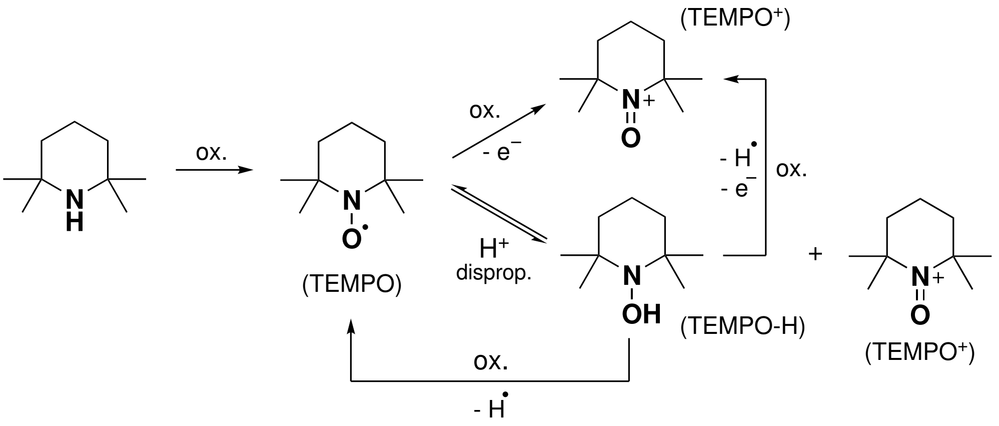

Scheme 4.1 Schematic representation of the redox chemistry involving TEMPO, the hydroxylamine TEMPO-H and the derived oxoammonium ion TEMPO$^+$.

TEMPO$^+$. Furthermore, in very acidic media ($pH < 2$), reversible disproportionation to the hydroxylamine TEMPO-H and the same oxoammonium ion can be observed.[134] Whereas TEMPO (and structurally related nitroxyl radicals[135, 136]) can be regarded as weaker oxidants, the corresponding oxoammonium ions were found to be suitable mediators for the oxidation of alcohols.[137] For such transformations of alcohols, TEMPO is usually utilized in catalytic quantities, together with a secondary oxidant capable of supplying the reactive oxoammonium ion TEMPO$^+$ from TEMPO, or from the reduced hydroxylamine form TEMPO-H. In this regard, the reaction mechanism for the formation of TEMPO$^+$ from the reduced TEMPO species, by reaction with the respective stoichiometric oxidant, is usually of a rather enigmatic nature. Although this step is rarely discussed in the relevant literature, it can be expected to be dependent on the nature of the utilized stoichiometric oxidant, and on the conditions of the oxidation reaction.

In contrast, the critical mechanistic step involving the reaction of the oxoammonium ion TEMPO$^+$ with the corresponding substrate alcohol has been subject to detailed studies. Accordingly, a complex mechanistic picture has been developed, involving two distinct mechanisms depending on the pH of the reaction medium.[134, 138] In basic media **(Scheme 4.2, a)** the reaction is thought to proceed *via* nucleophilic attack of an alkoxide onto the oxoammonium nitrogen. The resulting tetrahedral intermediate forms preferentially for sterically less crowded alcohols due to the bulky tetramethylated environment of the oxoammonium ion, and therefore primary alcohols react selectively over secondary alcohols. Noteworthy, due to the generally high stability constants of the intermediate, even small alkoxide concentrations (e.g. at pH 5) allow for this mechanism. Fragmentation of the intermediate (the overall rate-determining step) gives

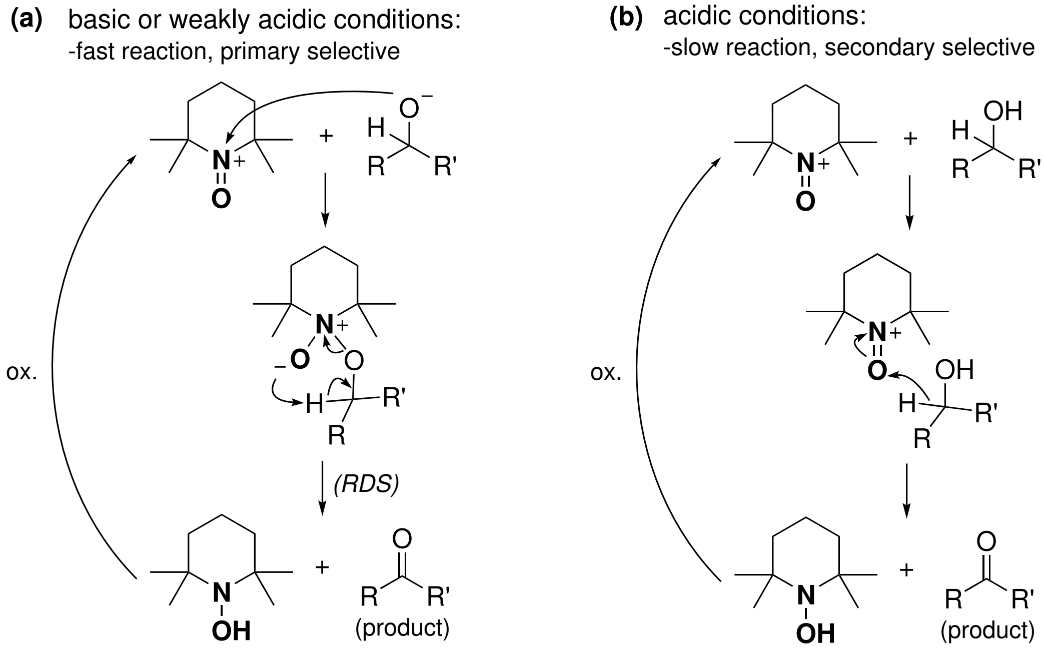
(a) basic or weakly acidic conditions:
-fast reaction, primary selective
(b) acidic conditions:
-slow reaction, secondary selective
ox.
(RDS)
(product)
ox.
(product)

Scheme 4.2 Catalytic cycles suggested for TEMPO-catalyzed oxidation reactions of alcohols, mechanistically depending on the pH of the solution.[134, 138] **(a)** Proposed mechanism under basic or weakly acidic conditions ($\mathrm{pH} \geqslant 5$). **(b)** Proposed mechanism under acidic conditions ($\mathrm{pH} < 5$). Counter ions and potential equilibrium steps are not shown. R, R' = H, organic residue. *RDS* = rate-determining step.

the carbonyl product and the hydroxylamine TEMPO-H, which can be converted to TEMPO or to the oxoammonium ion TEMPO^+ by the secondary oxidant. In acidic media **(Scheme 4.2, b)**, an alternative bimolecular mechanism is thought to proceed *via* hydride transfer of the alcohol to the oxoammonium ion oxygen. Since this hydride transfer is faster for higher substituted alcohols, secondary alcohols tend to react faster. However, the rate of this reaction is significantly lower as compared to the reaction under basic conditions. As a result, in many oxidation protocols, a buffer is added to neutralize any acidic species, for example derived from the stoichiometric oxidant (see below). In this way, a clean and fast reaction following mechanism **(a)** can be expected, exhibiting high selectivity for primary over secondary alcohols.

A large number of conditions involving diverse stoichiometric oxidants for TEMPO-catalyzed oxidations have been published to date.[139, 140] A widely employed alcohol oxidation protocol was introduced by Anelli *et al.* **(Scheme 4.3, a)**.[141] Sodium hypochlorite is used as a secondary oxidant, and the reaction is run in a biphasic solvent mixture (CH_2Cl_2/H_2O). Sodium hydrogen carbonate is added as a buffer, and a bromide salt (KBr) was found to have an accelerating effect on the reaction. Optionally, quaternary ammonium salts (Aliquat 336) can be added as phase-transfer catalysts to further increase the reaction rate. With this protocol, primary and secondary alcohols can be oxidized to the corresponding carbonyl products, and by controlling the reaction time and the amount of NaOCl, overoxidation of aldehydes (in hydrated form) to the carboxylic acids can be prevented. Although these reaction conditions can be regarded as generally mild, for specifically functionalized substrates, side reactions have to be considered. In this regard, vicinal diols can be cleaved under these conditions, and therefore only minimum amounts of the strong oxidant NaOCl should be used.[142] Likewise, lactols are easily converted to lactones with excessive oxidant.[143] Nevertheless, this method is frequently applied for otherwise challenging transformations. Due to the high selectivity of primary over secondary alcohols, this protocol can be regarded as a method of choice for such a selective transformation.[144] To overcome problems with side reactions, induced by NaOCl or by the derived acid HOCl, several modifications of this protocol have been developed, the most prevalent being the variant described by Piancatelli and Margarita **(Scheme 4.3, b)**.[145] In this reaction, PhI(OAc)$_2$ is used as a stoichiometric oxidant in combination with catalytic TEMPO. The reaction can be run in CH_2Cl_2 as the sole solvent, and thus, under anhydrous conditions. Notably, in this reaction, similarly high selectivities for primary alcohol oxidations in the presence of secondary alcohols were observed.

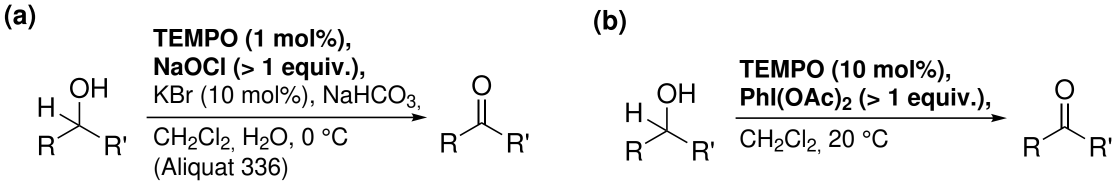

Scheme 4.3 **(a)** Anelli's protocol for TEMPO-catalyzed alcohol oxidation, using NaOCl in a biphasic medium.[141] **(b)** Piancatelli's and Margarita's protocol for TEMPO-catalyzed alcohol oxidation, using PhI(OAc)$_2$ in CH_2Cl_2.[145] R, R' = H, organic residue.

Although these protocols have found widespread application as synthetic tools, further investigations into the oxidation chemistry mediated by nitroxyl radicals are still being pursued. For example, sterically less demanding adamantane-derived nitroxyl radicals have been shown to be superior for the oxidation of sterically crowded secondary alcohols, for which TEMPO-based methods are unsuitable.[146] Furthermore, chiral nitroxyl radicals (or chiral oxoammonium species) have been developed, enabling the enantioselective oxidation of the alcohol substrates, for example in kinetic resolution by oxidation processes.[147]

4.2. Introduction to Higher Sugars

The vast majority of the naturally occurring carbohydrates belong to the pentoses or the hexoses, featuring a chain length of 5 or 6 consecutive carbon atoms, respectively. Accordingly, sugars with a chain length above 6 carbon atoms are commonly referred to as higher sugars. This interesting and diverse class of carbohydrates is associated with complex molecular structures and is frequently involved in many biological processes. An appropriate short introduction is given in a synthetic work by Baptistella and Coworkers.[148] Thus, higher-carbon sugars with 7 or 8 carbon atoms (heptoses and octoses) are frequently located in bacterial lipopolysaccharides, for example 3-deoxy-α-D-*manno*-oct-2-ulosonic acid (Kdo, **G** in **Scheme 1.2** on page 3) or L-*glycero*-D-*manno*-heptose (LDmanHep, **H** in **Scheme 1.2**). 9-Carbon sugars (nonoses) are prominently represented by the natural neuraminic acids/sialic acids family (like sialic acid **F** in **Scheme 1.1**), which are important components of saccharidic ligands targeted by lectins in biological recognition processes. Such heptoses, octoses and nonoses found in nature have been subject to intensive studies, and multiple reviews have been published on these well-known types of higher sugars.[10, 149–151] In contrast, higher sugars with 10 or more carbon atoms can be regarded as rare, some of them being found as the glycosidic components of natural products (see below).

Higher sugars in general have been attractive targets for synthetic carbohydrate chemistry. Typical synthetic strategies often involve conventional hexoses as starting materials and suitable homologation reactions for the chain elongation. Stereogenic centers in the target molecules, often hydroxylated, are frequently installed after chain elongation, for example *via* selective hydroxylation reactions of unsaturated intermediates.[152] A short summary of interesting synthetic strategies described in the literature is given below.

Early syntheses of higher sugars, as reported by R. Schaffer, were based on the aldol-selfcondensation of protected monosaccharides under basic conditions.[153, 154] In these experiments, carbon-branched higher sugars of purely synthetic origin could be isolated. Later, synthetic work on higher sugars frequently focussed on the targeted synthesis of unusual saccharides of natural origin. An interesting class of antibiotic natural products isolated from several strains of *Streptomyces* are the quinocyclines, which possess a tetracyclic anthraquinoid framework as the aglycon.[157] The glycosidic components of the quinocyclines have been identified to be unusual 4-*C*-branched 2,6-dideoxy L-sugars. For example, the glycosidic component of quinocycline A and isoquinocycline A was found to be the monosaccharide dihydrotrioxacarcinose B (depicted as its α-L-methyl glycoside **CK** in **Scheme 4.4**). In an early total synthesis of **CK**, Paulsen

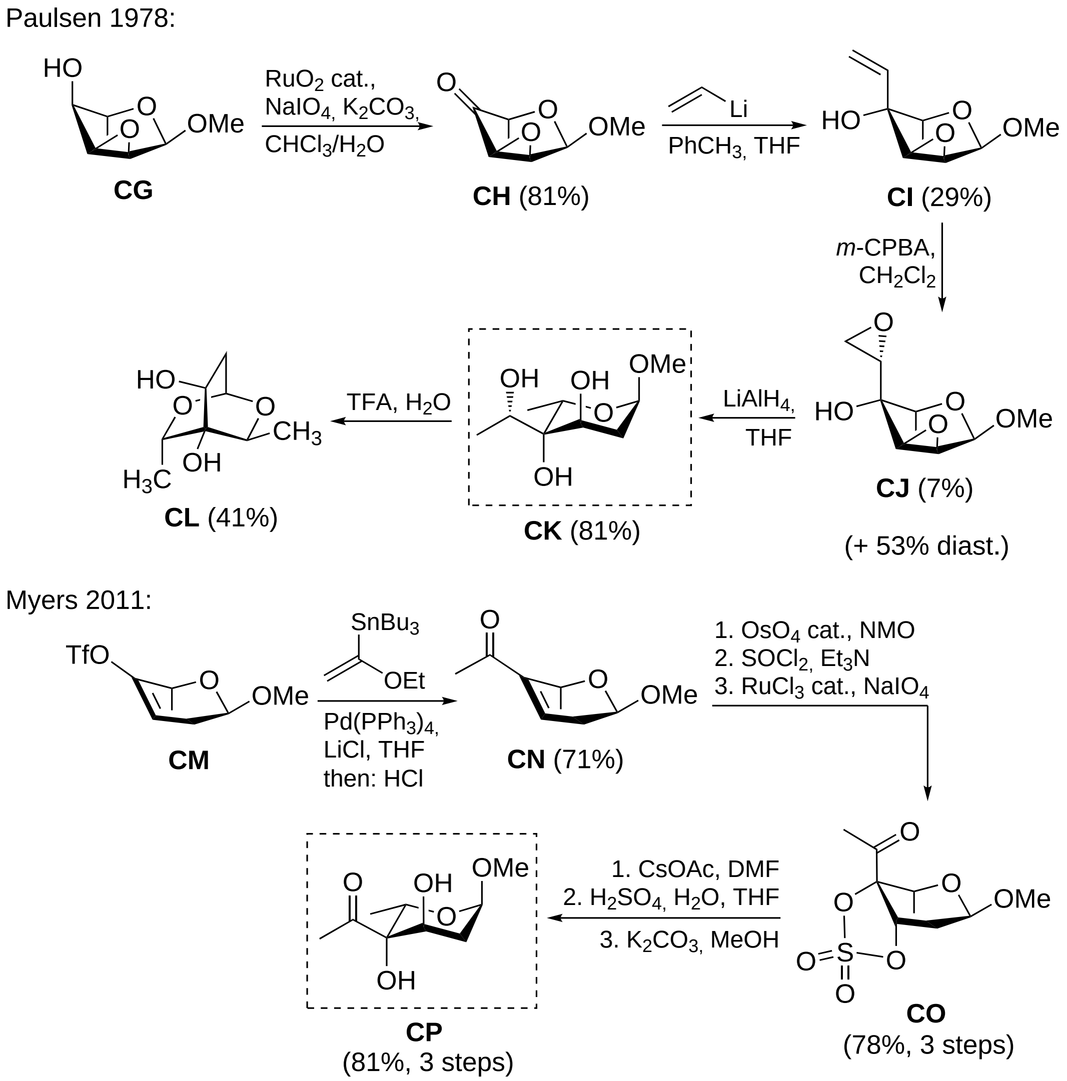
Paulsen 1978:
CG
RuO2 cat., NaIO4, K2CO3, CHCl3/H2O
CH (81%)
Li
PhCH3, THF
CI (29%)
m-CPBA, CH2Cl2
CJ (7%)
(+ 53% diast.)
LiAlH4, THF
CK (81%)
TFA, H2O
CL (41%)
Myers 2011:
CM
SnBu3
OEt
Pd(PPh3)4, LiCl, THF then: HCl
CN (71%)
1. OsO4 cat., NMO
2. SOCl2, Et3N
3. RuCl3 cat., NaIO4
CO
(78%, 3 steps)
1. CsOAc, DMF
2. H2SO4, H2O, THF
3. K2CO3, MeOH
CP
(81%, 3 steps)

Scheme 4.4 Top: Paulsen's synthesis of methyl α-dihydrotrioxacarcinoside B (structure **CK**) *via* vinylation/epoxidation.[155] Bottom: Myers' synthesis of methyl α-trioxacarcinoside B **CP** *via* Stille coupling/dihydroxylation.[156]

and Coworkers subjected epoxy alcohol **CG**, derived from L-rhamnal, to a ruthenium-based *C*-4 oxidation to provide 4-uloside **CH**.[155] Addition of vinyllithium gave vinyl-branched **CI**, together with other isomeric products. Epoxidation of the side chain gave, unfortunately, the wanted epoxide isomer **CJ** as the minor product. Reduction of the diepoxide with $LiAlH_4$ resulted in the formation of target compound **CK**. Although **CK** should be regarded as a 4-*C*-hydroxyethyl-branched hexose, the unusual sugar is sometimes referred to as an octose.[155] For reasons of structural elucidation, **CK** was treated with dilute trifluoroacetic acid to induce the formation of bicyclic **CL**, a suitable example for the peculiar structures that such higher sugars can possess. The related natural products quinocycline B and isoquinocycline B feature a structurally comparable glycosidic component referred to as trioxacarcinose B (depicted as its α-L-methyl glycoside **CP** in **Scheme 4.4**), formally arising from **CK** by oxidation of the side chain secondary alcohol to the ketone. In a modern total synthesis of **CP**, Myers and Coworkers employed a Stille reaction between vinyl triflate **CM** and an ethoxyvinylstannane to furnish, after acidic hydrolysis, enone **CN**.[156] Since the corresponding epoxide derived from **CN** (not shown) was unreactive, a sequence of *syn*-dihydroxylation, reaction with thionyl chloride and subsequent oxidation of the sulfur was used for the formation of the cyclic sulfate **CO**. This sulfate intermediate was more electrophilic than the epoxide, thereby enabling nucleophilic displacement with cesium acetate, followed by hydrolytic removal of the sulfate and deacetylation to give the target glycoside **CP**.

A class of compounds generally associated with structurally diverse higher sugars are the undecose nucleosides (see also **BA** in **Scheme 3.3** on page 31). A peculiar representative of this class, the anthelmintic natural product hikizimycin features an undecose core (termed hikosamine) consisting of a 4-deoxy-4-amino-glucopyranose linked *via* the *C*-5 to a fully oxygenated mannitol moiety (depicted as its α-methyl glycoside in peracetylated form **CV** in **Scheme 4.5**). In a synthetic approach to the hikosamine undecose, Danishefsky and Coworkers reacted D-galactose-derived aldehyde **CQ** with reactive diene **CR** in a $MgBr_2$-mediated Hetero-Diels-Alder reaction.[158] The obtained dihydropyran-4-one **CS** was subjected to Luche reduction of the enone, epoxidation with *syn*-selectivity with respect to the allylic hydroxyl group, and debenzoylation to provide **CT** with *manno*-configuration. Reduction of the hemiacetal and perbenzylation gave **CU**, which incorporated all required stereogenic centers of the side chain. Subsequent steps transformed the galactose residue (R) into a 4-deoxy-4-amino-glucopyranose, and the target methyl peracetyl-α-hikosaminide **CV** was available. In a different approach to the hikosamine undecose **(Scheme 4.5, bottom)**, Schreiber and Coworkers started from L-(+)-di-*iso*-propyl tartrate **CW**.[159] After benzylation, a two-directional elaboration of the chain started with Horner-Wadsworth-Emmons olefination under reducing conditions to give diene **CX**. Site-selective dihydroxylation and silylation provided **CY**, which incorporated 6 of the stereogenic centers required for the hikosamine structure. In subsequent steps involving sequential DIBAL-H reductions, Swern oxidations, olefinations and dihydroxylations, further two-directional elongation of the chain towards the hikosamine undecose could be achieved. Apart from the mentioned, other syntheses of the unusual hikosamine higher sugar were developed, including a modern two-fragment approach by Fürstner and Coworkers.[160]

As a prototypical example of a structurally unique higher sugar, Pérez and Coworkers isolated the natural product peltalosa **CZ** from roots of the Mexican plant *Psacalium*

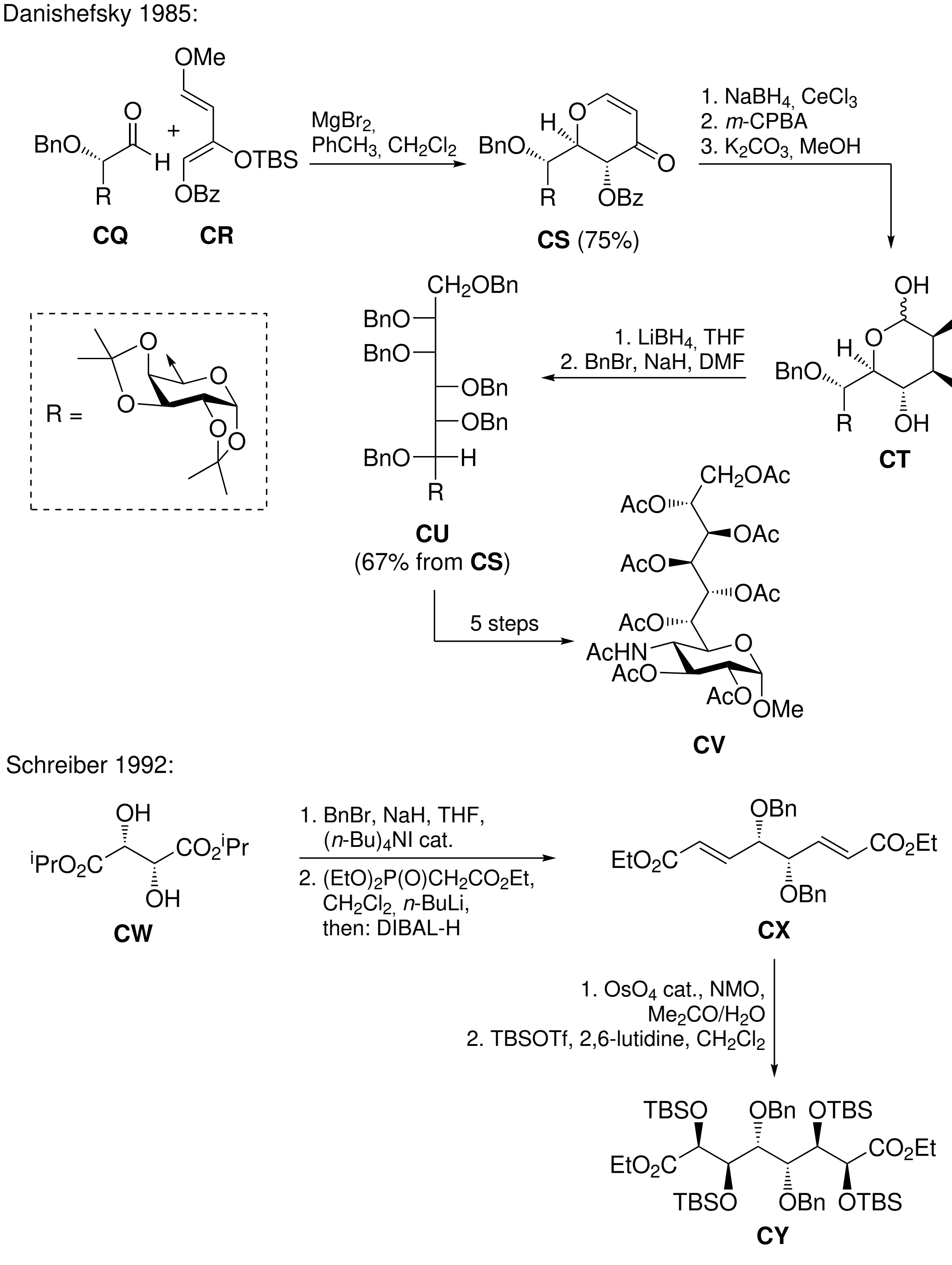
Danishefsky 1985:

Schreiber 1992:

OMe
BnO
H
R
OTBS
OBz
CQ
CR
MgBr$_2$, PhCH$_3$, CH$_2$Cl$_2$
CS (75%)
1. NaBH$_4$, CeCl$_3$
2. m-CPBA
3. K$_2$CO$_3$, MeOH
CT
1. LiBH$_4$, THF
2. BnBr, NaH, DMF
CH$_2$OBn
CU
(67% from CS)
R =
5 steps
CH$_2$OAc
AcO
OAc
AcHN
OMe
CV
^{i}PrO$_2$C
CO$_2$^{i}Pr
OH
CW
1. BnBr, NaH, THF, (n-Bu)$_4$NI cat.
2. (EtO)$_2$P(O)CH$_2$CO$_2$Et, CH$_2$Cl$_2$, n-BuLi, then: DIBAL-H
EtO$_2$C
CO$_2$Et
OBn
CX
1. OsO$_4$ cat., NMO, Me$_2$CO/H$_2$O
2. TBSOTf, 2,6-lutidine, CH$_2$Cl$_2$
TBSO
OTBS
CY

Scheme 4.5 Top: Danishefsky's approach to peracetylated methyl α-hikosaminide **CV** *via* Hetero-Diels-Alder reaction and epoxidation/hydride reductions.[158] Bottom: Schreiber's synthetic route for the intermediate **CY** towards the open-chain hikosamine.[159]

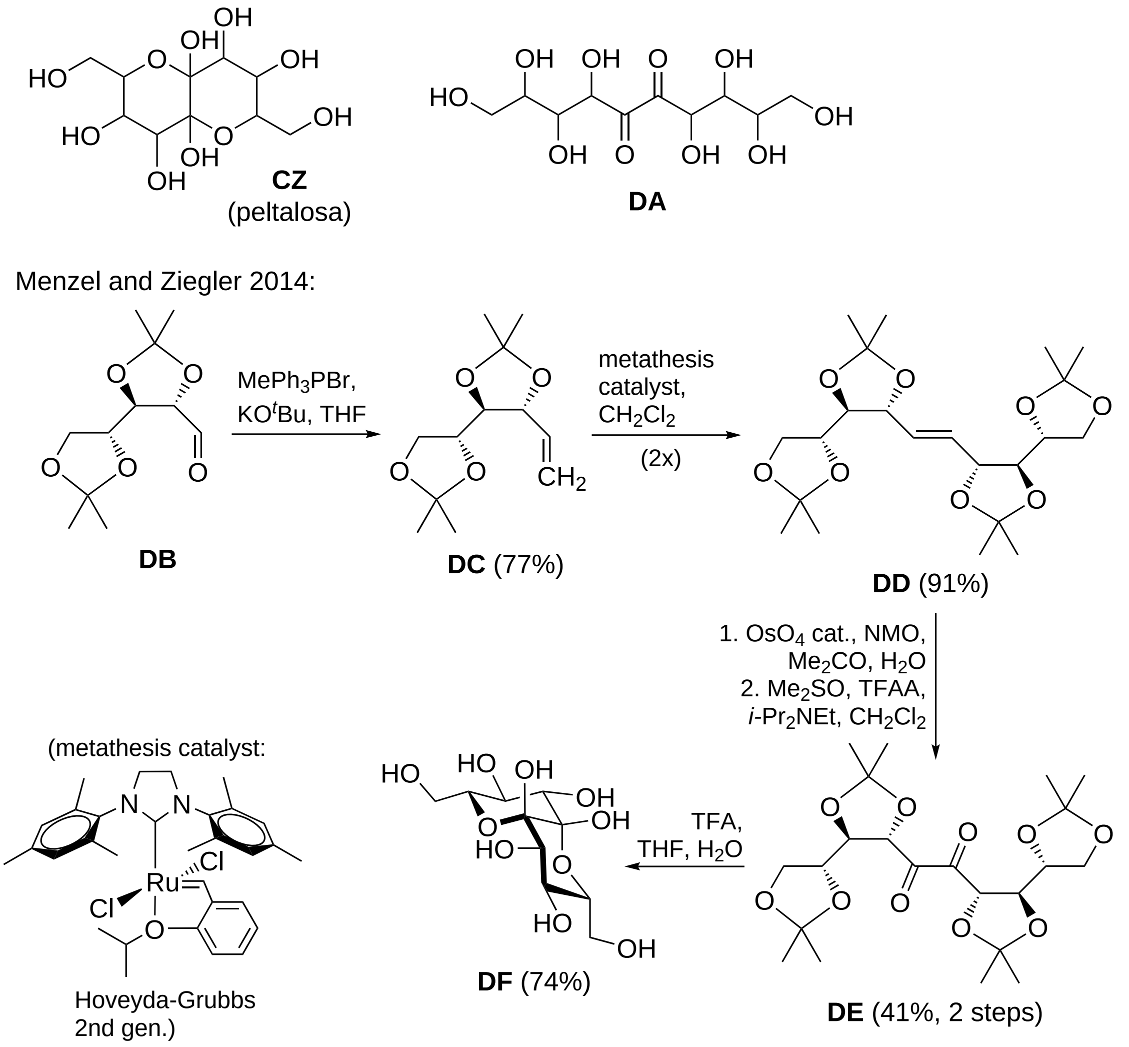
CZ
(peltalosa)
DA
Menzel and Ziegler 2014:
MePh3PBr,
KO*t*Bu, THF
metathesis
catalyst,
CH2Cl2
(2x)
DB
DC (77%)
DD (91%)
1. OsO4 cat., NMO,
Me2CO, H2O
2. Me2SO, TFAA,
i-Pr2NEt, CH2Cl2
TFA,
THF, H2O
DE (41%, 2 steps)
DF (74%)
(metathesis catalyst:
Hoveyda-Grubbs
2nd gen.)

Scheme 4.6 Top: proposed structures of the natural product peltalosa **CZ** and its open-chain diulose form **DA** (configurations unknown).[161] Bottom: Menzel and Ziegler's synthetic approach towards symmetrical 5,6-diulose **DF** with connectivity identical to **CZ**.[162]

peltatum in 2005.[161] The compound exhibited an interesting hypoglycemic activity, and was thus potentially interesting for the therapeutic treatment of type 2 diabetes mellitus. Although the structural characterization described by the authors did not allow for the assignment of the stereochemical configurations, mass spectra in combination with an unexpected simplicity of the NMR spectra suggested the structure of a C_2-symmetric decalin-like molecule **CZ (Scheme 4.6, top)**. Drawn in its corresponding open-chain isomeric form **DA**, the structure can be identified to be a symmetric deco-5,6-diulose. In a synthetic approach towards similar symmetric 5,6-diulose systems, Menzel and Ziegler utilized a sequence of Wittig-olefination and alkene metathesis homodimerization for the synthesis of arabinose-derived symmetrical dec-5-enitol **DD**

(Scheme 4.6, bottom).[162] The α-diketone could be constructed by a sequence of dihydroxylation followed by oxidation of the diol, but the latter turned out to be nontrivial. A modified Swern-type protocol employing DMSO/trifluoroacetic anhydride (TFAA) in combination with Hünig's base proceeded reliably, and the 5,6-diulose **DE** was obtained. After deprotection the diulose occupied a *cis*-decalin-type structure **DF** which was confirmed by X-ray crystallography. Although a comparison of the spectral properties of **DF** with those reported for the isolated **CZ** suggested that it was a stereoisomer of the natural product, this approach can be regarded as a general route to such structurally interesting higher-carbon diuloses.

In all of the examples given above, the syntheses involved oxidative functionalizations of alkene substrates *via* *syn*-dihydroxylation or epoxidation. These types of transformations can thus be regarded as essential reactions for the synthesis of higher sugars, but the prediction of the stereoselectivity of the product formation can be intricate for complex substrates. In this regard, S. Jarosz performed investigations on the stereochemical outcome of the osmoylation[163] and epoxidation[164] of the higher bis-glycosidic allylic alcohols **DG** and **DH** **(Scheme 4.7)**. Accordingly, *syn*-dihydroxylation of **DG** **(Scheme 4.7, a)** resulted in the formation of major isomer **DI** (d.r. = 86:14). This finding was in accordance with Kishi's empirical rule[105, 106], which suggests attack of osmium tetroxide from the face of the alkene opposite to that of the allylic hydroxyl in an eclipsed conformation, with the allylic hydrogen in plane with the alkene. Surprisingly, under the same conditions, the diastereoisomeric allyl alcohol **DH** was transformed into major isomer **DJ** (d.r. = 67:33), obviously *via* attack from the side of the allylic hydroxyl, and thus, in an "*anti*-Kishi" sense. In this case, by the author, this finding was attributed to a dominating repulsive effect of the furanose (Sug^2) ring oxygen over the repulsive effect of the allylic hydroxyl. An investigation of epoxidations of allylic alcohol **DG** revealed comparably false predictions of established models **(Scheme 4.7, b)**. Epoxidation of **DG** with *m*-CPBA gave **DK** (d.r. = 81:19), commonly designated as the *threo*-product. An analysis employing the Sharpless model[165] for acyclic allylic alcohols, which proposes a dihedral angle HO-C-C=C of 120° and peroxy acid attack from the side of the allylic hydroxyl, was in accordance, and also predicted the formation of the *threo*-product **DK**. In contrast, epoxidation of the same substrate **DG** with VO(acac)$_2$/*t*-BuOOH gave the same major *threo*-product **DK**, although a comparable analysis with the Sharpless model for vanadium-catalyzed epoxidations ([V]O-C-C=C: 50°) suggested the formation of the corresponding *erythro*-product, which was only observed as the minor component (d.r. = 63:37). Obviously, due to the crowded nature of the substrate allylic alcohols, additional steric factors result in deviations from the standard models that usually give good predictions for simpler substrates.

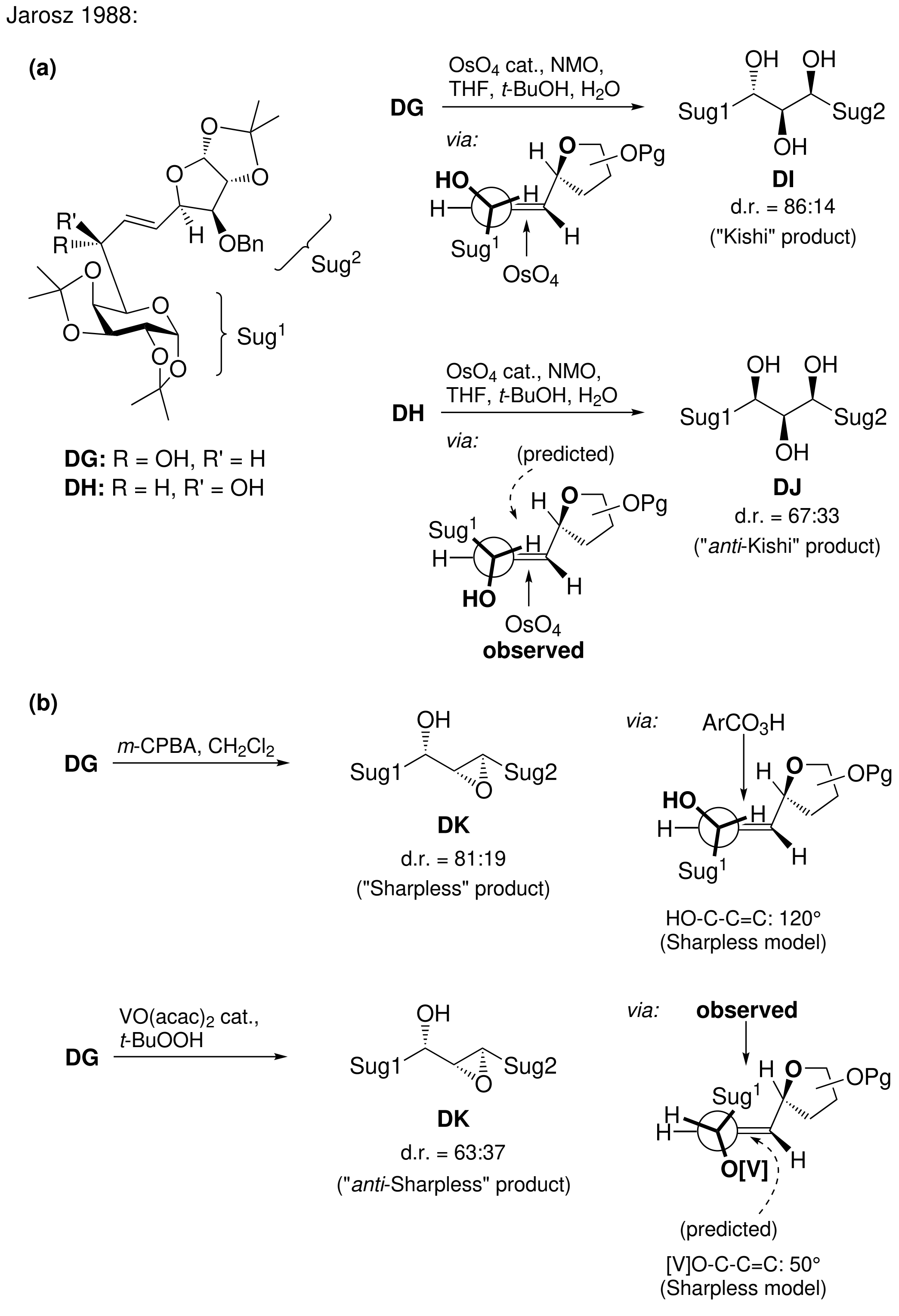
Jarosz 1988:
(a)
R'
R
O
OBn
H
Sug2
Sug1
DG: R = OH, R' = H
DH: R = H, R' = OH
DG
OsO4 cat., NMO, THF, t-BuOH, H2O
via:
HO
H
Sug1
OsO4
OPg
OH OH
Sug1 Sug2
OH
DI
d.r. = 86:14
("Kishi" product)
DH
OsO4 cat., NMO, THF, t-BuOH, H2O
via:
(predicted)
observed
OH OH
Sug1 Sug2
OH
DJ
d.r. = 67:33
("anti-Kishi" product)
(b)
DG
m-CPBA, CH2Cl2
OH
Sug1 Sug2
O
DK
d.r. = 81:19
("Sharpless" product)
via:
ArCO3H
HO-C-C=C: 120°
(Sharpless model)
DG
VO(acac)2 cat., t-BuOOH
OH
Sug1 Sug2
O
DK
d.r. = 63:37
("anti-Sharpless" product)
via:
observed
O[V]
(predicted)
[V]O-C-C=C: 50°
(Sharpless model)

Scheme 4.7 (**a**) Structures of higher sugar allylic alcohols **DG** and **DH**, major isomers **DI** and **DJ** formed in *syn*-dihydroxylations, and proposed modes of attack of osmium tetroxide. (**b**) Epoxidations of allylic alcohol **DG** and Sharpless' models for the predicted modes of attack.[163, 164]

Whereas the examples given above can be seen as a general introduction to strategies for the synthesis of higher sugars, the following section introduces a naturally occurring higher sugar with special relevance to this thesis. The unusual monosaccharide bradyrhizose **K** **(Scheme 1.3)** is structurally related to the target higher sugars **T-4**. Accordingly, a summary of published work on **K** is given below.

4.3. Introduction to Bradyrhizose: An Unusual Higher Monosaccharide

The reduction of atmospheric dinitrogen to biologically available ammonia as a nitrogen source is of tremendous ecological relevance. Industrially, this conversion is achieved in the Haber process. By far the most prevalent natural source of fixed nitrogen stems from symbioses of certain flowering plants (mostly legumes) with gram-negative soil bacteria capable of nitrogen-fixation, thus enabling the host plant to live in a potentially nitrogen-poor environment. On the side of the host plant, ca. 70% of all legume species, together with multiple other *actinorhizal* plants can potentially undergo such a symbiosis. On the side of the soil bacteria, hundreds of species of Proteobacteria (Alpha- and Betaproteobacteria) share the ability of nitrogen fixation in symbioses with legume host plants, and this type of bacteria is referred to as *rhizobia*. In contrast, symbioses of the non-legume actinorhizal plants can only be established by Actinobacteria of one genus (*Frankia*).[166, 167]

On a molecular level, bacterial nitrogen fixation is facilitated by the nitrogenase enzyme, a two-protein complex with Fe-S- and Mo-Fe-S-cluster core elements, which is capable of the reduction of molecular dinitrogen.[168] This reducing nitrogenase complex is irreversibly damaged by the action of atmospheric oxygen, however, the rhizobia themselves do rely on oxygen for respiratory purposes. On the level of the plant-rhizobium-symbiosis, this contradiction is addressed by the formation of nodules, symbiosis-specific organs, which are usually clearly visible at the roots of the host plant (comp. **Fig. 4.1**) or, less frequently, at the stem. These nodules are densely populated by the rhizobia, which then differentiate into nitrogen-fixing bacteroids.[170] The interior of the nodules is characterized by a low concentration of free oxygen, and a certain plant hemoglobin (*leghemoglobin*) is synthesized within the nodules to provide the guest bacteroids with oxygen, showing the high degree of sophistication achieved in such symbiotic relationships.[166, 167] From this perspective, an initiation of the symbiosis is required to result in the formation of nodules (a process termed *nodulation*) before nitrogen fixation within the nodules is feasible. This initiation process has been

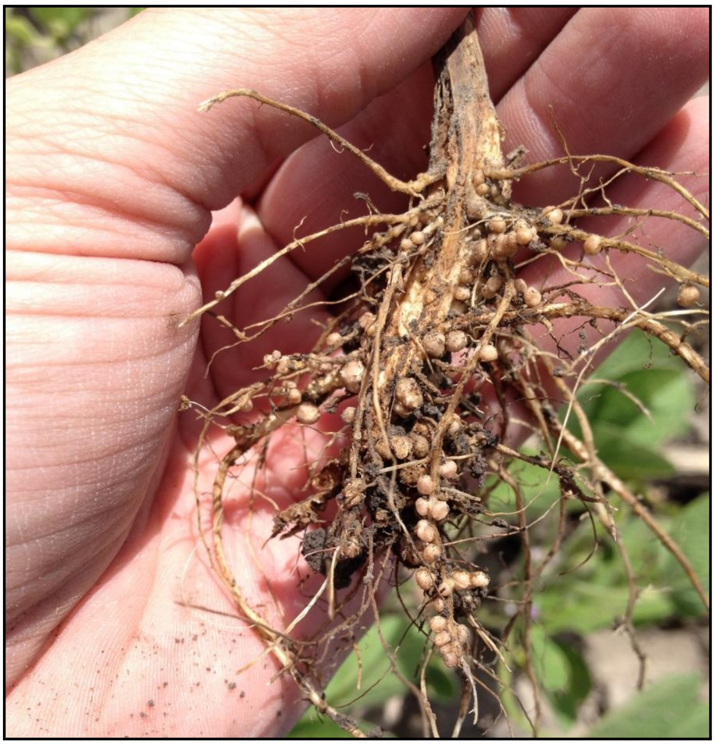

Figure 4.1 Nodulated soybean root. Picture taken in Dodge County, Wisconsin, U.S. Picture gratefully reprinted with permission from CropWatch.[169]

subject to detailed investigations, and at least three different modes of initiation are currently discussed. In this regard, the most prevalent and best understood mechanism, realized in efficient symbioses between most rhizobia and various legume plants, is referred to as the *Nod strategy*.[167] This type of mechanism relies on the mutual exchange of diffusible signaling substances between the potential host plant and the rhizobium. Initially, flavonoid signaling molecules are produced by the legume plant. As a result, in the rhizobia, nodulation genes (*nod genes*) are expressed, facilitating the biosynthesis of strain-specific lipochitooligosaccharides, which are universally designated as *Nod factors*. In the vast majority of rhizobia, three enzymes are involved in the biosynthesis of these lipochitooligosaccharides, and all three enzymes are encoded for by what is referred to as the canonical *nodABC* genes. In turn, in the host plant, receptor recognition of the Nod factors results in a biochemical cascade culminating in root (or stem) nodulation, and finally, in infection by the rhizobia.[166, 167, 171]

In 2007, Giraud *et al.* discovered that two photosynthetic strains of the genus *Bradyrhizobium* (*Bradyrhizobium* BTAi1 and ORS278) were capable of establishing nitrogen-fixing symbioses with the aquatic legume plants *Aeschynomene sensitiva* and *indica*, accompanied by nodulation of the plant's roots and of the stems.[171] Unexpectedly, although functional symbioses could be observed, the determination of the complete

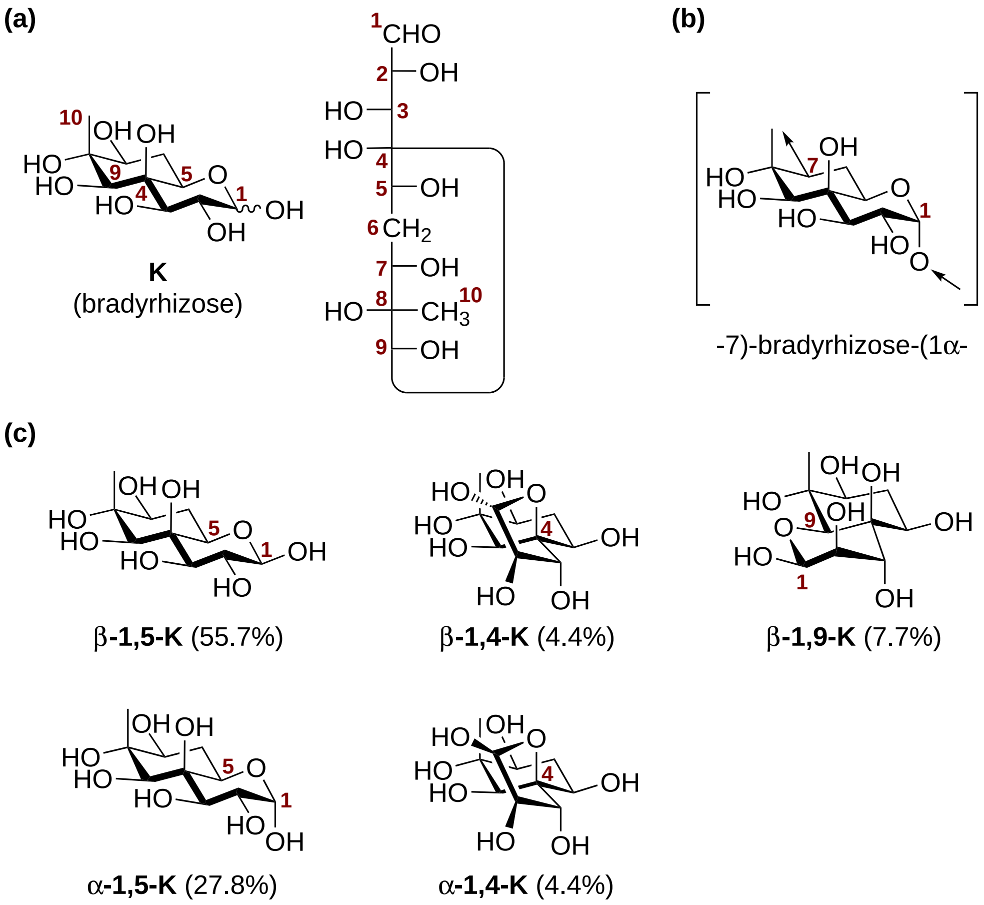

β-1,5-K (55.7%)
β-1,4-K (4.4%)
β-1,9-K (7.7%)
α-1,5-K (27.8%)
α-1,4-K (4.4%)

Scheme 4.8 **(a)** Structure **K** of the bradyrhizose monosaccharide and open-chain Fischer projection with carbocyclic moiety. **(b)** Repeating unit of the *Bradyrhizobium* BTAi1 O-antigen polysaccharide with α(1→7) connectivity. **(c)** Isomeric distribution of reducing bradyrhizose **K** in D_2O.[14]

genomic sequences of both *Bradyrhizobium* strains indicated the absence of the canonical *nodABC* genes. Since all other previously characterized rhizobia contained the *nodABC* genes, these findings indicated a completely novel mode of initiation of symbiosis. The question arose, how these types of Nod factor-independent symbioses are established. In this context, an involvement of the bacterial *Lipopolysaccharides* (LPS, **Fig. 1.1** on page 3) in the early recognition events of the symbiosis were investigated by Molinaro and Coworkers in 2011.[13] Due to the, in general, immunologically highly active nature of the LPS, and their known involvement in a plethora of bacterium-host-interaction processes (comp. **Chapter 1**), this question was addressed for *Bradyrhizobium* BTAi1. From dried cells of *Bradyrhizobium* BTAi1, Molinaro and Coworkers were able to isolate the LPS.[13] The O-antigen **(Fig. 1.1)** region of the extracted rhizobial LPS could be characterized, and its repeating unit was found to be composed of a single, structurally unique monosaccharide, which was designated *bradyrhizose* **K**.

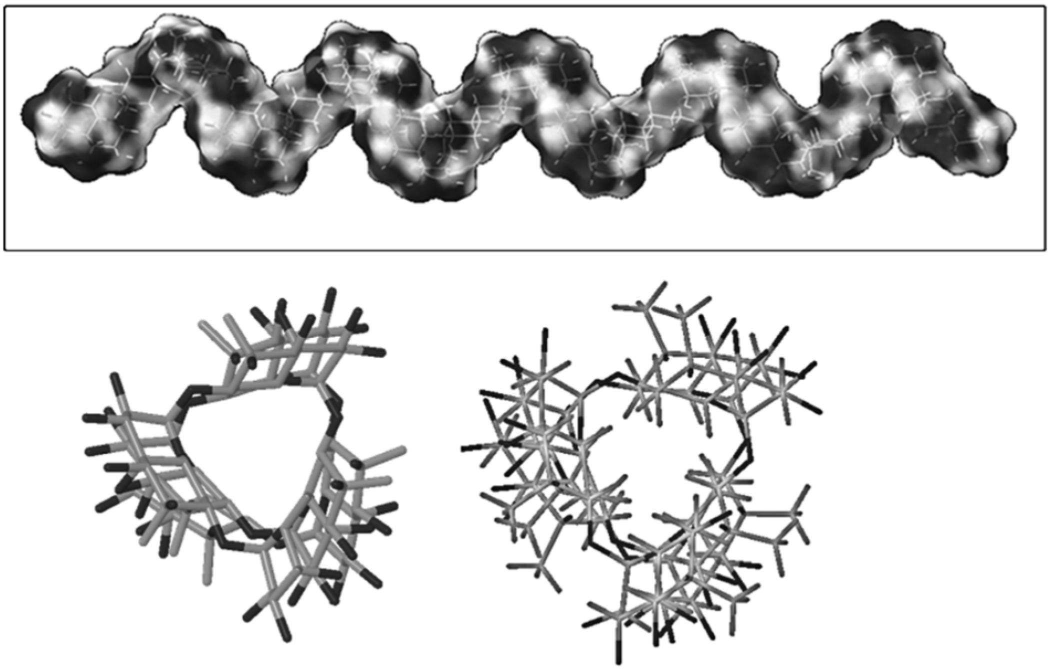

Figure 4.2 Results of molecular mechanics and dynamics calculations. Top: Connolly surface of the bradyrhizose eicohexasaccharide, showing a two-fold helicoidal conformation. Bottom: two representations of the calculated hydrophobic tunnel (bicyclic framework pointing inwards, hydroxyl and methyl groups pointing outwards) in the helicoidal conformation of a bradyrhizose octasaccharide. Figure gratefully reprinted with permission from John Wiley and Sons.[13]

The structure of **K (Scheme 4.8, a)** can be described as a methylated inositol, which is annulated to a galactose moiety in a *trans*-decalin-type fusion. Within the repeating unit of the O-antigen polysaccharide of *Bradyrhizobium* BTAi1 **(Scheme 4.8, b)**, the monosaccharide is connected *via* $\alpha(1\rightarrow7)$ linkages. Comparably, the LPS of *Bradyrhizobium* ORS278, the second strain for which absence of *nodABC* genes was observed, is also composed of $\alpha(1\rightarrow7)$-linked bradyrhizose units, but in this case the $\alpha(1\rightarrow9)$-linked isomers were found, too.[172] The structure of monomeric **K** is usually depicted in the shown 1,5-pyranose form, however, later structural studies by Yu, Molinaro and Coworkers revealed a complex mixture of isomers for the reducing monosaccharide **(Scheme 4.8, c)**.[14] Thus, in aqueous solution (D_2O), **K** exists in the α- and β-form of the major 1,5-pyranose (83.5% total isomeric contribution), together with the minor 1,4-spirofuranose form (α and β, 8.8%) and the minor 1,9-pyranose (β-isomer only, 7.7%). To study possible conformations adopted by the O-antigen structure (the bradyrhizose polysaccharide), the authors performed molecular mechanics and dynamics calculations. Thus, calculations on a bradyrhizose eicohexasaccharide **(Fig. 4.2, top)** suggested the preference for a right-handed two-fold helical conformation.

The bicyclic framework was found to point towards the inside of the helix, thus forming a “hydrophobic tunnel“, with all hydroxy and methyl substituents pointing outwards **(Fig. 4.2, bottom)**.[13]

The structurally unique bradyrhizose monosaccharide, together with the interesting conformational behavior suggested by computational results, raised the question whether the nature of the O-antigen of *Bradyrhizobium* BTAi1 was essential for the initiation of symbiosis with the host plant *Aeschynomene indica.* In subsequent immunological studies, *A. indica* and other model plants were subjected to either the intact LPS of *Bradyrhizobium* BTAi1, or to its O-antigen polysaccharide. A potential innate immune response was tracked by the elicitation of an oxidative burst caused by the generation of reactive oxygen species. Notably, neither the intact LPS, nor the O-antigen, triggered an immune response in the tested plants, including their host plant *A. indica*, and were thus not recognized as microbe-associated molecular patterns. This seemed to be the first evidence for a bacterial LPS unit which does not result in a defensive immune answer in plants. These results suggested that the structure of bradyrhizose **K**, and of the derived O-antigen, might be involved in the initiation of symbiosis. Specifically, the authors stated the hypothesis that the rhizobium *Bradyrhizobium* BTAi1 evolutionarily acquired the unusual O-antigen structure to evade being recognized by ist host plant *A. indica* as a hostile microbe.[13]

In 2015, the first total synthesis of bradyrhizose **K** was disclosed by Yu, Molinaro and Coworkers.[14] The synthesis of the monosaccharide could be achieved in 26 steps in an overall 9% yield. Starting with 2-*C*-alkenyl-branched glucal **DL (Scheme 4.9)**, which was available from direct Pd-catalyzed *C*-2-functionalization of tri-*O*-acetyl glucal, the axial *C*-2-OH was obtained from an epoxidation/epoxide opening sequence, giving *C*-2-branched mannoside **DM** after protecting group transformations. DIBAL-H reduction of the ester, silylation and acetylation gave **DN**, which was converted into the primary iodide **DO**. Dess-Martin oxidation and elimination of the iodide gave the unstable conjugated enone intermediate, which was directly treated with MeLi to install the axial methyl group in **DP**. Further protecting group manipulations gave **DQ**. In a $Hg(OAc)_2$-mediated Ferrier carbocyclization (Ferrier II reaction) as a key step **(Scheme 4.10)**, **DQ** was converted into the *keto*-inositol **DR**, which underwent reduction under Evans-Saksena conditions with $Me_4NHB(OAc)_3$ to give, after selective benzoylation of the equatorial hydroxyl group, **DS**. Dess-Martin oxidation, followed by axially-selective hydride reduction, gave the inverted product, which was then protected as the silyl ether **DT**. Dihydroxylation of the alkene under Sharpless conditions, with AD-mix α and $MeSO_2NH_2$, required additional co-oxidant ($K_2S_2O_8$), ligand ($(DHQ)_2PHAL$) and potassium osmate, and resulted in side products due to acetyl migration. Therefore, the

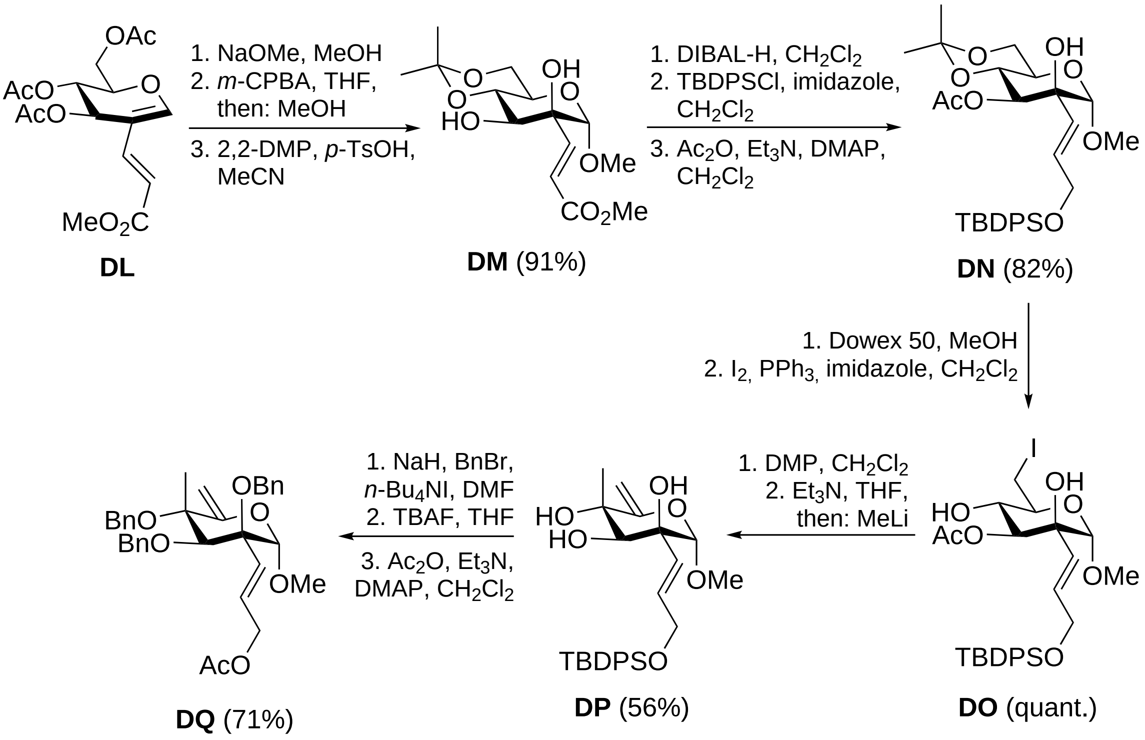
DL
1. NaOMe, MeOH
2. m-CPBA, THF, then: MeOH
3. 2,2-DMP, p-TsOH, MeCN
DM (91%)
1. DIBAL-H, CH2Cl2
2. TBDPSCl, imidazole, CH2Cl2
3. Ac2O, Et3N, DMAP, CH2Cl2
DN (82%)
1. Dowex 50, MeOH
2. I2, PPh3, imidazole, CH2Cl2
DO (quant.)
1. DMP, CH2Cl2
2. Et3N, THF, then: MeLi
DP (56%)
1. NaH, BnBr, n-Bu4NI, DMF
2. TBAF, THF
3. Ac2O, Et3N, DMAP, CH2Cl2
DQ (71%)

Scheme 4.9 Total synthesis of bradyrhizose **K** by Yu, Molinaro and Coworkers.[14] Synthesis of intermediate **DQ**.

crude mixture was subjected to selective deacetylation in the presence of the benzoyl group, with $Mg(OMe)_2$, to give the side chain triol **DU**. Selective oxidation of the primary alcohol in **DU** to the corresponding aldehyde was found to be challenging. For example, oxidation with TEMPO/$PhI(OAc)_2$ (comp. **Chapter 4.1**) resulted in partial oxidative diol cleavage. Under milder conditions, employing the combination TEMPO/trichloroisocyanuric acid (TCICA), clean conversion to the aldehyde was observed, but the following desilylation with TBAF was accompanied by epimerization of the α-stereogenic center. For this reason, **DU** was directly silylated to give **DV**, which was next treated with TEMPO/TCICA in the described method. Since partial overoxidation of the intermediately formed lactol to the corresponding lactone could not be prevented, the reaction was deliberately run until complete conversion to the lactone was observable, and subsequent DIBAL-H reduction furnished the wanted lactol **DW**. In the final step, hydrogenolytic debenzylation provided the target bradyrhizose **K**. In 2017, Yu, Molinaro and Coworkers developed an extension of this synthetic strategy to enable the synthesis of the corresponding bradyrhizose tetra- and pentasaccharides *via* glycosylation chemistry.[173] When these synthetic oligosaccharides were employed in plant immunological studies, in agreement with previous results using the natural bradyrhizose-containing material, no immune response was registered.

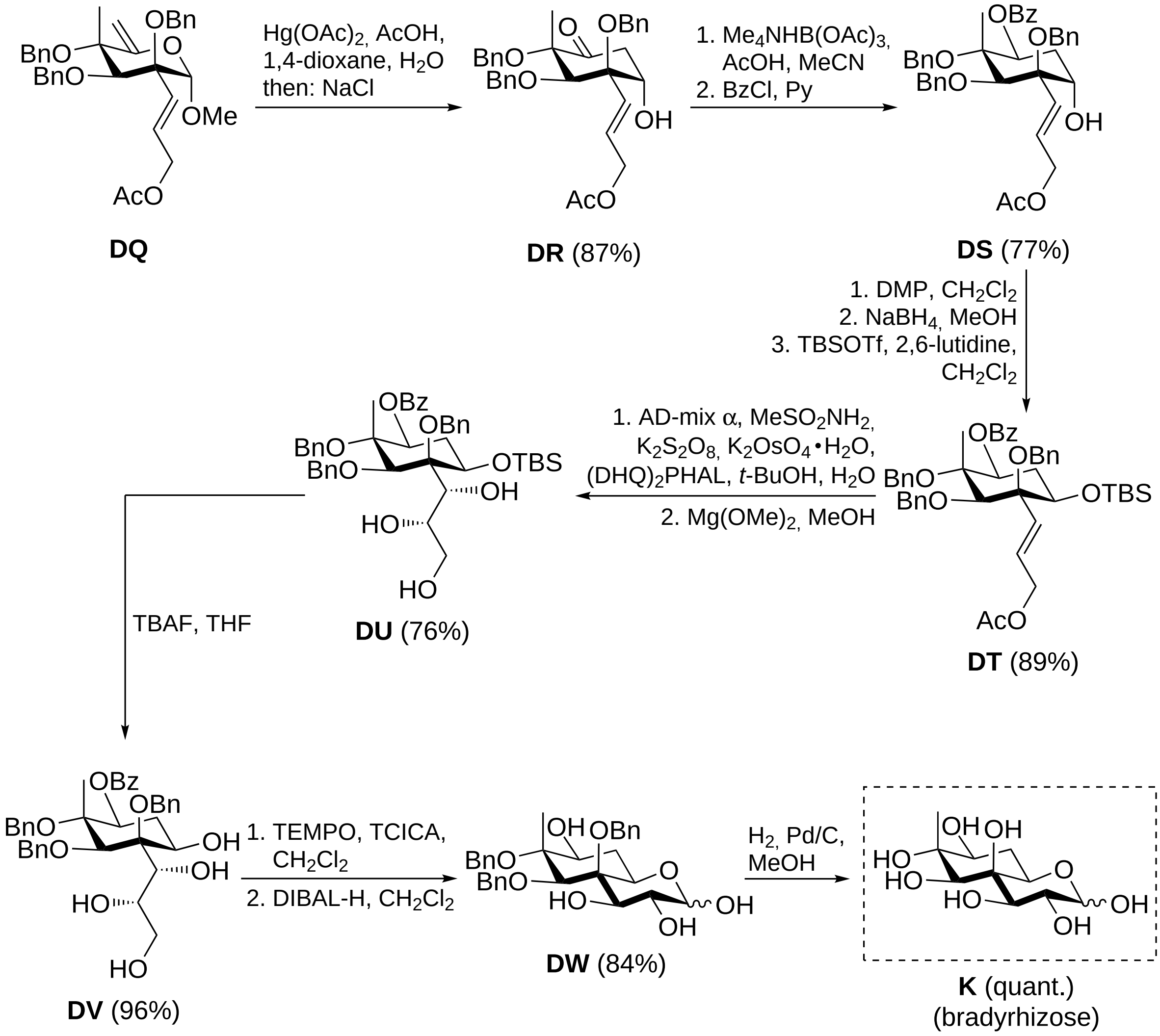
DQ
Hg(OAc)2, AcOH, 1,4-dioxane, H2O then: NaCl
DR (87%)
1. Me4NHB(OAc)3, AcOH, MeCN
2. BzCl, Py
DS (77%)
1. DMP, CH2Cl2
2. NaBH4, MeOH
3. TBSOTf, 2,6-lutidine, CH2Cl2
DT (89%)
1. AD-mix α, MeSO2NH2, K2S2O8, K2OsO4•H2O, (DHQ)2PHAL, t-BuOH, H2O
2. Mg(OMe)2, MeOH
DU (76%)
TBAF, THF
DV (96%)
1. TEMPO, TCICA, CH2Cl2
2. DIBAL-H, CH2Cl2
DW (84%)
H2, Pd/C, MeOH
K (quant.)
(bradyrhizose)

Scheme 4.10 Continued: Total synthesis of bradyrhizose **K** by Yu, Molinaro and Coworkers.[14] Completion of the synthesis.

In a recent publication in 2019, Lowary and Coworkers reported on a second synthetic approach to the bradyrhizose monosaccharide.[172] Based on a racemic synthesis and a late-stage resolution, both the natural D- and the L-enantiomer of **K** could be synthesized in 25 steps. The synthesis started from the known racemic orthoester **(±)-DX (Scheme 4.11)**, which was derived from *myo*-inositol (a *meso* compound). Swern oxidation gave a ketone, which displayed a high tendency for the formation of a hydrate upon purification. Therefore, the crude ketone was treated with MeMgBr to give the corresponding tertiary alcohol and, after benzylation, **(±)-DY** was obtained. Reductive opening of the orthoester with DIBAL-H, followed by the introduction of a tri-*iso*-propylsilyl (TIPS) protecting group provided intermediate **(±)-DZ**. A second DIBAL-H reduction of the benzylidene acetal resulted in the formation of two isomeric

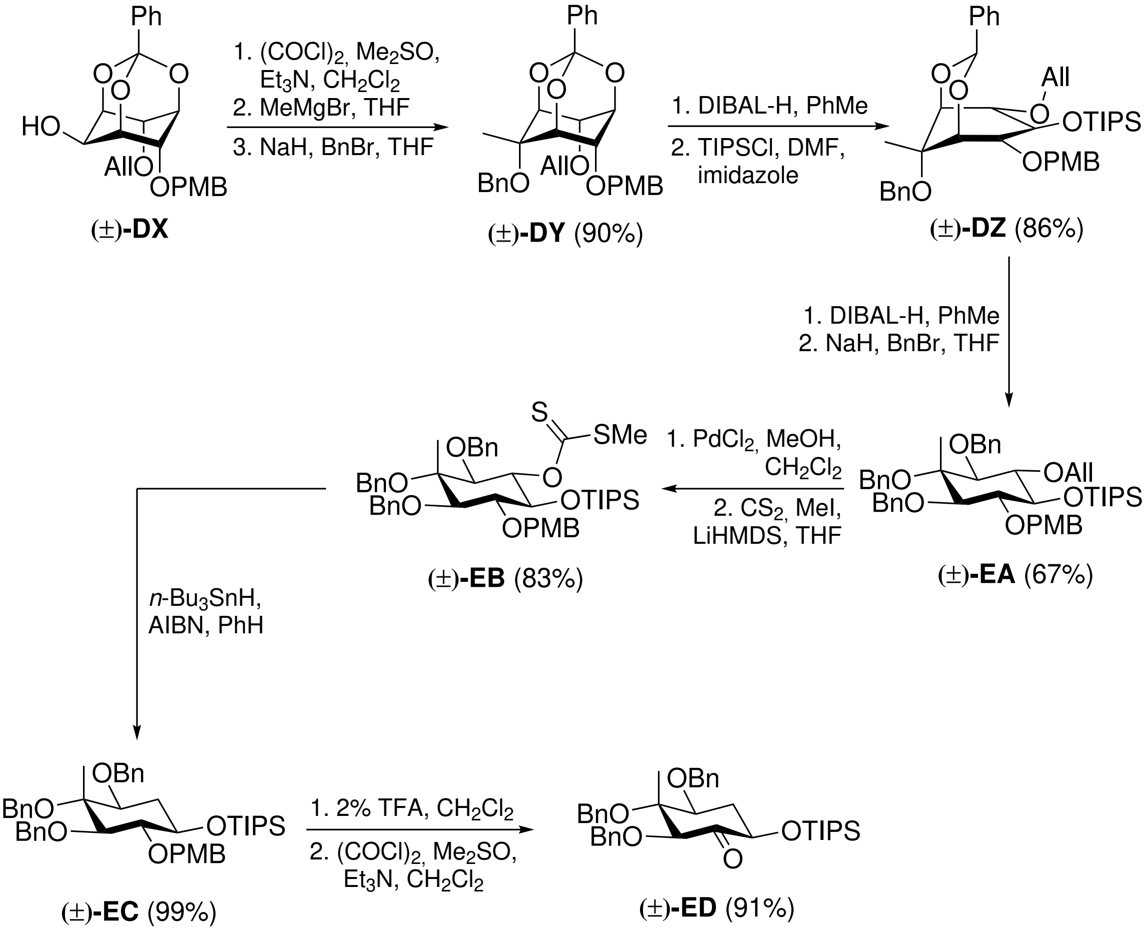
Ph
HO
AllO
OPMB
(±)-DX
1. (COCl)2, Me2SO, Et3N, CH2Cl2
2. MeMgBr, THF
3. NaH, BnBr, THF
BnO
(±)-DY (90%)
1. DIBAL-H, PhMe
2. TIPSCl, DMF, imidazole
All
OTIPS
(±)-DZ (86%)
1. DIBAL-H, PhMe
2. NaH, BnBr, THF
OBn
OAll
(±)-EA (67%)
1. PdCl2, MeOH, CH2Cl2
2. CS2, MeI, LiHMDS, THF
S
SMe
(±)-EB (83%)
n-Bu3SnH, AIBN, PhH
(±)-EC (99%)
1. 2% TFA, CH2Cl2
2. (COCl)2, Me2SO, Et3N, CH2Cl2
(±)-ED (91%)

Scheme 4.11 Total synthesis of bradyrhizose **K** by Lowary and Coworkers.[172] Synthesis of racemic intermediate **(±)-ED**. Only the D-enantiomers are shown.

alcohols as a mixture, which gave the single product **(±)-EA** upon benzylation. After Pd-catalyzed deallylation, the deprotected intermediate was reacted with CS_2/MeI in the presence of LiHMDS as a base, forming the xanthate **(±)-EB**. Next, Barton-McCombie deoxygenation gave **(±)-EC**, and upon acidic PMB-cleavage, followed by Swern oxidation, the key intermediate **(±)-ED** was obtained. The racemic synthesis continued **(Scheme 4.12)** with the addition of lithiated ethyl propiolate to the ketone functionality in **(±)-ED** with equatorial selectivity, giving alkynyl-branched inositol **(±)-EE**. Reduction to the (*E*)-alkene was successful with the Red-Al reagent, and desilylation gave **(±)-EF**. Direct dihydroxylation of **(±)-EF** under Sharpless AD conditions progressed reluctantly, and the corresponding spirolactone resulting from cleavage of the ethyl ester was isolated as a side product. Therefore, further protecting group transformations were required. Benzylation of the crowded tertiary alcohol in **(±)-EF** was not feasible, but a sequence of benzylidene acetal formation in the presence of camphorsulfonic acid (CSA), followed by regioselective reductive opening

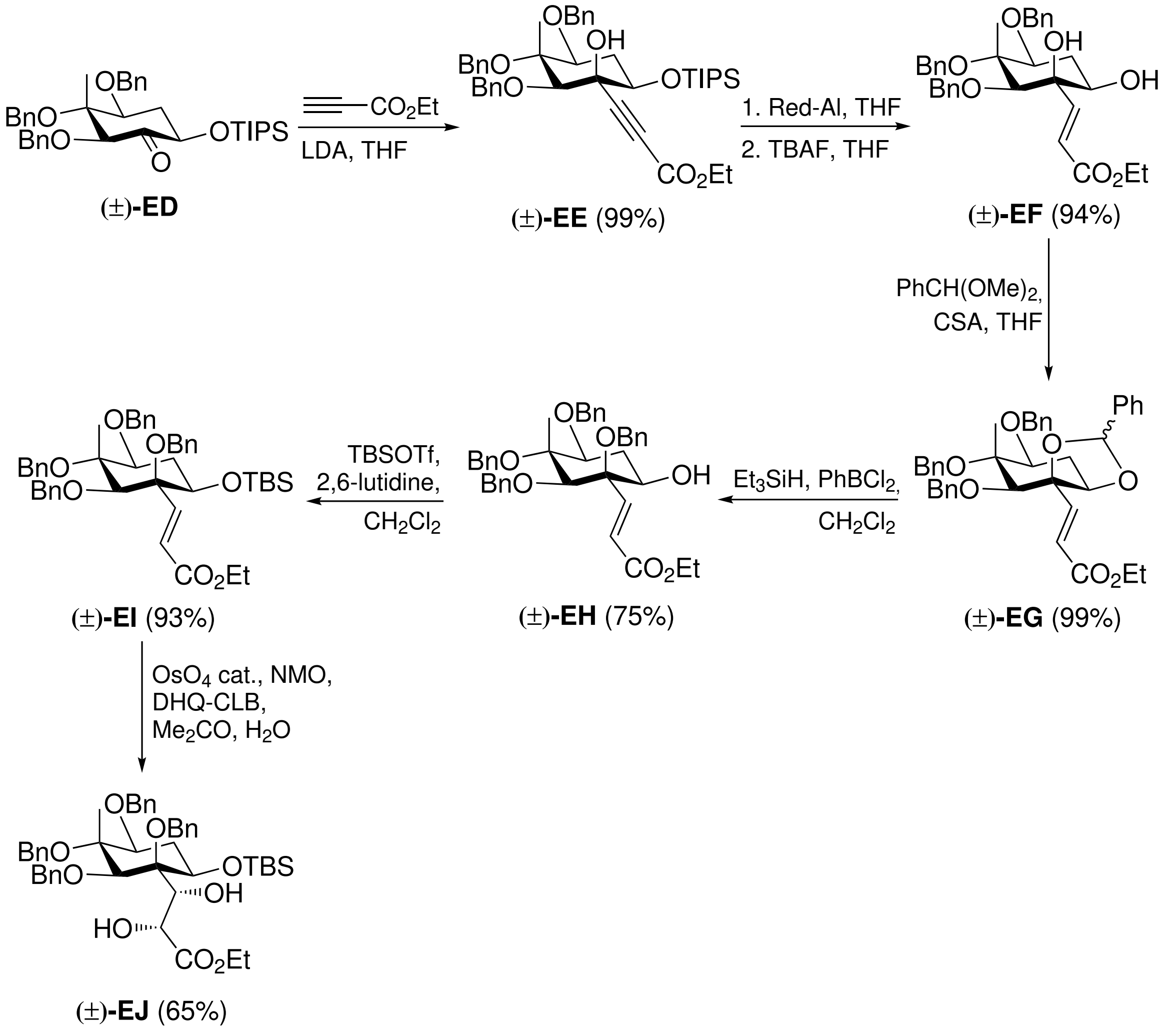
(±)-ED
CO2Et
LDA, THF
(±)-EE (99%)
1. Red-Al, THF
2. TBAF, THF
(±)-EF (94%)
PhCH(OMe)2,
CSA, THF
(±)-EG (99%)
Et3SiH, PhBCl2,
CH2Cl2
(±)-EH (75%)
TBSOTf,
2,6-lutidine,
CH2Cl2
(±)-EI (93%)
OsO4 cat., NMO,
DHQ-CLB,
Me2CO, H2O
(±)-EJ (65%)

Scheme 4.12 Continued: total synthesis of bradyrhizose **K** by Lowary and Coworkers.[172] Synthesis of racemic intermediate **(±)-EJ**. Only the D-enantiomers are shown.

with $Et_3SiH/PhBCl_2$ provided benzylated **(±)-EH**. Further protection of the secondary hydroxyl group was found to be necessary to obtain a suitable substrate for the subsequent dihydroxylation reaction, and therefore **(±)-EH** was converted into the silylated intermediate **(±)-EI**. The *syn*-dihydroxylation under conventional Sharpless AD conditions (K_2OsO_4 and the ligand $(DHQ)_2PHAL$) displayed only slow conversion, but an optimized procedure involving *O*-(4-chlorobenzoyl)hydroquinine (DHQ-CLB) as the ligand was capable of the transformation to the wanted side chain diol **(±)-EJ**. The resolution of this final racemic intermediate **(Scheme 4.13)** could be achieved by acylation with (*S*)-Mosher's acid [(*S*)-α-methoxy-α-(trifluoromethyl)phenylacetic acid, (*S*)-MTPA], which was found to react selectively with the L-enantiomer, giving acylated **L-EK** in 50% yield. Under these conditions, 36% of the corresponding D-enantiomer **D-EJ** could be reisolated. In the final stages of the synthesis of the natural D-enantiomer, unreacted **D-EJ** was desilylated with TBAF in the presence of NH_4F, giving a mixture of the desilylation product together with the lactone due to ester-cleavage. Reduction of this mixture with DIBAL-H provided **D-EL**, which was subjected to hydrogenolytic debenzylation to obtain the natural enantiomer D-bradyrhizose **D-K**. For the synthesis of the L-enantiomer, a deacylation step was required to remove the chiral auxiliary. However, common deacylation methods like NaOMe in MeOH were unsuccessful. Therefore, **L-EK** was treated with $LiBH_4$, which resulted in removal of the Mosher ester accompanied by complete reduction of the side chain to the primary alcohol. Subsequent desilylation provided the tetrol **L-EM**. Finally, comparable to the first total synthesis by Yu and Molinaro, selective primary alcohol oxidation was achieved with the combination TEMPO/TCICA to afford a mixture of the lactol and the lactone. DIBAL-H reduction of the mixture gave the lactol **L-EL**, and, after benzyl deprotection, L-bradyrhizose **L-K** was available. Following these syntheses of the D- and L-enantiomers of **K**, Lowary and Coworkers developed suitable derived glycosylation donor/acceptor partners to construct bradyrhizose disaccharides with variable stereochemical combinations (DD, DL, LD, LL, each in the form of the methyl glycoside) and with variable nature of the glycosidic linkage ($\alpha(1\rightarrow7)$, $\beta(1\rightarrow7)$, $\alpha(1\rightarrow8)$). When the thus obtained disaccharides were utilized in plant immunological tests with the model plant *Arabidopsis thaliana*, the majority of combinations were found to be immunologically silent, including the "natural" combination (DD, $\alpha(1\rightarrow7)$). However, some other combinations involving the L-enantiomer or other types of glycosidic linkages did result in the generation of an oxidative burst associated with a defensive immune response. These results seemed to be in agreement with the previously stated hypothesis, that the unusual structure of the bradyrhizose-containing O-antigens were evolutionarily acquired to be immunologically silent.

Based on these summarized interesting results regarding the chemical and biological properties of the natural bradyrhizose **K**, the synthesis of structurally comparable higher sugars was pursued in the context of this thesis. In this regard, the developed synthetic routes involve key transformations related to those in the summarized syntheses of natural **K**, for example represented by stereoselective dihydroxylations of alkenyl-branched intermediates, or by the selective primary alcohol oxidation. Following a successful synthesis of the desired analogs, a comparison of identified isomeric forms with those described for the complex isomeric mixture of bradyrhizose **K** was of special interest. The results obtained along these lines are given below.

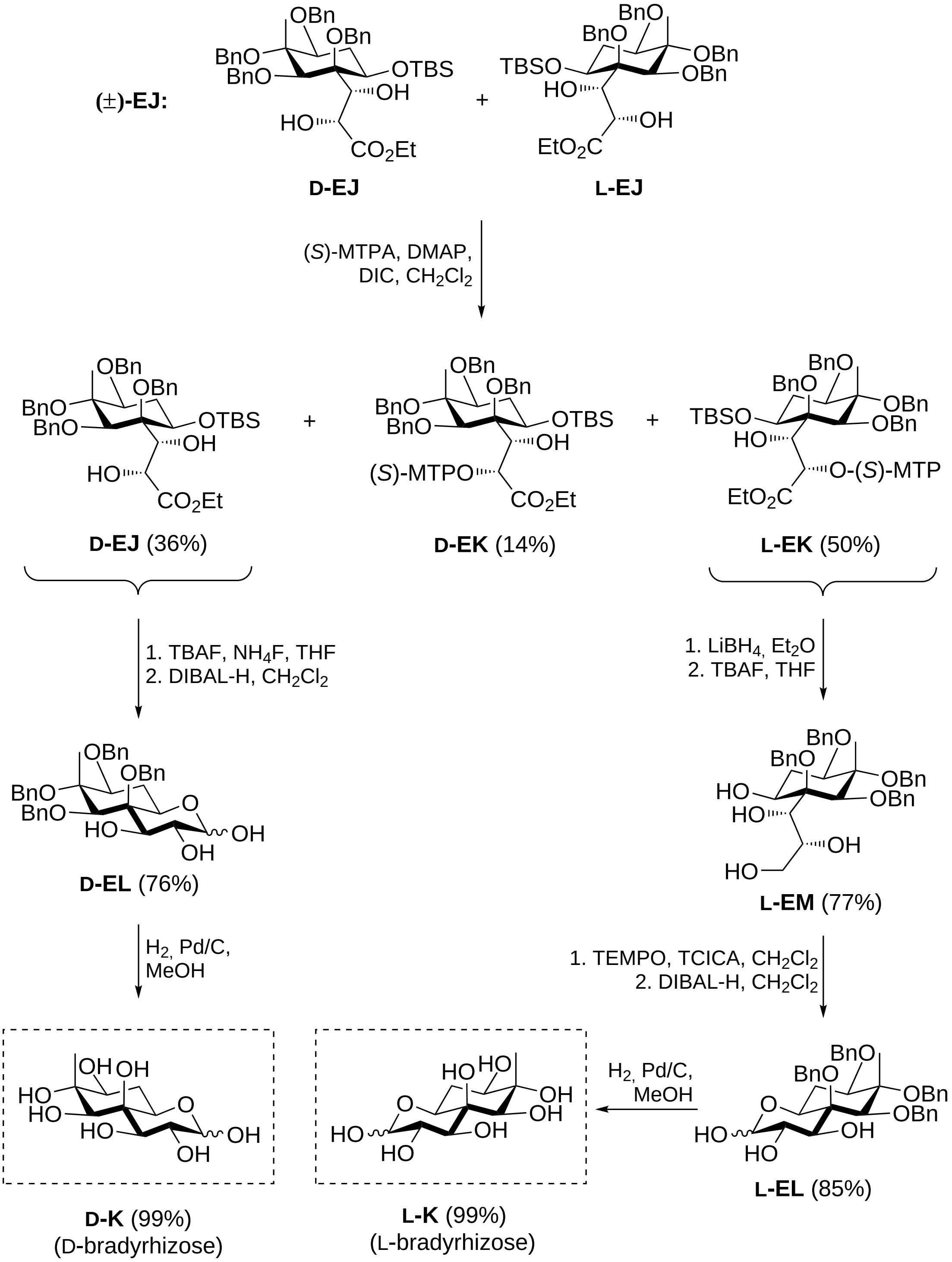
(±)-EJ:
D-EJ
L-EJ
(S)-MTPA, DMAP, DIC, CH2Cl2
D-EJ (36%)
D-EK (14%)
L-EK (50%)
1. TBAF, NH4F, THF
2. DIBAL-H, CH2Cl2
1. LiBH4, Et2O
2. TBAF, THF
D-EL (76%)
L-EM (77%)
H2, Pd/C, MeOH
1. TEMPO, TCICA, CH2Cl2
2. DIBAL-H, CH2Cl2
H2, Pd/C, MeOH
L-EL (85%)
D-K (99%)
(D-bradyrhizose)
L-K (99%)
(L-bradyrhizose)

Scheme 4.13 Continued: total synthesis of bradyrhizose **K** by Lowary and Coworkers.[172] Resolution of intermediate **(±)-EJ** and completion of the synthesis of enantiopure D-bradyrhizose **D-K** and L-bradyrhizose **L-K**.

4.4. Objective of this Chapter

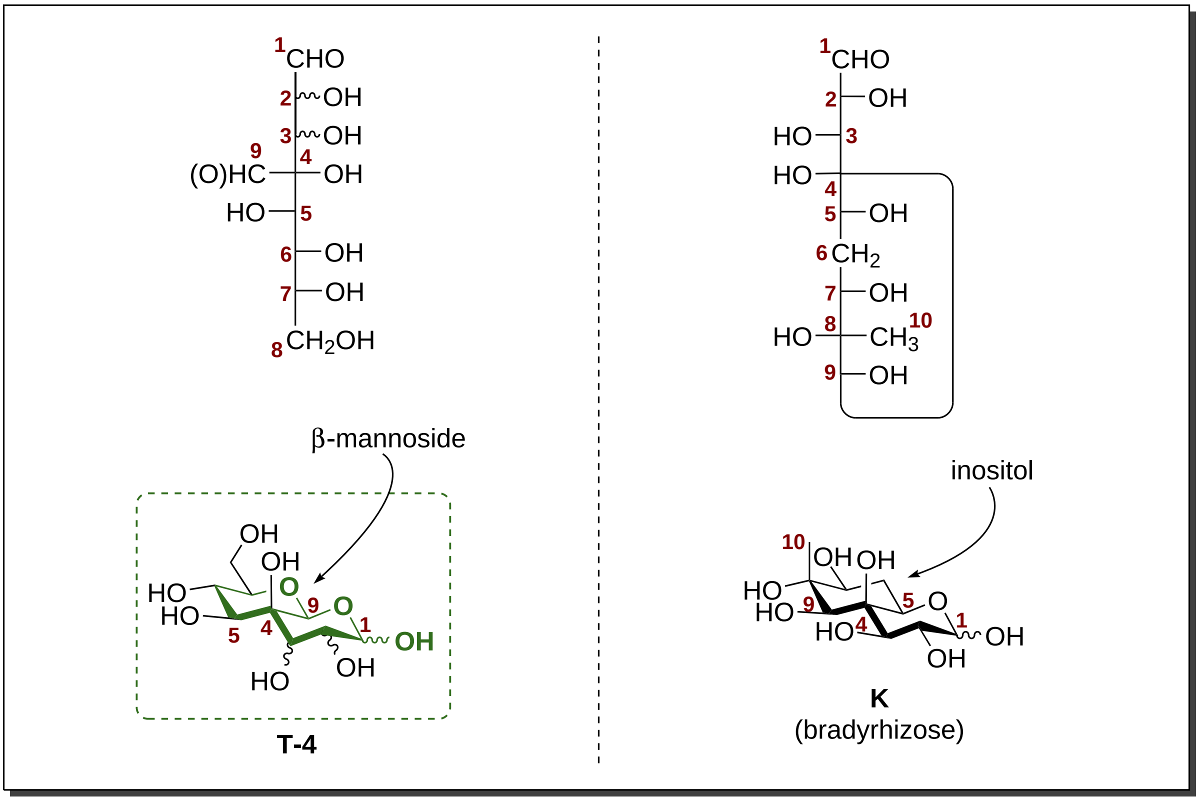

Scheme 4.14 Structural comparison of the major 1,5-pyranose isomer of natural monosaccharide bradyrhizose **K** with structurally related target compounds **T-4** of this chapter. For clarity, **T-4** is depicted in the (9*S*)-9,7-pyranose-1,9-pyranose isomeric form.

An interesting isomeric distribution of cyclic hemiacetal forms was characterized for the natural monosaccharide bradyrhizose **K** (**Scheme 4.8, (c)**, on page 70). Inspired by this, the following question was addressed: can generic target compounds of the general structure **T-4 (Scheme 4.14)** be obtained, in which the inositol moiety present in **K** is substituted for a conventional sugar with otherwise identical configurations of the hydroxylated stereogenic centers (a β-mannoside)? The open-chain forms of **T-4** can be regarded as 4-*C*-formyl-branched octoses, and thus, higher dialdoses. Therefore, as compared to carbocyclic monoaldehyde **K**, the presence of a second carbonyl functional group amenable to additional ring closures would potentially result in an increased number of cyclic hemiacetal isomers. As a consequence, it would be of interest to examine whether the intuitively anticipated (9*S*)-9,7-pyranose-1,9-pyranose isomeric forms **T-4** (the “bradyrhizose-type“ isomeric forms) can be identified to be the major isomers. Furthermore, a stereodivergent synthesis would allow for variable configurations of the

C-2/3 stereogenic centers. In this way, an influence of axial/equatorial substitution patterns within the annulated pyranose ring on the respective major cyclic hemiacetal forms could be examined. As a connection to the results described in **Chapter 3**, the anticipated “bradyrhizose-type“ isomeric forms of **T-4** are structurally related to the 1,2-annulated target compounds **T-3**. In this regard, target compounds **T-4** formally arise from oxidation of the proanomeric methylene group of the side chain in **T-3** to the reducing free hemiacetal. Since detailed structural studies on the non-reducing dioxadecalins **T-3** confirmed the *trans*-decalin geometry of the annulated framework, the respective reducing isomers of **T-4** could also be expected to exhibit a *trans*-decalin geometry with $^4C_1$ conformations of both pyranose moieties.

In earlier work in our group by M. Menzel, synthetic routes were explored towards the higher sugars of type **T-4**.[174] However, the structure of natural bradyrhizose **K** was not yet published at that time, and therefore these studies were motivated by a purely synthetic interest in the generic target compounds **T-4**, and when synthetic challenges were encountered, the project was abandoned.

In the course of this thesis, this project was reconsidered, and preliminary synthetic studies were performed on the synthetic approach that was initially proposed by Menzel and Ziegler.[174] According to this approach **(Scheme 4.15, a)**, benzyl β-2-uloside **2b** could be utilized as a substrate for the C-2-alkynylation with a metalated derivative of a suitably protected propiolaldehyde derivative, for example as its corresponding acetal. In this synthetic strategy, the required aldehyde oxidation state at the side chain C-9 (the later C-1 in **T-4**) would be installed in this early stage of the synthesis. Partial hydrogenation of the alkynylated intermediate, for example under Lindlar conditions, would give the acetal of a side chain (Z)-enal. Subsequently, *syn*- or *anti*-dihydroxylation could give the corresponding diol with variable stereochemistry and, after global deprotection and liberation of the side chain aldehyde, **T-4** could be obtained.

In a second approach explored in later synthetic studies **(Scheme 4.15, b)**, an analogous alkynylation of the 2-*keto* functionality could be conducted with unprotected propargyl alcohol, or with a protected propargyl alcohol derivative. In this way, either the free side chain propargyl alcohol derivative (R = H), or a derivative with a protecting group (R = Pg) orthogonally cleavable in the presence of the benzyl ether groups, would be accessible. Lindlar hydrogenation would give the side chain allyl alcohol derivative. Next, *syn*- or *anti*-dihydroxylation could be performed with either the protected (R = Pg) or the unprotected (R = H) allyl alcohol, giving the corresponding dihydroxylated intermediate with variable configurations of the C-7/8 diol stereogenic centers. In the key step, and comparable to the published syntheses of bradyrhizose

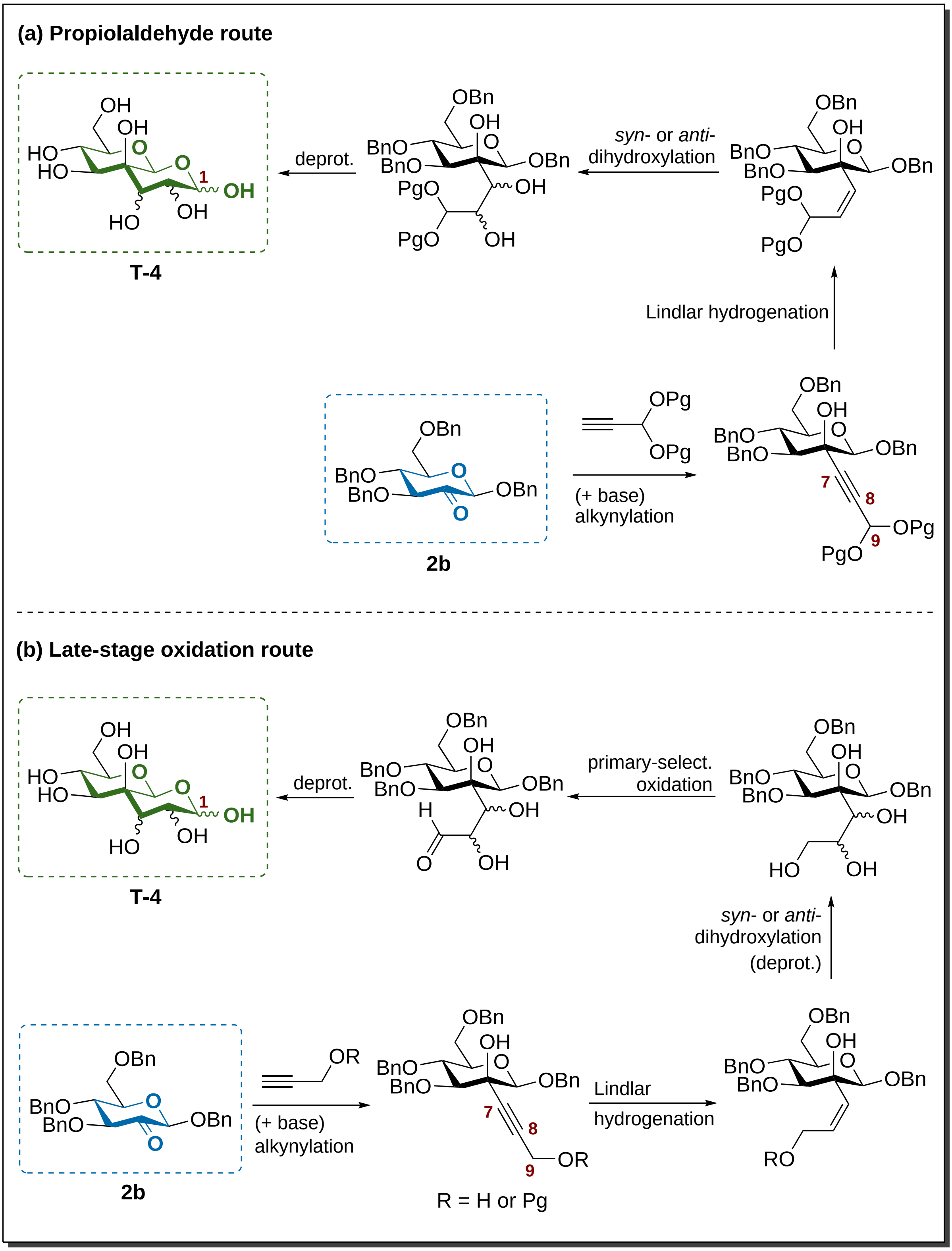
(a) Propiolaldehyde route
OH
OH
HO
HO
O
O
1
OH
HO
OH
T-4
deprot.
OBn
OH
BnO
BnO
O
OBn
PgO
OH
PgO
OH
syn- or anti-
dihydroxylation
OBn
OH
BnO
BnO
O
OBn
PgO
PgO
Lindlar hydrogenation
OBn
BnO
BnO
O
O
OBn
O
2b
OPg
OPg
(+ base)
alkynylation
OBn
OH
BnO
BnO
O
OBn
7
8
OPg
9
PgO
(b) Late-stage oxidation route
OH
OH
HO
HO
O
O
1
OH
HO
OH
T-4
deprot.
OBn
OH
BnO
BnO
O
OBn
H
OH
O
OH
primary-select.
oxidation
OBn
OH
BnO
BnO
O
OBn
OH
HO
OH
syn- or anti-
dihydroxylation
(deprot.)
OBn
BnO
BnO
O
OBn
O
2b
OR
(+ base)
alkynylation
OBn
OH
BnO
BnO
O
OBn
7
8
9
OR
R = H or Pg
Lindlar
hydrogenation
OBn
OH
BnO
BnO
O
OBn
RO

Scheme 4.15 Considered synthetic routes towards target compounds **T-4**. **(a)** Propiolaldehyde route **(b)** Late-stage oxidation route. For clarity, target compounds **T-4** are depicted in the (9S)-9,7-pyranose-1,9-pyranose isomeric form. Pg = protecting group.

K[14, 172], selective oxidation of the deprotected primary alcohol of the hydroxylated side chain could give the corresponding aldehyde. After global debenzylation of the parent pyranose moiety, target compounds **T-4** could be obtained. The results from following both the propiolaldehyde route as well as the late-stage oxidation route are reported below.

4.5. Results and Discussion

In a preceding analysis, the installation of the aldehyde oxidation state at the side chain *C*-9 *via* alkynylation with a propiolaldehyde acetal derivative **(Scheme 4.15, a)** was evaluated to be more promising. In contrast, the alternative selective oxidation step of the primary hydroxyl group **(Scheme 4.15, b)** could result in multiple competitive side reactions, and could thus be anticipated to be challenging. Consequently, initial synthetic efforts following the propiolaldehyde-route are described in **Section 4.5.1**.

4.5.1. Preliminary Synthetic Studies

According to the propiolaldehyde route proposed by Menzel and Ziegler[174], propiolaldehyde dibenzyl acetal[175] (Pg = Bn) would be a suitable C_3 building block for the alkynylation of the 2-*keto* functional group of 2-uloside **2b**. Specifically, the selection of the dibenzyl acetal would enable the cleavage of all protecting groups in one final deprotection step *via* hydrogenolytic debenzylation, and a second deprotection step to set free the side chain aldehyde could potentially be avoided. Following these lines of thought, propiolaldehyde dibenzyl acetal in THF was lithiated with *n*-BuLi at −80 °C, followed by the addition of 2-uloside **2b (Scheme 4.16)**. In this way, the novel 2-*C*-alkynyl mannoside **22** could be isolated in 85% yield. As observed for addition reactions to allyl 2-ulosides **1a** or **2a (Chapter 3)**, and in agreement with previous studies[101],

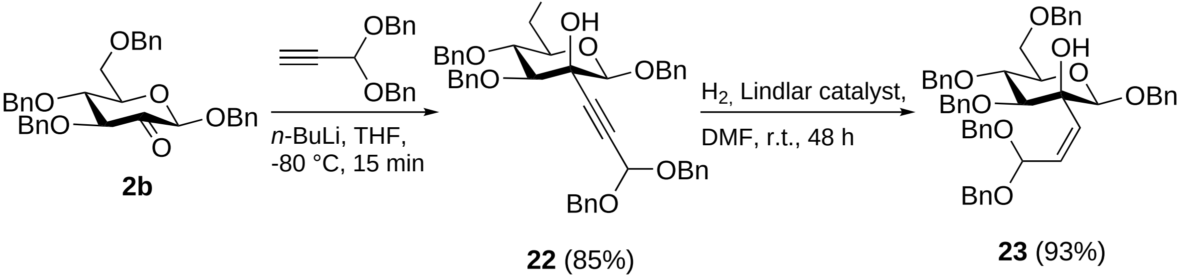

Scheme 4.16 Synthesis of 2-*C*-(*Z*)-alkenyl mannoside **23** *via* alkynylation and partial hydrogenation.

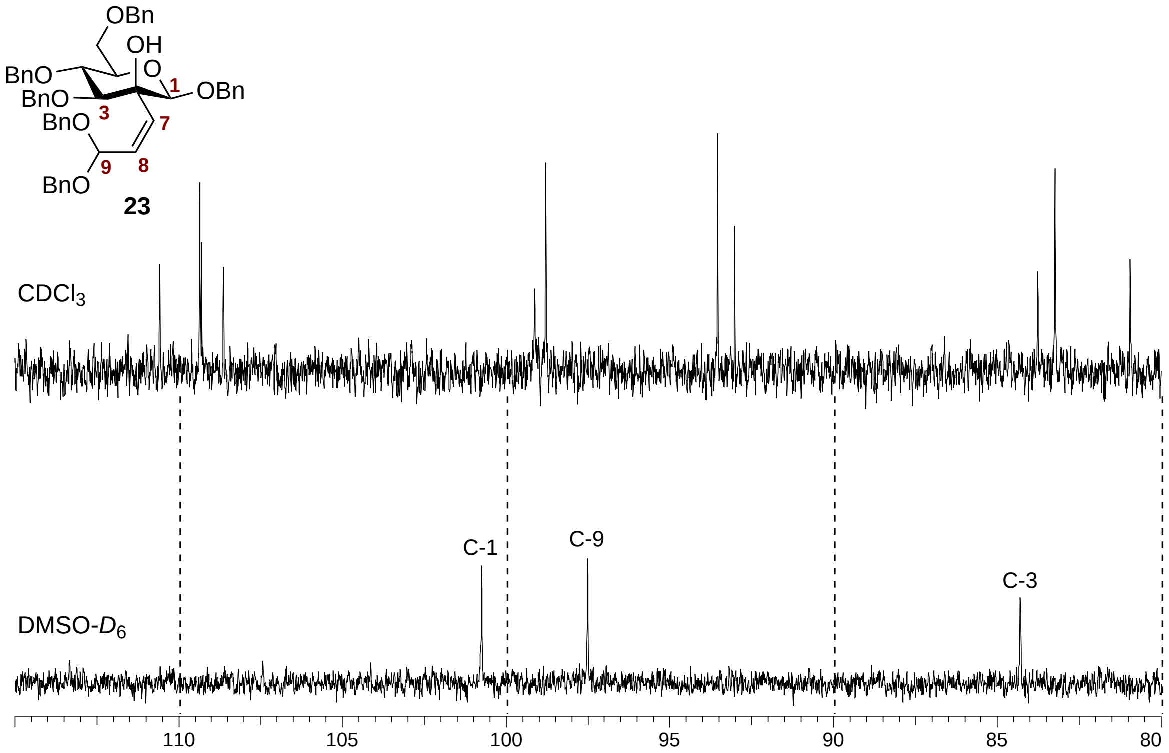

Figure 4.3 ^{13}C NMR spectra of **23** in CDCl$_3$ (top) and DMSO-D_6 (bottom) in the range 80–115 ppm. The shown spectra are unprocessed.

attack of the nucleophile proceeded solely *via* equatorial attack, giving the product with *manno*-configuration, and no diastereomeric side product could be detected. The subsequent partial hydrogenation of **22** employing Lindlar's catalyst[176], either in EtOAc or in MeOH with up to 30 wt% of the catalyst, proceeded very reluctantly, and only minor conversions of the starting alkyne were observable after several days. Switching the solvent to 1,4-dioxane had only a slightly accelerating effect on the rate of the partial hydrogenation. These observations could most probably be attributed to the sterical crowdedness around the alkyne functionality in **22** due to the substitution with the bulky dibenzyl acetal and the carbohydrate moiety. In addition, if still present in considerable amounts, the chromatographic separation of unreacted substrate **22** from alkene **23** was found to be challenging, and therefore a protocol resulting in complete conversion to **23** was desirable. Although the partial hydrogenation under Lindlar's conditions has been used frequently for the semihydrogenation of alkynes, often specific optimizations with respect to the individual substrate type are required, and solvent effects on the reaction are hard to assess.[160, 177–180] In the transformation of **22**, fortunately, a screening for suitable solvents revealed that DMF had a distinctly accelerating effect, and alkene **23** could be obtained in 93% yield after 2 days in

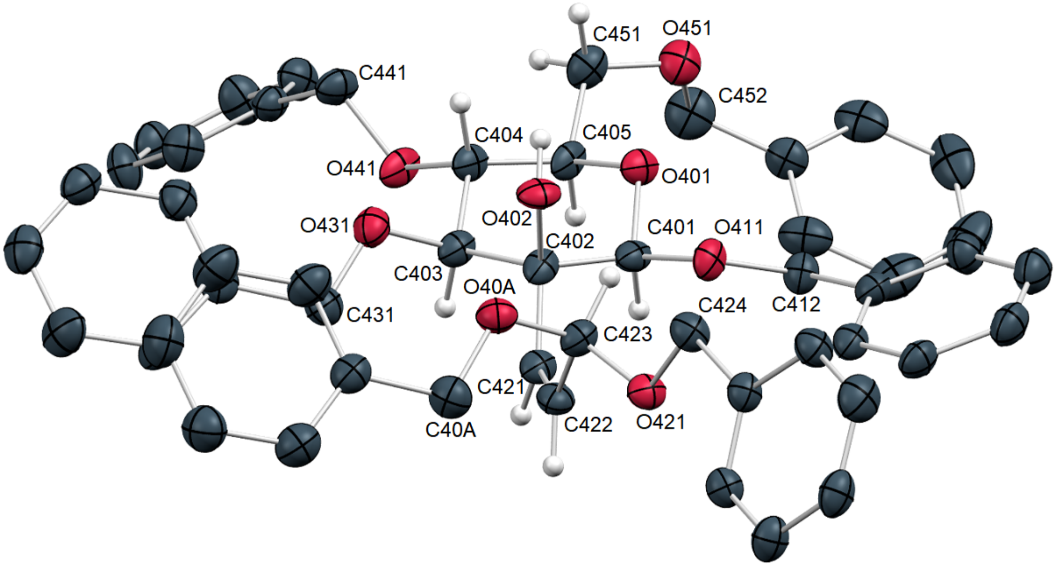

Figure 4.4 X-ray structure of (Z)-alkene **23**. One out of four molecules in the asymmetric unit is shown. Hydrogen atoms of the benzyl ethers are omitted for clarity. Ellipsoids are drawn at the 50% probability level. Red = oxygen, gray = carbon, white = hydrogen. Significant distances and torsion angles: C421-C422 1.325 Å, C402-C421-C422-C423 3.0°.

the presence of 50 wt% of the catalyst in DMF. The alkenyl-branched mannoside **23** exhibited remarkably complex ^{1}H and ^{13}C NMR spectra in $CDCl_3$ **(Fig. 4.3, top)**. A possible explanation could involve constrained rotation around the single bonds adjacent to the alkene moiety caused by the crowded substitution pattern, resulting in the observation of rotameric isomerism. When the same product sample was analyzed in DMSO-D_6 **(Fig. 4.3, bottom)**, simpler NMR spectra were obtained, and the structural characterization of **23** was feasible. The value of the vicinal alkene coupling constant ($J_{7,8} = 12.4$ Hz) was in a region rather suggestive for a Z-alkene, but also compatible with an E-alkene. Although usually low degrees of (E/Z)-isomerization are observed for Lindlar hydrogenations[177], an unambiguous characterization of the double bond (Z)-geometry in **23** was desirable. Apart from 2D NMR methods, single crystals of **23** suitable for X-ray structural analysis could be obtained from n-pentane/EtOAc. The molecular structure **(Fig. 4.4)** clearly confirmed the presence of a (Z)-alkene (C402-C421-C422-C423 3.0°) with a bond length as expected for an isolated double bond (C421-C422 1.325 Å). In the solid state, the benzyl residues of the sterically demanding dibenzyl acetal were found to be oriented towards each side of the side chain alkene functionality.

Table 4.1 Reaction screening on the *syn*-dihydroxylation of alkene **23**.

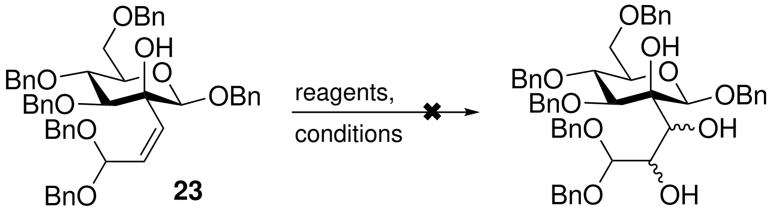

#	reagents	solvents	T, t	observation[a]
1	OsO_4 (4 to 100 mol%), NMO	Me_2CO, H_2O, *t*-BuOH	r.t. to 70 °C, 10 d	no react./ complex mixt.
2	AD-mix α, $MeSO_2NH_2$	H_2O, *t*-BuOH	r.t., 2 d, then: 40 °C, 1 h	decomp.[b]
3	AD-mix β, $MeSO_2NH_2$	H_2O, *t*-BuOH	r.t., 2 d then: 40 °C, 1 h	decomp.
4	OsO_4 (4 mol%), Me_3NO, pyridine	H_2O, *t*-BuOH	70 to 100 °C, 5 d	complex mixt.
5	OsO_4 (100 mol%), DMAP (2 equiv.)	H_2O, *t*-BuOH	r.t., 3 d, then: 40 °C, 24 h	no react.
6	$RuCl_3{\cdot}(H_2O)_3$ (7 mol%), $NaIO_4$	EtOAc, MeCN, H_2O	0 °C, 15 min, then: r.t.	complex mixt.

[a] Indicated by TLC analysis of the reaction mixture.

[b] ESI-MS of the crude decomposition product: $[M+Na]^+$ m/z 707 (proposed: debenzylation and dehydration).

To establish suitable methods for the subsequent side chain dihydroxylation of **23**, an initial screening involving common methods for the *syn*-dihydroxylation was performed **(Table 4.1)**. When **23** was subjected to classic Upjohn conditions[104] (entry 1) in the presence of NMO and catalytic amounts of OsO_4 at r.t., only traces of polar products could be identified *via* TLC. When up to 100 mol% of OsO_4 were added, and the temperature was elevated to 70 °C, the reaction mixture still contained major amounts of unreacted **23** after several days, together with a complex mixture of decomposition products. Next, the conditions of the Sharpless Asymmetric Dihydroxylation were explored (entries 2 and 3), and alkene **23** was treated with commercial AD-mix α or β in the presence of $MeSO_2NH_2$ according to the published protocol.[181] At r.t., the slow formation of a product with lower chromatographic mobility could be observed for both reactions. However, at this temperature, the reactions stopped after minor conversions. When higher temperatures (40 °C), and thus, unusual conditions for the Sharpless AD, were applied, one single product of high chromatographic mobility was formed in both transformations. Albeit, ESI-MS analysis of the crude product from the reaction with AD-mix α (entry 2) suggested decomposition of the substrate *via* a sequence of debenzylation and dehydration (m/z 707). Next, several methods with OsO_4 in combination with basic additives were tested. Typically, in this regard, pyridine is used as an additive, often in combination with Me_3NO as the secondary oxidant.[182, 183]. Application of this protocol to alkene **23** (entry 4) under forcing conditions (70 to 100 °C) resulted in complete conversion of the substrate, but a complex mixture of products with lower chromatographic mobility was formed. ESI-MS analysis suggested the presence of multiple decomposition products of lower molecular weight, and the desired diol product could not be identified. The complex of OsO_4 with two equivalents of DMAP has been described to be a powerful dihydroxylation reagent in stoichiometric reactions.[184] In the case of **23** (entry 5), these conditions could not affect the dihydroxylation of the substrate, even at elevated temperatures and prolonged reaction time (up to 40 °C, 4 d). Finally, a ruthenium-based method using catalytic $RuCl_3{\cdot}(H_2O)_3$ and stoichiometric $NaIO_4$ in biphasic EtOAc/MeCN/H_2O[185] (entry 6) resulted in no transformation at 0 °C, and in a complex mixture of decomposition products at r.t.

Since even drastic conditions (e.g. stoichiometric amounts of OsO_4 at 70 °C) could not affect the *syn*-dihydroxylation, **23** seemed to be an unsuitable substrate for the following steps of the synthesis. Most likely, the remarkably inert nature of the alkene functional group in **23** can be ascribed to the sterically crowded environment, caused by the dibenzyl acetal moiety and the benzyl groups at the carbohydrate positions 1 and 3. In addition, the axial hydroxyl group at the carbohydrate *C*-2 could possibly have an adverse effect on the accessibility of the alkene functionality. To study such influences of the substitution pattern around the side chain alkene, a series of routine protecting group manipulations was performed with alkyne **22 (Scheme 4.17)**. Acetylation of the tertiary axial *C*-2-OH required an excess of DMAP (2 equiv.)[186, 187] and forcing conditions (65 °C, 4 d) to give the propargyl acetate **24**, which was in turn transformed into (*Z*)-alkene **25** by applying the protocol for the Lindlar hydrogenation in DMF. Transformation of the dibenzyl acetal group in **22** into the dimethyl acetal **26** was achieved by iodine-catalyzed transacetalization[188] in methanol, and subsequent Lindlar hydrogenation gave dimethyl acetal **27** as a sterically less demanding substrate for dihydroxylation attempts. Similar iodine-catalyzed conditions with 1,3-dihydroxypropane were found to be unsuitable for the transacetalization of **22** into the 1,3-dioxane **28**, and only the corresponding free aldehyde could be detected. In contrast, classic Brønsted acid-catalyzed transacetalization conditions (1,3-dihydroxypropane, *p*-TsOH in toluene) gave **28** in good yield (84%). After Lindlar hydrogenation, **29** was available. Substitution of the acyclic dibenzyl acetal moiety for the cyclic dioxane

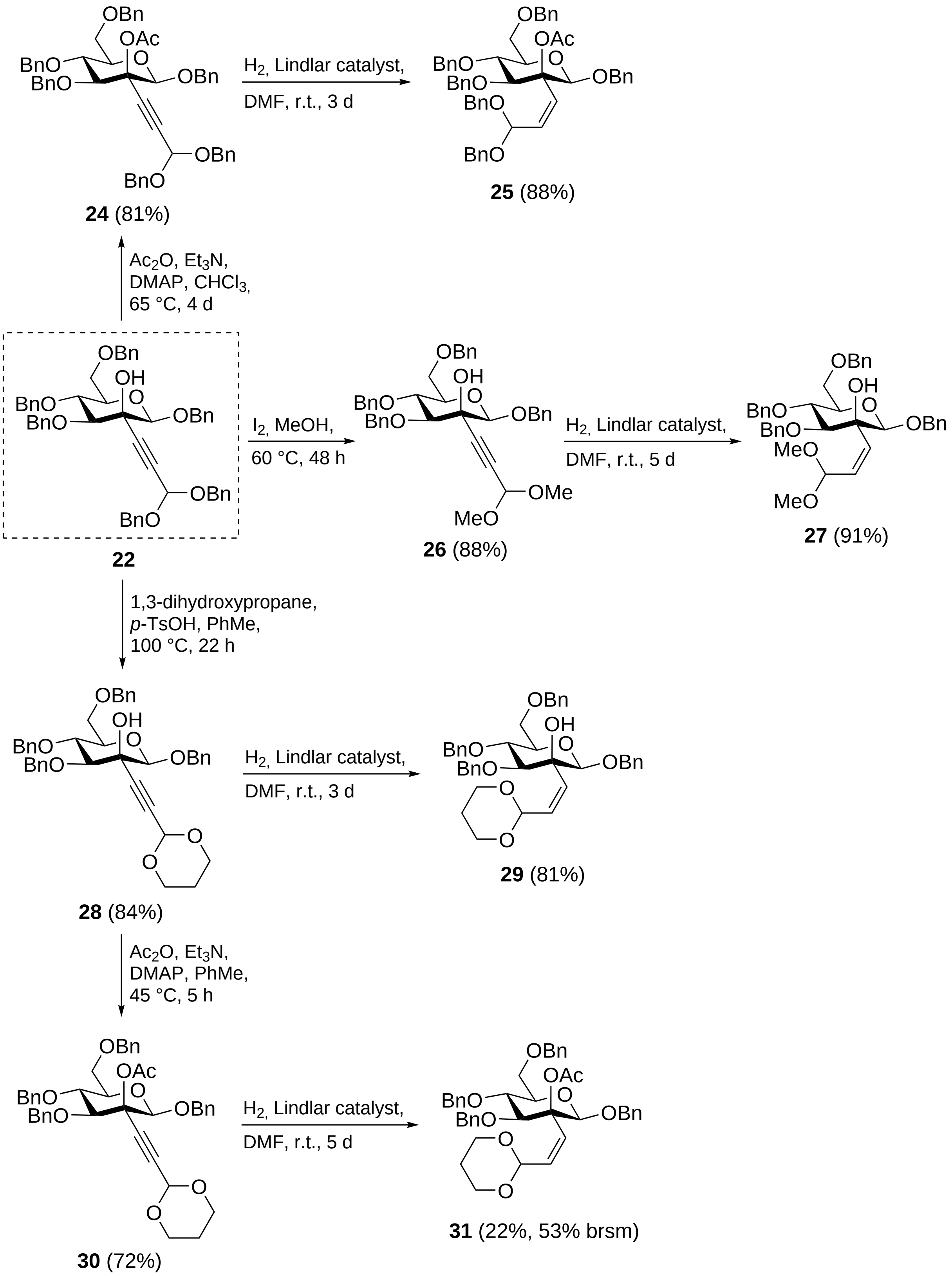
OBn
OAc
O
BnO
BnO
OBn
BnO
24 (81%)
H2, Lindlar catalyst,
DMF, r.t., 3 d
25 (88%)
Ac2O, Et3N,
DMAP, CHCl3,
65 °C, 4 d
OH
22
I2, MeOH,
60 °C, 48 h
MeO
OMe
26 (88%)
H2, Lindlar catalyst,
DMF, r.t., 5 d
27 (91%)
1,3-dihydroxypropane,
p-TsOH, PhMe,
100 °C, 22 h
28 (84%)
H2, Lindlar catalyst,
DMF, r.t., 3 d
29 (81%)
Ac2O, Et3N,
DMAP, PhMe,
45 °C, 5 h
30 (72%)
H2, Lindlar catalyst,
DMF, r.t., 5 d
31 (22%, 53% brsm)

Scheme 4.17 Protecting group diversifications of alkyne **22** and subsequent Lindlar hydrogenations, giving the corresponding (Z)-alkenes **25**, **27**, **29** and **31**. brsm = based on recovered starting material.

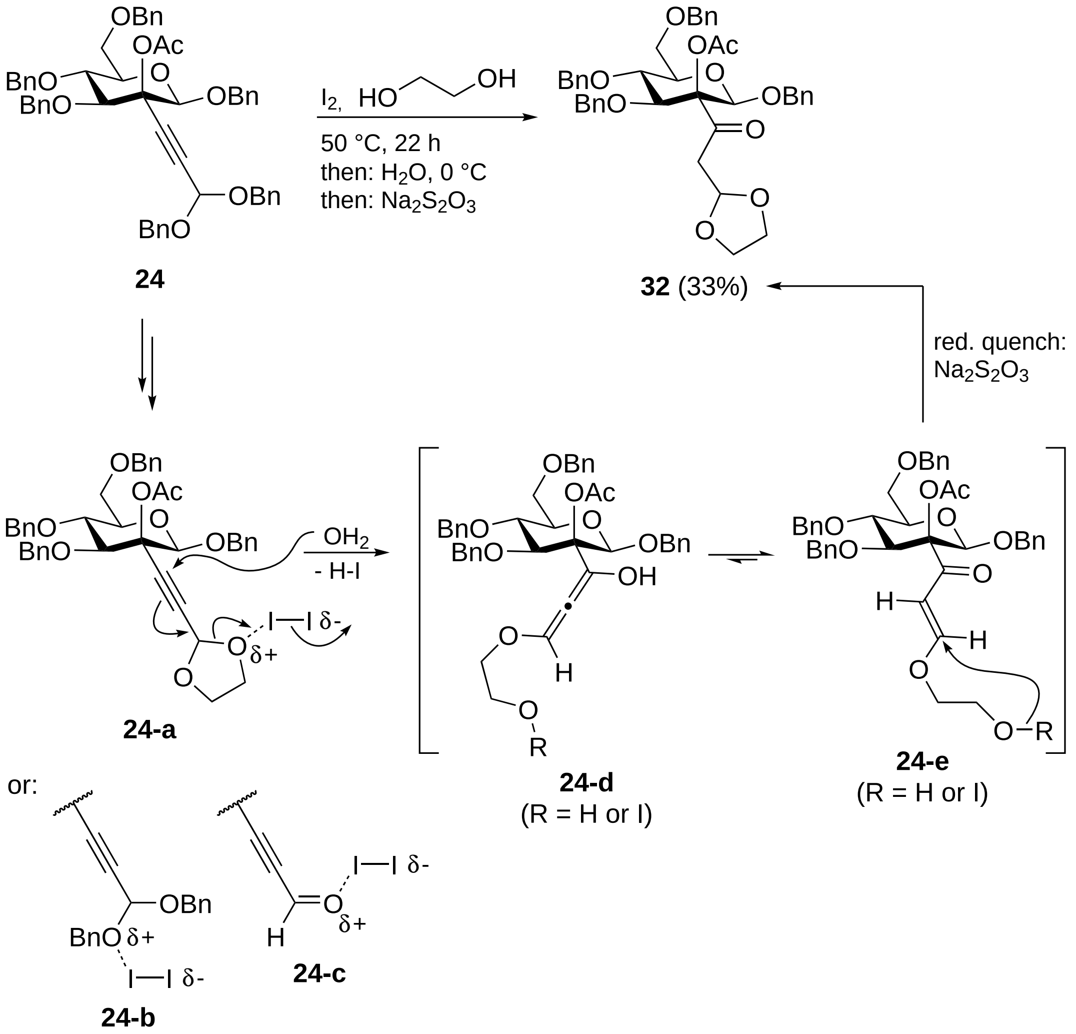

Scheme 4.18 Unwanted formation of ketone **32** from dibenzyl acetal **24** under iodine-catalyzed transacetalization conditions. A plausible mechanism is proposed.

protecting group in **29** was anticipated to result in a less conformationally flexible acetal group, and thus, easier access to the alkene functionality by the dihydroxylation reagent. Finally, acetylation of the tertiary *C*-2-OH in **28**, essentially as reported before, gave acetate **30** in 72% yield. The following partial hydrogenation proceeded, as opposed to the other hydrogenations, sluggishly, and gave under these unoptimized conditions **31** in a mediocre 22% yield, together with 59% of unreacted alkyne **30** (53% yield based on recovered substrate).

Several other protecting group transformations were explored, but remained unsuccessful. Among these, in an early attempt, acetylated dibenzyl acetal **24** was subjected to the conditions for iodine-catalyzed transacetalization in ethylene glycol for the anticipated introduction of a dioxolane protecting group **(Scheme 4.18)**. However, under these conditions, a complex reaction mixture was observed. After aqueous quenching and reductive workup of the reaction, *C*-7-ketone **32**, with a fully saturated side chain, could be isolated as one major product of the reaction (33% yield). The structure of **32** could be established from 2D NMR experiments, in combination with several characteristic properties of the ^{13}C NMR spectrum like a pronounced low-field shift of the quaternary carbohydrate *C*-2 (88.2 ppm), the absence of signals referring to the quaternary alkyne carbon atoms of the side chain, and a low-field signal (203.4 ppm) of a quaternary carbon indicative of the presence of a ketone. A plausible mechanistic explanation for the formation of **32** could involve iodine-activation of the wanted dioxolane in the form of **24-a** (or of another carbonyl derivative like dibenzyl acetal **24-b** or aldehyde **24-c**), followed by S_N2'-type hydration of the activated species and formation of a hydroxyallene, possibly in the form of a hypoiodite or the respective free alcohol (**24-d**). Given the fact that allenes are universally formed in reactions of propargyl systems under a variety of conditions, the formation of an allene intermediate is plausible.[189] Notably, since ice was added to the reaction mixture in the first step of the workup procedure, hydration after the transacetalization step (formation of **24-a**) seems to be likely. Tautomerization of the hydroxyallene would give the corresponding enone **24-e** which, upon reductively quenching with $Na_2S_2O_3$ in the second workup step, could undergo intramolecular conjugated addition and formation of the dioxolane. In a similar mechanism from **24-b** or **24-c**, external ethylene glycol could participate in the final conjugated addition step, followed by a cyclization step. Although **32** was isolated in only mediocre yield, the described reaction gives an impression of potential interesting side chain functionalizations starting from the *C*-2-branched propiolaldehyde derivatives.

Surprisingly, from the obtained (*Z*)-alkenes **25**, **27**, **29** and **31**, only the sterically least crowded dimethyl acetal **27** displayed complex NMR spectra in $CDCl_3$ similar to **23**. As opposed to **23**, however, in DMSO-D_6, rotameric isomerism was still observable for **27**, although to a lesser extent. In high-temperature NMR experiments (50 °C) in DMSO-D_6, severe decomposition of the dimethyl acetal was visible, and therefore the complete NMR-based structural elucidation of **27** was not feasible. In extended investigations on the side chain *syn*-dihydroxylation, the (*Z*)-alkenes **25**, **27** and **29** with an altered protecting group pattern were reacted under conditions similar to those applied to **23**. Since only insufficient amounts of pure material of **31** were available, no further transformations were explored with this substrate. The tested conditions for **25**, **27** and **29** involved both classic Upjohn dihydroxylation conditions (similar to entry 1, **Table 4.1** on page 85) as well as the combination Me_3NO/pyridine (similar to entry 4). However, in all reactions, none of the substrates reacted in a clean manner. Dimethyl acetal **27** was found to undergo rapid cleavage of the acetal group under all

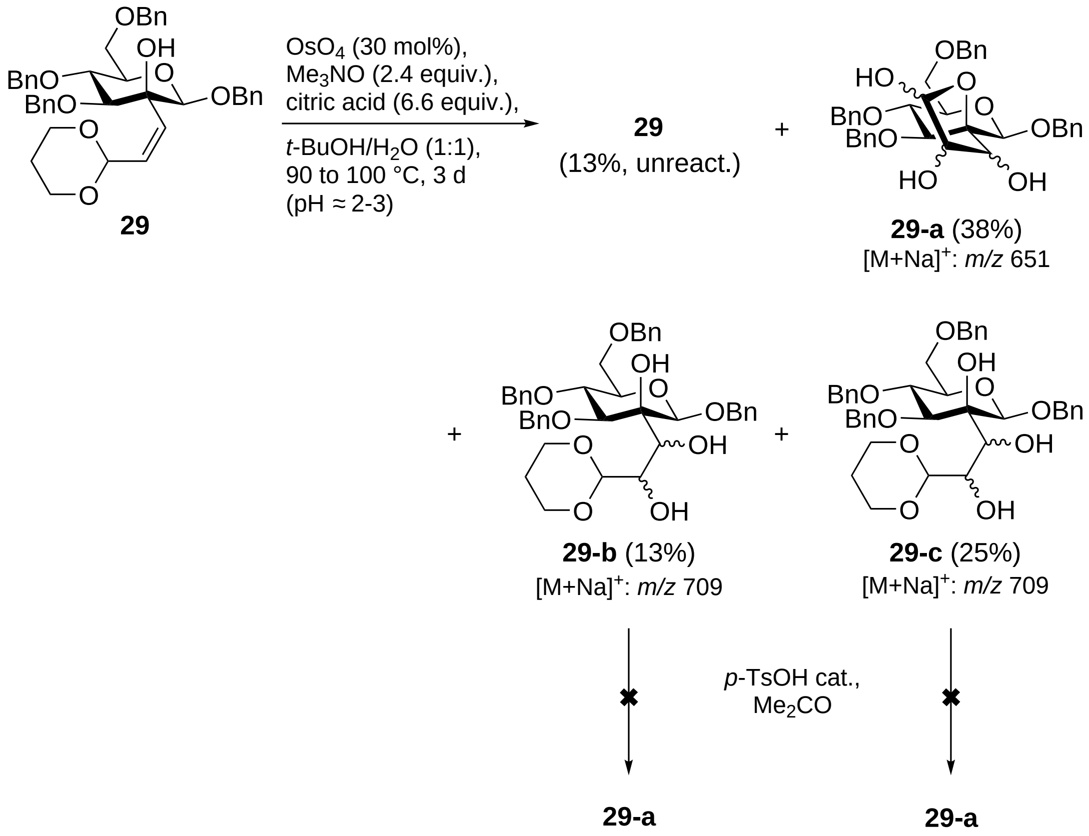
OsO4 (30 mol%), Me3NO (2.4 equiv.), citric acid (6.6 equiv.),
t-BuOH/H2O (1:1), 90 to 100 °C, 3 d (pH ≈ 2-3)
29
29 (13%, unreact.)
29-a (38%)
[M+Na]+: m/z 651
29-b (13%)
[M+Na]+: m/z 709
29-c (25%)
[M+Na]+: m/z 709
p-TsOH cat., Me2CO
29-a
29-a
OBn
OH
BnO
HO

Scheme 4.19 *syn*-Dihydroxylation of **29** in the presence of citric acid. The reaction was performed on a 30 mg scale. The given yields are isolated yields after chromatographic purification. Structures of products **29-a**, **29-b** and **29-c** are proposed structures, characterized only by ESI-MS analysis and ^{1}H NMR analysis (for **29-a**).

tested conditions, followed by decomposition reactions of the α,β-unsaturated aldehyde, resulting in complex mixtures. Substrates **25** and **29**, on the other hand, displayed similar behavior like the original substrate **23**, and required drastic conditions (similar to entries 1 and 4) to exhibit any transformation, resulting in mixtures of decomposition products.

In a final attempt, a reaction sequence of *syn*-dihydroxylation and acidic acetal cleavage was tested. Acidic additives like citric acid have been reported to be specifically beneficial for the *syn*-dihydroxylation of electron-deficient, otherwise challenging alkenes.[190] Application of these conditions to dioxane **29** was envisioned to result in the wanted dihydroxylation, followed by direct acid-catalyzed hydrolysis of the acetal and liberation of the aldehyde. Indeed, when **29** was reacted under standard dihydroxylation conditions in the presence of citric acid **(Scheme 4.19)**, at high temperatures (90 to 100 °C) the formation of three products with lower chromatographic mobility could be observed by TLC. Chromatographic purification of the crude product mixture provided, eluting in this is order, unreacted **29** (13%), followed by products **29-a** (38%), **29-b** (13%) and **29-c** (25%). ESI-MS analysis of **29-a** suggested cleavage of the dioxane and formation of the aldehyde. The ^{1}H NMR spectrum of **29-a**, although the purity of the sample did not allow for complete characterization, did not contain a deshielded signal significant for an aldehyde proton, and therefore lactol structure **29-a** could be proposed. Although the complete structure of the hemiacetal **29-a** could not be established, its proposed structure can be regarded as an interesting new class of spirofuranose-pyranose-hybrid molecules. In some structurally related intermediates *en route* to bradyrhizose **K**, the tendency to form comparable spirofuranose derivatives, e.g. as the derived lactones[172], has been described. Likewise, **K** itself was identified to form a minor 1,4-spirofuranose isomer with a related structure (**Scheme 4.8, (c)**, on page 70).[14] ESI-MS analyses of the isolated low-yield side products **29-b** and **29-c** suggested the formation of two diastereoisomers of the dihydroxylated product with intact dioxane group. From these isolated products, in preliminary studies **(Scheme 4.19)**, small-scale reactions for the dioxane cleavage in acetone in the presence of catalytic *p*-TsOH resulted in complex mixtures of products, and the clean formation of the free aldehyde, or of lactol **29-a**, could not be achieved. Most likely, under these conditions, the dioxane group is cleaved, however, the sensitive intermediate **29-a** undergoes subsequent acid-catalyzed decomposition reactions, for example debenzylation or dehydration reactions. Although the dihydroxylation of **29** in the presence of citric acid resulted in the promising formation of separable dihydroxylated products, several drawbacks were encountered. The reaction was run on a small scale (30 mg of **29**), but nevertheless a long reaction time at high temperatures (90 to 100 °C, 3 d) and large amounts (30 mol%) of OsO_4 were required to affect the major conversion of the substrate. In addition, the obtained dihydroxylated dioxanes **29-b** and **29-c** (proposed structures) could not be converted into the corresponding aldehyde, or into a spirofuranose comparable to **29-a**, without decomposition under acidic conditions.

For that reason, at this point, further investigations into the propiolaldehyde route were abandoned. The side chain dihydroxylation, which was found to be difficult with acetal substrates like **23**, was anticipated to be less challenging when performed with the corresponding allyl alcohol substrates as described in the late-stage oxidation route. Considering steric factors, the allyl alcohol intermediates traversed in this synthetic route should be more accessible for the dihydroxylation reagent than the corresponding unsaturated acetal intermediates. Furthermore, due to the absence of the inductively electron-withdrawing acetal group, the alkene functionality in the allyl alcohol intermediates would be expected to be a stronger nucleophile, and thus, more reactive in oxidation reactions.

4.5.2. Synthesis of the *syn*-Isomers

According to the suggested late-stage oxidation route (**Scheme 4.15, (b)**, on page 81) towards the target higher sugars **T-4**, alkynylation of the ketone **2b** with propargyl alcohol (R = H), or with a suitably protected derivative thereof (R = Pg), was expected to provide the alkynyl-branched mannosides in an addition reaction analogous to the synthesis of **22**. For the protected derivatives, the protecting group Pg was required to be orthogonally cleavable in the presence of the benzyl ether groups, since, after deprotection, the free primary alcohol should be transformed into the corresponding aldehyde in the pivotal primary-selective late-stage oxidation step. Furthermore, due to the highly basic conditions of the initial metalation/alkynylation sequence in the presence of organometallic bases like *n*-BuLi, only protecting groups with sufficient stability against base-induced cleavage would be adequate. As a suitable candidate, the tri-*iso*-propylsilyl (TIPS) protecting group was surmised to be sufficiently stable under highly basic conditions, and the selective fluoride-induced cleavage of the silylether could set free the primary alcohol at a later stage of the synthesis in a highly orthogonal manner. As a second option, the tetrahydro-2*H*-pyran-2-yl (THP) protecting group, an acetal protecting group highly stable under basic conditions, would allow for the selective hydrolytic cleavage of the acetal group under mildly acidic conditions that were expected to be compatible with the benzyl protecting groups.

Thus, in order to examine these protecting groups for their suitability in the required transformations, 2-uloside **2b**[37] was subjected to alkynylation reactions with a set of alkynes, including unprotected propargyl alcohol, TIPS-protected propargyl alcohol, and THP-protected propargyl alcohol **(Scheme 4.20)**. The addition of free propargyl alcohol could be achieved by employing a protocol published by Liang and Coworkers for the reaction of propargyl alcohols with simpler non-carbohydrate carbonyl substrates.[191] Ethylmagnesium bromide (2 equiv. based on propargyl alcohol) was used to form the corresponding propargyl alcohol-derived dianion equivalent at reflux temperature in THF, and the obtained solution was reacted with 2-uloside **2b** at ambient temperature to give propargyl alcohol derivative **33** in 63% yield in a rather unclean reaction. An analysis of the chromatographically isolated products of this reaction revealed the presence of unreacted 2-uloside **2b** (27%). Furthermore, the unwanted *gluco*-isomer **39** (5%) and the 3,2-enolone **40** (5%), originating from elimination of the 4-benzyloxy group, were obtained under these conditions **(Scheme 4.21, a)**. Interme-

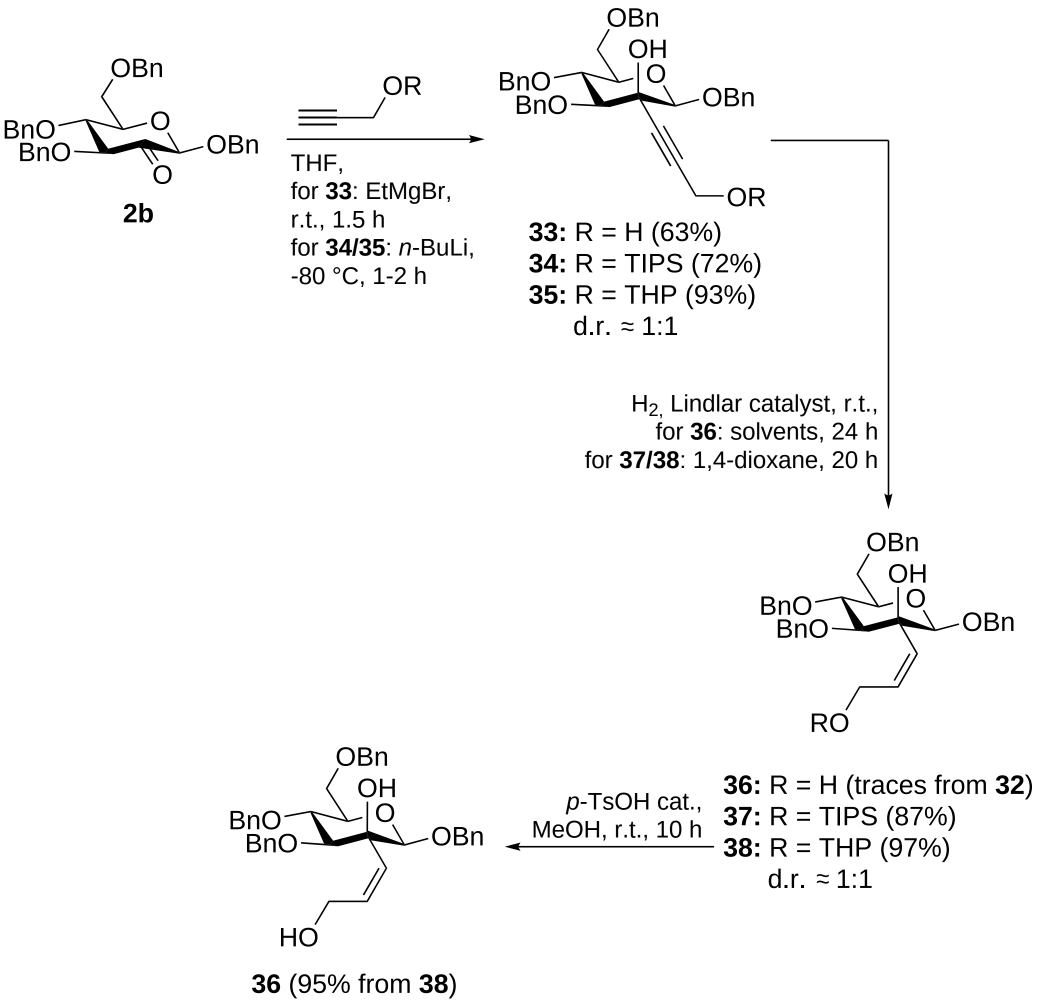
2b
OR
THF,
for 33: EtMgBr,
r.t., 1.5 h
for 34/35: n-BuLi,
-80 °C, 1-2 h
33: R = H (63%)
34: R = TIPS (72%)
35: R = THP (93%)
d.r. ≈ 1:1
H2, Lindlar catalyst, r.t.,
for 36: solvents, 24 h
for 37/38: 1,4-dioxane, 20 h
36: R = H (traces from 32)
37: R = TIPS (87%)
38: R = THP (97%)
d.r. ≈ 1:1
p-TsOH cat.,
MeOH, r.t., 10 h
36 (95% from 38)

Scheme 4.20 Synthesis of propargyl alcohol derivatives **33**–**35** and Lindlar hydrogenations, giving the derived allyl alcohol derivatives **36**–**38**.

diate **33** was, in addition, available from propiolaldehyde acetal **22**, which could be subjected to hydrolysis of the acetal group to obtain a crude mixture **(Scheme 4.21, b)**. Treatment of the crude hydrolysis product with $NaBH_4$ gave propargyl alcohol **33** in a 54% two-step yield. The corresponding protected derivatives **34** and **35** could be synthesized by utilizing the protocol described for the formation of **22**, which involved lithiation of the protected propargyl alcohol with *n*-BuLi, followed by the reaction with 2-uloside **2b** at −80 °C **(Scheme 4.20)**. In this way, TIPS-protected **34** was obtained in 72% yield, and THP-protected **35** in an excellent 93% yield. Due to the introduced stereogenic center at the THP protecting group, **35** was isolated as a 1:1 mixture of diastereoisomers. This can be regarded as a somewhat inconvenient feature of the THP protecting group, since the obtained protected products display highly complex NMR spectra. The subsequent partial hydrogenation of the alkyne proceeded only very

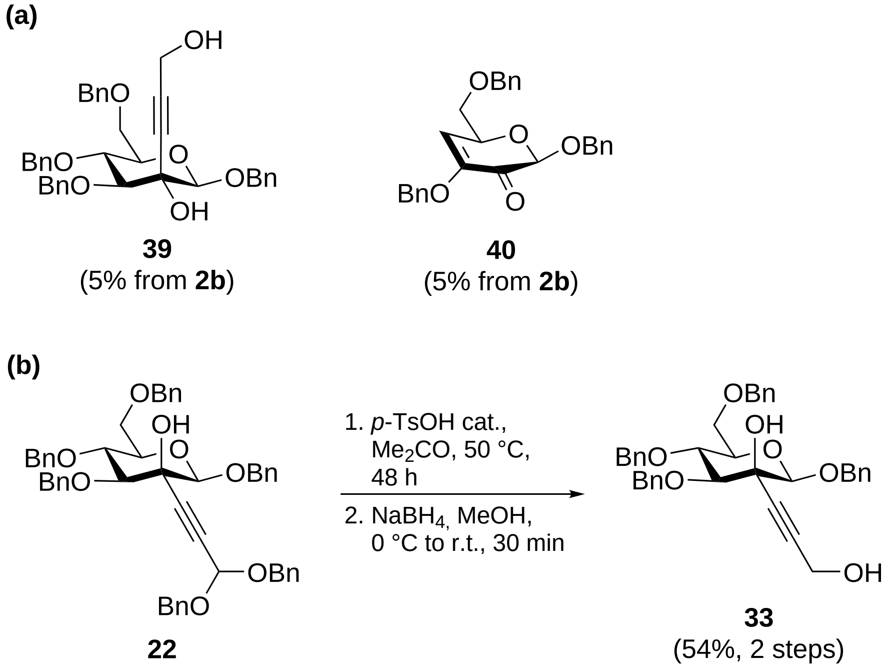

Scheme 4.21 **(a)** Side products **39** and **40**, as isolated in the formation of **33** from **2b**. **(b)** Synthesis of propargyl alcohol derivative **33** *via* acetal hydrolysis of **22**, followed by reduction of the intermediary propiolaldehyde.

reluctantly in the case of free propargyl alcohol **33**. The tested conditions involved different solvents (1,4-dioxane, acetonitrile, DMF or methanol), but only trace amounts of the wanted (Z)-alkene **36** could be isolated. In line with this, Lindlar hydrogenations of other free propargyl alcohol derivatives have been found to be erratic.[192] The Lindlar hydrogenations of the protected derivatives, however, proceeded smoothly in 1,4-dioxane, and gave TIPS-protected **37** (87%) or THP-protected **38** (97%) in good yields. According to the planned synthetic route, the dihydroxylation of the alkene functional group could be performed with the protected allyl alcohols **37** or **38**, followed by deprotection of the primary alcohol. However, bulky protecting groups could be expected to hamper access to the alkene functionality in the dihydroxylation step. Likewise, for a branched (E)-allyl alcohol *en route* to bradyrhizose **K**, Yu and Molinaro observed that a bulky TBDPS-protecting group had a retarding effect on the planned dihydroxylation.[14] Accordingly, deprotected allyl alcohol **36** was anticipated to be a more suitable substrate for alkene functionalizations. For that reason, since the synthetic route involving the THP-protected intermediates was evaluated as the most favorable, **38** was subjected to hydrolytic cleavage of the THP group, thus giving **36** in good yield (95%). In this way, key intermediate **36** could be routinely obtained on a 5 g scale and in a 86% three-step yield from 2-uloside **2b**. Given the fact that allyl alcohol

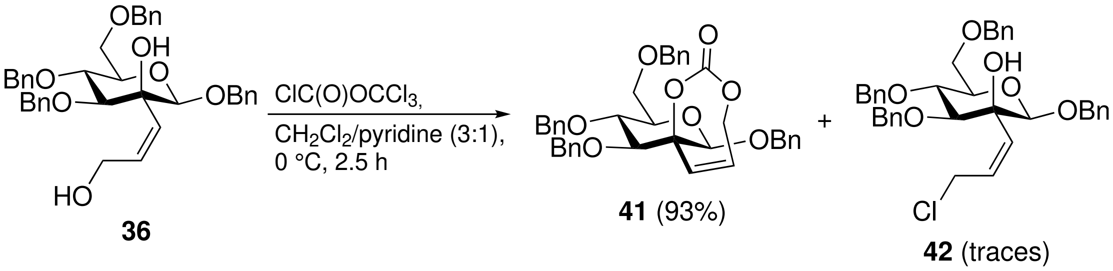
OBn
OH
O
BnO
BnO
OBn
HO
36
ClC(O)OCCl3,
CH2Cl2/pyridine (3:1),
0 °C, 2.5 h
O
OBn
O
O
O
BnO
BnO
OBn
41 (93%)
+
OBn
OH
O
BnO
BnO
OBn
Cl
42 (traces)

Scheme 4.22 Formation of spirocarbonate **41** from **36**, and allyl chloride **42**, identified as a low yield side-product.

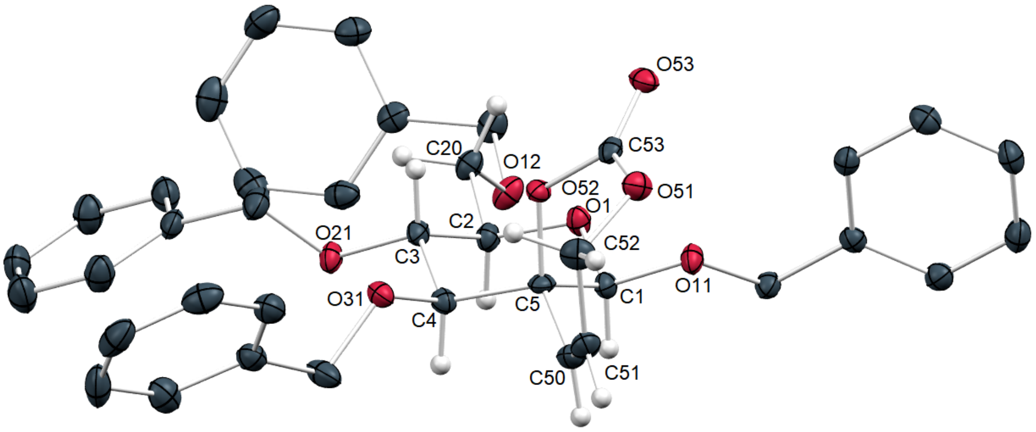
O53
C53
C20
O12
O52
O51
O1
C2
O21
C3
C52
O11
O31
C5
C1
C4
C50
C51

Figure 4.5 X-ray structure of spirocarbonate **41**. Hydrogen atoms of the benzyl ethers are omitted for clarity. Ellipsoids are drawn at the 50% probability level. Red = oxygen, gray = carbon, white = hydrogen. Significant distances and torsion angles: C53···O11 2.753 Å, O52-C5-C50-C51 6.9°, C50-C51-C52-O52 −55.5°.

derivatives are universally utilized intermediates for a large number of established alkene functionalization reactions, intermediate **36** with its 1,4-dihydroxyalk-2-ene pattern seemed to be an interesting substrate for the generation of carbohydrate structural diversity in general.

For synthetic purposes, some derivatizations of intermediate **36** were performed. One explored strategy involved protection of the 1,4-diol present in **36** with a suitable diol protecting group, resulting in the formation of a fully protected spirocyclic product. In such a protected derivative, due to the rigid fixation of the side chain within the spirocyclic arrangement, the alkene functionality could potentially be more easily approachable in a subsequent dihydroxylation step. In this context, protection of **36** in the form of a cyclic carbonate seemed to be an appropriate option, and this approach was initially explored in a Bachelor thesis by C. Jeuck.[193] When diol **36** was reacted with diphosgene (trichloromethyl chloroformate) in CH_2Cl_2 in the presence of pyridine **(Scheme 4.22)**, spirocarbonate **41** was formed in a clean reaction (93% yield), and only traces of a side product could be identified by TLC. When a similar reaction was conducted in pyridine as the sole solvent, comparable amounts of **41** were obtained, and the same side product could be isolated in low yield (2%). From this isolated material, its structure could be established to be allyl chloride **42**, most probably originating from direct conversion of the primary alcohol in **36** to the respective primary chloride by the action of diphosgene. The spirocarbonate **41** was obtained in the form of a crystalline solid, and single crystals could be obtained from *n*-pentane/acetone-D_6. X-ray structural analysis provided insight into the molecular structure **(Fig. 4.5)** of the interesting spirocyclic branched sugar, which was found to crystallize in the monoclinic space group $P2_1$ with $Z = 2$. Within the 1,3-dioxepin-2-one moiety involving the introduced carbonate, an almost planar orientation of the carbohydrate *O*-2 and *C*-2, the olefinic carbon atoms *C*-7 and *C*-8, and the *C*-9 methylene carbon (O52, C5, C50, C51, C52 in the crystal structure numbering) is observable. Accordingly, a small torsion angle around the *C*-2–*C*-7 bond can be observed (O52-C5-C50-C51 6.9°). The carbonate functional group adopts an orientation towards the anomeric oxygen (C53···O11 2.753 Å), with the carbonate carbon atom (C53) and one carbonate oxygen atom (O51) outside of the five-membered planar arrangement. A torsion angle approximate to gauche conformation of the atoms involving the former side chain allyl alcohol (C50-C51-C52-O52 −55.5°) demonstrates this sidewards orientation of the carbonate moiety.

The development of a synthetic route towards allyl alcohol **36** allowed for subsequent investigations into the continuation of the synthesis. In the following steps, *syn*-dihydroxylation of the alkene functionality in **36** was anticipated to install a 2,3-*syn*-diol side chain, whereas *anti*-dihydroxylation (e.g. a series of epoxidation and epoxide opening) could lead to target compounds **T-4** with a 2,3-*anti*-diol moiety as present in bradyrhizose **K**.

Along these lines, an examination of suitable conditions for the *syn*-dihydroxylation of **36** was performed **(Table 4.2)**. Furthermore, the spirocyclic carbonate **41** was included in these investigations to explore its synthetic applicability. When (*Z*)-alkene **36** was subjected to standard Upjohn conditions[104] (entry 1), no transformation could be observed over several days at elevated temperature (60 °C). Likewise, protocols involving basic additives like pyridine[115] (entry 2), methods that were suitable for the dihydroxylation of bicyclic intermediate **17** (**Scheme 3.11** on page 46), did not affect the dihydroxylation. The application of Sharpless AD conditions[181] (commercial AD-mix α or β, $MeSO_2NH_2$) to substrate **36** (entries 3 and 4) did, in both cases,

Table 4.2 Reaction screening on the *syn*-dihydroxylation of alkenes **36** and **41**.

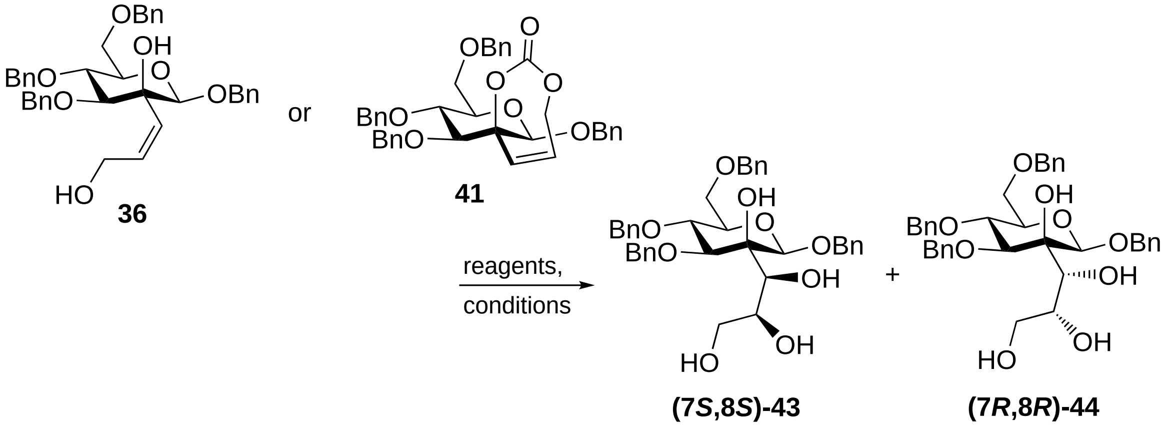

#	substr.	reagents	solvents	T, t	observation,[a] yield[b] (**43**+**44**), d.r.[c] (**43**/**44**)
1	**36**	OsO_4 (5 mol%), NMO	THF, H_2O, *t*-BuOH	r.t. to 60 °C, 8 d	no react.
2	**36**	OsO_4 (5 mol%), Me_3NO, pyridine (2 equiv.)	THF, H_2O, *t*-BuOH	r.t. to 60 °C, 8 d	no react.
3	**36**	AD-mix α, $MeSO_2NH_2$	H_2O, *t*-BuOH	0 °C to r.t., 3 d	no react.
4	**36**	AD-mix β, $MeSO_2NH_2$	H_2O, *t*-BuOH	0 °C to r.t., 3 d	no react.
5	**41**	OsO_4 (5 mol%), NMO	Me_2CO, H_2O, *t*-BuOH	55 °C, 24 h	no react.
6	**41**	OsO_4 (5 mol%), NMO, pyridine (2 equiv.)	Me_2CO, H_2O, *t*-BuOH	55 °C, 2 d	deprot. (**36**)
7	**36**	OsO_4 (2.8 mol%), NMO, citric acid (2 equiv.)	*t*-BuOH, H_2O	45 °C, 24 h	87%, 2.8:1
8[d]	**36**	OsO_4 (1.5 mol%), NMO, citric acid (2 equiv.)	*t*-BuOH, H_2O, MeCN	27 °C, 6 d	up to 96%, up to 6.6:1
9	**41**	OsO_4 (5 mol%), NMO, citric acid (2 equiv.)	*t*-BuOH, H_2O, MeCN	55 °C, 2 d	deprot. (**36**)

[a] Indicated by TLC analysis of the reaction mixture.

[b] Isolated yield.

[c] Determined by ^1H NMR integration.

[d] Experimental procedure given in **Chapter 6**.

not result in any transformation of the alkene. It should be noted that the included ligands of the PHAL-class are generally referred to as unsuitable for transformations of (Z)-alkenes, for which ligands of the IND-class were found to be superior.[194] However, this unsuitability usually only results in diminished enantioselectivities in asymmetric dihydroxylations. Therefore, since no reaction of **36** could be detected with the conventional PHAL-ligands, further investigations into Sharpless AD conditions with other ligand types were abandoned. Similarly, spirocarbonate **41** did not react under Upjohn dihydroxylation conditions (entry 5), and in the presence of pyridine (entry 6) only carbonate cleavage (formation of **36**) was noticeable. In light of the promising observations in the dihydroxylation of **29** (**Scheme 4.19** on page 90) with citric acid as an acidic additive[190], **36** was reacted with OsO_4/NMO in the presence of citric acid (entry 7). At 45 °C, full conversion of the substrate could be confirmed after 24 h, resulting in a mixture of major diol **(7*S*,8*S*)-43** and minor **(7*R*,8*R*)-44** (d.r. = 2.8:1) in good yield (87%).[195] The two diastereoisomers **43** and **44** were obtained as an inseparable mixture, and all efforts for the chromatographic separation remained unsuccessful. Noteworthy, the configurations of the introduced stereogenic centers at C-7/C-8 of the side chain diol moieties could not be determined from the obtained isomeric mixture, and complete structural characterizations relied on pure material of the separated diastereoisomers from a later stage of the synthesis (see below). Further optimized conditions could be found (entry 8), and involved running the reaction slightly above ambient temperature (27 °C) and the addition of acetonitrile as a co-solvent for solubility reasons. In this way, although in multiple experiments somewhat variable yields and diastereomeric ratios were obtained, the products **(7*S*,8*S*)-43** and **(7*R*,8*R*)-44** were typically formed in $>90\%$ yield and with d.r. $>4{:}1$. In a concluding experiment (entry 9), under analogous acidic conditions, spirocarbonate **41** was identified to be an unsuitable substrate, and only hydrolysis of the carbonate moiety and formation of **36** occurred as expected.

With an appropriate protocol for the *syn*-dihydroxylation at hand, a method for the separation of the isomers **(7*S*,8*S*)-43** and **(7*R*,8*R*)-44** was required. In this regard, fractional crystallization was found to result in an increased ratio of major **(7*S*,8*S*)-43** in the mother liquor, and a crystal fraction with an enriched content of **(7*R*,8*R*)-44** was obtained. Among several tested combinations of solvents, crystallization from *n*-hexane/chloroform (ca. 1:1) gave good results and provided sufficiently pure major isomer **(7*S*,8*S*)-43** from the mother liquor in 50% yield **(Scheme 4.23)**. From the precipitated crystal fraction, multiple analogous crystallization steps gave further **(7*S*,8*S*)-43** (65% total yield). Unfortunately, the minor isomer **(7*R*,8*R*)-44** was not available in isomeric purity *via* this crystallization protocol. In addition, this purification

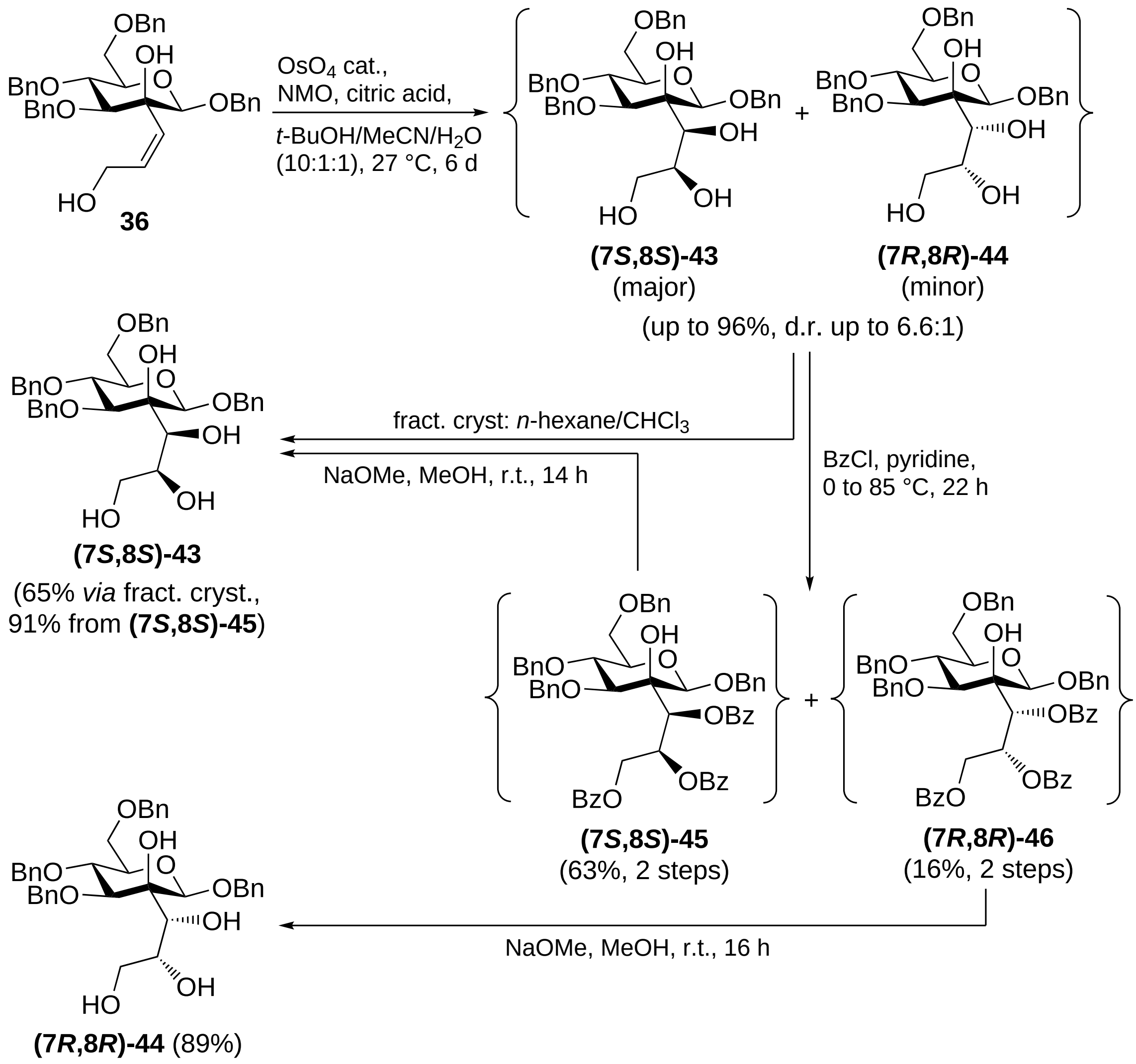
36
OsO₄ cat., NMO, citric acid,
t-BuOH/MeCN/H₂O (10:1:1), 27 °C, 6 d
(7S,8S)-43 (major)
(7R,8R)-44 (minor)
(up to 96%, d.r. up to 6.6:1)
fract. cryst: n-hexane/CHCl₃
NaOMe, MeOH, r.t., 14 h
BzCl, pyridine, 0 to 85 °C, 22 h
(7S,8S)-43
(65% via fract. cryst., 91% from (7S,8S)-45)
(7S,8S)-45 (63%, 2 steps)
(7R,8R)-46 (16%, 2 steps)
NaOMe, MeOH, r.t., 16 h
(7R,8R)-44 (89%)

Scheme 4.23 Synthesis of chromatographically inseparable **(7*S*,8*S*)-43** and **(7*R*,8*R*)-44**, and separation of the isomers *via* fractional crystallization or *via* chromatographically separable tribenzoates **(7*S*,8*S*)-45** and **(7*R*,8*R*)-46**.

method including multiple crystallization steps was found to be severely time-consuming. Therefore, in further experiments, derivatization of the mixture of diols to protected derivatives was anticipated to facilitate chromatographic purification. Acetylation under conventional conditions (Ac_2O, pyridine, DMAP, 0 °C to r.t.) gave a mixture of acetylated products, however, chromatographic separation of the two major products could not be achieved. In contrast, benzoylation of the side chain hydroxyl groups gave a mixture of tribenzoates **(7*S*,8*S*)-45** (63% over two steps) and **(7*R*,8*R*)-46** (16%), which could be separated by flash column chromatography. From these benzoyl-protected intermediates, pure major **(7*S*,8*S*)-43** and minor **(7*R*,8*R*)-44** were available by debenzoylation under Zemplén's conditions.

The *C*-7/*C*-8 configurations of the dihydroxylated intermediates **(7*S*,8*S*)-43** and **(7*R*,8*R*)-44** could, due to the conformational flexibility of the acyclic side chain, not be determined from simple interpretations of NOE contacts in H,H-NOESY NMR experiments. Possible methods for the determination of the stereochemical configuration based on derivatization exist, and would be an option in the present case. An established method developed by Rychnovsky and Coworkers would involve derivatization of diol stereogenic centers as the corresponding acetonides, followed by ^{13}C NMR analysis of the conformationally restricted cyclic acetals.[196] However, the 2,7,8,9-tetrahydroxylated motif in **43**/**44** was expected to give a mixture of 1,2- and 1,3-acetonides, as well as mono- and diacetonides, which would result in excessive further separation efforts. As a second established procedure, Mosher ester analysis would allow for the required determination of the secondary stereogenic centers.[197] In this regard, similar to tribenzoates **45**/**46**, the triacylated (*S*)- and (*R*)-MTPA (α-methoxy-α-trifluoromethylphenylacetyl) esters could possibly be accessible. Notably, this method is also suitable for the structural determination of complex natural products with polyhydroxylated frameworks.[198] Finally, X-ray structural analysis of **43**/**44**, or of a derivative, would unambiguously determine the *C*-7/*C*-8 configurations. In this context, however, all efforts to obtain single crystals from **(7*S*,8*S*)-43** or **(7*R*,8*R*)-44** were unsuccessful. Since derivatizations of the isomers could potentially facilitate the crystallization properties, such a strategy was explored next. A possible option would involve acylation with chiral camphanoyl chloride (3-oxo-4,7,7-trimethyl-2-oxabicyclo[2.2.1]heptane-1-carbonyl chloride). This method has application in derivatizations for the resolution of racemic alcohols[199], and has additionally been reported to frequently result in highly crystalline derivatized products.[200] To explore if the described camphanate method could not only facilitate clean crystallization, but also enable chromatographic separation of the isomers

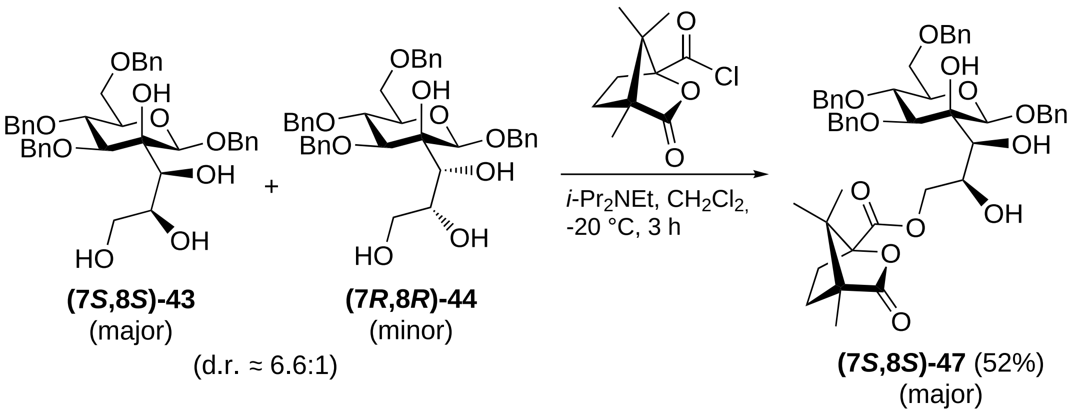

Scheme 4.24 Synthesis of primary major isomer-derived camphanate **(7*S*,8*S*)-47** *via* selective primary alcohol acylation.

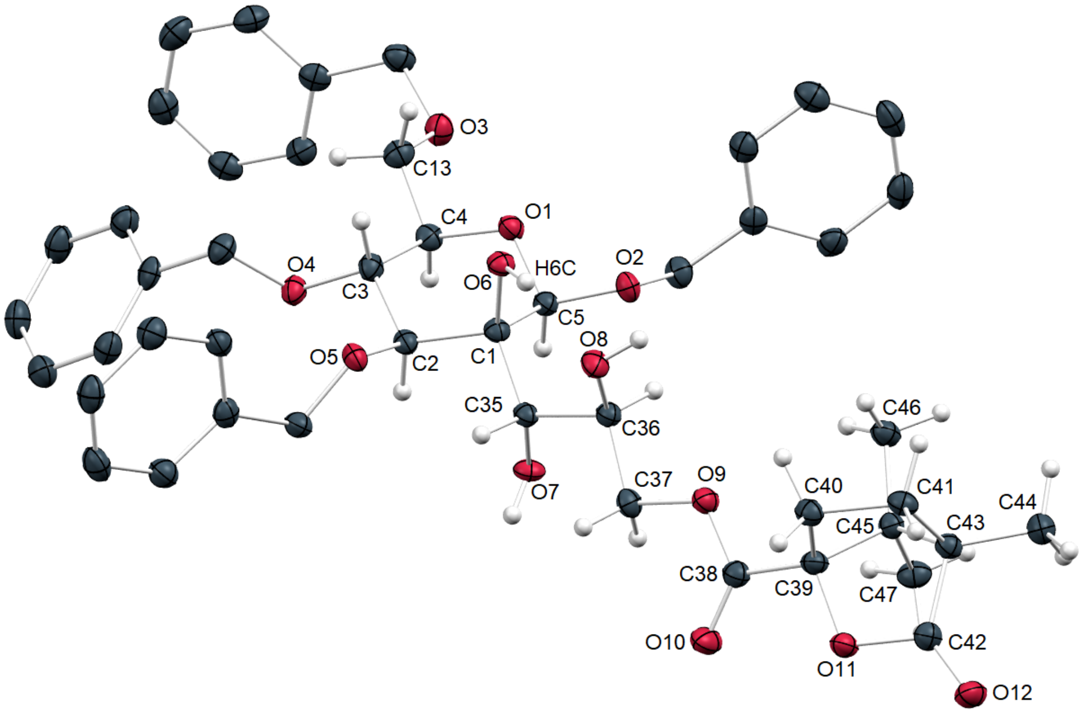

Figure 4.6 X-ray structure of primary camphanate **(7*S*,8*S*)-47**. Hydrogen atoms of the benzyl ethers are omitted for clarity. Ellipsoids are drawn at the 50% probability level. Red = oxygen, gray = carbon, white = hydrogen. Significant distances and angles: O8···H6C 1.961 Å, O8···O6 2.715 Å, O6-H6C···O8 153.9°.

43/**44** similar to the benzoylation route, the obtained mixture of **(7*S*,8*S*)-43** and **(7*R*,8*R*)-44** (d.r. ≈ 6.6:1) was reacted with one equivalent of (–)-(1*S*,4*R*)-camphanoyl chloride **(Scheme 4.24)** in the presence of Hünig's base (*i*-Pr_2NEt). Although some side products were observable by TLC control, as expected acylation of the primary hydroxyl groups occurred selectively. Chromatographic separation of the obtained isomers proved to be challenging, and had to be repeated multiple times, demonstrating that this derivatization method was unsuitable for separation purposes on a preparative scale. However, the major camphanate isomer **(7*S*,8*S*)-47** could be obtained as a single isomer in 52% yield. Fortunately, from diethyl ether/acetonitrile, single crystals of sufficient purity for X-ray structural analysis could be grown. In the solid state, the crystalline camphanate **(7*S*,8*S*)-47** occupied the monoclinic space group $P2_1$ with $Z = 2$ formula units in the unit cell. An analysis of the molecular structure **(Fig. 4.6)** revealed the (7*S*,8*S*)-configuration of the *syn*-diol moiety in **(7*S*,8*S*)-47**, and thus, indirectly, for major isomer **(7*S*,8*S*)-43**. Furthermore, by applying criteria identical to those of **Section 3.3.3** ($d_{O \cdots H} < 3.0$ Å and $\theta_{O-H \cdots O} > 90°$), an intramolecular hydrogen bond between the axial *C*-2-OH (O6-H6C) and the *O*-8 (O8) of the side chain was identified (O8···H6C 1.961 Å, O8···O6 2.715 Å, O6-H6C···O8 153.9°). Based on the determined (7*S*,8*S*)-configuration of this major isomer, the given structure for minor isomer **(7*R*,8*R*)-44** was established by assuming the reasonable *syn*-stereoselectivity of the osmium-based dihydroxylation. In addition, in conformationally fixed cyclic intermediates synthetically derived from **(7*R*,8*R*)-44**, significant NOE contacts in H,H-NOESY experiments confirmed the given structure indirectly.

An explanation for the observed stereoselectivity of the dihydroxylation of **36** would be of interest. A simple analysis of the modes of attack could involve the generally accepted "H in plane" conformations for *C*-9 according to Kishi's empirical rule (comp. **Scheme 4.7, (a)**, on page 67) and attack of OsO_4 from the opposite face of the alkene.[105, 106] However, due to the quaternary nature of *C*-2 and the presence of a second hydroxyl group, suitable orientations for both *C*-9 and the quaternary *C*-2 have to be proposed. An examination of the H,H-NOESY spectrum of alkene **36** in acetone-D_6 (**Fig. D.1** on page 304) revealed significant contacts between the alkene *H*-7 and both the axial carbohydrate *H*-1 and *H*-3, respectively. Consequently, an eclipsed relationship between the alkene double bond and the axial *C*-2-OH can be assumed **(Scheme 4.25, a)**. At *C*-9, two allylic hydrogen atoms (*H*-9a/b) could occupy an *anti*-periplanar orientation with respect to the *C*-2-OH, resulting in orientation of the *C*-9-OH either towards the carbohydrate *C*-3 (conformation **36-a**) or towards *C*-1 (**36-b**). It seems plausible to assume an overall seven-membered cyclic conformation, stabilized by the presence of an intramolecular hydrogen bond between *O*-9 and *O*-2. Notably, these proposed seven-membered cyclic conformations bear resemblance with the structure of seven-membered spirocarbonate **41** (**Fig. 4.5** on page 95). In the protic acidic medium (citric acid in *t*-BuOH/H_2O/MeCN) of the dihydroxylation reaction, the postulation of an intramolecular hydrogen bond seems to be inappropriate, since the saturation of all hydrogen bond acceptors by external donors has to be assumed. Taking into account that no transformation of **36** could be observed without the acidic additive (**Table 4.2** on page 97), the following circumstances are proposed **(Scheme 4.25, b)**: in the acidic medium, the absence of a stabilizing intramolecular hydrogen bond results in the preference for staggered conformations (**36-c** and **36-d**) with *anti*-periplanar orientation of the *C*-2-OH with respect to the alkene double bond. Possibly, in these conformations, attack of OsO_4 is facilitated due to decreased steric congestion around the alkene moiety, leading to the observed transformation of **36**. Two different "H in plane" conformations at *C*-9 can be formulated (**36-c** and **36-d**), resulting in four different modes of attack (i)–(iv) of OsO_4. Of these, (ii) and (iii) occur from the alkene face opposite to the *C*-9-OH, and thus, in "Kishi"-sense, whereas (i) and (iv) can be referred to as "*anti*-Kishi". From these considerations, although purely tentative, it can

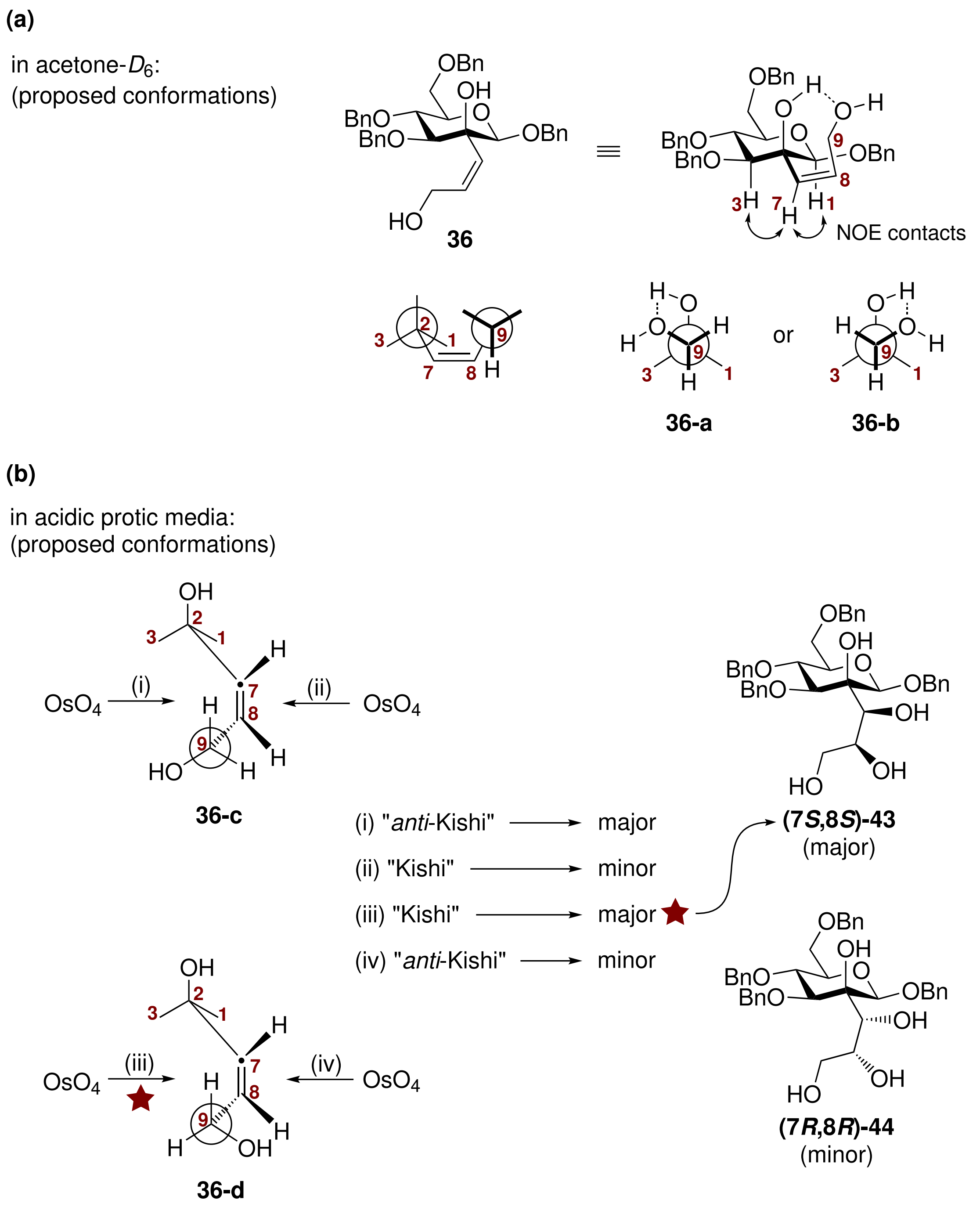
(a)
in acetone-D_6:
(proposed conformations)
OBn
OH
BnO
BnO
O
OBn
HO
36
≡
OBn
H
O
O
O
H
9
OBn
8
3H
7
H
H1
NOE contacts
3
2
1
7
8
H
9
H
O
H
O
H
3
9
1
H
36-a
or
O
H
H
O
H
3
9
1
H
36-b
(b)
in acidic protic media:
(proposed conformations)
OH
2
3
1
H
OsO4
(i)
(ii)
OsO4
H
7
8
9
HO
H
H
36-c
(i) "anti-Kishi" → major
(ii) "Kishi" → minor
(iii) "Kishi" → major
(iv) "anti-Kishi" → minor
OBn
OH
BnO
BnO
O
OBn
OH
OH
HO
(7S,8S)-43
(major)
OH
2
3
1
H
OsO4
(iii)
(iv)
OsO4
H
7
8
9
H
OH
H
36-d
OBn
OH
BnO
BnO
O
OBn
OH
OH
HO
(7R,8R)-44
(minor)

Scheme 4.25 **(a)** Proposed conformations of alkene **36** in acetone-D_6. Observed NOE contacts are indicated with arrows, and refer to the spectrum in **Fig. D.1** on page 304. In proposed conformations **36-a** and **36-b**, the interjacent alkene function is omitted for clarity. **(b)** Proposed reactive conformations **36-c** and **36-d** for the *syn*-dihydroxylation of **36** in acidic protic medium, *via* attack modes (i)–(iv).

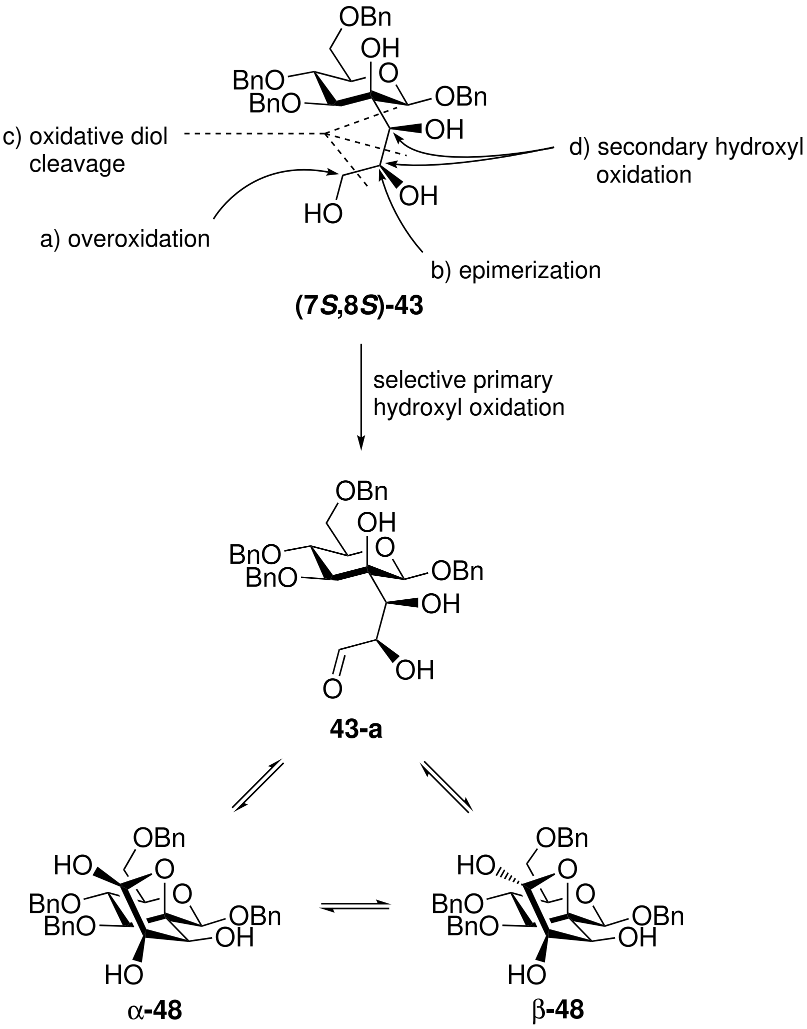
OBn
OH
BnO
BnO
O
OBn
OH
OH
HO
c) oxidative diol cleavage
d) secondary hydroxyl oxidation
a) overoxidation
b) epimerization
(7S,8S)-43
selective primary hydroxyl oxidation
43-a
α-48
β-48

Scheme 4.26 Desired selective primary alcohol oxidation of **(7*S*,8*S*)-43** to aldehyde **43-a**, or to the derived cyclic hemiacetals **α,β-48**. An analysis of anticipated competitive side reactions a)–d) is given.

be suggested that the major dihydroxylation product **(7*S*,8*S*)-43** is possibly formed *via* attack mode (iii) involving the substrate conformation **36-d**.

Following the general synthetic route (**Scheme 4.15, (b)**, on page 81), both *syn*-intermediates **(7*S*,8*S*)-43** and **(7*R*,8*R*)-44** serve as suitable substrates for the selective primary alcohol oxidation, which can be regarded as the key step of the overall synthesis. As demonstrated in an analysis of the desired reaction **(Scheme 4.26)**, the major substrate **(7*S*,8*S*)-43** could be transformed into the acyclic aldehyde **43-a** *via* selective oxidation of the primary *C*-9-OH group of the 2,7,8,9-tetrahydroxy moiety. Subsequently, based on previous observations (comp. **Scheme 4.19** on page 90), hemiacetal ring closure between the aldehyde functional group and the axial *C*-2-OH could be anticipated, resulting in an equilibrium between anomeric isomers **α-48** and **β-48**.

Several potential side reactions can be considered for the shown transformation. a) Overoxidation of the product aldehyde **43-a** (possibly *via* the hydrated intermediate) or of **α,β-48** would give either the unwanted free carboxylic acid, or the lactone. b) In the course of the oxidation, epimerization of the α-stereogenic center (at *C*-8) *via* the enol form has to be considered, e.g. from the formed aldehyde. c) Oxidative cleavage of vicinal diols, a ubiquitous side reaction in multiple oxidative transformations, could occur either from the substrate **(7*S*,8*S*)-43**, or from the wanted oxidized products. d) Finally, the unwanted oxidation of the secondary hydroxyl groups at *C*-7/*C*-8 to the corresponding ketones might be observed as a competitive side reaction.

A survey for comparable transformations suggested mild TEMPO-based oxidation protocols might be suitable (comp. **Chapter 4.1**), since several examples involving carbohydrate-derived polyol substrates have been described in the literature. In this context, Iadonisi and Coworkers **(Scheme 4.27, a)** reported on the selective primary oxidation of the 1,2-diol **EN** as a key step in a total synthesis of the unusual carbocyclic sugar caryose **J** (comp. **Scheme 1.3** on page 4).[201] The application of Anelli's protocol[141], involving TEMPO/NaOCl in biphasic H_2O/CH_2Cl_2 under phase-transfer conditions, gave the wanted hemiacetal products **α,β-EQ** and **α,β-ER** in 31% yield. Lactone **EO** (33%) was isolated as the major side product due to overoxidation. Significant amounts of unreacted **EN** were reisolated from the product mixture, however, increased amounts of the oxidant NaOCl resulted in a higher proportion of unwanted lactone **EO**. As an explanation, the authors surmised that the hydrophilic nature of the hemiacetal products **α,β-EQ** and **α,β-ER** might favor their overoxidation in the aqueous phase. Several variations of the originally biphasic oxidation protocol have been developed for specific synthetic challenges. In search of a convenient and mild synthetic access to sensitive dialdo-glycosides like **ET (Scheme 4.27, b)**, Ramström and Coworkers utilized the combination TEMPO/trichloroisocyanuric acid (TCICA) as a mild oxidizing system.[202] The high polarity of the substrate glycosides **ES** did not allow for the application of CH_2Cl_2 solvent mixtures. However, DMF as the solvent and slightly basic conditions ($NaHCO_3$ as a weak base) affected the clean formation of aldehydes **ET** *via* selective oxidation of the primary *C*-6 in the presence of unprotected *C*-2/3/4 hydroxyl groups. After an imine catch-and-release purification of the sensitive products with amino-functionalized column material, aldehydes **ET** or similar dialdo-glycosides could be isolated in excellent yields. Another relevant example was applied by Yu and Molinaro in their total synthesis of bradyrhizose **K (Scheme 4.27, c)**.[14] Preliminary experiments with the side chain triol **DU** and the combination TEMPO/$PhI(OAc)_2$[145] resulted in oxidative cleavage of the side chain. In contrast, with TEMPO/TCICA in unbuffered CH_2Cl_2, the aldehyde intermediate

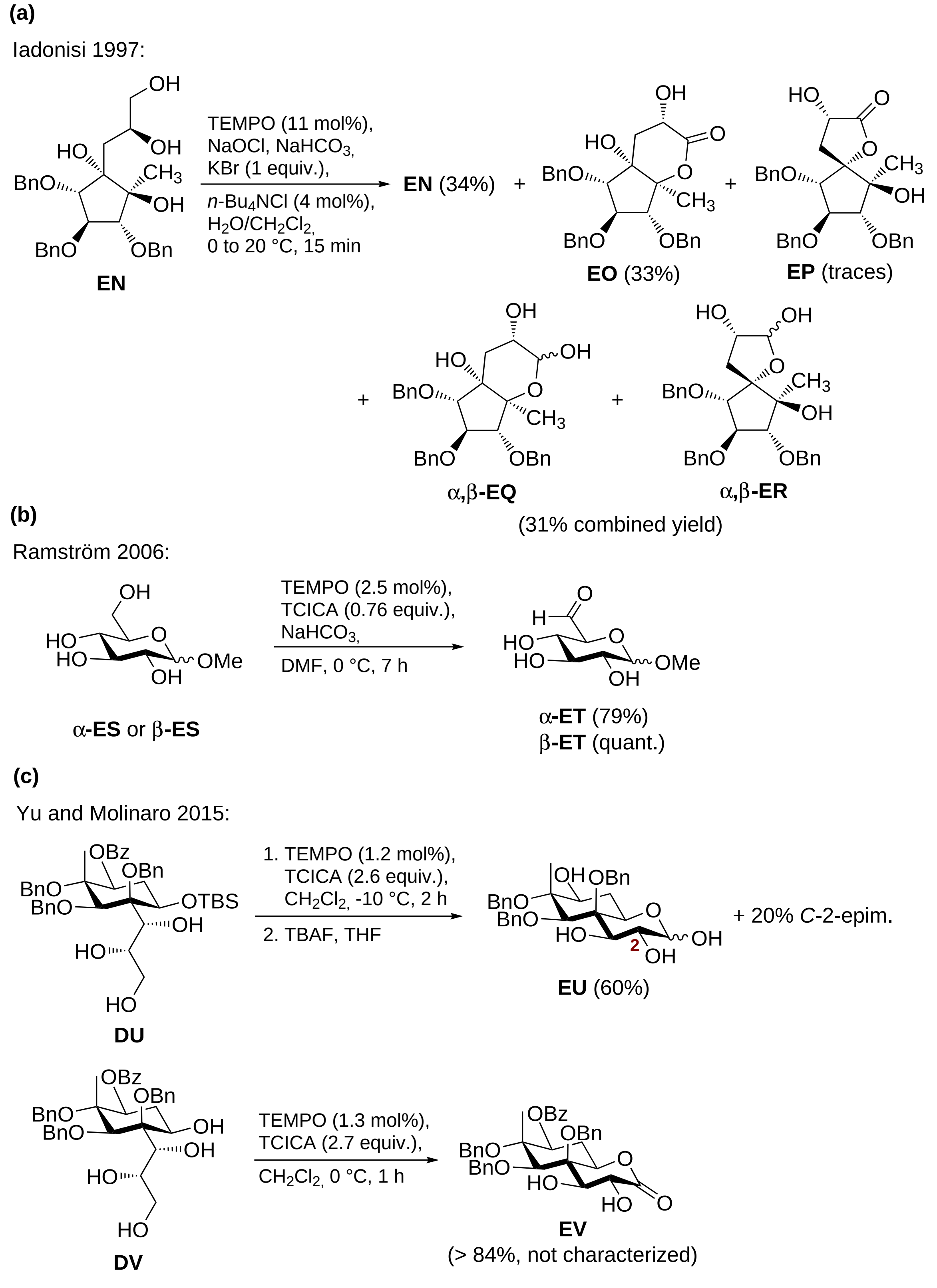
(a)
Iadonisi 1997:
TEMPO (11 mol%), NaOCl, NaHCO3, KBr (1 equiv.), n-Bu4NCl (4 mol%), H2O/CH2Cl2, 0 to 20 °C, 15 min
EN
EN (34%)
EO (33%)
EP (traces)
α,β-EQ
α,β-ER
(31% combined yield)
(b)
Ramström 2006:
TEMPO (2.5 mol%), TCICA (0.76 equiv.), NaHCO3, DMF, 0 °C, 7 h
α-ES or β-ES
α-ET (79%)
β-ET (quant.)
(c)
Yu and Molinaro 2015:
1. TEMPO (1.2 mol%), TCICA (2.6 equiv.), CH2Cl2, -10 °C, 2 h
2. TBAF, THF
DU
EU (60%)
+ 20% C-2-epim.
TEMPO (1.3 mol%), TCICA (2.7 equiv.), CH2Cl2, 0 °C, 1 h
DV
EV
(> 84%, not characterized)

Scheme 4.27 Selected examples: selective primary alcohol oxidations in carbohydrate substrates. **(a)** Iadonisi's oxidation of alcohol **EN**, utilizing TEMPO/NaOCl in biphasic H_2O/CH_2Cl_2.[201] **(b)** Ramström's protocol for the formation of dialdo-glycosides like **ET**, using TEMPO/trichloroisocyanuric acid (TCICA) in buffered DMF.[202] **(c)** Oxidation reactions with TEMPO/TCICA as published by Yu and Molinaro for synthetic intermediates **EU** and **EV**.[14]

could be obtained in good yield, and after desilylation the wanted lactol **EU** was available. However, in the following desilylation, significant amounts of the *C*-2-epimerized product were isolated from the reaction with TBAF, indicating that deprotection prior to the oxidation step would be favorable. The desilylated tetrol **DV** was reacted in a similar manner, but overoxidation to the lactone at low temperature (−30 °C) could not be prevented. At 0 °C, lactone **EV** was isolated as the major product, and was subjected to DIBAL-H reduction without further purification/characterization.

For the transformation of major isomer **(7*S*,8*S*)-43**, due to the structurally related substrates, the method applied by Yu and Molinaro (TEMPO/TCICA in unbuffered CH_2Cl_2) was investigated in preliminary attempts **(Table 4.3)**.[14] Under these conditions (entry 1), at low temperature (−40 °C), only slow conversion was observable. At −5 °C, a complex mixture of products was formed, and the desired hemiacetal product **α,β-48** could be isolated in only 12% yield after chromatography. An ESI-MS analysis of the mixture of side products with higher chromatographic mobility suggested substantial overoxidation to products of *keto*-lactone mass ($[M–H]^-$ m/z 623). When Ramström's conditions were applied (entry 2), at −8 °C, conversion to the product without significant overoxidation could be observed.[202] After chromatographic purification, **α,β-48** was obtained in 44% yield, however, the product still contained impurities of similar chromatographic mobility, possibly resulting from epimerization of the α-stereogenic center. Repeated chromatography of the impure product resulted in a severe loss of material. Possibly, the observed loss of material could originate from intermolecular acetal formations of the free hemiacetal products upon chromatography, and similar assumptions have been made to explain difficulties in the isolation of 1,6-dialdo-glycosides.[203] Furthermore, direct deprotection of impure **α,β-48** to the corresponding target higher sugar seemed to be no suitable option, since the separation of highly hydroxylated impurities from the polar target compounds could be expected to be difficult. For this reason, a protocol for the clean formation of **α,β-48** was required. Further variations from the published protocols revealed that in anhydrous ethyl acetate (entry 3), although a rather unusual solvent, the reaction proceeded with fast conversion at low temperatures (−35 °C). After an optimized, rapid chromatography procedure involving spherical silica, **α,β-48** was obtained in 62% yield (81% based on recovered substrate). Although a reduced complexity of the product mixture suggested a cleaner reaction in ethyl acetate, purified **α,β-48** still contained minor impurities. Repeated chromatography allowed for the isolation of the most pronounced side product in pure form, which was identified as the unexpected spiro-tetrahydrofuran **(7*S*,8*S*)-49 (Table 4.3)**. Detailed TLC control experiments under similar reaction conditions suggested that the side product **(7*S*,8*S*)-49** appeared upon reductive aqueous quenching (sat.

Table 4.3 Reaction screening on the TEMPO-based selective primary alcohol oxidation of major isomer **(7*S*,8*S*)-43**.

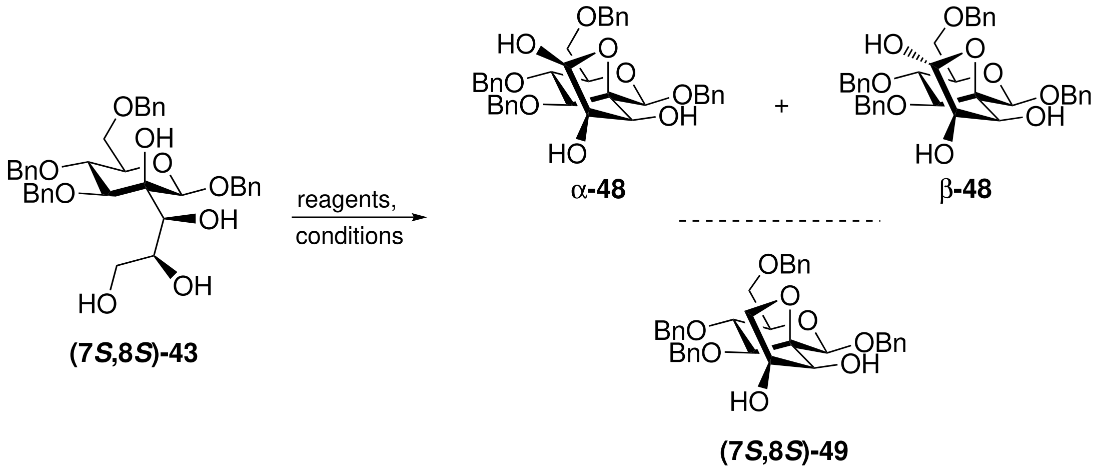

#	reagents	solvents	T, t	observation,[a] yield[b] (**α,β-48**)
1	TEMPO (2.6 mol%), TCICA (2.7 equiv.)	CH_2Cl_2	−40 to −5 °C, 24 h	complex mixt. 12% **α,β-48**, + overoxidation[c]
2	TEMPO (2.5 mol%), TCICA (0.76 equiv.), $NaHCO_3$ (30 equiv.)	DMF	−8 °C, 5 h	44% **α,β-48**[d]
3	TEMPO (2.5 mol%), TCICA (0.8 equiv.), $NaHCO_3$ (30 equiv.)	EtOAc	−35 to −15 °C, 4 h	62% **α,β-48**,[d] 81% brsm,[e] < 5% **(7*S*,8*S*)-49**
4[f]	TEMPO (3 mol%), TCICA (0.85 equiv.), MOPS (12 equiv.), then: Me_2S (2.7 equiv.)	EtOAc/PhMe (2:1)	−50 to −35 °C, 15 h −35 °C, 15 min	61% **α,β-48**, 72% brsm[e]

[a] Indicated by TLC analysis of the reaction mixture.

[b] Isolated yield.

[c] ESI-MS analysis: neg. mode: $[M\text{–}H]^-$ m/z 623 (proposed: *keto*-lactone).

[d] Product impurified after chromatography.

[e] brsm = based on recovered starting material.

[f] Experimental procedure given in **Chapter 6**. MOPS = 3-(*N*-morpholino)propanesulfonic acid. TCICA = trichloroisocyanuric acid.

$Na_2S_2O_5$) of the reaction mixture, indicating that it might possibly originate from *C*-9 deoxygenation by the reducing agent. Other explanations could involve the formation of the primary chloride from **(7*S*,8*S*)-43** by the stoichiometric reagent TCICA, followed by ring closure, or direct ring closure from the $TEMPO^+$-activated oxidation intermediate. From the reaction in ethyl acetate as described, further improvements to the conditions were made (entry 4): the addition of a non-polar co-solvent (toluene) was found to be beneficial for a clean reaction, and the reaction was run in high dilution (0.005 M). Since strictly anhydrous conditions were expected to minimize a possible epimerization of the α-stereogenic center, $NaHCO_3$ seemed to be an unsuitable buffer. As an unusual alternative, good results were obtained with 3-(*N*-morpholino)propanesulfonic acid (MOPS), an organic buffer with applications in biochemistry at near-neutral pH, which was added to the reaction as a heterogeneous buffer. The side product **(7*S*,8*S*)-49** was not formed in significant amounts upon quenching the reaction with aqueous $Na_2S_2O_3$ instead of $Na_2S_2O_5$. Nevertheless, a mild reductive non-aqueous quenching procedure was desirable to minimize product degradation, and thus, to obtain a product of higher purity. For that purpose, dimethyl sulfide in ethyl acetate was added as a reductive quench prior to the standard aqueous workup. In this way, after chromatographic purification, the desired **α,β-48** could routinely be isolated in high purity in 61% yield (72% based on recovered substrate) and on a 150 mg scale. In light of the aforementioned problems encountered in this transformation, and given the number of potential competitive side reactions (comp. **Scheme 4.26** on page 104), these results were evaluated as quite satisfactory. In addition, the developed conditions for the oxidation reaction could be expected to have potential applicability as a general oxidation protocol, given the mild and neutral conditions and the compatibility with low temperatures.

The obtained oxidation product **α,β-48** could be fully characterized, including the anomeric configurations of the interesting reducing spirofuranose-pyranose hybrid (for a clarification of anomeric configurations in the Fischer projection, see **Scheme 6.2, (a)**, on page 183). Initially, the major component of solid **α,β-48** was identified to be its α-anomer **α-48** ($\alpha/\beta \approx 11.1{:}1$, **Scheme 4.28**). In the NMR solvent acetone-D_6 at r.t., slow anomerization occurred, resulting in major **β-48** ($\alpha/\beta \approx 1{:}2.7$). The progression of the anomerization process could be monitored by accompanying NMR experiments (**Fig. 4.7** and **4.8**), which confirmed that equilibration to $\alpha/\beta \approx 1{:}2.7$ was complete after ca. 5–6 days. Although the mixture of anomers exhibited highly complex NMR spectra, this NMR-monitoring allowed for the complete assignment of all relevant signals, and thus, confirmed the purity of the obtained material. Unfortunately, attempts to monitor the mutarotation simultaneously remained unsuccessful due to limited solubility of the compound in acetone-D_6 and, as a result, observed precipitation

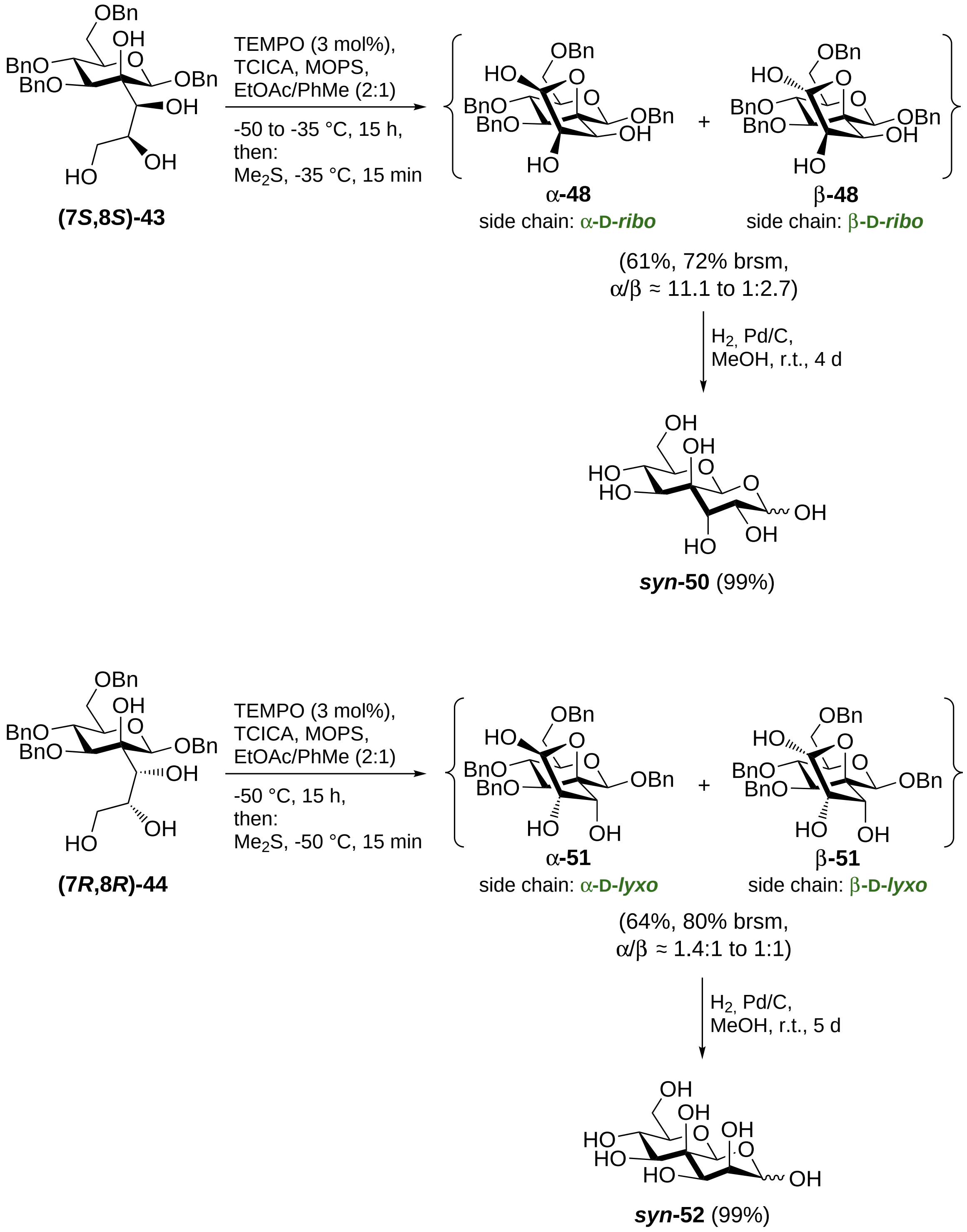
(7S,8S)-43
TEMPO (3 mol%), TCICA, MOPS, EtOAc/PhMe (2:1)
-50 to -35 °C, 15 h, then: Me2S, -35 °C, 15 min
α-48
side chain: α-D-ribo
β-48
side chain: β-D-ribo
(61%, 72% brsm, α/β ≈ 11.1 to 1:2.7)
H2, Pd/C, MeOH, r.t., 4 d
syn-50 (99%)
(7R,8R)-44
TEMPO (3 mol%), TCICA, MOPS, EtOAc/PhMe (2:1)
-50 °C, 15 h, then: Me2S, -50 °C, 15 min
α-51
side chain: α-D-lyxo
β-51
side chain: β-D-lyxo
(64%, 80% brsm, α/β ≈ 1.4:1 to 1:1)
H2, Pd/C, MeOH, r.t., 5 d
syn-52 (99%)

Scheme 4.28 Top: oxidative formation of spiro-ribofuranose **α,β-48**, and deprotection to target 4-*C*-formyl octose ***syn*-50**. Bottom: formation of minor isomer-derived spiro-lyxofuranose **α,β-51**, and deprotection to target 4-*C*-formyl octose ***syn*-52**. Anomeric ratios are given in acetone-D_6. For clarity, ***syn*-50** and ***syn*-52** are depicted in the (9*S*)-9,7-pyranose-1,9-pyranose isomeric form.

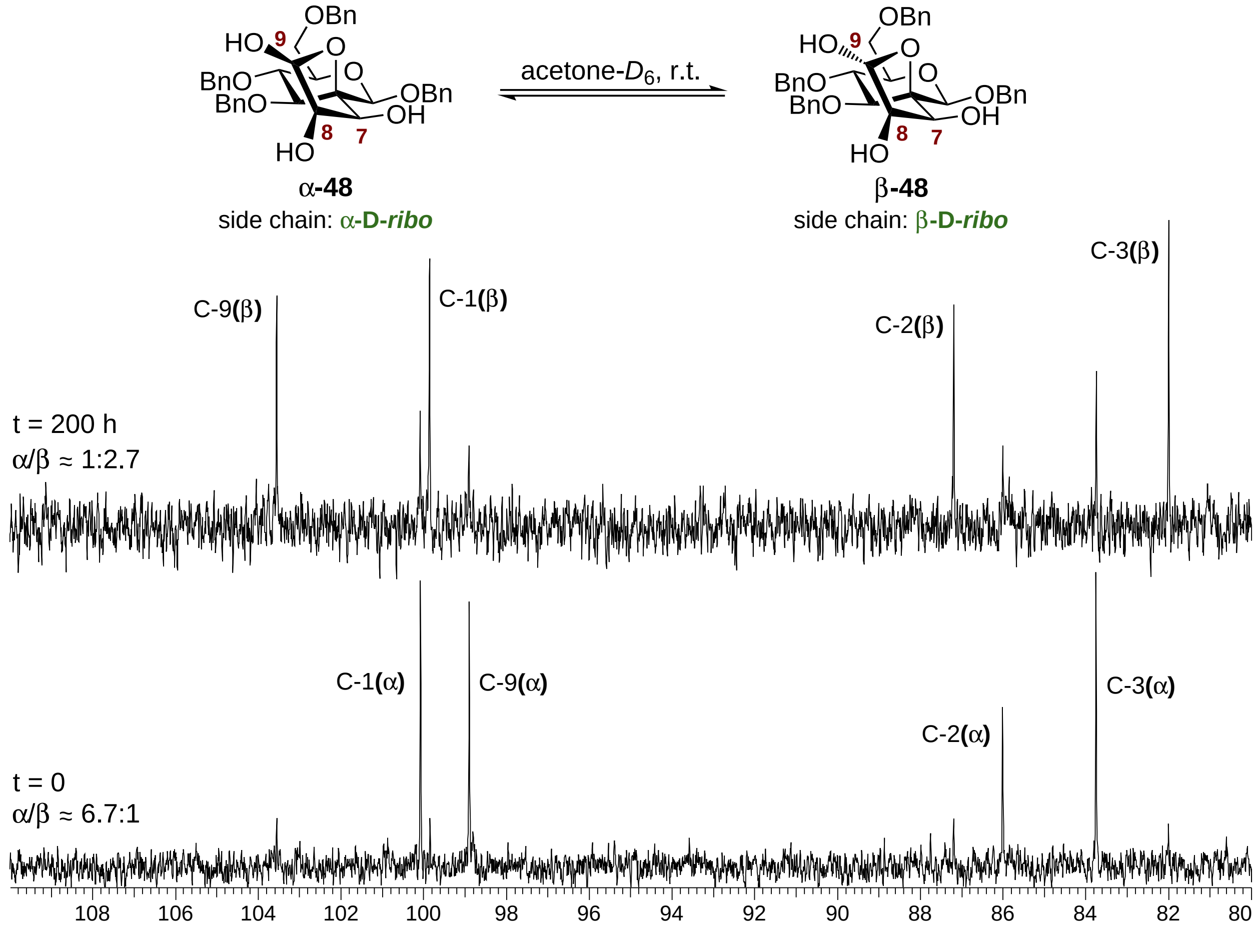

Figure 4.7 ^{13}C NMR-monitoring of the anomerization process of **α,β-48** at r.t. Spectra were recorded at 100.6 MHz in acetone-D_6 and are given in the range 80–110 ppm. Anomeric ratios were determined by integration of the corresponding proton spectra. The shown spectra are unprocessed.

when storing the sample over the required time of several days. Furthermore, initially measured changes in the specific rotation were small ($< 5°$), and therefore severely error-prone. The configurations of the stereogenic centers of the spiro-ribofuranose moiety in **α-48** could be unambiguously established by significant NOE contacts in H,H-NOESY experiments (**Fig. D.2** on page 305). In addition, it should be noted that the anomeric configurations in **α,β-48** and following similar spirofuranoses were fully consistent with published work on ^{13}C NMR chemical shift relations for structurally simpler furanosides.[204]

To complete the synthesis of the first target compound, **α,β-48** was subjected to hydrogenolytic debenzylation **(Scheme 4.28, top)** to yield ***syn*-50** in near-quantitative yield after RP-chromatographic purification (for characterization of target compounds, see **Section 4.5.4**). In a similar manner, application of the developed oxidation protocol

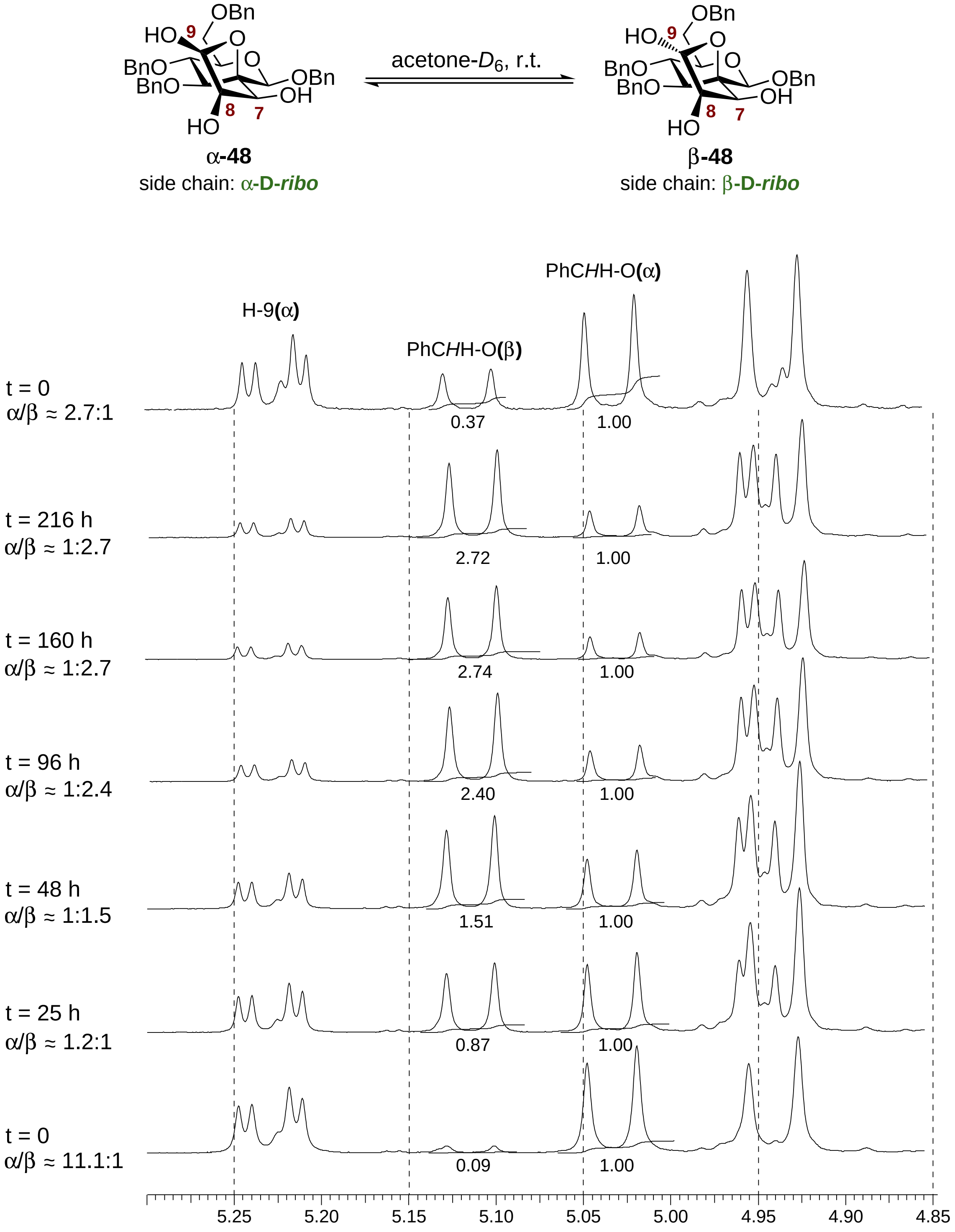

Figure 4.8 ^{1}H NMR-monitoring of the anomerization process of **α,β-48** at r.t. Spectra were recorded at 400.2 MHz in acetone-D_6 and are given in the range 4.85–5.30 ppm. Benzylic methylene protons of **α-48** and **β-48** were used for integration. The shown spectra are unprocessed. Top, t = 0: the original sample was evaporated, dried and redissolved in acetone-D_6 to demonstrate the reversibility of the epimerization process.

to minor isomer **(7*R*,8*R*)-44 (Scheme 4.28, bottom)** gave a mixture of spiro-lyxofuranoses **α,β-51** with α/β ≈ 1.4:1, slowly epimerizing to α/β ≈ 1:1 in acetone-D_6. Due to almost equal amounts of both anomers in solution, the 2D NMR spectra of lyxofuranoses **α,β-51** were more complex than for ribofuranose **α,β-48**. However, significant NOE contacts (**Fig. D.4** on page 307) between *H*-9 and *H*-8 (**β-51**) and between *H*-9 and OH-8 (**α-51**), respectively, allowed for the determination of the anomeric configurations. The mixture of spiro-lyxofuranoses **α,β-51** was, subsequently, subjected to global debenzylation to afford ***syn*-52** as the second target 4-*C*-formyl octose. Both target compounds could be obtained in a stereodivergent synthesis from the common alkene intermediate **36**. The synthetic route for both ***syn*-50** and ***syn*-52** included 14 steps from D-glucose, and proceeded in 9 steps/30% yield (major isomer, ***syn*-50**) and 9 steps/8% yield (minor isomer, ***syn*-52**), respectively, from the known 2-uloside **2b**. Based on the developed synthesis, an analogous synthesis of the corresponding *anti*-isomers was pursued next.

4.5.3. Synthesis of the *anti*-Isomers

Following the course of the late-stage oxidation route (**Scheme 4.15, (b)**, on page 81), the *anti*-isomers of target compounds **T-4** were anticipated to originate from nucleophilic epoxide opening of a side chain epoxide derived from alkene **36**. Thus, epoxidations of **36** were examined under a variety of conditions **(Scheme 4.29)**. Peracid epoxidation of **36** with *m*-CPBA resulted in the clean conversion to a mixture of epoxides (d.r. ≈ 5:1; ^{1}H NMR integration), of which major epoxide **(7*S*,8*S*)-53** could be isolated in 72% yield, together with 13% of the minor isomer **(7*R*,8*R*)-57**. Chromatographic separation of the isomers was found to be challenging due to comparable chromatographic mobility. Minor epoxide **(7*R*,8*R*)-57**, which eluted first, could only be separated from the following fractions of major **(7*S*,8*S*)-53** by optimized chromatographic conditions. Notably, the addition of Et_3N to the eluent (2%) was required, and significant loss of material upon chromatography was observed with lower amounts of the basic additive. The purification of *m*-CPBA prior to use (comp. **Section 6.3.1** on page 180) was found to be crucial for the reaction, since direct application of commercial material resulted in a sluggish and weakly reproducible reaction. Similarly, the addition of $NaHCO_3$ as a buffer was found to be detrimental to the reaction. Substitution of *m*-CPBA for magnesium monoperoxyphthalate ($MMPP \cdot (H_2O)_6$, $NaHCO_3$, 1,2-dichloroethane) required elevated temperatures (> 50 °C, 3 d), and gave the same major isomer **(7*S*,8*S*)-53** with lower diastereoselectivity (d.r. ≈ 2:1) and with only mediocre isolated yield (45%). When **36** was reacted with *t*-BuOOH in the presence of catalytic $VO(acac)_2$, the

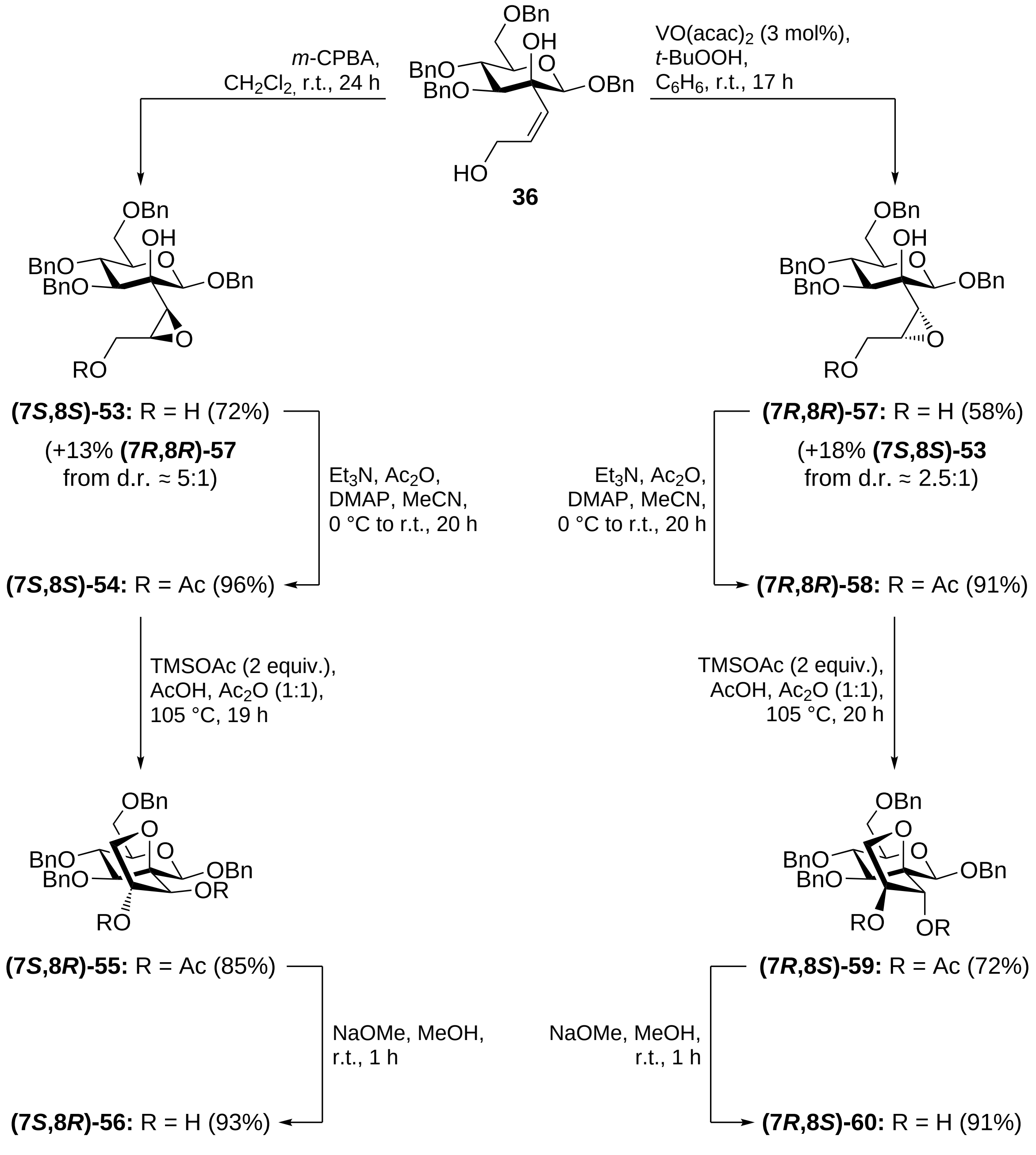
OBn
OH
O
BnO
BnO
OBn
HO
36
m-CPBA,
CH_2Cl_2, r.t., 24 h
VO(acac)$_2$ (3 mol%),
t-BuOOH,
C_6H_6, r.t., 17 h
RO
(7S,8S)-53: R = H (72%)
(+13% (7R,8R)-57
from d.r. ≈ 5:1)
(7R,8R)-57: R = H (58%)
(+18% (7S,8S)-53
from d.r. ≈ 2.5:1)
Et_3N, Ac_2O,
DMAP, MeCN,
0 °C to r.t., 20 h
(7S,8S)-54: R = Ac (96%)
(7R,8R)-58: R = Ac (91%)
TMSOAc (2 equiv.),
AcOH, Ac_2O (1:1),
105 °C, 19 h
105 °C, 20 h
OR
(7S,8R)-55: R = Ac (85%)
(7R,8S)-59: R = Ac (72%)
NaOMe, MeOH,
r.t., 1 h
(7S,8R)-56: R = H (93%)
(7R,8S)-60: R = H (91%)

Scheme 4.29 Diastereoselective epoxidations of alkene **36**, giving epoxides **(7*S*,8*S*)-53** and **(7*R*,8*R*)-57**, and derived epoxyacetates and spirotetrahydrofuran cyclization products.

formation of the other epoxide occurred with rather low selectivity (d.r. ≈ 2.5:1), and major epoxide **(7*R*,8*R*)-57** (58% yield) and minor isomer **(7*S*,8*S*)-53** (18%) could be isolated in a good overall yield of epoxides.

An explanation for the stereochemical outcome of the epoxidation reactions of **36** could involve an analysis of the reacting conformations of the allyloxy moiety according to the Sharpless model (comp. **Scheme 4.7, (b)** on page 67).[165] However, in the case of **36**, the presence of a second allyloxy moiety (the quaternary carbohydrate *C*-2-OH) has to be considered. In this regard, estimations of the preferred conformations could be expected to be intricate, since two sterically nearly identical carbohydrate sites (*C*-1 and *C*-3) are present. For peracid epoxidations, Sharpless and Coworkers suggested a reacting conformation with a HO-C-C=C dihedral angle of 120°, and peracid attack from the side of the allylic hydroxyl. Application of these requirements to the epoxidation of **36** with *m*-CPBA **(Scheme 4.30, a)** resulted in the proposed conformation **36-e**, which included two 120° dihedral angles (HO-C2-C=C and HO-C9-C=C). The depicted mode of attack of the peracid from the side of both hydroxyl groups illustrates the formation of **(7*S*,8*S*)-53** as the major epoxide. Minor epoxide **(7*R*,8*R*)-57** could, in this case, be either formed by an "*anti*-Sharpless" mode of attack from the top side of **36-e**, or *via* the second conformation featuring two 120° dihedral angles and upwards orientation of both hydroxyl groups (not shown). Alternatively, a fixed conformation with an intramolecular hydrogen-bonding interaction could be considered. In a conformation like **36-b**, the formation of major epoxide **(7*S*,8*S*)-53** would require the peracid attack to occur from the carbohydrate *C*-1 side.

In the epoxidation of **36** with VO(acac)$_2$/*t*-BuOOH **(Scheme 4.30, b)**, an analysis according to the Sharpless model would involve HO-C-C=C dihedral angles of 50°. Albeit, due to the presence of the Lewis acidic, pentavalent vanadium catalyst, it seems plausible to formulate a conformation like **36-f**, with the substrate diol forming a chelate complex with the vanadium peroxide moiety. The proposed conformation **36-f** would result in epoxidation from the carbohydrate *C*-3 side, and thus, the formation of major epoxide **(7*R*,8*R*)-57**. Putatively, this orientation would be more favorable than a corresponding chelate complex oriented towards the carbohydrate *C*-1 (related to **36-b**), and possible reasons could involve unfavorable interactions between the anionic complex ligands, and the carbohydrate ring oxygen lone pairs. However, the side differentiation seems to be rather weak, as expressed by significant concomitant formation of minor epoxide **(7*S*,8*S*)-53**.

In analogy to the formation of spirocarbonate **41** (**Scheme 4.22** on page 95), epoxide **(7*R*,8*R*)-57** was reacted with diphosgene, and the sensitive spiro-epoxycarbonate **(7*R*,8*R*)-61 (Scheme 4.31)** could be isolated in 81% yield after recrystallization.

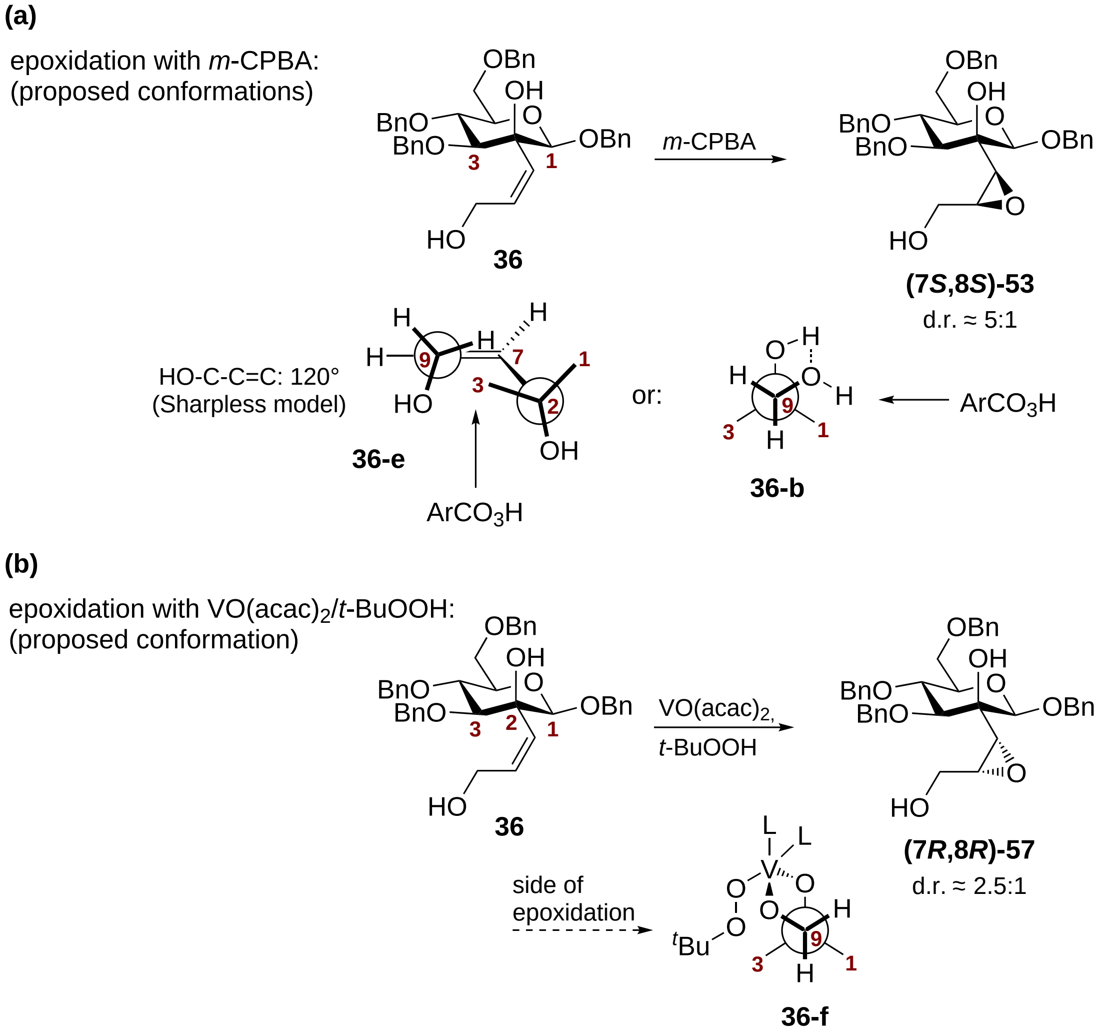
(a)
epoxidation with m-CPBA:
(proposed conformations)
OBn
OH
O
BnO
BnO
OBn
3
1
HO
36
m-CPBA
(7S,8S)-53
d.r. ≈ 5:1
HO-C-C=C: 120°
(Sharpless model)
H
H
H
9
7
3
1
2
HO
OH
36-e
ArCO3H
or:
O
H
O
H
H
9
3
1
H
36-b
ArCO3H
(b)
epoxidation with VO(acac)2/t-BuOOH:
(proposed conformation)
3
2
1
36
VO(acac)2,
t-BuOOH
(7R,8R)-57
d.r. ≈ 2.5:1
side of
epoxidation
L
L
V
O
O
O
O
tBu
H
9
3
1
H
36-f

Scheme 4.30 (a) Proposed conformations **36-e** or **36-b** for the epoxidation of **36** with *m*-CPBA, giving major epoxide **(7*S*,8*S*)-53**. (b) Proposed conformation **36-f** for the formation of major epoxide **(7*R*,8*R*)-57** in the epoxidation of **36** with VO(acac)$_2$/*t*-BuOOH. L = available ligand, e.g. *t*-BuO, acac.

Vapor diffusion of diethyl ether into the NMR sample of **(7*R*,8*R*)-61** in acetone-D_6 resulted in the crystallization of colorless plates suitable for X-ray crystallography. Crystalline **(7*R*,8*R*)-61** occupied the monoclinic space group $P2_1$, and $Z = 2$ formula units within the unit cell were found. An analysis of the molecular structure **(Fig. 4.9)** unambiguously confirmed the (7*R*,8*R*)-configurations of the side chain stereogenic centers of **(7*R*,8*R*)-61**, and thus, of the parent epoxide **(7*R*,8*R*)-57**. Apart from the presence of the epoxide, geometric properties of the seven-membered spirocarbonate moiety were found to be largely comparable to the structure of **41**, including an orientation of the carbonate functional group towards the anomeric oxygen (C9···O2 2.697 Å). Likewise, a near-planar arrangement of the former carbohydrate *C*-2-OH moiety and

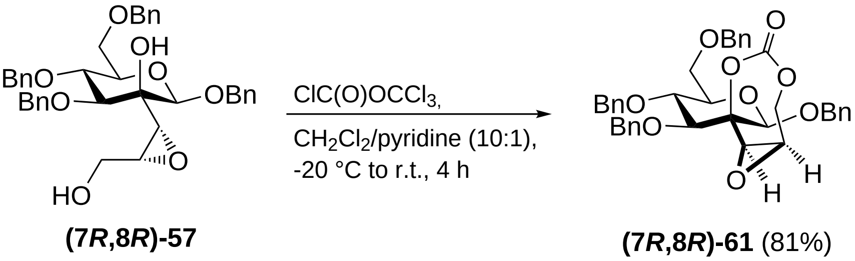

Scheme 4.31 Synthesis of spiro-epoxycarbonate **(7*R*,8*R*)-61** from epoxide **(7*R*,8*R*)-57**.

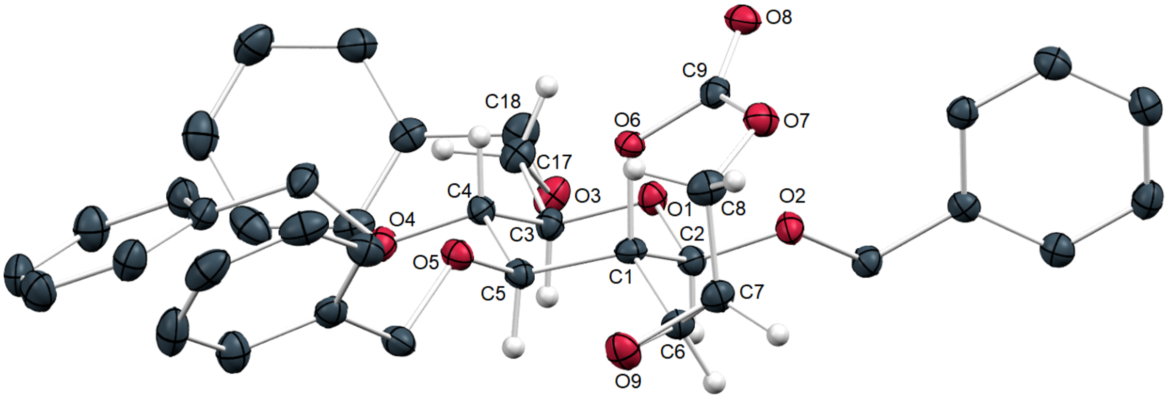

Figure 4.9 X-ray structure of spiro-epoxycarbonate **(7*R*,8*R*)-61**. Hydrogen atoms of the benzyl ethers are omitted for clarity. Ellipsoids are drawn at the 50% probability level. Red = oxygen, gray = carbon, white = hydrogen. Significant distances and torsion angles: C9···O2 2.697 Å, O6-C1-C6-C7 2.4°, C6-C7-C8-O7 −61.8°.

the side chain *C*-7/8/9 (in crystal structure numbering: O6, C1, C6, C7, C8) can be observed (comp. O6-C1-C6-C7 2.4°), with the former side chain *C*-9-OH involved in the carbonate functional group outside of this planar arrangement (C6-C7-C8-O7 −61.8°).

In following synthetic experiments, both diastereomeric epoxides **(7*S*,8*S*)-53** and **(7*R*,8*R*)-57** were subjected to conditions for nucleophilic epoxide opening for the anticipated formation of a side chain *anti*-diol moiety. In this regard, both acidic conditions (cat. *p*-TsOH in H_2O/THF, or: cat. $Sc(OTf)_3$ in H_2O/1,4-dioxane) and basic conditions (KOH in H_2O/1,4-dioxane, or: TBAF in H_2O/MeCN) were tested. However, in all cases, elevated temperatures were required to invoke a conversion, and the reactions resulted in inseparable complex mixtures of products. Likewise, for other reported epoxyalcohols in higher sugars, epoxide opening reactions have been described to be erratic.[164] To explain these observations, several potential side reactions have to be considered. Epoxide opening reactions of α-epoxy alcohols usually occur *via* regioselective attack at the β-position, and attack at the α-position is usually disfavored.[205] For steric reasons, in epoxides **(7*S*,8*S*)-53**/**(7*R*,8*R*)-57**, attack at the side chain *C*-8 seemed to be more plausible. However, competitive opening at *C*-7 would result in the concomitant formation of the diastereomeric *anti*-isomer. Furthermore, intramolecular side reactions have to be considered. Under forceful conditions, the unwanted cyclization of the 1,4-dihydroxy moiety to a spiro-tetrahydrofuran product seems to be plausible (comp. compound **(7*S*,8*S*)-49** on page 108), either with intact epoxide moiety, or from the wanted diol product. Apart from this, Payne rearrangement processes (epoxide migrations) are ubiquitous side reactions of epoxy alcohols under acidic or basic conditions.[206] Either initiated from the side chain *C*-9-OH, or from the carbohydrate *C*-2-OH, Payne rearrangements could result in the formation of isomeric epoxides, potentially leading to multiple derived epoxide opening or decomposition products of diverse stereochemistry.

As a result of these unsuccessful attempts for the direct epoxide opening, the introduction of protecting groups for the free hydroxyl groups of the epoxide substrates was anticipated to reduce the number of potential side reactions. For that purpose, acetylation of the primary *C*-9-OH in **(7*S*,8*S*)-53** and **(7*R*,8*R*)-57** (**Scheme 4.29** on page 114) was achieved under mild conditions (stoichiometric Et_3N/Ac_2O, cat. DMAP in MeCN at 0 °C), and gave the primary acetates **(7*S*,8*S*)-54** and **(7*R*,8*R*)-58**, respectively. Acetylation of the tertiary *C*-2-OH functionality was found to require harsh conditions in the case of other *C*-2-branched derivatives (comp. compound **24** on page 87), and was thus not performed with the sensitive epoxide substrates. For the following epoxide opening reactions of epoxyacetates **(7*S*,8*S*)-54** and **(7*R*,8*R*)-58**, basic conditions were anticipated to result in saponification of the acetate moiety, and thus acidic conditions were applied. Heating of **(7*S*,8*S*)-54** in a mixture of $AcOH/Ac_2O$ (1:1) at 105 °C, a method anticipated to give the fully acetylated product of the epoxide opening, resulted in the formation of one major product. The same product, albeit in a cleaner reaction, was formed when trimethylsilyl acetate (TMSOAc, 2 equiv.) was added to the reaction mixture as an additional Lewis acid. However, complete characterization of the product confirmed the structure of acetylated spiro-tetrahydrofuran **(7*S*,8*R*)-55**, obviously formed by intramolecular displacement of the *C*-9-acetate leaving group by the *C*-2-OH. Zemplén deacetylation of the *anti*-configured diacetate **(7*S*,8*R*)-55** provided **(7*S*,8*R*)-56**, which could be determined to be a stereoisomer of *syn*-configured spiro-tetrahydrofuran **(7*S*,8*S*)-49** (**Table 4.3** on page 108) by its spectral properties. From diastereomeric epoxyacetate **(7*R*,8*R*)-58**, similar conditions for epoxide opening gave the isomeric cyclization product **(7*R*,8*S*)-59**, or, after deprotection of the *anti*-diacetate, spiro-tetrahydrofuran **(7*R*,8*S*)-60**.

Due to the observed difficulties in the epoxide opening reactions, in a potential alternative to the planned synthetic route, oxidation of the primary hydroxyl group in

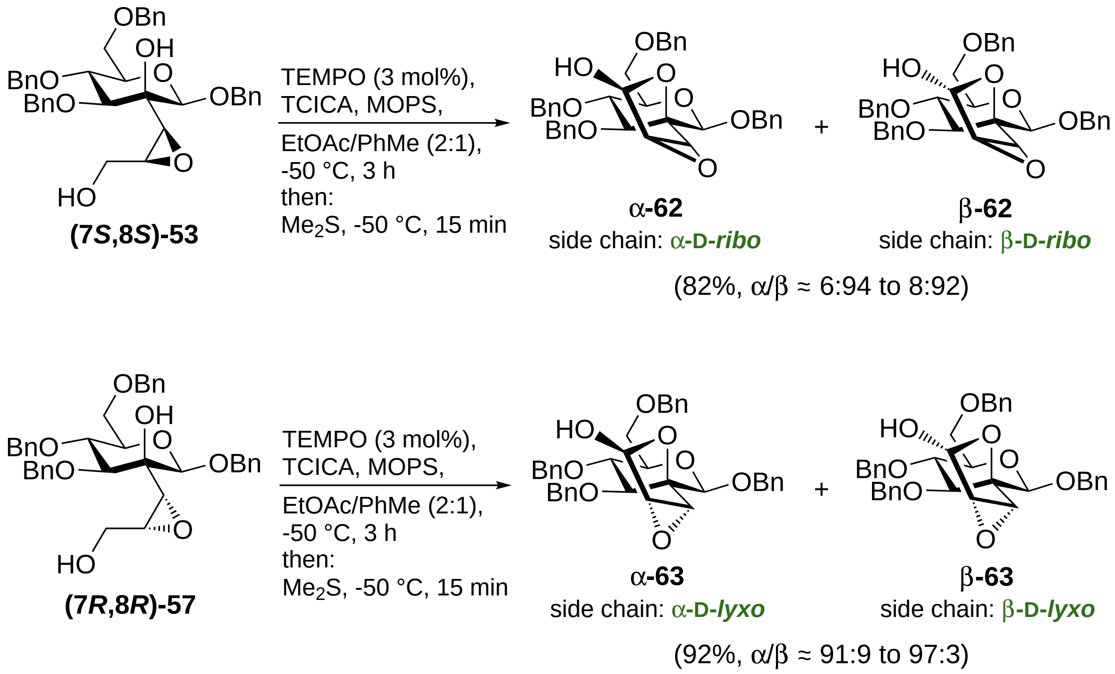

(7*S*,8*S*)-53 **α-62** **β-62**

(7*R*,8*R*)-57 **α-63** **β-63**

Scheme 4.32 Oxidative formation of 2,3-anhydro-ribofuranose **α,β-62** and 2,3-anhydro-lyxofuranose **α,β-63**. Anomeric ratios are given in acetone-D_6.

epoxides **(7*S*,8*S*)-53** and **(7*R*,8*R*)-57** to the corresponding aldehydes/lactols could be performed prior to epoxide opening. For this transformation, due to the absence of interfering secondary alcohols in the epoxide substrates, a variety of established oxidation methods like Dess-Martin oxidation or methods with activated DMSO seemed to be applicable. However, to further explore the developed oxidation protocol with TEMPO/TCICA in the presence of MOPS as a buffer, this method was used. Oxidation of **(7*S*,8*S*)-53** under the established conditions **(Scheme 4.32)** gave 2,3-anhydro-ribofuranose **α,β-62**, which could be isolated in good yield (82%). Likewise, under the same conditions, **(7*R*,8*R*)-57** was transformed into 2,3-anhydro-lyxofuranose **α,β-63** in an excellent 92% yield. Both reactions proceeded cleanly and with relatively fast conversions at low temperature (−50 °C, 3 h), demonstrating the potential applicability of the described oxidation protocol as a generally useful transformation. For both **α,β-62** and **α,β-63**, the respective 1,2-*trans*-isomer could be identified to be the major anomer (**β-62** and **α-63**, respectively) in acetone-D_6. The anomeric configurations could be deduced from the direct anomeric $^1J_{\mathrm{C9,H9}}$ coupling constants **(Fig. 4.10)** of the major isomers (**β-62**: 174.5, **α-63**: 174.3 Hz). The obtained values were fully consistent with published data on 2,3-anhydrofuranosides, which suggested coupling constants generally above 170 Hz in the case of 1,2-*trans*-relationships (1,2-*trans*: 171–174, 1,2-*cis*: 163–168 Hz).[207, 208] Apart from this, further confirmation for the anomeric configuration

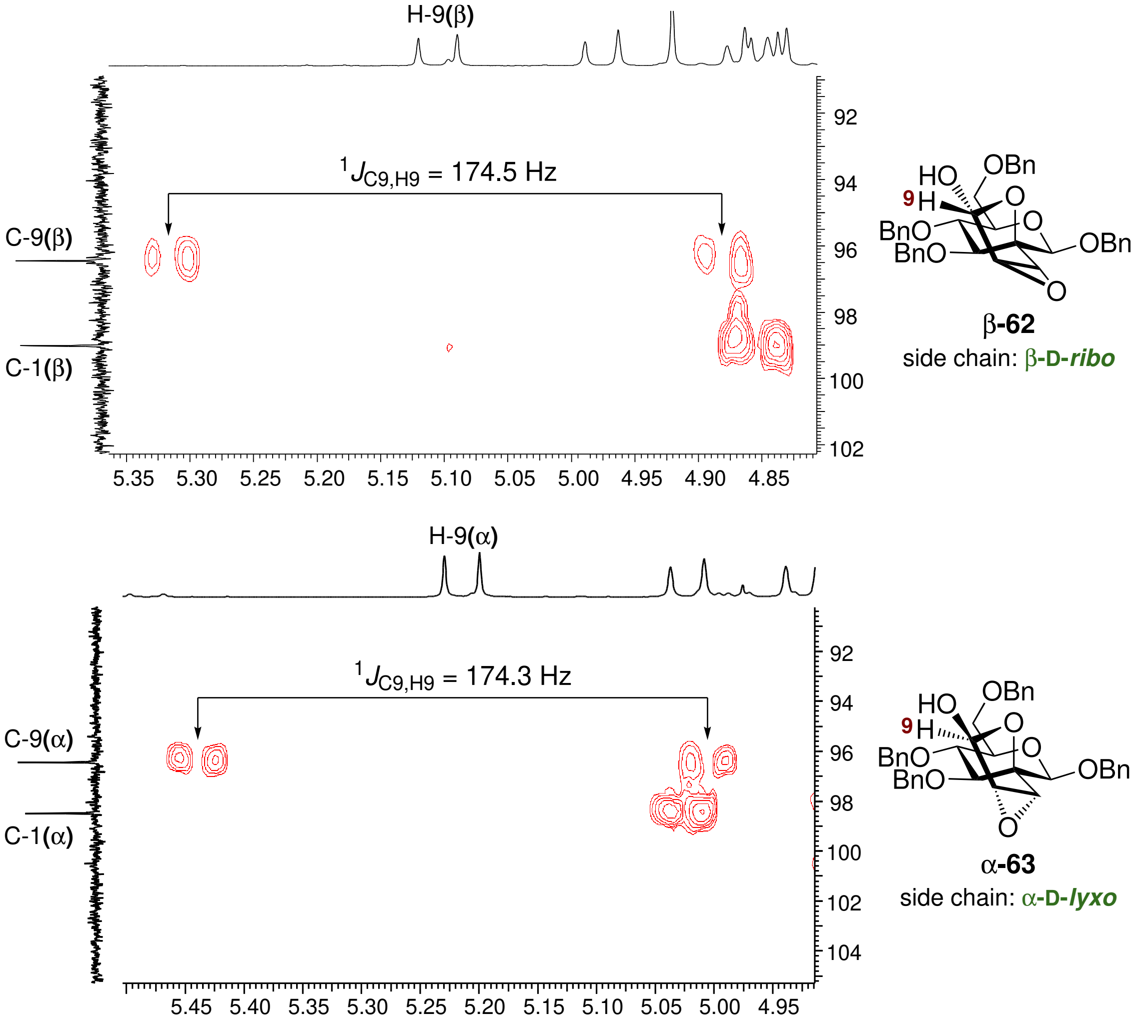

Figure 4.10 Sections of the C,H-HMBC spectra of **α,β-62** (top) and **α,β-63** (bottom) at 100.6 MHz/400.2 MHz in acetone-D_6. Visible residual signals of the $^1J_{\mathrm{C9,H9}}$ couplings of the major isomers are labeled, and were used to determine the values of the direct coupling constants.

of **α,β-63** could be obtained by X-ray structural analysis of a crystallized sample of the compound (monoclinic, $P2_1$, Z = 2). The molecular structure **(Fig. 4.11)** gave final confirmation for the anomeric α-configuration of the reducing furanose moiety. In a subsequent experiment, the crystalline sample of **α-63** was redissolved in acetone-D_6, and NMR analysis was performed in quick succession to minimize equilibration of the sample. The obtained ^{1}H NMR spectrum was ascribed to the α-isomer **α-63**, virtually in isomeric purity, which gave complete confirmation for the anomeric α-configuration both in solution and in the solid state.

Unfortunately, with 2,3-anhydrofuranoses **α,β-62** and **α,β-63** all efforts for epoxide opening, under similar conditions as given above for **(7*S*,8*S*)-53** and **(7*R*,8*R*)-57**,

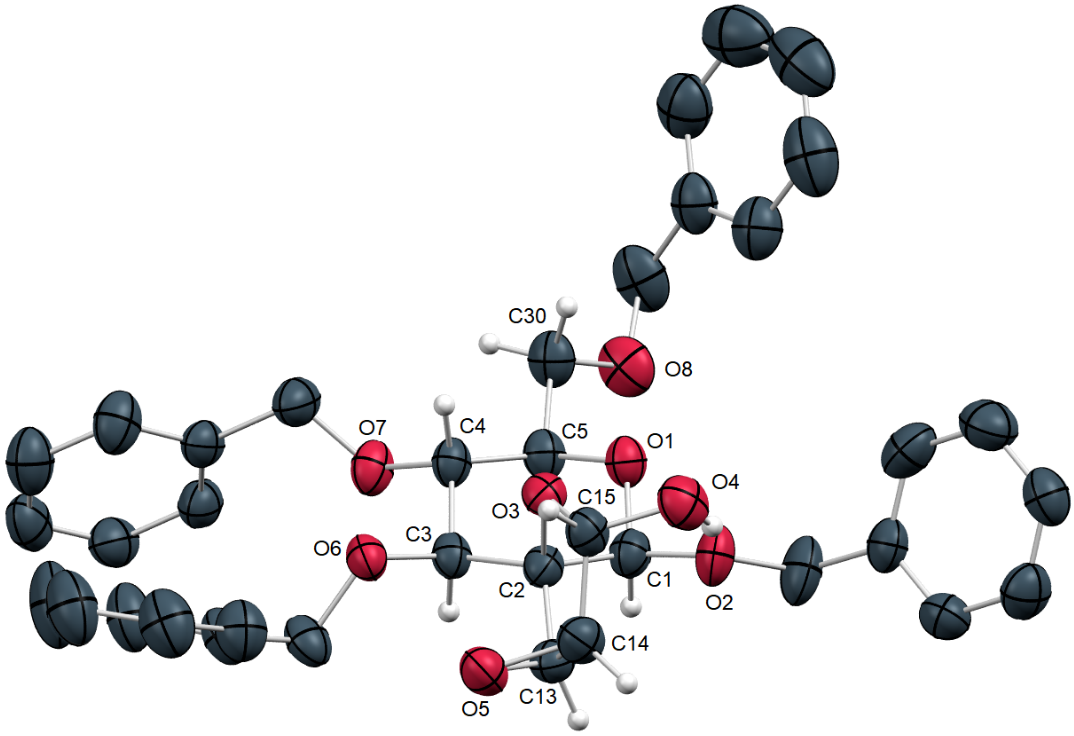

Figure 4.11 X-ray structure of compound **α-63**. Hydrogen atoms of the benzyl ethers and a disorder involving the *C*-3 benzyl group are omitted for clarity. Ellipsoids are drawn at the 50% probability level. Red = oxygen, gray = carbon, white = hydrogen.

failed due to unspecific decomposition of the starting anhydrofuranoses. As a result, another synthetic strategy was pursued in following experiments. Several Lewis acid-mediated methods have been developed for the direct conversion of acetone solutions of epoxide substrates into 1,2-acetonides as diol equivalents. The published methods include, amongst others, metal-based Lewis acids such as $SnCl_2$[209], $Er(OTf)_3$[210], MoO_2Cl_2[211], $CuSO_4$[212], or gold-based methods[213]. A survey for synthetic applications of these methods revealed a promising example published by Fuchs and Coworkers, which involved the $SnCl_2$-mediated epoxide opening of an epoxide-branched free hemiacetal carbohydrate derivative, for which other methods were unsuccessful.[214] When epoxide **(7*R*,8*R*)-57** (the major isomer resulting from epoxidation with $VO(acac)_2$/*t*-BuOOH) was reacted under conditions similar to those of Fuchs and Coworkers (30 mol% $SnCl_2$ in acetone at 55 °C), a mixture of multiple products was formed **(Scheme 4.33)**. Chromatographic purification of the mixture provided diacetonide **(7*R*,8*S*)-64** (28% yield), major monoacetonide **(7*R*,8*S*)-65** (44%), and minor monoacetonide **(7*R*,8*S*)-66** (15%), and the three *anti*-diol derivatives could

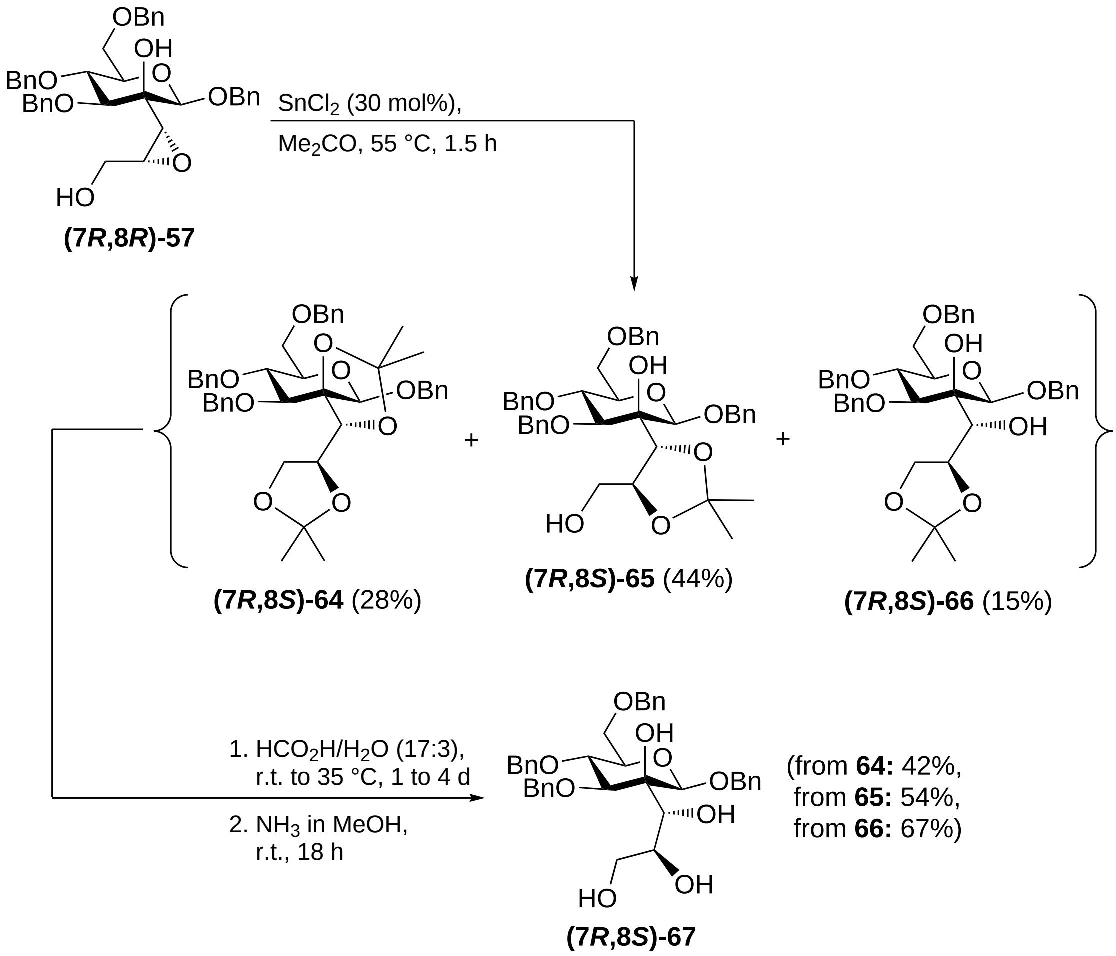
(7*R*,8*R*)-57
$SnCl_2$ (30 mol%),
Me_2CO, 55 °C, 1.5 h
(7*R*,8*S*)-64 (28%)
+
(7*R*,8*S*)-65 (44%)
+
(7*R*,8*S*)-66 (15%)
1. HCO_2H/H_2O (17:3), r.t. to 35 °C, 1 to 4 d
2. NH_3 in MeOH, r.t., 18 h
(7*R*,8*S*)-67
(from 64: 42%, from 65: 54%, from 66: 67%)

Scheme 4.33 Synthesis of *anti*-intermediate **(7*R*,8*S*)-67** from epoxide **(7*R*,8*R*)-57** *via* a sequence of $SnCl_2$-mediated epoxide opening and acetonide hydrolysis/formate cleavage.

be isolated and independently characterized in pure form. Attempts to enforce the complete conversion to diacetonide **(7*R*,8*S*)-64** over prolonged reaction times met with failure, since increased amounts of degradation products were obtained, and interfered with chromatographic separation of the acetonides. In the following step, which was performed for each individual acetonide derivative in an independent reaction, the anticipated hydrolytic acetal cleavages proved to be challenging. In several experiments (80% AcOH at 50 °C, or: cat. *p*-TsOH in 1,4-dioxane/H_2O at 80 °C, or: 1 M HCl/THF at 45 °C), severe decomposition of the acetonide substrates could be observed, putatively resulting from acidic debenzylation reactions, or from intramolecular reactions like the previously observed 1,4-diol cyclization (tetrahydrofuran formation). Best results were obtained upon mild hydrolysis of the acetonides in a mixture of formic acid and water, a method which has been reported before.[215, 216] The obtained crude

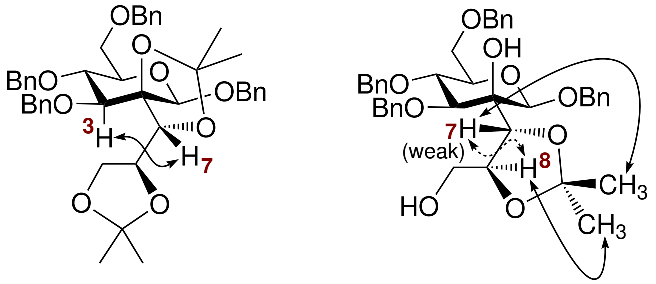

(7*R*,8*S*)-64 **(7*R*,8*S*)-65**

Scheme 4.34 Schematic representation of significant NOE contacts observed in H,H-NOESY experiments of diacetonide **(7*R*,8*S*)-64** and monoacetonide **(7*R*,8*S*)-65**.

mixtures of intermediate formates were deacylated in a successive step (NH_3 in MeOH), thus providing the wanted *anti*-diol intermediate **(7*R*,8*S*)-67** in satisfactory yields (42–67%). Notably, the identical product **(7*R*,8*S*)-67** was independently obtained from all three acetonides, therefore confirming the identical side chain configurations. The (7*R*,8*S*)-configuration of **(7*R*,8*S*)-67** was previously anticipated, since nucleophilic epoxide opening was assumed to occur selectively at the *C*-8 position due to steric factors related to the bulky carbohydrate moiety. Additionally, experimental evidence for the ascribed configuration could conveniently be obtained from H,H-NOESY experiments of the acetonide intermediates, which allowed for the determination of significant NOE contacts **(Scheme 4.34)** due to the conformationally locked nature of the cyclic acetal moieties. The (7*R*)-configuration was evident from a distinctive correlation between the axial carbohydrate *H*-3 and the side chain *H*-7 observed in the 2,7-locked diacetonide **(7*R*,8*S*)-64**. The respective (8*S*)-configuration followed from NOE contacts observed for the 7,8-locked monoacetonide **(7*R*,8*S*)-65**. An only weak *H*-7–*H*-8 correlation suggested the presence of an *anti*-realtionship. Furthermore, the two diastereotopic methyl groups of the isopropylidene moiety exhibited weak but visible NOE contacts to either the *H*-7, or the *H*-8, respectively, as would be expected in the given *anti*-configuration. These spectral properties, together with the transformation of all acetonides into one single deprotected product **(7*R*,8*S*)-67**, gave confirmation for the ascribed (7*R*,8*S*)-configuration.

In the final stages of the synthesis, advanced intermediate **(7*R*,8*S*)-67** was subjected to the previously developed TEMPO-based oxidation protocol to obtain spiroxylofuranose **α,β-68** **(Scheme 4.35)**. Surprisingly, under the conditions established for the *syn*-intermediates, overoxidation to xylonolactone **(7*R*,8*R*)-69** (84% yield) was the major pathway, and only minor amounts of **α,β-68** (6%) could be isolated. Running the reaction at lower temperature (−65 °C) retarded the overoxidation to some

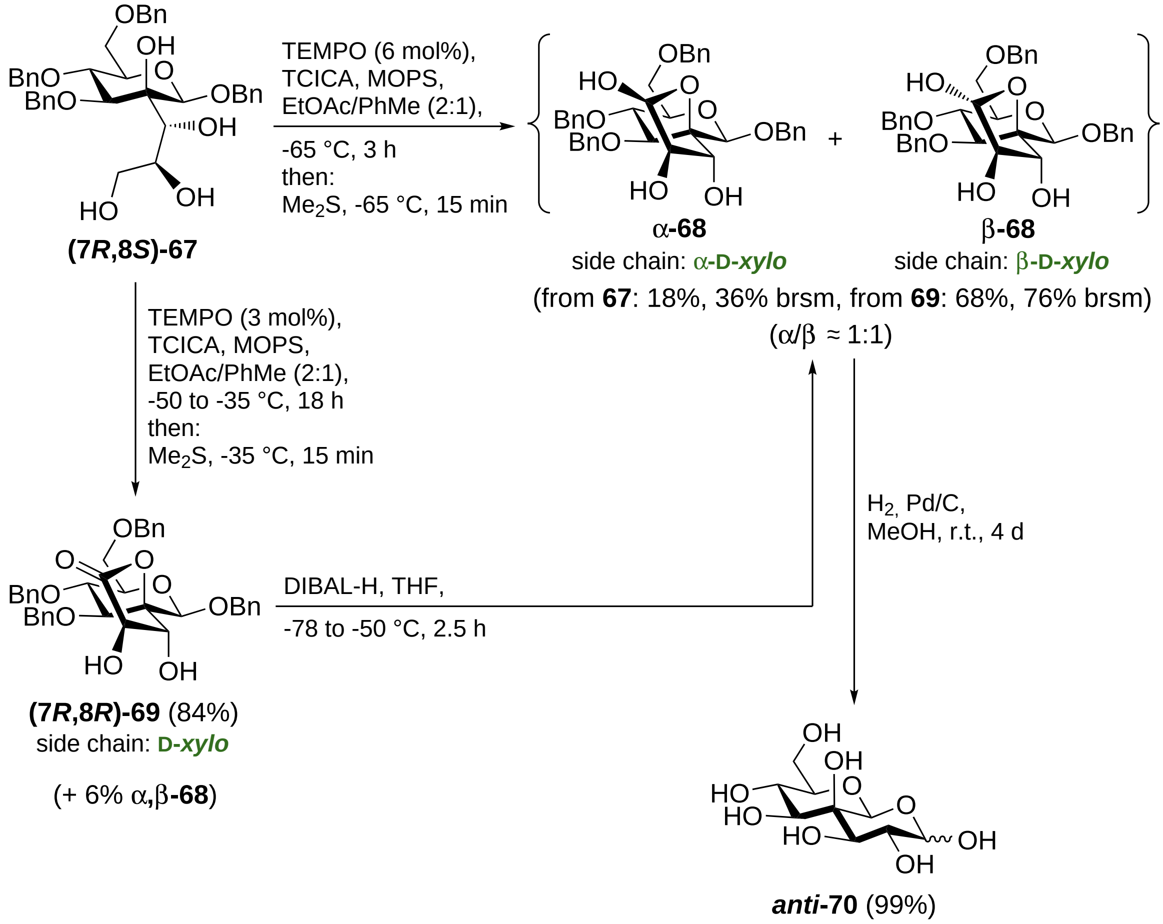
(7R,8S)-67
TEMPO (6 mol%), TCICA, MOPS, EtOAc/PhMe (2:1),
-65 °C, 3 h then: Me2S, -65 °C, 15 min
α-68
side chain: α-D-xylo
β-68
side chain: β-D-xylo
(from 67: 18%, 36% brsm, from 69: 68%, 76% brsm)
(α/β ≈ 1:1)
TEMPO (3 mol%), TCICA, MOPS, EtOAc/PhMe (2:1), -50 to -35 °C, 18 h then: Me2S, -35 °C, 15 min
(7R,8R)-69 (84%)
side chain: D-xylo
(+ 6% α,β-68)
DIBAL-H, THF,
-78 to -50 °C, 2.5 h
H2, Pd/C, MeOH, r.t., 4 d
anti-70 (99%)

Scheme 4.35 Oxidation of **(7*R*,8*S*)-67** to spiro-xylofuranose **α,β-68** in low yield, overoxidation to xylonolactone **(7*R*,8*R*)-69**, and deprotection to target 4-*C*-formyl octose ***anti*-70**. Anomeric ratios are given in acetone-D_6. For clarity, ***anti*-70** is depicted in the (9*S*)-9,7-pyranose-1,9-pyranose isomeric form.

degree, and upon interruption of the reaction at incomplete conversion, **α,β-68** could be obtained in higher, but still mediocre yield (18%, 36% brsm). Interestingly, for the corresponding *syn*-isomers, lactone formation did not occur to a significant amount. Obviously, the presence of the 7,8-*anti*-diol dramatically changes the susceptibility of **(7*R*,8*S*)-67** towards oxidation to the lactone. This observation seems to be somewhat in line with results by Yu and Molinaro in their total synthesis of bradyrhizose **K**.[14] In the published reaction, the authors observed overoxidation of substrate **DV**, also carrying a 2,3-*anti*-diol moiety, to the gluconolactone derivative **EV** (**Scheme 4.27, (c)**, on page 106). For the observed formation of xylonolactone **(7*R*,8*R*)-69**, an explanation for the altered reactivity in connection with the 7,8-*anti*-diol functionality seems to be intricate. A discussion of effects could involve, for example: (i) An increased nucleophilicity/basicity of the hemiacetal hydroxyl group in **α,β-68** involved (possibly in deprotonated form) in nucleophilic attack on the TEMPO-derived oxoammonium ion. (ii) Disfavored stabilizing hydrogen-bonding interactions in substrate **α,β-68**, or favored stabilizing hydrogen-bonding interactions in the product **(7*R*,8*R*)-69** or in the transition state of its formation, respectively, due to geometric circumstances. (iii) The putatively lower overall dipole moment of the *anti*-diol **(7*R*,8*R*)-69**, or of the transition state of its formation, as compared to the *syn*-derivatives. (iv) Stereoelectronic effects, e.g. hyperconjugative effects specifically viable in the *anti*-diol configuration. However, in this regard, further studies are required to determine a possible generality of these experimental observations concerning the oxidation behavior.

To provide sufficient material of the wanted spiro-xylofuranose **α,β-68**, lactone **(7*R*,8*R*)-69** was treated with DIBAL-H in THF at −78 °C. In this way, **α,β-68** was available in reasonable yield (68% from **69**), and amenable to full NMR characterization of the mixture of anomers (d.r. ≈ 1:1 in acetone-D_6). Although the configurations of the side chain stereogenic centers were indirectly concluded from NMR observations for the acetonides **64/65** (see above), an independent confirmation for the stereochemistry of **α,β-68** could be obtained from 2D NMR analyses. The (7*R*)-configuration followed from distinctive NOE contacts between the carbohydrate *H*-1 and *H*-7, and from the absence of corresponding NOE contacts between *H*-7–*H*-3 (**Fig. D.6** on page 309). Based on this, the (8*R*)-configuration was directly evident, since the sample was spectroscopically clearly distinguishable from the second (7*R*)-isomer **α,β-51**. The anomeric configurations could be established by significant magnitudes of vicinal coupling constants within the side chain, together with a comparison of ^{13}C NMR chemical shift values of the anomeric *C*-9 signals, which were found to be in sufficiently good agreement with those found for **α,β-48** with identical (8*R*)-configuration [**α,β-68**: 96.0 (α), 103.5 (β); **α,β-48**: 98.9 (α), 103.6 (β) ppm]. To complete the synthesis, **α,β-68** was deprotected, giving target compound ***anti*-70** in a completely analogous manner as previously described for the corresponding *syn*-isomers. The synthesis of ***anti*-70** proceeded in a total of 16 steps from D-glucose, and in 11 steps (13% yield) from the known *keto*-sugar **2b**.

Having established a synthesis for three target compounds (***syn*-50**, ***syn*-52** and ***anti*-70**), the remaining fourth isomer was anticipated to be available from the second epoxide isomer. Treatment of **(7*S*,8*S*)-53** under the conditions that were successfully applied to its isomer (cat. $SnCl_2$ in acetone) required somewhat lower loadings of the Lewis acid (10 mol% instead of 30 mol%) to react in a clean manner. Surprisingly, as opposed to the transformation of **(7*R*,8*R*)-57**, the formation of one major species was observable, essentially as the only significant product of the reaction in 68% yield **(Scheme 4.36)**. Complete characterization of the purified product revealed several

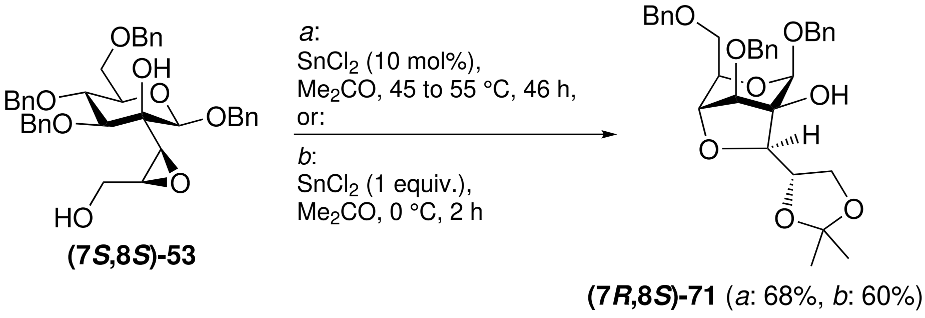

Scheme 4.36 Formation of bicyclic, conformationally locked $^1C_4$ pyranose **(7*R*,8*S*)-71** from epoxide **(7*S*,8*S*)-53**.

unexpected spectral properties that finally resulted in the ascribed structure **(7*R*,8*S*)-71**, which can be described as a $^1C_4$ system, which is conformationally locked by a linkage between the carbohydrate *O*-4 and the side chain *C*-7, thus forming a bicyclic framework with the carbohydrate substituents at positions 1,3,5 in triaxial orientation. The unusual structure of **(7*R*,8*S*)-71** could be established from the following analytical properties (for additional clarification, see **Scheme 4.37**): the loss of one benzyl group was evident from the mass spectra, as well as from ^{1}H NMR integration, which indicated the presence of 15 aromatic protons. C,H-HMBC measurements confirmed the positions of the remaining benzyl groups at *O*-1,3,6, and furthermore indicated the depicted *O*-4–*C*-7 ring closure by a distinct *H*-4–*C*-7 coupling. The $^1C_4$ conformation of the parent carbohydrate moiety followed tentatively, since the bridging *O*-4–*C*-7 connection would not be feasible for the bis(equatorial) orientation in a $^4C_1$ pyranose form. Spectroscopic evidence for a $^1C_4$-like conformation was a small coupling constant $J_{4,5} = 2.6$ Hz, which was inconsistent with a 1,2-diaxial, and rather suggestive for a 1,2-equatorial relationship. Likewise, the coupling constant $J_{3,4} = 5.7$ Hz was smaller than conventionally anticipated for *manno*-configured pyranoses, but larger than expected for a clean bis(equatorial) orientation[128], therefore indicating a distortion of the $^1C_4$ chair geometry probably caused by the rigid 2,4-connecting bicyclic framework. Similarly, distinct NOE contacts between *H*-3,4,5 were significant for spatial proximity and inconsistent with *trans*-diaxial relationships. The configuration of the side chain *C*-7 followed from a strong correlation between *H*-7 and the equatorial *H*-1. The determination of the (8*S*)-configuration required a detailed analysis of long-range NOE contacts (not shown) observed for the diastereotopic methyl groups of the acetonide moiety, in combination with a distinct *H*-3–*H*-8 correlation (as indicated in **Scheme 4.37**).

Since the reaction of **(7*S*,8*S*)-53** in the presence of 10 mol% $SnCl_2$ required prolonged reaction times (46 h at 45–55 °C) for complete conversion, a second experiment was conducted in the presence of equimolar amounts of the Lewis acid (**Scheme 4.36**, reaction

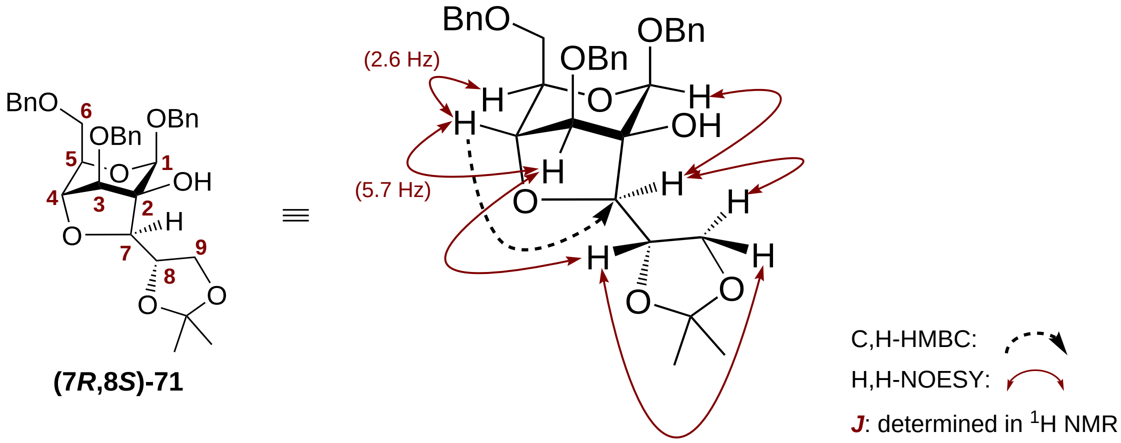

(7*R*,8*S*)-71

Scheme 4.37 Schematic representation of selected correlations in H,H-NOESY (red solid arrow) and C,H-HMBC (dashed black arrow) experiments as observed for **(7*R*,8*S*)-71**. Given values for coupling constants were determined in the ^{1}H NMR spectrum.

b). In this case, complete conversion of the epoxide occurred at 0 °C after 2 h, albeit, the isolated product was, similarly, **(7*R*,8*S*)-71** (60% yield). Concludingly, an extended optimization of the conditions for the desired reaction seemed to be futile, since formation of the unwanted product **(7*R*,8*S*)-71** was observed under two distinctly different conditions. To explain the unusual reaction, plausible mechanistic pictures were developed based on the following rationale: in epoxide **(7*S*,8*S*)-53**, direct epoxide opening at *C*-8 seems to be less favorable as compared to diastereomeric epoxide **(7*R*,8*R*)-57**, possibly due to conformational circumstances. Therefore, longer reaction times or higher loadings of Lewis acid are required, and deprotection/rearrangement steps occur. One possible mechanism **(Scheme 4.38, left)** could involve the formation of the oxetane **53-a** *via* intramolecular $SnCl_2$-mediated displacement of the *C*-4-benzyloxy group. In the putative oxetane intermediate, the epoxide could be converted into the anticipated 7,8-acetonide **53-b** *via* attack at *C*-7, resulting in the required (7*R*,8*S*)-stereochemistry. In the final step, acetonide migration to the *C*-8,9 position and oxetane opening by the liberated *O*-7 would give the product **(7*R*,8*S*)-71**. However, both the initial oxetane formation step, and the oxetane opening step by the remote *O*-7 of the equatorial side chain, seem to be questionable. Another mechanism **(Scheme 4.38, right)** could involve Lewis acid-catalyzed formation of an activated *C*-9 hemiacetal species **53-c**. This intermediate could be trapped intramolecularly by the remote *O*-4, accompanied by nucleophile-assisted debenzylation. Due to the nine-membered cyclic acetonide moiety in **53-d**, a $^1C_4$-like conformation of the pyranose moiety could be feasible, leading to a prearranged structure with *O*-4 and the intact epoxide in spatial proximity. Thus, a

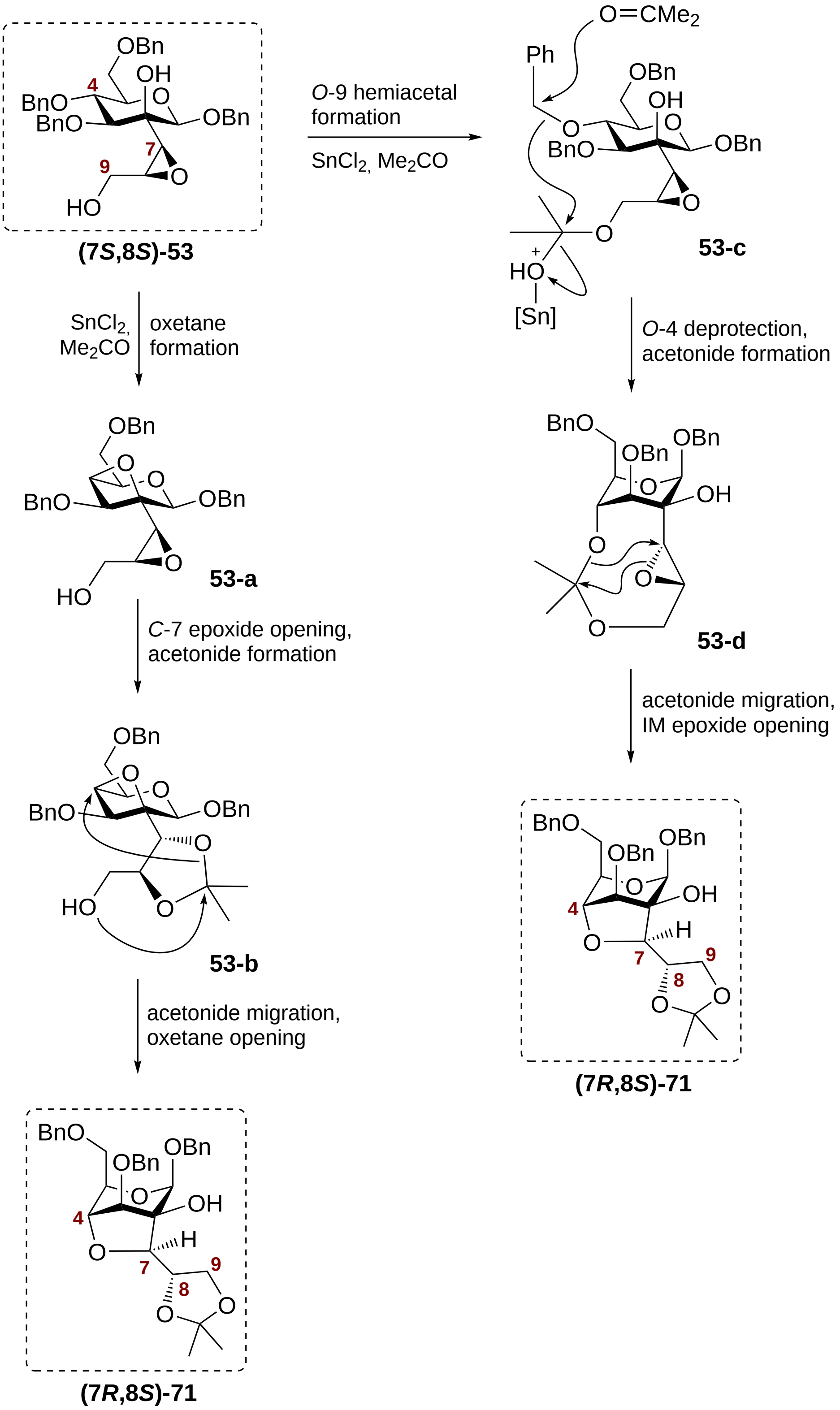
(7S,8S)-53
O-9 hemiacetal formation
SnCl2, Me2CO
53-c
SnCl2, Me2CO
oxetane formation
O-4 deprotection, acetonide formation
53-a
53-d
C-7 epoxide opening, acetonide formation
acetonide migration, IM epoxide opening
53-b
(7R,8S)-71
acetonide migration, oxetane opening
(7R,8S)-71

Scheme 4.38 Plausible mechanistic suggestions for the formation of **(7*R*,8*S*)-71** from epoxide **(7*S*,8*S*)-53**.

Lewis acid-mediated cascade, featuring epoxide opening by *O*-4 and acetonide migration to *C*-8,9 could result in the formation of **(7*R*,8*S*)-71**.

In following experiments, other Lewis acids were explored for the transformation of epoxide **(7*S*,8*S*)-53** under otherwise similar conditions in acetone. However, all reactions either resulted in complex inseparable mixtures of products ($Er(OTf)_3$[210], MoO_2Cl_2[211], $Sn(OTf)_2$), or did not lead to any visible transformation of the epoxide (SnF_2). Since a synthesis of the most desirable *anti*-isomer ***anti*-70** with side chain configurations similar to those of the natural product bradyrhizose **K** was successfully developed, further investigations into the synthesis of the second *anti*-isomer were abandoned at this point.

4.5.4. Characterization of the Target Compounds

The obtained 4-*C*-formyl octoses ***syn*-50**, ***syn*-52** and ***anti*-70** were initially characterized by HR-ESI-TOF-MS (positive and negative mode), which confirmed the complete absence of partially benzylated residues in the products, and gave a preliminary indication for the purity of the compounds. Following this, all three target compounds were subjected to detailed NMR-based analyses in D_2O, upon which the ^1H NMR spectra once again confirmed the absence of aromatic impurities in the products. ***syn*-50**, ***syn*-52** and ***anti*-70** each exhibited highly complex NMR spectra, which indicated the presence of a large number of isomeric forms (>5 isomers) for each target compound. However, due to the complexity of the ^1H NMR spectra, as well as limited sensitivity of the ^{13}C NMR experiments, no precise absolute numbers can be given. Noteworthy, for ***syn*-50**, ***syn*-52** and ***anti*-70**, the presence of free aldehyde isomers could be ruled out, since the ^1H NMR spectra exhibited no corresponding deshielded signal significant for an aldehyde.

To support a following 2D NMR-based structural characterization of the major isomeric forms present in solution, a qualitative analysis of plausible isomeric forms was performed (**Scheme 4.39** and **Scheme 4.40**). From the open-chain dialdehyde form (depicted as ***syn*-50**), two pyranose ring closures are feasible (9,7-pyr and 1,5-pyr, **Scheme 4.39**). 9,7-Pyranose formation results in a number of possible following ring closures, for example the intuitively assumed “bradyrhizose-type“ (9*S*)-9,7-pyranose-1,9-pyranose isomeric form, resembling the major isomer of bradyrhizose **K** (comp. **Scheme 4.8** on page 70). Similarly, the bicyclic 9,7-pyranose-1,5-pyranose form and the spirocyclic 9,7-pyranose-1,4-furanose form (resembling the spirofuranose intermediates traversed in the synthesis) are related to the minor isomers identified for the natural product **K**. In this manner, several other potential isomeric forms can be derived

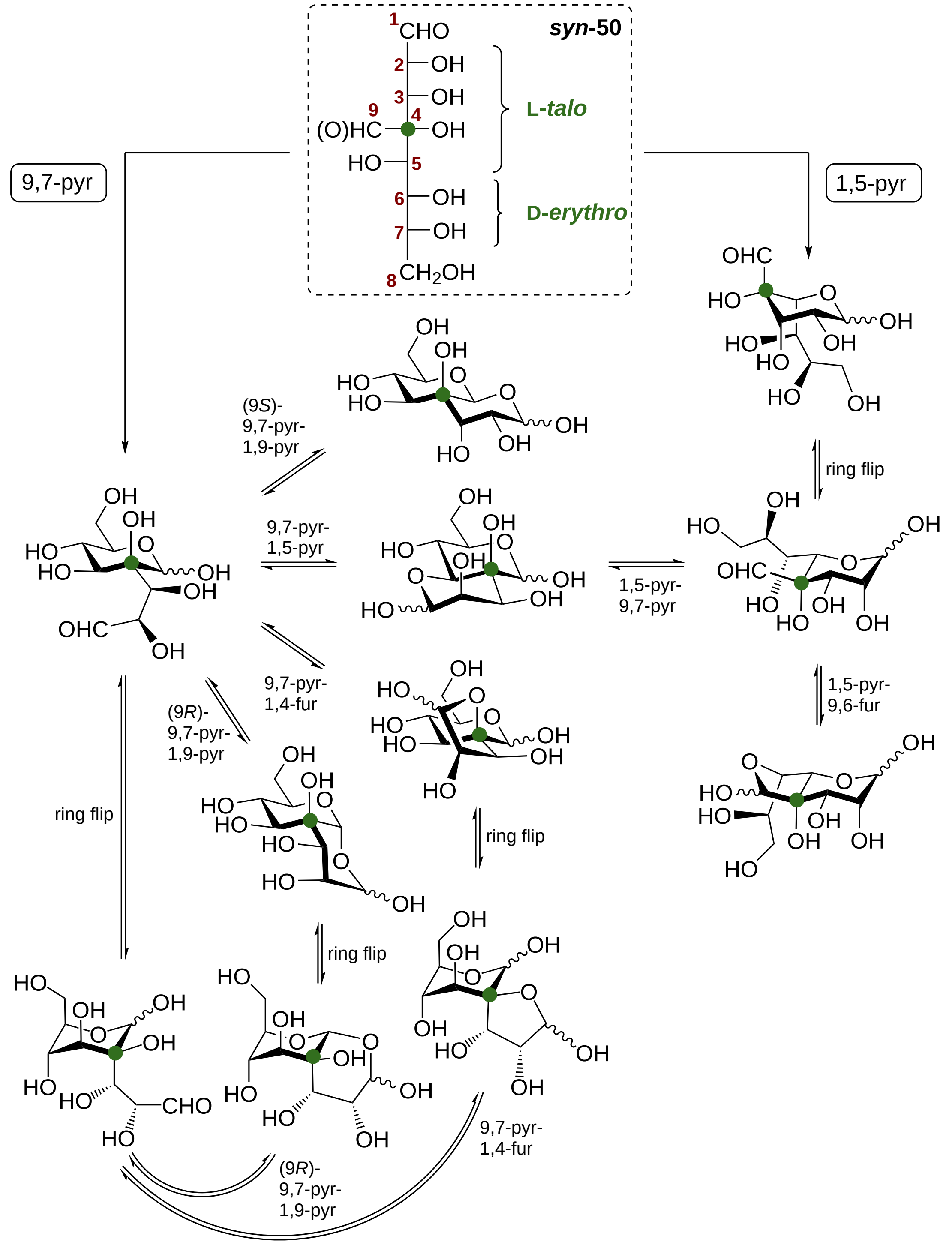
syn-50
1 CHO
2 OH
3 OH
9 (O)HC
4 OH
HO 5
6 OH
7 OH
8 CH2OH
L-talo
D-erythro
9,7-pyr
1,5-pyr
(9S)-9,7-pyr-1,9-pyr
9,7-pyr-1,5-pyr
1,5-pyr-9,7-pyr
9,7-pyr-1,4-fur
(9R)-9,7-pyr-1,9-pyr
ring flip
1,5-pyr-9,6-fur
OHC
CHO
HO
OH
O

Scheme 4.39 Analysis of plausible isomers of target compound ***syn*-50**. **Part I: Isomers including 9,7-pyranose and 1,5-pyranose isomeric forms.** Isomers are only given for free aldehydes, furanoses and pyranoses (not for bridged cycles). Ring flip (pyranoses only) as well as α/β-isomerism (wavy bond) is shown where possible. The quaternary *C*-4 is indicated with a green dot. pyr = pyranose, fur = furanose.

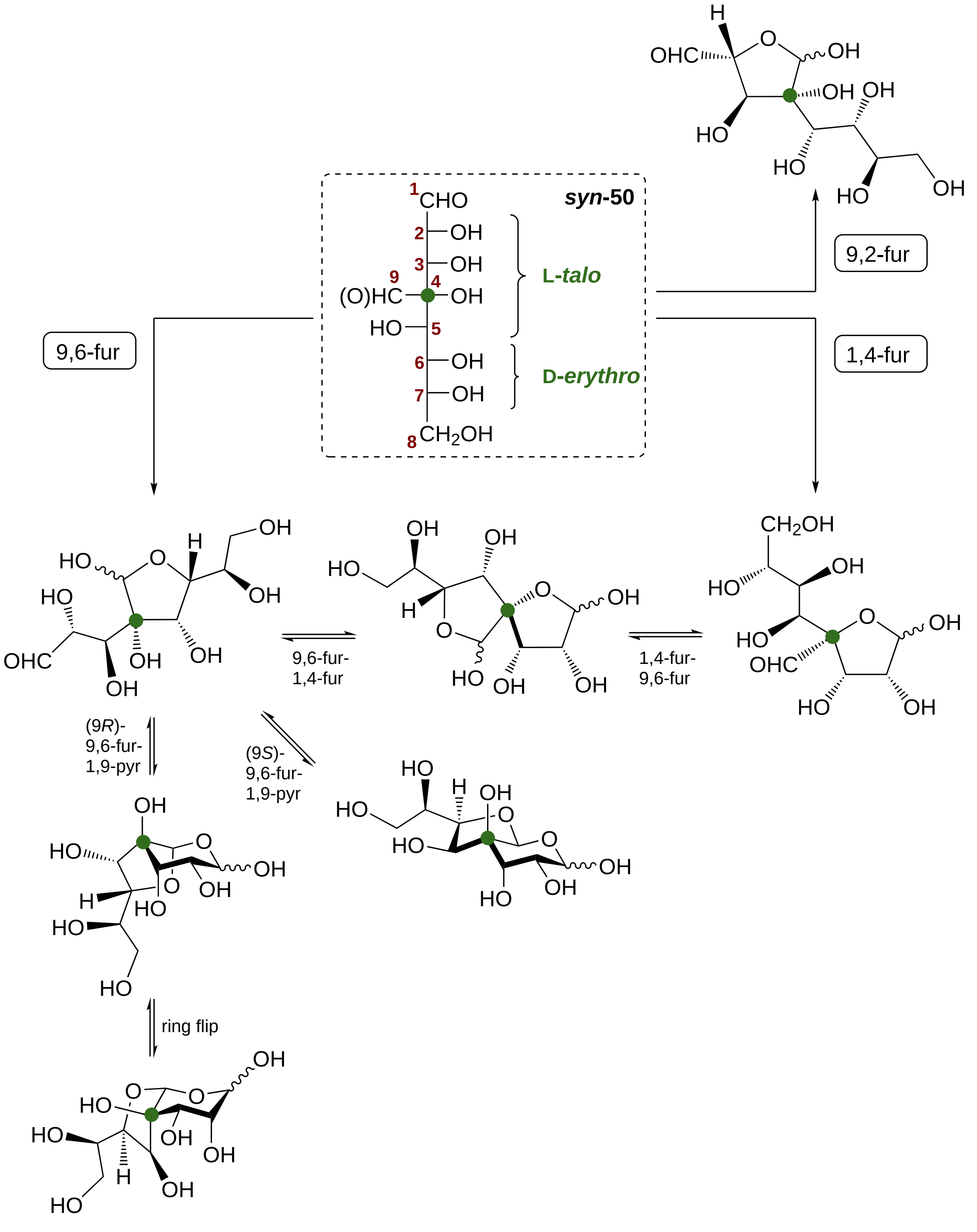
syn-50
L-talo
D-erythro
9,6-fur
9,2-fur
1,4-fur
9,6-fur-1,4-fur
1,4-fur-9,6-fur
(9R)-9,6-fur-1,9-pyr
(9S)-9,6-fur-1,9-pyr
ring flip

Scheme 4.40 Analysis of plausible isomers of target compound ***syn*-50**. **Part II: Isomers including 9,6-furanose, 1,4-furanose and 9,2-furanose isomeric forms.** Isomers are only given for free aldehydes, furanoses and pyranoses (not for bridged cycles). Ring flip (pyranoses only) as well as α/β-isomerism (wavy bond) is shown where possible. The quaternary *C*-4 is indicated with a green dot. pyr = pyranose, fur = furanose. Isomers given in **Scheme 4.39** are not reproduced.

from the 9,7-pyranose and 1,5-pyranose ring closures. Notably, the given analysis only involved pyranose and furanose isomers, and smaller or larger cyclic forms, as well as possible bridged cyclic forms, were disregarded. Nevertheless, as depicted, the number of potential individual isomers is significantly increased by considering following ring flip isomerism (only given for pyranoses), and by considering putative anomeric mixtures for all isomers due to the presence of (either one or two) free hemiacetal functionalities. In addition to these pyranose ring closures, several furanose ring closures are feasible from the acyclic isomer (9,6-fur, 1,4-fur and 9,2-fur, **Scheme 4.40**).

In total, the given set of plausible isomers includes 47 individual isomeric forms, taking into account the presence of α- and β-anomeric isomers for each hemiacetal functionality. Subtraction of the number of free aldehyde isomers, not present according to preliminary NMR studies, results in a total of 32 potential isomers (constitutional isomers and diastereoisomers). Furthermore, by disregarding ring flip isomerism or α,β-isomerism, five individual constitutional isomers can be identified. Noteworthy, for target compounds ***syn*-52** and ***anti*-70**, a completely analogous analysis can be given (not shown). Based on the analysis of potential isomeric forms for ***syn*-50**, 2D NMR analyses were utilized to gain insight into the major isomeric forms of the compounds in D_2O (for ^{1}H NMR spectra of the anomeric regions, see **Fig. 4.12** on page 135. For selected 2D NMR spectra, see **Appendix D**). All NMR analyses were performed on samples of the concentration 0.075 mmol/mL, and thus, with the same concentration used for the synthesis-derived bradyrhizose **K**.[14] Surprisingly, detailed NMR investigations confirmed that the intuitively anticipated, "bradyrhizose-type" 9,7-pyranose-1,9-pyranose isomer was no major constituent of the isomeric mixture of ***syn*-50**. Instead, the annulated 1,5-pyranose-9,7-pyranose isomer, both in the 1,9-diaxial (1*R*,9*S*)-form ***syn*-50-A** (49% isomeric contribution) and in the (1*S*,9*S*)-form ***syn*-50-B** (37%) could be identified (for a summary of results, see **Table 4.4** on page 134). The ring closures for these isomers were evident from distinct long-range couplings in C,H-HMBC experiments (H-1–C-5/H-5–C-1). The *C*-1 anomeric configuration of ***syn*-50-B** could be determined from a *H*-1–*H*-5 NOE contact, which confirmed the 1,3-diaxial relationships expected for this isomer. Furthermore, the ascribed anomeric configurations at *C*-1 and *C*-9 were fully supported by the determined $^1J_{\mathrm{C,H}}$ coupling constants, which were in good agreement with the ranges expected for axial (158–160 Hz) or equatorial (170 Hz) anomeric protons.[99, 100] Comparably, for target compound ***syn*-52**, the 1,5-pyranose-9,7-pyranose ring closures were favored, too. In this case, the diequatorial (1*S*,9*R*)-form ***syn*-52-A** (66% isomeric contribution) was identified, largely from similar spectral properties as given above, and all other isomeric forms were negligible ($<$ 13% contribution). For ***anti*-70**, two major isomers could be identified, however, the determined ${}^{1}J_{\mathrm{C1,H1}}$ coupling constants (175.4 and 175.5 Hz) were inconsistent with α- or β-anomeric configurations in pyranoses, and rather suggestive for a furanose. For both identified isomers, a pronounced long-range coupling between H-1–C-4 (C,H-HMBC), as well as a significant low-field shift of the quaternary *C*-4 (the former carbohydrate *C*-2) as compared to the other isomers (84.2 vs. 74.0–75.8 ppm) also suggested the presence of a spirofuranose form (related to synthetic intermediate **α,β-68**). The major isomer could be determined to be ***anti*-70-A** with (1*S*,9*S*)-configuration (47% isomeric contribution). The minor isomer ***anti*-70-B** (10% isomeric contribution) was found to be the corresponding 9-equatorial isomer with (1*S*,9*R*)-configuration and similarly α-configured xylofuranose moiety. The *C*-1 anomeric α-configurations were deduced from specific NOE contacts (H-1–H-2), combined with further spectral properties (^{13}C chemical shifts of *C*-1: 94.8, 94.4 ppm; ^{1}H NMR: ${}^{3}J_{1,2} = 4.7$, 5.0 Hz) that were in agreement with literature data reported for simpler xylofuranosides.[217] It should be noted that the NMR spectral data obtained for compounds ***syn*-50**, ***syn*-52** and ***anti*-70** as stated here remained practically unchanged upon storing the solutions in D_2O for several days at ambient temperature. Thus, good evidence was obtained that equilibration of the isomeric mixtures was completed. The results described here demonstrate that the anticipated “bradyrhizose-type“ isomers (the potential (9*S*)-9,7-pyranose-1,9-pyranose isomeric forms) are not major constituents of aqueous solutions of the target compounds **T-4**. Especially in the case of ***anti*-70**, the isomer with side chain configurations identical to the natural bradyrhizose **K**, these findings seem to be remarkable. In the putative (9*S*)-9,7-pyranose-1,9-pyranose isomer of ***anti*-70** (**Scheme 4.41** on page 136), both hydroxyl groups at the 2,3-positions are equatorially-oriented, similar to the major 1,5-pyranose isomer of bradyrhizose **K**. Nevertheless, this intuitively favorable isomeric form was not found as a major constituent of solutions of ***anti*-70**. The alternate 1,5-pyranose-9,7-pyranose isomer (the major form found for ***syn*-50** and ***syn*-52**) with 2,3-diaxial configuration seems to be unfavorable, too. Instead, the 1,4-spiro-xylofuranose forms ***anti*-70-A** and ***anti*-70-B** are preferred. Remarkably, xylose is typically a pentose with high conformational stability, and furanose forms are usually only trace constituents in aqueous solution.[218, 219]

The fact that the 9,7-pyranose-1,9-pyranose isomers seem to be unfavorable for the three 4-*C*-formyl octoses ***syn*-50**, ***syn*-52** and ***anti*-70** can be addressed, in a qualitative manner, by considering the special role of hemiacetal functionalities in hydrogen-bonding interactions of glycosides. Both theoretical and experimental studies have confirmed that the hemiacetal group is a comparably poor hydrogen bond acceptor, but the strongest hydrogen bond donor in carbohydrates.[131, 220, 221] Computational results suggested, for example, that the monohydration of glucose proceeds preferentially

Table 4.4 Major isomers of target 4-*C*-formyl octoses ***syn*-50**, ***syn*-52** and ***anti*-70** in aqueous solution (D_2O) and key NMR data of the anomeric regions.

compound **T-4**	major isomers[a]	ratio[b]	anomeric *H*-1[c] anomeric *C*-1	anomeric *H*-9[c] anomeric *C*-9	key NMR features[d]
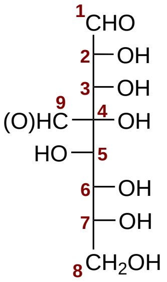 ***syn*-50**	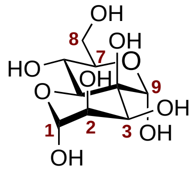 ***syn*-50-A**	49%	5.29 (d, 1.2 Hz)[e] 95.4	5.15 (s) 93.0	H-1-C-5 (HMBC) H-9-C-7 (HMBC) H-3-H-5 (NOESY) $^1J_{C1,H1}$ = 172.2 Hz[f] $^1J_{C9,H9}$ = 172.0 Hz
	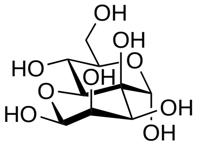 ***syn*-50-B**	37%	4.86 (d, 0.7 Hz)[e] 94.7	5.15 (s) 93.2	H-5-C-1 (HMBC) H-9-C-7 (HMBC) H-1-H-5 (NOESY) H-3-H-5 (NOESY) $^1J_{C1,H1}$ = 161.8 Hz $^1J_{C9,H9}$ = 172.0 Hz
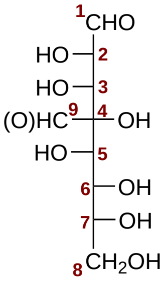 ***syn*-52**	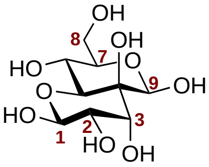 ***syn*-52-A**	66%[g]	4.86 (d, 8.4 Hz) 95.1	4.99 (s) 93.9	H-5-C-1 (HMBC) H-7-C-9 (HMBC) H-1-H-5 (NOESY) H-5-H-9 (NOESY) H-7-H-9 (NOESY) $^1J_{C1,H1}$ = 163.1 Hz $^1J_{C9,H9}$ = 164.3 Hz
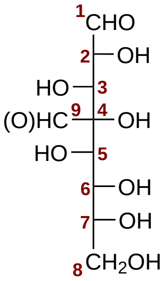 ***anti*-70**	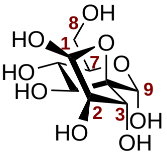 ***anti*-70-A**	47%	5.27 (d, 4.7 Hz) 94.8	5.01 (s) 97.4	H-1-C-4 (HMBC) H-9-C-7 (HMBC) H-1-H-2 (NOESY) H-9-H-3 (NOESY) $^1J_{C1,H1}$ = 175.4 Hz $^1J_{C9,H9}$ = 170.9 Hz
	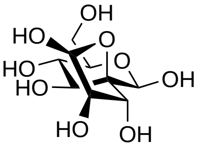 ***anti*-70-B**	10%	5.31 (d, 5.0 Hz) 94.4	4.75 (s)[h] 93.5	H-1-C-4 (HMBC) H-9-C-7 (HMBC) H-1-H-2 (NOESY) H-9-H-5 (NOESY) H-9-H-7 (NOESY) $^1J_{C1,H1}$ = 175.5 Hz $^1J_{C9,H9}$ = 161.7 Hz

[a] In solution: 0.075 mmol/mL in D_2O at 25 °C. After NMR analysis, the samples were stored for several days in D_2O. Unchanged spectral properties confirmed complete equilibration.

[b] Determined by ^1H NMR integration: combined anomeric integration of the isomer in relation to total anomeric signal integration (4.6–5.5 ppm) in baseline-corrected spectra.

[c] NMR signals [ppm] and coupling constants [Hz] in D_2O at 700.3/176.1 MHz.

[d] Key NMR correlations observed in the corresponding experiments.

[e] Weakly resolved doublet.

[f] Determined in F2-coupled C,H-HSQC experiments.

[g] Only observed isomer with > 12% contribution.

[h] Partially obscured by solvent signal.

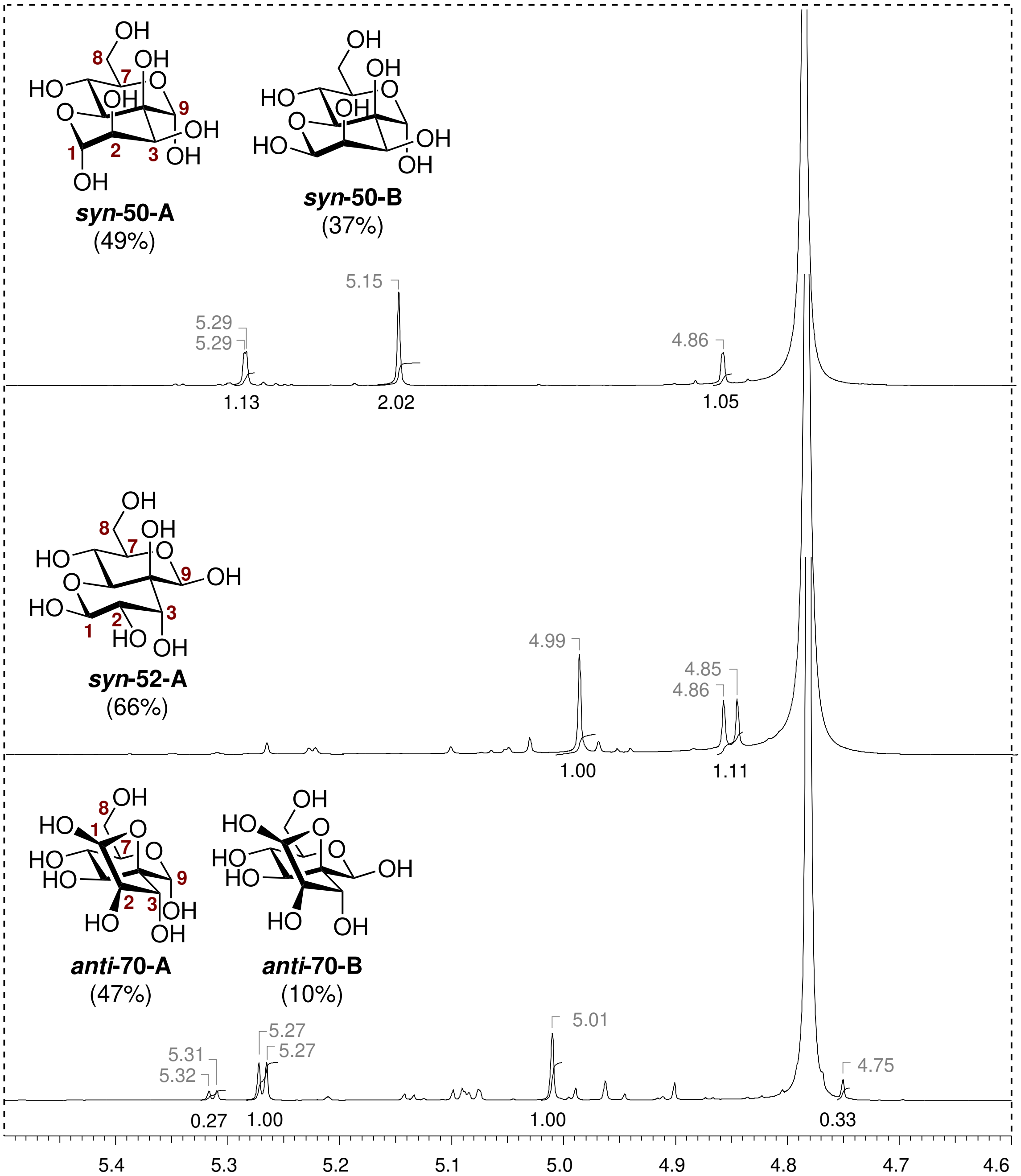

Figure 4.12 Anomeric regions (4.6–5.5 ppm) of the ^{1}H NMR spectra of the identified isomers for 4-*C*-formyl octoses ***syn*-50**, ***syn*-52** and ***anti*-70** in D_2O at 700.3 MHz. For signal assignments, see **Table 4.4**. The shown spectra are unprocessed. The ratios of the isomers were determined by integration of corresponding baseline-corrected spectra (not shown).

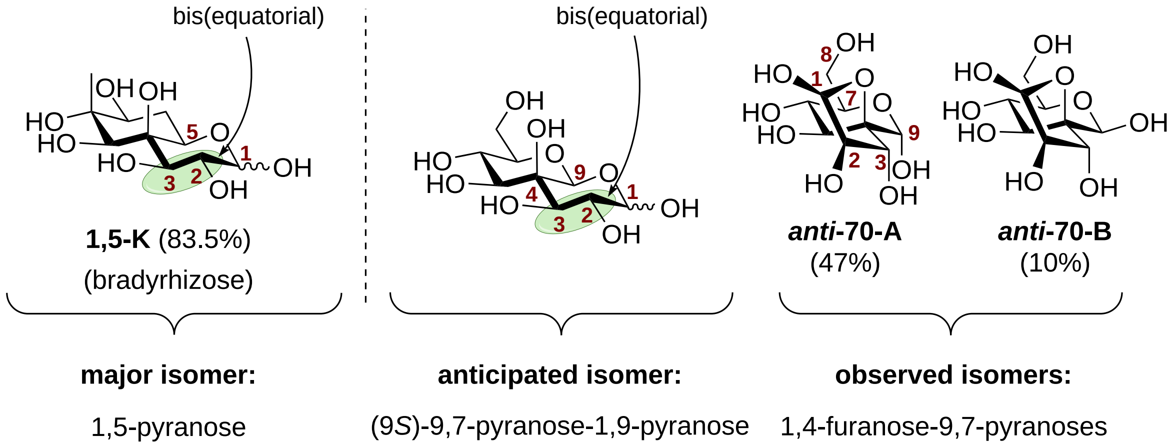
bis(equatorial)
bis(equatorial)
1,5-K (83.5%)
(bradyrhizose)
anti-70-A
(47%)
anti-70-B
(10%)
major isomer:
1,5-pyranose
anticipated isomer:
(9S)-9,7-pyranose-1,9-pyranose
observed isomers:
1,4-furanose-9,7-pyranoses

Scheme 4.41 Structural comparison of the major 1,5-pyranose isomer of bradyrhizose **K** (left) with the anticipated and observed isomers for target compound ***anti*-70**.

at the exocyclic hemiacetal oxygen (the *C*-1-OH).[222] From this perspective, the "bradyrhizose-type" isomers [(9*S*)-9,7-pyranose-1,9-pyranose forms] can be referred to as proximal acetal-hemiacetal forms, featuring one acetal functionality (*C*-9), and one hemiacetal functionality (*C*-1). All identified isomers, in contrast, are bis(hemiacetal) forms, with both *C*-1 and *C*-9 carrying a hemiacetal group. Along these lines, the observations described here could be explained by a higher number of hemiacetal functionalities in the observed isomers as compared to the anticipated isomers (2 vs. 1), and thus, favorable hydration properties (e.g. hydration enthalpies). In the natural monosaccharide bradyrhizose **K**, due to the inositol moiety, only one aldehyde is present, and thus, one hemiacetal functionality can be established. Understandably, the major isomeric form is isomer **1,5-K**, exhibiting the sterically favorable 2,3-bis(equatorial) configuration.

4.6. Summary of this Chapter

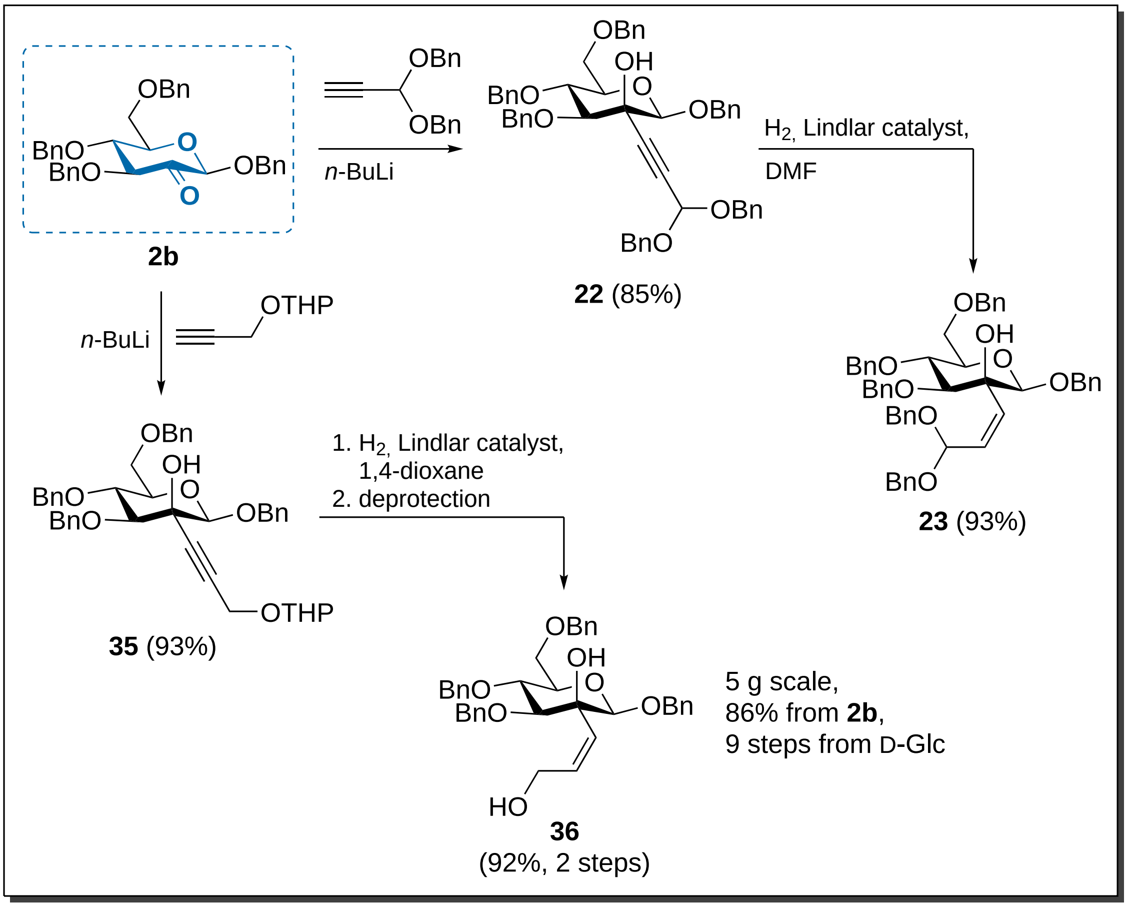

2b
n-BuLi
22 (85%)
H2, Lindlar catalyst,
DMF
23 (93%)
n-BuLi
OTHP
35 (93%)
1. H2, Lindlar catalyst,
1,4-dioxane
2. deprotection
36
(92%, 2 steps)
5 g scale,
86% from 2b,
9 steps from D-Glc

Scheme 4.42 Synthesis of 2-*C*-(*Z*)-alkenyl mannosides **23** and **36** *via* alkynylation and Lindlar hydrogenation.

Starting from the known benzyl 2-uloside **2b**[37], preliminary synthetic studies towards the target 4-*C*-formyl octoses **T-4** were performed following a route proposed by Menzel and Ziegler.[174] Thus, equatorially-selective alkynylation of the ketone **2b** with propiolaldehyde dibenzyl acetal afforded the novel 2-*C*-alkynyl mannoside **22 (Scheme 4.42)**. Extensive investigations revealed that the following partial hydrogenation of **22** under Lindlar conditions proceeded smoothly in DMF, which was found to be the preferable solvent for semihydrogenations of sterically crowded 2-*C*-alkynyl branched glycosides. In this way, (*Z*)-alkene **23** was available. The structure of **23**, which displayed solvent-dependent rotameric isomerism effects in NMR experiments, was additionally confirmed by X-ray crystallography. Routine protecting group manipulations of alkyne **22** provided, after similar partial hydrogenations of the alkyne moieties, an extended set of 2-*C*-alkynyl and 2-*C*-(*Z*)-alkenyl mannosides with an acetal-protected γ-aldehyde functionality. Subsequently, osmium-based *syn*-dihydroxylations of the alkene moiety

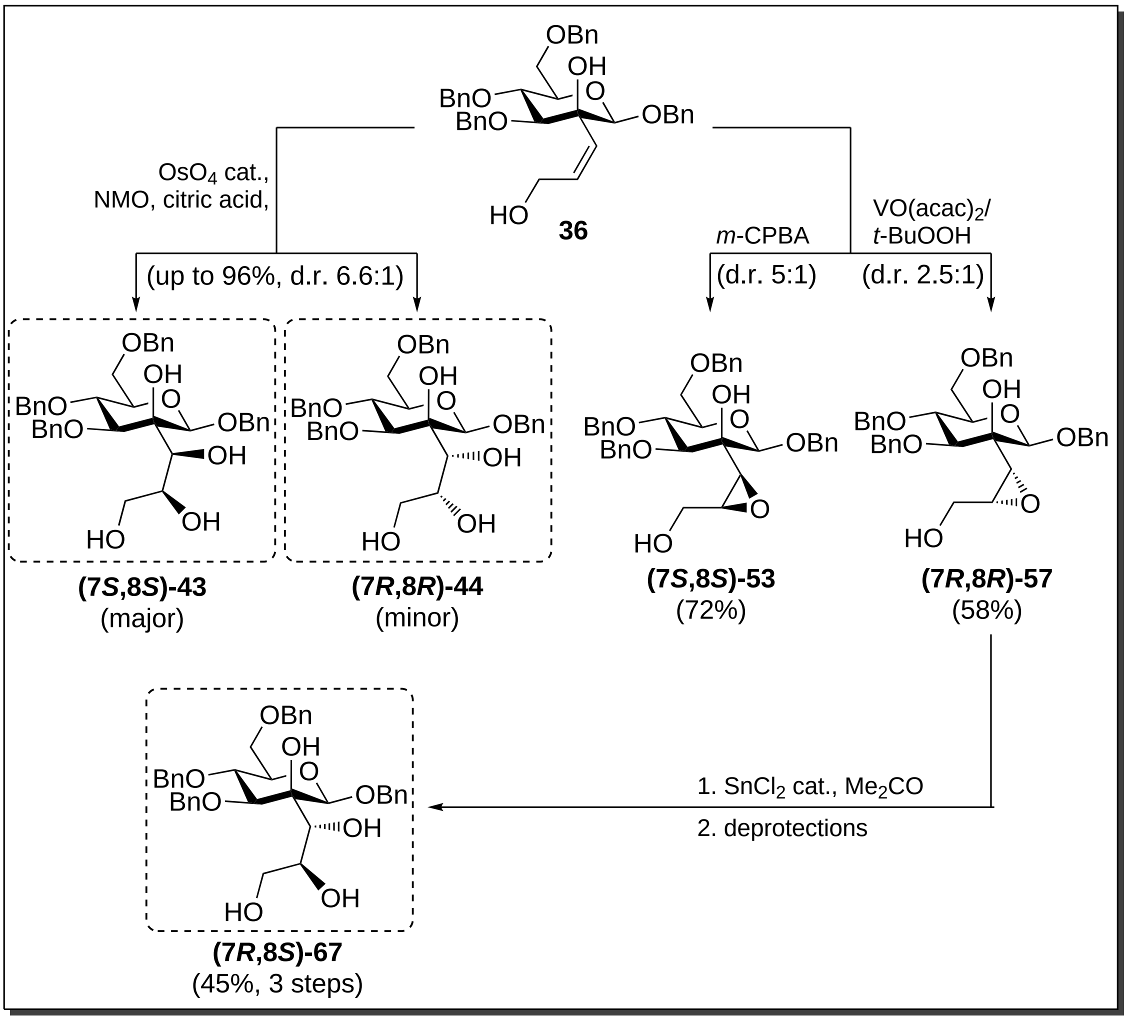
OBn
OH
BnO
BnO
O
OBn
HO
36
OsO4 cat.,
NMO, citric acid,
(up to 96%, d.r. 6.6:1)
m-CPBA
(d.r. 5:1)
VO(acac)2/
t-BuOOH
(d.r. 2.5:1)
OH
OH
(7S,8S)-43
(major)
(7R,8R)-44
(minor)
(7S,8S)-53
(72%)
(7R,8R)-57
(58%)
1. SnCl2 cat., Me2CO
2. deprotections
(7R,8S)-67
(45%, 3 steps)

Scheme 4.43 Synthesis of tetrols **(7*S*,8*S*)-43**, **(7*R*,8*R*)-44** and **(7*R*,8*S*)-67** with diverse configurations of the side chain diol moiety.

in **23** or derivatives thereof were explored. However, even forceful conditions could not affect the desired transformation of the sterically crowded (Z)-alkene substrates.

In an alternate route, comparable alkynylations of **2b** were performed with protected propargyl alcohol derivatives, giving THP-protected **35** or similar derivatives with other protecting groups. Partial hydrogenation of the alkyne and subsequent deprotection provided allyl alcohol **36** as a suitable key substrate. From **36**, oxidative functionalizations of the double bond enabled an exploration of the chemical space of 2-C-branched mannosides, and of derived 2-spiroannulated molecular patterns. The osmoylation of **36** was found to require the addition of citric acid, whereas conventional methods without additives or protocols with basic additives did not affect the dihydroxylation **(Scheme 4.43)**. The successful *syn*-dihydroxylation provided major isomer **(7*S*,8*S*)-43** and minor isomer **(7*R*,8*R*)-44**, which could be separated either by fractional crystallization or by employing derivatization techniques. Furthermore, epoxidations of **36** were examined. Peracid epoxidation with *m*-CPBA provided epoxyalcohol **(7*S*,8*S*)-53** as the major isomer. In contrast, vanadium-catalyzed epoxidation with the combination VO(acac)$_2$/*t*-BuOOH resulted in the formation of **(7*R*,8*R*)-57** as the major epoxide isomer. The following epoxide opening towards the desired *anti*-diol intermediates proved to be challenging. In this regard, a protocol involving SnCl$_2$-mediated epoxide opening in acetone, followed by deprotection reactions, was found to be suitable for the transformation of epoxide **(7*R*,8*R*)-57** into *anti*-diol **(7*R*,8*S*)-67** as a third intermediate with a fully hydroxylated side chain. A similar procedure from epoxide **(7*S*,8*S*)-53**, however, gave only an unwanted debenzylation/rearrangement product. The depicted stereochemistry of all side chain functionalized intermediates could be fully established by 2D NMR spectroscopy. Furthermore, X-ray structural analyses of derivatization products confirmed these spectroscopic results indirectly.

The synthesis continued with the obtained tetrols **(7*S*,8*S*)-43**, **(7*R*,8*R*)-44** and **(7*R*,8*S*)-67**, which were subjected to selective primary alcohol oxidations. Published procedures suggested mild and selective TEMPO-based oxidation protocols as a suitable method, however, under reported conditions, the reactions proceeded sluggishly and gave impure products. A new optimized procedure could be developed by utilizing the known combination catalytic TEMPO/trichloroisocyanuric acid (TCICA). Improvements over published protocols involved 3-(*N*-morpholino)propanesulfonic acid (MOPS) as an organic buffer to ensure anhydrous conditions, ethyl acetate/toluene as the solvent mixture at low temperatures (−65 to −35 °C), and a reductive quench with dimethyl sulfide prior to aqueous workup **(Scheme 4.44)**. In this way, the *syn*-configured tetrol substrates **(7*S*,8*S*)-43** and **(7*R*,8*R*)-44** were cleanly converted into the corresponding reducing spirofuranose-pyranose hybrids **α,β-48** and **α,β-51**. *Via* the optimized oxidation protocol, these reducing furanose intermediates were obtained in high purity, whereas other methods gave impure products and required extensive multiple chromatography steps which led to severe loss of material of the sensitive free hemiacetals. In the case of the *anti*-isomer **(7*R*,8*S*)-67**, major overoxidation to the lactone occurred, thus demanding a following reduction step with DIBAL-H to afford the lactol **α,β-68** in reasonable yield. The obtained products could be fully characterized by multiple analytical methods. Notably, the α- and β-components of the novel reducing spirofuranose-pyranose hybrids could be independently characterized by NMR spectroscopy to a large extent. Furthermore, related synthetic explorations afforded previously undescribed molecular frameworks **(Scheme 4.44, bottom)** like the corresponding spiro-tetrahydrofuran cyclization products **(7*S*,8*S*)-49**/**(7*S*,8*R*)-56**/**(7*R*,8*S*)-60**, spiro-epoxycarbonate **(7*R*,8*R*)-61**,

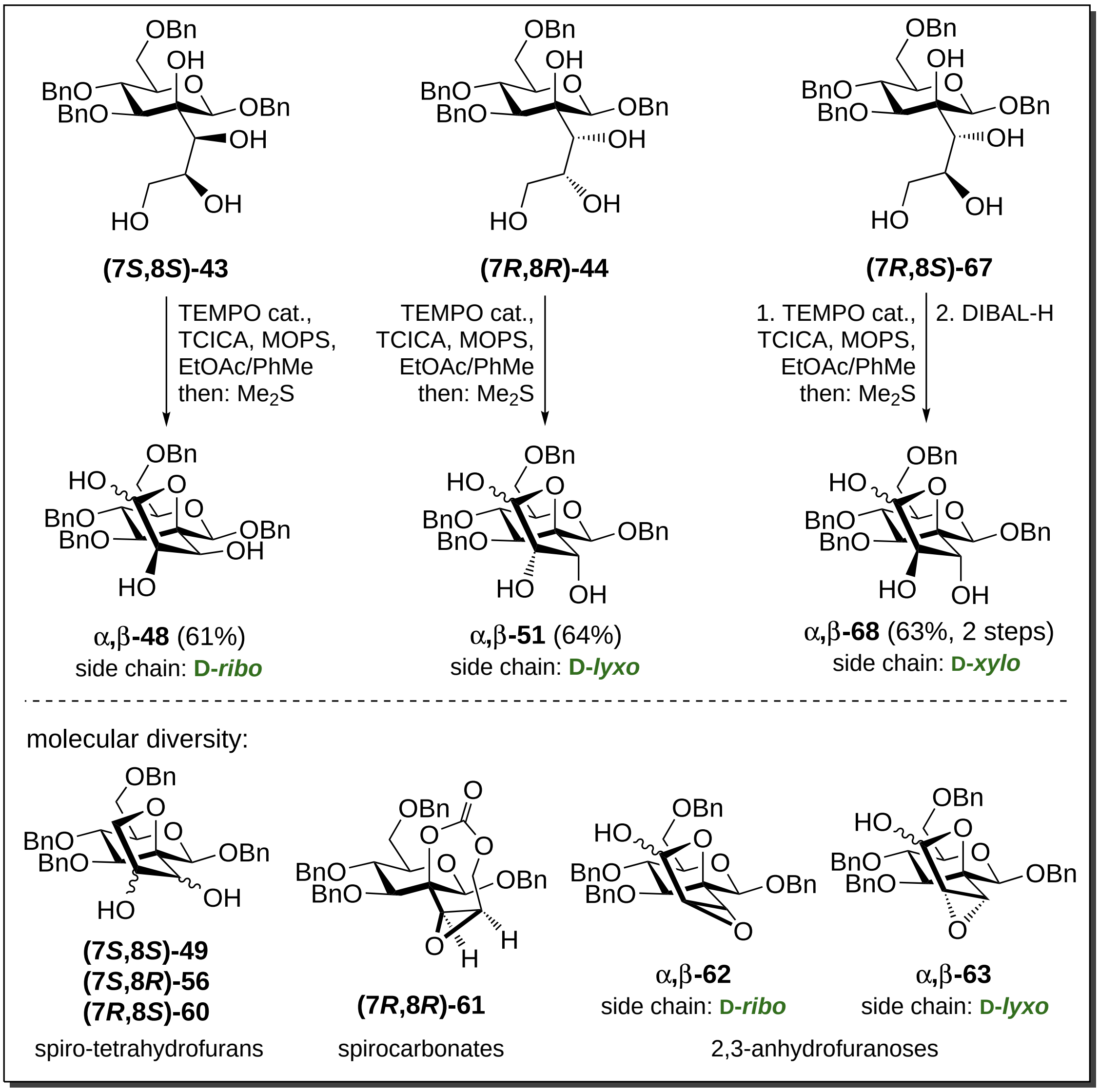
(7S,8S)-43
(7R,8R)-44
(7R,8S)-67
TEMPO cat., TCICA, MOPS, EtOAc/PhMe then: Me2S
TEMPO cat., TCICA, MOPS, EtOAc/PhMe then: Me2S
1. TEMPO cat., TCICA, MOPS, EtOAc/PhMe then: Me2S
2. DIBAL-H
α,β-48 (61%)
side chain: D-ribo
α,β-51 (64%)
side chain: D-lyxo
α,β-68 (63%, 2 steps)
side chain: D-xylo
molecular diversity:
(7S,8S)-49
(7S,8R)-56
(7R,8S)-60
spiro-tetrahydrofurans
(7R,8R)-61
spirocarbonates
α,β-62
side chain: D-ribo
α,β-63
side chain: D-lyxo
2,3-anhydrofuranoses

Scheme 4.44 Top: oxidative synthesis of spirofuranoses **α,β-48**, **α,β-51** and **α,β-68**. Bottom: molecular diversity of related 2-spiroannulated frameworks.

or the epoxide-derived 2,3-anhydrofuranoses **α,β-62**/**α,β-63** as an addition to the structural diversity of 2-*C*-branched glycosides and 2-spiroannulated carbohydrates.

Debenzylation of the spirofuranoses **α,β-48**, **α,β-51** and **α,β-68** provided the corresponding target 4-*C*-formyl octoses ***syn*-50**, ***syn*-52** and ***anti*-70**, each as a complex mixture of isomers **(Scheme 4.45)**. Detailed NMR studies in D_2O revealed the structures of the 1,5-pyranose-9,7-pyranose (***syn*-50** and ***syn*-52**) or the 1,4-furanose-9,7-pyranose (***anti*-70**) hemiacetal forms, and these species could be identified as the major isomeric forms in solution. In contrast, the initially anticipated isomeric forms of target compounds **T-4 (Scheme 4.45, bottom)**, the (9*S*)-9,7-pyranose-1,9-pyranose forms with structural analogy to the natural monosaccharide bradyrhizose **K**, were

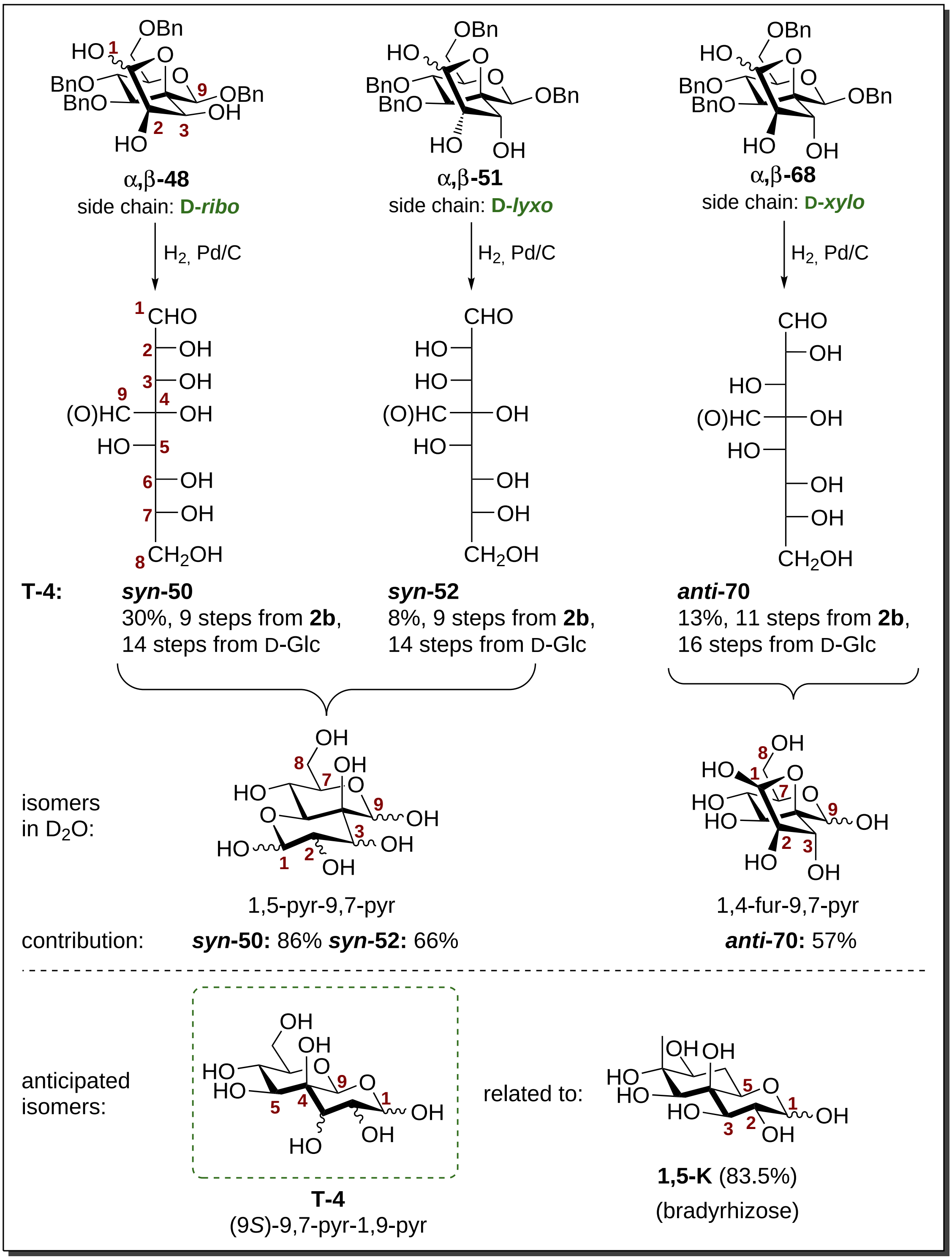
OBn
HO
BnO
BnO
O
OBn
OH
HO
1
2
3
9
α,β-48
side chain: D-ribo
α,β-51
side chain: D-lyxo
α,β-68
side chain: D-xylo
H2, Pd/C
CHO
OH
(O)HC
CH2OH
1
2
3
4
5
6
7
8
9
T-4:
syn-50
30%, 9 steps from 2b,
14 steps from D-Glc
syn-52
8%, 9 steps from 2b,
14 steps from D-Glc
anti-70
13%, 11 steps from 2b,
16 steps from D-Glc
isomers
in D2O:
1,5-pyr-9,7-pyr
1,4-fur-9,7-pyr
contribution:
syn-50: 86% syn-52: 66%
anti-70: 57%
anticipated
isomers:
T-4
(9S)-9,7-pyr-1,9-pyr
related to:
1,5-K (83.5%)
(bradyrhizose)

Scheme 4.45 Top: synthesis of target 4-C-formyl octoses **T-4**, represented by ***syn*-50**, ***syn*-52** and ***anti*-70**. The major isomers identified in D_2O are shown. Bottom: initially anticipated isomeric form of **T-4** and related structure of the major 1,5-pyranose isomer of bradyrhizose **K**. pyr = pyranose, fur = furanose.

not identified as major constituents. These results suggest that for higher sugars of type **T-4**, isomeric forms with two hemiacetal functionalities are favorable, and thereby preferred over the acetal-hemiacetal isomeric forms of initially anticipated compounds **T-4**. Obviously, substitution of the inositol moiety in bradyrhizose **K** for a conventional monosaccharide (β-mannoside) results in an alteration of the isomeric distribution. For this reason, target compounds ***syn*-50**, ***syn*-52** and ***anti*-70** seem to be inadequate as structural analogs for the natural product **K**. Nevertheless, detailed structural investigations into isomeric equilibria of higher sugars are rare, and therefore the described results can be seen as an addition to the synthesis and characterization of complex higher sugars.

5. Cyclopent-2-enones from 2-Uloside Precursors

As covered in **Chapter 2**, benzylated 2-ulosides **2a-c** with diverse anomeric substituents could be obtained by Dess-Martin oxidation (**Scheme 2.14** on page 24), and were thus available as precursors for the synthesis of higher sugar analogs as reported in **Chapters 3** and **4**. In reactions involving precursors **2a** and **2b**, the following observations were made: allyl 2-uloside **2a** exhibited a high tendency to form the corresponding 3,2-enolone **3b** *via* elimination of benzyl alcohol, either under the conditions of its formation, or upon chromatographic purification (**Scheme 2.13** on page 21). In contrast, the corresponding benzyl 2-uloside **2b** was more resistant, and required highly basic conditions to afford 3,2-enolone **40** as a side product in the ketone alkynylation reaction (**Scheme 4.21, (a)**, on page 94).

In light of the interesting downstream chemistry of structurally similar 3,2-enolones (comp. **Section 2.1.2**), further transformations of the 3,2-enolone intermediates derived from **2a-c** were explored in the course of this thesis. These results are covered in this chapter.

5.1. Introduction to Carbohydrate-Derived 3,2-Enolones and 3,2-Enones

Within the area of carbohydrate-based building blocks, sugars incorporating an α,β-unsaturated carbonyl moiety have attracted interest due to the high synthetic versatility of the enone functional group. As a result, several review articles have been published focussing on such unsaturated carbohydrate derivatives.[113, 223] The incorporation of a ketone functionality at position 2 of a pyranose and of an unsaturation at positions 3/4 results in what can be referred to as a hex-3-enopyranoside-2-ulose according to carbohydrate nomenclature.[16, 113] Apart from this, the following nomenclature is frequently applied for reasons of convenience: 4-deoxy-hex-3-enopyranoside-2-uloses can be referred to as carbohydrate 3,2-enolones **(Scheme 5.1)**, thus emphasizing the

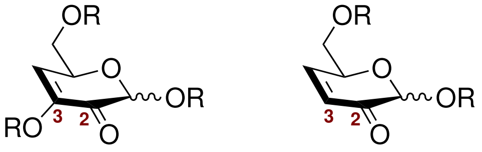

3,2-enolone 3,2-enone

Scheme 5.1 General structures of carbohydrate-derived 3,2-enolones and 3,2-enones. R = protecting groups.

presence of an α-ketoenol arrangement. Frequently, the protecting group at *O*-3 is an ester, and these protected derivatives can be designated as 3,2-enolone esters.[48, 113] Accordingly, the corresponding 3,4-dideoxy derivatives can be referred to as carbohydrate 3,2-enones. In a pyranose system, an α,β-unsaturated carbonyl moiety can similarly be established with the carbonyl functionality at *C*-1 (lactones), *C*-3 or *C*-4. Although these regioisomers feature a comparably diverse chemistry[113, 223], this introduction will focus on reactions of the relevant 3,2-enolones and the related 3,2-enones.

Carbohydrate 3,2-enones can be routinely obtained from simple 2-oxyglycals *via* a Lewis acid-mediated Ferrier-type glycosylation/elimination cascade.[223] Due to this convenient synthetic accessibility, carbohydrate 3,2-enones have been frequently applied as building blocks for the synthesis of 4-*C*-branched sugars by means of conjugated addition reactions to the Michael system. For example, Fraser-Reid and Coworkers reported on the cuprate addition of the tritylated 3,2-enone **EW**, which provided the *C*-4 methylated product **EX** *via* selective axial attack of the reagent **(Scheme 5.2)**.[224] A similar strategy was employed by Tatsuta and Coworkers, who reacted enone **EY** with a sulfonyl-stabilized carbanion. After intramolecular trapping of the enolate intermediate, the glycoside-annulated hydroquinone **EZ** could be obtained.[225] Several contributions to such conjugated addition reactions of carbohydrate 3,2-enones have been published by Varela and Coworkers. Accordingly, in one example, enone **FA** was treated with ethanethiol in the presence of a catalytic amine base to afford the corresponding 3,4-dideoxy-4-thiohexopyranos-2-uloside **FB** in a *thia*-Michael reaction with selectivity for axial attack.[226] Further examinations suggested that the configuration at the anomeric position provided the steric bias for the diastereoselectivity, since otherwise similar β-configured substrates resulted in selective equatorial attack at the *C*-4.[227]

Apart from conjugated addition reactions, other transformations of carbohydrate 3,2-enones include, for example, Diels-Alder reactions. In this regard, Varela and Coworkers reacted 3,2-enone **FC** with cyclopentadiene in toluene **(Scheme 5.3, top)**.[228] The cycloaddition occurred selectively from the β-face, and gave annulated 2-ulosides **FD/FE** as an *endo*/*exo* mixture. Noteworthy, Diels-Alder reactions have also been investigated

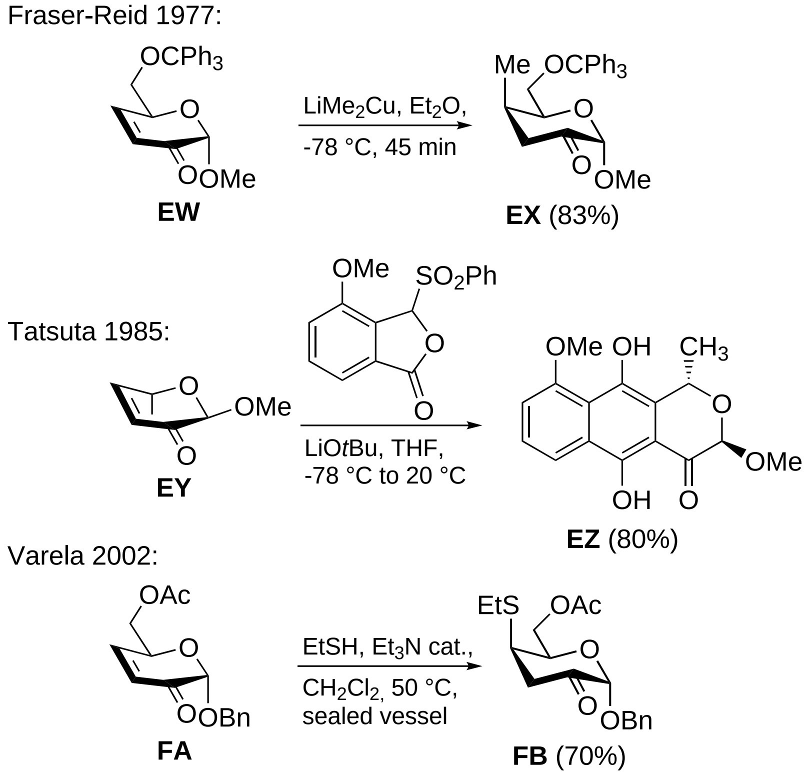
Fraser-Reid 1977:
OCPh3
O
O
OMe
EW
LiMe2Cu, Et2O,
-78 °C, 45 min
Me
OCPh3
O
O
OMe
EX (83%)
Tatsuta 1985:
O
OMe
O
EY
OMe
SO2Ph
O
O
LiOtBu, THF,
-78 °C to 20 °C
OMe OH CH3
O
OMe
OH O
EZ (80%)
Varela 2002:
OAc
O
O
OBn
FA
EtSH, Et3N cat.,
CH2Cl2, 50 °C,
sealed vessel
EtS
OAc
O
O
OBn
FB (70%)

Scheme 5.2 *C*-4 functionalizations of carbohydrate 3,2-enones **EW**[224], **EY**[225] and **FA**[226] *via* conjugated addition reactions.

with carbohydrate 3,2-enolone substrates, although these displayed a significantly lower dienophilicity as compared to 3,2-enones. Lichtenthaler and Coworkers treated 3,2-enolone ester **FF** with cyclopentadiene in CH_2Cl_2 **(Scheme 5.3, bottom)**.[229] The thermal reaction required high temperatures (200 °C, 48 h), and therefore high pressure (15 kbar) and Lewis acid-catalyzed ($TiCl_4$) procedures were explored. Suitable conditions could be found, and provided the *endo*-product **FG** *via* selective attack from the α-face.

Other synthetically useful addition reactions to carbohydrate 3,2-enolones do exist, however, these transformations frequently suffer from low predictability of the synthetic outcome. Lichtenthaler and Coworkers performed a detailed investigation on the reactivity of benzoylated 1,5-anhydro-3,2-enolone **FH (Scheme 5.4)**.[53] The cuprate addition (CuI, MeLi) to **FH** provided 4-*C*-methylated **FI** with equatorial selectivity, albeit in a mediocre 40% yield. In contrast, in the presence of lithium enolates, 1,2-addition occurred at the *C*-2, accompanied by an unexpected *O*-3–*O*-2 benzoyl migration and formation of the 3-ulose product **FJ**. Unexpectedly, under nitroaldol conditions, double addition occurred at the *C*-2, and the 2,2-bis(nitromethyl) product **FK** was formed. Similar transformations involving the conventional 3,2-enolones (not

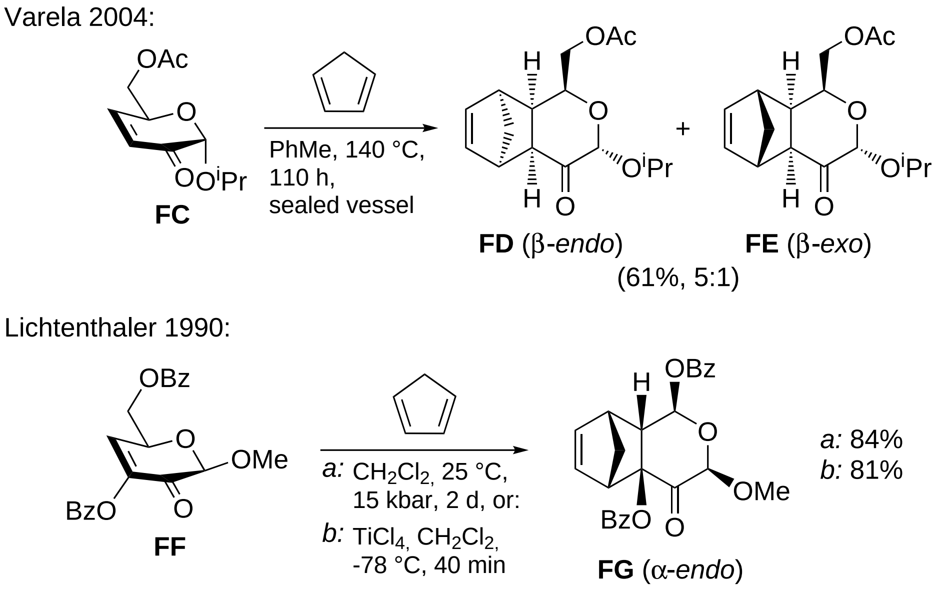
Varela 2004:
OAc
O
O
O^iPr
FC
PhMe, 140 °C,
110 h,
sealed vessel
H
OAc
O
O^iPr
H
O
+
FD (β-endo)
FE (β-exo)
(61%, 5:1)
Lichtenthaler 1990:
OBz
O
OMe
BzO
O
FF
a: CH2Cl2, 25 °C,
15 kbar, 2 d, or:
b: TiCl4, CH2Cl2,
-78 °C, 40 min
H
OBz
O
OMe
BzO
O
FG (α-endo)
a: 84%
b: 81%

Scheme 5.3 Diels-Alder reactions of carbohydrate 3,2-enone **FC**[228] and 3,2-enolone ester **FF**[229].

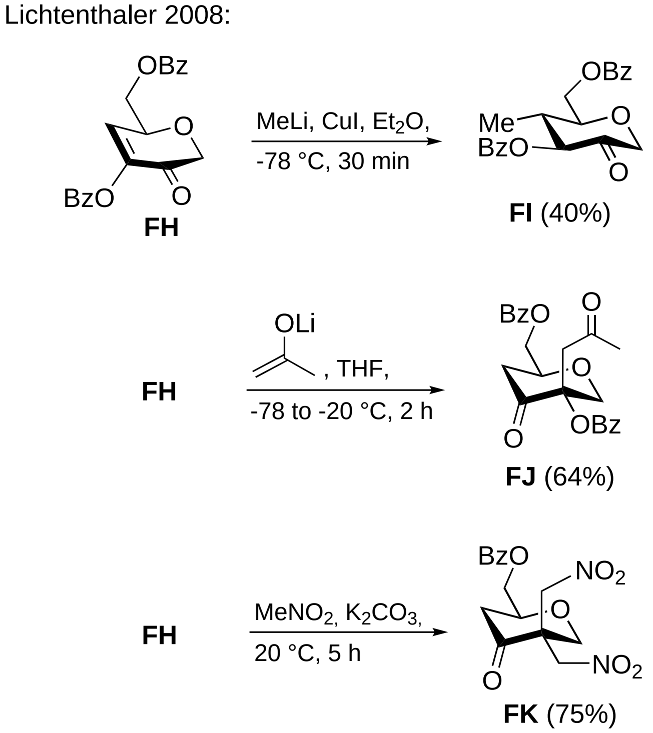
Lichtenthaler 2008:
OBz
O
BzO
O
FH
MeLi, CuI, Et2O,
-78 °C, 30 min
OBz
Me
BzO
O
O
FI (40%)
FH
OLi
, THF,
-78 to -20 °C, 2 h
BzO
O
O
O
OBz
FJ (64%)
FH
MeNO2, K2CO3,
20 °C, 5 h
BzO
NO2
O
O
NO2
FK (75%)

Scheme 5.4 Observed transformations of 1,5-anhydro-3,2-enolone ester **FH**, involving 1,4-addition and 1,2-addition reactions.[53]

the 1-deoxy derivatives like **FH**) seem to be underexplored. However, an examination of the diverse degradation reactions of carbohydrate 3,2-enolones **(Section 2.1.2)** suggests that under basic, as well as under acidic conditions, several potential side reactions have to be considered.

In 2001, Zou and Coworkers reported on an interesting rearrangement reaction of a carbohydrate 3,2-enolone.[230] When *C*-glycosidic α-allyl 3,2-enolone **FL** or the corresponding β-isomer **FM** were subjected to basic conditions (K_2CO_3 or Et_3N in MeOH), from both substrates one identical product could be isolated and identified to be the 5-hydroxycyclopent-2-enone **(±)-FN**, notably as a racemic mixture **(Scheme**

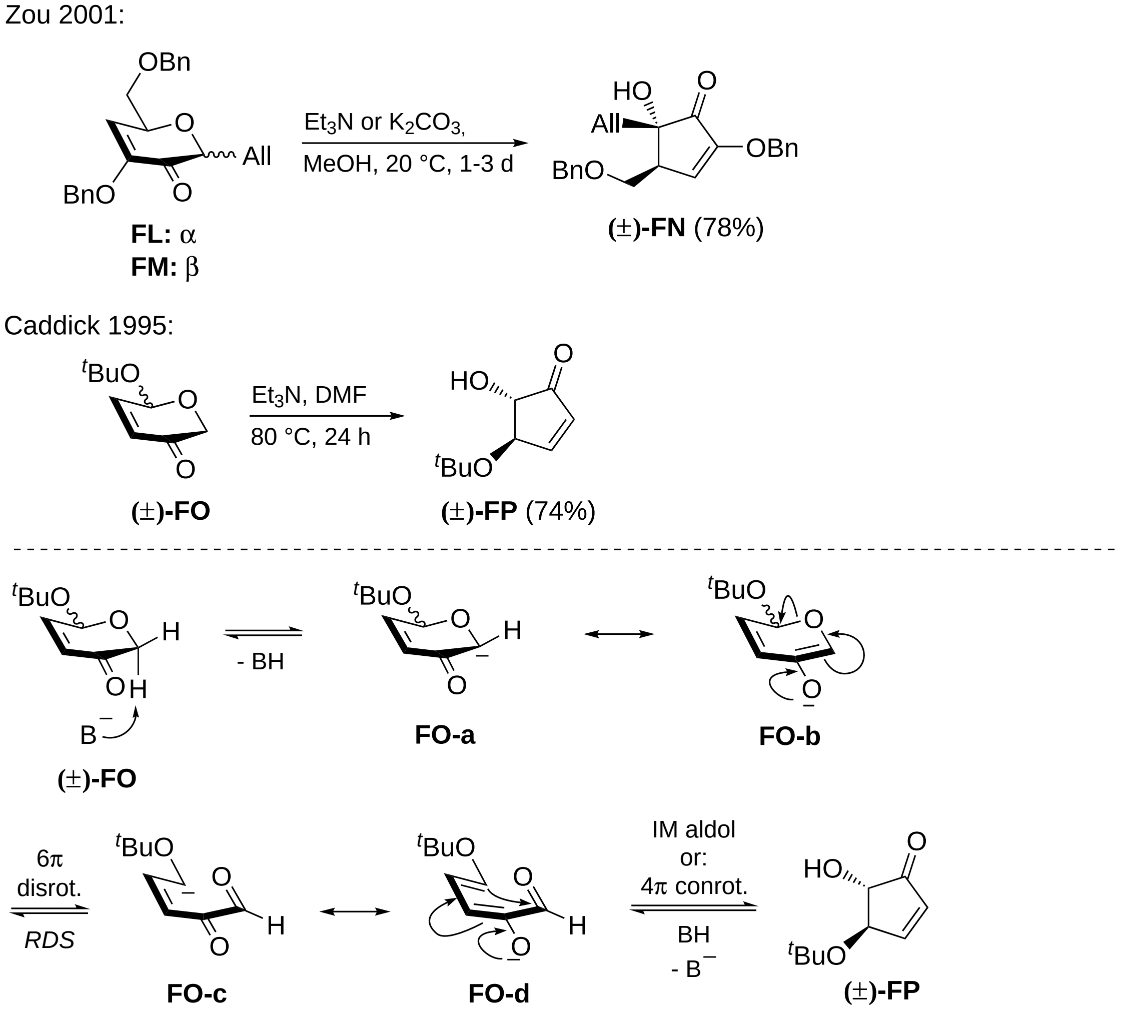
Zou 2001:
OBn
O
All
BnO
O
FL: α
FM: β
Et3N or K2CO3,
MeOH, 20 °C, 1-3 d
HO
O
All
OBn
BnO
(±)-FN (78%)
Caddick 1995:
tBuO
O
O
(±)-FO
Et3N, DMF
80 °C, 24 h
HO
O
tBuO
(±)-FP (74%)
tBuO
O
H
OH
B−
(±)-FO
- BH
tBuO
O
H
O
FO-a
tBuO
O
O
FO-b
6π
disrot.
RDS
tBuO
O
H
O
FO-c
tBuO
O
H
O
FO-d
IM aldol
or:
4π conrot.
BH
- B−
HO
O
tBuO
(±)-FP

Scheme 5.5 Top: published base-induced rearrangement reactions of dihydropyran-3-ones, giving racemic 5-hydroxycyclopent-2-enones **(±)-FN**[230] and **(±)-FP**[231]. Bottom: generally accepted mechanism involving 6π electrocyclic ring opening, followed by ring closure *via* intramolecular aldol addition or 4π electrocyclic reaction. B^- = basic reagent. *RDS* = rate-determining step. Counter ion not shown.

5.5). Previously, Caddick and Coworkers published a comparable rearrangement of the racemic enone **(±)-FO**. Upon treatment with Et_3N in DMF, the dihydropyran-3-one underwent rearrangement into 5-hydroxycyclopent-2-enone **(±)-FP**, which exhibited a 4,5-*trans*-configuration comparable to **(±)-FN**.[231] Prior to these two reports, Kolb and Hoffmann published a similar rearrangement of dihydropyran-3-ones into 5-hydroxycyclopent-2-enones (not shown).[232] In their optimized procedure, the authors treated the substrates with a buffer of $PhCO_2H$/KOAc (1:2) in DMF at 80 °C to invoke the rearrangement. However, following experiments indicated that the reaction was dependent on proton catalysis, rather than a base-induced process.

For the rearrangements described by Zou[230] and Caddick[231], a generally accepted mechanism can be given by taking into account mechanistic considerations by the authors, including following publications by the Caddick group.[233–238] Thus, as exemplified for the transformation of **(±)-FO**, deprotonation at the C-2 of the dihydropyran-3-one (related to the carbohydrate C-1) gives the enolate **FO-a/FO-b (Scheme 5.5, bottom)**. Subsequently, a 6π disrotatory electrocyclic ring opening would occur, putatively supported by the anionic enolate oxygen, giving the open-chain vinylogous enolate **FO-c/FO-d**, notably an achiral intermediate. The final cyclization would proceed either in the sense of an intramolecular aldol addition, or in a (charge-promoted) 4π conrotatory electrocyclic ring closure. Computational results reported by the Caddick group suggested that the formation of **FO-c/FO-d** (the ring opening) is the rate-determining step of the overall reaction.[238] For the following step **FO-d→(±)-FP**, rotational isomerizations and the final cyclization step are energetically advantageous for the formation of the 4,5-*trans*-isomer **(±)-FP**, which was found to be both the kinetic and the thermodynamic product.

Notably, a comparison of this type of rearrangements with known base-induced degradation reactions of 3,2-enolones (**Scheme 2.7** on page 15) suggests that the initial deprotonation/enolate formation step is crucial for the outcome of the reaction: thus, deprotonation at the carbohydrate C-5 (C-6 in the pyran numbering) is associated with elimination processes (represented by the formation of **AS**), whereas deprotonation at the carbohydrate C-1 results in the described ring contraction to racemic cyclopentenones. However, the chemistry of dihydropyran-3-one systems seems to be complex, and dependent on the individual substrate and the reaction conditions. Therefore, other factors like the absence of a leaving group at the carbohydrate C-1 in substrates **(±)-FL/FM/FO** have to be taken into account.

5.2. Objective of this Chapter

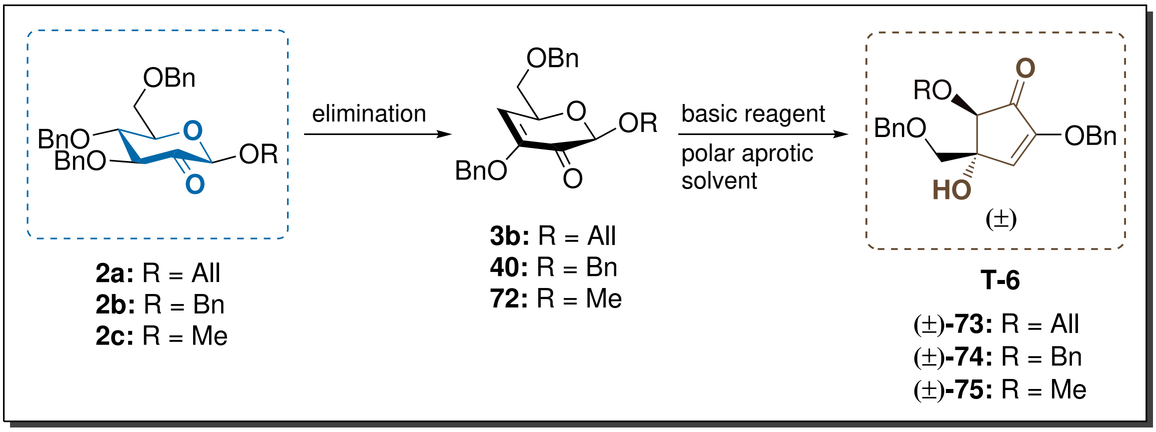

Scheme 5.6 Schematic representation of the synthetic routes described in this chapter.

In preceding transformations, both allyl 2-uloside **2a** and benzyl 2-uloside **2b** were observed to undergo elimination to the corresponding 3,2-enolones **3b** and **40** in the presence of bases **(Scheme 5.6)**. Inspired by this, suitable conditions were examined to deliberately invoke this elimination under basic conditions. As a third, structurally simpler substrate, methyl 2-uloside **2c** was included in these investigations. In following experiments, the thus obtained 3,2-enolones **3b**, **40** and **72** were reacted in the presence of nucleophilic/basic reagents to explore their applicability as unsaturated carbohydrate building blocks. Under optimized conditions, the formation of racemic *C*-4 quaternary 4-hydroxycyclopent-2-enones **(±)-73**, **(±)-74** and **(±)-75** occurred in a previously undescribed rearrangement. Further investigations into this interesting transformation, including effects of the solvent and of the nature of the base, were performed. A plausible mechanistic picture for the title reaction was established in the context of related published reactions. The results obtained along these lines are covered in this chapter.

5.3. Results and Discussion

Initial experiments for the formation of 3,2-enolones **3b**, **40** and **72** from the corresponding 2-ulosides **2a,b,c** startet with an examination of conditions decribed in the literature for similar transformations (comp. **Section 2.1.2** on page 13). These early investigations, including the preliminary observation of the title reaction, were in part elaborated by R. M. Oechsner in the course of a bachelor thesis.[239]

5.3.1. Synthesis of 3,2-Enolone Substrates

In general, ester-protected 2-ulosides undergo elimination to the 3,2-enolone esters cleanly under a variety of conditions. A protocol frequently applied, in this regard, involves simple heating of the acylated 2-ulosides in wet benzene in the presence of $NaHCO_3$ as a weak base (comp. formation of **AQ**, **Scheme 2.6** on page 14).[38, 51, 56] Starting from these conditions in the case of benzylated 2-ulosides **2a,b,c**, minor variations were required. To account for the poor benzyloxide leaving group at position 4, a stronger base (K_2CO_3) was applied. Furthermore, the solvent was changed from benzene to toluene for toxicity reasons. Thus, when 2-ulosides **2b,c** were stirred in wet toluene in the presence of K_2CO_3 at 80–95 °C, smooth elimination to 3,2-enolones **40** and **72** was observable, and the products could be isolated in 85–90% yield **(Scheme 5.7)**. In the transformation of the sensitive allyl 2-uloside **2a** to **3b**, crude material as obtained from the Dess-Martin oxidation of **7** was subjected to the elimination, since chromatographic purification of **2a** resulted in a severe loss of material.

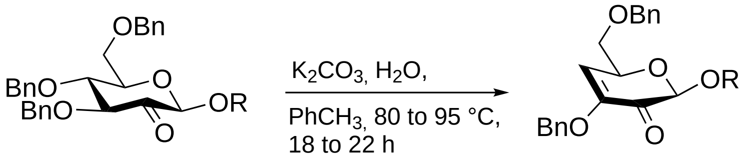

2a: R = All (crude)
2b: R = Bn
2c: R = Me

3b: R = All (70%, 2 steps, from **7**)
40: R = Bn (90%)
72: R = Me (85%)

Scheme 5.7 Formation of 3,2-enolones **3b**, **40** and **72** from 2-ulosides **2a,b,c**.

Analytical data obtained for 3,2-enolones **3b**, **40** and **72** were largely comparable to published data on similar systems. In this regard, the determination of the $J_{4,5}$ coupling constant of the H-4 (a doublet) allowed for a conformational analysis. Dihydropyran-3-ones usually occupy either envelope conformations with the ring oxygen above or below the plane (${}^{O}E$ or E_{O}), or half-chair conformations (${}^{O}H_2$ or ${}^{2}H_{O}$).[229] Lichtenthaler and Coworkers deduced the following circumstances from spectroscopic data on a set of α- and β-configured 3,2-enolones **(Scheme 5.8, top)**.[56, 229] Accordingly, α-configured 3,2-enolones **FQ** and **AQ** feature coupling constants $J_{4,5}$ in the range 1.8–2.0 Hz. These values are in agreement with a 90° orientation of the quasi-axial H-5 with respect to the five-carbon envelope plane as established in an ${}^{O}E$ conformation. Possibly, for α-3,2-enolones, this conformation is favorable owing to the anomeric effect. In contrast, for β-configured 3,2-enolone **FF**, $J_{4,5} = 3.5\,\mathrm{Hz}$ was found, relating to a quasi-equatorial orientation of H-5 as realized in an E_{O} conformation. Furthermore, the authors proposed a slight distortion of the envelope conformation, caused by steric repulsions between the

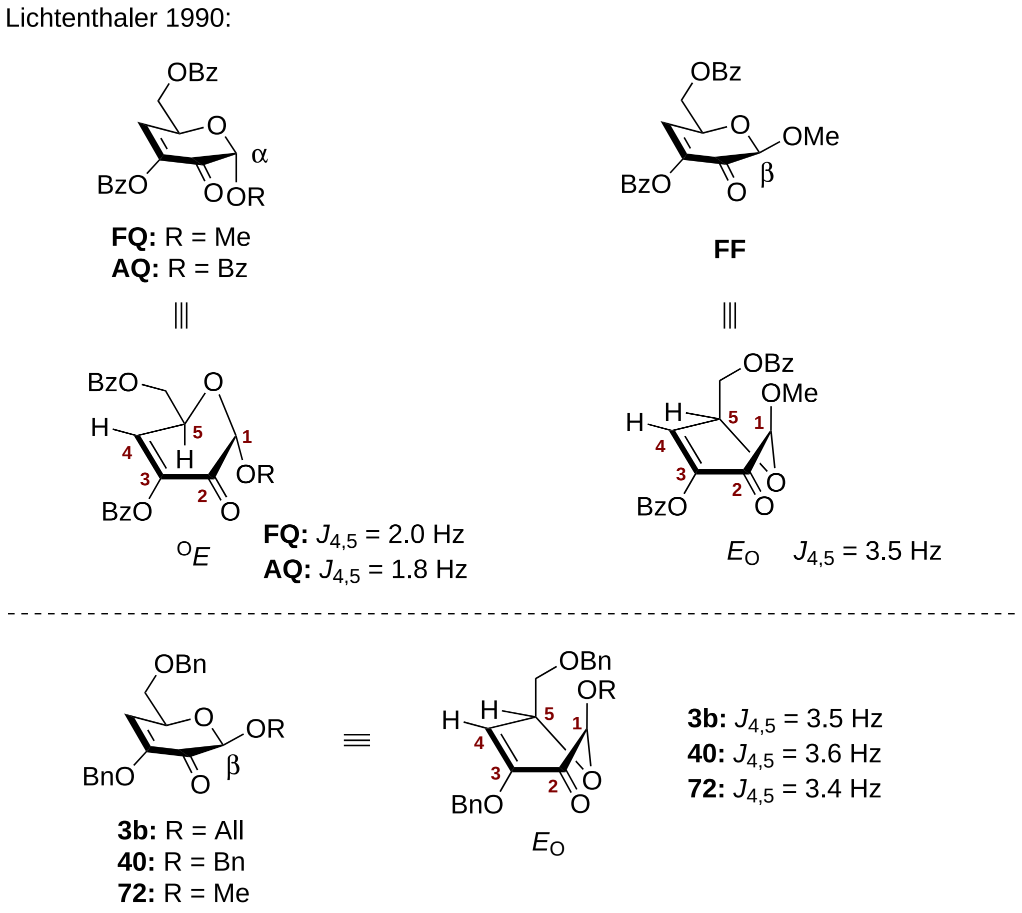
Lichtenthaler 1990:
OBz
O
α
BzO
O
OR
FQ: R = Me
AQ: R = Bz
OBz
O
OMe
β
BzO
O
FF
BzO
O
H
5
1
4
H
OR
3
2
BzO
O
^{O}E
FQ: $J_{4,5}$ = 2.0 Hz
AQ: $J_{4,5}$ = 1.8 Hz
OBz
OMe
H
H
5
1
4
3
O
2
BzO
O
E_O
$J_{4,5}$ = 3.5 Hz
OBn
O
OR
β
BnO
O
3b: R = All
40: R = Bn
72: R = Me
≡
OBn
OR
H
H
5
1
4
3
O
2
BnO
O
E_O
3b: $J_{4,5}$ = 3.5 Hz
40: $J_{4,5}$ = 3.6 Hz
72: $J_{4,5}$ = 3.4 Hz

Scheme 5.8 Top: proposed conformations of α-3,2-enolones **FQ/AQ** (^{O}E; *H*-5 quasi-axial) and β-3,2-enolone **FF** (E_O; *H*-5 quasi-equatorial) by Lichtenthaler and Coworkers.[56, 229] Published values of the significant coupling constant $J_{4,5}$ are given in $CDCl_3$. Bottom: proposed E_O conformation for β-3,2-enolones **3b**, **40** and **72**. Values for $J_{4,5}$ are given in $CDCl_3$ (**3b**) or acetone-D_6 (**40** and **72**).

bis(quasi-axial) substituents at positions 1 and 5. For β-3,2-enolones **3b**, **40** and **72**, values for $J_{4,5}$ in the range 3.4–3.6 Hz **(Scheme 5.8, bottom)** were in good agreement with these suggestions, and thus indicated the preference for an E_O conformation of these 3,2-enolone intermediates in the respective NMR solvent.

5.3.2. Base-induced Rearrangement: Formation of Cyclopent-2-enones

Further investigations into the chemistry of the obtained 3,2-enolones **3b**, **40** and **72** started with the benzyl derivative **40**, which was subjected to standard *thia*-Michael conditions[227] involving ethanethiol and a catalytic amine base in CH_2Cl_2 to explore possible reactivities with nucleophilic reagents **(Scheme 5.9, top)**. Surprisingly, **40** was found to be unreactive even under forcing conditions (100 °C, sealed vessel). Obviously, the α,β-unsaturated carbonyl moiety in carbohydrate 3,2-enolone ethers of this type is no suitable electrophile for conjugated addition reactions, most certainly due to the presence of a donor oxygen substituent at the α-position (*C*-3). Next, **40** was reacted in the presence of highly nucleophilic sodium thiophenolate in DMF at 80 °C **(Scheme 5.9, bottom)**. Under these conditions, the formation of a single product was observable by TLC. After workup and chromatographic purification of the crude product, the obtained mass spectra suggested a molecular weight identical to the substrate **40**, and thus, a product probably originating from a rearrangement reaction. Albeit, the isolated material exhibited no significant optical rotation, which was indicative of a racemic mixture or of an achiral product. Eventually, by means of 2D NMR experiments, the structure of 2,5-bis(benzyloxy)-4-benzyloxymethyl-4-hydroxycyclopent-2-enone **(±)-74** could be established, which was obviously formed in the reaction as a racemic mixture in 70% yield. In addition, chiral column HPLC experiments provided further confirmation for a racemic mixture by the presence of two detectable species with near-identical integration **(Appendix B)**.

A literature survey for comparable rearrangements revealed transformations published by Caddick[231] and Zou[230], which afforded cyclopent-2-enones from dihydropyran-3-ones in putatively similar reactions (**Scheme 5.5** on page 147). However, in the published procedures, the formation of the 5-hydroxy-substituted cyclopentenones occurred, whereas the transformation of **40** afforded the 4-hydroxy-substituted cyclopentenone **(±)-74**. NMR Spectroscopically, this difference was evident from the

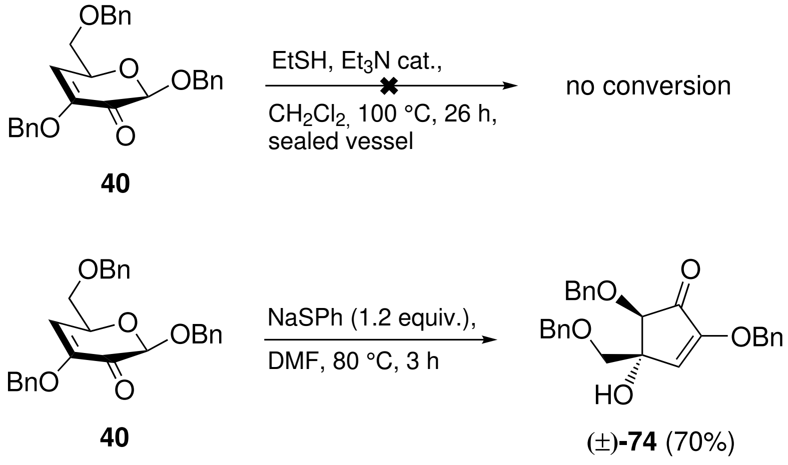

Scheme 5.9 Preliminary experiments for the reaction of 3,2-enolone **40** with nucleophilic reagents, and initial formation of cyclopent-2-enone **(±)-74**.[239]

cyclopentenone ring protons. For literature compound **(±)-FN**, the olefinic proton *H*-3 (6.30 ppm in $CDCl_3$) appeared as a doublet due to vicinal coupling with the adjacent tertiary *H*-4 ($J_{3,4} = 2.0$ Hz).[230] For **(±)-74**, in contrast, both the olefinic *H*-3 (6.35 ppm in acetone-*D6*) as well as the tertiary *H*-5 (4.14 ppm) appeared as clean singlets.

Synthetic strategies for cyclopent-2-enones, and especially for the prominent 4-hydroxycyclopent-2-enone motif, are of interest. For example, various compounds carrying this framework have been extracted from natural sources, and the cyclopentenone pharmacophore is frequently associated with interesting biological activities.[240–245] In this context, biological and chemical properties of cyclopent-2-enones have been outlined in a large number of review articles.[246–250] For this reason, the observed unexpected formation of cyclopentenones from carbohydrate 3,2-enolone synthons seemed to be an interesting addition to the available synthetic methods. Therefore, a systematic examination of this reaction was performed.

An initial experiment was designed based on the following observation reported by Zou and Coworkers[230]: β-configured 2-uloside **BU** underwent rapid elimination in 1 h to 3,2-enolone **FM** by using 1% K_2CO_3 or 10% Et_3N as a base in methanol **(Scheme 5.10, top)**. Under the same conditions, upon extending the reaction time to 3 d, the described rearrangement into **(±)-FN** occurred. Related to this transformation, 2-uloside **2b** was subjected to identical conditions **(Scheme 5.10, bottom)** to examine if a similar

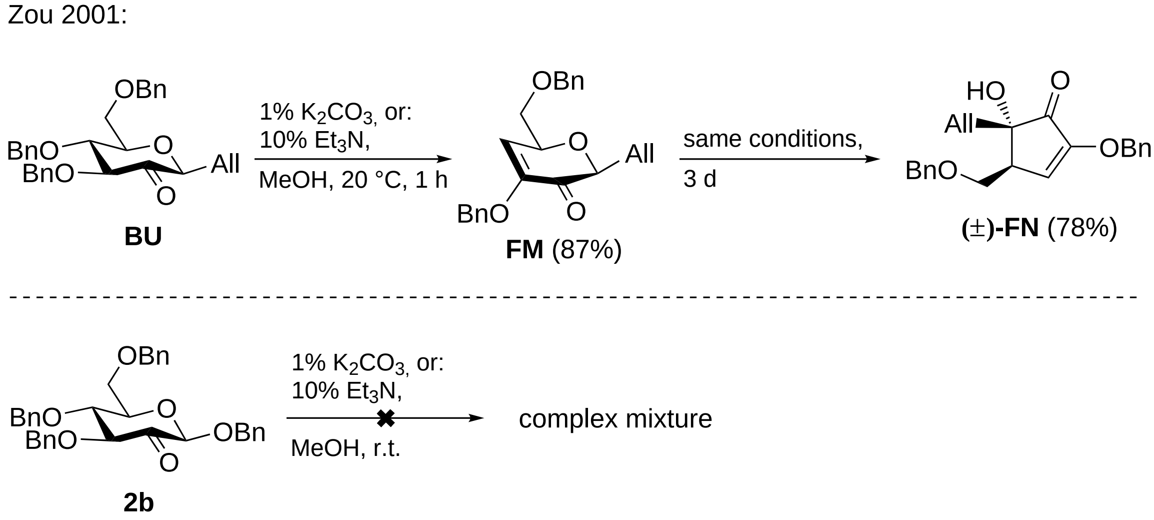

Scheme 5.10 Top: published procedure by Zou and Coworkers, including base-induced elimination of 2-uloside **BU** towards 3,2-enolone **FM**, followed by rearrangement into cyclopent-2-enone **(±)-FN** upon prolonged reaction time.[230] Bottom: unoptimized transformation of 2-uloside **2b** under similar conditions, resulting in a complex mixture.

cascade of elimination and rearrangement was feasible. However, TLC control suggested the formation of plentiful products, and likewise ^{1}H NMR analysis of the crude reaction mixture was indicative of a complex mixture. Obviously, the conditions published by Zou and Coworkers were unsuitable for *O*-glycosidic substrates of type **2** (or the derived 3,2-enolones). In addition, this finding emphasized a strong influence of the solvent on the elimination and the following rearrangement reactions. In this context, it is noteworthy that in the elimination reaction (formation of **40** from **2b**) K_2CO_3 was also used as the base, albeit in nonpolar toluene at 80 °C. Under these conditions, clean elimination to **40** occurred without observable premature rearrangement into **(±)-74**. In contrast, with K_2CO_3 in the highly polar protic methanol, fast reaction of **2b** to multiple products can be observed even at ambient temperature.

As a consequence of these preliminary experiments, further variations started from the initially identified conditions (NaSPh in DMF). A reaction screening for the transformation of **40** into **(±)-74** included a selection of various basic/nucleophilic reagents and solvents **(Table 5.1)**. Starting from the initial procedure, which utilized NaSPh as a stoichiometric reagent (1.2 equiv.) in DMF (entry 1), the possibility of a catalytic reaction seemed to be plausible. Under similar conditions, using 0.15 equiv. of NaSPh (entry 2), the reaction proceeded cleanly, but with only low conversion to **(±)-74** after 48 h. In extended examinations on the rearrangement reaction described by Caddick and Coworkers, catalytic amounts of DABCO (1,4-diazabicyclo[2.2.2]octane) as a nucleophilic amine base in *t*-BuOH were identified as appropriate conditions.[238] Related to this, **40** was reacted in the presence of catalytic DABCO (entry 3) in DMF. Although formation of **(±)-74** occurred, the reaction proceeded in an unclean manner and several side products were formed. To further include an alkoxide base in the reaction screening, catalytic amounts of KO*t*Bu (entry 4) were examined in the reaction of **40**. In this case, the clean transformation was observable at 40 °C, and **(±)-74** was isolated in 64% yield after 5 h, together with 26% of unreacted **40**. An extension of the reaction time to 8 h, however, resulted in a complex mixture and diminished yield (entry 5), indicating that the product **(±)-74** was unstable under the conditions of its formation. Similar experiments involving the basic reagents NaSPh, DABCO and KO*t*Bu were conducted in protic solvents like *t*-BuOH (entries 6–8), or in the more polar 2,2,2-trifluoroethanol (TFE, entries 9–11), but in these cases only low conversions or multiple side products could be observed. Concluding experiments involved the most promising reagent KO*t*Bu in different solvents. Thus, in MeCN (entry 12), decomposition of the substrate **40** was observed at room temperature. In THF at 60 °C (entry 13), the product **(±)-74** was formed, albeit in only low amounts (4%) after 24 h. Finally, fast conversion was

Table 5.1 Reaction screening on the rearrangement of 3,2-enolone **40** into 4-hydroxycyclopent-2-enone **(±)-74**.[a]

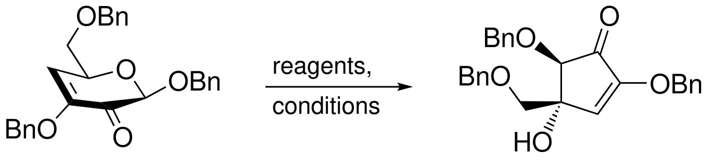

40 (±)-**74**

#	reagent (equiv.)	solvent	T, t	recov. **40**[b]	**(±)-74**[b]
1	NaSPh (1.2)	DMF	80 °C, 3 h	–	70%
2	NaSPh (0.15)	DMF	80 °C, 48 h	62%	22%
3	DABCO (0.15)	DMF	80 °C, 6 h	–	53%[c]
4	KO*t*Bu (0.15)	DMF	40 °C, 5 h	26%	64%
5	KO*t*Bu (0.15)	DMF	40 °C, 8 h	–	47%[c]
6	NaSPh (0.15)	*t*-BuOH	80 °C, 4 h	–	no react.
7	DABCO (0.15)	*t*-BuOH	80 °C, 24 h	4%[c,d]	21%[c,d]
8	KO*t*Bu (0.15)	*t*-BuOH	80 °C, 48 h	51%	8%
9	NaSPh (0.15)	TFE	70 °C, 24 h	–	no react.
10	DABCO (0.15)	TFE	70 °C, 24 h	71%[c,d]	9%[c,d]
11	KO*t*Bu (0.15)	TFE	70 °C, 24 h	65%[c,d]	3%[c,d]
12	KO*t*Bu (0.15)	MeCN	r.t., 24 h	–	decomp.[c]
13	KO*t*Bu (0.15)	THF	60 °C, 24 h	66%	4%
14	KO*t*Bu (0.15)	DMSO	r.t., 1 h	–	45%[c]

[a] Reactions were run under an atmosphere of nitrogen with 50 mg of **40** in 1.7 mL of anhydrous solvent. When TLC control indicated completion, quenching (acetate buffer pH 5), aqueous workup (CH_2Cl_2/H_2O), drying (Na_2SO_4), filtration and evaporation gave the crude product. For DMF: co-evaporation with *n*-heptane. For DMSO: addition of 5 mL H_2O followed by repeated freeze-drying. Purification by automated flash column chromatography (20 g SiO_2; *n*-hexane/*i*-PrOH, 20:1; 14 mL/min; UV detection at 260 nm) gave the product. DABCO = 1,4-diazabicyclo[2.2.2]octane. TFE = 2,2,2-trifluoroethanol.

[b] Chromatographically isolated. Average value of two independent identical experiments.

[c] Complex mixture of products.

[d] Estimated by ^1H NMR integration of a chromatographically inseparable mixture.

observed in DMSO (entry 14) at room temperature. However, after 1 h, the product was obtained as a mixture including several side products.

These results suggested that, in general, polar aprotic solvents are beneficial for the reaction. Highly polar solvents (DMSO, MeCN) can be associated with fast conversion of the substrate at ambient temperature, however, the reactions proceed unclean and with several side products, probably resulting from partial degradation of the cyclopentenone product **(±)-74** under these conditions. The initially utilized DMF seems to be a suitable solvent, with KO*t*Bu as the base suggesting a promising tradeoff between fast conversion and negligible product degradation, provided the reaction is stopped at major conversion. It should be noted that purified KO*t*Bu (see **Section 6.3.1** on page 180), in these and the following experiments, was added in the form of a solution in DMF (2 mg/mL). Upon standing of the stock solution for longer than 30 min, base-mediated degradation of DMF[251] resulted in a decreased concentration of the base, therefore exhibiting weakly reproducible and slow conversions in the rearrangement reaction when using this reagent. As a consequence, freshly prepared solutions of KO*t*Bu in DMF had to be employed. This seems to suggest that, under the conditions of the rearrangement (80 °C in DMF), KO*t*Bu similarly reacts with the solvent. A plausible explanation could involve a (partially) autocatalytic mechanism, in which a deprotonated 4-hydroxycyclopentenone product (an alkoxide base), originating from the reaction induced under sufficiently high starting concentration of KO*t*Bu, functions as a base in the transformation of a second substrate molecule.

Starting from the identified conditions (KO*t*Bu in DMF, entries 4 and 5), 3,2-enolone substrates **3b**, **40** and **72** were next subjected to the rearrangement reaction **(Table 5.2)**. Furthermore, to explore a possible two-step reaction cascade involving elimination and skeletal rearrangement, 2-ulosides **2b,c** were reacted under similar conditions. In the case of the sensitive allyl 2-uloside **2a**, which could not be obtained in purified form without substantially diminished yield, only the two-step reaction (rearrangement of **3b**) was investigated. For the transformation of **40** (entry 1), a smaller amount of KO*t*Bu was applied (0.05 equiv.) to prevent extensive product degradation. Elevated temperatures (90 °C) were required in this case, but the product **(±)-74** was obtained in good yield (78%). In a similar manner, 2-uloside **2b** underwent the reaction cascade into **(±)-74** in a 85% two-step yield (entry 2). In this case, at 50 °C, TLC suggested the clean formation of the intermediate **40**, which was converted to the cyclopentenone product upon raising the temperature to 90 °C. The allyl derivative **3b** (entry 3) was found to be more reative, and the reaction in the presence of KO*t*Bu (0.05 equiv.) proceeded at r.t. However, **(±)-73** was isolated in a mediocre 55% yield, most probably due to base-induced double bond migration of the allyl moiety, which was also observed

Table 5.2 Optimized conditions for the formation of **(±)-73,74,75**.[a]

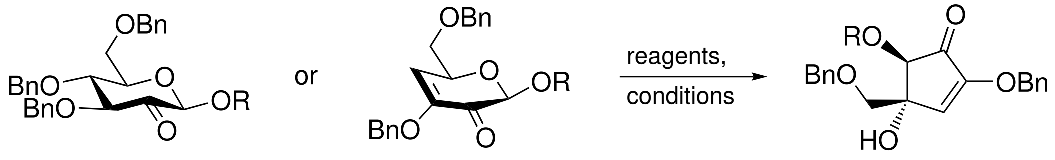

2b: R = Bn
2c: R = Me

3b: R = All
40: R = Bn
72: R = Me

(±)**-73:** R = All
(±)**-74:** R = Bn
(±)**-75:** R = Me

#	substrate (R)	reagent (equiv.)	solvent	T, t[b]	product (yield)[c]
1	**40** (Bn)	KO*t*Bu (0.05)	DMF	90 °C, 28 h	**(±)-74** (78%)
2	**2b** (Bn)	KO*t*Bu (0.05)	DMF	50 to 90 °C, 30 h	**(±)-74** (85%)
3	**3b** (All)	KO*t*Bu (0.05)	DMF	r.t., 2 h	**(±)-73** (55%)
4	**3b** (All)	NaSPh (0.50)	DMF	90 °C, 22 h	**(±)-73** (66%)
5	**72** (Me)	KO*t*Bu (0.05)	DMF	90 °C, 75 min	**(±)-75** (71%), **(±)-76** (8%)
6	**2c** (Me)	KO*t*Bu (0.10)	DMF	50 to 90 °C, 42 h	**(±)-75** (61%)

[a] Experimental procedures are given in **Chapter 6**.
[b] Reaction time until total consumption of the starting material (TLC).
[c] Chromatographically isolated.

by Zou and Coworkers.[230] For that reason, a substoichiometric amount (0.50 equiv.) of NaSPh at 90 °C (entry 4) was applied, and in this way **(±)-73** could be isolated in 66% yield. Methyl 3,2-enolone **72** (entry 5) underwent rearrangement into **(±)-75** in 71% yield under the established conditions with KO*t*Bu as the base. For this transformation, a side product could be isolated in minor amounts (8%) and NMR spectroscopically identified to be the 4,5-*cis*-configured *C*-5 epimerization product **(±)-76 (Scheme 5.11)**. In a similar manner but with 0.1 equiv. of the base (entry 6), 2-uloside **2c** was transformed in the cascade reaction to give **(±)-75** in an acceptable 61% yield. In this case, the epimerization product **(±)-76** was not identified in significant amounts.

An analysis of the H,H-NOESY spectra for isomers **(±)-75** and **(±)-76** (**Scheme 5.11**; for spectra, see **Appendix D**) provided further confirmations for the assigned structures and, specifically, for the *C*-4/5 relative configurations. Accordingly, **(±)-75** exhibited a correlation between the *C*-4-OH (clearly visible in acetone-D_6) and the *H*-5. On the other hand, **(±)-76** showed the expected correlations between the *C*-4-OH and the *C*-5-OMe, and between the *C*-4-CH_2 and *H*-5, respectively. Apart from these spectroscopic properties, an additional structural proof could be obtained for major

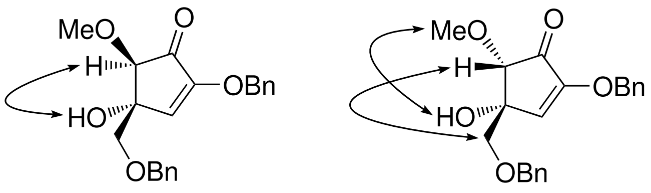

(±)-75 **(±)-76**

Scheme 5.11 Significant NOE contacts observed for cyclopentenones **(±)-75** and **(±)-76** in acetone-D_6 at 600.1 MHz. For H,H-NOESY spectra, see **Appendix D**.

isomer **(±)-75**, which could be crystallized from a solution in toluene/*n*-pentane. X-ray structural analysis of the racemic compound (orthorhombic space group $Pna2_1$; $Z = 4$ formula units in the unit cell) gave further confirmation for the assigned structure, and for the 4,5-*trans*-configuration **(Fig. 5.1)**. The torsion angle involving the α,β-unstaturated carbonyl (O1-C1-C2-C3 167.4°) as well as the torsion angle involving *C*-4/5 (O1-C1-C5-C4 −157.1°) both indicated a distortion of the cyclopentenone framework. In comparison, structurally related, but *C*-4-monosubstituted/*C*-5-unsubstituted cyclopent-2-enones feature torsion angles significantly closer to 180° (e.g. O1-C1-C2-C3 −177.6°, O1-C1-

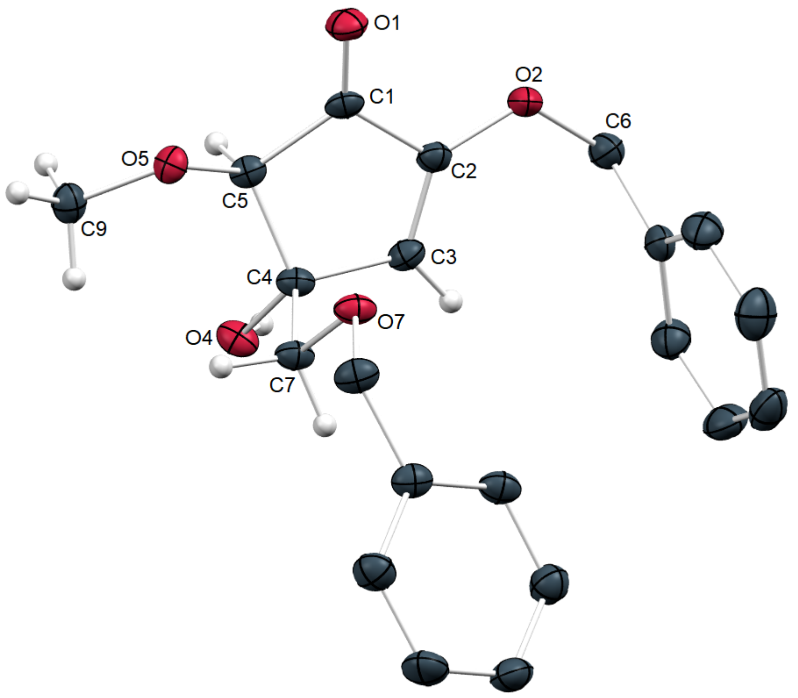

Figure 5.1 X-ray structure of compound **(±)-75**. Hydrogen atoms of the benzyl ethers are omitted for clarity. Ellipsoids are drawn at the 50% probability level. Red = oxygen, gray = carbon, white = hydrogen. Significant torsion angles: O1-C1-C2-C3 167.4°, O1-C1-C5-C4 −157.1°.

C5-C4 −178.0° for 2-hydroxy-4-methoxymethylcyclopent-2-enone[252]). Most probably, higher deviations from 180°, as found for **(±)-75**, can be explained by considering unfavorable steric repulsions, caused by the *C*-4/5 functionalizations of the compound.

5.3.3. Mechanistic Considerations

In the published rearrangements by Zou and Caddick, the formation of 5-hydroxy-substituted cyclopent-2-enones is observed. An explanation can be obtained from the generally accepted mechanism for these transformations **(Scheme 5.12, b)**.[230, 231, 233–238] Thus, in the final ring closure step, the formal *C*-5 to *C*-1 addition of the enolate intermediate **FO-d** provides the corresponding 5-hydroxycyclopent-2-enones. Inspired by this, a plausible mechanistic picture for the here described rearrangement was developed **(Scheme 5.12, a)**. According to this, deprotonation/enolization would occur at the *C*-5, giving the vinylogous enolate **40-a/40-b**. Putatively, deprotonation at the anomeric *C*-1 might be unfavorable due to repulsive interactions with the anomeric oxygen substituent, which is not present in Caddick's 1-deoxy system **(±)-FO** or Zou's *C*-glycosides **FL/FM** (comp. **Scheme 5.5** on page 147). Subsequently, a 6π disrotatory electrocyclic ring opening can give the achiral cyclic enolate **40-c/40-d**. In the final step, 4π conrotatory electrocyclic ring closure or an intramolecular aldol addition would result in the formation of **(±)-74**. Notably, this final step features a formal *C*-1 to *C*-5 addition, and therefore gives the 4-hydroxy-substituted cyclopent-2-enones as observed.

Apart from the related rearrangements by Zou and Caddick[230, 231, 233–238], several other reactions published in the literature are supportive for the proposed mechanism. For the 6π electrocyclic ring opening step (**40-a/40-b** to **40-c/40-d**), analogous processes have been described for the formation of other donor-acceptor-substituted diene intermediates.[232] Notably, in some published examples, a complex chemistry involving equilibria between electrocyclization and retro-cyclization processes was observed.[253, 254] Focussing on the second step (**40-c/40-d** to **(±)-74**), similar processes, both base- or acid-catalyzed, are usually referred to as a Nazarov-type conrotatory 4π electrocyclic process.[254–257] As an experimental evidence, such transformations frequently proceed with high diastereoselectivities associated with an electrocyclic reaction. In this context, Nieto Faza and Coworkers performed computational studies on oxygenated pentadienyl cation intermediates, as for example traversed in the Piancatelli rearrangement[255], to gain insight into the mechanistic nature of the cyclization reactions.[256] According to these theoretical studies, such cyclization processes probably proceed in a 4π electrocyclic ring closure supported by charge polarization.

(a)

proposed mechanism - this work:

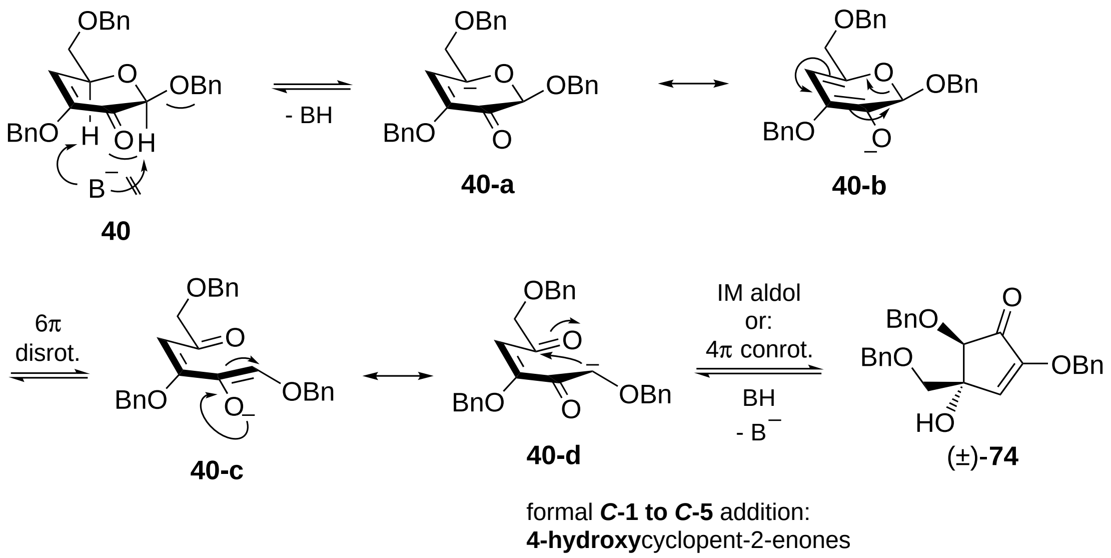
OBn
BnO
H
OH
B−
40
- BH
40-a
40-b
6π
disrot.
40-c
40-d
IM aldol
or:
4π conrot.
BH
- B−
(±)-74
formal **C-1 to C-5** addition:
4-hydroxycyclopent-2-enones

(b)

generally accepted mechanism - Zou 2001 and Caddick 1995:

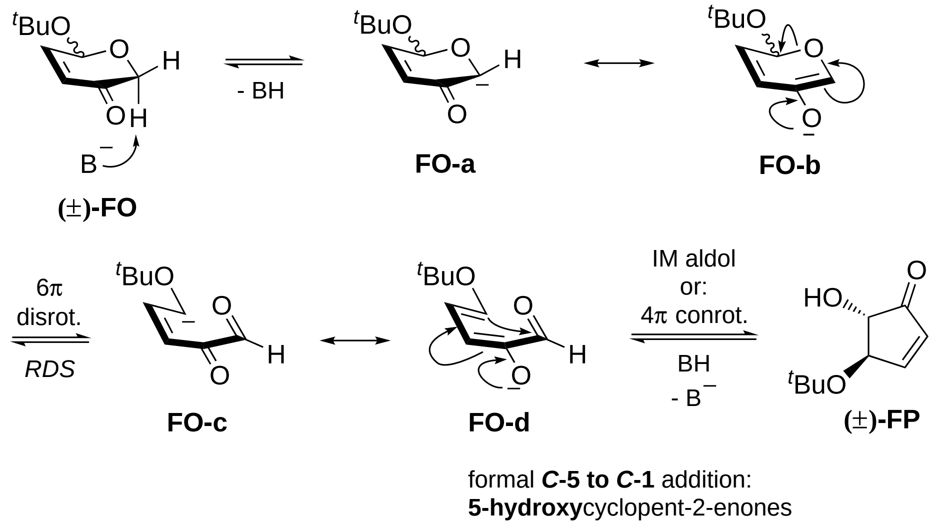
ᵗBuO
H
OH
B−
(±)-FO
- BH
FO-a
FO-b
6π
disrot.
RDS
FO-c
FO-d
IM aldol
or:
4π conrot.
BH
- B−
HO
(±)-FP
formal **C-5 to C-1** addition:
5-hydroxycyclopent-2-enones

Scheme 5.12 **(a)** Plausible mechanism for the formation of 4-hydroxycyclopent-2-enones, exemplified by the formation of **(±)-74** from **40**. The ring closure step features a formal *C*-1 to *C*-5 addition. **(b)** Proposed mechanism for published formations of 5-hydroxycyclopent-2-enones, exemplified by the formation of **(±)-FP** from **(±)-FO**.[230, 231, 238] The ring closure step features a formal *C*-5 to *C*-1 addition. B⁻ = basic reagent. *RDS* = rate-determining step. Counter ion not shown.

It should be noted that the rearrangement reaction described here exhibited some experimental distinctions from the literature transformations. Caddick and Coworkers, in later studies on the rearrangement of **(±)-FO**, found that the use of protic solvents (DABCO in *t*-BuOH) provided an improved yield of the product **(±)-FP**.[238] This beneficial effect was attributed to the stabilization of enolate intermediates by the protic solvent. However, for the described reaction of **40**, protic solvents were found to be unsuitable for the formation of **(±)-74** (**Table 5.1** on page 155, entries 6–11), although the proposed mechanism involves similar anionic enolate intermediates. Owing to these contradictory observations, alternative mechanistic pathways for the transformation of **40** to **(±)-74** were considered.

A possible alternative to the proposed mechanism could involve initial conjugated addition of the nucleophilic base, and formation of the *C*-4 branched intermediate **40-e**, which could undergo elimination to the common vinylogous enolate intermediate **40-b (Scheme 5.13, a)**. However, this pathway seems unlikely since no intermediate addition products could be isolated or observed by TLC or NMR analysis of the crude reaction mixtures. Furthermore, the reactivity trends for the nucleophilic reagents (rapid conversion of **40** with KO*t*Bu, significantly slower conversion with NaSPh), and the fact that **40** was inert under *thia*-Michael conditions, seem to be contradictive for such a pathway. In addition, mechanisms involving radical intermediates can be discussed. Thus, reaction of **40** with the base acting as a single electron reductant could provide, after α-cleavage and α-hydrogen abstraction, common intermediate **40-c (b)**. Furthermore, the reaction of open-chain enolate **40-c** could proceed *via* an intramolecular single electron transfer (SET), giving diradical **40-h** and, after radical recombination, the product **(±)-74 (c)**. Finally, a cyclic intermediate, for example vinylogous enolate **40-a**, could undergo homolytic cleavage of the *O*-5–*C*-1 bond and formation of diradical **40-i (d)**. A following intramolecular electron transfer step could give diradical **40-h** and, after recombination, **(±)-74**. Comparable diradical intermediates, similar to **40-h**, have in part been discussed as intermediates by Caddick and Coworkers.[235, 238]

To gain further insight into mechanistic features of the title reaction towards cyclopent-2-enones of type **(±)-74**, a series of additional experiments was performed. In these reactions 3,2-enolone **40** was subjected to the rearrangement under a variety of conditions involving other reagent/solvent combinations, or in the presence of additives.

(a)
conjugate addition/elimination pathway:

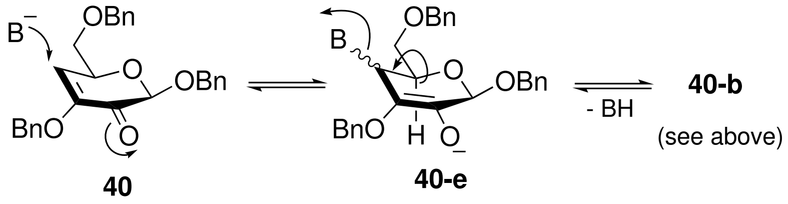
B⁻
OBn
O
OBn
BnO
O
40
B
OBn
O
OBn
BnO
H
O
40-e
- BH
40-b
(see above)

(b)
single electron transfer pathway:

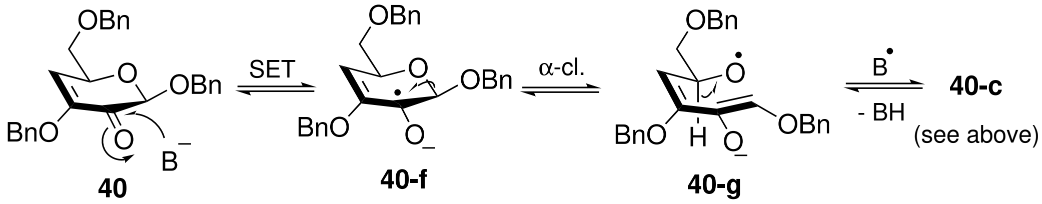
OBn
O
OBn
BnO
O
B⁻
40
SET
OBn
O
OBn
BnO
O
40-f
α-cl.
OBn
O
OBn
BnO
H
O
40-g
B•
- BH
40-c
(see above)

(c)
diradical pathway: IM single electron transfer

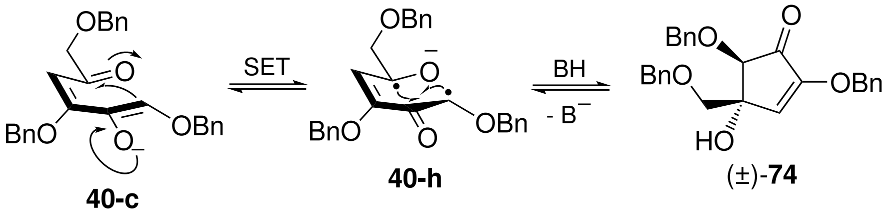
OBn
O
OBn
BnO
O
40-c
SET
OBn
O
OBn
BnO
O
40-h
BH
- B⁻
O
BnO
BnO
OBn
HO
(±)-74

(d)
diradical pathway: homolytic cleavage

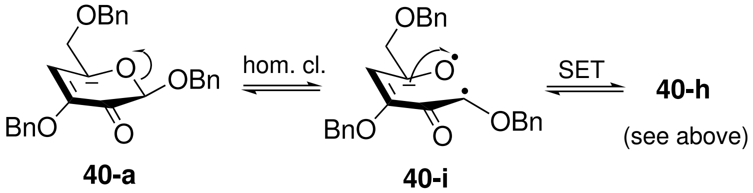
OBn
O
OBn
BnO
O
40-a
hom. cl.
OBn
O
OBn
BnO
O
40-i
SET
40-h
(see above)

Scheme 5.13 Alternatively considered mechanisms for the formation of (±)-**74** from **40**. (**a**) Conjugated addition and elimination pathway. (**b**) Single electron transfer pathway. (**c**) Diradical pathway *via* intramolecular single electron transfer. (**d**) Diradical pathway *via* homolytic cleavage. B^{-} = basic reagent. SET = single electron transfer. Counter ion not shown.

Radical-Scavenging Experiments

In mechanistic studies performed by Caddick and Coworkers, dihydropyran-3-one **(±)-FO** was subjected to the rearrangement into **(±)-FP** in the presence of the radical scavenger TEMPO (1 equiv., 2.5 equiv. DABCO in *N*,*N*-dimethylacetamide at 40 °C) .[238] Simultaneous GC monitoring of the formation of **(±)-FP** confirmed that the reaction with TEMPO proceeded with practically the same rate as a control reaction without TEMPO. Thus, the authors concluded that a mechanism involving radical intermediates was unlikely.

A similar experiment with **40** in the presence of TEMPO, under the optimized reaction conditions, was designed. Due to the base-induced solvent degradation, as discussed above, the rearrangement processes exhibited significant variations concerning the reaction rate of identical reactions. Thus, time-dependent monitoring of the product formation, similar to the experiment by Caddick[238], seemed to be inappropriate to determine the influence of the radical scavenger TEMPO. However, ESI-MS studies of TEMPO addition products have been applied to track radical intermediates in biologically relevant reactions of proteins.[258] Inspired by this, the analysis of TEMPO scavenging products in reactions of **40** by ESI-MS analysis seemed to be a suitable method. Accordingly, after reacting **40** under the established conditions in the presence of TEMPO **(Scheme 5.14, a)**, ^{1}H NMR integration of the crude product was applied to determine the yield of unreacted **40** (11%) and of the product **(±)-74** (30%), which was obviously formed in a somewhat diminished yield. The following ESI-MS analysis of the crude product (**Scheme 5.14, (b)**, spectrum i) exhibited the expected signals of substrate/product mass ($[M+Na]^+$ m/z 453; $[M+K]^+$ m/z 469). In addition, signals in conformity with TEMPO adduct species of potential diradical intermediates were observable, as exemplified by m/z 588 ($[M+\dot{H}+TEMP\dot{O}+H^+]$ or $[M+H\text{-}TEMPO+H^+]$) and by m/z 743 ($[M+2\,TEMP\dot{O}+H^+]$). However, suitable reference samples containing TEMPO as a neat unreacted mixture with **40** and **(±)-74** (spectrum ii), or obtained in a similar reaction in the absence of the base (spectrum iii) also exhibited the signal at m/z 588. Concludingly, this signal can most likely be attributed to be a spectrometer adduct of TEMPO-H, which is formed by hydrogen abstraction of a closed-shell species. In contrast, m/z 743 could only be observed for the original reaction. A following high resolution ESI-TOF-MS analysis for the corresponding signal (calcd. for $C_{45}H_{63}N_2O_7$ $[M+2\,TEMP\dot{O}+H^+]$: 743.4630, found: 743.4628) was also found to be in agreement with a potential double TEMPO adduct. It was furthermore observed that handling of the TEMPO-containing crude reaction samples at ambient temperature resulted in an observable signal, reduced by two mass units, at m/z 586. Observation of this species

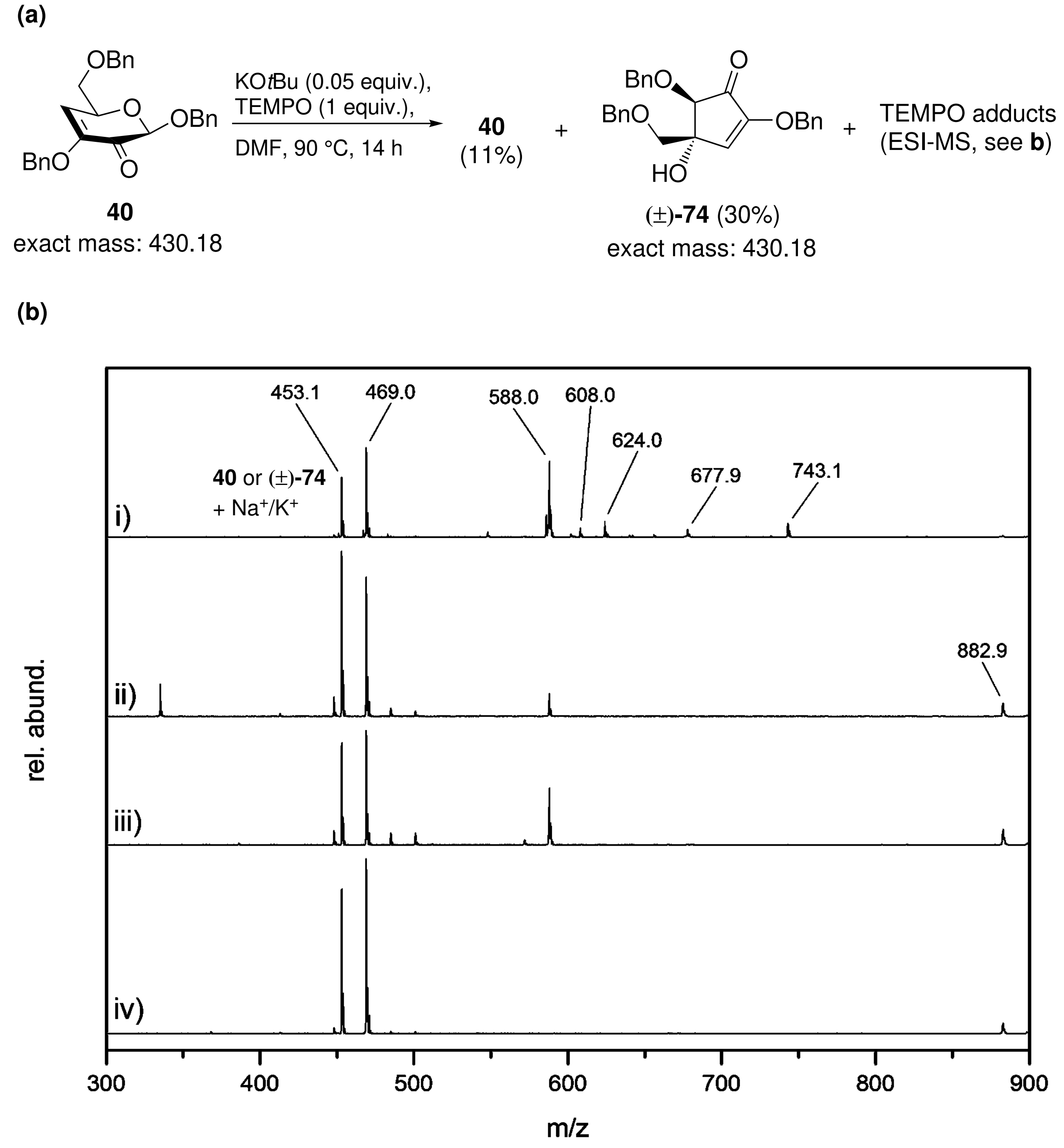

Scheme 5.14 Radical scavenging experiments. **(a)** Reaction of **40** in the presence of TEMPO. Yields determined by ^{1}H NMR integration with benzaldehyde as an internal standard. **(b)** ESI-MS spectra of radical scavenging products and reference samples. Material obtained as stated below was dissolved in MeOH (35 µg/mL) and injected. Conditions for reactions: anhydrous, degassed DMF, 90 °C, 14 h. Sample preparation: **i)-scavenging sample:** substrate **40** (36 mg; 0.084 mmol) and TEMPO (0.084 mmol) in DMF (2.5 mL) was reacted with 235 µL of KO*t*Bu in DMF (2 mg/mL; 4.2 µmol). Workup as described for the synthetic scale provided the crude sample. **ii)-not reacted:** a neat mixture of **40**, **(±)-74** and TEMPO (1:1:7) was analyzed. **iii)-no base:** substrate **40** (17 mg; 0.039 mmol) and TEMPO (0.039 mmol) in DMF (1.3 mL) were reacted. **iv)-no TEMPO:** substrate **40** (44 mg; 0.102 mmol) in DMF (2.7 mL) with 285 µL of KO*t*Bu in DMF (2 mg/mL; 5.0 µmol) were reacted.

could, most likely, be attributed either to dehydrogenation (double hydrogen abstraction) of **40/(±)-74** by residual TEMPO, or to an adduct containing the TEMPO-derived oxoammonium ion ([M+TEMPO$^+$]).

Based on the described results of radical scavenging experiments, involving a diminished yield in the formation of **(±)-74** in the presence of TEMPO together with the identification of potential TEMPO adduct species by ESI-MS, a mechanism featuring radical intermediates cannot be ruled out. However, especially under the forceful conditions of the reaction (90 °C in DMF), the inertness of TEMPO towards closed-shell species like the substrate/product or the solvent seems to be questionable. In this regard, TEMPO-induced side reactions like hydrogen abstractions or single electron oxidation reactions have to be considered, since such side reactions would diminish the significance of the obtained results for the general mechanism of the reaction.[139, 259, 260]

Several attempts were undertaken to track potential radical intermediates by EPR monitoring of the reaction of **40**. However, in this regard, all efforts remained unfruitful. Direct EPR-monitoring of the prototype transformation of **40** (for experimental details, see **Chapter 6.1** on page 179) in the temperature range 20–100 °C only provided unreproducible and unspecific signals of weak intensity (not shown). Following analogous experiments were performed utilizing *N*-*tert*-butyl-α-phenylnitrone[261, 262] (PBN) as a spin trapping agent (0.25 or 1.0 equiv.; 20–100 °C). These experiments resulted, albeit also weakly reproducible, in low-intensity signals associated with nitroxyl radical products (after 2–3 h at 40 °C, or after 5 min at 100 °C). However, similar signals were observable for a reference sample containing no substrate **40**, but PBN and KO*t*Bu (1:1) in DMF, thus indicating an origin related to the base-induced decomposition of PBN or degradation reactions involving the solvent DMF.

Concludingly, the radical scavenging results described here seem to be ambiguous. TEMPO radical scavenging in combination with ESI-MS analysis provided signals in conformity with TEMPO adduct species of radical/diradical intermediates. However, due to the questionable inertness of TEMPO under the forcing reaction conditions, and since no radical intermediates could be directly observed *via* EPR spectroscopy, the proposed mechanism involving non-radical intermediates (**Scheme 5.12, (a)** on page 160) seems to be the most plausible mechanism.

Isolation of Colored Side Products

The rearrangement reactions described here exhibited a striking property: reaction conditions which displayed significant formation of the cyclopentenone product (**Table**

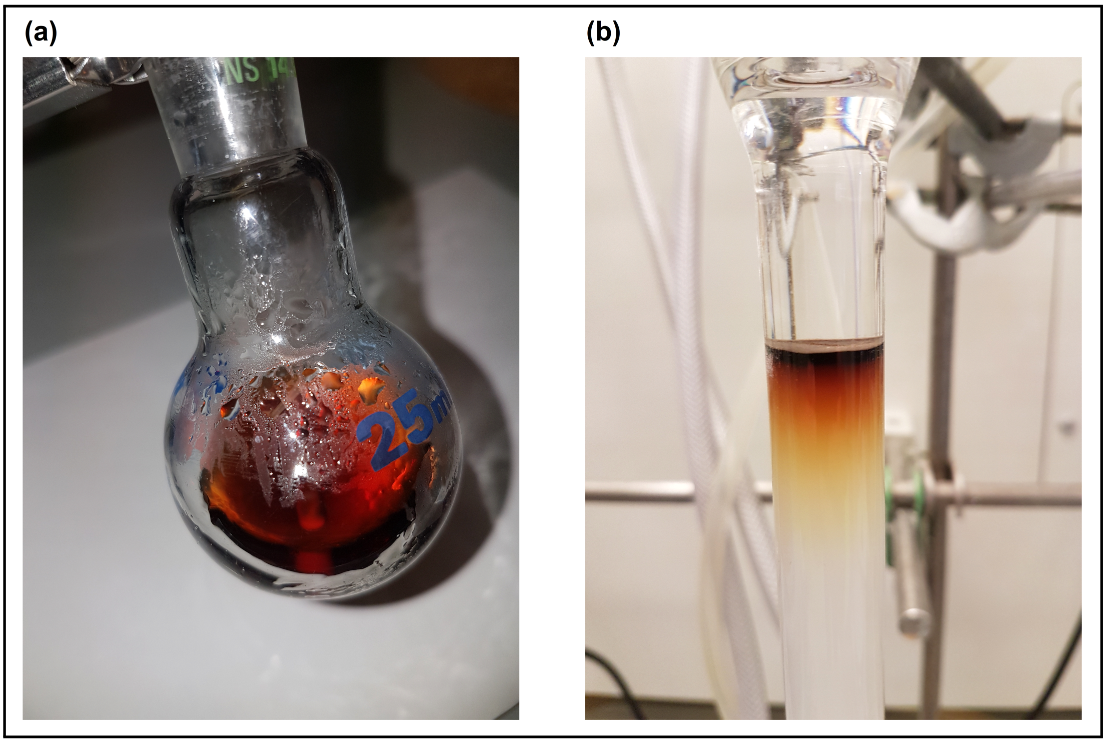

Figure 5.2 **(a)** Red coloring of the reaction mixture in the transformation of **40** into **(±)-74**. The picture refers to the reaction in **Scheme 5.15, (a)**. **(b)** Colored residue upon column chromatography (SiO$_2$) of the crude product obtained from the reaction in **Scheme 5.15, (a)**.

5.1 on page 155, entries 1, 4, 5, 14) were accompanied by an instant, clearly visible deep red coloring of the homogeneous reaction mixtures **(Fig. 5.2, a)**. Likewise, reactions in which only slow conversion to the product **(±)-74** occurred (entries 2 and 7), the coloring appeared with a delay of several hours. A suitable reference sample (2 mg/mL KO*t*Bu in DMF at 90 °C) without the substrate **40** did not display a coloration, thereby precluding an effect related to the solvent degradation. In the comparable literature reactions towards 5-hydroxycyclopent-2-enones, Zou and Coworkers did not report on any coloration of the reaction mixtures.[230] On the other hand, for the transformation of **(±)-FO** with Et$_3$N in DMF, Caddick and Coworkers reported on a black reaction mixture. In light of the proposed mechanism for the formation of 4-hydroxycyclopent-2-enones, involving the highly conjugated open-chain intermediates of type **40-c/40-d** (**Scheme 5.12, (a)** on page 160), it seemed likely that the observed intense coloring might originate from such donor-acceptor-substituted diene intermediates, or from derived condensation/degradation products.

In a prototype reaction of 3,2-enolone **40 (Scheme 5.15, a)** with an increased amount of KO*t*Bu (0.15 equiv.) in DMF, after neutralization (acetate buffer pH 5)

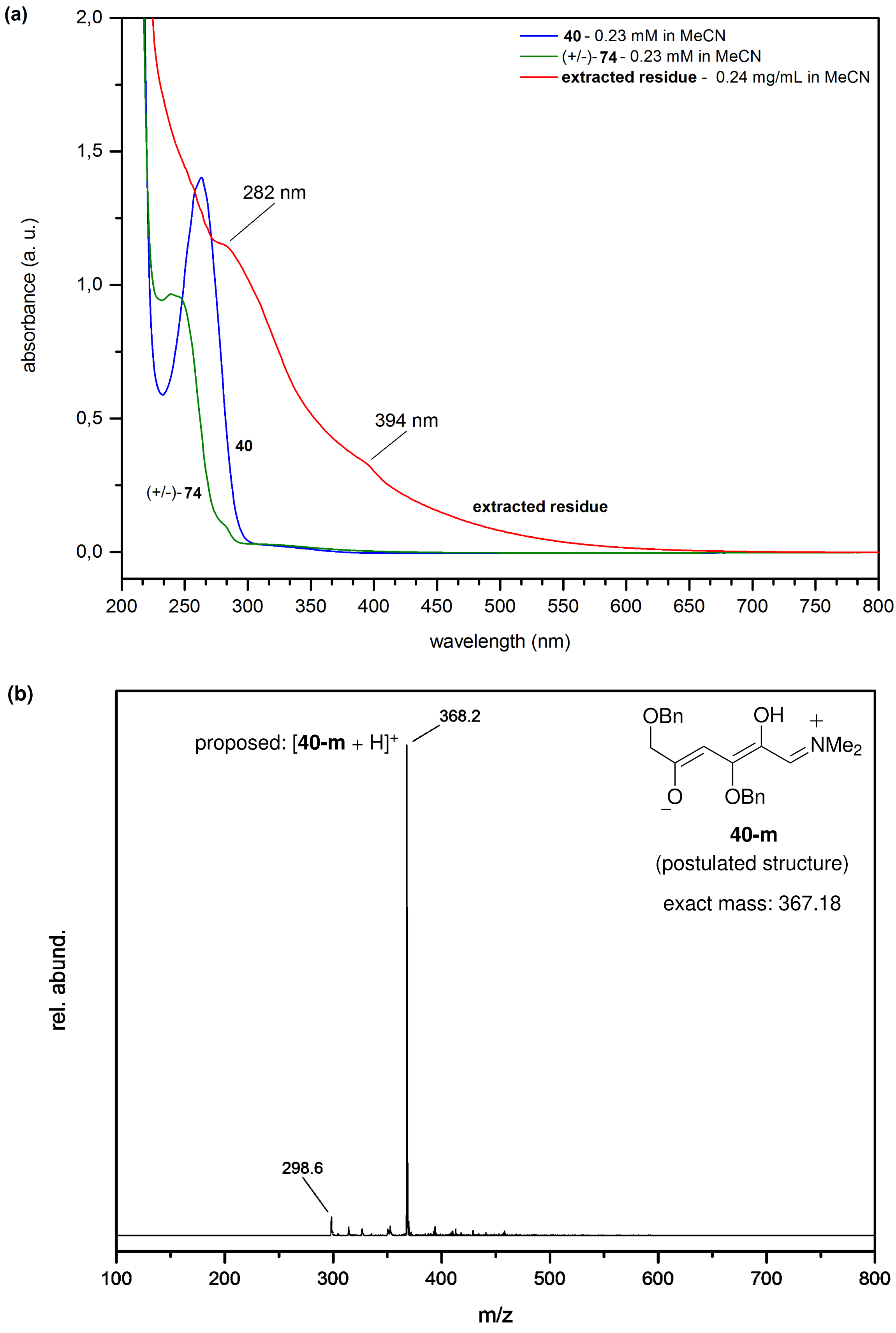

Figure 5.3 (a) UV/Vis spectrum of the extracted chromatography residue from the reaction of **40** in **Scheme 5.15, (a)**. (b) ESI-MS spectrum of the extracted residue.

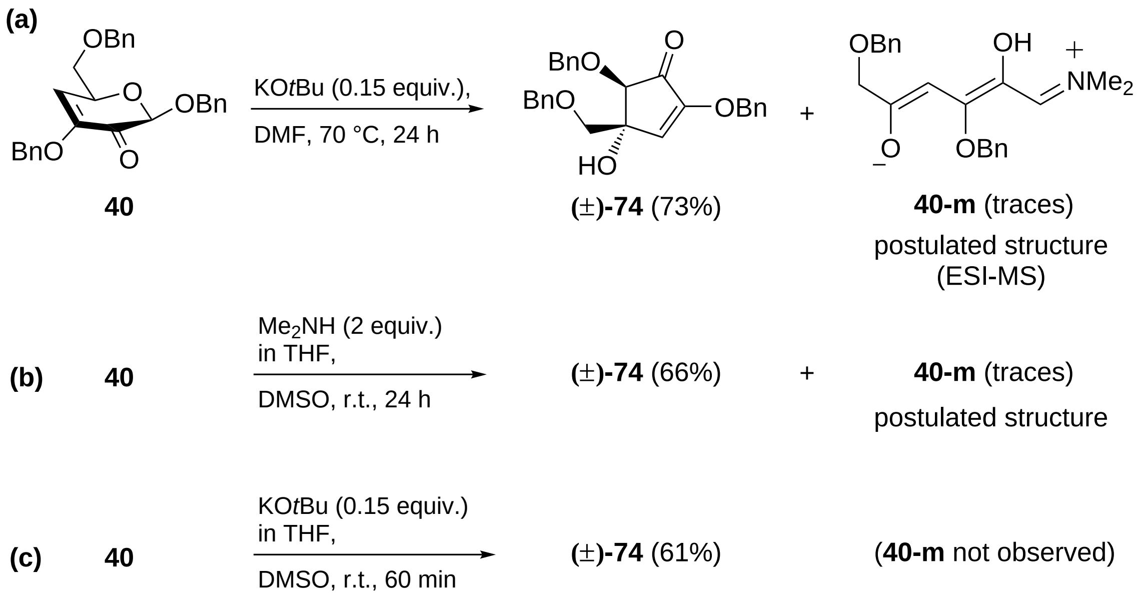
(a)
OBn
O
OBn
BnO
O
40
KOtBu (0.15 equiv.),
DMF, 70 °C, 24 h
BnO
BnO
O
OBn
HO
(±)-74 (73%)
+
OBn
OH
+
NMe2
O
−
OBn
40-m (traces)
postulated structure
(ESI-MS)
(b)
40
Me2NH (2 equiv.)
in THF,
DMSO, r.t., 24 h
(±)-74 (66%)
+
40-m (traces)
postulated structure
(c)
40
KOtBu (0.15 equiv.)
in THF,
DMSO, r.t., 60 min
(±)-74 (61%)
(40-m not observed)

Scheme 5.15 Reactions for the extraction of colored side products. **(a)** Reaction of **40** with KO*t*Bu in DMF. The structure of proposed side product **40-m** is shown. **(b)** Reaction utilizing Me_2NH as the sole base in DMSO. **(c)** Reaction with KO*t*Bu in DMSO. Yields were determined by ^{1}H NMR integration with benzaldehyde as an internal standard.

and following complete evaporation of the volatile components, a dark brown oil was obtained as the crude product. ^{1}H NMR integration was used to determine the yield of **(±)-74** (73%), followed by chromatographic purification of the crude oil. Upon silica gel chromatography, a brownish-red residue was obtained **(Fig. 5.2, b)**, which did not display chromatographic mobility even in increasingly polar solvents (toluene/ethyl acetate, 10:1 to 1:1, then 100% ethyl acetate, then 100% acetonitrile). By extraction of this residue from the silica gel layer with methanol, filtration and evaporation, a brownish residue could be obtained. Extraction of the colored parts with acetone provided, after evaporation, traces of a red oil (1 mg from 78 mg of **40**). NMR spectroscopic analysis of the sample was not feasible, and provided only weakly reproducible spectra with unspecific broad signals in several solvents. However, UV/Vis spectra in acetonitrile could be obtained **(Fig. 5.3, a)**. As compared to the substrate **40** and the product **(±)-74**, an increased absorbance starting around 650 nm was noticeable, together with shoulders at 394 nm and 282 nm, respectively.

ESI-MS analysis of the same extracted material provided a remarkably simple spectrum, featuring essentially one high intensity signal at m/z 368 **(Fig. 5.3, b)**. This mass-to-charge ratio seemed to be consistent with a species of substrate/product mass, undergoing substitution of one benzyloxy group with a dimethylamino group. High

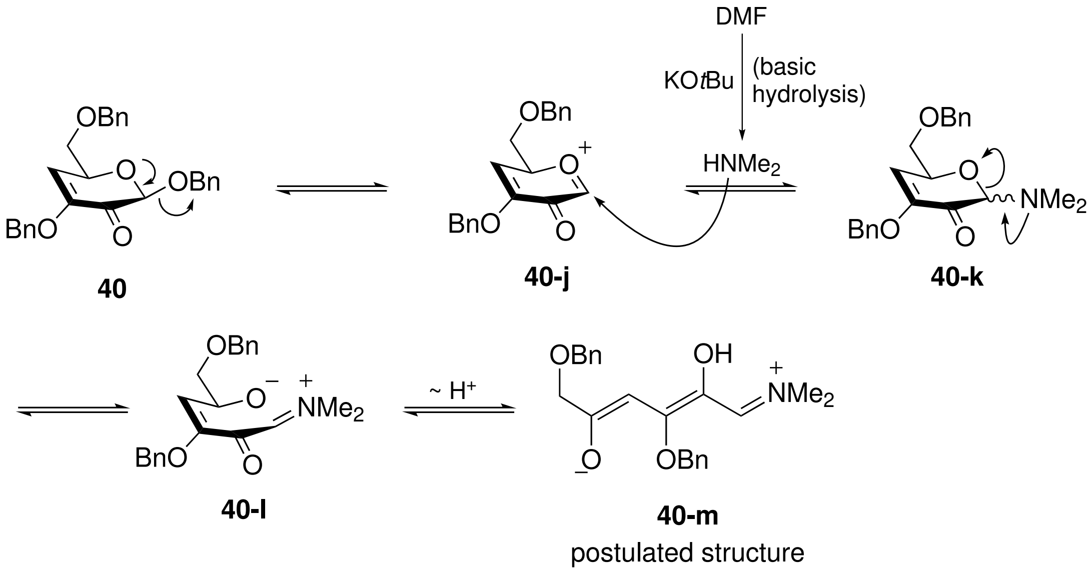

Scheme 5.16 Mechanistic suggestions for the formation of side product **40-m** (proposed structure) *via* reaction with Me$_2$NH from base-induced DMF decomposition.

resolution ESI-TOF-MS analysis was, likewise, found to be compatible with these results (calcd. for $C_{22}H_{26}NO_4$ $[M+H]^+$: 368.1856, found: 368.1858). To account for these considerations, the following mechanistic explanation is proposed **(Scheme 5.16)**. Basic hydrolysis of the solvent DMF by KO*t*Bu[251] results in the formation of dimethylamine, thus present in the reaction mixture. Substrate **40** undergoes explusion of the anomeric benzyloxide group and formation of the glycosyl cation **40-j** (the tautomeric form of a 3-oxidopyrylium ion). The anomeric cation is trapped by dimethylamine, giving the *N*-glycoside **40-k**. Subsequent ring opening and tautomerization reactions could provide the conjugated iminium ion **40-m** (or a tautomeric form of it) as the proposed side product. Notably, the structure of **40-m** is purely tentative. However, it seemed to be in good agreement with the observation that the colored residue remained chromatographically immobile when basic eluents (10% Et_3N in EtOAc) were employed, which seemed to be suggestive for a zwitterionic iminium species of type **40-m**, rather than for anomeric amine **40-k** of the same molar mass.

To find further evidence for the suggested role of DMF-derived dimethylamine, two additional experiments were performed. When a reaction of **40** was conducted with dimethylamine as the sole base in DMSO **(Scheme 5.15, b)**, the same product **(±)-74** was formed in good yield (66%). Extraction of the chromatographic residue as described above and analysis by ESI-MS gave a similarly intensive signal at m/z 368, thereby suggesting the formation of the same low-yield side product. In contrast, when the reaction was run with KO*t*Bu in DMSO **(Scheme 5.15, c)**, and thus in the absence of a source of dimethylamine, the derived ESI-MS spectrum exhibited no corresponding signal at m/z 368. In this case, from the visually comparable brownish-red residue, only mass-to-charge ratios consistent with dehydration products of the substrate/product mass could be obtained.

The proposed structure of the donor-substituted conjugated iminium ion **40-m** is closely related to the Stenhouse salts (or: pyridinium dyes/pentamethine dyes), a highly colored family of pentadienyl iminium dyes.[263, 264] In connection with the title reaction, this class of compounds is widely known to undergo 4π electrocyclic ring closure reactions to amino-substituted cyclopent-2-enone derivatives, for example in processes like the *aza*-Piancatelli reaction (the acid-catalyzed reaction of furfuryl alcohols with amines), or in the ring opening/ring closure cascade of furfural-derived imines.[257, 265] Likewise, 4π electrocyclic ring closures of the corresponding 1-oxo derivatives of stenhouse salt species (the non-iminium derivatives) are ubiquitously discussed in processes like the original Piancatelli rearrangement, the acid-catalyzed transformation of furfuryl alcohols into 4-hydroxycyclopent-2-enones.[249, 255, 264, 266] In this regard, the given considerations can be regarded as an initial classification of the title reaction within the complex field of the isomerization chemistry of unsaturated five- and six-membered rings.

Isomerization Studies

The proposed mechanism for the described transformation of 3,2-enolones into 4-hydroxycyclopent-2-enones (**Scheme 5.12, (a)** on page 160) suggests equilibria between all intermediate species. Thus, the reaction of product **(±)-74** in a 4π electrocyclic ring opening or in a retro-aldol reaction, followed by 6π electrocyclic ring closure, could potentially afford the original substrate **40**, albeit as a racemic mixture. In this context, in mechanistically comparable transformations published in the literature, complex quilibria involving five- and six-membered cyclic products have been observed.[254]

Thus, in order to gain insight into the reversibility of the described transformation, cyclopent-2-enone **(±)-74** was reacted under conditions similar to its original formation **(Scheme 5.17, top)**. The reaction proceeded reluctantly even in the presence of increased amounts of KO*t*Bu (0.15 equiv.) at 70 °C. After 24 h, the reaction mixture contained large amounts of unreacted substrate **(±)-74** (43%), together with two minor products **(±)-77** (20%) and **(±)-78** (16%). Chromatographic purification of the mixture provided pure samples of **(±)-77** and **(±)-78** in 17% and 16% isolated yields, respectively, and both isomers were determined to be of the same molar mass like **(±)-74** by ESI-MS analysis and, likewise, obtained in racemic form. Following NMR

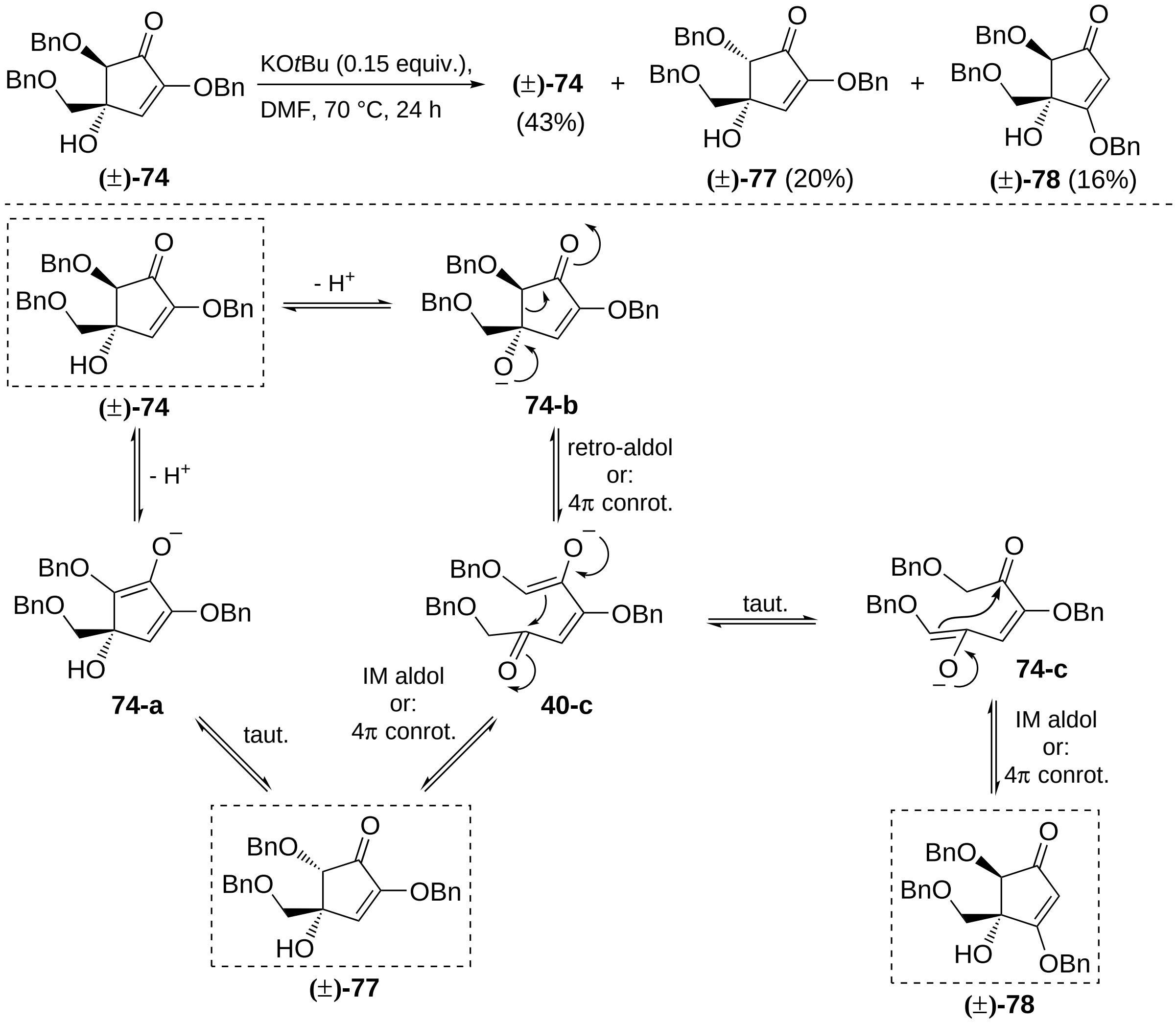

Scheme 5.17 Top: reaction of cyclopentenone **(±)-74** under the rearrangement conditions, affording diastereoisomeric **(±)-77** and regioisomeric **(±)-78**. Yields were determined by ^{1}H NMR integration with benzaldehyde as an internal standard. Bottom: plausible mechanism for the isomerizations.

analyses fully disclosed the structure of the C-5 isomerized 4,5-*cis*-configured **(±)-77** (comparable to the methyl derivative **(±)-76**). Remarkably, **(±)-78** was established to be the corresponding regioisomeric 3-benzyloxy derivative. As compared to **(±)-74**, the ^{13}C NMR spectrum of **(±)-78** featured a significantly deshielded signal for the C-3 (183.2 vs. 127.3 ppm) associated with a vinylogous ester, and a high-field signal for C-2 (104.3 vs. 155.2 ppm).

From a mechanistic perspective **(Scheme 5.17, bottom)**, the formation of the C-5 epimerization product **(±)-77** can, in a straightforward manner, be explained by formation of the intermediate enolate **74-a**, which can undergo tautomerization to minor isomer **(±)-77** or back to major isomer **(±)-74**. Alternatively, deprotonation of the free hydroxyl group in **(±)-74** gives the alkoxide **74-b**. From this intermediate, ring opening (either in an electrocyclic reaction or in a retro-aldol reaction) gives the enolate **40-c** proposed as the open chain intermediate in the original rearrangement process. **40-c** can cyclize to the originally unfavored 4,5-*cis*-isomer **(±)-77**, or back to major isomer **74-b**. To account for the formation of the 3-benzyloxy isomer, the double keto-enol tautomerization of **40-c** could give enolate **74-c**, followed by ring closure to **(±)-78**. In this way, the observed formation of **(±)-78** serves as a good evidence for the existence of open-chain intermediate species of the type **40-c/74-c** within the overall mechanistic picture.

Concluding Remarks

As a clarification, the title reaction for the transformation of carbohydrate-derived 3,2-enolones into 4-hydroxycyclopent-2-enones can be discussed in the context of widely known related transformations of five- and six-membered unsaturated carbocycles and heterocycles **(Scheme 5.18)**. Thus, furfuryl alcohols, available from the reduction of biomass-derived furfural, can be converted into 4-hydroxycyclopent-2-enones in the Piancatelli rearrangement under Lewis or Brønsted acid catalysis.[249, 255, 264, 266] Alternatively, furfuryl alcohols can undergo ring expansion into dihydropyran-3-one systems, a process initiated under oxidative conditions (e.g. Br_2 or NBS) which is referred to as the Achmatowicz reaction.[267, 268] Highly functionalized (oxygenated) dihydropyran-3-one systems can further be obtained from carbohydrate sources by

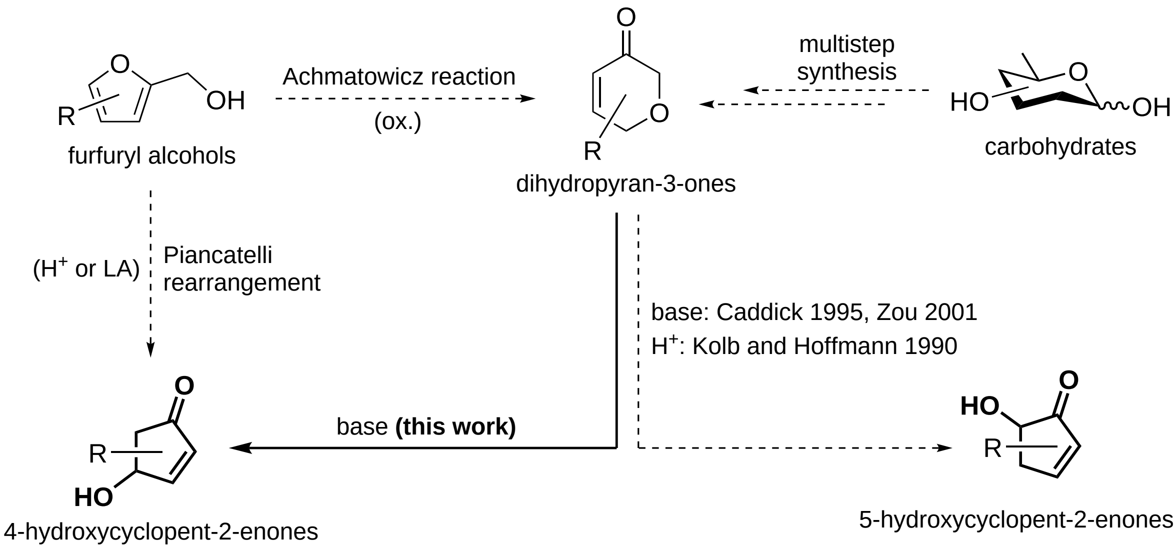
O
R
OH
furfuryl alcohols
Achmatowicz reaction
(ox.)
O
O
R
dihydropyran-3-ones
multistep
synthesis
HO
O
OH
carbohydrates
(H+ or LA)
Piancatelli
rearrangement
base: Caddick 1995, Zou 2001
H+: Kolb and Hoffmann 1990
O
R
HO
4-hydroxycyclopent-2-enones
base (this work)
O
HO
R
5-hydroxycyclopent-2-enones

Scheme 5.18 Schematic representation of the title reaction in the context of related transformations.

multistep carbohydrate transformations, resulting in enantiopure dihydropyran-3-ones (carbohydrate 3,2-enolones). As previously described, Caddick and Coworkers demonstrated that such dihydropyran-3-ones can undergo a base-induced rearrangement into 5-hydroxycyclopent-2-enones.[231] In a similar transformation using carbohydrate-derived enantiopure dihydropyran-3-ones, Zou and Coworkers demonstrated a similar rearrangement to 5-hydroxycyclopent-2-enones, albeit also in racemic form due to a proposed achiral open chain intermediate.[230] Comparable rearrangements by Kolb and Hoffmann, which proceeded under Brønsted acid catalysis, suggest that a wide array of conditions can initiate such a rearrangement.[232] In this context, the title reaction constitutes a novel method for the synthesis of the corresponding regioisomeric 4-hydroxycyclopent-2-enones from dihydropyran-3-ones.

However, the developed rearrangement comprises some drawbacks: a) Since the literature reactions towards 5-hydroxycyclopent-2-enones proceed under very similar conditions as compared to the title reaction (basic reagents in polar protic or aprotic solvents), it seems likely that the rearrangement is restricted to a narrow substrate scope of *O*-glycosidic 3,2-enolones. Furthermore, the highly basic conditions can be expected to be incompatible with ester-protected carbohydrate substrates, which constitute the majority of published potential carbohydrate 3,2-enolone substrates. b) A cumbersome multistep synthesis is required to obtain the carbohydrate substrates for the rearrangement (from D-glucose: 6 steps towards the 2-uloside substrates, 7 steps towards the 3,2-enolones). c) Only racemic products can be obtained. Putatively, an achiral open chain intermediate is formed, resulting in complete loss of stereoinformation present in the carbohydrate substrate. Since carbohydrates are frequently employed as chiral building blocks towards enantiopure products in what is referred to as the chiral pool approach, this can be regarded as a severe disadvantage.

With the goal of developing an asymmetric protocol of their rearrangement towards 5-hydroxycyclopent-2-enones, Caddick and Coworkers employed chiral cinchona alkaloid bases like quinine or quinidine. However, only a low level of enantioselectivity was observed (ee $< 6\%$).[237] In contrast, the lipase-based kinetic resolution provided the acetylated and the non-acetylated products in good enanomeric excesses (ee $> 95\%$).[238] Apart from this, multiple approaches towards chiral cyclopent-2-enones in general have been published, including an asymmetric Piancatelli rearrangement employing chiral BINOL-derived Brønsted acids.[250, 265] This seems to suggest that extended investigations into the title rearrangement, including hitherto unexplored acidic conditions, could potentially facilitate an asymmetric reaction. In this regard, the results described here offer a detailed examination of this transformation which might be valuable concerning further investigations.

5.3.4. Antimicrobial Activity Screenings

Compounds featuring the cyclopent-2-enone structural motif have been isolated from natural sources, for example represented by the clavulone prostanoids.[242, 243, 269] In part, such structures been associated with biological activities, including antibiotic[241, 245] and cytotoxic[244, 246, 270] properties.[248] Likewise, a number of dihydropyran-3-one systems with interesting biological activities have been identified.[271–274] From this perspective, a screening for potential activities of the 3,2-enolone substrates, and of the derived cyclopent-2-enones formed in the title reaction, was of interest.

Antimicrobial screenings involving the 3,2-enolones **3b**, **40** and **72**, as well as the racemic cyclopent-2-enones **(±)-73**, **(±)-74**, **(±)-75** and **(±)-76**, were performed by the CO-ADD initiative (The Community for Open Antimicrobial Drug Discovery), located at the University of Queensland, Australia (for screening details and results, see **Appendix C**). The antimicrobial activity was determined by the measurement of the percentage of growth inhibition, and included the following selection of five bacteria and two fungi: *Staphylococcus aureus* (ATCC 43300), *Escherichia coli* (ATCC 25922), *Klebsiella pneumoniae* (ATCC 700603), *Acinetobacter baumannii* (ATCC 19606), *Pseudomonas aeruginosa* (ATCC 27853), *Candida albicans* (ATCC 90028), *Cryptococcus neoformans var. grubii* (H99, ATCC 208821). The screening samples were prepared using stock solutions of the respective compound in DMSO (32 µg/mL). Albeit, no significant antimicrobial activity of the tested compounds against the involved bacterial and fungal strains could be found.

5.4. Summary of this Chapter

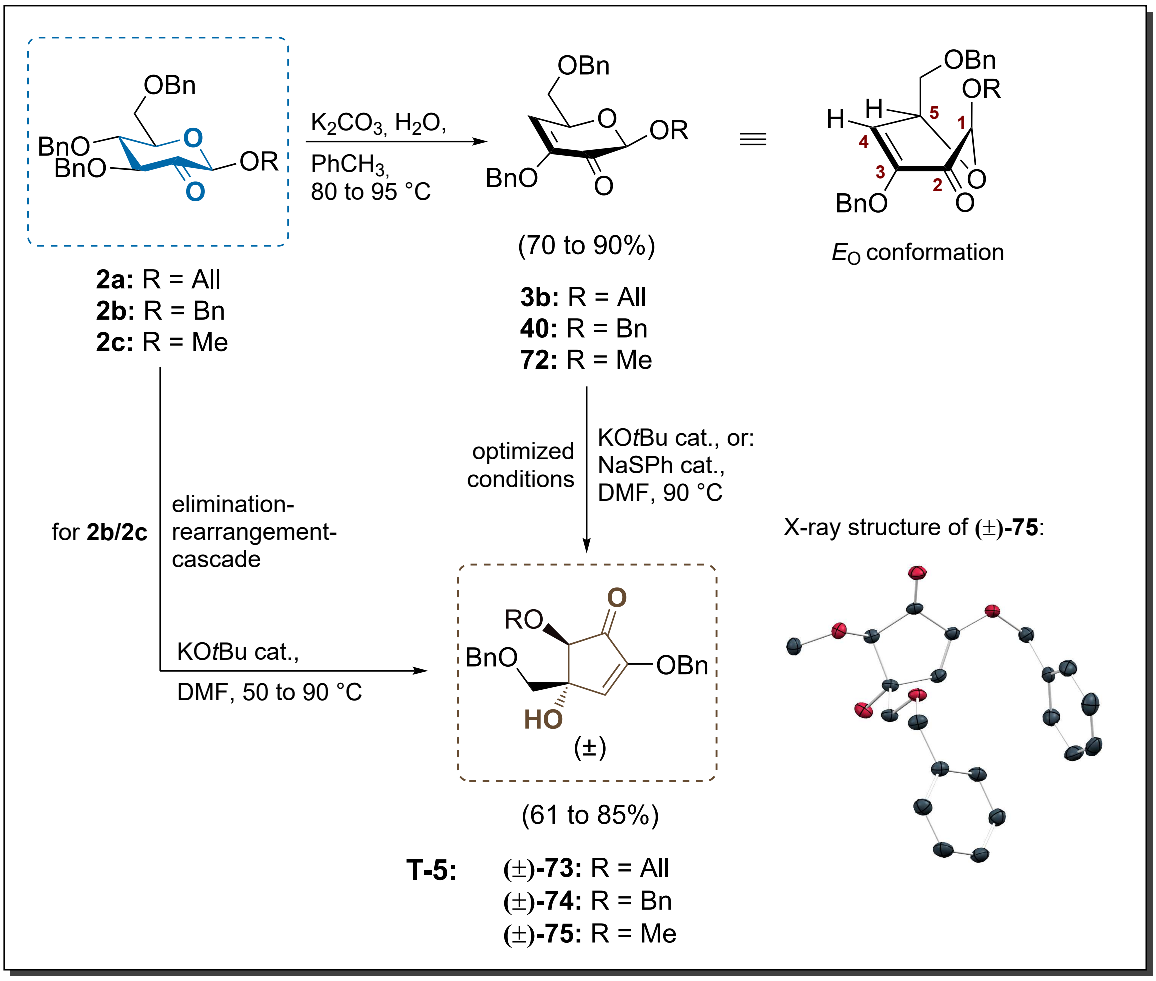
OBn
BnO
BnO
O
O
OR
2a: R = All
2b: R = Bn
2c: R = Me
K2CO3, H2O,
PhCH3,
80 to 95 °C
OBn
O
OR
BnO
O
(70 to 90%)
3b: R = All
40: R = Bn
72: R = Me
≡
OBn
OR
H
H
5
1
4
3
2
BnO
O
O
EO conformation
for 2b/2c
elimination-
rearrangement-
cascade
KOtBu cat.,
DMF, 50 to 90 °C
optimized
conditions
KOtBu cat., or:
NaSPh cat.,
DMF, 90 °C
RO
O
BnO
OBn
HO
(±)
(61 to 85%)
T-5:
(±)-73: R = All
(±)-74: R = Bn
(±)-75: R = Me
X-ray structure of (±)-75:

Scheme 5.19 Synthetic routes described in this chapter. Formation of racemic cyclopent-2-enones **(±)-73**, **(±)-74** and **(±)-75** from 2-ulosides **2a,b,c** by a sequence of elimination and base-mediated rearrangement.

Treatment of 2-uloside precursors **2a,b,c** with K_2CO_3 in wet toluene allowed for the clean formation of the carbohydrate 3,2-enolones **3b**, **40** and **72** *via* elimination of benzyl alcohol **(Scheme 5.19)**. In reactivity studies involving these intermediates, the α-oxygenated α,β-unsaturated carbonyl moiety was found to be inert towards the conjugated addition of nucleophilic reagents. In contrast, by employing catalytic amounts of basic KO*t*Bu or NaSPh in the polar aprotic solvent DMF, a previously undescribed rearrangement reaction afforded racemic 2-benzyloxy-4-hydroxycyclopent-2-enones **(±)-73,74,75** in generally good yields (61–85%). Likewise, 2-ulosides **2b** and **2c** could be directly converted into the respective cyclopent-2-enone products in an elimination-rearrangement cascade reaction. The structures of the racemic products could be fully established by using multiple methods including 2D NMR spectroscopy, chiral column HPLC, and X-ray crystallography on a crystalline sample obtained for the methyl derivative **(±)-75**.

In contrast to the described title reaction, affording the 4-hydroxycyclopent-2-enones, similar published rearrangements of dihydropyran-3-ones provide the corresponding 5-hydroxycyclopent-2-enone products. To explain these differences, a plausible mechanism was developed and discussed in the context of literature transformations. Further experimental studies gave insight into potential side products formed in the reaction. In this regard, an analysis of downstream isomerization processes from **(±)-73,74,75** towards diastereo- and regioisomeric cyclopent-2-enones completed the proposed mechanistic picture involving achiral, open chain enolate intermediates.

6. Experimental Part

6.1. Instruments and Techniques

For the isolation, purification and characterization of the compounds described in this thesis, the following instruments and techniques were used:

Analytical Thin-layer Chromatography (TLC): Reactions were monitored by TLC on Polygram Sil G/UV plates from Macherey-Nagel and the detection of spots was affected by inspection of the plates under UV light, by charring with H_2SO_4 (5% in EtOH), by staining with an alkaline aqueous solution of $KMnO_4$, or by staining with $(NH_4)_2MoO_4/Ce(SO_4)_2$ in dilute sulfuric acid.

Preparative Flash Column Chromatography: Preparative Chromatography for purification of the compounds was performed on silica gel (0.032–0.063 mm mesh) from Macherey-Nagel. For a typical chromatography procedure, the mass of silica gel used was equal to 50–200 times the mass of the crude product subjected to chromatography. Spherical SiO_2 (Reprosil 70 Si, 50 µm) was purchased from Dr. Maisch GmbH. This material was used for challenging purifications of compound mixtures with similar chromatographic mobility. Typically, the amount of spherical SiO_2 was equal to 200–300 times the mass of the crude product (ca. 50–200 mg of crude material in combination with 15–50 g of spherical SiO_2). After purification, the columns were rinsed with THF and acetone, and this way used ca. 5–10 times. RP-C18 silica gel 100 (fully endcapped) was purchased from Sigma-Aldrich. For all described RP-chromatographic purifications, columns with 10 g of RP material were used.

Chiral High-Performance Liquid Chromatography (HPLC): Chiral HPLC experiments of compounds **(±)-73**, **(±)-74** and **(±)-75** were performed with a Sykam S 1121 HPLC machine in combination with the column Reprosil Chiral-NR (8 µm, 150 × 4.6 mm) by Dr. Maisch GmbH. Isocratic *n*-hexane/*iso*-propyl alcohol (**(±)-73** and **(±)-74**: 90:10; **(±)-75**: 100:7) was used as the eluent with a flow of 1.6 mL/min (for **(±)-73** and **(±)-74**) or 2 mL/min (**(±)-75**). Detection of compounds was performed by UV detection at 254 nm. Samples of 1.8 mg of the compound were dissolved in 1 mL of the eluent (for **(±)-75**: addition of 200 µL $CHCl_3$) and injected into the system (**(±)-73** and **(±)-74**: 5 µL; **(±)-75**: 10 µL). Data processing and integration was done with the software PeakSimple 4.49 64 bit. Chromatograms are given in **Appendix B**.

Melting Points: Melting points were determined with a Büchi Melting Point M-560 apparatus.

Optical Rotations: Optical rotations were measured with a Perkin-Elmer Polarimeter 341 in a 10 cm glass cuvette at 20 °C and at a wavelength of 589 nm.

Mass Spectrometry (MS): The following spectrometers were used for the measurement of the corresponding mass spectra: FAB-MS: Finnigan model TSQ 70. ESI-MS: Bruker Daltonics ESQUIRE 3000 Plus. ESI-TOF-HRMS: Bruker Daltonics maXis 4g. ESI-FTICR-HRMS: Bruker Daltonics Apex II.

Nuclear Magnetic Resonance (NMR): NMR spectra were recorded with the following spectrometers: Bruker Avance III HD 400 (^1H: 400.2 MHz; ^{13}C: 100.6 MHz), Bruker Avance III HDX 600 (^1H: 600.2 MHz; ^{13}C: 150.9 MHz), Bruker Avance III HDX 700 (^1H: 700.3 MHz; ^{13}C: 176.1 MHz). Values of the chemical shift δ [ppm] are given in relation to tetramethylsilane. Solvent residual signals were used for referencing[275]: acetone-D_6: 2.05 (^1H) and 29.84 (^{13}C), $CDCl_3$: 7.26 (^1H) and 77.16 (^{13}C), CD_3OD: 3.31 (^1H) and 49.00 (^{13}C), DMSO-D_6: 2.50 (^1H) and 39.52 ppm (^{13}C). Spectra measured in D_2O were calibrated for residual or added (0.5%) MeOH (^1H: 3.34 ppm, ^{13}C: 49.50 ppm). ^{13}C NMR spectra were measured with broadband decoupling. The assignment of signals was supported by DEPT-135 spectra and 2D NMR spectra, including H,H-COSY, C,H-HSQC, F2-coupled C,H-HSQC, C,H-HMBC, H,H-NOESY, H,H-TOCSY and TOCSY-HSQC. The following abbreviations are used for the splitting patterns of signals: s (singlet), bs (broad singlet), d (doublet), t (triplet), q (quartet), dd (doublet of doublets), ddd (doublet of doublet of doublets), dddd (doublet of doublet of doublet of doublets), dt (doublet of triplets), m (multiplet). For diastereotopic methylene protons like the carbohydrate *H*-6, the signal appearing at a higher chemical shift was designated Ha, the one appearing at lower chemical shift Hb. In isomeric mixtures, corresponding signals are marked with an asterisk, if observable. For isomeric mixtures of complex carbohydrates, signal assignments, splitting patterns and integrations are only given where possible. Copies of ^1H and ^{13}C spectra are given in **Appendix E**.

Elemental Analysis (Combustion Analysis): Elemental analyses were performed with a HEKAtech Euro 3000 CHN analyzer.

UV/Vis Spectroscopy: UV/Vis spectra were recorded on a PerkinElmer Lambda 35 spectrometer using a 1 cm quartz glass cuvette.

X-ray Crystallography: X-ray data were collected on a Bruker SMART APEX II DUO diffractometer (for **11**: Bruker APEX II CCD) equipped with an IµS microfocus sealed tube and QUAZAR optics, using CuK_α radiation (λ = 1.54178 Å) or MoK_α radiation (λ = 0.71073 Å). Corrections for absorption effects were applied using SADABS.[276] The structures were solved by direct methods using SHELXS[277] and SHELXL/SHELXLE[278] for structure refinement. Complete crystallographic data have been deposited with the Cambridge Crystallographic Data Centre. This information can be obtained free of charge from `https://www.ccdc.cam.ac.uk` *via* the corresponding CCDC numbers of the structures. The CCDC numbers, techniques used for crystallization and crystal structure data/refinement parameters are given in **Appendix A**.

Electron Paramagnetic Resonance (EPR): EPR spectra were recorded with a Bruker EMX micro spectrometer in the X-band range. In a typical reaction, the substrate **40** (24 mg; 0.056 mmol) was dissolved in anhydrous, degassed DMF (290 µL) at 0 °C. A freshly prepared solution of KO*t*Bu 4 mg/mL in DMF (250 µL) was added, and the sample was stored at 0 °C until the EPR measurement of aliquotic samples was performed in quick succession. During measurement, the aliquotic sample was heated in the range 20–100 °C (20 °C steps; 5 min resting time at each temperature). In spin trapping experiments, a solution of **40** (16 mg; 0.037 mmol) in anhydrous degassed DMF (525 µL) at 0 °C was treated with *N*-*tert*-butyl-α-phenylnitrone (PBN; 0.25 equiv. or 1.0 equiv.), and then with a freshly prepared solution of KO*t*Bu 4 mg/mL in DMF (255 µL). The sample was stored at 0 °C until the EPR measurement of aliquotic samples as described above commenced.

6.2. General Methods

Non-aqueous reactions were run in oven-dried glassware and in anhydrous solvents using standard Schlenk techniques in combination with nitrogen as an inert gas for the exclusion of oxygen and humidity. If not stated otherwise, the given yields correspond to isolated yields of solvent-free material obtained after the respective method of purification (flash column chromatography, recrystallization or distillation).

6.3. Reagents and Materials

Commercial chemicals were purchased from the following suppliers: abcr, Acros Organics, Alfa Aesar, AppliChem, Carbolution, Carl Roth, euriso-top, Fisher Scientific, Fluka, Glycon Biochemicals, Merck, Riedel-de-Haën, Sigma-Aldrich, Strem Chemicals, TCI, Th. Geyer. If not mentioned otherwise below, all reagents were used as received. Dry solvents were either purchased in anhydrous form, or in technical grade and dried *via* the following standard methods: acetone ($CaSO_4$), acetonitrile (purchased from Acros), benzene (CaH_2), CH_2Cl_2 (P_4O_{10}), $CHCl_3$ (P_4O_{10}), 1,4-dioxane (Na/benzophenone), DMF (P_4O_{10}), DMSO (purchased from Sigma-Aldrich), EtOAc ($CaSO_4$), MeOH (Mg/I_2), *n*-hexane (Na/benzophenone), nitromethane ($CaCl_2$), toluene (purchased from Acros), THF (Na/benzophenone). After drying with the described method and distillation, solvents were stored under an atmosphere of nitrogen over activated molecular sieves 3 Å (not for acetone). Degassed solvents were obtained by using the freeze-pump-thaw technique.

6.3.1. Key Reagents, Prepared Reagents and Purified Reagents

The following list comprises a selection of critical reagents for key reactions and the corresponding commercial supplier. Furthermore, prepared reagents as well as purchased reagents that were purified prior to use are included.

- acetate buffer pH 5: NaOAc (1.6 g) and AcOH (337 µL) dissolved in water (200 mL).
- allyl alcohol: commercial material (Fluka) was stirred over CaH_2 at r.t. for 12 h followed by distillation.
- benzyl chloride: commercial material (Fluka) was dried over $MgSO_4$, filtered and distilled.
- *n*-BuLi: purchased from Acros Organics.
- *tert*-butyl hydroperoxide: purchased from Sigma-Aldrich.
- camphanoyl chloride: purchased from Sigma-Aldrich.
- Dess-Martin periodinane: prepared *via* the $KBrO_3$ route.[279]
- DIBAL-H: purchased from Sigma-Aldrich.
- dimethylsulfide: purchased from Acros Organics.

- diphosgene: purchased from Acros Organics.
- Hoveyda-Grubbs catalyst 2nd generation: purchased from Sigma-Aldrich.
- KO*t*Bu: commercial material (Acros Organics) was suspended in anhydrous THF (25 m%), filtered, and the filtrate was evaporated to dryness to give pure material.
- Lindlar catalyst: contains 5% Pd; purchased from Sigma-Aldrich.
- *m*-CPBA: commercial material (Sigma-Aldrich) was washed with phosphate buffer pH 7.4 and water, then dried.
- MOPS: purchased from Carl Roth.
- OsO_4: purchased from Riedel-de-Haën.
- Pd 10% on activated charcoal: purchased from Acros Organics.
- propiolaldehyde dibenzyl acetal: prepared *via* the route by Fliegel *et al.*[175]
- 2-(2-propynyloxy)tetrahydropyran: prepared *via* the route by McCune *et al.*[280]
- pyridine: anhydrous material was purchased from Sigma-Aldrich.
- $SnCl_2$: purchased from Fluka.
- TEMPO: purchased from abcr.
- TCICA: commercial material (Sigma-Aldrich) was recrystallized from 1,2-dichloroethane.
- TMSOAc: purchased from Acros Organics.
- tri-*iso*-propyl(prop-2-yn-1-yloxy)silane: prepared *via* the route by Barros *et al.*[281]
- vinylmagnesium bromide: purchased from Acros Organics.
- $VO(acac)_2$: purchased from Acros Organics.

6.4. Numbering, Nomenclature and Fischer Projections

In 2-*C*-branched carbohydrate precursors, the side chain is numbered in the order *C*2-*C*7-*C*8-*C*9, and this numbering is also used for the given NMR assignments. For the bicyclic carbohydrates in **Chapter 3**, the nomenclature is, in accordance with IUPAC recommendations[16] for fused systems (2-Carb-35.2), in the following form: substituents-(carbohydrate)[connection]annulation. Substituents on the annulated ring precede the name, and the locants of the separated systems, and not those of the total system numbering, are used. Substituents on the parent carbohydrate are given within the parentheses. As a major difference of this method as compared to standard heterocyclic nomenclature, the carbohydrate moiety is always cited first. For clarity, the NMR assignment numbering of the 2-*C*-branched carbohydrates was retained for the annulated compounds (side chain: *C*2-*C*7-*C*8-*C*9). The described procedure is illustrated in **Scheme 6.1, (a)**. The nomenclature of spirocyclic carbohydrate intermediates of **Chapter 4** is in conformity with IUPAC recommendations[16] for

(a)

3,6-Dihydro(3,4,6-tri-*O*-benzyl-1-deoxy-β-D-mannopyranoso)[1,2-*b*]-2*H*-pyran **(17)**:

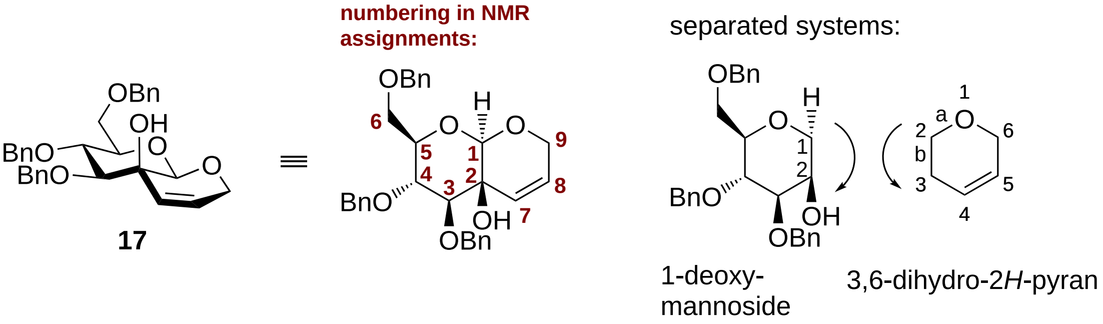
17
numbering in NMR assignments:
separated systems:
OBn
OH
BnO
BnO
O
O
≡
H
6
5
1
9
4
3
2
8
7
OH
OBn
a
b
1
2
3
4
5
6
1-deoxy-mannoside
3,6-dihydro-2H-pyran

(3*S*,4*R*)-3,4-Dihydroxytetrahydro(3,4,6-tri-*O*-benzyl-1-deoxy-β-D-mannopyranoso)[2,1-*e*]-2*H*-pyran **(18)**:

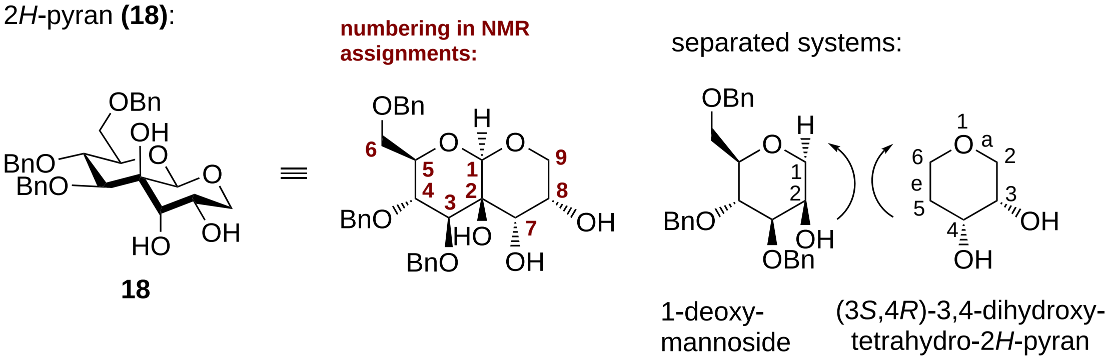
18
numbering in NMR assignments:
separated systems:
OBn
OH
BnO
BnO
HO
OH
≡
H
6
5
1
9
4
3
2
8
7
OH
BnO
HO
e
1
2
3
4
5
6
1-deoxy-mannoside
(3S,4R)-3,4-dihydroxy-tetrahydro-2H-pyran

(b)

(2*S*,2'*R*/*S*,3'*R*,4'*S*)-1,3,4,6-Tetra-*O*-benzyl-2',3',4'-trihydroxyspiro[2-deoxy-β-D-manno-pyranose-2,5'-tetrahydrofuran] **(α,β-48)**:

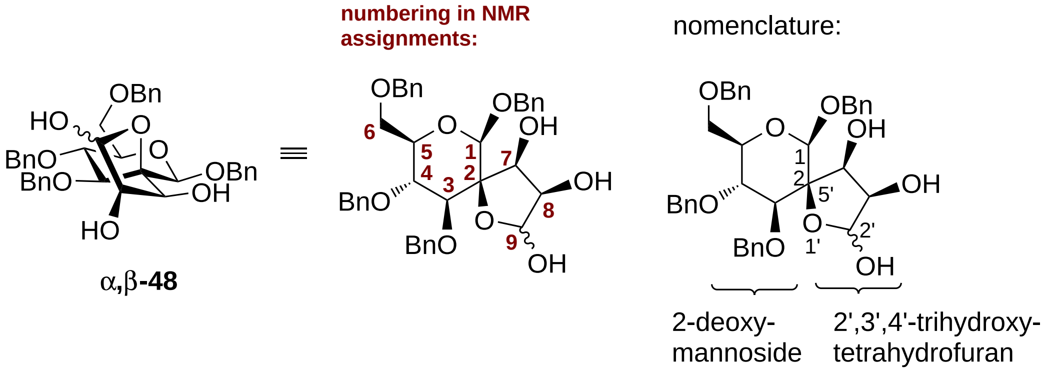
α,β-48
numbering in NMR assignments:
nomenclature:
OBn
HO
BnO
BnO
OH
≡
6
5
1
7
4
3
2
8
9
OH
1'
2'
5'
2-deoxy-mannoside
2',3',4'-trihydroxy-tetrahydrofuran

Scheme 6.1 (a) Clarification of numbering and nomenclature of annulated carbohydrate derivatives of **Chapter 3**, exemplified for compounds **17** and **18**. (b) Numbering and nomenclature of spirocyclic carbohydrates of **Chapter 4**, exemplified for compound **α,β-48**.

(a)

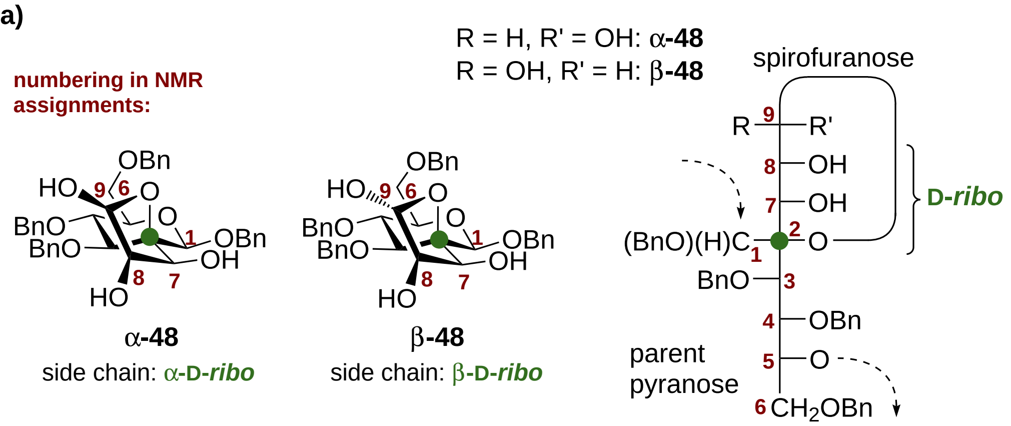
numbering in NMR assignments:
R = H, R' = OH: α-48
R = OH, R' = H: β-48
spirofuranose
OBn
HO
9
6
O
BnO
BnO
O
1
OBn
OH
8
7
HO
α-48
side chain: α-D-ribo
β-48
side chain: β-D-ribo
R
R'
OH
OH
D-ribo
(BnO)(H)C
2
O
BnO
3
4
OBn
parent pyranose
5
O
6
CH2OBn

(b)

4-*C*-formyl-D-*erythro*-L-*talo*-octose (***syn*-50**):

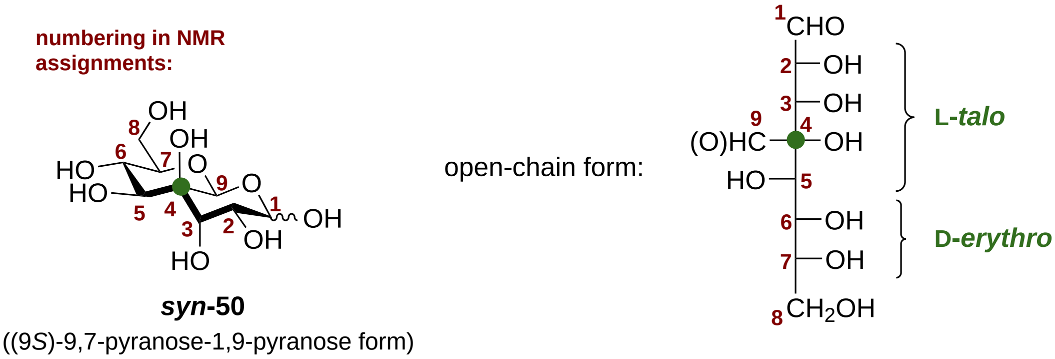
numbering in NMR assignments:
8
OH
6
OH
HO
7
O
HO
9
O
5
4
1
OH
3
2
OH
HO
syn-50
((9S)-9,7-pyranose-1,9-pyranose form)
open-chain form:
1
CHO
2
OH
3
OH
L-talo
9
4
(O)HC
OH
HO
5
6
OH
D-erythro
7
OH
8
CH2OH

Scheme 6.2 **(a)** Fischer projection of **α,β-48**. Dashed arrows indicate the parent pyranose moiety. **(b)** Numbering, nomenclature and Fischer projection of 4-*C*-formyl octose ***syn*-50**. A green dot indicates the quaternary *C*-4. For clarity, ***syn*-50** is depicted in the (9*S*)-9,7-pyranose-1,9-pyranose isomeric form.

spirocyclic carbohydrates (2-Carb-35.3) and follows the general pattern substituents-spiro[carbohydrate-connection-heterocycle] which is illustrated in **Scheme 6.1, (b)**. Substituents of the carbohydrate moiety are given in carbohydrate numbering, followed by heterocycle substituents with accentuated heterocycle numbering. The determination of the anomeric configurations of the spirocyclic carbohydrates is based on the Fischer projections of the spiro-compounds as depicted in **Scheme 6.2, (a)**. The numbering and nomenclature of deprotected target octoses of **Chapter 4** is in accordance with IUPAC recommendations[16] for aldoses with multiple configurational prefixes (2-Carb-8.3). This procedure is based on the Fischer projections of the compounds as illustrated in **Scheme 6.2, (b)**. For these higher carbohydrates, the numbering for NMR assignment is consistent with carbohydrate numbering, in which the longest chain is numbered first, with position 1 being the higher oxidized carbon atom at the top position in the Fischer projection. Consequently, following the synthetic route for these compounds, the former side chain *C*-9 in **α,β-48** equals the *C*-1 in ***syn*-50** after deprotection.

6.5. Synthetic Procedures

Allyl 3,4,6-tri-*O*-benzyl-β-D-*arabino*-hexopyranoside-2-ulose (2a):

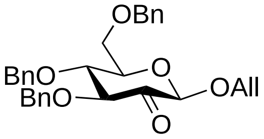

***Via* Koenigs-Knorr glycosylation of AD**: to a suspension of MS 3 Å (1.1 g) and Ag_2CO_3 (2.59 g; 9.39 mmol) in dry CH_2Cl_2 (16 mL) was added first allyl alcohol (0.49 mL; 7.11 mmol) and then dropwise a solution of 3,4,6-tri-*O*-benzyl-α-D-*arabino*-hexopyranos-2-ulosyl bromide **AD**[43] (1.45 g; 2.84 mmol) in dry CH_2Cl_2 (8 mL). The reaction was stirred for 5 min. Filtration through a pad of Celite and evaporation of the solvent yielded a clear oil which was purified by flash column chromatography (SiO_2, chloroform/methanol, 100:1). The slightly impurified product (875 mg) was purified by multiple chromatography steps (SiO_2, 100% chloroform) to yield pure **2a** as a colorless solid in minor yields (< 10%).

***Via* optimized Dess-Martin oxidation of 7**: to a solution of allyl glucoside **7**[61] (1.70 g; 3.47 mmol) in anhydrous CH_2Cl_2 (55 mL) was added $NaHCO_3$ (2.9 g). Next, Dess-Martin reagent (5.88 g; 13.86 mmol) was portionwise added over 30 min. The reaction was stirred for 24 h at r.t. and diluted with CH_2Cl_2 (260 mL). The solution was washed with water (130 mL), sat. $NaHCO_3$/0.2 M $Na_2S_2O_3$ (1:1, 3 × 210 mL) and water (210 mL). The organic phase was dried over Na_2SO_4. Filtration and evaporation of the solvent yielded crude **2a** (83% crude yield), which was used for following transformations without further purification. Repeated flash column chromatography (SiO_2, 100% chloroform) resulted in diminished yields (typically < 10%) of pure **2a** as a colorless solid. Analytical data corresponded fully to those obtained from **2a** *via* glycosylation of **AD** (see above).

$[\alpha]_D^{20}$ −38.7 (c = 1.0, $CHCl_3$); ^1H NMR (400.2 MHz, $CDCl_3$) δ: 7.43–7.29 (m, 13H, H_{Ar}), 7.23–7.20 (m, 2H, H_{Ar}), 6.01–5.92 (m, 1H, allyl: O-CH_2-C*H*=CH_2), 5.35 (dd, 1H, J_{trans} = 17.2, J_{gem} = 1.2 Hz, allyl: O-CH_2-CH=C*H*H), 5.26 (d, 1H, J_{cis} = 10.4 Hz, allyl: O-CH_2-CH=CH*H*), 5.01 (d, 1H, *J* = 11.4 Hz, CH_2Ph), 4.92–4.82 (m, 2H, CH_2Ph, H-1), 4.65–4.53 (m, 4H, CH_2Ph), 4.42 (dd, 1H, J_{gem} = 12.7, J_{vic} = 5.0 Hz, allyl: O-C*H*H-CH=CH_2), 4.27–4.19 (m, 2H, H-3, allyl: O-CH*H*-CH=CH_2), 3.96–3.84 (m, 2H, H-4, H-5), 3.80–3.72 (m, 2H, H-6a, H-6b); ^{13}C NMR (100.6 MHz, CDCl$_3$) δ: 197.4 (C-2), 138.0, 137.8, 137.4 ($3 \times$ C$_{\text{Ar,q.}}$), 133.2 (allyl: O-CH$_2$-CH=CH$_2$), 128.6–127.8 (C$_{\text{Ar}}$), 118.8 (allyl: O-CH$_2$-CH=CH$_2$), 98.0 (C-1), 85.7 (C-3), 80.1 (C-4), 75.9 (C-5), 75.0 (CH$_2$Ph), 73.6 (CH$_2$Ph), 73.6 (CH$_2$Ph), 69.9 (allyl: O-CH$_2$-CH=CH$_2$), 69.1 (C-6); FAB-MS m/z 511 [M+Na]$^+$; HR-ESI-FTICR calcd. for $C_{31}H_{36}O_7Na$ [M+Na+MeOH]$^+$: 543.2353. Found: 543.2350; Anal. calcd. for $C_{30}H_{32}O_6$: C, 73.75; H, 6.60. Found: C, 73.57; H, 6.64.

Benzyl 3,4,6-tri-*O*-benzyl-β-D-*arabino*-hexopyranoside-2-ulose (2b):

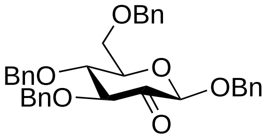

To a solution of glucoside **11**[62] (1.65 g; 3.05 mmol) in CH$_2$Cl$_2$ (100 mL) was added Dess-Martin periodinane (2.85 g; 6.71 mmol) in portions over 15 min at r.t., and the mixture was stirred until TLC (toluene/ethyl acetate, 4:1) indicated complete transformation of the starting material (16 h). The solution was diluted with CH$_2$Cl$_2$ (100 mL) and washed with water (80 mL), sat. NaHCO$_3$/0.2 M Na$_2$S$_2$O$_3$ (1:1, $3 \times$ 210 mL) and with water (80 mL). The organic layer was dried with Na$_2$SO$_4$, filtered and concentrated to dryness. The crude product was suspended in toluene/acetone (20 mL/15 mL), and the suspension was purified by flash column chromatography (SiO$_2$, toluene/acetone, 20:1) to afford pure ketone **2b** (1.58 g; 96%) as a colorless solid. Crystals suitable for X-ray structural analysis were obtained from *n*-pentane/ethyl acetate/chloroform. Analytical data corresponded to published data.[37]

Additional characterization data: ^{13}C NMR (100.6 MHz, CDCl$_3$) δ: 197.4 (C-2), 138.1, 137.8, 137.4, 136.2 ($4 \times$ C$_{\text{Ar,q.}}$), 128.6–127.8 (C$_{\text{Ar}}$), 97.4 (C-1), 85.8 (C-3), 80.1 (C-4), 75.9 (C-5), 75.0, 73.6, 73.6, 70.3 ($4 \times$ CH$_2$Ph), 69.1 (C-6); Anal. calcd. for $C_{34}H_{34}O_6$: C, 75.82; H, 6.36. Found: C, 75.54; H, 6.35.

Methyl 3,4,6-tri-*O*-benzyl-β-D-*arabino*-hexopyranoside-2-ulose (2c):

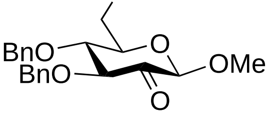

To a solution of methyl glucoside **8**[67, 69] (0.80 g; 1.72 mmol) in anhydrous CH$_2$Cl$_2$ (56 mL) was added Dess-Martin periodinane (1.61 g; 3.79 mmol) portionwise over 15 min at r.t. After 18 h, TLC (toluene/ethyl acetate, 4:1) indicated complete consumption of the starting material. The reaction mixture was diluted with CH$_2$Cl$_2$ (60 mL) and washed with water (150 mL), sat. $NaHCO_3$/0.2 M $Na_2S_2O_3$ (1:1, 3 × 50 mL) and water (50 mL). The organic phase was dried over Na_2SO_4, filtered, and evaporated to dryness. The crude oil was purified by flash column chromatography (SiO_2, toluene/acetone, 10:1) to give pure ketone **2c** (0.77 g; 96%) as a colorless solid. Analytical data corresponded to published data.[69]

Additional characterization data: ^{1}H NMR (400.2 MHz, $CDCl_3$) δ: 7.43–7.38 (m, 2H, H_{Ar}), 7.37–7.25 (m, 12H, H_{Ar}), 7.22–7.15 (m, 2H, H_{Ar}), 4.99 (d, 1H, J_{gem} = 11.5 Hz, CH_2Ph), 4.86 (d, 1H, J_{gem} = 10.9 Hz, CH_2Ph), 4.72 (s, 1H, H-1), 4.63–4.53 (m, 4H, CH_2Ph), 4.24 (d, 1H, $J_{3,4}$ = 8.4 Hz, H-3), 3.93–3.82 (m, 2H, H-4, H-5), 3.80–3.70 (m, 2H, H-6a, H-6b), 3.60 (s, 3H, CH_3); ^{13}C NMR (100.6 MHz, $CDCl_3$) δ: 197.3 (C-2), 138.0, 137.8, 137.4 (3 × $C_{Ar,q.}$), 128.6–127.9 (C_{Ar}), 100.2 (C-1), 85.7 (C-3), 80.2 (C-4), 75.9 (C-5), 75.1 (CH_2Ph), 73.7 (2 × CH_2Ph), 69.0 (C-6), 57.0 (CH_3); HR-ESI-TOF calcd. for $C_{28}H_{30}O_6Na$ $[M+Na]^+$: 517.2197. Found: 517.2201; Anal. calcd. for $C_{28}H_{30}O_6$: C, 72.71; H, 6.54. Found: C, 72.42; H, 6.69.

Allyl 3,6-di-*O*-benzoyl-4-deoxy-β-D-*glycero*-hex-3-enopyranoside-2-ulose (3a):

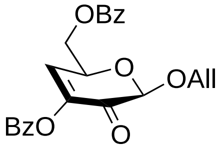

Isolated from the Koenigs-Knorr glycosylation of **AB**: a suspension of 3,4,6-tri-*O*-benzoyl-α-D-*arabino*-hexopyranos-2-ulosyl bromide **AB**[42] (1.52 g; 2.75 mmol), MS 3 Å (2 g) and Ag_2CO_3 (1.14 g; 4.12 mmol) in dry CH_2Cl_2 (30 mL) was stirred for 30 min at r.t. Allyl alcohol (0.56 mL; 8.25 mmol) was added, and the suspension was stirred for 3 h until TLC (toluene/ethyl acetate, 4:1) showed complete conversion of the starting material. Filtration through a layer of Celite, evaporation of the solvent and flash column chromatography (SiO_2, toluene/ethyl acetate, 10:1) of the residue afforded 3,2-enolone **3a** (346 mg; 31%) as a colorless solid.

R_f = 0.22 (toluene/ethyl acetate, 60:1); ^{1}H NMR (400.2 MHz, $CDCl_3$) δ: 8.15–8.07 (m, 4H, H_{Ar}), 7.65–7.57 (m, 2H, H_{Ar}), 7.52–7.44 (m, 4H, H_{Ar}), 6.92 (d, 1H, $J_{4,5}$ = 3.3 Hz, H-4), 6.02–5.89 (m, 1H, allyl: O-CH_2-C*H*=CH_2), 5.36 (dddd, 1H, J_{trans} = 17.2, J_{gem} = 1.5, 2 × ^4J = 1.5 Hz, allyl: O-CH_2-CH=C*H*H), 5.26 (dddd, 1H, J_{cis} = 10.4, J_{gem} = 1.3, 2 × ^4J = 1.3 Hz, allyl: O-CH_2-CH=CH*H*), 5.17 (s, 1H, H-1), 5.10 (ddd, 1H, $J_{5,6a}$ = 6.9, $J_{5,6b}$ = 6.0, $J_{4,5}$ = 3.5 Hz, H-5), 4.74 (dd, 1H, $J_{6a,6b}$ = 11.1, $J_{5,6a}$ = 7.0 Hz, H-6a), 4.65 (dd, 1H, $J_{6a,6b}$ = 11.4, $J_{5,6b}$ = 6.1 Hz, H-6b), 4.43 (dddd, 1H, J_{gem} = 12.6, ^3J = 5.3, 2 × ^4J = 1.5 Hz, allyl: O-C*H*H-CH=CH_2), 4.26 (dddd, 1H, J_{gem} = 12.9, ^3J = 6.3, 2 × ^4J = 1.3 Hz, allyl: O-CH*H*-CH=CH_2); ^{13}C NMR (100.6 MHz,

$CDCl_3$) δ: 182.6 (C-2), 166.2, 163.9 (2 x benzoyl C=O), 142.3 (C-3), 134.2, 133.6 (2 × C_{Ar}), 133.0 (allyl: O-CH_2-*C*H=CH_2), 132.6 (C-4), 130.5–128.3 (C_{Ar}), 118.9 (allyl: O-CH_2-CH=*C*H_2), 97.8 (C-1), 71.2 (C-5), 70.0 (allyl: O-*C*H_2-CH=CH_2), 66.3 (C-6); FAB-MS *m/z* 431 $[M+Na]^+$; HR-ESI-TOF calcd. for $C_{23}H_{20}O_7Na$ $[M+Na]^+$: 431.1101. Found: 431.1102.

Allyl 3,6-di-*O*-benzyl-4-deoxy-β-D-*glycero*-hex-3-enopyranoside-2-ulose (3b):

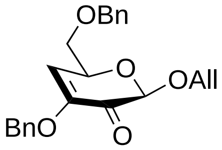

As a side product: Isolated in the unoptimized unbuffered Dess-Martin oxidation of **7** and subsequent unoptimized Grignard addition: to a solution of glucoside **7**[61] (0.95 g; 1.93 mmol) in anhydrous CH_2Cl_2 (30 mL) was added Dess-Martin reagent (1.06 g; 2.50 mmol) portionwise over 15 min at r.t. The reaction was stirred for 2 h and then diluted with CH_2Cl_2 (70 mL). The solution was washed with a half-saturated K_2CO_3 solution (3 × 25 mL) and water (3 × 25 mL). The organic phase was dried over Na_2SO_4, filtered and evaporated. The crude solid (1.4 g) was extracted with *n*-hexane/$CHCl_3$ 6:1 and filtered. Evaporation of the filtrate afforded a colorless solid (1.1 g), which was purified by flash column chromatography (SiO_2, *n*-hexane/chloroform, 2:1) to yield 1.01 g of slightly impurified **2a**. The product was dissolved in anhydrous THF and cooled to −78 °C. 2.1 mL (2.1 mmol) of vinylmagnesium bromide 1 M in THF was added over 10 min, and after 45 min another 0.3 mL (0.3 mmol) of the vinylmagnesium bromide solution was added. After 15 min TLC (toluene/ethyl acetate, 4:1) showed no more progression of the reaction. At −78 °C, 5 mL of sat. NH_4Cl was added dropwise and the reaction was allowed to warm to r.t. The suspension was diluted with CH_2Cl_2 (120 mL) and washed with water (3 × 50 mL). Drying of the organic phase over Na_2SO_4, filtration and evaporation of the solvent yielded a colorless oil, which was purified by flash column chromatography (SiO_2, toluene/acetone, 25:1). **3b** (110 mg; 15%) was isolated as the component with higher chromatographic mobility alongside with **16** (575 mg; 58%).

Synthesized from 7: To allyl glucoside **7**[61] (607 mg; 1.24 mmol) in anhydrous CH_2Cl_2 (25 mL) was portionwise added Dess-Martin periodinane (765 mg; 1.80 mmol) over 10 min at r.t. After 15 h TLC control (toluene/ethyl acetate, 4:1) indicated completion of the reaction, and the suspension was diluted with CH_2Cl_2 (100 mL), washed with sat. $NaHCO_3$/0.2 M $Na_2S_2O_3$ (1:1, 3 × 50 mL) and water (50 mL). The organic phase was dried over Na_2SO_4, filtered, and evaporated to dryness to give 608 mg of crude **2a**. The crude product was dissolved in toluene (25 mL) and water (0.75 mL). K_2CO_3 (288 mg; 2.08 mmol) was added, and the suspension was stirred at 80 °C for 18 h, when TLC (toluene/ethyl acetate, 4:1) indicated complete consumption of the starting material. The reaction mixture was diluted with toluene (50 mL), allowed to cool to r.t., washed with water (2 × 20 mL) and dried over Na_2SO_4. Filtration and evaporation of the solvents yielded a colorless oil, which was purified by flash column chromatography (SiO_2, toluene/ethyl acetate, 8:1) to give 3,2-enolone **3b** (325 mg; 70% over two steps) as a colorless oil.

R_f = 0.67 (toluene/ethyl acetate, 4:1); $[\alpha]_D^{20}$ −95.5 (c = 1.0, $CHCl_3$); UV (acetonitrile) λ_{max} (log ϵ) 263 (3.90), 326 nm (sh, 2.13); ^{1}H NMR (400.2 MHz, $CDCl_3$) δ: 7.40–7.29 (m, 10H, H_{Ar}), 5.99 (d, 1H, $J_{4,5}$ = 3.5 Hz, H-4), 5.90 (dddd, 1H, J_{trans} = 17.2, J_{cis} = 10.4, J_{vic} = 6.1, J_{vic} = 5.3 Hz, allyl: O-CH_2-C*H*=CH_2), 5.31 (dddd, 1H, J_{trans} = 17.2, J_{gem} = 1.5, 2 × ^4J = 1.4 Hz, allyl: O-CH_2-CH=C*H*H), 5.23 (dddd, 1H, J_{cis} = 10.4, J_{gem} = 1.5, 2 × ^4J = 1.4 Hz, allyl: O-CH_2-CH=CH*H*), 5.00 (s, 1H, H-1), 4.91 (d, 1H, J = 12.1 Hz, CH_2Ph), 4.87 (d, 1H, J = 12.1 Hz, CH_2Ph), 4.75 (ddd, 1H, $J_{4,5}$ = 3.5, $J_{5,6b}$ = 6.9, $J_{5,6a}$ = 6.5 Hz, H-5), 4.57 (d, 1H, J = 12.0 Hz, CH_2Ph), 4.53 (d, 1H, J = 12.0 Hz, CH_2Ph), 4.31 (dddd, 1H, J_{gem} = 12.7, J_{vic} = 5.3, 2 × ^4J = 1.5 Hz, allyl: O-C*H*H-CH=CH_2), 4.16 (dddd, 1H, J_{gem} = 12.7, J_{vic} = 6.1, 2 × ^4J = 1.4 Hz, allyl: O-CH*H*-CH=CH_2), 3.80 (dd, 1H, $J_{6a,6b}$ = 9.2, $J_{5,6a}$ = 6.5 Hz, H-6a), 3.60 (dd, 1H, $J_{6a,6b}$ = 9.2, $J_{5,6b}$ = 6.9 Hz, H-6b); ^{13}C NMR (100.6 MHz, $CDCl_3$) δ: 184.6 (C-2), 147.0 (C-3), 137.8, 135.6 (2 × $C_{Ar,q.}$), 133.3 (allyl: O-CH_2-*C*H=CH_2), 128.8–127.5 (C_{Ar}), 118.3 (allyl: O-CH_2-CH=*C*H_2), 116.8 (C-4), 97.9 (C-1), 73.6 (CH_2Ph), 73.1 (C-6), 72.0 (C-5), 70.0 (CH_2Ph), 69.5 (allyl: O-*C*H_2-CH=CH_2); HR-ESI-TOF calcd. for $C_{23}H_{24}O_5Na$ $[M+Na]^+$: 403.1516. Found: 403.1515; Anal. calcd. for $C_{23}H_{24}O_5$: C, 72.61; H, 6.36. Found: C, 72.67; H, 6.53.

2,3,5-Tri-*O*-benzyl-D-*arabino*-1,4-lactone (4):

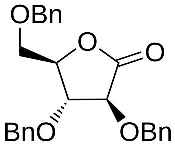

A solution of 3,4,6-tri-*O*-benzyl-α-D-*arabino*-hexopyranos-2-ulosyl bromide **AD**[43] (950 mg; 1.86 mmol) in dry CH_2Cl_2 (8 mL) was slowly added to a suspension of allyl alcohol (314 µL; 4.65 mmol), MS 3 Å (700 mg) and Ag_2CO_3 (1.79 g; 6.14 mmol) in dry CH_2Cl_2 (12 mL) and the mixture was stirred at r.t. for 5 min. Filtration through a layer of Celite and evaporation of the volatile components gave a complex mixture of compounds as observed by TLC (toluene/ethyl acetate, 20:1). Chromatographic purification of the residue (toluene/ethyl acetate, 20:1) afforded **4** (80 mg; 10%) as a colorless solid. Analytical data corresponded to published data.[59, 60] The formation of **4** could not be reproduced.

3,4,6-Tri-*O*-acetyl-1,2-*O*-(1-methoxyethylidene)-α-D-glucopyranose (5):

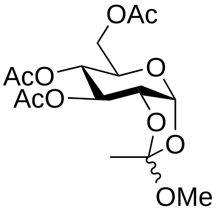

Based on a method published by Nepogodiev *et al.*[62] for the synthesis of **9**, a solution of 2,3,4,6-tetra-*O*-acetyl-α-D-glucopyranosyl bromide **AV** (15.2 g; 37.0 mmol) in dry $MeNO_2$ (45 mL) at r.t. was treated with 2,4,6-collidine (9.80 mL; 73.92 mmol), MeOH (7.47 mL; 184.8 mmol) and *n*-Bu_4NBr (2.50 g; 7.76 mmol). After 28 h, TLC control (toluene/ethyl acetate, 4:1, + 1% Et_3N) confirmed completion of the reaction, and a white precipitate had formed. Dilution with $CHCl_3$ (300 mL), washing with water (3 × 300 mL), drying (Na_2SO_4), filtration and evaporation of the volatile parts gave a yellow oil. Purification by flash column chromatography (SiO_2, toluene/ethyl acetate, 25:1 to 16:1, + 2% Et_3N) gave orthoester **5** (12.41 g; 93%) in the form of a colorless oil as an isomeric mixture (*exo*/*endo* = 12:1). Analytical data corresponded to published data.[63].

3,4,6-Tri-*O*-benzyl-1,2-*O*-(1-methoxyethylidene)-α-D-glucopyranose (6):

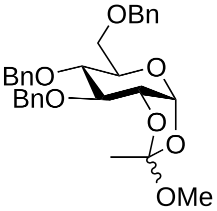

According to a similar reaction as published by Nepogodiev *et al.*[62] for the synthesis of **10**, acetylated orthoester **5** (6.63 g; 18.29 mmol) was dissolved in anhydrous benzyl chloride (50 mL) and treated with NaOH (11.46 g; 286.50 mmol). The vigorously stirred mixture was heated to 135 °C for 3 h, when TLC control (toluene, + 2% Et_3N) confirmed complete conversion. The reaction was allowed to cool to r.t., diluted with Et_2O (500 mL) and washed with water (3 × 200 mL, addition of brine to facilitate phase separation). Drying (Na_2SO_4), filtration and evaporation of the volatile parts gave a yellow oil. Purification by flash column chromatography (SiO_2, toluene/petroleum ether

60–90, 2:1, + 2% Et_3N) gave orthoester **6** (6.0 g; 65%) as a colorless oil as an isomeric mixture (*exo*/*endo*: n. d.). Analytical data corresponded to published data.[282, 283]

Allyl 3,4,6-tri-*O*-benzyl-β-D-glucopyranoside (7):

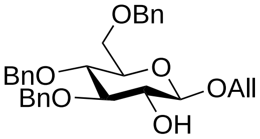

As described by Draghetti *et al.*[61], benzylated orthoester **6** (9.54 g; 18.83 mmol) in anhydrous allyl alcohol (41 mL) was cooled to 0 °C and treated with TMSOTf (255 µL; 1.41 mmol). The solution was stirred at 0 °C for 30 min, when TLC (toluene/ethyl acetate, 4:1) indicated absence of the starting material. The reaction was quenched at 0 °C by the dropwise addition of Et_3N (2 mL) in CH_2Cl_2 (20 mL), allowed to warm to r.t., and diluted with CH_2Cl_2 (250 mL). Washing with sat. $NaHCO_3$ (2 × 75 mL) and water (2 × 75 mL), drying (Na_2SO_4), filtration and evaporation of the volatile parts provided a brown oil. The crude product was dissolved in MeOH (120 mL), and NaOMe 25% in MeOH (750 µL) was added dropwise at r.t. After a reaction time of 18 h, neutralization with Dowex H^+ ion exchange resin, filtration and evaporation to dryness gave a brown oil. Flash column chromatography (SiO_2, toluene/ethyl acetate, 12:1) gave allyl glucoside **7** (6.10 g; 66%, 2 steps) as a colorless oil. Analytical data corresponded to published data.[284]

Methyl 3,4,6-tri-*O*-benzyl-β-D-glucopyranoside (8):

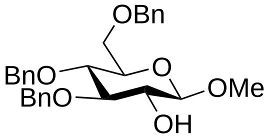

As described by Draghetti *et al.*[61] for the synthesis of **7**, benzylated orthoester **6** (1.26 g; 2.48 mmol) in anhydrous MeOH (5.5 mL) was cooled to 0 °C, and TMSOTf (40 µL; 0.22 mmol) was added. The solution was stirred at 0 °C for 30 min, when TLC (toluene/ethyl acetate, 4:1) indicated absence of the starting material. The reaction was quenched at 0 °C by the dropwise addition of Et_3N (0.5 mL) in CH_2Cl_2 (5 mL), allowed to warm to r.t., and diluted with CH_2Cl_2 (40 mL). Washing with sat. $NaHCO_3$ (2 × 15 mL) and water (2 × 15 mL), drying (Na_2SO_4), filtration and evaporation to dryness gave a brown oil. The crude oil was dissolved in MeOH (20 mL), and NaOMe 25% in MeOH (100 µL) was added dropwise at r.t. After a reaction time of 18 h, neutralization with Dowex H^+ ion exchange resin, filtration and evaporation of the solvent gave a brown oil, which was purified by flash column chromatography (SiO_2, toluene/ethyl acetate, 12:1) to give methyl glucoside **8** (920 mg; 80%, 2 steps) as a colorless solid. Analytical data corresponded to published data.[67]

3,4,6-Tri-*O*-acetyl-1,2-*O*-(1-benzyloxyethylidene)-α-D-glucopyranose (9):

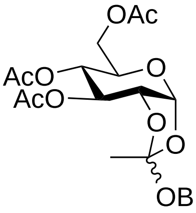

According to Nepogodiev *et al.*[62], 2,3,4,6-tetra-*O*-acetyl-α-D-glucopyranosyl bromide **AV** (23.20 g; 56.41 mmol) was dissolved in anhydrous $MeNO_2$ (75 mL) and was treated with 2,4,6-collidine (15.0 mL; 113.14 mmol) and benzyl alcohol (29.3 mL; 282.1 mmol). Next, *n*-Bu_4NBr (3.78 g; 11.72 mmol) was added, and the mixture was stirred at r.t. for 24 h, when a white precipitate had formed and TLC (toluene/ethyl acetate, 4:1, + 2% Et_3N) confirmed complete consumption of the starting material. Dilution with $CHCl_3$ (700 mL), washing with water (3 × 350 mL), drying (Na_2SO_4), filtration and evaporation of the volatile parts gave an oil. Purification by flash column chromatography (SiO_2, toluene to toluene/ethyl acetate 10:1, + 2% Et_3N) gave orthoester **9** (20.49 g; 83%) in the form of a colorless oil as an isomeric mixture (*exo*/*endo* = 25:1). Analytical data corresponded to published data.[62]

3,4,6-Tri-*O*-benzyl-1,2-*O*-(1-benzyloxyethylidene)-α-D-glucopyranose (10):

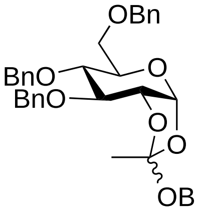

As described by Nepogodiev *et al.*[62], to acetylated orthoester **9** (25.50 g; 58.16 mmol) in anhydrous benzyl chloride (150 mL) was added NaOH (36.50 g; 912.5 mmol), and the vigorously stirred mixture was heated to 135 °C for 5 h, when TLC (toluene, + 2% Et_3N) confirmed complete transformation. The suspension was allowed to cool to r.t., diluted with water (300 mL) and extracted with Et_2O (2 × 300 mL). The combined organic extracted were washed with water (3 × 300 mL), dried (Na_2SO_4), and filtered. Evaporation of the volatile parts, followed by evaporation of benzyl chloride at 65 °C to complete dryness, gave a crude brown oil. Purification by flash column chromatography (SiO_2, toluene, + 2% Et_3N) gave benzylated orthoester **10** (28.27 g; 83%) as an isomeric mixture (*exo*/*endo* = 25:1) in the form of a brownish oil. Analytical data corresponded to published data.[62]

Benzyl 3,4,6-tri-*O*-benzyl-β-D-glucopyranoside (11):

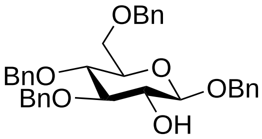

According to a protocol published by Nepogodiev *et al.*[62], benzylated orthoester **10** (28.27 g; 48.52 mmol) in anhydrous $MeNO_2$ (150 mL) was treated with $HgBr_2$ (1.23 g; 3.41 mmol). The mixture was heated to 93 °C for 5.5 h, when TLC (toluene/ethyl acetate, 4:1) indicated complete conversion. The reaction was allowed to cool to r.t., and $CHCl_3$ (500 mL) was added. Washing of the mixture with water (4 × 200 mL), drying (Na_2SO_4), filtration and evaporation of the solvents gave a crude brown oil (41.4 g). Of this crude product, a fraction of 21.90 g (53 m%) was suspended in MeOH (100 mL), and CH_2Cl_2 (100 mL) was added. To the clear solution was added NaOMe 25% in MeOH (500 µL) at r.t. After 5 d, a second portion of NaOMe was added (200 µL). After a total reaction time of 7 d, the reaction mixture was neutralized by the addition of Dowex H^+ ion exchange resin, filtered and evaporated to dryness. Flash column chromatography (SiO_2, toluene/ethyl acetate, 15:1) provided benzyl glucoside **11** (11.82 g; 85%, 2 steps, based on reacted fraction of the crude product). Analytical data corresponded to published data.[62]

Allyl 3,4,6-tri-*O*-benzoyl-2-*C*-vinyl-β-D-mannopyranoside (12):

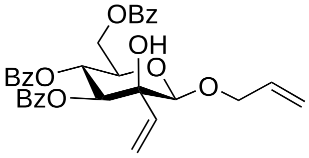

A suspension of benzoylated ulosyl bromide **AB**[42] (801 mg; 1.45 mmol), MS 3 Å (650 mg) and Ag_2CO_3 (400 mg; 1.45 mmol) in anhydrous CH_2Cl_2 (15 mL) was stirred at r.t. for 30 min. Subsequently, allyl alcohol (108 µL; 1.60 mmol) was added, and stirring was continued for 3 h until TLC (toluene/ethyl acetate, 4:1) showed complete conversion of the starting material. The suspension was filtered through a layer of Celite and concentrated under reduced pressure to give crude **1a**. The crude material was dissolved in anhydrous THF (25 mL) and cooled to −80 °C. Vinylmagnesium bromide 0.7 M in THF (2.49 mL; 1.74 mmol) was added dropwise and the reaction was stirred for 30 min at −80 °C until TLC (toluene/ethyl acetate, 12:1) showed complete conversion of the starting material. Sat. NH_4Cl (5 ml) was added dropwise, and the mixture was allowed to warm to r.t. The suspension was extracted with CH_2Cl_2 (3 × 15 mL), and the combined organic extracts were washed with brine (20 mL), dried (Na_2SO_4), filtered and concentrated *in vacuo*. Flash column chromatography (SiO_2, toluene/ethyl acetate, 25:1) of the residue gave diene **12** (236 mg; 29% over two steps) as a white foam. An analytical sample was recrystallized from cyclohexane.

M.p. 118 °C (cyclohexane); $R_f = 0.14$ (toluene/ethyl acetate, 18:1); $[\alpha]_D^{20}$ −186.2 (c = 0.5, $CHCl_3$); ^1H NMR (400.2 MHz, acetone-D_6) δ: 8.06–8.01 (m, 2H, H_{Ar}), 7.95–7.85 (m, 4H, H_{Ar}), 7.65–7.36 (m, 9H, H_{Ar}), 5.95–5.85 (m, 3H, H-4, allyl: -CH_2-C*H*=CH_2, vinyl: -C*H*=CH_2), 5.70 (d, 1H, $J_{3,4} = 9.9$ Hz, H-3), 5.51 (dd, 1H, $J_{trans} = 17.2$, $J_{gem} = 1.8$ Hz, vinyl: -CH=C*H*H), 5.28 (dddd, 1H, $J_{trans} = 17.2$, $J_{gem} = 1.8$ Hz, 2 × $^4J = 1.8$ Hz, allyl: -CH_2-CH=C*H*H), 5.19–5.11 (m, 2H, allyl: -CH_2-CH=CH*H*, vinyl: -CH=CH*H*), 5.01 (s, 1H, H-1), 4.61 (dd, 1H, $J_{6a,6b} = 11.9$, $J_{5,6a} = 3.0$ Hz, H-6a), 4.52 (dd, 1H, $J_{6a,6b} = 11.9$, $J_{5,6b} = 5.3$ Hz, H-6b), 4.38–4.29 (m, 2H, allyl: O-C*H*H-CH=CH_2, H-5), 4.27 (d, 1H, $J = 1.0$ Hz, OH), 4.18 (dddd, 1H, $J_{gem} = 13.2$, $^3J = 5.9$, 2 × $^4J = 1.6$ Hz, allyl: O-CH*H*-CH=CH_2); ^{13}C NMR (100.6 MHz, acetone-D_6) δ: 166.5, 166.3, 166.1 (3 × benzoyl C=O), 137.9 (vinyl: -*C*H=CH_2), 135.1 (allyl: -CH_2-*C*H=CH_2), 134.2, 134.0, 134.0 (3 × $C_{Ar,q.}$), 131.0–129.3 (C_{Ar}), 117.3 (allyl: -CH_2-CH=*C*H_2), 117.0 (vinyl: -CH=*C*H_2), 102.0 (C-1), 77.9 (C-2), 75.2 (C-3), 72.8 (C-5), 70.6 (allyl: -*C*H_2-CH=CH_2), 69.5 (C-4), 64.3 (C-6); FAB-MS m/z 581 $[M+Na]^+$; HR-ESI-TOF calcd. for $C_{32}H_{30}O_9Na$ $[M+Na]^+$: 581.1782. Found: 581.1780; Anal. calcd. for $C_{32}H_{30}O_9$: C, 68.81; H, 5.41. Found: C, 68.99; H, 5.39.

3,6-Dihydro(3,4,6-tri-*O*-benzoyl-1-deoxy-β-D-mannopyranoso)[1,2-*b*]-2*H*-pyran (13):

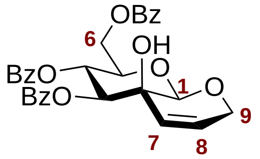

A mixture of diene **12** (513 mg; 0.92 mmol) and Hoveyda-Grubbs catalyst 2nd gen. (50 mg; 9 mol%) in CH_2Cl_2 (50 mL) was stirred at r.t. while a thin stream of nitrogen was slowly conducted through the mixture. After a total reaction time of 28 h, TLC (toluene/acetone, 20:1) showed complete conversion of the starting material. Concentration of the mixture under reduced pressure and flash column chromatography (SiO_2, toluene/acetone, 20:1) of the residue gave alkene **13** (431 mg; 88%) as a colorless solid. An analytical sample was recrystallized from *n*-hexane/ethyl acetate.

M.p. 129–135 °C (*n*-hexane/ethyl acetate, decomp.); $R_f = 0.11$ (toluene/acetone, 20:1); $[\alpha]_D^{20}$ −43.0 (c = 1.0, $CHCl_3$); ^1H NMR (400.2 MHz, $CDCl_3$) δ: 8.07–8.00 (m, 4H,

H_{Ar}), 7.90–7.85 (m, 2H, H_{Ar}), 7.55–7.43 (m, 3H, H_{Ar}), 7.41–7.28 (m, 6H, H_{Ar}) 6.07 (dd, 1H, $J_{4,5} = J_{3,4} = 9.7$ Hz, H-4), 5.98–5.90 (m, 2H, H-7, H-8), 5.52 (d, 1H, $J_{3,4} = 9.5$ Hz, H-3), 4.80 (s, 1H, H-1), 4.66 (dd, 1H, $J_{6a,6b} = 12.3$, $J_{5,6a} = 2.9$ Hz, H-6a), 4.53–4-46 (m, 3H, H-6b, H-9a, H-9b), 4.18 (ddd, 1H, $J_{4,5} = 9.9$, $J_{5,6b} = 5.2$, $J_{5,6a} = 2.9$ Hz, H-5), 2.44 (bs, 1H, OH); ^{13}C NMR (100.6 MHz, $CDCl_3$) δ: 166.6, 166.4, 165.4 (3 × benzoyl C=O), 133.6, 133.4, 133.1 ($C_{Ar,q.}$), 130.1 (C-8), 130.0–128.4 (C_{Ar}), 125.1 (C-7), 99.1 (C-1), 74.1 (C-3), 74.1 (C-5), 68.3 (C-4), 67.8 (C-2), 67.1 (C-9), 63.5 (C-6); FAB-MS m/z 553 $[M+Na]^+$, 531 $[M+H]^+$; HR-ESI-TOF calcd. for $C_{30}H_{26}O_9Na$ $[M+Na]^+$: 553.1469. Found: 553.1478; Anal. calcd. for $C_{30}H_{26}O_9$: C, 67.92; H, 4.94. Found: C, 68.04; H, 5.37.

(3*S*,4*R*)-3,4-Dihydroxytetrahydro(3,4,6-tri-*O*-benzoyl-1-deoxy-β-D-mannopyranoso)[2,1-*e*]-2*H*-pyran (14):

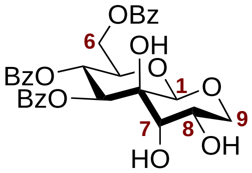

NMO (190 mg; 1.65 mmol) was added to a solution of alkene **13** (673 mg; 1.27 mmol) in a mixture of acetone (15 mL), water (5 mL) and *t*-BuOH (2 mL), followed by 100 µL of an aqueous 2% OsO_4 solution. The mixture was stirred at 45 °C for several days, until TLC (toluene/ethyl acetate, 4:1) indicated no further progress of the reaction. A second portion of NMO (190 mg; 1.65 mmol) and OsO_4 solution (125 µL) was added, and stirring was continued (in total 12 d) until TLC showed complete conversion of the starting material. $Na_2S_2O_3$ (0.6 g) was added at r.t., the mixture was stirred for 30 min and diluted with water (80 mL). The resulting solution was extracted with ethyl acetate (3 × 80 mL) and the combined extracts were washed with 1 M HCl (2 × 100 mL), sat. $NaHCO_3$ (2 × 100 mL) and brine (100 mL), dried over Na_2SO_4, filtered and concentrated *in vacuo*. Recrystallization of the residue from toluene/acetone gave triol **14** (531 mg; 74%) as a colorless solid.

M.p. 193–194 °C (toluene/acetone, decomp.); $R_f = 0.13$ (toluene-ethyl acetate, 4:1); $[\alpha]_D^{20}$ −28.8 (c = 1.0, acetone); ^{1}H NMR (400.2 MHz, acetone-D_6) δ: 8.07–7.91 (m, 6H, H_{Ar}), 7.65–7.54 (m, 3H, H_{Ar}), 7.51–7.39 (m, 6H, H_{Ar}), 6.00–5.93 (m, 2H, H-4, H-3), 5.05 (s, 1H, H-1), 4.58 (dd, 1H, $J_{6a,6b} = 12.1$, $J_{5,6a} = 2.8$ Hz, H-6a), 4.50 (dd, 1H, $J_{6a,6b} = 12.1$, $J_{5,6b} = 5.1$ Hz, H-6b), 4.46 (bs, 1H, C-2-O*H*), 4.38–4.29 (m, 2H, C-5-O*H*, H-5), 4.24–4.15 (m, 1H, H-8), 3.98–3.92 (m, 1H, H-7), 3.86–3.80 (m, 1H, C-8-O*H*), 3.76 (dd, 1H, $J_{9a,9b} = 10.9$, $J_{8,9a} = 5.8$ Hz, H-9a), 3.67 (dd, 1H, $J_{9a,9b} = 10.9$, $J_{8,9b} = 10.9$ Hz, H-9b); ^{13}C NMR (100.6 MHz, acetone-D_6) δ: 166.7, 166.4, 166.2 (3 × C=O), 134.2, 134.2, 133.9 ($C_{Ar,q.}$), 130.9–129.3 (C_{Ar}), 98.4 (C-1), 74.1 (C-2), 73.8 (C-5), 73.6 (C-4), 70.0 (C-7), 69.8 (C-3), 65.8 (C-9), 64.7 (C-8), 64.1 (C-6); FAB-MS m/z 587 $[M+Na]^+$, 565 $[M+H]^+$; HR-ESI-TOF calcd. for $C_{30}H_{28}O_{11}Na$ $[M+Na]^+$: 587.1524. Found: 587.1524; Anal. calcd. for $C_{30}H_{28}O_{11}$: C, 63.83; H, 5.00. Found: C, 63.42; H, 5.16.

(3*S*,4*R*)-3,4-Dihydroxytetrahydro(1-deoxy-β-D-mannopyranoso)[2,1-*e*]-2*H*-pyran (*syn*-15):

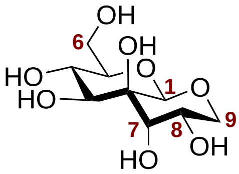

From 14: A catalytic amount of NaOMe 25% in MeOH (80 µL) was added to a solution of tribenzoate **14** (258 mg; 0.46 mmol) in MeOH (15 mL) and the solution was stirred at r.t. for 15–20 min until TLC (toluene/ethyl acetate, 8:1) indicated complete conversion of the starting material. The solution was neutralized by the addition of Dowex H^+ ion exchange resin, filtered and concentrated under reduced pressure. Washing of the remaining colorless oil several times with *n*-hexane/ethyl acetate (1:1), followed by co-evaporation with toluene and washing of the residue with $CHCl_3$, gave ***syn*-15** (88 mg, 76%) as a colorless solid.

From 18: Pd 10% on activated charcoal (60 mg; 43 wt%) was added to a solution of **18** (141 mg; 0.27 mmol) in MeOH (10 mL). The suspension was stirred under an atmosphere of hydrogen at r.t. for 18 h. When TLC (chloroform/methanol, 5:1) showed completion of the reaction the solvent was evaporated and the residue was suspended in MeCN/H_2O 4:1 (24 mL). The suspension was centrifuged and the clear phase was separated. The solid residue was again suspended in MeCN/H_2O and centrifuged again. The combined clear phases were evaporated and the residual oil was purified by RP-C18 chromatography (MeCN/H_2O, 2:1) to provide pure hexol ***syn*-15** (68 mg; quant.) as an oil. Crystals suitable for X-ray structural analysis were obtained from a saturated solution of ***syn*-15** in methanol/water.

M.p. 240 °C (methanol/water, decomp.); $R_f = 0.17$ (chloroform/methanol, 5:1); $[\alpha]_D^{20}$ 22.5 (c = 0.93, D_2O); ^1H NMR (400.2 MHz, D_2O) δ: 4.74 (s, 1H, H-1), 4.18 (ddd, 1H, $J_{8,9ab} = 11.3$, 5.6, $J_{7,8} = 3.2$ Hz, H-8), 4.06 (d, 1H, $J_{7,8} = 3.1$ Hz, H-7), 3.92–3.82 (m, 3H, H-6a, H-9a, H-3), 3.75 (dd, 1H, $J_{6a,6b} = 12.5$, $J_{5,6b} = 5.9$ Hz, H-6b), 3.69–3.62 (m, 2H, H-4, H-9b), 3.46 (ddd, 1H, $J_{4,5} = 10.0$, $J_{5,6b} = 5.9$, $J_{5,6a} = 2.2$ Hz, H-5); ^{13}C NMR (100.6 MHz, D_2O) δ: 97.5 (C-1), 78.0 (C-5), 73.8 (C-2), 71.9 (C-3), 68.5 (C-7), 68.2 (C-4), 64.7 (C-9), 64.3 (C-8), 61.3 (C-6); ESI-MS m/z 286 $[M+Cl]^-$; HR-ESI-TOF calcd. for $C_9H_{16}O_8Na$ [M+Na]$^+$: 275.0737. Found: 275.0741; Anal. calcd. for $C_9H_{16}O_8$: C, 42.86; H, 6.39. Found: C, 42.53; H, 6.46.

Allyl 3,4,6-tri-*O*-benzyl-2-*C*-vinyl-β-D-mannopyranoside (16):

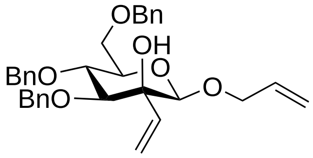

Crude **2a** as described above from the Dess-Martin oxidation of 1.70 g (3.47 mmol) of **7** was dissolved in anhydrous THF (65 mL) and cooled to −78 °C. Vinylmagnesium bromide 1 M in THF (6.97 mL; 6.97 mmol) was constantly added dropwise over 2 h by using a programmable syringe pump. After completion of the addition, the solution was stirred for another 30 min at −78 °C, neutralized by the dropwise addition of sat. NH_4Cl (4 mL) and allowed to warm to r.t. The reaction mixture was diluted with CH_2Cl_2 (260 mL), washed with water (3 × 130 mL) and dried over Na_2SO_4. Filtration and evaporation of the solvents gave a colorless oil which was purified by flash column chromatography (SiO_2, toluene/acetone, 25:1) to provide diene **16** (1.49 g; 83% over two steps) in the form of a colorless oil.

$R_f = 0.56$ (toluene/ethyl acetate, 4:1); $[\alpha]_D^{20}$ −30.4 (c = 1.0, $CHCl_3$); ^{1}H NMR (400.2 MHz, $CDCl_3$) δ: 7.39–7.26 (m, 13H, H_{Ar}), 7.22–7.19 (m, 2H, H_{Ar}), 5.89 (dddd, 1H, J_{trans} = 17.2, J_{cis} = 10.4, J_{vic} = 6.4, 4.9 Hz, allyl: O-CH_2-C*H*=CH_2), 5.79 (dd, 1H, J_{trans} = 17.1, J_{cis} = 10.5 Hz, vinyl: -C*H*=CH_2), 5.62 (dd, 1H, J_{trans} = 17.1, J_{gem} = 1.5 Hz vinyl: -CH=C*H*H), 5.37 (dd, 1H, J_{cis} = 10.5, J_{gem} = 1.5 Hz, vinyl: -CH=CH*H*), 5.29 (dddd, 1H, J_{trans} = 17.2, J_{gem} = 1.6, 2 × ^4J = 1.6 Hz, allyl: O-CH_2-CH=C*H*H), 5.20 (dddd, 1H, J_{cis} = 10.4, J_{gem} = 1.6, 2 × ^4J = 1.4 Hz, allyl: O-CH_2-CH=CH*H*), 4.83 (d, 1H, J_{gem} = 10.4 Hz, CH_2Ph), 4.76 (d, 1H, J_{gem} = 10.6 Hz, CH_2Ph), 4.71 (d, 1H, J_{gem} = 10.6 Hz, CH_2Ph), 4.66 (d, 1H, J_{gem} = 12.2 Hz, CH_2Ph), 4.62–4.54 (m, 2H, CH_2Ph), 4.43–4.35 (m, 2H, H-1, allyl: O-C*H*H-CH=CH_2, visible coupling constants: J_{gem} = 13.1, J_{vic} = 4.8, 2 × ^4J = 1.5 Hz), 4.13 (dddd, 1H, J_{gem} = 13.1, J_{vic} = 6.5, 2 × ^4J = 1.2 Hz, allyl: O-CH*H*-CH=CH_2), 3.91 (dd, $J_{4,5}$ = $J_{3,4}$ = 9.5 Hz, H-4), 3.81 (dd, 1H, $J_{6a,6b}$ = 10.9, $J_{5,6a}$ = 2.1 Hz, H-6a), 3.75 (dd, 1H, $J_{6a,6b}$ = 10.9, $J_{5,6b}$ = 5.1 Hz, H-6b), 3.55–3.49 (m, 2H, H-5, H-3, visible coupling constants: $J_{3,4}$ = 9.1 Hz), 2.56 (bs, 1H, OH); ^{13}C NMR (100.2 MHz, $CDCl_3$) δ: 138.4, 138.2, 137.8 (3 × $C_{Ar,q.}$), 137.6 (vinyl: -*C*H=CH_2), 133.8 (allyl: O-CH_2-*C*H=CH_2), 128.5–127.7 (C_{Ar}), 117.9 (allyl: O-CH_2-CH=*C*H_2), 117.0 (vinyl: -CH=*C*H_2), 100.3 (C-1), 84.3 (C-3), 77.3 (C-2), 76.0 (C-4), 76.0 (CH_2Ph), 75.4 (C-5), 75.2 (CH_2Ph), 73.6 (CH_2Ph), 69.9 (allyl: O-*C*H_2-CH=CH_2), 69.2 (C-6); HR-ESI-TOF calcd. for $C_{32}H_{36}O_6Na$ [M+Na]$^+$:

539.2404. Found: 539.2404; Anal. calcd. for $C_{32}H_{36}O_6$: C, 74.40; H, 7.02. Found: C, 73.94; H, 7.17.

3,6-Dihydro(3,4,6-tri-*O*-benzyl-1-deoxy-β-D-mannopyranoso)[1,2-*b*]-2*H*-pyran (17):

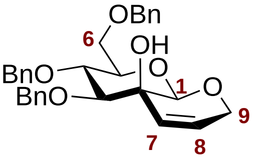

To a solution of diolefin **16** (705 mg; 1.36 mmol) in dry CH_2Cl_2 (35 mL) was added Hoveyda-Grubbs catalyst 2nd gen. (14 mg; 0.022 mmol; 1.6 mol%) and the green solution was stirred for 24 h at r.t. When TLC (toluene/ethyl acetate, 4:1) indicated complete consumption of the starting material, the solvent was evaporated. To the brown residue in 5 mL CH_2Cl_2, di(ethylene glycol) vinyl ether was added as a ruthenium scavenger[126] and the solution was stirred at r.t. for 1.5 h. The solvent was evaporated and the brown oil was purified by flash column chromatography (SiO_2, toluene/ethyl acetate, 5:1) to yield bicyclic alkene **17** (629 mg; 94%) as a colorless solid. Crystals of **17** suitable for X-ray structural analysis were obtained from *n*-hexane/ethyl acetate.

M.p. 118 °C (*n*-hexane/ethyl acetate); $R_f = 0.11$ (toluene/ethyl acetate, 4:1); $[\alpha]_D^{20}$ 17.7 (c = 1.0, $CHCl_3$); ^1H NMR (400.2 MHz, $CDCl_3$) δ: 7.40–7.25 (m, 13H, H_{Ar}), 7.22–7.15 (m, 2H, H_{Ar}), 5.96 (ddd, 1H, $J_{7,8} = 10.0$, $J_{7,9a} = 2.0$, $J_{7,9b} = 2.0$ Hz, H-7), 5.80 (ddd, 1H, $J_{7,8} = 10.0$, $J_{8,9a} = 3.1$, $J_{8,9b} = 1.8$ Hz, H-8), 4.99 (d, 1H, $J_{gem} = 11.5$ Hz, CH_2Ph), 4.82 (d, 1H, $J_{gem} = 10.8$ Hz, CH_2Ph), 4.73–4.67 (m, 2H, CH_2Ph), 4.62–4.55 (m, 2H, CH_2Ph), 4.44–4.37 (m, 2H, H-1, H-9a), 4.33 (ddd, 1H, $J_{9a,9b} = 17.3$, $J_{8,9b} = 2.1$, $J_{7,9b} = 2.1$ Hz, H-9b), 4.17 (dd, 1H, $J_{4,5} = 9.7$, $J_{3,4} = 9.0$ Hz, H-4), 3.84–3.76 (m, 2H, H-6a, H-6b), 3.61 (ddd, 1H, $J_{4,5} = 9.8$, $J_{5,6a} = 4.2$, $J_{5,6b} = 2.5$ Hz, H-5), 3.39 (d, 1H, $J_{3,4} = 9.0$ Hz, H-3), 2.22 (bs, 1H, OH); ^{13}C NMR (100.6 MHz, $CDCl_3$) δ: 138.3, 138.1, 138.1 (3 × $C_{Ar,q.}$), 129.3 (C-8), 128.6–127.7 (C_{Ar}), 126.0 (C-7), 99.3 (C-1), 82.6 (C-3), 77.2 (C-5), 76.8 (C-4), 75.9 (CH_2Ph), 75.3 (CH_2Ph), 73.7 (CH_2Ph), 68.9 (C-6), 68.3 (C-2), 66.9 (C-9); HR-ESI-TOF calcd. for $C_{30}H_{32}O_6Na$ $[M+Na]^+$: 511.2091. Found: 511.2092; Anal. calcd. for $C_{30}H_{32}O_6$: C, 73.75; H, 6.60. Found: C, 73.64; H, 6.60.

(3*S*,4*R*)-3,4-Dihydroxytetrahydro(3,4,6-tri-*O*-benzyl-1-deoxy-β-D-mannopyranoso)[2,1-*e*]-2*H*-pyran (18):

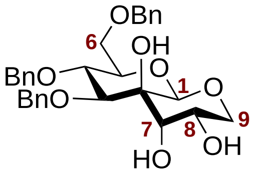

A solution of alkene **17** (139 mg; 0.28 mmol) in THF (4 mL) and water (1.5 mL) was treated with pyridine (23 µL; 0.28 mmol) and trimethylamine *N*-oxide (63 mg; 0.57 mmol). Then, 80 µL of a solution of OsO_4 (1% in water) was added and the reaction mixture was stirred at 60 °C. When TLC (toluene/ethyl acetate, 1:1) indicated no further progress of the reaction after 3 d, 20 µL of OsO_4 1% solution and 15 mg (0.14 mmol) of trimethylamine *N*-oxide was added and heating was continued. After 5 d TLC showed complete transformation of the substrate and the reaction mixture was allowed to cool to r.t. $Na_2S_2O_3$ (50 mg) was added and the solution was stirred for 30 min. Dilution with water/brine (30 mL/10 mL), extraction with EtOAc (3 × 30 mL), drying (Na_2SO_4), filtration and evaporation of the volatile parts provided a colorless oil. Purification by flash column chromatography (SiO_2, toluene/ethyl acetate, 1:1) yielded triol **18** (141 mg; 95%) as a colorless foam. An analytical sample was recrystallized from *n*-hexane/ethyl acetate.

M.p. 143 °C (*n*-hexane/ethyl acetate); $R_f = 0.17$ (toluene/ethyl acetate, 1:1); $[\alpha]^{20}_{D}$ 45.0 (c = 1.0, $CHCl_3$); ^1H NMR (400.2 MHz, acetone-D_6) δ: 7.43–7.23 (m, 15H, H_{Ar}), 4.93–4.88 (m, 2H, CH_2Ph), 4.82 (d, 1H, $J_{gem} = 11.1$ Hz, CH_2Ph), 4.68 (s, 1H, H-1), 4.65–4.59 (m, 2H, CH_2Ph), 4.53 (d, 1H, $J_{gem} = 12.1$ Hz, CH_2Ph), 4.24–4.16 (m, 1H, H-8), 4.15–4.11 (m, 1H, H-7), 4.09–4.03 (m, 1H, OH), 4.01–3.91 (m, 3H, OH, H-3, H-4), 3.77–3.73 (m, 2H, H-6a, H-6b), 3.69 (dd, 1H, $J_{9a,9b} = 10.9$, $J_{8,9a} = 5.6$ Hz, H-9a), 3.61 (dd, 1H, $J_{9a,9b} = 10.9$, $J_{8,9b} = 10.8$ Hz, H-9b), 3.54 (ddd, 1H, $J_{4,5} = 9.3$, $J_{5,6a} = 3.3$, $J_{5,6b} = 3.3$ Hz, H-5), 3.44 (bs, 1H, C-2-OH); ^{13}C NMR (100.6 MHz, acetone-D_6) δ: 142.2, 139.8, 139.7 (3 × $C_{Ar,q.}$), 129.0–128.1 (C_{Ar}), 98.4 (C-1), 81.8 (C-3), 77.3 (C-4), 77.1 (C-5), 75.7 (CH_2Ph), 75.4 (CH_2Ph), 74.4 (C-2), 73.7 (CH_2Ph), 70.4 (C-7), 70.1 (C-6), 65.5 (C-9), 65.1 (C-8); HR-ESI-TOF calcd. for $C_{30}H_{34}O_8Na$ $[M+Na]^+$: 545.2146. Found: 545.2146; Anal. calcd. for $C_{30}H_{34}O_8$: C, 68.95; H, 6.56. Found: C, 69.25; H, 6.72.

(3*R*,4*S*)-3,4-Epoxytetrahydro(3,4,6-tri-*O*-benzyl-1-deoxy-β-D-mannopyranoso)[2,1-*e*]-2*H*-pyran (19):

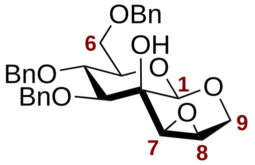

Alkene **17** (92 mg; 0.188 mmol) was dissolved in anhydrous toluene (6 mL) and VO(acac)$_2$ (2 mg; 0.008 mmol; 4 mol%) was added. The blue solution was treated with *t*-BuOOH 5.5 M in decane (41 µL; 0.226 mmol) upon which the solution turned red immediately, and was then stirred at 60 °C for 18 h when TLC (petroleum ether 60–90/ethyl acetate, 1:1, + 2% Et_3N) indicated no further progress of the reaction. A second portion of *t*-BuOOH solution (10 µL; 0.055 mmol) was added, and stirring at 60 °C was continued. After a total reaction time of 48 h the reaction was diluted with toluene (30 mL) and allowed to cool to r.t. The solution was washed with ice-cold half-sat. $Na_2S_2O_3$ (3 × 15 mL) and water (20 mL). Drying over Na_2SO_4, filtration and evaporation of the solvent afforded a colorless oil which was recrystallized from *n*-hexane/ethyl acetate to yield 57 mg of epoxide **19** as a colorless crystalline solid. Chromatographic purification (SiO_2, petroleum ether 60–90/ethyl acetate, 1.5:1, + 0.25% Et_3N) of the residue from the evaporated mother liquor yielded an additional 11 mg of epoxide **19** (68 mg; 72% total yield).

M.p. 142 °C (*n*-hexane/ethyl acetate); $R_f = 0.35$ (petroleum ether 60–90/ethyl acetate, 1.5:1, + 2% Et_3N); $[\alpha]_D^{20}$ 53.7 (c = 1.0, $CHCl_3$); ^1H NMR (400.2 MHz, $CDCl_3$) δ: 7.42–7.25 (m, 13H, H_{Ar}), 7.24–7.17 (m, 2H, H_{Ar}), 5.08 (d, 1H, $J_{gem} = 11.9$ Hz, CH_2Ph), 4.85 (d, 1H, $J_{gem} = 10.8$ Hz, CH_2Ph), 4.74 (d, 1H, $J_{gem} = 11.9$ Hz, CH_2Ph), 4.69 (d, 1H, $J_{gem} = 12.1$ Hz, CH_2Ph), 4.61 (d, 1H, $J_{gem} = 10.8$ Hz, CH_2Ph), 4.56 (d, 1H, $J_{gem} = 12.2$ Hz, CH_2Ph), 4.31–4.19 (m, 2H, H-4, H-9a), 4.01–3.94 (m, 2H, H-9b, H-1), 3.82–3.74 (m, 2H, H-6a, H-6b), 3.56 (dddd, 1H, $J_{4,5} = 9.9$, $J_{5,6a} = 2.3$, $J_{5,6b} = 2.3$, $^4J = 2.3$ Hz, H-5), 3.47 (d, 1H, $J_{3,4} = 9.1$ Hz, H-3), 3.11–3.05 (m, 2H, H-8, H-7), 2.85 (bs, 1H, OH); ^{13}C NMR (100.6 MHz, $CDCl_3$) δ: 138.2, 137.9, 137.8 (3 × $C_{Ar,q.}$), 128.7–127.7 (C_{Ar}), 99.6 (C-1), 80.3 (C-3), 77.2 (C-5), 76.9 (C-4), 75.4 (CH_2Ph), 75.3 (CH_2Ph), 73.8 (CH_2Ph), 68.7 (C-6), 67.2 (C-2), 64.8 (C-9), 52.5 (C-7), 51.6 (C-8); HR-ESI-TOF calcd. for $C_{30}H_{32}O_7Na$ $[M+Na]^+$: 527.2040. Found: 527.2043; Anal. calcd. for $C_{30}H_{32}O_7$: C, 71.41; H, 6.39. Found: C, 71.45; H, 6.57.

(3*R*,4*R*)-3,4-Dihydroxytetrahydro(3,4,6-tri-*O*-benzyl-1-deoxy-β-D-mannopyranoso)[2,1-*e*]-2*H*-pyran (20):

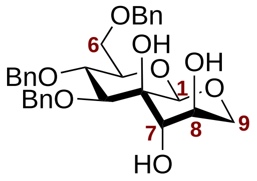

To a solution of epoxide **19** (225 mg; 0.446 mmol) in DMSO (16 mL) and water (4 mL) was added KOH (349 mg) and the reaction mixture was stirred at 35 °C for 7 d, when

TLC (toluene/ethyl acetate, 1:3) indicated complete conversion of the starting material. After cooling to r.t., NH_4Cl (333 mg) was added and the solution was stirred for 15 min. Brine (40 mL) was added and the solution was extracted with ethyl acetate (4 × 40 mL). The combined organic extracts were washed with water (5 × 40 mL) and dried over Na_2SO_4, filtered and evaporated to provide a yellow oil. Flash column chromatography (SiO_2, toluene/ethyl acetate, 1.5:1) yielded **20** (145 mg; 62%) as a colorless solid. An analytical sample was recrystallized from *n*-hexane/ethyl acetate.

M.p. 150 °C (*n*-hexane/ethyl acetate); $R_f = 0.32$ (toluene/ethyl acetate, 1:3); $[\alpha]_D^{20}$ 75.8 (c = 1.0, $CHCl_3$); ^1H NMR (400.2 MHz, acetone-D_6) δ: 7.44–7.24 (m, 15H, H_{Ar}), 4.94–4.84 (m, 2H, CH_2Ph), 4.81 (d, 1H, $J_{gem} = 11.1$ Hz, CH_2Ph), 4.70–4.59 (m, 5H, 2 × OH, H-1, 2 × CH_2Ph), 4.55 (d, 1H, $J_{gem} = 12.0$ Hz, CH_2Ph), 4.27 (bs, 1H, *C*-2-OH), 4.19–4.15 (m, 1H, H-7), 4.04 (dd, 1H, $J_{9a,9b} = 12.3$, $J_{8,9a} = 1.3$ Hz, H-9a), 4.00–3.91 (m, 2H, H-3, H-4), 3.87 (ddd, 1H, $J_{9a,9b} = 12.2$, $J_{8,9b} = 1.3$, $^4J = 1.3$ Hz, H-9b), 3.79–3.73 (m, 2H, H-6a, H-6b), 3.68–3.62 (m, 1H, H-8), 3.58–3.52 (m, 1H, H-5); ^{13}C NMR (100.6 MHz, acetone-D_6) δ: 140.2, 139.7, 139.7 (3 × $C_{Ar,q.}$), 129.0–128.1 (C_{Ar}), 98.8 (C-1), 81.6 (C-3), 77.2 (C-4), 77.1 (C-5), 75.6 (CH_2Ph), 75.3 (CH_2Ph), 74.5 (C-2), 73.7 (CH_2Ph), 70.8 (C-8), 70.1 (C-6), 68.7 (C-7), 68.6 (C-9); HR-ESI-TOF calcd. for $C_{30}H_{34}O_8Na$ $[M+Na]^+$: 545.2146. Found: 545.2152; Anal. calcd. for $C_{30}H_{34}O_8$: C, 68.95; H, 6.56. Found: C, 68.67; H, 6.70.

(3*R*,4*R*)-3,4-Dihydroxytetrahydro(1-deoxy-β-D-mannopyranoso)[2,1-*e*]-2*H*-pyran (*anti*-21):

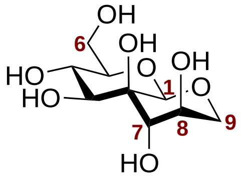

Triol **20** (90 mg; 0.172 mmol) was dissolved in MeOH (6.4 mL). Pd 10% on activated charcoal (38 mg; 42 wt%) was added, and the suspension was stirred at r.t. under an atmosphere of hydrogen for 20 h. TLC control (chloroform/methanol, 5:1) indicated complete transformation of the starting material. After evaporation of the solvent, the residue was suspended in MeCN/H_2O 4:1, centrifuged, and the clear phase was separated. The solid residue was suspended in MeCN/H_2O and centrifuged again. Evaporation of the combined clear phases yielded a colorless oil. Purification by RP-C18 chromatography (MeCN/H_2O, 2:1) gave ***anti*-21** (39 mg; 90%) as a colorless solid.

$R_f = 0.08$ (chloroform/methanol, 5:1); $[\alpha]_D^{20}$ 19.4 (c = 1.0, H_2O); ^1H NMR (400.2 MHz, D_2O) δ: 4.72 (s, 1H, H-1), 4.10–3.99 (m, 3H, H-7, H-9a, H-9b), 3.91 (dd, 1H,

$J_{6a,6b}$ = 12.5, $J_{5,6a}$ = 2.2 Hz, H-6a), 3.82–3.79 (m, 1H, H-8), 3.78–3.72 (m, 2H, H-3, H-6b), 3.65 (dd, 1H, $J_{3,4}$ = 9.7, $J_{4,5}$ = 9.7 Hz, H-4), 3.47 (ddd, 1H, $J_{4,5}$ = 9.9, $J_{5,6b}$ = 6.2, $J_{5,6a}$ = 2.2 Hz, H-5); ^{13}C NMR (100.6 MHz, D_2O) δ: 97.9 (C-1), 78.0 (C-5), 73.4 (C-2), 71.8 (C-3), 69.3 (C-8), 68.2 (C-4), 68.0 (C-9), 67.1 (C-7), 61.4 (C-6); HR-ESI-TOF calcd. for $C_9H_{16}O_8Na$ $[M+Na]^+$: 275.0737. Found: 275.0740; HR-ESI-TOF calcd. for $C_9H_{15}O_8$ $[M-H]^-$: 251.0772. Found: 251.0773; Anal. calcd. for $C_9H_{16}O_8$: C, 42.86; H, 6.39. Found: C, 42.67; H, 6.82.

Benzyl 3,4,6-tri-*O*-benzyl-2-*C*-(3,3-dibenzyloxypropyn-1-yl)-β-D-mannopyranoside (22):

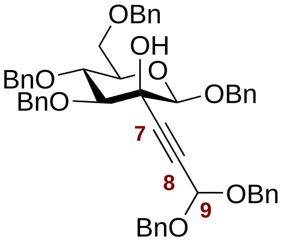

Propiolaldehyde dibenzyl acetal[175] (1.02 g; 4.04 mmol) was dissolved in anhydrous THF (35 mL) and cooled to −80 °C. *n*-BuLi (1.50 mL; 4.04 mmol; 2.7 M in *n*-heptane) was added dropwise, and stirring at −80 °C was continued for 2.5 h. Next, benzyl 2-uloside **2b**[37] (1.98 g; 3.67 mmol) in 30 mL THF was added dropwise over 15 min. After stirring for another 15 min, the reaction was quenched by the dropwise addition of brine (25 mL) at −80 °C. The mixture was diluted with $CHCl_3$ (200 mL) and washed with water, sat. NH_4Cl, sat. $NaHCO_3$ and water (100 mL each). Drying of the organic phase (Na_2SO_4), filtration, evaporation of the solvents and purification of the residue by flash column chromatography (SiO_2, toluene/acetone, 20:1) afforded alkyne **22** (2.47 g; 85%) as a colorless solid. An analytical sample was recrystallized from *n*-hexane/ethyl acetate.

M.p. 85 °C (*n*-hexane/ethyl acetate); $R_f = 0.65$ (toluene/ethyl acetate, 4:1); $[\alpha]_D^{20}$ 3.5 (c = 1.0, $CHCl_3$); ^{1}H NMR (400.2 MHz, $CDCl_3$) δ: 7.50–7.21 (m, 30H, H_{Ar}), 5.57 (s, 1H, H-9), 5.14 (d, 1H, J_{gem} = 10.6 Hz, CH_2Ph), 5.04 (d, 1H, J_{gem} = 12.1 Hz, CH_2Ph), 4.95 (d, 1H, J_{gem} = 10.6 Hz, CH_2Ph), 4.88 (d, 1H, J_{gem} = 11.1 Hz, CH_2Ph), 4.85–4.78 (m, 3H, CH_2Ph), 4.74–4.63 (m, 4H, CH_2Ph), 4.59 (d, 1H, J_{gem} = 10.9 Hz, CH_2Ph), 4.56 (s, 1H, H-1), 3.91–3.76 (m, 3H, H-4, H-6a, H-6b), 3.71 (d, 1H, $J_{3,4}$ = 9.1 Hz, H-3), 3.52 (ddd, 1H, $J_{4,5}$ = 9.9, $J_{5,6ab}$ = 5.1, 1.9 Hz, H-5), 3.10 (bs, 1H, OH); ^{13}C NMR (100.6 MHz, $CDCl_3$) δ: 138.2, 138.1, 137.8 137.4, 137.3, 136.7 (6 × $C_{Ar,q.}$), 128.5–127.7 (C_{Ar}), 99.7 (C-1), 90.7 (C-9), 85.3 (C-3), 85.1 (C-7), 80.8 (C-8), 76.1 (CH_2Ph), 75.3 (C-5), 75.2 (CH_2Ph), 75.0 (C-4), 73.6 (CH_2Ph), 71.6 (C-2), 70.8 (CH_2Ph), 69.0 (C-6), 67.5 (C-9-O-CH_2Ph), 67.4 (C-9-O-CH_2Ph); HR-ESI-TOF calcd. for $C_{51}H_{50}O_8Na$ $[M+Na]^+$: 813.3398. Found: 813.3384; Anal. calcd. for $C_{51}H_{50}O_8$: C, 77.45; H, 6.37. Found: C, 77.21; H, 6.40.

Benzyl 3,4,6-tri-*O*-benzyl-2-*C*-{(*Z*)-3,3-dibenzyloxyprop-1-en-1-yl}-β-D-mannopyranoside (23):

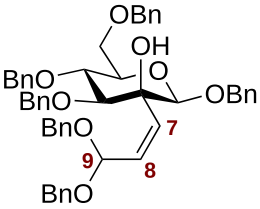

A solution of alkyne **22** (129 mg; 0.163 mmol) in anhydrous DMF (2 mL) was treated with Lindlar catalyst (64 mg; 50 wt%). The mixture was stirred under an atmosphere of hydrogen at r.t. for 48 h, when TLC (toluene/ethyl acetate, 4:1) indicated complete conversion. Dilution with CH_2Cl_2, filtration through a layer of Celite, evaporation of the volatile parts and co-evaporation of residual DMF with *n*-heptane gave a crude oil. Flash column chromatography (SiO_2, toluene/acetone, 20:1) gave (*Z*)-alkene **23** (120 mg; 93%) as a colorless solid. An analytical sample was recrystallized from *n*-hexane/ethyl acetate. Crystals suitable for X-ray structural analysis were obtained from *n*-pentane/ethyl acetate.

M.p. 95 °C (*n*-hexane/ethyl acetate); $R_f = 0.76$ (toluene/ethyl acetate, 4:1); $[\alpha]_D^{20}$ −34.0 (c = 0.5, $CHCl_3$); ^{1}H NMR (400.2 MHz, DMSO-D_6) δ: 7.40–7.15 (m, 30H, H_{Ar}), 6.19 (d, 1H, $J_{8,9} = 6.8$ Hz, H-9), 5.74 (dd, 1H, $J_{7,8} = 12.4$, $J_{8,9} = 6.8$ Hz, H-8), 5.67 (d, $J_{7,8} = 12.4$ Hz, H-7), 4.80 (d, $J_{gem} = 12.4$ Hz, CH_2Ph), 4.76–4.46 (m, 11H, CH_2Ph, H-1), 4.43 (d, $J_{gem} = 11.6$ Hz, CH_2Ph), 4.34 (bs, 1H, OH), 3.78–3.63 (m, 4H, H-3, H-4, H-6a, H-6b), 3.58–3.52 (m, 1H, H-5); ^{13}C NMR (100.6 MHz, DMSO-D_6) δ: 138.5, 138.5, 138.4, 138.4, 138.3, 137.7 (6 × $C_{Ar,q.}$), 133.2 (C-7), 129.8 (C-8), 128.2–127.2 (C_{Ar}), 100.7 (C-1), 97.5 (C-9), 84.3 (C-3), 78.7 (C-2), 75.6 (C-4), 74.9 (CH_2Ph), 74.5 (C-5), 74.1 (CH_2Ph), 72.3 (CH_2Ph), 70.2 (CH_2Ph), 69.1 (C-6), 67.5 (CH_2Ph), 66.3 (CH_2Ph); HR-ESI-TOF calcd. for $C_{51}H_{52}O_8Na$ $[M+Na]^+$: 815.3554. Found: 815.3544; Anal. calcd. for $C_{51}H_{52}O_8$: C, 77.25; H, 6.61. Found: C, 77.31; H, 6.56.

Benzyl 2-*O*-acetyl-3,4,6-tri-*O*-benzyl-2-*C*-(3,3-dibenzyloxypropyn-1-yl)-β-D-mannopyranoside (24):

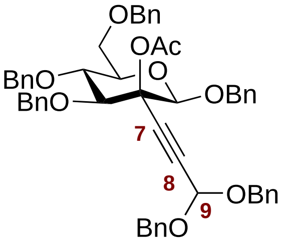

A solution tertiary alcohol **22** (394 mg; 0.50 mmol) in $CHCl_3$ (4 mL) was treated with Ac_2O (4 mL), Et_3N (76 µL; 0.548 mmol) and DMAP (122 mg; 1.0 mmol). The mixture was heated to 65 °C for 4 d, when TLC (toluene/ethyl acetate, 4:1) indicated complete conversion of the starting material. The reaction mixture was diluted with $CHCl_3$ (50 mL) and poured onto ice-cold sat. $NaHCO_3$ (50 mL). The organic layer was separated and washed with sat. $NaHCO_3$ and water (20 mL each), then dried (Na_2SO_4), filtered, concentrated *in vacuo* and co-evaporated with toluene (2 × 10 mL). Flash column chromatography of the residue (SiO_2, toluene/acetone, 50:1) gave acetate **24** (335 mg; 81%) in the form of a colorless oil.

$R_f = 0.70$ (toluene/ethyl acetate, 4:1); $[\alpha]_D^{20}$ −11.7 (c = 0.85, $CHCl_3$); ^1H NMR (400.2 MHz, $CDCl_3$) δ: 7.43–7.18 (m, 28H, H_{Ar}), 7.15–7.10 (m, 2H, H_{Ar}), 5.53 (s, 1H, H-9), 5.30 (d, 1H, J_{gem} = 10.9 Hz, CH_2Ph), 4.97 (d, 1H, J_{gem} = 12.4 Hz, CH_2Ph), 4.87–4.62 (m, 8H, CH_2Ph), 4.56 (d, 1H, J_{gem} = 12.1 Hz, CH_2Ph), 4.51–4.44 (m, 2H, H-1, CH_2Ph), 3.79–3.67 (m, 4H, H-6a, H-6b, H-3), 3.49 (ddd, 1H, $J_{4,5}$ = 9.6, $J_{5,6}$ = 4.5, 2.5 Hz, H-5), 2.18 (s, 3H, CH_3); ^{13}C NMR (100.6 MHz, $CDCl_3$) δ: 168.3 (acetyl C=O), 138.3, 138.2, 138.0, 137.6, 137.6, 136.7 (6 × $C_{Ar,q.}$), 128.7–127.7 (C_{Ar}), 100.6 (C-1), 91.0 (C-9), 86.1 (C-3), 84.4 (C-7), 82.2 (C.8), 75.7 (C-5), 75.4 (CH_2Ph), 2 × 75.2 (CH_2Ph, C-2), 74.7 (C-4), 73.6 (CH_2Ph), 71.2 (CH_2Ph), 69.2 (C-6), 67.6 (CH_2Ph), 67.6 (CH_2Ph), 22.2 (CH_3); HR-ESI-TOF calcd. for $C_{53}H_{52}O_9Na$ $[M+Na]^+$: 855.3504. Found: 855.3505; Anal. calcd. for $C_{53}H_{52}O_9$: C, 76.42; H, 6.29. Found: C, 76.36; H, 6.32.

Benzyl 2-*O*-acetyl-3,4,6-tri-*O*-benzyl-2-*C*-{(*Z*)-3,3-dibenzyloxyprop-1-en-1-yl}-β-D-mannopyranoside (25):

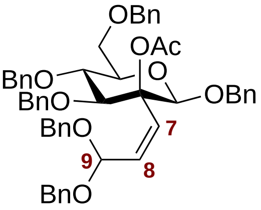

Alkyne **24** (249 mg; 0.299 mmol) in anhydrous DMF (3 mL) was treated with Lindlar catalyst (113 mg; 45 wt%). The mixture was stirred under an atmosphere of hydrogen at r.t. for 3 d, when TLC (toluene/ethyl acetate, 4:1) indicated complete conversion. Dilution with CH_2Cl_2, filtration through a layer of Celite, evaporation of the volatile parts and co-evaporation of residual DMF with *n*-heptane gave alkene **25** (220 mg; 88%) as a colorless oil in high purity without further purification.

$R_f = 0.78$ (toluene/ethyl acetate, 2:1); $[\alpha]_D^{20}$ −18.6 (c = 1, $CHCl_3$); ^1H NMR (400.2 MHz, $CDCl_3$) δ: 7.35–7.16 (m, 30H, H_{Ar}), 6.21 (d, 1H, $J_{7,8}$ = 12.4 Hz, H-7), 5.76 (dd, 1H, $J_{7,8}$ = 12.4, $J_{8,9}$ = 7.8 Hz, H-8), 5.67 (d, 1H, $J_{8,9}$ = 7.8 Hz, H-9), 5.27 (s, 1H, H-1), 4.87 (d, 1H, J_{gem} = 11.6 Hz, CH_2Ph), 4.65–4.55 (m, 3H, CH_2Ph), 4.51–4.46 (m, 3H, CH_2Ph), 4.44–4.37 (m, 5H, CH_2Ph), 4.95–4.82 (m, 4H, H-5, H-3, H-6a, H-4), 3.77 (dd, 1H, $J_{6a,6b}$ = 9.6, $J_{5,6b}$ = 5.8 Hz, H-6b), 1.83 (s, 3H, CH_3); ^{13}C NMR (100.6 MHz, $CDCl_3$) δ: 169.4 (acetyl C=O), 138.5, 138.4, 138.2, 138.1, 138.0, 137.8 (6 × $C_{Ar,q.}$), 133.1 (C-7), 128.6–127.5 (C_{Ar}), 127.1 (C-8), 99.8 (C-1), 95.8 (C-9), 80.2 (C-2), 79.7 (C-3), 75.1 (*C-4), 74.9 (*C-5; assignments may be interchanged), 74.8 (CH_2Ph), 73.3 (CH_2Ph), 72.3 (CH_2Ph), 71.1 (CH_2Ph), 70.6 (C-6), 66.9 (CH_2Ph), 65.2 (CH_2Ph), 22.2 (CH_3); HR-ESI-TOF calcd. for $C_{53}H_{54}O_9Na$ $[M+Na]^+$: 857.3660. Found: 857.3663; Anal. calcd. for $C_{53}H_{54}O_9$: C, 76.24; H, 6.52. Found: C, 76.14; H, 6.48.

Benzyl 3,4,6-tri-*O*-benzyl-2-*C*-(3,3-dimethoxypropyn-1-yl)-β-D-mannopyranoside (26):

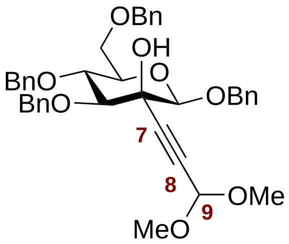

Dibenzyl acetal **22** (301 mg; 0.38 mmol) was dissolved in anhydrous MeOH (20 mL) and I_2 (200 mg; 0.79 mmol) was added. The solution was stirred at 60 °C for 48 h until TLC (toluene/ethyl acetate, 4:1) indicated complete consumption of the starting material. The reaction mixture was cooled to 0 °C, treated with solid $Na_2S_2O_3$ (1.0 g), stirred for 15 min and allowed to warm to r.t. Next, $CHCl_3$ (100 mL) was added, and the organic layer was washed with water (2 × 30 mL) and brine (30 mL). The solution was dried (Na_2SO_4), filtered and concentrated *in vacuo*. Flash column chromatographic purification of the residue (SiO_2, toluene/acetone, 20:1) afforded dimethyl acetal **26** (213 mg; 88%) as a colorless oil.

$R_f = 0.30$ (toluene/ethyl acetate, 4:1); $[\alpha]_D^{20}$ −6.7 (c = 1, $CHCl_3$); ^1H NMR (400.2 MHz, $CDCl_3$) δ: 7.48–7.27 (m, 18H, H_{Ar}), 7.22–7.15 (m, 2H, H_{Ar}), 5.18 (s, 1H, H-9), 5.08 (d, 1H, J_{gem} = 10.9 Hz, CH_2Ph), 5.00 (d, 1H, J_{gem} = 12.1 Hz, CH_2Ph), 4.90 (d, 1H, J_{gem} = 10.9 Hz, CH_2Ph), 4.85–4.74 (m, 2H, CH_2Ph), 4.70–4.51 (m, 4H, CH_2Ph, H-1), 3.86–3.67 (m, 4H, H-4, H-6a, H-6b, H-3, visible coupling constants: $J_{3,4}$ = 9.1 Hz), 3.52–3.45 (m, 1H, H-5), 3.36 (s, 6H, 2 × CH_3), 3.04 (bs, 1H, OH); ^{13}C NMR (100.6 MHz, $CDCl_3$) δ: 138.3, 138.1, 137.9 136.8 (4 × $C_{\text{Ar,q.}}$), 128.5–127.7 (C_{Ar}), 99.9 (C-1), 93.1 (C-9), 85.4 (C-3), 84.9 (C-7), 80.5 (C-8), 76.1 (CH_2Ph), 75.4 (C-5), 75.2 (CH_2Ph), 75.0 (C-4), 73.6 (CH_2Ph), 71.7 (C-2), 70.9 (CH_2Ph), 69.1 (C-6), 52.8 (CH_3), 52.6 (CH_3); HR-ESI-TOF calcd. for $C_{39}H_{42}O_8Na$ $[M+Na]^+$: 661.2772. Found: 661.2777; Anal. calcd. for $C_{39}H_{42}O_8$: C, 73.33; H, 6.63. Found: C, 73.04; H, 6.65.

Benzyl 3,4,6-tri-*O*-benzyl-2-*C*-{(*Z*)-3,3-dimethoxyprop-1-en-1-yl}-β-D-mannopyranoside (27):

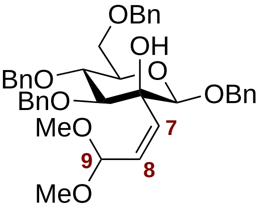

Alkyne **26** (95 mg; 0.149 mmol) in anhydrous DMF (3 mL) was treated with Lindlar catalyst (71 mg; 75 wt%) and stirred under an atmosphere of hydrogen for 5 d when TLC (toluene/ethyl acetate, 4:1) indicated complete conversion. Dilution with CH_2Cl_2, filtration through a layer of Celite, evaporation of the volatile parts and co-evaporation of residual DMF with *n*-heptane gave the crude product. Flash column chromatographic purification (SiO_2, toluene, + 2% Et_3N) provided alkene **27** (87 mg; 91%) in the form of a colorless, amorphous solid.

$R_f = 0.23$ (toluene, + 2% Et_3N); $[\alpha]_D^{20}$ −57.0 (c = 1, $CHCl_3$); ^1H NMR (400.2 MHz, DMSO-D_6) δ: rotameric isomerism, significant signals: 5.69 (d, 1H, $J_{8,9}$ = 6.3 Hz, H-9), 5.59 (d, 1H, $J_{7,8}$ = 12.4 Hz, H-7), 5.54 (dd, 1H, $J_{7,8}$ = 12.4, $J_{8,9}$ = 6.3 Hz, H-8), 3.14 (s, 6H, 2 × CH_3); ^{13}C NMR (100.6 MHz, DMSO-D_6) δ: rotameric isomerism, significant signals: 133.2 (C-7), 129.8 (C-8), 100.7 (C-1), 99.0 (C-9), 74.5 (C-5), 52.8, 51.6 (2 × CH_3); HR-ESI-TOF calcd. for $C_{39}H_{44}O_8Na$ $[M+Na]^+$: 663.2928. Found: 663.2933; Anal. calcd. for $C_{39}H_{44}O_8$: C, 73.10; H, 6.92. Found: C, 72.97; H, 7.01.

Benzyl 3,4,6-tri-*O*-benzyl-2-*C*-{(1,3-dioxan-2-yl)ethynyl}-β-D-mannopyranoside (28):

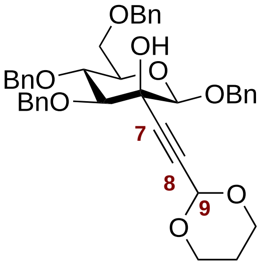

To a solution of dibenzyl acetal **22** (465 mg; 0.59 mmol) in anhydrous toluene (15 mL) was added 1,3-dihydroxypropane (426 µL; 5.88 mmol) and a catalytic amount of *p*-TsOH·H_2O (14 mg). The solution was stirred at 100 °C for 22 h, when TLC (toluene/ethyl acetate, 4:1) indicated the complete transformation of the starting material. The reaction mixture was diluted with toluene (20 mL) and washed with sat. $NaHCO_3$ (20 mL) and water (20 mL). After drying (Na_2SO_4), filtration and concentration *in vacuo*, flash column chromatographic purification of the residue (SiO_2, toluene/ethyl acetate, 7:1) afforded dioxane **28** (320 mg; 84%) as a colorless amorphous solid.

$R_f = 0.26$ (toluene/ethyl acetate, 4:1); $[\alpha]_D^{20}$ −2.4 (c = 1, $CHCl_3$); ^{1}H NMR (400.2 MHz, $CDCl_3$) δ: 7.48–7.42 (m, 4H, H_{Ar}), 7.40–7.26 (m, 14H, H_{Ar}), 7.21–7.16 (m, 2H, H_{Ar}), 5.46 (s, 1H, H-9), 5.10 (d, 1H, J_{gem} = 10.9 Hz, CH_2Ph), 5.01 (d, 1H, J_{gem} = 12.4 Hz, CH_2Ph), 4.91 (d, 1H, J_{gem} = 10.9 Hz, CH_2Ph), 4.85–4.76 (m, 2H, CH_2Ph), 4.69–4.52 (m, 4H, CH_2Ph, H-1), 4.22–4.15 (m, 2H, -CH_2-CH_2-CH_2-), 3.86–3.69 (m, 6H, -CH_2-CH_2-CH_2-, H-6a, H-6b, H-4, H-3, visible coupling constants: $J_{3,4}$ = 8.8 Hz), 3.48 (ddd, 1H, $J_{4,5}$ = 9.8, $J_{5,6}$ = 5.1, 2.0 Hz, H-5), 3.07 (bs, 1H, OH), 1.81–1.67 (m, 2H, -CH_2-CH_2-CH_2-); ^{13}C NMR (100.6 MHz, $CDCl_3$) δ: 138.3, 138.1, 137.9, 136.9 (4 × $C_{Ar,q.}$), 128.5–127.7 (C_{Ar}), 99.9 (C-1), 90.2 (C-9), 85.4 (C-3), 85.1 (C-7), 80.7 (C-8), 76.1 (CH_2Ph), 75.4 (C-5), 75.2 (CH_2Ph), 75.0 (C-4), 73.6 (CH_2Ph), 71.7 (C-2), 70.9 (CH_2Ph), 69.1 (C-6), 64.6 (-CH$_2$-CH_2-CH_2-), 64.6 (-CH_2-CH_2-CH$_2$-), 25.7 (-CH_2-CH$_2$-CH_2-); HR-ESI-TOF calcd. for $C_{40}H_{42}O_8Na$ $[M+Na]^+$: 673.2772. Found: 673.2777; Anal. calcd. for $C_{40}H_{42}O_8$: C, 73.83; H, 6.51. Found: C, 73.67; H, 6.66.

Benzyl 3,4,6-tri-*O*-benzyl-2-*C*-{(*Z*)-2-(1,3-dioxan-2-yl)vinyl}-β-D-mannopyranoside (29):

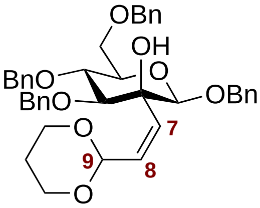

Alkyne **28** (239 mg; 0.367 mmol) in anhydrous DMF (5 mL) was treated with Lindlar catalyst (144 mg; 60 wt%) and stirred under an atmosphere of hydrogen for 3 d, when

TLC (toluene/ethyl acetate, 4:1) suggested the completion of the reaction. Dilution with CH_2Cl_2, filtration through a layer of Celite, evaporation of the volatile parts and co-evaporation of residual DMF with *n*-heptane gave pure alkene **29** (194 mg; 81%) as a colorless, amorphous solid.

$R_f = 0.65$ (toluene/ethyl acetate, 2:1); $[\alpha]_D^{20}$ –61.2 (c = 1, $CHCl_3$); ^1H NMR (400.2 MHz, $CDCl_3$) δ: 7.41–7.25 (m, 18H, H_{Ar}), 7.23–7.17 (m, 2H, H_{Ar}), 5.80 (d, 1H, $J_{8,9}$ = 5.1 Hz, H-9), 5.70 (dd, 1H, $J_{7,8}$ = 12.1, $J_{8,9}$ = 5.2 Hz, H-8), 5.33 (d, 1H, $J_{7,8}$ = 12.1 Hz, H-7), 4.93 (d, 1H, J_{gem} = 12.1 Hz, CH_2Ph), 4.86 (d, 1H, J_{gem} = 10.9 Hz, CH_2Ph), 4.76–4.52 (m, 6H, CH_2Ph), 4.26 (s, 1H, H-1), 4.10–4.01 (m, 2H, -CH_2-CH_2-CH_2-), 3.92–3.72 (m, 6H, H-4, OH, -CH_2-CH_2-CH_2-, H-6a, H-6b), 3.49–3.43 (m, 1H, H-5), 3.40 (d, 1H, $J_{3,4}$ = 9.1 Hz, H-3), 2.17–2.03 (m, 1H, -CH_2-C*Ha*Hb-CH_2-), 1.31 (d, 1H, J_{vic} = 13.4 Hz, -CH_2-CHa*Hb*-CH_2-); ^{13}C NMR (100.6 MHz, $CDCl_3$) δ: 138.5, 138.4, 138.0, 137.2 (4 × $C_{Ar,q.}$), 133.2 (C-7), 132.2 (C-8), 128.8–127.7 (C_{Ar}), 99.8 (C-1), 98.5 (C-9), 84.6 (C-3), 78.7 (C-2), 2 × 76.1 (C-4, CH_2Ph), 75.5 (C-5), 75.2 (CH_2Ph), 73.7 (CH_2Ph), 70.4 (CH_2Ph), 69.5 (C-6), 66.7 (-*C*H_2-CH_2-CH_2-), 66.6 (-CH_2-CH_2-*C*H_2-), 25.6 (CH_2-*C*H_2-CH_2-); HR-ESI-TOF calcd. for $C_{40}H_{44}O_8Na$ $[M+Na]^+$: 675.2932. Found: 675.2928; Anal. calcd. for $C_{40}H_{44}O_8$: C, 73.60; H, 6.79. Found: C, 73.65; H, 6.88.

Benzyl 2-*O*-acetyl-3,4,6-tri-*O*-benzyl-2-*C*-{(1,3-dioxan-2-yl)ethynyl}-β-D-mannopyranoside (30):

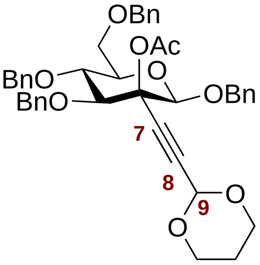

The tertiary alcohol **28** (128 mg; 0.197 mmol) was dissolved in anhydrous toluene (2 mL) and treated with Ac_2O (2 mL), Et_3N (30 µL; 0.22 mmol) and DMAP (24 mg; 0.197 mmol). The mixture was heated to 45 °C for 5 h, when TLC (toluene/ethyl acetate, 4:1) suggested complete conversion of the starting material. The reaction mixture was allowed to cool to r.t., and was next diluted with toluene (30 mL) and poured onto ice-cold sat. $NaHCO_3$ (20 mL). After stirring for 1 h, the organic layer was separated and washed with sat. $NaHCO_3$ (2 × 15 mL, to neutral solution) and water (20 mL). Drying (Na_2SO_4), filtration and evaporation of the solvents *in vacuo* gave a brown oil, which was purified by flash column chromatography (SiO_2, toluene/acetone, 60:1) to give acetate **30** (85 mg; 72%) as a yellowish oil.

$R_f = 0.76$ (toluene/ethyl acetate, 4:1); $[\alpha]_D^{20}$ −28.3 (c = 1, $CHCl_3$); ^{1}H NMR (400.2 MHz, $CDCl_3$) δ: 7.48–7.27 (m, 18H, H_{Ar}), 7.17–7.12 (m, 2H, H_{Ar}), 5.54 (s, 1H, H-9), 5.31 (d, 1H, $J_{gem} = 10.6$ Hz, CH_2Ph), 5.00 (d, 1H, $J_{gem} = 12.4$ Hz, CH_2Ph), 4.83–4.78 (m, 2H, CH_2Ph), 4.75 (d, 1H, $J_{gem} = 12.4$ Hz, CH_2Ph), 4.68 (d, 1H, $J_{gem} = 12.1$ Hz, CH_2Ph), 4.61–4.55 (m, 2H, CH_2Ph, H-1), 4.49 (d, 1H, $J_{gem} = 10.9$ Hz, CH_2Ph), 4.36–4.26 (m, 2H, -C*Ha*Hb-CH_2-CH_2-, -CH_2-CH_2-C*Ha*Hb-), 3.87–3.70 (m, 6H, -CHa*Hb*-CH_2-CH_2-, -CH_2-CH_2-CHa*Hb*-, H-3, H-4, H-6a, H-6b), 3.53 (ddd, 1H, $J_{4,5} = 9.9$, $J_{5,6} = 4.3$, 2.5 Hz, H-5), 2.20 (s, 3H, CH_3), 1.91–1.80 (m, 1H, -CH_2-C*Ha*Hb-CH_2-), 1.71–1.61 (m, 1H, -CH_2-CHa*Hb*-CH_2-); ^{13}C NMR (100.6 MHz, $CDCl_3$) δ: 168.5 (acetyl C=O), 138.3, 138.1, 138.0, 136.8 (4 × $C_{Ar,q.}$), 128.7–127.7 (C_{Ar}), 100.8 (C-1), 89.7 (C-9), 86.1 (C-3), 84.0 (C-7), 82.4 (C-8), 75.6 (C-5), 75.4 (CH_2Ph), 75.2 (C-2), 75.2 (CH_2Ph), 74.6 (C-4), 73.5 (CH_2Ph), 71.3 (CH_2Ph), 69.1 (C-6), 2 × 63.7 (-*C*H_2-CH_2-CH_2-, -CH_2-CH_2-*C*H_2-), 25.9 (-CH_2-*C*H_2-CH_2-), 22.2 (CH_3); HR-ESI-TOF calcd. for $C_{42}H_{44}O_9Na$ $[M+Na]^+$: 715.2878. Found: 715.2879; Anal. calcd. for $C_{42}H_{44}O_9$: C, 72.81; H, 6.40. Found: C, 72.79; H, 6.47.

Benzyl 2-*O*-acetyl-3,4,6-tri-*O*-benzyl-2-*C*-{(*Z*)-2-(1,3-dioxan-2-yl)vinyl}-β-D-mannopyranoside (31):

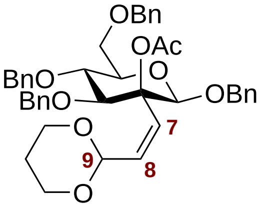

To a solution of alkyne **30** (82 mg; 0.118 mmol) in anhydrous DMF (3 mL) was added Lindlar catalyst (44 mg; 54 wt%), and the mixture was stirred under an atmosphere of hydrogen for 5 d, when no more conversion could be observed. TLC (toluene/ethyl acetate, 4:1) suggested the presence of unreacted **30** and of a product with lower chromatographic mobility. Dilution with CH_2Cl_2, filtration through a layer of Celite, evaporation of the volatile parts and co-evaporation of residual DMF with *n*-heptane gave a crude mixture. Flash column chromatographic purification (SiO_2, toluene/acetone, 60:1) provided substrate **30** (48 mg; 0.069 mmol) together with alkene **31** (18 mg; 22%; 53% brsm) in the form of a colorless oil.

$R_f = 0.45$ (toluene/ethyl acetate, 4:1); $[\alpha]_D^{20}$ –20.9 (c = 1, $CHCl_3$); ^{1}H NMR (400.2 MHz, $CDCl_3$) δ: 7.38–7.24 (m, 18H, H_{Ar}), 7.23–7.19 (m, 2H, H_{Ar}), 6.11 (dd, 1H, $J_{7,8} = 12.6$, $J_{7,9} = 0.7$ Hz, H-7), 5.48 (dd, 1H, $J_{7,8} = 12.7$, $J_{8,9} = 6.5$ Hz, H-8), 5.21 (dd, 1H, $J_{8,9} = 6.6$, $J_{7,9} = 0.6$ Hz, H-9), 5.12 (s, 1H, H-1), 4.90 (d, 1H, $J_{gem} = 12.7$ Hz, CH_2Ph), 4.76 (d, 1H, $J_{gem} = 11.4$ Hz, CH_2Ph), 4.69–4.63 (m, 2H, CH_2Ph), 4.54 (d, 1H, J_{gem} =

11.9 Hz, CH_2Ph), 4.51–4.43 (m, 3H, CH_2Ph), 4.06 (d, 1H, $J_{3,4}$ = 6.0 Hz, H-3), 4.04–3.96 (m, 2H, -C*Ha*Hb-CH_2-CH_2-, -CH_2-CH_2-C*Ha*Hb-), 3.91–3.76 (m, 4H, H-6a, H-4, H-5, H-6b), 3.54 (ddd, 1H, J = 11.9, 11.9, 2.4 Hz, -CHa*Hb*-CH_2-CH_2-), 3.44 (ddd, 1H, J = 11.9, 11.9, 2.4 Hz, -CH_2-CH_2-CHa*Hb*-), 2.11–1.97 (m, 4H, -CH_2-C*Ha*Hb-CH_2-, CH_3), 1.26–1.20 (m, 1H, -CH_2-CHa*Hb*-CH_2-); ^{13}C NMR (100.6 MHz, $CDCl_3$) δ: 168.9 (acetyl C=O), 138.6, 138.4, 138.1, 137.5 (4 × $C_{Ar,q.}$), 132.6 (C-7), 128.5–127.6 (C_{Ar}), 127.5 (C-8), 99.7 (C-1), 97.9 (C-9), 81.4 (C-2), 81.3 (C-3), 75.5 (*C-5), 75.0 (*C-4, assignments may be interchanged), 74.9 (CH_2Ph), 73.4 (CH_2Ph), 73.2 (CH_2Ph), 70.9 (CH_2Ph), 70.5 (C-6), 66.6 (-*C*H_2-CH_2-CH_2-), 66.6 (-CH_2-CH_2-*C*H_2-), 25.6 (-CH_2-*C*H_2-CH_2-), 21.9 (CH_3); HR-ESI-TOF calcd. for $C_{42}H_{46}O_9Na$ $[M+Na]^+$: 717.3034. Found: 717.3040; Anal. calcd. for $C_{42}H_{46}O_9$: C, 72.60; H, 6.67. Found: C, 72.27; H, 6.99.

Benzyl 2-*O*-acetyl-3,4,6-tri-*O*-benzyl-2-*C*-{(1,3-dioxolan-2-yl)acetyl}-β-D-mannopyranoside (32):

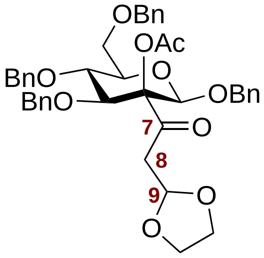

To acetylated dibenzyl acetal **24** (62 mg; 0.074 mmol) in ethylene glycol (5 mL) was added I_2 (50 mg), and the mixture was heated to 50 °C for 22 h. TLC (toluene/acetone, 20:1) indicated the presence of multiple products. The reaction mixture was cooled to 0 °C by the addition of ice. Next, $Na_2S_2O_3$ (90 mg) was added, and the suspension was stirred for 15 min until it had completely decolorized. $CHCl_3$ (50 mL) and water (20 ml) were added, and the organic layer was separated. Washing with sat. $NaHCO_3$ (20 mL) and water (2 × 20 mL), drying (Na_2SO_4), filtration and evaporation of the volatile components *in vacuo* gave a crude oil. Flash column chromatography (SiO_2, toluene/acetone, 20:1) afforded ketone **32** (17 mg; 33%) in the form of a colorless oil.

$R_f = 0.22$ (toluene/acetone, 20:1); $[\alpha]_D^{20}$ −52.9 (c = 1, $CHCl_3$); ^{1}H NMR (400.2 MHz, $CDCl_3$) δ: 7.37–7.22 (m, 18H, H_{Ar}), 7.11–7.06 (m, 2H, H_{Ar}), 5.15 (dd, 1H, $J_{8a,9}$ = 5.3, $J_{8b,9}$ = 4.2 Hz, H-9), 4.93 (d, 1H, J_{gem} = 11.4 Hz, CH_2Ph), 4.75–4.69 (m, 2H, CH_2Ph), 4.67–4.46 (m, 6H, CH_2Ph, H-1, H-3), 4.43 (d, 1H, J_{gem} = 10.9 Hz, CH_2Ph), 3.89–3.68 (m, 7H, 2 × *dioxolane* CH_2, H-4, H-6a, H-6b), 3.58 (ddd, 1H, $J_{4,5}$ = 9.6, $J_{5,6}$ = 4.6, 2.8 Hz, H-5), 3.14 (dd, 1H, $J_{8a,8b}$ = 16.9, $J_{8a,9}$ = 5.3 Hz, H-8a), 3.07 (dd, 1H, $J_{8a,8b}$ = 16.9, $J_{8b,9}$ = 4.2 Hz, H-8b), 2.23 (s, 3H, CH_3); ^{13}C NMR (100.6 MHz, $CDCl_3$) δ: 203.3 (C-7), 170.2 (acetyl C=O), 138.5, 138.3, 138.1, 136.4 (4 × $C_{Ar,q.}$), 128.5–127.6 (C_{Ar}), 101.4 (C-9), 99.7 (C-1), 88.2 (C-2), 80.9 (C-3), 75.8 (C-4), 75.7 (C-5), 75.1 (CH_2Ph), 74.9 (CH_2Ph), 73.6 (CH_2Ph), 71.4 (CH_2Ph), 69.3 (C-6), 64.9 (*dioxolane* CH_2), 64.8 (*dioxolane* CH_2), 45.2 (C-8), 21.5 (CH_3); HR-ESI-TOF calcd. for $C_{41}H_{44}O_{10}Na$ $[M+Na]^+$: 719.2827. Found: 719.2822.

Benzyl 3,4,6-tri-*O*-benzyl-2-*C*-(3-hydroxyprop-1-yn-1-yl)-β-D-mannopyranoside (33):

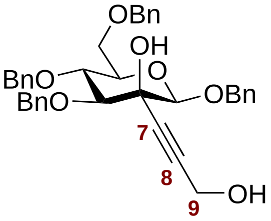

From 2b: 43 µL of propargyl alcohol (0.74 mmol) in anhydrous THF (5 mL) was dropwise treated with 1.49 mL of ethylmagnesium bromide (1 M in THF; 1.49 mmol) at r.t. The mixture was heated to 80 °C for 1.5 h, and then allowed to cool to r.t. Next, this solution was added dropwise to benzyl 2-uloside **2b**[37] (0.20 g; 0.37 mmol) in anhydrous THF (5 mL) at r.t. with a programmable syringe pump (addition rate: 0.12 mL/min). The reaction mixture was stirred for another 30 min, when TLC control (toluene/ethyl acetate, 4:1) showed complete consumption of the starting material. The solution was cooled to 0 °C and dropwise treated with sat. NH_4Cl (2 mL). After dilution with $CHCl_3$ (100 mL) and water (25 mL), and washing of the organic part with sat. NH_4Cl (25 mL), sat. $NaHCO_3$ (25 mL) and water (25 mL), the organic phase was dried (Na_2SO_4), filtered and evaporated to give a crude oil. Flash column chromatographic purification (SiO_2, toluene/ethyl acetate, 4:1) yielded alkynol **33** (138 mg; 63%) as a colorless resin. As side products with higher chromatographic mobility, *gluco*-derivative **39** (11 mg; 5%) and 3,2-enolone **40** (9 mg; 5%) were obtained.

From 22: A solution of dibenzyl acetal **22** (297 mg; 0.38 mmol) in anhydrous acetone (20 mL) was treated with a catalytic amount of *p*-TsOH·H_2O (30 mg). The solution was stirred at 50 °C for 48 h. TLC (toluene/ethyl acetate, 4:1) suggested the presence of multiple products, and the solution was neutralized by the addition of Et_3N (50 µL) at r.t., and was then evaporated to dryness. Flash column chromatographic purification (SiO_2, toluene/acetone, 20:1) gave a mixture of products as a yellow oil (170 mg). This crude mixture was dissolved in MeOH (10 mL) and cooled to 0 °C. $NaBH_4$ (19 mg; 0.50 mmol) was added, and stirring at 0 °C was continued for 30 min. TLC control (toluene/ethyl acetate, 4:1) confirmed the formation of a major product with lower chromatographic mobility, and the mixture was neutralized by the addition of sat.

NH_4Cl (200 µL). Stirring at 0 °C was continued until no further gas evolved from the solution, which was then allowed to warm to r.t. Evaporation of all volatile components *in vacuo* gave a crude product, which was dissolved in CH_2Cl_2 (50 mL), washed with water (2 × 20 mL) and dried (Na_2SO_4). Filtration, evaporation of the solvents, and flash column chromatographic purification (SiO_2, toluene/ethyl acetate, 6:1 to 4:1) gave alkynol **33** (121 mg; 54% over two steps) as a colorless resin.

$R_f = 0.08$ (toluene/ethyl acetate, 4:1); $[\alpha]_D^{20}$ −9.5 (c = 1, $CHCl_3$); ^1H NMR (400.2 MHz, $CDCl_3$) δ: 7.48–7.25 (m, 18H, H_{Ar}), 7.23–7.13 (m, 2H, H_{Ar}), 5.06–4.95 (m, 2H, CH_2Ph), 4.91 (d, 1H, J_{gem} = 11.0 Hz, CH_2Ph), 4.81 (d, 1H, J_{gem} = 10.9 Hz, CH_2Ph), 4.75 (d, 1H, J_{gem} = 12.3 Hz, CH_2Ph), 4.66 (d, 1H, J_{gem} = 12.2 Hz, CH_2Ph), 4.59 (d, 1H, J_{gem} = 12.1 Hz, CH_2Ph), 4.53 (d, 1H, J_{gem} = 10.9 Hz, CH_2Ph), 4.48 (s, 1H, H-1), 4.20 (s, 2H, H-9a, H-9b), 3.85–3.70 (m, 3H, H-4, H-6a, H-6b), 3.64 (d, 1H, $J_{3,4}$ = 9.2 Hz, H-3), 3.52–3.43 (m, 1H, H-5); ^{13}C NMR (100.6 MHz, $CDCl_3$) δ: 138.2, 138.1, 138.1, 136.9 (4 × $C_{Ar,q.}$), 128.5–127.7 (C_{Ar}), 100.0 (C-1), 85.5 (C-3), 84.6 (C-7), 84.2 (C-8), 76.0 (CH_2Ph), 75.3 (C-5), 75.2 (CH_2Ph), 75.2 (C-4), 73.6 (CH_2Ph), 71.7 (C-2), 70.9 (CH_2Ph), 69.1 (C-6), 51.0 (C-9); HR-ESI-TOF calcd. for $C_{37}H_{38}O_7Na$ $[M+Na]^+$: 617.2510. Found: 617.2506; Anal. calcd. for $C_{37}H_{38}O_7$: C, 74.73; H, 6.44. Found: C, 74.67; H, 6.64.

Benzyl 3,4,6-tri-*O*-benzyl-2-*C*-{3-(tri-*iso*-propylsilyloxy)prop-1-yn-1-yl}-β-D-mannopyranoside (34):

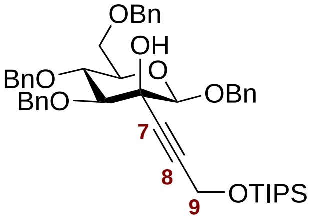

Tri-*iso*-propyl(prop-2-yn-1-yloxy)silane[281] (235 µL; 0.93 mmol) in anhydrous THF (14 mL) was cooled to −80 °C. Next, *n*-BuLi (2.5 M in *n*-hexane; 360 µL; 0.19 mmol) was added dropwise, and the reaction mixture was stirred for 60 min at −80 °C. Benzyl 2-uloside **2b**[37] (387 mg; 0.72 mmol) in THF (6 mL) was slowly added with a programmable syringe pump (addition rate: 0.17 mL/min), and the cooled solution was stirred for 1 h. TLC reaction control (toluene/ethyl acetate, 4:1) showed complete conversion, and the reaction was quenched by the dropwise addition of sat. NH_4Cl (3 mL). The suspension was allowed to warm to r.t. and was diluted with $CHCl_3$ (80 mL) and water (20 mL). The organic phase was washed with sat. $NaHCO_3$ (25 mL) and water (25 mL), dried (Na_2SO_4), filtered and evaporated to dryness. Flash column chromatographic purification (SiO_2, toluene/acetone, 25:1) of the crude material provided silyl ether **34** (293 mg; 72%) as a colorless, highly viscous oil.

$R_f = 0.65$ (toluene/ethyl acetate, 4:1); $[\alpha]_D^{20}$ −8.3 (c = 1, $CHCl_3$); ^1H NMR (400.2 MHz, $CDCl_3$) δ: 7.44–7.24 (m, 18H, H_{Ar}), 7.17–7.12 (m, 2H, H_{Ar}), 5.12 (d, 1H, J_{gem} = 10.8 Hz, CH_2Ph), 4.98 (d, 1H, J_{gem} = 12.2 Hz, CH_2Ph), 4.87 (d, 1H, J_{gem} = 10.8 Hz, CH_2Ph), 4.79 (d, 1H, J_{gem} = 10.9 Hz, CH_2Ph), 4.74 (d, 1H, J_{gem} = 12.2 Hz, CH_2Ph), 4.64 (d, 1H, J_{gem} = 12.2 Hz, CH_2Ph), 4.57 (d, 1H, J_{gem} = 12.1 Hz, CH_2Ph), 4.53–4.47 (m, 2H, CH_2Ph, H-1), 4.45–4.36 (m, 2H, H-9a, H-9b), 3.79–3.68 (m, 3H, H-4, H-6a, H-6b), 3.66 (d, 1H, $J_{3,4}$ = 9.1 Hz, H-3), 3.46 (ddd, 1H, $J_{4,5}$ = 9.9, $J_{5,6a}$ = 5.4, $J_{5,6b}$ = 2.0 Hz, H-5), 1.11–1.01 (m, 21H, *i*-Pr); ^{13}C NMR (100.6 MHz, $CDCl_3$) δ: 138.4, 138.2, 138.1, 137.0 (4 × $C_{Ar,q.}$), 128.5–127.7 (C_{Ar}), 100.3 (C-1), 85.8 (C-3), 84.6 (C-7), 83.4 (C-8), 76.1 (CH_2Ph), 75.4 (C-5), 75.3 (CH_2Ph), 75.1 (C-4), 73.7 (CH_2Ph), 71.7 (C-2), 71.1 (CH_2Ph), 69.2 (C-6), 52.1 (C-9), 18.1 ($(H_3\mathit{C})_2CH\text{-}Si$), 12.1 ($(H_3C)_2\mathit{C}H\text{-}Si$); HR-ESI-TOF calcd. for $C_{46}H_{58}O_7SiNa$ $[M+Na]^+$: 773.3844. Found: 773.3840; Anal. calcd. for $C_{46}H_{58}O_7Si$: C, 73.56; H, 7.78. Found: C, 73.36; H, 7.73.

Benzyl 3,4,6-tri-*O*-benzyl-2-*C*-{3-[(2*R*/*S*)-tetrahydro-2*H*-pyran-2-yloxy]-prop-1-yn-1-yl}-β-D-mannopyranoside (35):

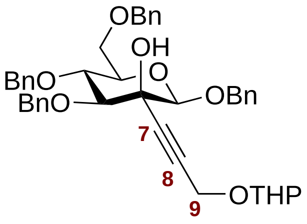

2-(2-Propynyloxy)tetrahydropyran[280](1.87 mL; 13.32 mmol) was dissolved in anhydrous THF (200 mL) and cooled to −80 °C. Next, *n*-BuLi (5.55 mL; 13.88 mmol; 2.5 M in *n*-hexane) was added dropwise, and the reaction mixture was stirred at −80 °C for 1 h. Benzyl 2-uloside **2b**[37] (5.98 g; 11.10 mmol) was dissolved in anhydrous THF (100 mL) at r.t. and was slowly added dropwise to the cooled solution *via* a cannula (addition over 50 min). When the addition was complete, the mixture was stirred for another 10 min at −80 °C, when TLC (toluene/ethyl acetate, 4:1) indicated complete consumption of the starting material. The reaction was quenched by the dropwise addition of brine (50 mL), and was then allowed to warm to r.t. Dilution with CH_2Cl_2 (700 mL), washing with water, sat. $NaHCO_3$ and water (150 mL each) and drying over Na_2SO_4 provided, after filtration and evaporation, a colorless oil (8 g). Purification by flash column chromatography (SiO_2, toluene/ethyl acetate, 5.5:1) gave THP-protected alkynol **35** (7.0 g; 93%) as a diastereomeric mixture (ca. 1:1) in the form of a colorless oil.

R_f = 0.45 (toluene/ethyl acetate, 4:1); ^{1}H NMR (400.2 MHz, $CDCl_3$): δ: 7.44–7.25 (m, 18H, H_{Ar}), 7.18–7.13 (m, 2H, H_{Ar}), 5.07 (d, 1H, J_{gem} = 10.8 Hz, CH_2Ph), 4.98 (d, 1H, J_{gem} = 12.4 Hz, CH_2Ph), 4.87 (d, 1H, J_{gem} = 10.8 Hz, CH_2Ph), 4.82–4.72 (m, 3H, CH_2Ph, *pyran* H-2), 4.64 (d, 1H, J_{gem} = 12.1 Hz, CH_2Ph), 4.57 (d, 1H, J_{gem} = 12.1 Hz, CH_2Ph), 4.53–4.47 (m, 2H, CH_2Ph, H-1), 4.35–4.22 (m, 2H, H-9ab), 3.84–3.74 (m, 3H, *pyran* H-6a, H-4, H-6a), 3.71 (dd, 1H, $J_{6a,6b}$ = 10.9, $J_{5,6b}$ = 5.3 Hz, H-6b), 3.65 (d, 1H, $J_{3,4}$ = 9.1 Hz, H-3), 3.52–3.42 (m, 2H, H-5, *pyran* H-6b), 2.96 (bs, 1H, OH), 1.83–1.41 (m, 6H, *pyran* H-3ab, *pyran* H-4ab, *pyran* H-5ab); ^{13}C NMR (100.6 MHz, $CDCl_3$) mixture of diastereoisomers(*): δ: 138.4, 138.2, 138.0, 137.0 (4 × $C_{Ar,q.}$), 128.5–127.7 (C_{Ar}), 100.1 (C-1), 100.1 (C-1*), 96.9 (*pyran* C-2), 85.7 (C-3), 85.6 (C-3*), 85.0 (C-7), 84.9 (C-7*), 82.1 (C-8), 82.1 (C-8*), 76.1 (CH_2Ph), 76.1 (CH_2Ph*), 75.4 (C-5), 75.3 (CH_2Ph), 75.2 (C-4), 75.1 (C4*), 73.7 (CH_2Ph), 71.7 (C-2), 71.0 (CH_2Ph), 70.9 (CH_2Ph*), 69.2 (C-6), 62.2 (*pyran* C-6), 62.1 (*pyran* C-6*), 54.3 (C-9), 54.2 (C-9*), 30.3 (*pyran* C-3), 25.5 (*pyran* C-5), 19.2 (*pyran* C-4), 19.1 (*pyran* C-4*); HR-ESI-TOF calcd. for $C_{42}H_{46}O_8Na$ $[M+Na]^+$: 701.3085. Found: 701.3085; Anal. calcd. for $C_{42}H_{46}O_8$: C, 74.31; H, 6.83. Found: C, 74.12; H, 6.85.

Benzyl 3,4,6-tri-*O*-benzyl-2-*C*-{(*Z*)-3-hydroxyprop-1-en-1-yl}-β-D-mannopyranoside (36):

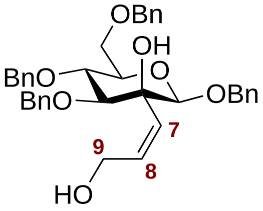

To a solution of THP-protected allyl alcohol **38** (6.78 g; 9.96 mmol) in MeOH (200 mL) was added a catalytic amount of *p*-TsOH·H_2O (100 mg) and the mixture was stirred at r.t. for 10 h. TLC reaction monitoring (toluene/ethyl acetate, 4:1) indicated complete conversion. After neutralization with Et_3N (1 mL) and stirring for 15 min, evaporation of the volatile parts yielded a colorless oil (6 g). Flash column chromatography (SiO_2, toluene/ethyl acetate, 2.5:1) gave pure allyl alcohol **36** (5.65 g; 95%) as a colorless oil.

R_f = 0.21 (toluene/ethyl acetate, 4:1); $[\alpha]_D^{20}$ −59.2 (c = 1, $CHCl_3$); ^{1}H NMR (400.2 MHz, acetone-D_6) δ: 7.43–7.21 (m, 20H, H_{Ar}), 5.81 (ddd, 1H, $J_{7,8}$ = 12.0, $J_{8,9a}$ = 5.9, $J_{8,9b}$ = 5.9 Hz, H-8), 5.43 (ddd, 1H, $J_{7,8}$ = 12.2, $J_{7,9a}$ = 1.7, $J_{7,9b}$ = 1.7 Hz, H-7), 4.87 (d, 1H, J_{gem} = 12.2 Hz, CH_2Ph), 4.83–4.74 (m, 3H, CH_2Ph), 4.69–4.55 (m, 5H, CH_2Ph, H-1), 4.51 (ddd, 1H, $J_{9a,9b}$ = 14.1, $J_{8,9a}$ = 6.0, $J_{7,9a}$ = 1.6 Hz, H-9a), 4.39 (ddd, 1H, $J_{9a,9b}$ = 13.9, $J_{8,9b}$ = 5.8, $J_{7,9b}$ = 1.5 Hz, H-9b), 3.96 (bs, 1H, OH), 3.89 (dd, 1H, $J_{3,4}$ = 9.4, $J_{4,5}$ = 9.4 Hz, H-4), 3.83 (dd, 1H, $J_{6a,6b}$ = 11.0, $J_{5,6a}$ = 2.1 Hz, H-6a), 3.77 (dd, 1H, $J_{6a,6b}$ = 11.0, $J_{5,6b}$ = 5.3 Hz, H-6b), 3.61–3.53 (m, 2H, H-3, H-5); ^{13}C NMR (100.6 MHz, acetone-D_6) δ: 139.9, 139.9, 139.8, 138.9 (4 × $C_{Ar,q.}$), 135.7 (C-8), 130.5 (C-7), 129.1–128.2 (C_{Ar}), 102.2 (C-1), 86.2 (C-3), 79.2 (C-2), 76.9 (C-4), 76.4 (CH_2Ph), 76.3 (C-5), 75.4 (CH_2Ph), 73.8 (CH_2Ph), 71.1 (CH_2Ph), 70.3 (C-6), 59.7 (C-9); HR-ESI-TOF calcd. for $C_{37}H_{40}O_7Na$ $[M+Na]^+$: 619.2666. Found: 619.2667; Anal. calcd. for $C_{37}H_{40}O_7$: C, 74.47; H, 6.76. Found: C, 74.17; H, 6.87.

Benzyl 3,4,6-tri-*O*-benzyl-2-*C*-{(*Z*)-3-[tri-*iso*-propylsilyloxy]prop-1-en-1-yl}-β-D-mannopyranoside (37):

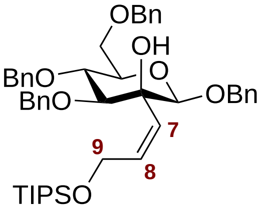

To alkyne **34** (73 mg; 0.098 mmol) in 1,4-dioxane (3.5 mL) was added Lindlar catalyst (24 mg; 33 wt%) and the reaction mixture was stirred under an atmosphere of hydrogen at r.t. After 21 h, when TLC (toluene/ethyl acetate, 4:1) indicated no further progression of the reaction, another portion of Lindlar catalyst (15 mg; 20 wt%) was added, and stirring under the hydrogen atmosphere was continued for another 22 h. The suspension was diluted with EtOAc (20 mL), filtered through a layer of Celite, and evaporated *in vacuo* to give a crude oil. Flash column chromatographic purification (SiO_2, 100% toluene to toluene/ethyl acetate, 9:1) yielded TIPS-protected allyl alcohol **37** (64 mg; 87%) in the form of a colorless oil.

$R_f = 0.83$ (toluene/ethyl acetate, 4:1); $[\alpha]_D^{20}$ −45.8 (c = 1, $CHCl_3$); ^{1}H NMR (400.2 MHz, $CDCl_3$) δ: 7.39–7.25 (m, 18H, H_{Ar}), 7.18–7.12 (m, 2H, H_{Ar}), 5.81 (ddd, 1H, $J_{7,8}$ = 12.2, $J_{8,9a}$ = 5.3, $J_{8,9b}$ = 5.3 Hz, H-8), 5.10 (ddd, 1H, $J_{7,8}$ = 12.2, $J_{7,9a}$ = 2.0, $J_{7,9b}$ = 2.0 Hz, H-7), 4.91 (d, 1H, J_{gem} = 12.2 Hz, CH_2Ph), 4.82–4.70 (m, 4H, CH_2Ph, H-9a), 4.68–4.56 (m, 4H, CH_2Ph, H-9b), 4.53 (d, 1H, J_{gem} = 10.9 Hz, CH_2Ph), 4.29 (s, 1H, H-1), 3.86 (dd, 1H, $J_{3,4}$ = 9.4, $J_{4,5}$ = 9.4 Hz, H-4), 3.80 (dd, 1H, $J_{6a,6b}$ = 10.9, $J_{5,6a}$ = 2.0 Hz, H-6a), 3.74 (dd, 1H, $J_{6a,6b}$ = 10.9, $J_{5,6b}$ = 5.3 Hz, H-6b), 3.47–3.40 (m, 2H, H-5, H-3), 2.91 (bs, 1H, OH), 1.09–0.99 (m, 21H, *i*-Pr); ^{13}C NMR (100.6 MHz, $CDCl_3$) δ: 138.5, 138.3, 138.2, 137.2 (4 × $C_{Ar,q.}$), 137.0 (C-8), 128.5–127.7 (C_{Ar}), 127.6 (C-7), 100.3 (C-1), 85.3 (C-3), 78.6 (C-2), 76.1 (C-4), 76.0 (CH_2Ph), 75.4 (C-5), 75.2 (CH_2Ph), 73.7 (CH_2Ph), 70.5 (CH_2Ph), 69.4 (C-6), 60.9 (C-9), 18.2 ($(H_3C)_2CH$-Si), 12.1 ($(H_3C)_2CH$-Si); HR-ESI-TOF calcd. for $C_{46}H_{60}O_7SiNa$ $[M+Na]^+$: 775.4001. Found: 775.3997; Anal. calcd. for $C_{46}H_{60}O_7Si$: C, 73.37; H, 8.03. Found: C, 73.23; H, 8.04.

Benzyl 3,4,6-tri-*O*-benzyl-2-*C*-{(*Z*)-3-[(2*R*/*S*)-tetrahydro-2*H*-pyran-2-yloxy]prop-1-en-1-yl}-β-D-mannopyranoside (38):

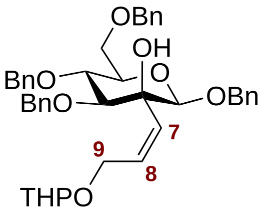

Alkyne **35** (7.0 g; 10.31 mmol) in 1,4-dioxane (200 mL) was treated with Lindlar catalyst (3.5 g; 50 wt%) and stirred under an atmosphere of hydrogen at r.t. After 20 h, TLC (toluene/ethyl acetate, 4:1) showed complete conversion. Filtration through a layer of Celite and evaporation of the solvent *in vacuo* gave a crude oil. Flash column chromatography (SiO_2, toluene/ethyl acetate, 8:1 to 5:1) provided THP-protected allyl alcohol **38** (6.80 g; 97%) as a mixture of diastereoisomers (ca. 1:1) in the form of a colorless oil.

$R_f = 0.61$ (toluene/ethyl acetate, 4:1); ^{1}H NMR (400.2 MHz, $CDCl_3$) mixture of diastereoisomers(*): δ: 7.40–7.22 (m, 18H, H_{Ar}), 7.19–7.14 (m, 2H, H_{Ar}), 5.85–5.72 (m, 1H, H-8), 5.32–5.24 (m, 1H, H-7), 4.97–4.88 (m, 1H, CH_2Ph), 4.85–4.76 (m, 2H, CH_2Ph), 4.74–4.58 (m, 6H, CH_2Ph, H-9a, *pyran* H-2, *pyran* H-2*, H-9a*), 4.57–4.51 (m, 1H, CH_2Ph), 4.45 (ddd, 0.5H, $J_{gem} = 13.5$, $J_{8*,9b*} = 6.7$, $J_{7*,9b*} = 1.4$ Hz, H-9b*), 4.37 (ddd, 0.5H, $J_{gem} = 13.4$, $J_{8,9b} = 5.6$, $J_{7,9b} = 1.6$ Hz, H-9b), 4.33 (s, 0.5H, H-1), 4.31 (s, 0.5H, H-1*), 3.93–3.85 (m, 1H, H-4), 3.84–3.72 (m, 3H, H-6a, H-6b, *pyran* H-6a), 3.68–3.51 (m, 1H, OH), 3.50–3.37 (m, 3H, H-5, *pyran* H-6b, H-3), 1.84–1.72 (m, 1H, *pyran* H-4a), 1.69–1.40 (m, 5H, *pyran* H-3ab, *pyran* H-5ab, *pyran* H-4b); ^{13}C NMR (100.6 MHz, $CDCl_3$) mixture of diastereoisomers(*): δ: 138.5, 138.3, 138.2, 138.1, 137.3, 137.2 ($C_{Ar,q.}$), 132.2 (C-8), 131.6 (C-8*), 131.3 (C-7), 130.4 (C-7*), 128.5–127.7 (C_{Ar}), 100.8 (C-1), 100.5 (C-1*), 98.0 (*pyran* C-2), 97.1 (*pyran* C-2*), 85.3 (C-3), 85.1 (C-3*), 78.7 (C-2), 78.5 (C-2*), 76.2 (CH_2Ph), 76.1 (C-4), 75.5 (C-5), 75.2 (CH_2Ph), 73.7 (CH_2Ph), 70.8 (CH_2Ph), 70.7 (CH_2Ph*), 69.5 (C-6), 64.3 (C-9*), 63.5 (C-9), 62.1 (*pyran* C-6), 62.0 (*pyran* C-6*), 30.6 (*pyran* C-3), 30.5 (*pyran* C-3*), 25.5 (*pyran* C-5), 25.5 (*pyran* C-5*), 19.4 (*pyran* C-4), 19.3 (*pyran* C-4*); HR-ESI-TOF calcd. for $C_{42}H_{48}O_8Na$ $[M+Na]^+$: 703.3241. Found: 703.3243; Anal. calcd. for $C_{42}H_{48}O_8$: C, 74.09; H, 7.11. Found: C, 73.99; H, 7.18.

Benzyl 3,4,6-tri-*O*-benzyl-2-*C*-(3-hydroxyprop-1-yn-1-yl)-β-D-glucopyranoside (39):

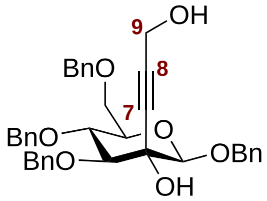

Isolated as a minor side product (11 mg; 5%) in the formation of **33** from **2b** (0.20 g; 0.37 mmol) as described on page 210.

$R_f = 0.17$ (toluene/ethyl acetate, 4:1); ^{1}H NMR (400.2 MHz, $CDCl_3$) δ: 7.44–7.23 (m, 18H, H_{Ar}), 7.18–7.12 (m, 2H, H_{Ar}), 5.04–4.95 (m, 2H, CH_2Ph), 4.88–4.79 (m, 2H, CH_2Ph), 4.71–4.64 (m, 2H, CH_2Ph), 4.57–4.49 (m, 2H, CH_2Ph), 4.29 (s, 3H, H-1, H-9a, H-9b), 3.82–3.73 (m, 3H, H-4, H-6a, H-6b), 3.60 (d, 1H, $J_{3,4} = 9.2$ Hz, H-3), 3.50 (ddd, 1H, $J_{4,5} = 9.8$, $J_{5,6a} = 3.3$, $J_{5,6b} = 3.3$ Hz, H-5), 2.45 (bs, 2H, 2 × OH); ^{13}C NMR (100.6 MHz, $CDCl_3$) δ: 138.6, 138.3, 138.2, 136.8 (4 × $C_{Ar,q.}$), 128.6–127.8 (C_{Ar}), 101.6 (C-1), 86.2 (C-7), 85.8 (C-3), 82.1 (C-8), 76.9 (C-4), 76.0 (C-5), 75.5 (CH_2Ph), 75.3 (CH_2Ph), 75.0 (C-2), 73.6 (CH_2Ph), 71.3 (CH_2Ph), 69.0 (C-6), 51.4 (C-9); HR-ESI-TOF calcd. for $C_{37}H_{38}O_7Na$ $[M+Na]^+$: 617.2510. Found: 617.2509.

Benzyl 3,6-di-*O*-benzyl-4-deoxy-β-D-*glycero*-hex-3-enopyranoside-2-ulose (40):

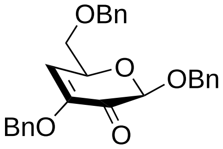

As a side product: Isolated as a minor product (9 mg; 5%) in the formation of **33** from **2b** (0.20 g; 0.37 mmol) as described on page 210.

Synthesized from 2b: 2-Uloside **2b**[37] (0.97 g; 1.80 mmol) was dissolved in toluene (38 mL), and water (2.6 mL) was added. Next, the mixture was treated with K_2CO_3 (0.50 g; 3.62 mmol), and the suspension was stirred at 95 °C. After 22 h, TLC (toluene/ ethyl acetate, 4:1) suggested complete conversion of the substrate, and the reaction mixture was diluted with toluene (50 mL) and allowed to cool to r.t. The suspension was washed with water (3 × 20 mL), dried (Na_2SO_4), and filtered. The solvent was evaporated *in vacuo*, and the resulting yellow oil was purified by flash column chromatography (SiO_2, toluene/ethyl acetate, 8:1) to give benzyl 3,2-enolone **40** (0.71 g; 92%) as a colorless oil.

$R_f = 0.71$ (toluene/ethyl acetate, 4:1); $[\alpha]_D^{20}$ −108.9 (c = 1, $CHCl_3$). UV (acetonitrile) λ_{max} (log ϵ) 263 (3.78), 337 nm (sh, 1.86); ^{1}H NMR (400.2 MHz, acetone-D_6) δ: 7.45–7.27 (m, 15H, H_{Ar}), 6.29 (d, 1H, $J_{4,5} = 3.6$ Hz, H-4), 5.07 (s, 1H, H-1), 4.92–

4.85 (m, 4H, H-5, CH_2Ph), 4.70 (d, 1H, J_{gem} = 11.9 Hz, CH_2Ph), 4.62–4.55 (m, 2H, CH_2Ph), 3.88 (dd, 1H, $J_{6a,6b}$ = 9.7, $J_{5,6a}$ = 7.0 Hz, H-6a), 3.71 (dd, 1H, $J_{6a,6b}$ = 9.8, $J_{5,6b}$ = 6.1 Hz, H-6b); ^{13}C NMR (100.6 MHz, acetone-D_6) δ: 184.9 (C-2), 147.9 (C-3), 139.4, 138.3, 137.3 (3 × $C_{Ar,q.}$), 129.3–128.4 (C_{Ar}), 117.6 (C-4), 99.0 (C-1), 74.0 (C-6), 73.7 (CH_2Ph), 73.0 (C-5), 70.8 (CH_2Ph), 70.3 (CH_2Ph). HR-ESI-TOF: calcd. for $C_{27}H_{26}O_5Na$ $[M+Na]^+$ 453.1672. Found 453.1675. Anal. calcd. for $C_{27}H_{26}O_5$: calcd. C, 75.33; H, 6.09. Found: C, 75.37; H, 6.15.

(2*S*)-1,3,4,6-Tetra-*O*-benzyl-4'7'-dihydrospiro[2-deoxy-β-D-mannopyranose-2,4'-[1,3]-dioxepin-2-one] (41):

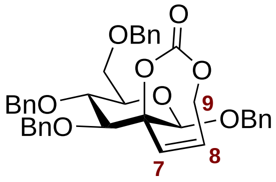

Diol **36** (205 mg; 0.344 mmol) in anhydrous CH_2Cl_2/pyridine (3:1, 40 mL) was cooled to 0 °C. Subsequently, trichloromethyl chloroformate (diphosgene; 45 µL; 0.378 mmol) in CH_2Cl_2 (2 mL) was slowly added dropwise. When the addition was complete, stirring at 0 °C was continued for 2.5 h, when TLC (toluene/ethyl acetate, 4:1) suggested complete conversion to a product of higher chromatographic mobility. The reaction mixture was treated with water (1 mL) and allowed to warm to r.t. The volatile components were evaporated *in vacuo*, followed by co-evaporation of residual pyridine with toluene. The crude product was dissolved in CH_2Cl_2 (80 mL) and washed with sat. $NaHCO_3$ (20 mL) and water (20 mL). Drying (Na_2SO_4), filtration and evaporation gave a crude product, which was purified by flash column chromatography (SiO_2, toluene/ethyl acetate, 7:1) to give spirocarbonate **41** (200 mg; 93%) as a colorless solid. An analytical sample was recrystallized from *n*-hexane/ethyl acetate (1:1). Single crystals for X-ray structural analysis were obtained from *n*-pentane/acetone-D_6.

M.p. 142–143 °C (*n*-hexane/ethyl acetate); $R_f = 0.62$ (toluene/ ethyl acetate, 4:1); $[\alpha]_D^{20}$ −77.3 (c = 1, $CHCl_3$); ^{1}H NMR (400.2 MHz, acetone-D_6) δ: 7.46–7.19 (m, 20H, H_{Ar}), 6.24 (ddd, 1H, $J_{7,8}$ = 11.1, $J_{8,9b}$ = 5.9, $J_{8,9a}$ = 4.9 Hz, H-8), 5.89 (d, 1H, $J_{7,8}$ = 11.1 Hz, H-7), 4.92–4.84 (m, 2H, CH_2Ph), 4.79–4.59 (m, 8H, CH_2Ph, H-1, H-9a), 4.54 (dd, 1H, $J_{9a,9b}$ = 14.1, $J_{8,9b}$ = 6.2 Hz, H-9a), 4.13 (dd, 1H, $J_{3,4}$ = 9.5, $J_{4,5}$ = 9.5 Hz, H-4), 3.90 (d, 1H, $J_{3,4}$ = 9.3 Hz, H-3), 3.86–3.77 (m, 2H, H-6a, H-6b), 3.63 (ddd, 1H, $J_{4,5}$ = 9.9, $J_{5,6a}$ = 4.9, $J_{5,6b}$ = 2.1 Hz, H-5); ^{13}C NMR (100.6 MHz, acetone-D_6) δ: 153.4 (OC(=O)O), 139.9, 139.6, 139.3, 138.6 (4 × $C_{Ar,q.}$), 131.3 (C-7), 129.1–129.0 (C_{Ar}), 128.9 (C-8), 128.8–128.2 (C_{Ar}), 100.4 (C-1), 89.2 (C-2), 85.4 (C-3), 76.8 (C-5), 76.4 (CH$_2$Ph), 75.9 (C-4), 75.6 (CH$_2$Ph), 73.9 (CH$_2$Ph), 71.2 (CH$_2$Ph), 70.0 (C-6), 64.2 (C-9); HR-ESI-TOF calcd. for $C_{38}H_{38}O_8Na$ [M+Na]$^+$: 645.2459. Found: 645.2467; Anal. calcd. for $C_{38}H_{38}O_8$: C, 73.29; H, 6.15. Found: C, 73.08; H, 6.21.

Benzyl 3,4,6-tri-*O*-benzyl-2-*C*-{(*Z*)-3-chloroprop-1-en-1-yl}-β-D-mannopyranoside (42):

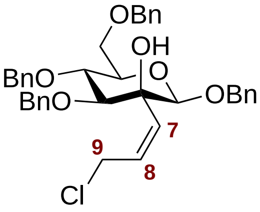

In a procedure similar to the synthesis of spirocarbonate **41** above, diol **36** (100 mg; 0.168 mmol) in anhydrous pyridine (20 mL) was treated with neat trichloromethyl chloroformate (22 µL; 0.184 mmol) at 0 °C. After a reaction time of 1 h at 0 °C, workup and chromatography as described above provided allyl chloride **42** (2 mg; 2%) as a side product with higher chromatographic mobility, together with spirocarbonate **41** (103 mg; 94%).

R$_f$ = 0.73 (toluene/ethyl acetate, 4:1); $[\alpha]_D^{20}$ −35.5 (c = 0.27, CHCl$_3$); ^{1}H NMR (600.1 MHz, acetone-D_6) δ: 7.43–7.21 (m, 20H, H$_{Ar}$), 5.75 (ddd, 1H, $J_{7,8}$ = 11.8, $J_{8,9a}$ = 6.8, $J_{8,9b}$ = 6.8 Hz, H-8), 5.89 (d, 1H, $J_{7,8}$ = 11.1 Hz, H-7), 5.53 (ddd, 1H, $J_{7,8}$ = 11.6, $^4J_{7,9ab}$ = 1.3, 1.3 Hz, H-7), 4.87 (d, 1H, J_{gem} = 12.1 Hz, CH$_2$Ph), 4.83–4.72 (m, 4H, H-9a, CH$_2$Ph), 4.68–4.58 (m, 5H, CH$_2$Ph, H-1), 4.50 (ddd, 1H, $J_{9a,9b}$ = 12.3, $J_{8,9b}$ = 6.8, $^4J_{7,9b}$ = 1.3 Hz, H-9b), 3.92 (dd, 1H, $J_{3,4}$ = 9.4, $J_{4,5}$ = 9.4 Hz, H-4), 3.83 (dd, 1H, $J_{6a,6b}$ = 11.0, $J_{5,6a}$ = 2.0 Hz, H-6a), 3.80–3.75 (m, 2H, H-6b, OH), 3.60 (d, 1H, $J_{3,4}$ = 9.2 Hz, H-3), 3.57 (ddd, 1H, $J_{4,5}$ = 9.8, $J_{5,6b}$ = 5.1, $J_{5,6a}$ = 1.8 Hz, H-5); ^{13}C NMR (150.9 MHz, acetone-D_6) δ: 139.9, 139.7, 139.7, 138.7 (4 × C$_{Ar,q.}$), 132.6 (C-7), 132.1 (C-8), 129.1–128.2 (C$_{Ar}$), 101.9 (C-1), 85.8 (C-3), 79.3 (C-2), 76.9 (C-4), 76.4 (CH$_2$Ph), 76.3 (C-5), 75.4 (CH$_2$Ph), 73.8 (CH$_2$Ph), 71.2 (CH$_2$Ph), 70.2 (C-6), 42.7 (C-9); HR-ESI-TOF calcd. for $C_{37}H_{39}ClO_6Na$ [M+Na]$^+$: 637.2327. Found: 637.2327.

Benzyl 3,4,6-tri-*O*-benzyl-2-*C*-{(1*S*,2*S*)-1,2,3-trihydroxyprop-1-yl}-β-D-mannopyranoside [(7*S*,8*S*)-43]:

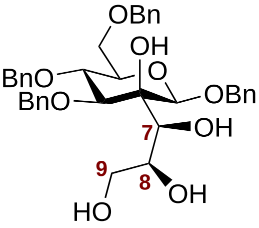

From 36: Alkene **36** (406 mg; 0.68 mmol) in a mixture of *t*-BuOH (10 mL), MeCN (1 mL) and H_2O (1 mL) was treated with citric acid (261 mg; 1.36 mmol) and NMO (159 mg; 1.36 mmol). The solution was slightly heated to 27 °C. OsO_4 1% aqueous solution (150 µL; 0.9 mol%) was added, and the mixture was stirred at 27 °C for 3 d. TLC control (toluene/ethyl acetate, 1:1) showed reluctant further progression after this time, and additional H_2O (1 mL) and OsO_4 (100 µL; 0.6 mol%) was added. Stirring was continued for 3 d. Next, $Na_2S_2O_3$ (100 mg) was added, and the solution was stirred for 60 min, diluted with brine and sat. $NaHCO_3$ (1:1, 30 mL), extracted with CH_2Cl_2 (3 × 50 mL), dried (Na_2SO_4), filtered and evaporated to dryness. The crude residue was purified by flash column chromatography (SiO_2, chloroform/acetonitrile, 6:1 to 4:1) to give a mixture of *syn*-diols **(7*S*,8*S*)-43** and **(7*R*,8*R*)-44** (381 mg; 89%; d.r. ≈ 6.6:1) as a colorless solid. Of this mixture of isomers, 262 mg (69% of total material) was subjected to fractional crystallization from *n*-hexane/$CHCl_3$ (ca. 1:1). The major isomer **(7*S*,8*S*)-43** was obtained from the mother liquor collected after typically 18 h at r.t. Repeated analogous crystallizations of the precipitated fractions and collection of the mother liquor (NMR analysis for confirmation of purity) provided pure **(7*S*,8*S*)-43** (184 mg; 65% from **36**, based on crystallized material fraction).

From (7*S*,8*S*)-45: Tribenzoate **(7*S*,8*S*)-45** (528 mg; 0.56 mmol) in MeOH (18 mL) was dropwise treated with NaOMe (150 µL; 30% in MeOH) at r.t. After 14 h, TLC reaction control (toluene/ethyl acetate, 4:1) confirmed complete conversion of the starting material. The solution was neutralized by the addition of Dowex H^+ ion exchange resin, filtered, and evaporated *in vacuo* to give a crude oil. Purification by flash column chromatography (SiO_2, chloroform/acetonitrile, 4:1) provided **(7*S*,8*S*)-43** (322 mg; 91%) as a colorless solid. An analytical sample was recrystallized from *n*-hexane/$CHCl_3$.

M.p. 140–141 °C (*n*-hexane/$CHCl_3$). $R_f = 0.48$ (toluene/ethyl acetate, 1:1); $[\alpha]_D^{20}$ −9.9 (c = 1, $CHCl_3$); ^1H NMR (400.2 MHz, CD_3OD) δ: 7.45–7.40 (m, 2H, H_{Ar}), 7.40–7.24 (m, 16H, H_{Ar}), 7.20–7.16 (m, 2H, H_{Ar}), 4.95–4.89 (m, 2H, CH_2Ph), 4.85 (s, 1H, H-1), 4.81 (d, 1H, J_{gem} = 11.0 Hz, CH_2Ph), 4.74 (d, 1H, J_{gem} = 11.1 Hz, CH_2Ph), 4.68 (d, 1H, J_{gem} = 11.6 Hz, CH_2Ph), 4.63–4.53 (m, 3H, CH_2Ph), 4.28–4.21 (m, 1H, H-8), 4.02 (d, 1H, $J_{7,8}$ = 9.4 Hz, H-7), 3.89 (d, 1H, $J_{3,4}$ = 9.4 Hz, H-3), 3.84 (dd, 1H, $J_{3,4}$ = 9.4, $J_{4,5}$ = 9.4 Hz, H-4), 3.79–3.68 (m, 3H, H-6a, H-6b, H-9a), 3.61 (dd, 1H, $J_{9a,9b}$ = 11.4, $J_{8,9b}$ = 5.0 Hz, H-9b), 3.50–3.43 (m, 1H, H-5); ^{13}C NMR (100.6 MHz, CD_3OD) δ: 139.9, 139.6, 139.5, 138.9 (4 × $C_{Ar,q.}$), 129.4–128.6 (C_{Ar}), 101.1 (C-1), 83.3 (C-3), 80.3 (C-2), 78.0 (C-4), 77.0 (CH_2Ph), 76.2 (C-5), 75.8 (CH_2Ph), 74.6 (C-8), 74.5 (CH_2Ph), 72.0 (CH_2Ph), 70.4 (C-6), 69.1 (C-7), 65.7 (C-9); HR-ESI-TOF calcd. for $C_{37}H_{42}O_9Na$

$[M+Na]^+$: 653.2721. Found: 653.2725; Anal. calcd. for $C_{37}H_{42}O_9$: C, 70.46; H, 6.71. Found: C, 70.17; H, 6.90.

Benzyl 3,4,6-tri-*O*-benzyl-2-*C*-{(1*R*,2*R*)-1,2,3-trihydroxyprop-1-yl}-β-D-mannopyranoside [(7*R*,8*R*)-44]:

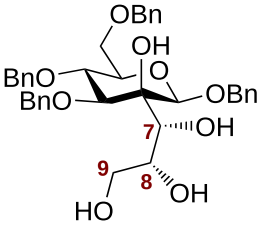

To tribenzoate **(7*R*,8*R*)-46** (270 mg; 0.29 mmol) in MeOH (10 mL) was dropwise added NaOMe (100 µL; 30% in MeOH) at r.t. After 16 h TLC (toluene/ethyl acetate, 4:1) confirmed complete conversion of the starting material. Neutralization with Dowex H^+ ion exchange resin, filtration and evaporation of the volatile parts *in vacuo* gave a crude oil. Purification by flash column chromatography (SiO_2, chloroform/acetonitrile, 4:1) gave minor tetrol **(7*R*,8*R*)-44** (160 mg; 89%) in the form of a colorless solid. An analytical sample was recrystallized from *n*-hexane/$CHCl_3$.

M.p. 152 °C (*n*-hexane/$CHCl_3$). $R_f = 0.46$ (toluene/ethyl acetate, 1:1); $[\alpha]_D^{20}$ −38.1 (c = 1, $CHCl_3$); ^1H NMR (600.1 MHz, CD_3OD) δ: 7.44–7.41 (m, 2H, H_{Ar}), 7.40–7.36 (m, 2H, H_{Ar}), 7.36–7.22 (m, 14H, H_{Ar}), 7.17–7.13 (m, 2H, H_{Ar}), 4.94–4.90 (m, 2H, CH_2Ph), 4.83 (d, 1H, $J_{gem} = 11.4$ Hz, CH_2Ph), 4.75 (s, 1H, H-1), 4.73 (d, 1H, $J_{gem} = 11.0$ Hz, CH_2Ph), 4.67 (d, 1H, $J_{gem} = 11.5$ Hz, CH_2Ph), 4.63 (d, 1H, $J_{gem} = 12.0$ Hz, CH_2Ph), 4.59–4.55 (m, 2H, CH_2Ph), 4.06 (d, 1H, $J_{3,4} = 9.4$ Hz, H-3), 4.01–3.96 (m, 2H, H-7, H-8), 3.94 (dd, 1H, $J_{3,4} = 9.7$, $J_{4,5} = 9.7$ Hz, H-4), 3.78 (dd, 1H, $J_{6a,6b} = 10.9$, $J_{5,6a} = 2.1$ Hz, H-6a), 3.76–3.70 (m, 2H, H-6b, H-9a), 3.62–3.58 (m, 1H, H-9b), 3.47 (ddd, 1H, $J_{4,5} = 9.7$, $J_{5,6b} = 5.4$, $J_{5,6a} = 2.1$ Hz, H-5); ^{13}C NMR (150.9 MHz, CD_3OD) δ: 140.0, 139.6, 139.5, 138.9 (4 × $C_{Ar,q.}$), 129.4–128.4 (C_{Ar}), 101.7 (C-1), 82.6 (C-3), 79.3 (C-2), 78.8 (C-4), 76.3 (C-5), 75.9 (CH_2Ph), 75.7 (CH_2Ph), 74.5 (C-8), 74.5 (CH_2Ph), 72.1 (CH_2Ph), 70.3 (C-6), 70.1 (C-7), 65.7 (C-9); HR-ESI-TOF calcd. for $C_{37}H_{42}O_9Na$ $[M+Na]^+$: 653.2721. Found: 653.2733; Anal. calcd. for $C_{37}H_{42}O_9$: C, 70.46; H, 6.71. Found: C, 70.23; H, 6.70.

Benzyl 3,4,6-tri-*O*-benzyl-2-*C*-{(1*S*,2*S*)-1,2,3-tribenzoyloxyprop-1-yl}-β-D-mannopyranoside [(7*S*,8*S*)-45]:

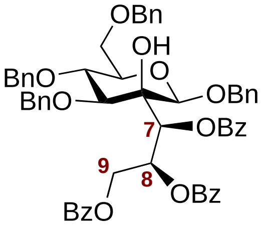

Alkene **36** (449 mg; 0.75 mmol) was subjected to the osmium-based dihydroxylation as reported above on page 219 to give crude **(7*S*,8*S*)-43** and **(7*R*,8*R*)-44**. After flash column chromatographic purification (SiO_2, chloroform/acetonitrile, 6:1 to 4:1) the mixture of isomers (466 mg; 0.74 mmol) was dissolved in anhydrous pyridine (7 mL) and cooled to 0 °C. The solution was dropwise treated with benzoyl chloride (562 µL; 4.88 mmol), stirred for 5 min, and allowed to warm to r.t. Subsequently, the reaction mixture was heated to 75 °C for 15 h. More benzoyl chloride (100 µL; 0.87 mmol) was added, and the temperature was elevated to 85 °C for 7 h. Next, MeOH (3 mL) was slowly added dropwise at r.t., and the reaction mixture was stirred for 15 min. Evaporation of the volatile parts, followed by co-evaporation of residual pyridine with toluene (10 mL), gave a crude product. Flash column chromatography (SiO_2, toluene/ethyl acetate, 24:1 to 18:1) gave major tribenzoate **(7*S*,8*S*)-45** (448 mg; 63%, 2 steps) and minor tribenzoate **(7*R*,8*R*)-46** (110 mg; 16%, 2 steps), both as a colorless foam. Analytical data for major **(7*S*,8*S*)-45**:

$R_f = 0.64$ (toluene/ethyl acetate, 4:1); $[\alpha]_D^{20}$ −70.9 (c = 1, $CHCl_3$); ^{1}H NMR (400.2 MHz, acetone-D_6) δ: 8.02–7.98 (m, 2H, H_{Ar}), 7.86–7.80 (m, 4H, H_{Ar}), 7.63–7.24 (m, 29H, H_{Ar}), 6.50–6.45 (m, 1H, H-8), 6.28 (d, 1H, $J_{7,8}$ = 4.0 Hz, H-7), 5.03 (d, 1H, J_{gem} = 11.6 Hz, CH_2Ph), 4.99–4.88 (m, 4H, H-1, H-9a, CH_2Ph), 4.82–4.77 (m, 2H, CH_2Ph), 4.72–4.65 (m, 2H, CH_2Ph), 4.62 (d, 1H, J_{gem} = 12.2 Hz, CH_2Ph), 4.48 (dd, 1H, $J_{9a,9b}$ = 12.1, $J_{8,9b}$ = 5.9 Hz, H-9b), 4.21 (s, 1H, OH), 4.03 (dd, 1H, J_{vic} = 9.7, 9.2 Hz, H-4), 3.86 (dd, 1H, $J_{6a,6b}$ = 11.1, $J_{5,6a}$ = 2.1 Hz, H-6a), 3.80 (dd, 1H, $J_{6a,6b}$ = 11.1, $J_{5,6b}$ = 5.4 Hz, H-6b), 3.68–3.59 (m, 2H, H-3, H-5); ^{13}C NMR (100.6 MHz, acetone-D_6) δ: 166.5, 166.3, 166.1 (3 × benzoyl C=O), 139.8, 139.6, 139.5, 137.7 (4 × $C_{Ar,q.}$), 134.4, 133.9, 133.8 (C_{Ar}), 131.4–128.2 (C_{Ar}, $C_{Ar,q.}$), 99.2 (C-1), 82.3 (C-3), 78.5 (C-4), 77.0 (C-2), 76.1 (CH_2Ph), 76.0 (C-5), 75.2 (CH_2Ph), 73.8 (CH_2Ph), 73.5 (C-7), 72.4 (C-8), 70.6 (CH_2Ph), 70.0 (C-6), 64.1 (C-9); HR-ESI-TOF calcd. for $C_{58}H_{54}O_{12}Na$ $[M+Na]^+$: 965.3508. Found: 965.3506; Anal. calcd. for $C_{58}H_{54}O_{12}$: C, 73.87; H, 5.77. Found: C, 73.99; H, 5.85.

Benzyl 3,4,6-tri-*O*-benzyl-2-*C*-{(1*R*,2*R*)-1,2,3-tribenzoyloxyprop-1-yl}-β-D-mannopyranoside [(7*R*,8*R*)-46]:

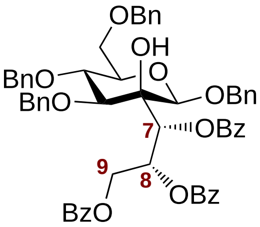

Isolated as the minor component (110 mg; 16%, 2 steps) as a colorless foam from the benzoylation of **(7*S*,8*S*)-43** and **(7*R*,8*R*)-44** as described above.

$R_f = 0.69$ (toluene/ethyl acetate, 4:1); $[\alpha]_D^{20}$ 41.8 (c = 1, $CHCl_3$); ^{1}H NMR (400.2 MHz, acetone-D_6) δ: 8.12–8.06 (m, 2H, H_{Ar}), 8.01–7.95 (m, 2H, H_{Ar}), 7.86–7.81 (m, 2H, H_{Ar}), 7.66–7.44 (m, 9H, H_{Ar}), 7.43–7.18 (m, 20H, H_{Ar}), 6.53 (ddd, 1H, $J_{7,8} = 5.6$, $J_{8,9b} = 5.6$, $J_{8,9a} = 2.7$ Hz, H-8), 6.31 (d, 1H, $J_{7,8} = 5.6$ Hz, H-7), 5.16 (d, 1H, $J_{gem} = 11.6$ Hz, CH_2Ph), 5.03 (d, 1H, $J_{gem} = 11.6$ Hz, CH_2Ph), 4.99 (d, 1H, $J_{gem} = 11.0$ Hz, CH_2Ph), 4.95–4.88 (m, 2H, H-9a, H-1), 4.82–4.72 (m, 2H, CH_2Ph), 4.70–4.63 (m, 2H, CH_2Ph), 4.59 (d, 1H, $J_{gem} = 12.2$ Hz, CH_2Ph), 4.48 (dd, 1H, $J_{9a,9b} = 12.2$, $J_{8,9b} = 5.6$ Hz, H-9b), 4.19 (dd, 1H, $J_{3,4} = 9.2$, $J_{4,5} = 9.2$ Hz, H-4), 4.07 (d, 1H, $J_{3,4} = 8.9$ Hz, H-3), 4.02 (s, 1H, OH), 3.86–3.78 (m, 2H, H-6a, H-6b), 3.68–3.62 (m, 1H, H-5); ^{13}C NMR (100.6 MHz, acetone-D_6) δ: 166.4, 166.2, 165.9 (3 × benzoyl C=O), 139.7, 139.5, 139.4, 138.5 (4 × $C_{Ar,q.}$), 134.3–128.0 (C_{Ar}, $C_{Ar,q.}$), 100.5 (C-1), 82.5 (C-3), 77.9 (C-4), 77.6 (C-2), 76.0 (C-5), 75.4 (CH_2Ph), 75.1 (CH_2Ph), 73.7 (CH_2Ph), 73.0 (C-7), 72.3 (C-8), 71.9 (CH_2Ph), 69.9 (C-6), 64.2 (C-9); HR-ESI-TOF calcd. for $C_{58}H_{54}O_{12}Na$ $[M+Na]^+$: 965.3508. Found: 965.3509; Anal. calcd. for $C_{58}H_{54}O_{12}$: C, 73.87; H, 5.77. Found C, 73.60; H, 6.08.

Benzyl 3,4,6-tri-*O*-benzyl-2-*C*-{(1*S*,2*S*)-3-[(1*S*,4*R*)-3-oxo-4,7,7-trimethyl-2-oxabicyclo[2.2.1]heptane-1-carbonyl]oxy-1,2-dihydroxyprop-1-yl}-β-D-mannopyranoside [(7*S*,8*S*)-47]:

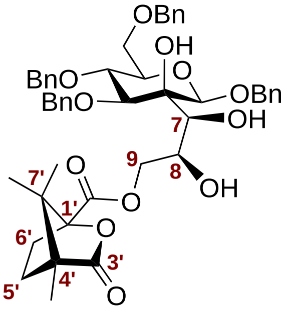

A mixture of *syn*-tetrols **(7*S*,8*S*)-43** and **(7*R*,8*R*)-44** (154 mg; 0.244 mmol; d.r. ≈ 6.6:1), as obtained from the osmium-based dihydroxylation reported on page 219 after chromatography, was dissolved in anhydrous CH_2Cl_2 (10 mL). Next, *i*-Pr_2NEt (83 µL; 0.488 mmol) was added at −20 °C, followed by the dropwise addition of (–)-(1*S*,4*R*)-

camphanoyl chloride (53 mg; 0.244 mmol) in CH_2Cl_2 (2 mL). The solution was stirred for 3 h at 0 °C, when TLC reaction control (toluene/ethyl acetate, 4:1) indicated complete consumption of the starting materials and the formation of multiple products. The reaction mixture was evaporated to dryness *in vacuo*. Multiple successive chromatographic purification steps (spherical SiO_2, toluene/ethyl acetate, 5:1 to 4:1, and: chloroform/acetonitrile, 30:1 to 18:1) provided major primary camphanate **(7*S*,8*S*)-47** (107 mg; 52%) as a colorless solid. Single crystals for X-ray structural analysis were grown from diethyl ether/acetonitrile.

$R_f = 0.16$ (toluene/ethyl acetate, 4:1); $[\alpha]_D^{20}$ −14.3 (c = 1, $CHCl_3$); ^{1}H NMR (400.2 MHz, acetone-D_6) δ: 7.47–7.38 (m, 6H, H_{Ar}), 7.40–7.22 (m, 14H, H_{Ar}), 5.03 (d, 1H, $J_{gem} = 11.5$ Hz, CH_2Ph), 4.98–4.92 (m, 2H, CH_2Ph, H-1), 4.87 (d, $J_{gem} = 11.5$ Hz, CH_2Ph), 4.79 (d, $J_{gem} = 11.1$ Hz, CH_2Ph), 4.73–4.53 (m, 8H, CH_2Ph, 3 × OH, H-8), 4.48 (dd, 1H, $J_{9a,9b} = 11.5$, $J_{8,9a} = 2.6$ Hz, H-9a), 4.29 (dd, 1H, $J_{9a,9b} = 11.5$, $J_{8,9b} = 4.7$ Hz, H-9b), 4.19–4.13 (m, 1H, H-7), 4.02–3.94 (m, 2H, H-3, H-4), 3.85 (dd, 1H, $J_{6a,6b} = 11.0$, $J_{5,6a} = 2.2$ Hz, H-6a), 3.78 (dd, 1H, $J_{6a,6b} = 11.0$, $J_{5,6a} = 5.3$ Hz, H-6b), 3.60–3.53 (m, 1H, H-5), 2.35–2.27 (m, 1H, H-6'a), 1.86–1.72 (m, 2H, H-6'b, H-5'a), 1.46 (ddd, 1H, $J_{gem} = 14.2$, $J_{vic} = 10.2$, 5.0 Hz, H-5'b), 0.99 (s, 3H, C-4'-CH_3), 0.96 (s, 3H, C(CH_3)(CH_3)), 0.84 (s, 3H, C(CH_3)(CH_3)); ^{13}C NMR (100.6 MHz, acetone-D_6) δ: 178.5 (C-3'=O), 167.9 ((C-1')-*C*=O), 140.1, 139.9, 139.7, 138.9 (4 × $C_{Ar,q.}$), 129.1–128.0 (C_{Ar}), 100.6 (C-1), 92.0 (C-1'), 82.7 (C-3), 79.8 (C-2), 77.8 (C-4), 76.3 (C-5), 75.8 (CH_2Ph), 75.2 (CH_2Ph), 73.8 (CH_2Ph), 72.2 (C-8), 71.2 (CH_2Ph), 70.3 (C-6), 68.8 (C-7), 67.9 (C-9), 55.2 (C-7'), 54.6 (C-4'), 31.2 (C-6'), 29.6 (C-5'), 17.1 (C(*C*H_3)(CH_3)), 16.9 (C(CH_3)(*C*H_3)), 9.9 (C-4'-*C*H_3); HR-ESI-TOF calcd. for $C_{47}H_{54}O_{12}Na$ $[M+Na]^+$: 833.3508. Found: 833.3505; Anal. calcd. for $C_{47}H_{54}O_{12}$: C, 69.61; H, 6.71. Found: C, 69.55; H, 6.79.

(2*S*,2'*R*/*S*,3'*R*,4'*S*)-1,3,4,6-Tetra-*O*-benzyl-2',3',4'-trihydroxyspiro[2-deoxy-β-D-mannopyranose-2,5'-tetrahydrofuran] (α,β-48):

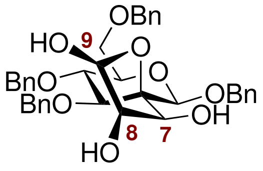

α-48
side chain: α-D-*ribo*

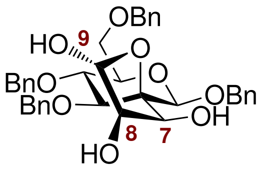

β-48
side chain: β-D-*ribo*

To major tetrol **(7*S*,8*S*)-43** (139 mg; 0.220 mmol) in anhydrous EtOAc/toluene (2:1, 36 mL) was added 3-(*N*-morpholino)propanesulfonic acid (MOPS; 554 mg; 2.64 mmol) and the suspension was stirred vigorously. The mixture was cooled to −50 °C, and

TEMPO 1 mg/mL in EtOAc (1.0 mL; 3 mol%) was added. Next, trichloroisocyanuric acid (TCICA) 10 mg/mL in EtOAc (4.4 mL; 0.187 mmol) was slowly added dropwise over 15 min. After complete addition, the pale yellow mixture was stirred for 1 h, allowed to warm to −35 °C, and stirred for 14 h at this temperature. TLC control (toluene/ethyl acetate, 1:1) showed major conversion, and Me_2S (44 µL; 0.60 mmol) in EtOAc (1 mL) was added dropwise, upon which the yellowish reaction mixture decolorized rapidly. Stirring of the suspension was continued for 15 min at −35 °C. After dilution with EtOAc (30 mL) and washing with brine/sat. $Na_2S_2O_3$ (10:1, 2 × 20 mL), the organic phase was dried (Na_2SO_4), filtered and evaporated *in vacuo* to give crude **48** (158 mg). Flash column chromatographic purification (spherical SiO_2, toluene/*n*-hexane/acetone, 8:8:5, + 0.25% Et_3N) gave **α,β-48** (84 mg; 61%; 72% brsm) as a colorless solid with higher chromatographic mobility, along with recovered **(7*S*,8*S*)-43** (21 mg). Solid **α,β-48** contained **α-48** as the major component (α/β ≈ 11.1:1 in acetone-D_6), and at r.t. in acetone-D_6, isomerization was observed, giving **β-48** as the major isomer after ca. 5–6 d (α/β ≈ 1:2.7). An analytical sample of **α,β-48** was recrystallized from Et_2O/CH_2Cl_2.

M.p. 162–164 °C (Et_2O/CH_2Cl_2, decomp.); $R_f = 0.60$ (toluene/ethyl acetate, 1:1); $[\alpha]_D^{20}$ −16.2 (α/β ≈ 2.7:1, c = 0.5, acetone-D_6), −13.8 (α/β ≈ 1:1.7, c = 0.5, acetone-D_6); selected signals for **α-48**: ^{1}H NMR (400.2 MHz, acetone-D_6) δ: 7.49–7.24 (m, 20H, H_{Ar}), 5.23 (dd, 1H, $J_{9,OH} = 11.5$, $J_{8,9} = 3.1$ Hz, H-9), 5.03 (d, 1H, $J_{gem} = 11.4$ Hz, CH_2Ph), 4.94 (d, 1H, $J_{gem} = 11.3$ Hz, CH_2Ph), 4.69 (H-1), 4.56 (H-7), 4.15 (d, 1H, $J_{7,OH} = 7.1$ Hz, C-7-OH), 3.94 (d, 1H, $J_{8,OH} = 10.8$ Hz, C-8-OH), 3.91–3.80 (m, 3H, H-4, H-6a, H-6b), 3.77–3.72 (m, 1H, H-8), 3.66 (d, 1H, $J_{3,4} = 9.4$ Hz, H-3), 3.57 (ddd, 1H, $J_{4,5} = 9.8$, $J_{5,6a} = 4.9$, $J_{5,6b} = 2.1$ Hz, H-5); ^{13}C NMR (100.6 MHz, acetone-D_6) δ: 139.8, 139.6, 139.6, 137.9 (4 × $C_{Ar,q.}$), 129.3–128.2 (C_{Ar}), 100.1 (C-1), 98.9 (C-9), 86.0 (C-2), 83.8 (C-3), 78.6 (C-4), 76.5 (CH_2Ph), 76.3 (C-5), 75.3 (CH_2Ph), 73.9 (CH_2Ph), 72.8 (C-7), 72.6 (C-8), 72.1 (CH_2Ph), 70.0 (C-6); selected signals for **β-48**: ^{1}H NMR (400.2 MHz, acetone-D_6) δ: 7.49–7.23 (m, 20H, H_{Ar}), 5.11 (d, 1H, $J_{gem} = 11.0$ Hz, CH_2Ph), 4.97–4.91 (m, 2H, H-9, CH_2Ph), 4.85–4.79 (m, 2H, CH_2Ph), 4.71 (H-1), 4.15 (d, 1H, $J = 8.3$ Hz, OH), 3.88 (H-4), 3.75 (d, 1H, $J_{3,4} = 9.5$ Hz, H-3), 3.61 (H-5, H-8); ^{13}C NMR (100.6 MHz, acetone-D_6) δ: 139.7, 139.5, 138.4, 137.7 (4 × $C_{Ar,q.}$), 129.5–128.2 (C_{Ar}), 103.6 (C-9), 99.9 (C-1), 87.2 (C-2), 82.0 (C-3), 78.6 (C-4), 77.3 (C-8), 77.2 (CH_2Ph), 76.2 (C-5), 75.3 (CH_2Ph), 73.9 (CH_2Ph), 72.1 (CH_2Ph), 71.6 (C-7), 69.9

(C-6); HR-ESI-TOF calcd. for $C_{37}H_{40}O_9Na$ $[M+Na]^+$: 651.2565. Found: 651.2563; Anal. calcd. for $C_{37}H_{40}O_9$: C, 70.68; H, 6.41. Found: C, 70.37; H, 6.61.

(2*S*,3'*S*,4'*S*)-1,3,4,6-Tetra-*O*-benzyl-3',4'-dihydroxyspiro[2-deoxy-β-D-mannopyranose-2,2'-tetrahydrofuran] [(7*S*,8*S*)-49]:

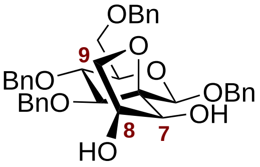

Isolated as a colorless solid in low yields (< 5%) from the synthesis of **α,β-48** as described above upon quenching with sat. $Na_2S_2O_5$ (2 mL) at −40 °C, aqueous workup (brine), and chromatography as described.

$R_f = 0.65$ (toluene/ethyl acetate, 1:1); $[\alpha]_D^{20}$ −15.7 (c = 0.5, $CHCl_3$); ^{1}H NMR (400.2 MHz, acetone-D_6) δ: 7.48–7.24 (m, 20H, H_{Ar}), 5.02 (d, 1H, $J_{gem} = 11.5$ Hz, CH_2Ph), 4.93 (d, 1H, $J_{gem} = 11.1$ Hz, CH_2Ph), 4.77 (d, 1H, $J_{gem} = 11.1$ Hz, CH_2Ph), 4.75–4.70 (m, 2H, CH_2Ph), 4.70–4.64 (m, 3H, H-1, CH_2Ph), 4.64–4.59 (m, 1H, CH_2Ph), 4.56–4.51 (m, 1H, H-7), 4.00–3.85 (m, 4H, H-8, H-9a, H-4, OH), 3.85–3.78 (m, 2H, H-6a, H-6b), 3.76–3.69 (m, 3H, H-9b, H-3, OH), 3.67 (d, 1H, $J_{3,4} = 9.3$ Hz, H-3), 3.56 (ddd, 1H, $J_{4,5} = 9.9$, $J_{5,6ab} = 4.8$, 2.2 Hz, H-5); ^{13}C NMR (100.6 MHz, acetone-D_6) δ: 139.8, 139.7, 139.6, 137.9 (4 × $C_{Ar,q.}$), 129.5–128.1 (C_{Ar}), 100.4 (C-1), 85.3 (C-2), 84.3 (C-3), 78.7 (C-4), 76.6 (CH_2Ph), 76.2 (C-5), 75.4 (C-9), 75.3 (CH_2Ph), 74.3 (C-7), 73.9 (CH_2Ph), 72.9 (C-8), 71.9 (CH_2Ph), 70.0 (C-6); HR-ESI-TOF calcd. for $C_{37}H_{40}O_8Na$ $[M+Na]^+$: 635.2615. Found: 635.2618.

4-*C*-Formyl-D-*erythro*-L-*talo*-octose (*syn*-50):

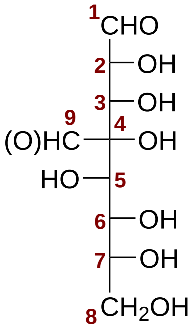

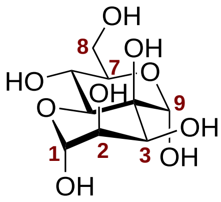

***syn*-50-A**
(49%)

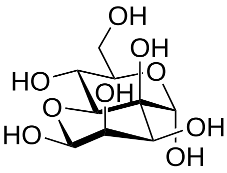

***syn*-50-B**
(37%)

A solution of **α,β-48** (64 mg; 0.102 mmol) in MeOH (6.5 mL) was treated with Pd 10% on activated charcoal (250 mg), and the suspension was stirred under an atmosphere of hydrogen for 4 d. TLC reaction control (chloroform/methanol, 2:1) showed complete conversion to a mixture of products without observable fluorescence quenching, and with low chromatographic mobility. The reaction mixture was diluted with MeOH (10 mL), filtered through a layer of Celite, and the filter pad was thoroughly rinsed with MeOH. The collected filtrate was evaporated to dryness to give a colorless oil. RP-chromatographic purification (RP-C18 silica gel, methanol/water, 1:1) gave, after partial evaporation and freeze-drying from residual water over several days, ***syn*-50** (27 mg; 99%) as a colorless foam. The compound was isolated as a mixture of isomers.

$R_f = 0.39$ (chloroform/methanol, 2:1); $[\alpha]_{\mathrm{D}}^{20}$ 10.6 (c = 0.5, H_2O); identified isomers: **(1*R*,9*S*)-4-*C*-formyl-D-*erythro*-L-*talo*-octo-1,5-pyranose-9,7-pyranose** (***syn*-50-A**, 49% isomeric contribution in D_2O), selected signals: ^{1}H NMR (700.3 MHz, D_2O) δ: 5.29 (d, 1H, $J_{1,2}$ = 1.2 Hz, H-1), 5.15 (s, 1H, H-9), 4.13 (d, 1H, $J_{5,6}$ = 8.7 Hz, H-5), 4.07 (d, 1H, $J_{2,3}$ = 3.4 Hz, H-3), 3.91 (dd, 1H, $J_{2,3}$ = 3.4, $J_{1,2}$ = 1.5 Hz, H-2), 3.90–3.82 (m, H-6, H-7), 3.79–3.75 (m, 2H, H-8a, H-8b); ^{13}C NMR (176.1 MHz, D_2O) δ: 95.4 (C-1), 93.0 (C-9), 75.8 (C-4), 73.2 (C-7), 71.7 (C-2), 70.9 (C-5), 65.5 (C-6), 64.7 (C-3), 61.5 (C-8); **(1*S*,9*S*)-4-*C*-formyl-D-*erythro*-L-*talo*-octo-1,5-pyranose-9,7-pyranose** (***syn*-50-B**, 37% isomeric contribution in D_2O), selected signals: ^{1}H NMR (700.3 MHz, D_2O) δ: 5.15 (s, 1H, H-9), 4.86 (d, 1H, $J_{1,2}$ = 0.7 Hz, H-1), 3.96 (dd, 1H, $J_{2,3}$ = 3.3, $J_{1,2}$ = 0.7 Hz, H-2), 3.93 (d, 1H, $J_{2,3}$ = 3.3 Hz, H-3), 3.90–3.82 (m, H-6, H-7, H-8a, H-8b), 3.58 (d, 1H, $J_{5,6}$ = 9.3 Hz, H-5); ^{13}C NMR (176.1 MHz, D_2O) δ: 94.7 (C-1), 93.2 (C-9), 75.7 (C-5), 74.7 (C-4), 73.0 (C-7), 72.4 (C-2), 68.1 (C-3), 65.6 (C-6), 61.5 (C-8); HR-ESI-TOF calcd. for $C_9H_{16}O_9Na$ $[M+Na]^+$: 291.0687. Found: 291.0688; HR-ESI-TOF calcd. for $C_9H_{15}O_9$ $[M-H]^-$: 267.0722. Found: 267.0726; Anal. calcd. for $C_9H_{16}O_9 \cdot H_2O$: C, 37.77; H, 6.34. Found: C, 37.64; H, 6.37.

(2*S*,2'*R*/*S*,3'*S*,4'*R*)-1,3,4,6-Tetra-*O*-benzyl-2',3',4'-trihydroxyspiro[2-deoxy-β-D-mannopyranose-2,5'-tetrahydrofuran] (α,β-51):

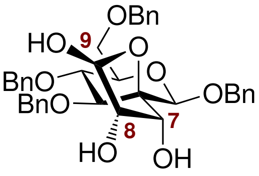

α-51

side chain: α-D-*lyxo*

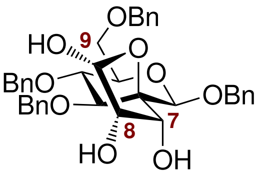

β-51

side chain: β-D-*lyxo*

To minor tetrol **(7*R*,8*R*)-44** (158 mg; 0.251 mmol) in anhydrous EtOAc/toluene (2:1, 40.5 mL) was added MOPS (629 mg; 3.01 mmol), and the vigorously stirred suspension was cooled to −50 °C. TEMPO 1 mg/mL in EtOAc (1.2 mL; 3 mol%) was added, followed by the dropwise addition of TCICA 10 mg/mL in EtOAc (5.0 mL; 0.213 mmol) over 15 min. The yellowish mixture was stirred for 15 h at −50 °C, after which time TLC control (toluene/ethyl acetate, 1:1) indicated major conversion. Me_2S (66 µL;

0.90 mmol) in EtOAc (1 mL) was added dropwise, and the decolorized reaction mixture was stirred for 15 min at −50 °C. Dilution with EtOAc (20 mL), washing with brine/sat. $Na_2S_2O_3$ (10:1, 2 × 20 mL), drying (Na_2SO_4), filtration and evaporation of the volatile parts gave crude **51** (158 mg). Purification by flash column chromatography (spherical SiO_2, toluene/*n*-hexane/acetone, 8:5:8, + 0.25% Et_3N) gave **α,β-51** (101 mg; 64%; 80% brsm) as a colorless solid with higher chromatographic mobility, alongside with recovered **(7*R*,8*R*)-44** (31 mg). The product **α,β-51** was initially isolated as a mixture with α/β ≈ 1.4:1 in acetone-D_6, and at r.t. in solution epimerization to α/β ≈ 1:1 was observable. An analytical sample was recrystallized from Et_2O/CH_2Cl_2.

M.p. 193 °C (Et_2O/CH_2Cl_2, decomp.); $R_f = 0.60$ (toluene/ethyl acetate, 1:1); $[\alpha]_D^{20}$ −42.4 (α/β ≈ 1:1, c = 0.5, acetone-D_6); selected signals for **α-51**: ^{1}H NMR (400.2 MHz, acetone-D_6) δ: 7.46–7.23 (m, 20H, H_{Ar}), 4.92 (H-9), 4.70 (H-1), 4.69 (H-7), 4.44–4.40 (m, 1H, C-7-OH), 4.20 (d, 1H, $J_{8,OH}$ = 11.9 Hz, C-8-OH), 4.05–3.92 (m, H-4, C-9-OH), 3.89–3.80 (m, H-6a, H-6b), 3.75 (H-3), 3.66–3.60 (m, 2H, H-5, H-8); ^{13}C NMR (150.9 MHz, acetone-D_6) δ: 138.9–137.0 ($C_{Ar,q.}$), 128.5–127.3 (C_{Ar}), 102.6 (C-9), 98.5 (C-1), 87.6 (C-2), 79.7 (C-3), 77.8 (C-4), 76.4 (C-8), 75.3 (C-5), 70.8 (C-7), 69.0 (C–6); selected signals for **β-51**: ^{1}H NMR (400.2 MHz, acetone-D_6) δ: 7.46–7.23 (m, 20H, H_{Ar}), 5.17–5.11 (m, 1H, H-9), 4.62 (H-1), 4.56 (C-9-OH), 4.53 (H-7), 4.05–3.92 (m, H-4), 3.89–3.80 (m, H-6a, H-6b), 3.78 (H-8), 3.75 (H-3), 3.57 (ddd, 1H, $J_{4,5}$ = 9.8, $J_{5,6a}$ = 4.3, $J_{5,6b}$ = 2.3 Hz, H-5); ^{13}C NMR (150.9 MHz, acetone-D_6) δ: 138.9–137.0 ($C_{Ar,q.}$), 128.5–127.3 (C_{Ar}), 100.6 (C-1), 97.9 (C-9), 86.4 (C-2), 80.3 (C-3), 77.9 (C-4), 75.2 (C-5), 71.9 (C-7), 71.8 (C-8), 69.0 (C-6); HR-ESI-TOF calcd. for $C_{37}H_{40}O_9Na$ $[M+Na]^+$: 651.2565. Found: 651.2565; Anal. calcd. for $C_{37}H_{40}O_9$: C, 70.68; H, 6.41. Found: C, 70.50; H, 6.47.

4-*C*-Formyl-D-*erythro*-L-*gulo*-octose (*syn*-52):

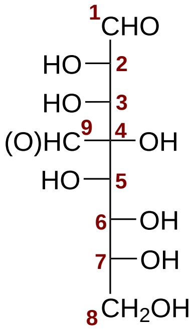

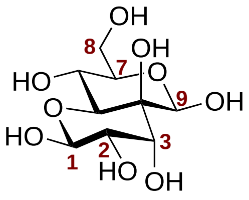

***syn*-52-A**
(66%)

To **α,β-51** (54 mg; 0.086 mmol) in MeOH (7.5 mL) was added Pd 10% on activated charcoal (211 mg), and the suspension was stirred under an atmosphere of hydrogen for 5 d. After this time, TLC (chloroform/methanol, 2:1) showed complete conversion to a mixture of products without detectable fluorescence quenching, and with low chromatographic mobility. The suspension was diluted with MeOH (10 mL), filtered through Celite, and the filter pad was thoroughly rinsed with MeOH. The obtained filtrate was evaporated to dryness *in vacuo* to give a colorless oil. RP-chromatographic purification (RP-C18 silica gel, methanol/water, 1:1) gave, after partial evaporation and freeze-drying from residual water, ***syn*-52** (23 mg; 99%) as a colorless foam. The compound was isolated as a mixture of isomers.

$R_f = 0.39$ (chloroform/methanol, 2:1); $[\alpha]_D^{20}$ −4.4 (c = 0.5, H_2O); identified isomer: **(1*S*,9*R*)-4-*C*-formyl-D-*erythro*-L-*gulo*-octo-1,5-pyranose-9,7-pyranose** (**syn-52-A**, 66% isomeric contribution in D_2O), selected signals: ^{1}H NMR (700.3 MHz, D_2O) δ: 4.99 (s, 1H, H-9), 4.86 (d, 1H, $J_{1,2}$ = 8.4 Hz, H-1), 3.97 (d, 1H, $J_{2,3}$ = 3.4 Hz, H-3), 3.91–3.88 (m, H-8a), 3.78 (d, 1H, $J_{5,6}$ = 9.7 Hz, H-5), 3.76–3.69 (m, 3H, H-8b, H-6, H-2), 3.44–3.40 (m, 1H, H-7); ^{13}C NMR (176.1 MHz, D_2O) δ: 95.1 (C-1), 93.9 (C-9), 77.0 (C-7), 75.6 (C-5), 74.0 (C-4), 70.6 (C-3), 70.1 (C-2), 65.7 (C-6), 61.4 (C-8); HR-ESI-TOF calcd. for $C_9H_{16}O_9Na$ $[M+Na]^+$: 291.0687. Found: 291.0685; HR-ESI-TOF calcd. for $C_9H_{15}O_9$ $[M–H]^-$: 267.0722. Found: 267.0724; Anal. calcd. for $C_9H_{16}O_9 \cdot 2H_2O$: C, 35.53; H, 6.63. Found: C, 35.69; H, 6.54.

Benzyl 3,4,6-tri-*O*-benzyl-2-*C*-{(2*S*,3*S*)-2-hydroxymethyloxiran-3-yl}-β-D-mannopyranoside [(7*S*,8*S*)-53]:

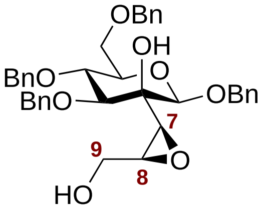

Alkene **36** (190 mg; 0.318 mmol) was dissolved in anhydrous CH_2Cl_2 (12 mL), and purified *m*-CPBA 100 mg/mL in CH_2Cl_2 (0.714 mL; 71.4 mg; 0.414 mmol) was slowly added dropwise at r.t. After 24 h, TLC (toluene/*n*-hexane/acetone, 1:1:1, + 0.5% Et_3N) suggested complete consumption of the substrate, and the reaction was quenched by the addition of sat. $Na_2S_2O_3$ (1 mL). After stirring for 15 min, the reaction mixture was diluted with CH_2Cl_2 (30 mL), and washed with sat. $NaHCO_3$ (2 × 10 mL) and water (10 mL). Drying of the organic layer (Na_2SO_4), filtration and evaporation of the volatile parts yielded the crude product as a mixture of diastereoisomers (d.r. ≈ 5:1). Purification by flash column chromatography (spherical SiO_2, toluene/*n*-hexane/acetone, 1:1:0.2 to 1:1:0.25, + 2% Et_3N) gave pure major epoxide **(7*S*,8*S*)-53** (140 mg; 72%) as a colorless oil, alongside with minor **(7*R*,8*R*)-57** (25 mg; 13%) with higher chromatographic mobility.

$R_f = 0.18$ (toluene/n-hexane/acetone, 2:2:1, + 0.5% Et_3N); $[\alpha]_D^{20}$ −37.2 (c = 1, $CHCl_3$); ^1H NMR (400.2 MHz, acetone-D_6) δ: 7.49–7.17 (m, 20H, H_{Ar}), 4.94–4.87 (m, 2H, CH_2Ph), 4.82–4.76 (m, 2H, CH_2Ph), 4.75–4.58 (m, 5H, H-1, CH_2Ph), 4.06–3.97 (m, H-9a, H-4), 3.87–3.75 (m, 3H, H-9b, H-6a, H-6b), 3.71 (d, 1H, $J_{3,4}$ = 9.3 Hz, H-3), 3.66–3.56 (m, 2H, H-5, OH), 3.29 (s, 1H, OH), 3.00 (ddd, 1H, $J_{8,9ab}$ = 7.3, 2.7, $J_{7,8}$ = 4.3 Hz, H-8), 2.94 (d, 1H, $J_{7,8}$ = 4.3 Hz, H-7); ^{13}C NMR (100.6 MHz, acetone-D_6) δ: 139.8, 139.6, 139.4, 138.9 (4 × $C_{Ar,q.}$), 129.1–128.2 (C_{Ar}), 102.6 (C-1), 82.7 (C-3), 77.1 (C-4), 76.3 (C-5), 76.2 (CH_2Ph), 75.5 (C-2), 75.4 (CH_2Ph), 73.8 (CH_2Ph), 71.0 (CH_2Ph), 70.1 (C-6), 61.5 (C-9), 58.2 (C-8), 57.9 (C-7); HR-ESI-TOF calcd. for $C_{37}H_{40}O_8Na$ $[M+Na]^+$: 635.2615. Found: 635.2615; Anal. calcd. for $C_{37}H_{40}O_8$: C, 72.53; H, 6.58. Found: C, 72.52; H, 6.75.

Benzyl 3,4,6-tri-*O*-benzyl-2-*C*-{(2*S*,3*S*)-2-acetoxymethyloxiran-3-yl}-β-D-mannopyranoside [(7*S*,8*S*)-54]:

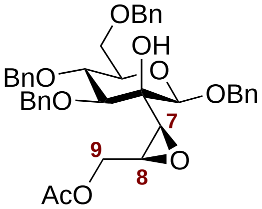

A solution of epoxyalcohol **(7*S*,8*S*)-53** (217 mg; 0.354 mmol) in anhydrous MeCN (20 mL) was treated with catalytic amounts of DMAP (8 mg) at 0 °C. Then, Et_3N in MeCN (1.48 mL; 50 µL/mL; 0.531 mmol) was added dropwise, followed by Ac_2O in MeCN (1.0 mL; 50 µL/mL; 0.531 mmol), and the mixture was slowly allowed to warm to r.t. After 20 h, TLC control (toluene/n-hexane/acetone, 1:1:1, + 0.5% Et_3N) indicated completion of the reaction, and the solution was neutralized by the addition of $NaHCO_3$ (300 mg), followed by stirring for 15 min. Dilution with CH_2Cl_2 (50 mL), washing with sat. $NaHCO_3$ (15 mL) and sat. NaCl (15 mL), drying (Na_2SO_4), filtration and evaporation of the solvents gave a colorless oil. Purification of the crude product by flash column chromatography (SiO_2, toluene/n-hexane/acetone, 1:1:0.2, + 2% Et_3N) yielded pure epoxyacetate **(7*S*,8*S*)-54** (222 mg; 96%) as a colorless oil.

$R_f = 0.76$ (toluene/n-hexane/acetone, 1:1:1, + 0.5% Et_3N); $[\alpha]_D^{20}$ −52.2 (c = 1, $CHCl_3$); ^1H NMR (400.2 MHz, acetone-D_6) δ: 7.48–7.19 (m, 20H, H_{Ar}), 4.96–4.88 (m, 2H, CH_2Ph), 4.85–4.75 (m, 2H, CH_2Ph), 4.75–4.63 (m, 4H, H-1, CH_2Ph), 4.60 (d, 1H, J_{gem} = 12.2 Hz, CH_2Ph), 4.54 (dd, 1H, $J_{9a,9b}$ = 13.0, $J_{8,9a}$ = 7.6 Hz, H-9a), 4.42 (dd, 1H, $J_{9a,9b}$ = 13.1, $J_{8,9b}$ = 1.8 Hz, H-9b), 4.02 (dd, 1H, $J_{3,4}$ = 9.5, $J_{4,5}$ = 9.5 Hz, H-4), 3.87–3.78 (m, 2H, H-6a, H-6b), 3.75 (d, 1H, $J_{3,4}$ = 9.4 Hz, H-3), 3.60 (ddd, 1H, $J_{4,5}$ = 9.7, $J_{5,6ab}$ = 4.7, 2.3 Hz, H-5), 3.40 (d, 1H, J = 1.2 Hz, OH), 3.06–2.98 (m, 2H, H-8, H-7), 1.94 (s, 3H, CH_3); ^{13}C NMR (100.6 MHz, acetone-D_6) δ: 170.7 (acetyl C=O), 139.8, 139.6, 139.2, 138.8 (4 × $C_{Ar,q.}$), 129.1–128.2 (C_{Ar}), 102.3 (C-1), 82.5 (C-3), 77.1 (C-4), 76.3 (C-5), 76.3 (CH_2Ph), 75.4 (CH_2Ph), 75.3 (C-2), 73.8 (CH_2Ph), 70.9 (CH_2Ph), 70.1 (C-6), 64.8 (C-9), 57.4 (C-7), 54.5 (C-8); HR-ESI-TOF calcd. for $C_{39}H_{42}O_9Na$ [M+Na]$^+$: 677.2721. Found: 677.2721; Anal. calcd. for $C_{39}H_{42}O_9$: C, 71.54; H, 6.47. Found: C, 71.34; H, 6.52.

(2*S*,3'*S*,4'*R*)-1,3,4,6-Tetra-*O*-benzyl-3',4'-bis(acetoxy)spiro[2-deoxy-β-D-mannopyranose-2,2'-tetrahydrofuran] [(7*S*,8*R*)-55]:

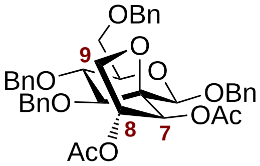

Epoxyacetate **(7*S*,8*S*)-54** (101 mg; 0.154 mmol) in 5 mL of degassed HOAc/Ac_2O (1:1, preheated at 75 °C for 18 h) was treated with TMSOAc (46 µL; 0.309 mmol), and the solution was heated to 105 °C for 19 h. TLC reaction control (toluene/*n*-hexane/acetone, 2:2:1, + 0.5% Et_3N) indicated complete conversion. The mixture was poured onto ice-cold sat. $NaHCO_3$ (30 mL), stirred for 15 min and diluted with CH_2Cl_2 (30 mL). After separation of the phases, the aqueous phase was extracted with CH_2Cl_2 (2 × 20 mL), and the combined organic extracts were washed with sat. $NaHCO_3$ and water (15 mL each). Drying (Na_2SO_4), filtration and evaporation of the solvents *in vacuo* gave a yellow oil. Flash column chromatography (SiO_2, toluene/*n*-hexane/acetone, 2:2:0.25 to 2:2:0.35) yielded spiro-tetrahydrofuran **(7*S*,8*R*)-55** (91 mg; 85%) as a colorless oil.

$R_f = 0.60$ (toluene/*n*-hexane/acetone, 2:2:1, + 0.5% Et_3N); $[\alpha]_D^{20}$ −40.4 (c = 1, $CHCl_3$); ^{1}H NMR (400.2 MHz, acetone-D_6) δ: 7.52–7.24 (m, 20H, H_{Ar}), 5.94 (d, 1H, $J_{7,8}$ = 6.2 Hz, H-7), 5.49 (ddd, 1H, $J_{8,9a}$ = 7.7, $J_{7,8}$ = 6.1, $J_{8,9b}$ = 6.1 Hz, H-8), 4.97 (d, 1H, J_{gem} = 10.8 Hz, CH_2Ph), 4.93–4.86 (m, 2H, CH_2Ph), 4.81 (d, 1H, J_{gem} = 11.1 Hz, CH_2Ph), 4.74 (d, 1H, J_{gem} = 11.6 Hz, CH_2Ph), 4.68–4.63 (m, 3H, H-1, CH_2Ph), 4.59 (d, 1H, J_{gem} = 12.1 Hz, CH_2Ph), 4.42 (dd, 1H, $J_{9a,9b}$ = 8.9, $J_{8,9a}$ = 7.7 Hz, H-9a), 3.87–3.74 (m, 3H, H-4, H-6a, H-6b), 3.69 (d, 1H, $J_{3,4}$ = 9.5 Hz, H-3), 3.64 (dd, 1H, $J_{9a,9b}$ = 8.9, $J_{8,9b}$ = 6.0 Hz, H-9b), 3.50 (ddd, 1H, $J_{4,5}$ = 9.8, $J_{5,6ab}$ = 5.0, 2.1 Hz, H-5), 2.03 (s, 3H, CH_3), 1.97 (s, 3H, CH_3); ^{13}C NMR (100.6 MHz, acetone-D_6) δ: 171.1, 170.9 (2 × acetyl C=O), 139.8, 139.8, 139.6, 138.6 (4 × $C_{Ar,q.}$), 129.2–128.2 (C_{Ar}), 101.0 (C-1), 85.1 (C-2), 81.8 (C-3), 78.2 (C-4), 78.0 (C-8), 76.5 (C-7), 76.2 (CH_2Ph), 76.0 (C-5), 75.3 (CH_2Ph), 73.8 (CH_2Ph), 71.8 (CH_2Ph), 71.4 (C-9), 70.0 (C-6), 20.8, 20.7 (2

× CH_3); HR-ESI-TOF calcd. for $C_{41}H_{44}O_{10}Na$ $[M+Na]^+$: 719.2827. Found: 719.2827; Anal. calcd. for $C_{41}H_{44}O_{10}$: C, 70.67; H, 6.37. Found: C, 70.45; H, 6.44.

(2*S*,3'*S*,4'*R*)-1,3,4,6-Tetra-*O*-benzyl-3',4'-dihydroxyspiro[2-deoxy-β-D-mannopyranose-2,2'-tetrahydrofuran] [(7*S*,8*R*)-56]:

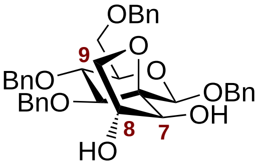

A solution of diacetate **(7*S*,8*R*)-55** (89 mg; 0.128 mmol) in MeOH (3 mL) was treated with cat. NaOMe (30 µL; 25% in MeOH). The mixture was stirred at r.t. for 1 h, when TLC (toluene/*n*-hexane/acetone, 2:2:1, + 0.5% Et_3N) indicated formation of a single product. Neutralization with Dowex H^+ ion exchange resin, filtration and evaporation yielded a colorless solid. Flash column chromatography (SiO_2, chloroform/acetonitrile, 4:1) gave diol **(7*S*,8*R*)-56** (73 mg; 93%) as a colorless solid.

$R_f = 0.28$ (toluene/*n*-hexane/acetone, 2:2:1, + 0.5% Et_3N); $[\alpha]_D^{20}$ −50.1 (c = 1, $CHCl_3$); ^1H NMR (400.2 MHz, acetone-D_6) δ: 7.50–7.22 (m, 20H, H_{Ar}), 5.00 (d, 1H, J_{gem} = 11.3 Hz, CH_2Ph), 4.89 (d, 1H, J_{gem} = 11.5 Hz, CH_2Ph), 4.81–4.74 (m, 2H, CH_2Ph), 4.72 (s, 1H, H-1), 4.69–4.51 (m, 5H, CH_2Ph, H-8), 4.46 (dd, 1H, $J_{7,8}$ = 6.4, $J_{7,OH}$ = 6.4 Hz, H-7), 4.39 (d, 1H, $J_{7,OH}$ = 6.4 Hz, OH), 4.18 (d, 1H, $J_{8,OH}$ = 5.4 Hz, OH), 4.06 (dd, 1H, $J_{8,9a}$ = 7.7, $J_{9a,9b}$ = 7.7 Hz, H-9a), 3.89–3.75 (m, 3H, H-4, H-6a, H-6b), 3.65 (d, 1H, $J_{3,4}$ = 9.5 Hz, H-3), 3.56 (dd, 1H, $J_{8,9b}$ = 7.8, $J_{9a,9b}$ = 7.8 Hz, H-9b), 3.50 (ddd, 1H, $J_{4,5}$ = 9.7, $J_{5,6ab}$ = 5.0, 2.1 Hz, H-5); ^{13}C NMR (100.6 MHz, acetone-D_6) δ: 139.8, 139.8, 139.7, 139.3 (4 × $C_{Ar,q.}$), 129.1–128.2 (C_{Ar}), 101.9 (C-1), 85.5 (C-2), 82.6 (C-3), 79.1 (C-7), 78.3 (C-4), 76.4 (C-8), 76.4 (CH_2Ph), 76.1 (C-5), 75.2 (CH_2Ph), 73.8 (CH_2Ph), 72.7 (C-9), 71.7 (CH_2Ph), 70.2 (C-6); HR-ESI-TOF calcd. for $C_{37}H_{40}O_8Na$ $[M+Na]^+$: 635.2615. Found: 635.2616; Anal. calcd. for $C_{37}H_{40}O_8$: C, 72.53; H, 6.58. Found: C, 72.56; H, 6.66.

Benzyl 3,4,6-tri-*O*-benzyl-2-*C*-{(2*R*,3*R*)-2-hydroxymethyloxiran-3-yl}-β-D-mannopyranoside [(7*R*,8*R*)-57]:

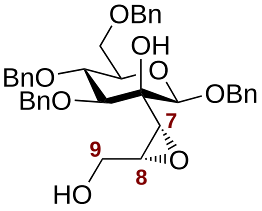

To alkene **36** (1.85 g; 3.10 mmol) in anhydrous benzene (115 mL) was added VO(acac)$_2$ (24 mg; 2.9 mol%) at r.t. The blue solution was treated with *t*-BuOOH (5.5 M in nonane; 620 µL; 3.41 mmol), upon which the solution turned deep red. The reaction mixture was stirred for 17 h at r.t., after which time TLC (toluene/*n*-hexane/acetone, 1:1:1, + 0.5% Et$_3$N) indicated complete conversion. The reaction was quenched by the addition of sat. Na$_2$S$_2$O$_3$ (5 mL) and stirred for 15 min. Dilution with toluene (300 mL), washing with water (3 × 100 mL), drying (Na$_2$SO$_4$), filtration and evaporation of the volatile components yielded the crude product as a mixture of diastereoisomers (d.r. ≈ 2.5:1). Purification by flash column chromatography (spherical SiO$_2$, toluene/*n*-hexane/acetone, 1:1:0.2 to 1:1:0.25, + 2% Et$_3$N) provided pure major epoxide **(7*R*,8*R*)-57** (1.1 g; 58%) as a colorless solid, together with minor **(7*S*,8*S*)-53** (342 mg; 18%) with lower chromatographic mobility. An analytical sample was crystallized from toluene/*n*-hexane/chloroform.

M.p. 119 °C (toluene/*n*-hexane/chloroform); $R_f = 0.22$ (toluene/*n*-hexane/acetone, 2:2:1, + 0.5% Et$_3$N); $[\alpha]_D^{20}$ −60.9 (c = 1, CHCl$_3$); ^{1}H NMR (400.2 MHz, acetone-D_6) δ: 7.48–7.22 (m, 20H, H$_{Ar}$), 4.96 (d, 1H, J_{gem} = 10.3 Hz, CH$_2$Ph), 4.89 (d, 1H, J_{gem} = 11.9 Hz, CH$_2$Ph), 4.80 (d, 1H, J_{gem} = 11.1 Hz, CH$_2$Ph), 4.77–4.71 (m, 2H, CH$_2$Ph, H-1), 4.70–4.56 (m, 4H, CH$_2$Ph), 3.99 (dd, 1H, $J_{9a,9b}$ = 13.0, $J_{8,9a}$ = 7.0 Hz, H-9a), 3.94–3.73 (m, 5H, H-9b, H-3, H6a, H-6b, H-4), 3.63 (bs, 1H, OH), 3.58 (ddd, 1H, $J_{4,5}$ = 9.7, $J_{5,6ab}$ = 5.3, 2.0 Hz, H-5), 3.34 (bs, 1H, OH), 3.10 (d, 1H, $J_{7,8}$ = 4.3 Hz, H-7), 3.08–3.03 (m, 1H, H-8); ^{13}C NMR (100.6 MHz, acetone-D_6) δ: 139.8, 139.8, 139.7, 138.5 (4 × C$_{Ar,q.}$), 129.2–128.2 (C$_{Ar}$), 100.1 (C-1), 87.2 (C-3), 76.9 (C-4), 76.3 (C-5), 75.7 (CH$_2$Ph), 75.5 (CH$_2$Ph), 74.7 (C-2), 73.8 (CH$_2$Ph), 71.3 (CH$_2$Ph), 70.2 (C-6), 61.4 (C-9), 59.2 (C-7), 58.9 (C-8); HR-ESI-TOF calcd. for C$_{37}$H$_{40}$O$_8$Na [M+Na]$^+$: 635.2615. Found: 635.2613; Anal. calcd. for C$_{37}$H$_{40}$O$_8$: C, 72.53; H, 6.58. Found: C, 72.40; H, 6.62.

Benzyl 3,4,6-tri-*O*-benzyl-2-*C*-{(2*R*,3*R*)-2-acetoxymethyloxiran-3-yl}-β-D-mannopyranoside [(7*R*,8*R*)-58]:

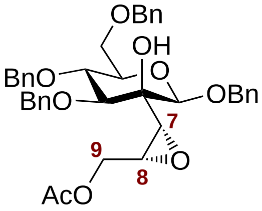

To epoxyalcohol **(7*R*,8*R*)-57** (186 mg; 0.304 mmol) in anhydrous MeCN (17 mL) was added a catalytic amount of DMAP (8 mg) at 0 °C. Next, Et$_3$N in MeCN (1.26 mL; 50 µL/mL; 0.456 mmol), followed by Ac$_2$O in MeCN (0.86 mL; 50 µL/mL; 0.456 mmol) was added dropwise, and the reaction mixture was allowed to warm to r.t. After 20 h, TLC (toluene/*n*-hexane/acetone, 1:1:1, + 0.5% Et_3N) indicated complete conversion, and the solution was neutralized by the addition of $NaHCO_3$ (300 mg) and was stirred for 15 min. Dilution with CH_2Cl_2 (50 mL), washing with sat. $NaHCO_3$ (15 mL) and brine (15 mL), drying (Na_2SO_4), filtration and evaporation of the volatile components gave a colorless oil. Purification of the crude product by flash column chromatography (SiO_2, toluene/*n*-hexane/acetone, 1:1:0.2, + 2% Et_3N) yielded pure epoxyacetate **(7*R*,8*R*)-58** (182 mg; 91%) as a colorless solid.

$R_f = 0.76$ (toluene/*n*-hexane/acetone, 1:1:1, + 0.5% Et_3N); $[\alpha]_D^{20}$ −30.8 (c = 1, $CHCl_3$); ^1H NMR (400.2 MHz, acetone-D_6) δ: 7.48–7.21 (m, 20H, H_{Ar}), 4.95 (d, 1H, J_{gem} = 10.4 Hz, CH_2Ph), 4.89 (d, 1H, J_{gem} = 12.0 Hz, CH_2Ph), 4.82–4.72 (m, 3H, CH_2Ph, H-1), 4.71–4.50 (m, 6H, CH_2Ph, H9a, H-9b), 3.89 (d, 1H, $J_{3,4}$ = 8.9 Hz, H-3), 3.86–3.74 (m, 3H, H-4, H6a, H-6b), 3.59 (ddd, 1H, $J_{4,5}$ = 9.7, $J_{5,6ab}$ = 5.1, 2.0 Hz, H-5), 3.44 (bs, 1H, OH), 3.17 (d, 1H, $J_{7,8}$ = 4.4 Hz, H-7), 3.16–3.11 (m, 1H, H-8), 2.00 (s, 3H, CH_3); ^{13}C NMR (100.6 MHz, acetone-D_6) δ: 170.8 (acetyl C=O), 139.8, 139.7, 139.5, 138.4 (4 × $C_{Ar,q.}$), 129.2–128.2 (C_{Ar}), 99.8 (C-1), 86.9 (C-3), 76.9 (C-4), 76.3 (C-5), 75.7 (CH_2Ph), 75.5 (CH_2Ph), 74.5 (C-2), 73.8 (CH_2Ph), 71.3 (CH_2Ph), 70.2 (C-6), 64.7 (C-9), 58.7 (C-7), 55.5 (C-8), 20.8 (CH_3); HR-ESI-TOF calcd. for $C_{39}H_{42}O_9Na$ $[M+Na]^+$: 677.2721. Found: 677.2727; Anal. calcd. for $C_{39}H_{42}O_9$: C, 71.54; H, 6.47. Found: C, 71.59; H, 6.54.

(2*S*,3'*R*,4'*S*)-1,3,4,6-Tetra-*O*-benzyl-3',4'-bis(acetoxy)spiro[2-deoxy-β-D-mannopyranose-2,2'-tetrahydrofuran] [(7*R*,8*S*)-59]:

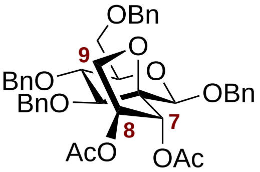

To epoxyacetate **(7*R*,8*R*)-58** (182 mg; 0.278 mmol) in 9 mL of degassed HOAc/Ac_2O (1:1, preheated at 75 °C for 18 h) was added TMSOAc (83 µL; 0.556 mmol) at r.t., and the solution was then heated to 105 °C for 20 h. TLC control (toluene/*n*-hexane/acetone, 2:2:1, + 0.5% Et_3N) indicated complete conversion. The mixture was poured onto ice-cold sat. $NaHCO_3$ (50 mL), stirred for 15 min and diluted with CH_2Cl_2 (50 mL). After separation of the phases, and extraction of the aqueous phase with CH_2Cl_2 (20 mL), the combined organic parts were washed with sat. $NaHCO_3$ (2 × 50 mL) and water (50 mL). The organic phases were dried (Na_2SO_4), filtered and evaporated *in vacuo* to give a yellow oil. Flash column chromatography (SiO_2, toluene/*n*-hexane/acetone, 2:2:0.20 to 2:2:0.25) yielded spirotetrahydrofuran **(7*R*,8*S*)-59** (143 mg; 72%) as a colorless oil.

$\mathrm{R_f} = 0.63$ (toluene/n-hexane/acetone, 2:2:1, + 0.5% $\mathrm{Et_3N}$); $[\alpha]_{\mathrm{D}}^{20}$ −3.4 (c = 1, $\mathrm{CHCl_3}$); ^{1}H NMR (400.2 MHz, acetone-D_6) δ: 7.50–7.23 (m, 20H, $\mathrm{H_{Ar}}$), 5.87 (d, 1H, $J_{7,8} = 6.9\,\mathrm{Hz}$, H-7), 5.54 (ddd, 1H, $J_{8,9\mathrm{a}} = 7.2$, $J_{8,9\mathrm{b}} = 7.2$, $J_{7,8} = 7.2\,\mathrm{Hz}$, H-8), 4.99–4.89 (m, 3H, $\mathrm{CH_2Ph}$), 4.78 (d, 1H, $J_{\mathrm{gem}} = 11.0\,\mathrm{Hz}$, $\mathrm{CH_2Ph}$), 4.73–4.63 (m, 4H, $\mathrm{CH_2Ph}$, H-1), 4.59 (d, 1H, $J_{\mathrm{gem}} = 12.1\,\mathrm{Hz}$, $\mathrm{CH_2Ph}$), 4.41–4.35 (m, 1H, H-9a), 3.95 (dd, 1H, $J_{3,4} = 9.7$, $J_{4,5} = 9.7\,\mathrm{Hz}$, H-4), 3.85–3.76 (m, 2H, H-6a, H-6b), 3.68–3.61 (m, 2H, H-3, H-9b), 3.50 (ddd, 1H, $J_{4,5} = 9.9$, $J_{5,6\mathrm{ab}} = 4.2, 2.7\,\mathrm{Hz}$, H-5), 2.20 (s, 3H, $\mathrm{CH_3}$), 1.97 (s, 3H, $\mathrm{CH_3}$); ^{13}C NMR (100.6 MHz, acetone-D_6) δ: 170.8, 170.8 (2 × acetyl C=O), 139.8, 139.7, 139.5, 138.9 (4 × $\mathrm{C_{Ar,q.}}$), 129.2–128.2 ($\mathrm{C_{Ar}}$), 101.1 (C-1), 86.2 (C-2), 82.1 (C-3), 78.5 (C-4), 77.6 (C-8), 77.1 (C-7), 76.1 (C-5), 75.4 ($\mathrm{CH_2Ph}$), 75.4 ($\mathrm{CH_2Ph}$), 73.8 ($\mathrm{CH_2Ph}$), 72.2 ($\mathrm{CH_2Ph}$), 70.6 (C-9), 69.8 (C-6), 21.1, 20.6 (2 × $\mathrm{CH_3}$); HR-ESI-TOF calcd. for $\mathrm{C_{41}H_{44}O_{10}Na}$ $[\mathrm{M+Na}]^+$: 719.2827. Found: 719.2826; Anal. calcd. for $\mathrm{C_{41}H_{44}O_{10}}$: C, 70.67; H, 6.37. Found: C, 70.72; H, 6.44.

(2*S*,3'*R*,4'*S*)-1,3,4,6-Tetra-*O*-benzyl-3',4'-dihydroxyspiro[2-deoxy-β-D-mannopyranose-2,2'-tetrahydrofuran] [(7*R*,8*S*)-60]:

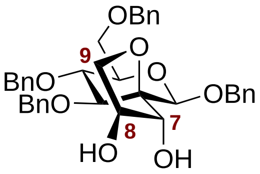

A solution of diacetate **(7*R*,8*S*)-59** (132 mg; 0.189 mmol) in MeOH (4.5 mL) was treated with NaOMe (50 µL; 25% in MeOH) and stirred at r.t. for 1.5 h. After this time, TLC (toluene/n-hexane/acetone, 2:2:1, + 0.5% $\mathrm{Et_3N}$) indicated complete consumption of the starting material, and the mixture was neutralized by the addition of Dowex $\mathrm{H^+}$ ion exchange resin. Filtration and evaporation to dryness gave a colorless solid, which was purified by flash column chromatography ($\mathrm{SiO_2}$, chloroform/acetonitrile, 4:1) to give diol **(7*R*,8*S*)-60** (105 mg; 91%) as a colorless solid.

$\mathrm{R_f} = 0.25$ (toluene/n-hexane/acetone, 2:2:1, + 0.5% $\mathrm{Et_3N}$); $[\alpha]_{\mathrm{D}}^{20}$ −44.0 (c = 1, $\mathrm{CHCl_3}$); ^{1}H NMR (400.2 MHz, acetone-D_6) δ: 7.44–7.19 (m, 20H, $\mathrm{H_{Ar}}$), 5.06 (d, 1H, $J_{\mathrm{gem}} = 11.0\,\mathrm{Hz}$, $\mathrm{CH_2Ph}$), 4.92 (d, 1H, $J_{\mathrm{gem}} = 12.1\,\mathrm{Hz}$, $\mathrm{CH_2Ph}$), 4.84 (d, 1H, $J_{\mathrm{gem}} = 10.9\,\mathrm{Hz}$, $\mathrm{CH_2Ph}$), 4.81–4.76 (m, 2H, $\mathrm{CH_2Ph}$, OH), 4.69–4.57 (m, 5H, H-1, $\mathrm{CH_2Ph}$), 4.53–4.43 (m, 2H, H-7, H-8), 4.20 (d, 1H, $J_{8,\mathrm{OH}} = 5.3\,\mathrm{Hz}$, OH), 4.10–4.03 (m, 1H, H-9a), 3.91–3.72 (m, 4H, H-4, H-6a, H-6b, H-3), 3.58–3.52 (m, 1H, H-9b), 3.48 (ddd, 1H, $J_{4,5} = 9.8$, $J_{5,6\mathrm{ab}} = 5.0, 2.0\,\mathrm{Hz}$, H-5); ^{13}C NMR (100.6 MHz, acetone-D_6) δ: 140.6, 139.8, 139.8, 139.1 (4 × $\mathrm{C_{Ar,q.}}$), 129.1–127.8 ($\mathrm{C_{Ar}}$), 101.3 (C-1), 86.5 (C-2), 81.9 (C-3), 79.1 (C-7 or C-8), 78.5 (C-4), 76.9 (C-7 or C-8), 76.1 (C-5), 75.4 ($\mathrm{CH_2Ph}$), 74.3 ($\mathrm{CH_2Ph}$), 73.8 ($\mathrm{CH_2Ph}$), 72.4 (C-9), 71.3 ($\mathrm{CH_2Ph}$), 70.2 (C-6); HR-ESI-TOF calcd. for $\mathrm{C_{37}H_{40}O_8Na}$

[M+Na]$^+$: 635.2615. Found: 635.2617; Anal. calcd. for $C_{37}H_{40}O_8$: C, 72.53; H, 6.58. Found: C, 72.22; H, 6.66.

(2*S*,5'*R*,6'*R*)-1,3,4,6-Tetra-*O*-benzyl-spiro[2-deoxy-β-D-mannopyranose-2,4'-(oxirano[2,3-*e*]-[1,3]-dioxepan-2-one)] [(7*R*,8*R*)-61]:

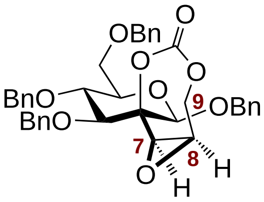

Epoxide **(7*R*,8*R*)-57** (82 mg; 0.134 mmol) in anhydrous CH_2Cl_2/pyridine (10:1, 11 mL) was cooled to −20 °C, and trichloromethyl chloroformate (diphosgene; 18 µL; 0.147 mmol) in CH_2Cl_2 (1 mL) was added dropwise. After the addition, stirring at −20 °C was continued for 3.5 h, and the reaction was then allowed to warm to r.t. After a total reaction time of 4 h, TLC (toluene/*n*-hexane/acetone, 1:1:1, + 0.5% Et_3N) indicated completion of the reaction. The reaction mixture was dropwise treated with water (0.5 mL), diluted with CH_2Cl_2 (30 mL), washed with brine (3 × 10 mL) and dried (Na_2SO_4). Filtration and evaporation yielded a crude solid, which was co-evaporated with toluene (10 mL) prior to recrystallization from toluene/acetone (2.4:1) to give **(7*R*,8*R*)-61** (69 mg; 81%) as a colorless crystalline solid. Single crystals for X-ray structural analysis were obtained from diethyl ether/acetone-D_6.

M.p. 158 °C (toluene/acetone); $R_f = 0.77$ (toluene/*n*-hexane/acetone, 1:1:1, + 0.5% Et_3N); $[\alpha]_D^{20}$ −91.9 (c = 1, $CHCl_3$); ^{1}H NMR (400.2 MHz, acetone-D_6) δ: 7.47–7.16 (m, 20H, H_{Ar}), 5.11 (d, 1H, J_{gem} = 10.8 Hz, CH_2Ph), 4.98–4.91 (m, 2H, CH_2Ph, H-1), 4.76–4.68 (m, 4H, CH_2Ph), 4.65 (dd, 1H, $J_{9a,9b}$ = 13.1, $J_{8,9a}$ = 1.4 Hz, H-9a), 4.62–4.57 (m, 2H, CH_2Ph), 4.33 (dd, 1H, $J_{9a,9b}$ = 13.1, $J_{8,9b}$ = 4.4 Hz, H-9b), 4.13–4.05 (m, 2H, H-3, H-4), 3.84 (dd, 1H, $J_{6a,6b}$ = 11.3, $J_{5,6a}$ = 2.0 Hz, H-6a), 3.80 (dd, 1H, $J_{6a,6b}$ = 11.3, $J_{5,6b}$ = 5.3 Hz, H-6b), 3.72–3.64 (m, 1H, H-5), 3.52–3.45 (m, 2H, H-8, H-7); ^{13}C NMR (100.6 MHz, acetone-D_6) δ: 151.4 (OC(=O)O), 139.9, 139.8, 139.5, 138.3 (4 × $C_{Ar,q.}$), 129.3–127.9 (C_{Ar}), 100.7 (C-1), 85.2 (C-3), 83.6 (C-2), 76.9 (C-5), 76.5 (C-4), 75.8 (CH_2Ph), 75.8 (CH_2Ph), 73.9 (CH_2Ph), 71.5 (CH_2Ph), 70.0 (C-6), 64.0 (C-9), 56.7 (C-7), 51.1 (C-8); HR-ESI-TOF calcd. for $C_{38}H_{38}O_9Na$ [M+Na]$^+$: 661.2408. Found: 661.2412; Anal. calcd. for $C_{38}H_{38}O_9$: C, 71.46; H, 6.00. Found: C, 71.18; H, 6.19.

(2*S*,2'*R*/*S*,3'*R*,4'*S*)-1,3,4,6-Tetra-*O*-benzyl-2'-hydroxyspiro[2-deoxy-β-D-mannopyranose-2,5'-(oxirano[2,3-*c*]-tetrahydrofuran)] (α,β-62):

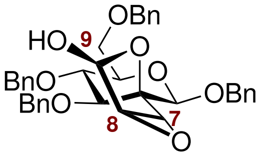

α-62
side chain: α-D-*ribo*

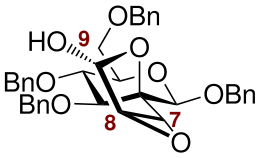

β-62
side chain: β-D-*ribo*

Epoxy alcohol **(7*S*,8*S*)-53** (260 mg; 0.424 mmol) in anhydrous EtOAc/toluene (2:1, 67 mL) was treated with MOPS (1.06 g; 5.09 mmol), and the vigorously stirred mixture was cooled to −50 °C. TEMPO 1 mg/mL in EtOAc (2.0 mL; 3 mol%) was added, followed by dropwise addition of TCICA 20 mg/mL in EtOAc (7.4 mL; 0.636 mmol) over 15 min. The pale yellow suspension was vigorously stirred for 3 h at −50 °C, after which time TLC (toluene/*n*-hexane/acetone, 1:1:1, + 0.5% Et_3N) showed complete conversion of the starting material. Next, Me_2S (150 µL; 2.0 mmol) in EtOAc (2 mL) was added dropwise to the reaction mixture at −50 °C, and stirring of the decolorized mixture continued for 15 min. After dilution with EtOAc (50 mL) and washing with sat. $NaHCO_3$/sat. $Na_2S_2O_3$ (10:1, 2 × 30 mL), the organic phase was dried (Na_2SO_4), filtered and the solvents evaporated to dryness to give crude **62** (260 mg). Flash column chromatographic purification (spherical SiO_2, toluene/*n*-hexane/acetone, 10:10:1, + 2% Et_3N) gave **α,β-62** (211 mg; 82%) as a colorless oil. The major component of the isomeric mixture was determined to be **β-62** in acetone-D_6 (α/β ≈ 6:94 to 8:92).

$R_f = 0.69$ (toluene/*n*-hexane/acetone, 1:1:1, + 0.5% Et_3N); $[\alpha]_D^{20}$ −9.2 (α/β ≈ 8:92, c = 0.5, acetone-D_6); selected signals for **α-62**: ^1H NMR (400.2 MHz, acetone-D_6) δ: 5.49 (H-9), 4.83 (H-1), 4.76 (OH), 3.58 (H-5); ^{13}C NMR (100.6 MHz, acetone-D_6) δ: 99.9 (C-1); selected signals for **β-62**: ^1H NMR (400.2 MHz, acetone-D_6) δ: 7.49–7.20 (m, 20H, H_{Ar}), 5.11 (d, 1H, $J_{9,OH}$ = 12.2 Hz, H-9), 4.98 (d, 1H, J_{gem} = 10.4 Hz, CH_2Ph), 4.92 (s, 1H, H-1), 4.89–4.82 (m, 3H, CH_2Ph), 4.73–4.67 (m, 2H, CH_2Ph), 4.65 (d, 1H, J_{gem} = 12.2 Hz, CH_2Ph), 4.58 (d, 1H, J_{gem} = 12.2 Hz, CH_2Ph), 4.53 (d, 1H, $J_{9,OH}$ = 12.2 Hz, OH), 3.96 (d, 1H, $J_{3,4}$ = 9.3 Hz, H-3), 3.88–3.78 (m, 4H, H-4, H-6a, H-6b, H-7), 3.65 (ddd, 1H, $J_{4,5}$ = 9.1, $J_{5,6ab}$ = 4.7, 2.5 Hz, H-5), 3.53 (d, 1H, $J_{7,8}$ = 2.7 Hz, H-8); ^{13}C NMR (100.6 MHz, acetone-D_6) δ: 139.7, 139.5, 139.4, 137.9 (4 × $C_{Ar,q.}$), 129.9–128.0 (C_{Ar}), 99.9 (C-1), 97.4 (C-9), 85.0 (C-2), 82.6 (C-3), 77.6 (C-4), 77.1 (CH_2Ph), 76.6 (C-5), 75.3 (CH_2Ph), 73.8 (CH_2Ph), 70.6 (CH_2Ph), 70.1 (C-6), 56.9 (C-8), 56.5 (C-7); HR-ESI-TOF calcd. for $C_{37}H_{38}O_8Na$ $[M+Na]^+$: 633.2459. Found: 633.2459; Anal. calcd. for $C_{37}H_{38}O_8$: C, 72.77; H, 6.27. Found: C, 72.73; H, 6.37.

(2*S*,2'*R*/*S*,3'*S*,4'*R*)-1,3,4,6-Tetra-*O*-benzyl-2'-hydroxyspiro[2-deoxy-β-D-mannopyranose-2,5'-(oxirano[2,3-*c*]-tetrahydrofuran)] (α,β-63):

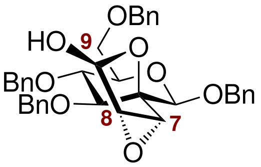

α-63
side chain: α-D-*lyxo*

+

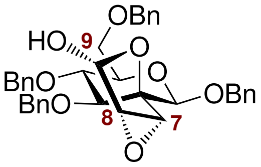

β-63
side chain: β-D-*lyxo*

To epoxy alcohol **(7*R*,8*R*)-57** (303 mg; 0.496 mmol) in anhydrous EtOAc/toluene (2:1, 78 mL) was added MOPS (1.25 g; 5.95 mmol), and the vigorously stirred suspension was cooled to −50 °C. TEMPO 1 mg/mL in EtOAc (2.3 mL; 3 mol%) was added, and then dropwise TCICA 20 mg/mL in EtOAc (8.7 mL; 0.744 mmol) slowly over 15 min. The pale yellow suspension was stirred for 3 h at −50 °C, when TLC control (toluene/*n*-hexane/acetone, 1:1:1, + 0.5% Et_3N) showed complete consumption of the starting material. Me_2S (170 µL; 2.3 mmol) in EtOAc (2 mL) was added dropwise at −50 °C, and stirring of the cooled decolorized mixture was continued for 15 min. Dilution with EtOAc (50 mL), washing with sat. $NaHCO_3$/sat. $Na_2S_2O_3$ (10:1, 2 × 30 mL), drying of the organic layer (Na_2SO_4), filtration and evaporation to dryness gave crude **63** (260 mg). Flash column chromatographic purification (spherical SiO_2, toluene/*n*-hexane/acetone, 10:10:3, + 2% Et_3N) gave **α,β-63** (280 mg; 92%) as a colorless foam. The major component of the isomeric mixture was identified to be **α-63** in acetone-D_6 (α/β ≈ 91:9 to 97:3). Single crystals of **α-63** suitable for X-ray structural analysis were obtained from toluene/CH_2Cl_2.

$R_f = 0.67$ (toluene/*n*-hexane/acetone, 1:1:1, + 0.5% Et_3N); $[\alpha]_D^{20}$ −68.4 (α/β ≈ 97:3, c = 0.5, acetone-D_6); selected signals for **α-63**: ^{1}H NMR (400.2 MHz, acetone-D_6) δ: 7.50–7.20 (m, 20H, H_{Ar}), 5.20 (d, 1H, $J_{9,OH}$ = 12.0 Hz, H-9), 5.01 (d, 1H, J_{gem} = 11.5 Hz, CH_2Ph), 4.91 (d, 1H, J_{gem} = 10.4 Hz, CH_2Ph), 4.83 (s, 1H, H-1), 4.82–4.74 (m, 2H, CH_2Ph), 4.65–4.52 (m, 4H, CH_2Ph), 4.32 (d, 1H, $J_{9,OH}$ = 12.0 Hz, OH), 4.01 (d, 1H, $J_{3,4}$ = 8.9 Hz, H-3), 3.94 (d, 1H, $J_{7,8}$ = 2.7 Hz, H-7), 3.85 (H-6a), 3.79–3.71 (m, 2H, H-6b, H-4), 3.64 (ddd, 1H, $J_{4,5}$ = 9.3, $J_{5,6b}$ = 5.4, $J_{5,6a}$ = 2.2 Hz, H-5), 3.58 (d, 1H, $J_{7,8}$ = 2.7 Hz, H-8); ^{13}C NMR (100.6 MHz, acetone-D_6) δ: 139.9, 139.8, 139.8, 137.6 (4 × $C_{Ar,q.}$), 129.5–128.1 (C_{Ar}), 99.4 (C-1), 97.3 (C-9), 83.6 (C-2), 82.5 (C-3), 76.7 (C-4), 76.7 (C-5), 75.4 (CH_2Ph), 75.2 (CH_2Ph), 73.8 (CH_2Ph), 72.0 (CH_2Ph), 70.4 (C-6), 57.3 (C-7), 56.9 (C-8); selected signals for **β-63**: ^{1}H NMR (400.2 MHz, acetone-D_6) δ: 5.47 (H-9), 4.96 (H-1), 4.71 (OH), 4.23 (d, 1H, $J_{3,4}$ = 9.1 Hz, H-3), 3.67 (H-5); ^{13}C NMR (100.6 MHz, acetone-D_6) δ: 98.9 (C-1), 98.0 (C-9), 81.7 (C-3); HR-ESI-TOF calcd. for

$C_{37}H_{38}O_8Na$ $[M+Na]^+$: 633.2459. Found: 633.2447; Anal. calcd. for $C_{37}H_{38}O_8$: C, 72.77; H, 6.27. Found: C, 72.61; H, 6.29.

(2*S*,4'*R*)-1,3,4,6-Tetra-*O*-benzyl-2',2'-dimethyl-4'-{(1*S*)-1,2-O-isopropylidene-1,2-dihydroxyethyl}spiro[2-deoxy-β-D-mannopyranose-2,5'-[1,3]-dioxolane] [(7*R*,8*S*)-64]:

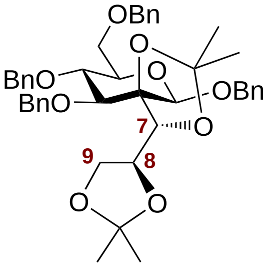

To epoxide **(7*R*,8*R*)-57** (1.39 g; 2.26 mmol) in anhydrous acetone (115 mL) at r.t. was dropwise added a freshly prepared solution of $SnCl_2$ 10 mg/mL in acetone (12.9 mL; 30 mol%). The solution was heated to 55 °C for 1.5 h, after which time TLC (toluene/*n*-hexane/acetone, 2:2:1, + 0.5% Et_3N) indicated complete conversion of the substrate epoxide, and the formation of multiple products. The reaction mixture was allowed to cool to r.t. and was slowly treated with sat. $NaHCO_3$ (4 mL). Next, the mixture was diluted with water (100 mL), extracted with CH_2Cl_2 (3 × 150 mL), and the combined organic extracts were dried (Na_2SO_4). Filtration and evaporation of the volatile parts *in vacuo* yielded a crude oil. Flash column chromatographic purification (SiO_2, toluene/*n*-hexane/acetone, 2:2:0.4 to 2:2:0.8) gave, eluting in this order, **(7*R*,8*S*)-64** (446 mg; 28%) as a yellowish oil with high chromatographic mobility, **(7*R*,8*S*)-66** (223 mg; 15%) as a colorless oil with medium mobility and **(7*R*,8*S*)-65** (667 mg; 44%) as a colorless oil with low chromatographic mobility. Analytical data for **(7*R*,8*S*)-64**:

$R_f = 0.58$ (toluene/*n*-hexane/acetone, 2:2:1, + 0.5% Et_3N); $[\alpha]_D^{20}$ −47.4 (c = 0.5, $CHCl_3$); ^1H NMR (600.1 MHz, acetone-D_6) δ: 7.49–7.23 (m, 20H, H_{Ar}), 5.03 (d, 1H, J_{gem} = 11.4 Hz, CH_2Ph), 4.90 (d, 1H, J_{gem} = 11.7 Hz, CH_2Ph), 4.80 (d, 1H, J_{gem} = 11.0 Hz, CH_2Ph), 4.72–4.65 (m, 3H, CH_2Ph), 4.61 (d, 1H, J_{gem} = 11.9 Hz, CH_2Ph), 4.42–4.38 (m, 2H, H-8, H-1), 4.25 (d, 1H, $J_{7,8}$ = 8.4 Hz, H-7), 3.89–3.84 (m, 3H, H-9a, H-4, H-6a), 3.80 (dd, 1H, $J_{6a,6b}$ = 11.0, $J_{5,6b}$ = 5.2 Hz, H-6b), 3.64 (dd, 1H, $J_{9a,9b}$ = 8.0, $J_{8,9b}$ = 8.0 Hz, H-9b), 3.58 (ddd, 1H, $J_{4,5}$ = 9.9, $J_{5,6b}$ = 5.3, $J_{5,6a}$ = 2.0 Hz, H-5), 3.47 (d, 1H, $J_{3,4}$ = 9.4 Hz, H-3), 1.44 (s, 3H, CH_3), 1.35 (s, 3H, CH_3), 1.30 (s, 3H, CH_3), 1.23 (s, 3H, CH_3); ^{13}C NMR (150.9 MHz, acetone-D_6) δ: 139.8, 139.5, 139.5, 138.4 (4 × $C_{Ar,q.}$), 129.3–128.3 (C_{Ar}), 110.4 (Me_2CO_2), 109.2 (Me_2CO_2), 99.9 (C-1), 85.7 (C-2), 81.7 (C-3), 79.3 (C-7), 79.2 (C-4), 76.6 (CH_2Ph), 76.0 (C-5), 75.5 (C-8), 75.3 (CH_2Ph), 73.9 (CH_2Ph), 70.6 (CH_2Ph), 70.0 (C-6), 66.1 (C-9), 27.2 (CH_3), 27.2 (CH_3), 27.1

(CH_3), 25.9 (CH_3); HR-ESI-TOF calcd. for $C_{43}H_{50}O_9Na$ $[M+Na]^+$: 733.3347. Found: 733.3352. Anal. calcd. for $C_{43}H_{50}O_9$: C, 72.65; H, 7.09. Found: C, 72.72; H, 7.20.

Benzyl 3,4,6-tri-*O*-benzyl-2-*C*-{(1*R*,2*S*)-1,2-*O*-isopropylidene-1,2,3-trihydroxyprop-1-yl}-β-D-mannopyranoside [(7*R*,8*S*)-65]:

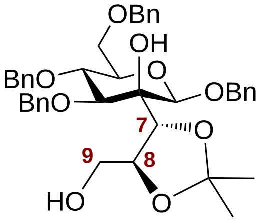

Isolated as the major product (667 mg; 44%) in the form of a colorless oil in the $SnCl_2$-mediated epoxide opening of **(7*R*,8*R*)-57** as described above.

$R_f = 0.28$ (toluene/*n*-hexane/acetone, 2:2:1, + 0.5% Et_3N); $[\alpha]_D^{20}$ −34.6 (c = 0.5, $CHCl_3$); ^1H NMR (600.1 MHz, acetone-D_6) δ: 7.43–7.21 (m, 20H, H_{Ar}), 4.99 (d, 1H, $J_{gem} = 11.0$ Hz, CH_2Ph), 4.91–4.85 (m, 2H, CH_2Ph), 4.79–4.74 (m, 2H, H-8, CH_2Ph), 4.72–4.64 (m, 3H, CH_2Ph), 4.63–4.59 (m, 2H, H-1, CH_2Ph), 4.29 (d, 1H, $J_{7,8} = 8.3$ Hz, H-7), 4.16 (s, 1H, OH), 4.04 (dd, $J_{4,5} = 9.7$, $J_{3,4} = 9.4$ Hz, H-4), 3.95–3.91 (m, 2H, H-3, OH), 3.83 (dd, 1H, $J_{6a,6b} = 11.0$, $J_{5,6a} = 2.0$ Hz, H-6a), 3.80 (dd, 1H, $J_{6a,6b} = 11.0$, $J_{5,6b} = 4.8$ Hz, H-6b), 3.67 (ddd, 1H, $J_{9a,9b} = 11.0$, $J_{9a,OH} = 6.2$, $J_{8,9a} = 4.8$ Hz, H-9a), 3.64–3.59 (m, 1H, H-9b), 3.55 (ddd, 1H, $J_{4,5} = 9.7$, $J_{5,6b} = 4.8$, $J_{5,6a} = 2.2$ Hz, H-5), 1.46 (s, 3H, CH_3), 1.35 (s, 3H, CH_3); ^{13}C NMR (150.9 MHz, acetone-D_6) δ: 139.8, 139.7, 139.6, 138.8 (4 × $C_{Ar,q.}$), 129.1–128.1 (C_{Ar}), 109.0 (Me_2CO_2), 101.0 (C-1), 81.6 (C-3), 79.2 (C-7), 78.7 (C-8), 78.4 (C-4), 76.1 (C-2), 76.1 (C-5), 75.3 (CH_2Ph), 75.0 (CH_2Ph), 73.8 (CH_2Ph), 71.1 (CH_2Ph), 70.1 (C-6), 64.7 (C-9), 27.7 (CH_3), 27.1 (CH_3); HR-ESI-TOF calcd. for $C_{40}H_{46}O_9Na$ $[M+Na]^+$: 693.3034. Found: 693.3027. Anal. calcd. for $C_{40}H_{46}O_9$: C, 71.62; H, 6.91. Found: C, 71.78; H, 7.07.

Benzyl 3,4,6-tri-*O*-benzyl-2-*C*-{(1*R*,2*S*)-2,3-*O*-isopropylidene-1,2,3-trihydroxyprop-1-yl}-β-D-mannopyranoside [(7*R*,8*S*)-66]:

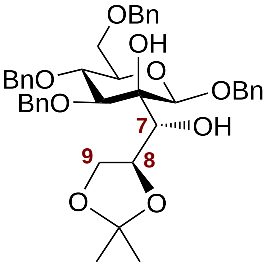

Isolated as the minor product (223 mg; 15%) in the form of a colorless oil in the $SnCl_2$-mediated epoxide opening of **(7*R*,8*R*)-57** as described above.

$R_f = 0.39$ (toluene/n-hexane/acetone, 2:2:1, + 0.5% Et_3N); $[\alpha]_D^{20}$ +7.8 (c = 0.5, $CHCl_3$); ^1H NMR (400.2 MHz, acetone-D_6) δ: 7.44–7.24 (m, 20H, H_{Ar}), 5.01 (d, 1H, $J_{gem} = 11.5$ Hz, CH_2Ph), 4.92 (d, 1H, $J_{gem} = 11.7$ Hz, CH_2Ph), 4.85–4.78 (m, 3H, H-1, CH_2Ph), 4.70–4.65 (m, 3H, CH_2Ph), 4.60 (d, 1H, $J_{gem} = 12.4$ Hz, CH_2Ph), 4.45 (ddd, 1H, $J_{8,9b} = 7.8$, $J_{8,9a} = 6.3$, $J_{7,8} = 6.3$ Hz, H-8), 4.04 (dd, $J_{4,5} = 9.5$, $J_{3,4} = 9.5$ Hz, H-4), 3.95–3.88 (m, 3H, H-3, H-9a, H-7), 3.87–3.80 (m, 3H, OH, H-6a, H-6b), 3.74 (dd, 1H, $J_{8,9b} = 8.1$, $J_{9a,9b} = 8.1$ Hz, H-9b), 3.58–3.53 (m, 2H, H-5, OH), 1.26 (s, 3H, CH_3), 1.16 (s, 3H, CH_3); ^{13}C NMR (100.6 MHz, acetone-D_6) δ: 139.9, 139.9, 139.7, 138.9 (4 × $C_{Ar,q.}$), 129.1–128.2 (C_{Ar}), 108.5 (Me_2CO_2), 101.6 (C-1), 81.4 (C-3), 78.4 (C-4), 77.8 (C-2), 77.3 (C-8), 76.2 (C-5), 75.4 (CH_2Ph), 75.1 (CH_2Ph), 73.8 (C-7), 73.8 (CH_2Ph), 71.5 (CH_2Ph), 70.1 (C-6), 68.0 (C-9), 27.0 (CH_3), 26.1 (CH_3); HR-ESI-TOF calcd. for $C_{40}H_{46}O_9Na$ $[M+Na]^+$: 693.3034. Found: 693.3034. Anal. calcd. for $C_{40}H_{46}O_9$: C, 71.62; H, 6.91. Found: C, 71.33; H, 6.91.

Benzyl 3,4,6-tri-*O*-benzyl-2-*C*-{(1*R*,2*S*)-1,2,3-trihydroxyprop-1-yl}-β-D-mannopyranoside [(7*R*,8*S*)-67]:

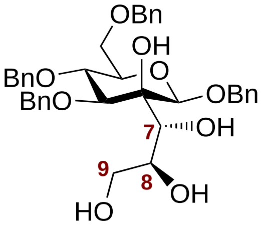

From (7*R*,8*S*)-64: Diacetonide **(7*R*,8*S*)-64** (446 mg; 0.627 mmol) in a mixture of formic acid (21.5 mL) and water (3.8 mL) was heated to 35 °C for 4 d. Simultaneous reaction monitoring of aliquotic samples *via* ESI-MS confirmed the absence of acetonide species after this time. The solution was allowed to cool to r.t., diluted with water (20 mL), extracted with CH_2Cl_2 (3 × 50 mL), saturated with NaCl and once more extracted with CH_2Cl_2 (50 mL). The combined organic extracts were washed with sat. $NaHCO_3$ (2 × 50 mL) and water (50 mL), dried (Na_2SO_4), filtered and evaporated to give a crude brown oil. This crude product was dissolved in MeOH (25 mL), and NH_3 7 N in MeOH (10 mL) was added. After 18 h at r.t., TLC (toluene/ethyl acetate, 1:1) confirmed complete saponification of formate species and formation of one major product of low chromatographic mobility. The reaction mixture was evaporated to dryness, and the crude product was purified by flash column chromatography (SiO_2, chloroform/acetonitrile, 4:1) to give tetrol **(7*R*,8*S*)-67** (167 mg; 42% over 2 steps) as a colorless solid.

From (7*R*,8*S*)-65: In an analogous procedure with **(7*R*,8*S*)-65** (667 mg; 0.994 mmol), reaction in formic acid/water at r.t. for 3 d, and then at 35 °C for 1 d gave, after formate cleavage as described above, tetrol **(7*R*,8*S*)-67** (339 mg; 54% over 2 steps).

From (7*R*,8*S*)-66: In an analogous procedure with **(7*R*,8*S*)-66** (223 mg; 0.332 mmol), reaction in formic acid/water at r.t. for 1 d gave, after formate cleavage as described above, tetrol **(7*R*,8*S*)-67** (141 mg; 67% over 2 steps).

$R_f = 0.21$ (toluene/ethyl acetate, 1:1); $[\alpha]_D^{20}$ −9.2 (c = 1, $CHCl_3$); ^1H NMR (400.2 MHz, CD_3OD) δ: 7.45–7.23 (m, 18H, H_{Ar}), 7.18–7.13 (m, 2H, H_{Ar}), 4.95–4.87 (m, 3H, CH_2Ph, H-1), 4.79 (d, 1H, J_{gem} = 11.0 Hz, CH_2Ph), 4.71 (d, 1H, J_{gem} = 11.0 Hz, CH_2Ph), 4.66–4.61 (m, 2H, CH_2Ph), 4.60–4.53 (m, 2H, CH_2Ph), 4.04 (d, 1H, $J_{7,8}$ = 2.5 Hz, H-7), 4.02–3.94 (m, 2H, H-4, H-8), 3.82–3.73 (m, 3H, H-3, H-6a, H-6b), 3.64–3.49 (m, 3H, H-9a, H-9b, H-5); ^{13}C NMR (100.6 MHz, CD_3OD) δ: 139.7, 139.5, 139.4, 138.9 (4 × $C_{Ar,q.}$), 129.5–128.6 (C_{Ar}), 102.7 (C-1), 82.1 (C-3), 78.5 (C-2), 78.5 (C-4), 76.2 (C-5), 76.0 (CH_2Ph), 75.8 (CH_2Ph), 74.5 (CH_2Ph), 72.6 (C-7), 72.5 (CH_2Ph), 71.2 (C-8), 70.2 (C-6), 65.0 (C-9); HR-ESI-TOF calcd. for $C_{37}H_{42}O_9Na$ $[M+Na]^+$: 653.2721. Found: 653.2722; Anal. calcd. for $C_{37}H_{42}O_9$: C, 70.46; H, 6.71. Found: C, 70.31; H, 6.82.

(2*S*,2'*R*/*S*,3'*R*,4'*R*)-1,3,4,6-Tetra-*O*-benzyl-2',3',4'-trihydroxyspiro[2-deoxy-β-D-mannopyranose-2,5'-tetrahydrofuran] (α,β-68):

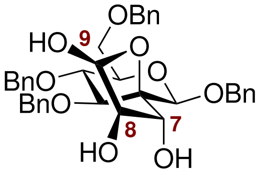

α-68

side chain: α-D-*xylo*

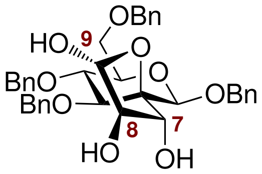

β-68

side chain: β-D-*xylo*

From (7*R*,8*S*)-67: To **(7*R*,8*S*)-67** (100 mg; 0.159 mmol) in anhydrous EtOAc/toluene (2:1, 25.5 mL) was added MOPS (399 mg; 1.90 mmol), and the vigorously stirred suspension was cooled to −65 °C. Next, TEMPO 1 mg/mL in EtOAc (1.49 mL; 6 mol%) was added, followed by the dropwise addition of a solution of TCICA 10 mg/mL in EtOAc (3.1 mL; 0.135 mmol) over 15 min. The resulting pale yellow mixture was stirred for 3 h at −65 °C. Next, Me_2S (70 µL; 0.85 mmol) in EtOAc (1 mL) was added dropwise at −65 °C, and stirring of the decolorized reaction mixture continued for 15 min. After dilution with EtOAc (20 mL) and washing with brine/sat. $Na_2S_2O_3$ (10:1, 2 × 15 mL), the organic layer was dried (Na_2SO_4), filtered and evaporated to dryness to give crude **68** (111 mg). Flash column chromatographic purification (spherical SiO_2, toluene/*n*-hexane/acetone, 4:4:3, + 0.5% Et_3N) gave **α,β-68** (18 mg; 18%; 36% brsm) as a colorless solid with higher chromatographic mobility, along with recovered **(7*R*,8*S*)-67** (50 mg).

From (7*R*,8*R*)-69: A solution of lactone **(7*R*,8*R*)-69** (89 mg; 0.142 mmol) in anhydrous THF (6 mL) was cooled to −78 °C, and a solution of DIBAL-H (1.42 mL; 1 M in THF; 1.42 mmol) was slowly added dropwise. The reaction mixture was stirred at −78 °C for 1 h, allowed to warm to −50 °C, and stirred for another 1 h. TLC (toluene/ethyl acetate, 1:1) showed major conversion of the substrate lactone, and MeOH (0.5 mL) was added dropwise at −50 °C. Next, 10% HCl (0.5 mL) was also added dropwise, and the mixture was stirred for 10 min at −50 °C. CH_2Cl_2 (10 mL) was added, and the mixture was allowed to warm to r.t. Water (5 mL) was added, followed by extraction with EtOAc (2 × 20 mL) and CH_2Cl_2 (2 × 20 mL). The combined organic extracts were dried (Na_2SO_4), filtered and evaporated to give a crude solid (85 mg). Purification by flash column chromatography (SiO_2, toluene/*n*-hexane/acetone, 2:2:0.8 to 2:2:1) gave **α,β-68** (61 mg; 68%; 76% brsm) along with recovered substrate **(7*R*,8*R*)-69** (9 mg). **α,β-68** was isolated as a mixture of isomers with α/β ≈ 1:1 in acetone-D_6.

$R_f = 0.46$ (toluene/ethyl acetate, 1:1); $[\alpha]_D^{20}$ −21.8 (α/β ≈ 1:1, c = 0.5, acetone-D_6); selected signals for **α-68**: ^{1}H NMR (600.1 MHz, acetone-D_6) δ: 7.45–7.23 (m, 20H, H_{Ar}), 5.14 (dd, 1H, $J_{9,OH} = 6.1$, $J_{8,9} = 6.1$ Hz, H-9), 4.90 (C-7-OH), 4.61 (H-1), 4.40 (m, 1H, visible: $J = 8.1$, 4.8 Hz, H-7), 4.26–4.20 (m, 2H, H-8, C-9-OH), 3.89 (dd, 1H, $J_{3,4} = 9.7$, $J_{4,5} = 9.7$ Hz, H-4), 3.85–3.77 (m, 3H, H-6a, H-6b, H-3), 3.55–3.48 (m, 2H, H-5, C-8-OH); ^{13}C NMR (150.9 MHz, acetone-D_6) δ: 99.5 (C-1), 96.0 (C-9), 86.1 (C-2), 81.2 (C-3), 78.4 (C-4), 78.4 (C-8), 76.6 (C-7), 76.3 or 76.1 (C-5), 70.1 (C-6); selected signals for **β-68**: ^{1}H NMR (600.1 MHz, acetone-D_6) δ: 7.45–7.23 (m, 20H, H_{Ar}), 4.94 (H-9), 4.90 (C-7-OH), 4.61 (H-1), 4.59 (C-9-OH), 4.47 (dd, 1H, $J = 7.0$, 5.0 Hz, H-7), 4.44–4.38 (m, 1H, C-8-OH), 4.10–4.06 (m, 1H, H-8), 3.93 (dd, 1H, $J_{3,4} = 9.0$, $J_{4,5} = 9.0$ Hz, H-4), 3.85–3.77 (m, 3H, H-6a, H-6b, H-3), 3.55–3.48 (m, 1H, H-5); ^{13}C NMR (150.9 MHz, acetone-D_6) δ: 103.5 (C-9), 100.5 (C-1), 86.9 (C-2), 84.2 (C-8), 81.3 (C-3), 78.4 (C-4), 77.8 (C-7), 76.3 or 76.1 (C-5), 70.1 (C-6); HR-ESI-TOF calcd. for $C_{37}H_{40}O_9Na$ $[M+Na]^+$: 651.2565. Found: 651.2559; Anal. calcd. for $C_{37}H_{40}O_9$: C, 70.68; H, 6.41. Found: C, 70.47; H, 6.62.

(2*S*,3'*R*,4'*R*)-1,3,4,6-Tetra-*O*-benzyl-3',4'-dihydroxyspiro[2-deoxy-β-D-mannopyranose-2,5'-tetrahydrofuran-2-one] (7*R*,8*R*)-69:

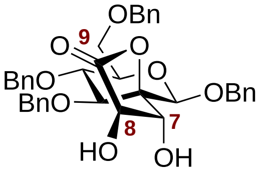

A solution of **(7*R*,8*S*)-67** (199 mg; 0.316 mmol) in anhydrous EtOAc/toluene (2:1, 50 mL) was treated with MOPS (794 mg; 3.79 mmol), and the vigorously stirred mixture was cooled to −50 °C. Next, TEMPO 1 mg/mL in EtOAc (1.48 mL; 3 mol%) was added. Subsequently, TCICA 20 mg/mL in EtOAc (5.9 mL; 0.506 mmol) was slowly added dropwise over 15 min, and the resulting pale yellow mixture was stirred for 30 min at −50 °C. The reaction was allowed to slowly warm to −35 °C and stirred at this temperature for 17 h, after which time TLC (toluene/ethyl acetate, 1:1) showed essentially complete conversion. Next, Me_2S (175 µL; 2.37 mmol) in EtOAc (2 mL) was added dropwise, and stirring of the rapidly decolorizing reaction mixture continued for 15 min at −35 °C. After dilution with EtOAc (50 mL) and washing with brine/sat. $Na_2S_2O_3$ (10:1, 3 × 30 mL) and water (30 mL), the organic phase was dried (Na_2SO_4), filtered and evaporated to dryness to give crude **(7*R*,8*R*)-69** (220 mg). Flash column chromatographic purification (SiO_2, toluene/*n*-hexane/acetone, 10:10:4 to 10:10:5.5) gave pure lactone **(7*R*,8*R*)-69** (166 mg; 84%) as a colorless solid with higher chromatographic mobility, along with **α,β-68** (12 mg; 6%) as a side product. An analytical sample was recrystallized from *n*-hexane/ethyl acetate.

M.p. 172 °C (*n*-hexane/ethyl acetate, decomp.). $R_f = 0.72$ (toluene/ethyl acetate, 1:1); $[\alpha]_D^{20}$ −43.7 (c = 1, $CHCl_3$); ^{1}H NMR (400.2 MHz, acetone-D_6) δ: 7.45–7.20 (m, 20H, H_{Ar}), 5.59 (d, 1H, $J_{7,OH} = 5.1$ Hz, C-7-OH), 5.15 (d, 1H, $J_{8,OH} = 5.8$ Hz, C-8-OH), 5.05 (d, 1H, $J_{gem} = 11.0$ Hz, CH_2Ph), 4.97–4.88 (m, 2H, CH_2Ph), 4.82–4.77 (m, 2H, H-1, CH_2Ph), 4.73–4.59 (m, 5H, CH_2Ph, H-7), 4.58 (dd, 1H, $J_{7,8} = 8.4$, $J_{8,OH} = 5.9$ Hz, H-8), 4.08 (d, 1H, $J_{3,4} = 9.5$ Hz, H-3), 3.91 (dd, $J_{4,5} = 9.8$, $J_{3,4} = 9.8$ Hz, H-4), 3.88–3.81 (m, 2H, H-6a, H-6b), 3.63 (ddd, 1H, $J_{4,5} = 9.8$, $J_{5,6ab} = 4.3$, 2.4 Hz, H-5); ^{13}C NMR (100.6 MHz, acetone-D_6) δ: 174.4 (C-9), 139.7, 139.5, 139.4, 138.3 (4 × $C_{Ar,q.}$), 129.2–128.0 (C_{Ar}), 98.7 (C-1), 86.0 (C-2), 80.0 (C-3), 78.3 (C-4), 76.1 (C-5), 75.6 (CH_2Ph), 75.3 (C-7), 74.8 (CH_2Ph), 74.7 (C-8), 73.9 (CH_2Ph), 71.6 (CH_2Ph), 69.7 (C-6); HR-ESI-TOF calcd. for $C_{37}H_{48}O_9Na$ $[M+Na]^+$: 649.2408. Found: 649.2409; Anal. calcd. for $C_{37}H_{38}O_9$: C, 70.91; H, 6.11. Found: C, 70.68; H, 6.36.

4-*C*-Formyl-D-*erythro*-L-*ido*-octose (*anti*-70):

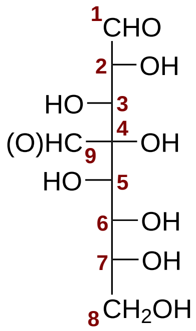

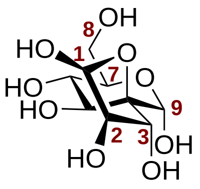

***anti*-70-A**
(47%)

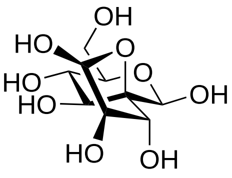

***anti*-70-B**
(10%)

To a solution of **α,β-68** (29 mg; 0.045 mmol) in MeOH (4 mL) was added Pd 10% on activated charcoal (112 mg), and the suspension was stirred under an atmosphere of hydrogen for 4 d. TLC control (chloroform/methanol, 2:1) indicated complete conversion to a mixture of products without observable fluorescence quenching. The reaction mixture was diluted with MeOH (5 mL), filtered through a layer of Celite, and the filter pad was thoroughly rinsed with MeOH. The collected filtrate was evaporated to dryness to give a colorless oil. RP-chromatographic purification (RP-C18 silica gel, methanol/water, 1:1) gave, after partial evaporation and freeze-drying from residual water over several days, ***anti*-70** (12 mg; 99%) as a colorless foam. The compound was isolated as a mixture of isomers.

$R_f = 0.14$–0.64 (chloroform/methanol, 2:1); $[\alpha]_D^{20}$ 42.8 (c = 0.5, H_2O); identified isomers: **(1*S*,9*S*)-4-*C*-formyl-D-*erythro*-L-*ido*-octo-1,4-furanose-9,7-pyranose** (***anti*-70-A**, 47% isomeric contribution in D_2O), selected signals: ^{1}H NMR (700.3 MHz, D_2O) δ: 5.27 (d, 1H, $J_{1,2} = 4.7$ Hz, H-1), 5.01 (s, 1H, H-9), 4.25 (dd, 1H, $J_{2,3} = 9.0$, $J_{1,2} = 4.7$ Hz, H-2), 4.14 (d, 1H, $J_{2,3} = 9.0$ Hz, H-3), 3.94 (d, 1H, $J_{5,6} = 9.7$ Hz, H-5), 3.86 (H-8a), 3.82 (H-7), 3.73 (dd, 1H, $J_{8a,8b} = 11.8$, $J_{7,8b} = 6.0$ Hz, H8b), 3.53 (dd, 1H, $J_{5,6} = 9.7$, $J_{6,7} = 9.7$ Hz, H-6); ^{13}C NMR (176.1 MHz, D_2O) δ: 97.4 (C-9), 94.8 (C-1), 84.2 (C-4), 77.4 (C-3), 76.4 (C-2), 72.3 (C-7), 69.6 (C-5), 68.8 (C-6), 61.6 (C-8); **(1*S*,9*R*)-4-*C*-formyl-D-*erythro*-L-*ido*-octo-1,4-furanose-9,7-pyranose** (***anti*-70-B**, 10% isomeric contribution in D_2O), selected signals: ^{1}H NMR (700.3 MHz, D_2O) δ: 5.31 (d, 1H, $J_{1,2} = 5.0$ Hz, H-1), 4.75 (s, 1H, H-9), 4.30 (dd, 1H, $J_{2,3} = 8.8$, $J_{1,2} = 5.0$ Hz, H-2), 4.25 (H-3), 3.76 (H-5), 3.41 (H-7); ^{13}C NMR (176.1 MHz, D_2O) δ: 94.4 (C-1), 93.5 (C-9), 76.4 (C-2), 76.4 (C-7), 74.8 (C-3), 71.2 (C-5), 68.5 (C-6), 61.5 (C-8); HR-ESI-TOF calcd. for $C_9H_{16}O_9Na$ $[M+Na]^+$: 291.0687. Found: 291.0689; HR-ESI-TOF calcd. for $C_9H_{15}O_9$ $[M-H]^-$: 267.0722. Found: 267.0723; Anal. calcd. for $C_9H_{16}O_9 \cdot H_2O$: C, 37.77; H, 6.34. Found: C, 37.69; H, 6.56.

1,3,6-Tri-*O*-benzyl-2-*C*,4-*O*-{(1*R*,2*S*)-2,3-*O*-isopropylidene-2,3-dihydroxy-*n*-prop-1-ylidene}-β-D-mannopyranose-$^1C_4$ (7*R*,8*S*)-71:

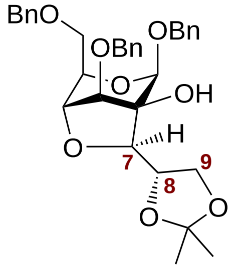

Method *a*: To a solution of epoxide **(7*S*,8*S*)-53** (91 mg; 0.149 mmol) in anhydrous acetone (4 mL) was dropwise added a freshly prepared solution of $SnCl_2$ in acetone

(141 µL; 10 mg/mL; 5 mol%), and the mixture was heated to 45 °C for 24 h. A second portion of $SnCl_2$ in acetone (5 mol%) was added, and the solution was heated to 55 °C for another 22 h. TLC reaction control (toluene/*n*-hexane/acetone, 2:2:1, + 0.5% Et_3N) confirmed the formation of one major product, and the reaction mixture was allowed to cool to r.t. Next, sat. $NaHCO_3$ (1 mL) was added dropwise, the solution was diluted with water (10 mL) and extracted with CH_2Cl_2 (3 × 20 mL). Drying (Na_2SO_4) of the organic parts, filtration and evaporation of the volatile components gave a yellow oil, which was purified by flash column chromatography (SiO_2, toluene/*n*-hexane/acetone, 2:2:1) to give acetonide **(7*R*,8*S*)-71** (57 mg; 68%) as a colorless solid. An analytical sample was recrystallized from *n*-hexane/acetone.

Method *b*: Starting from epoxide **(7*S*,8*S*)-53** (71 mg; 0.116 mmol) in acetone (3 mL) with $SnCl_2$ in acetone (2.2 mL; 10 mg/mL; 1 equiv.), reaction for 2 h at 0 °C, workup and chromatography as described above gave **(7*R*,8*S*)-71** (39 mg; 60%).

M.p. 134 °C (*n*-hexane/acetone); $R_f = 0.45$ (toluene/*n*-hexane/acetone, 2:2:1, + 0.5% Et_3N); $[\alpha]_D^{20}$ −15.1 (c = 1, $CHCl_3$); ^1H NMR (400.2 MHz, acetone-D_6) δ: 7.37–7.19 (m, 15H, H_{Ar}), 4.94 (d, 1H, $J_{gem} = 11.7$ Hz, CH_2Ph), 4.86–4.82 (m, 2H, CH_2Ph, H-1), 4.70–4.67 (m, 2H, OH, CH_2Ph), 4.51 (d, 1H, $J_{3,4} = 5.7$ Hz, H-3), 4.46 (d, 1H, $J_{gem} = 11.7$ Hz, CH_2Ph), 4.38–4.30 (m, 3H, H-4, CH_2Ph, visible coupling constants: $J_{4,5} = 2.6$ Hz), 4.23 (ddd, 1H, $J_{8,9b} = 7.6$, $J_{8,9a} = 6.8$, $J_{7,8} = 5.3$ Hz, H-8), 4.10–4.00 (m, 3H, H-5, H-9a, H-6a), 3.94 (d, 1H, $J_{7,8} = 5.3$ Hz, H-7), 3.87 (dd, 1H, $J_{6a,6b} = 9.9$, $J_{5,6b} = 5.3$ Hz, H-6b), 3.79 (dd, 1H, $J_{9a,9b} = 8.3$, $J_{8,9b} = 7.9$ Hz, H-9b), 1.34 (s, 3H, CH_3), 1.31 (s, 3H, CH_3); ^{13}C NMR (150.9 MHz, acetone-D_6) δ: 139.7, 139.6, 139.4 (3 × $C_{Ar,q.}$), 129.0–127.9 (C_{Ar}), 109.3 (Me_2CO_2), 104.9 (C-1), 81.7 (C-7), 80.0 (C-3), 77.5 (C-5), 76.7 (C-8), 76.1 (C-2), 73.9 (C-4), 73.6 (CH_2Ph), 73.5 (CH_2Ph), 71.2 (C-6), 70.7 (CH_2Ph), 66.7 (C-9), 26.6 (CH_3), 26.1 (CH_3); HR-ESI-TOF calcd. for $C_{33}H_{38}O_8Na$ $[M+Na]^+$: 585.2459. Found: 585.2464; Anal. calcd. for $C_{33}H_{38}O_8$: C, 70.44; H, 6.81. Found: C, 70.48; H, 6.81.

Methyl 3,6-di-*O*-benzyl-4-deoxy-β-D-*glycero*-hex-3-enopyranoside-2-ulose (72):

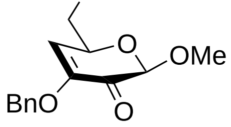

To methyl 2-uloside **2c**[69] (229 mg; 0.50 mmol) in toluene (10 mL) and water (0.33 mL) was added K_2CO_3 (110 mg; 0.80 mmol), and the mixture was stirred at 80 °C for 20 h. TLC control (toluene/ethyl acetate, 4:1) indicated complete conversion, and the emulsion was diluted with toluene (30 mL), allowed to cool to r.t., and washed with water (2 × 10 mL). Drying of the organic phase (Na_2SO_4), filtration and evaporation of the volatile parts gave a colorless oil. Purification by flash column chromatography (SiO_2, toluene/ethyl acetate, 6:1) yielded methyl 3,2-enolone **72** (150 mg; 85%) as a colorless oil.

$R_f = 0.51$ (toluene/ethyl acetate, 4:1); $[\alpha]_D^{20}$ −81.0 (c = 1, $CHCl_3$). UV (acetonitrile) λ_{max} (log ϵ) 263 (3.70), 317 nm (sh, 1.10); ^1H NMR (400.2 MHz, acetone-D_6) δ: 7.45–7.27 (m, 10H, H_{Ar}), 6.27 (d, 1H, $J_{4,5} = 3.4$ Hz, H-4), 4.94–4.87 (m, 2H, CH_2Ph), 4.86 (s, 1H, H-1), 4.83 (ddd, 1H, $J_{5,6a} = 6.4$, $J_{5,6b} = 6.4$, $J_{4,5} = 3.4$ Hz, H-5), 4.64–4.57 (m, 2H, CH_2Ph), 3.81 (dd, 1H, $J_{6a,6b} = 9.7$, $J_{5,6a} = 6.9$ Hz, H-6a), 3.67 (dd, 1H, $J_{6a,6b} = 9.7$, $J_{5,6b} = 6.1$ Hz, H-6b), 3.47 (s, 3H, CH_3); ^{13}C NMR (100.6 MHz, acetone-D_6) δ: 185.0 (C-2), 147.9 (C-3), 139.4, 137.3 (2 × $C_{Ar,q.}$), 129.3, 129.2, 128.9, 128.6, 128.4 (C_{Ar}), 117.5 (C-4), 100.9 (C-1), 74.0 (C-6), 73.7 (CH_2Ph), 72.9 (C-5), 70.3 (CH_2Ph), 56.2 (CH_3); HR-ESI-TOF calcd. for $C_{21}H_{22}O_5Na$ $[M+Na]^+$: 377.1359. Found: 377.1360. Anal. calcd. for $C_{21}H_{22}O_5$: C, 71.17; H, 6.26. Found: C, 70.81; H, 6.39.

***rac*-(4*R*/*S*,5*R*/*S*)-5-Allyloxy-2-benzyloxy-4-benzyloxymethyl-4-hydroxy-cyclopent-2-enone** [(±)-**73**]:

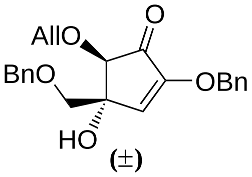

To allyl 3,2-enolone **3b** (170 mg; 0.447 mmol) in anhydrous DMF (8.0 mL) was added NaSPh (30 mg; 0.223 mmol) at r.t., and after 25 min the reaction mixture was heated to 90 °C for 22 h. TLC reaction control (toluene/ethyl acetate, 4:1) confirmed completion of the reaction, and the red solution was allowed to cool to r.t. and neutralized with acetate buffer pH 5 (1 mL). Dilution with CH_2Cl_2 (70 mL), washing with water (20 mL), drying (Na_2SO_4), filtration and evaporation *in vacuo* gave a brown oil. Residual DMF was removed by co-evaporation with *n*-heptane (10 mL), and purification by flash column chromatography (SiO_2, toluene/ethyl acetate, 11:1) gave cyclopentenone **(±)-73** (113 mg; 66%) as a colorless oil.

$R_f = 0.47$ (toluene/ethyl acetate, 4:1); $[\alpha]_D^{20}$ 0 (c = 1, $CHCl_3$); UV (acetonitrile) λ_{max} (log ϵ) 248 (3.90), 323 nm (1.67); ^1H NMR (700.3 MHz, acetone-D_6) δ: 7.42–7.40 (m, 2H, H_{Ar}), 7.39–7.35 (m, 2H, H_{Ar}), 7.35–7.29 (m, 5H, H_{Ar}), 7.27–7.24 (m, 1H, H_{Ar}), 6.33 (s, 1H, H-3), 5.94 (dddd, 1H, $J_{trans} = 17.3$, $J_{cis} = 10.5$, 2 × $J_{vic} = 5.2$ Hz, $H_2C{=}CH\text{-}CH_2\text{-}$), 5.36 (dddd, 1H, $J_{trans} = 17.3$, $J_{gem} = 1.8$, 2 × $^4J = 1.8$ Hz, $H_aH_bC{=}CH\text{-}CH_2\text{-}$), 5.16–

5.14 (m, 1H, visible coupling constant: $J_{cis} = 10.5\,\text{Hz}$, Ha*Hb*C=CH-CH$_2$-), 5.03–4.98 [m, 2H, PhC*H*$_2$O-(C-2)], 4.81 (bs, 1H, OH), 4.52–4.48 (m, 2H, PhC*H*$_2$O-CH$_2$), 4.43 (dddd, 1H, $J_{\text{gem}} = 13.3$, $J_{\text{vic}} = 5.2$, $2 \times {}^4J = 1.6\,\text{Hz}$, H$_2$C=CH-C*Ha*Hb-), 4.32 (dddd, 1H, $J_{\text{gem}} = 13.3$, $J_{\text{vic}} = 5.2$, $2 \times {}^4J = 1.6\,\text{Hz}$, H$_2$C=CH-CHa*Hb*-), 4.06 (s, 1H, H-5), 3.63 (d, 1H, $J_{\text{gem}} = 9.3\,\text{Hz}$, PhCH$_2$O-C*Ha*Hb), 3.57 (d, 1H, $J_{\text{gem}} = 9.3\,\text{Hz}$, PhCH$_2$OCHa*Hb*); ^{13}C NMR (176.1 MHz, acetone-D_6) δ: 196.1 (C-1), 155.2 (C-2), 139.6, 137.0 ($2 \times$ C$_{\text{Ar,q.}}$), 135.7 (H$_2$C=*C*H-CH$_2$-), 129.3, 129.0, 129.0, 128.6, 128.2, 128.1 (C$_{\text{Ar}}$), 127.1 (C-3), 116.8 (H$_2$*C*=CH-CH$_2$-), 87.0 (C-5), 77.9 (C-4), 74.3 (PhCH$_2$O-*C*H$_2$), 73.8 (Ph*C*H$_2$O-CH$_2$), 73.1 (H$_2$C=CH-*C*H$_2$-), 71.8 [Ph*C*H$_2$O-(C-2)]; HR-ESI-TOF calcd. for $C_{23}H_{24}O_5Na$ $[M+Na]^+$: 403.1516. Found: 403.1518; Anal. calcd. for $C_{23}H_{24}O_5$: C, 72.61; H, 6.36. Found: C, 72.65; H, 6.59.

***rac*-(4*R/S*,5*R/S*)-2,5-Bis(benzyloxy)-4-benzyloxymethyl-4-hydroxycyclopent-2-enone [(±)-74]:**

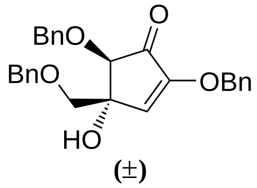

From 40: Benzyl 3,2-enolone **40** (195 mg; 0.453 mmol) was dissolved in anhydrous DMF (11.8 mL), and a freshly prepared solution of KO*t*Bu 2 mg/mL in DMF (1.25 mL; 0.023 mmol) was dropwise added. The resulting yellow solution was heated to 90 °C, upon which the color of the solution changed into a deep red. After 28 h, TLC (toluene/ethyl acetate, 4:1) indicated complete consumption of the starting material, and the reaction was allowed to cool to r.t. The reaction mixture was neutralized by the addition of acetate buffer pH 5 (1 mL). Next, the solution was diluted with CH$_2$Cl$_2$ (50 mL), washed with water (2 × 15 mL), dried (Na$_2$SO$_4$), filtered, and evaporated to dryness. Residual DMF was removed by co-evaporation with *n*-heptane (10 mL) to give a brown oil. Purification by flash column chromatography (SiO$_2$, toluene/ethyl acetate, 10:1) gave cyclopentenone **(±)-74** (153 mg; 78%) as a colorless oil.

From 2b: To a solution of benzyl 2-uloside **2b**[37] (243 mg; 0.451 mmol) in anhydrous DMF (14.8 mL) was dropwise added a freshly prepared solution of KO*t*Bu 2 mg/mL in DMF (1.25 mL; 0.023 mmol). The solution was heated to 50 °C and stirred for 3 h. TLC (toluene/ethyl acetate, 4:1) indicated complete conversion of the starting material to the intermediate 3,2-enolone **40**, and the temperature was elevated to 90 °C. The dark red solution was stirred at this temperature for 30 h, after which time TLC suggested completion of the reaction. The solution was allowed to cool to r.t., and was then neutralized by the addition of acetate buffer pH 5 (1 mL). Dilution with CH_2Cl_2 (50 mL), washing with water (2 × 15 mL), drying (Na_2SO_4), filtration and evaporation gave a brown oil, which was co-evaporated with *n*-heptane (10 mL) to remove residual DMF. The crude product was purified by flash column chromatography (SiO_2, toluene/ethyl acetate, 10:1) to yield cyclopentenone **(±)-74** (166 mg; 85%) as a colorless oil.

$R_f = 0.52$ (toluene/ethyl acetate, 4:1). $[\alpha]_D^{20}$ 0 (c = 1, $CHCl_3$). UV (acetonitrile) λ_{max} (log ϵ) 239 (3.62), 246 (3.61), 284 (sh, 2.57), 316 nm (sh, 2.09). ^1H NMR (700.3 MHz, acetone-D_6) δ: 7.45–7.40 (m, 4H, H_{Ar}), 7.39–7.33 (m, 5H, H_{Ar}), 7.31–7.28 (m, 5H, H_{Ar}), 7.26–7.23 (m, 1H, H_{Ar}), 6.35 (s, 1H, H-3), 5.03–4.98 [m, 3H, PhCH_2O-(C-2), PhC*Ha*HbO-(C-5)], 4.89–4.85 [m, 2H, PhCHa*Hb*O-(C-5), OH], 4.52–4.48 (m, 2H, PhCH_2O-CH_2), 4.14 (s, 1H, H-5), 3.67 (d, 1H, J_{gem} = 9.3 Hz, $PhCH_2O$-C*Ha*Hb), 3.63 (d, 1H, J_{gem} = 9.3 Hz, $PhCH_2O$-CHa*Hb*); ^{13}C NMR (176.1 MHz, acetone-D_6) δ: 196.2 (C-1), 155.2 (C-2), 139.5, 139.3, 137.0 (3 × $C_{Ar,q.}$), 129.3, 129.1, 129.0, 129.0, 128.6, 128.4, 128.3, 128.2, 128.1 (C_{Ar}), 127.1 (C-3), 87.1 (C-5), 78.0 (C-4), 74.3 ($PhCH_2O$-CH_2), 74.0 [Ph*C*H_2O-(C-5)], 73.8 (Ph*C*H_2O-CH_2), 71.8 [Ph*C*H_2O-(C-2)]; HR-ESI-TOF calcd. for $C_{27}H_{26}O_5Na$ $[M+Na]^+$: 453.1672. Found: 453.1675. Anal. calcd. for $C_{27}H_{26}O_5$: C, 75.33; H, 6.09. Found: C, 75.01; H, 6.25.

rac-(4*R*/*S*,5*R*/*S*)-2-Benzyloxy-4-benzyloxymethyl-4-hydroxy-5-methoxy-cyclopent-2-enone [(±)-75]:

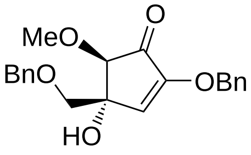

(±)

From 72: To a solution of methyl 3,2-enolone **72** (83 mg; 0.234 mmol) in anhydrous DMF (8.3 mL) was added a freshly prepared solution of KO*t*Bu 2 mg/mL in DMF (0.65 mL; 0.012 mmol), and the yellow solution was heated to 90 °C. The resulting deep red reaction mixture was stirred at 90 °C for 75 min, after which time TLC (toluene/ethyl acetate, 4.1) indicated complete conversion of the starting material. The solution was allowed to cool to r.t. and was then neutralized with acetate buffer pH 5 (1 mL). Dilution with CH_2Cl_2 (50 mL), washing with water (20 mL), drying (Na_2SO_4), filtration and evaporation of the volatile parts gave a yellow oil. Residual DMF was removed by co-evaporation of the crude product with *n*-heptane (10 mL). Purification by flash column chromatography (SiO_2, toluene/ethyl acetate, 10:1) yielded, as a side product, **(±)-76** (7 mg; 8%) with higher chromatographic mobility, together with **(±)-75** (59 mg; 71%) as the major isomer in the form of a colorless oil.

From 2c: A solution of methyl 2-uloside **2c**[69] (113 mg; 0.244 mmol) in anhydrous DMF (8 mL) at r.t. was treated with a freshly prepared solution of KO*t*Bu 2 mg/mL in DMF (0.68 mL; 0.012 mmol), and the yellow reaction mixture was stirred for 24 h at r.t. TLC reaction control (toluene/ethyl acetate, 4:1) indicated the complete formation of the intermediate **72**. Next, the temperature was elevated to 50 °C, and two additional portions of KO*t*Bu 2 mg/mL in DMF (2 × 0.68 mL; 0.024 mmol) were added when TLC showed reluctant further progression of the reaction. After stirring at 50 °C for a total reaction time of 18 h, the red solution was allowed to cool to r.t. The mixture was neutralized with acetate buffer pH 5 (1 mL), diluted with CH_2Cl_2 (50 mL), washed with water (2 × 25 mL), dried (Na_2SO_4), filtered and evaporated. The resulting brown oil was co-evaporated with *n*-heptane (10 mL), and purified by flash column chromatography (SiO_2, toluene/ethyl acetate, 9:1) to provide **(±)-75** (53 mg; 61%) as a colorless oil. Single crystals of **(±)-75** suitable for X-ray crystallography were obtained from toluene/*n*-pentane. Analytical data for **(±)-75:**

$R_f = 0.52$ (toluene/ ethyl acetate, 4:1); $[\alpha]_D^{20}$ 0 (c = 1, $CHCl_3$); UV (acetonitrile) λ_{max} (log ϵ) 248 (3.99), 323 nm (sh, 1.90); ^1H NMR (600.1 MHz, acetone-D_6) δ: 7.43–7.40 (m, 2H, H_{Ar}), 7.39–7.28 (m, 7H, H_{Ar}), 7.28–7.24 (m, 1H, H_{Ar}), 6.32 (s, 1H, H-3), 5.03–4.97 [m, 2H, $PhCH_2O$(C-2)], 4.75 (bs, 1H, OH), 4.52–4.47 (m, 2H, $PhCH_2O$-CH_2), 3.88 (s, 1H, H-5), 3.64 (s, 3H, CH_3), 3.61 (d, 1H, J_{gem} = 9.3 Hz, $PhCH_2O$-C*Ha*Hb), 3.53 (d, 1H, J_{gem} = 9.3 Hz, $PhCH_2O$-CHa*Hb*); ^{13}C NMR (100.6 MHz, acetone-D_6) δ: 196.2 (C-1), 155.1 (C-2), 139.6, 137.0 (2 × $C_{Ar,q.}$), 129.3, 129.0, 129.0, 128.6, 128.2, 128.1 (C_{Ar}), 127.1 (C-3), 89.4 (C-5), 77.8 (C-4), 74.3 ($PhCH_2O$-*C*H_2), 73.8 (Ph*C*H_2O-CH_2), 71.8 [Ph*C*H_2O-(C-2)], 60.4 (CH_3); HR-ESI-TOF calcd. for $C_{21}H_{22}O_5Na$ $[M+Na]^+$: 377.1359. Found: 377.1361; Anal. calcd. for $C_{21}H_{22}O_5$: C, 71.17; H, 6.26. Found: C, 71.35; H 6.47.

***rac*-(4*R*/*S*,5*S*/*R*)-2-Benzyloxy-4-benzyloxymethyl-4-hydroxy-5-methoxycyclopent-2-enone [(±)-76]:**

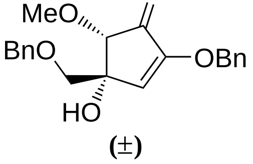

Isolated as the minor diastereoisomer (7 mg; 8%) in the formation of **(±)-75** from **72** as described above:

$R_f = 0.55$ (toluene/ethyl acetate, 4:1); $[\alpha]_D^{20}$ 0 (c = 1, $CHCl_3$). ^1H NMR (600.1 MHz, acetone-D_6) δ: 7.44–7.41 (m, 2H, H_{Ar}), 7.40–7.33 (m, 7H, H_{Ar}), 7.31–7.27 (m, 1H, H_{Ar}), 6.42 (s, 1H, 3H), 5.02-4.98 [m, 2H, PhCH_2O-(C-2)], 4.62–4.56 (m, 2H, PhCH_2OCH$_2$), 3.96 (bs, 1H, OH), 3.82 (s, 1H, H-5), 3.65 (d, 1H, J_{gem} = 9.4 Hz, PhCH$_2$O-C*Ha*Hb), 3.60–3.57 (m, 4H, PhCH$_2$O-CHa*Hb*, CH$_3$); ^{13}C NMR (100.6 MHz, acetone-D_6) δ: 198.3 (C-1), 156.9 (C-2), 139.4, 137.0 (2 × $C_{\mathrm{Ar,q.}}$), 129.3, 129.2, 129.0, 128.7, 128.6, 128.6, 128.5 (C_{Ar}), 128.4 (C-3), 81.2 (C-5), 75.3 (PhCH$_2$O-*C*H$_2$), 74.0 (Ph*C*H$_2$O-CH$_2$), 72.1 [Ph*C*H$_2$O-(C-2)], 60.0 (CH$_3$); HR-ESI-TOF calcd. for $C_{21}H_{22}O_5Na$ [M+Na]$^+$: 377.1359. Found: 377.1358.

***rac*-(4*R*/*S*,5*S*/*R*)-2,5-Bis(benzyloxy)-4-benzyloxymethyl-4-hydroxycyclopent-2-enone** [**(±)-77**]:

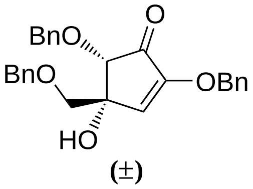

(±)

To a solution of 5-benzyloxycyclopent-2-enone **(±)-74** (69 mg; 0.160 mmol) in anhydrous DMF (3.3 mL) was added a freshly prepared solution of KO*t*Bu 2 mg/mL in DMF (1.35 mL; 0.024 mmol), and the reaction mixture was heated to 70 °C. After 24 h, the mixture was allowed to cool to r.t., and acetate buffer pH 5 (1 mL) was added to the dark brown solution. All volatile components were evaporated *in vacuo*. Benzaldehyde (19.2 mg) was added to the crude product mixture as an internal integration standard to determine the amount of unreacted **(±)-74** (43%), of diastereoisomer **(±)-77** (20%), and of regioisomer **(±)-78** (16%) by ^{1}H NMR integration. Chromatographic purification (SiO$_2$, toluene/ethyl acetate, 12:1 to 10:1) afforded **(±)-77** (12 mg, 17%) as a yellow oil as the product with higher chromatographic mobility, along with **(±)-78** (11 mg, 16%). Analytical data for **(±)-77:**

R_f = 0.54 (toluene/ethyl acetate, 4:1); $[\alpha]_D^{20}$ 0 (c = 1, CHCl$_3$); ^{1}H NMR (600.1 MHz, acetone-D_6) δ: 7.45–7.27 (m, 15H, H_{Ar}), 6.43 (s, 1H, H-3), 5.02–5.00 [m, 2H, PhCH_2O-(C-2)], 4.90 [d, 1H, J_{gem} = 11.9 Hz, PhC*Ha*HbO-(C-5)], 4.85 [d, 1H, J_{gem} = 11.9 Hz, PhCHa*Hb*O-(C-5)], 4.53 (d, 1H, J_{gem} = 12.1 Hz, PhC*Ha*HbO-CH$_2$), 4.50 (d, 1H, J_{gem} = 11.9 Hz, PhCHa*Hb*O-CH$_2$), 4.10 (bs, 1H, OH), 4.08 (s, 1H, H-5), 3.60 (d, 1H, J_{gem} = 9.4 Hz, PhCH$_2$O-C*Ha*Hb), 3.57 (d, 1H, J_{gem} = 9.4 Hz, PhCH$_2$O-CHa*Hb*); ^{13}C NMR (150.9 MHz, acetone-D_6) δ: 198.6 (C-1), 157.0 (C-2), 139.3, 139.1, 137.0 (3 × $C_{\mathrm{Ar,q.}}$), 129.4, 129.1, 129.1, 129.1, 128.9, 128.7 (C_{Ar}), 128.7 (C-3), 128.6, 128.5, 128.4 (C_{Ar}), 78.9 (C-5), 75.1 (PhCH$_2$O-*C*H$_2$), 74.7 (C-4), 74.0 (Ph*C*H$_2$O-CH$_2$), 73.8 [Ph*C*H$_2$O-(C-

5)], 72.1 [Ph*C*H$_2$O-(C-2)]; HR-ESI-TOF calcd. for $C_{27}H_{26}O_5Na$ $[M+Na]^+$: 453.1672. Found: 453.1674.

***rac*-(4*R*/*S*,5*R*/*S*)-3,5-Bis(benzyloxy)-4-benzyloxymethyl-4-hydroxycyclopent-2-enone [(±)-78]:**

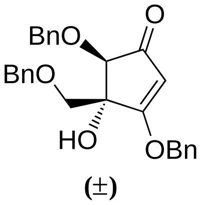

Cyclopent-2-enone **(±)-78** (11 mg; 16%) was isolated as a minor regioisomer, together with **(±)-77**, in the transformation of **(±)-74** as described above. Analytical data for **(±)-78:**

$R_f = 0.42$ (toluene/ethyl acetate, 4:1); $[\alpha]_D^{20}$ 0 (c = 1, $CHCl_3$); ^{1}H NMR (600.1 MHz, acetone-D_6) δ: 7.47–7.44 (m, 4H, H_{Ar}), 7.40–7.32 (m, 5H, H_{Ar}), 7.29–7.21 (m, 6H, H_{Ar}), 5.46 (s, 1H, H-2), 5.19–5.13 [m, 2H, PhC*H*$_2$O-(C-3)], 5.07–5.04 [m, 2H, OH, PhC*Ha*HbO-(C-5)], 4.87 [d, 1H, J_{gem} = 12.1 Hz, PhCHa*Hb*O-(C-5)], 4.54 (d, 1H, J_{gem} = 12.1 Hz, PhC*Ha*HbO-CH$_2$), 4.48 (d, 1H, J_{gem} = 12.1 Hz, PhCHa*Hb*O-CH$_2$), 4.16 (s, 1H, H-5), 3.78–3.76 (m, 2H, PhCH$_2$O-C*H*$_2$); ^{13}C NMR (150.9 MHz, acetone-D_6) δ: 197.9 (C-1), 183.2 (C-3), 139.6, 139.5, 136.2 (3 × $C_{Ar,q.}$), 129.4, 129.2, 129.0, 129.0, 128.8, 128.3, 128.3, 128.2, 128.1 (C_{Ar}), 104.3 (C-2), 87.0 (C-5), 80.2 (C-4), 74.1 [Ph*C*H$_2$-O-(C-5)], 73.9 (Ph*C*H$_2$O-CH$_2$), 73.7 [Ph*C*H$_2$O-(C-3)], 71.6 (PhCH$_2$O-*C*H$_2$); HR-ESI-TOF calcd. for $C_{27}H_{26}O_5Na$ $[M+Na]^+$: 453.1672. Found: 453.1672.

7. Summary of Results

In the course of this thesis, synthetic and structural studies have been performed on complex carbohydrate scaffolds of interest. In this regard, the results described here offer a contribution to the chemistry of higher-carbon sugars with structural relations to either naturally occurring complex sugars, or to carbohydrate analogs with potential biological applications. Detailed investigations into the reactivities of the synthetic intermediates provided further insight into widely employed classes of carbohydrate building blocks. Compound classes with special relevance to the synthetic routes described here are 2-*keto*-sugars (2-ulosides) and 2-*C*-branched sugars. Consequently, this thesis contains contributions to the chemistry of these important carbohydrate frameworks.

As universal intermediates towards the target structures of this thesis, 3,4,6-*O*-benzylated β-2-ulosides of type **2** were required. In this regard, preliminary examinations focussed on the synthesis of the unknown allyl 2-uloside **2a**, a sensitive intermediate prone to elimination of the 4-benzyloxy group. Whereas glycosylation-based methods with the corresponding 2-ulosyl bromide donor met with failure, Dess-Martin oxidation of the respective 2-*O*-unprotected glucoside **7** proved to be suitable and provided the sensitive 2-*keto*-sugar **2a** reliably. The corresponding benzyl 2-uloside **2b** and methyl 2-uloside **2c**, which have both been prepared previously by other methods, could also be obtained in this way from the known 2-*O*-unprotected glucosides **8** and **11**. X-ray structural analyses on both the known glucoside **11** and the corresponding known 2-uloside **2b** provided insight into structural features of 2-*keto*-sugars, and confirmed that **2b** occupied a distorted $^4C_1$ conformation.

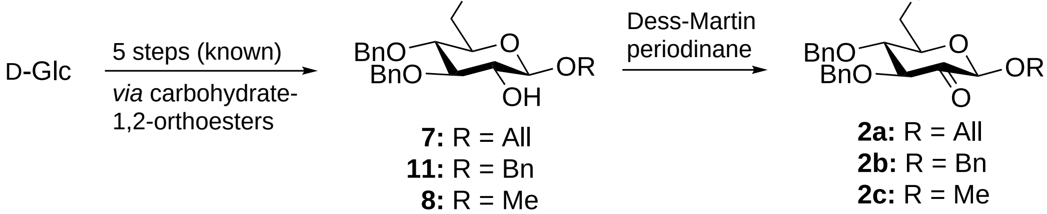

7: R = All
11: R = Bn
8: R = Me

2a: R = All
2b: R = Bn
2c: R = Me

(83 to 96%)

β-2-Ulosides structurally similar to intermediates **2a,b,c** have been shown to undergo carbonyl addition reactions with equatorial selectivity, giving the respective carbon-branched mannoside products. In this way, derived from ketones **2a,b**, various novel 2-*C*-branched mannosides could be synthesized by the reaction with Grignard reagents or alkynyllithium nucleophiles. The obtained products included the vinyl-branched allyl mannoside **16**, as well as 2-*C*-(*Z*)-alkenyl branched mannosides **23** or **36**, both derived from Lindlar hydrogenation of the respective alkynes. This set of unsaturated branched mannosides could be extended by routine protecting group transformations, or by reacting substrates **2** with other metalated alkynes in a similar manner. The Lindlar hydrogenations of alkynes of type **22** required optimized conditions, and DMF as the solvent was found to significantly accelerate the semihydrogenations of these sterically crowded branched alkynes. The structure of **23**, which exhibited rotameric isomerism in NMR experiments, was furthermore confirmed by X-ray crystallography. Apart from serving as intermediates in the target-oriented syntheses as described below, these molecular scaffolds can be expected to be useful carbohydrate building blocks due to the straightforward functionalization of the introduced unsaturations.

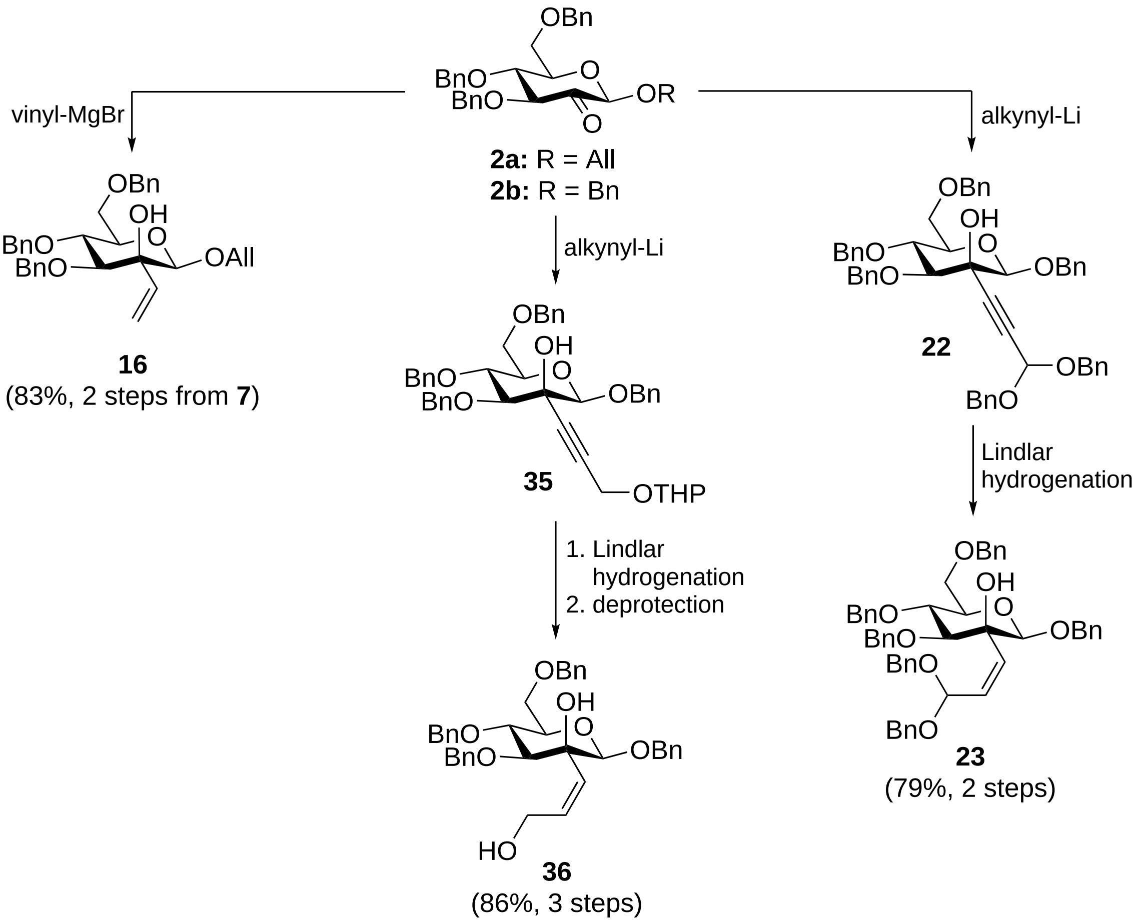
OBn
BnO
BnO
O
OR
O
2a: R = All
2b: R = Bn
vinyl-MgBr
alkynyl-Li
alkynyl-Li
OBn
OH
O
OAll
16
(83%, 2 steps from 7)
OTHP
35
1. Lindlar hydrogenation
2. deprotection
HO
36
(86%, 3 steps)
22
Lindlar hydrogenation
23
(79%, 2 steps)

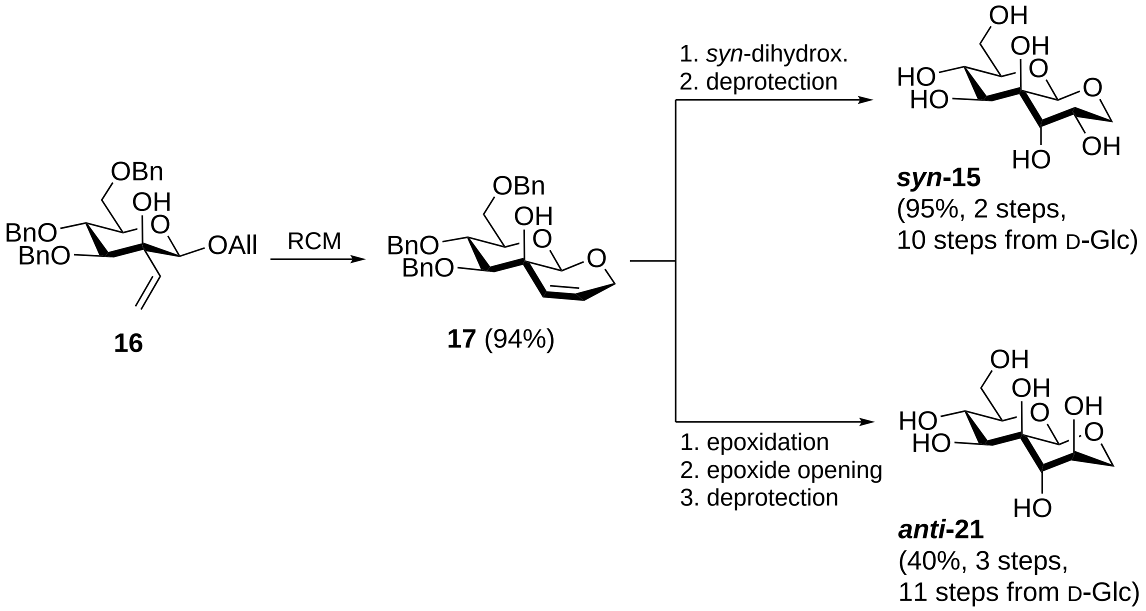

In one target-oriented synthetic project, the synthesis of 1,2-annulated bicyclic carbohydrates was explored. Such rigid, conformationally fixed sugar derivatives have been shown to act as carbohydrate mimetic inhibitors for several natural glycosidases, an enzyme class widely associated with severe diseases, and thus, medicinally relevant. Starting from vinyl-branched mannoside **16**, a synthetic strategy involving ring-closing metathesis followed by *syn*-dihydroxylation or epoxidation/epoxide opening provided target structures ***syn*-15** and ***anti*-21**, which can be described as polyhydroxylated 2,10-dioxadecalin derivatives. Both highly polar bicyclic sugars exhibited a *trans*-decalin core structure, and were amenable to full NMR characterization in D_2O. The structure of ***syn*-15** could additionally be confirmed by X-ray crystallography, which provided insight into a dense network of hydrogen-bonding interactions of the hydroxyl-rich sugar hybrid in the solid state. Structurally related 1,2-annulated sugars have been reported before. However, the developed synthetic strategy involving allyl 2-uloside **2a** facilitated the synthesis of such frameworks with the traditionally challenging β-*manno*-configuration. In this regard, the results discussed here are a valuable contribution to synthetic strategies for bicyclic carbohydrate mimetics.

In contrast to these conformationally rigid annulated sugars, a second project targeted the synthesis of structurally diverse reducing sugars with multiple cyclic hemiacetal forms. Inspired by the annulated major isomer of the unusual natural monosaccharide bradyrhizose (structure **K**), the synthesis of similar cyclic hemiacetals with a conventional pyranose (β-mannose) instead of the carbasugar moiety was pursued. The natural bradyrhizose **K** was isolated from Gram-negative nitrogen-fixing soil bacteria,

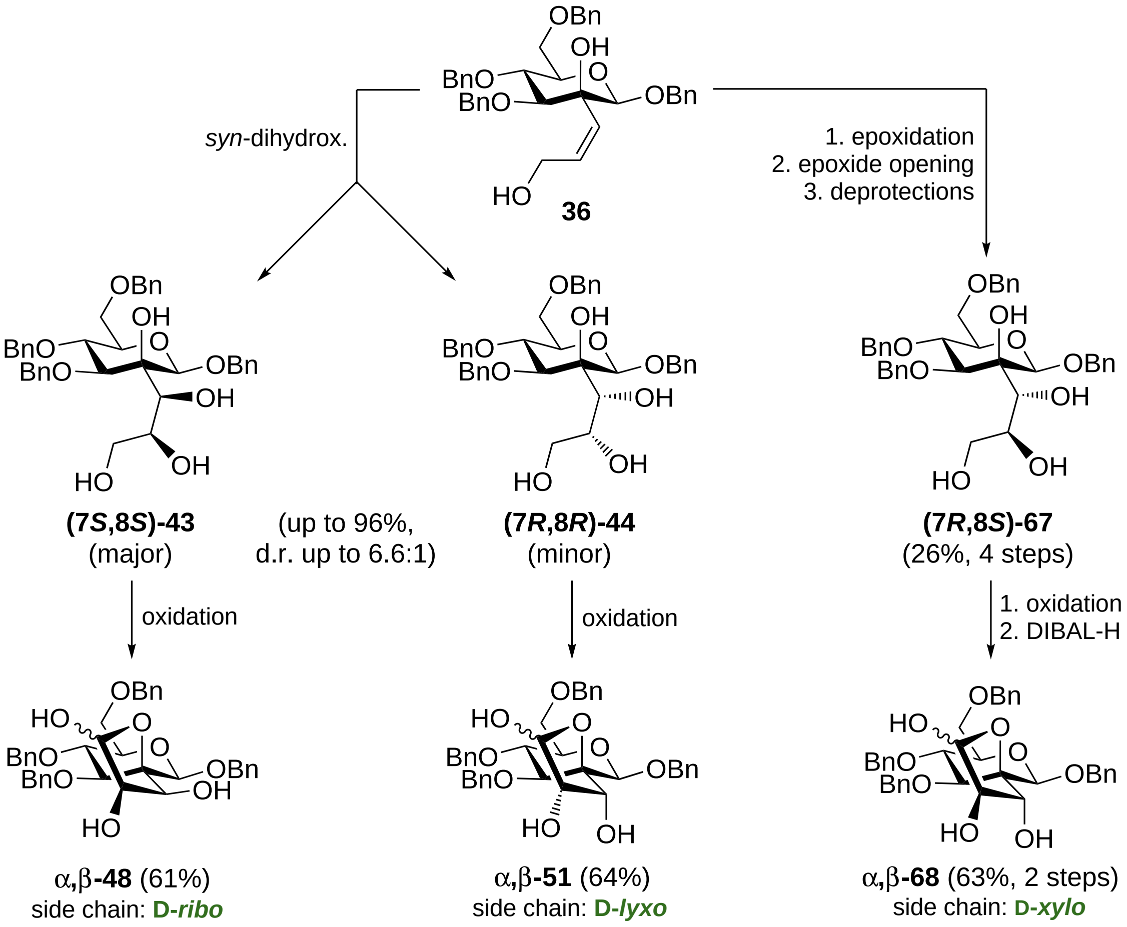
syn-dihydrox.
36
1. epoxidation
2. epoxide opening
3. deprotections
(7S,8S)-43
(major)
(up to 96%,
d.r. up to 6.6:1)
(7R,8R)-44
(minor)
(7R,8S)-67
(26%, 4 steps)
oxidation
oxidation
1. oxidation
2. DIBAL-H
α,β-48 (61%)
side chain: D-ribo
α,β-51 (64%)
side chain: D-lyxo
α,β-68 (63%, 2 steps)
side chain: D-xylo

and its unusual structure is believed to play a role in the initiation of symbiosis with legume host plants. Due to these biological aspects, and due to an interesting equilibrium of hemiacetal isomers of **K**, the synthesis of these higher sugar analogs was desirable. In an optimized synthetic approach towards such structures, side chain allyl alcohol **36** was transformed into the fully hydroxylated propyl-branched mannosides **(7*S*,8*S*)-43**, **(7*R*,8*R*)-44** and **(7*R*,8*S*)-67** *via* osmium-based *syn*-dihydroxylation or *via* an epoxidation/epoxide opening sequence. The configurations of the hydroxylated side chains of these intermediates could be fully established by NMR experiments and X-ray structural analyses of suitable derivatization products. Subsequently, selective oxidation of the primary alcohol functionalities gave spirofuranose-pyranoses **α,β-48**, **α,β-51** and **α,β-68** with diverse stereochemical configurations of the furanose moieties (D-*ribo*, -*lyxo* and -*xylo*, respectively). Selective oxidation methods utilizing catalytic TEMPO under reported conditions failed to give these intermediates in a clean manner. Therefore, a novel oxidation protocol involving TEMPO/trichloroisocyanuric acid in connection with an optimized solvent/buffer system had to be established, and proved to be an effective and mild oxidation method for other sensitive substrates. In the transformation of the *anti*-isomer **(7*R*,8*S*)-67**, overoxidation to the lactone occurred, and therefore a following reduction step was required to provide the wanted hemiacetal **α,β-68**. The obtained spirofuranose-pyranose hybrid molecules constituted a new class of structurally interesting complex carbohydrates, and could be fully characterized as α/β-mixtures *via* 2D NMR experiments. In the final global debenzylation step, these spirofuranoses liberated the target molecules, represented by the 4-*C*-formyl branched octoses ***syn*-50**, ***syn*-52** and ***anti*-70** in the open-chain forms. Detailed NMR-based structural investigations into the major cyclic hemiacetal forms in D_2O revealed that the anticipated bradyrhizose-type acetal-hemiacetal-isomers (see bottom) did not represent major isomeric forms of the compounds. Instead, the respective bis(hemiacetal) forms

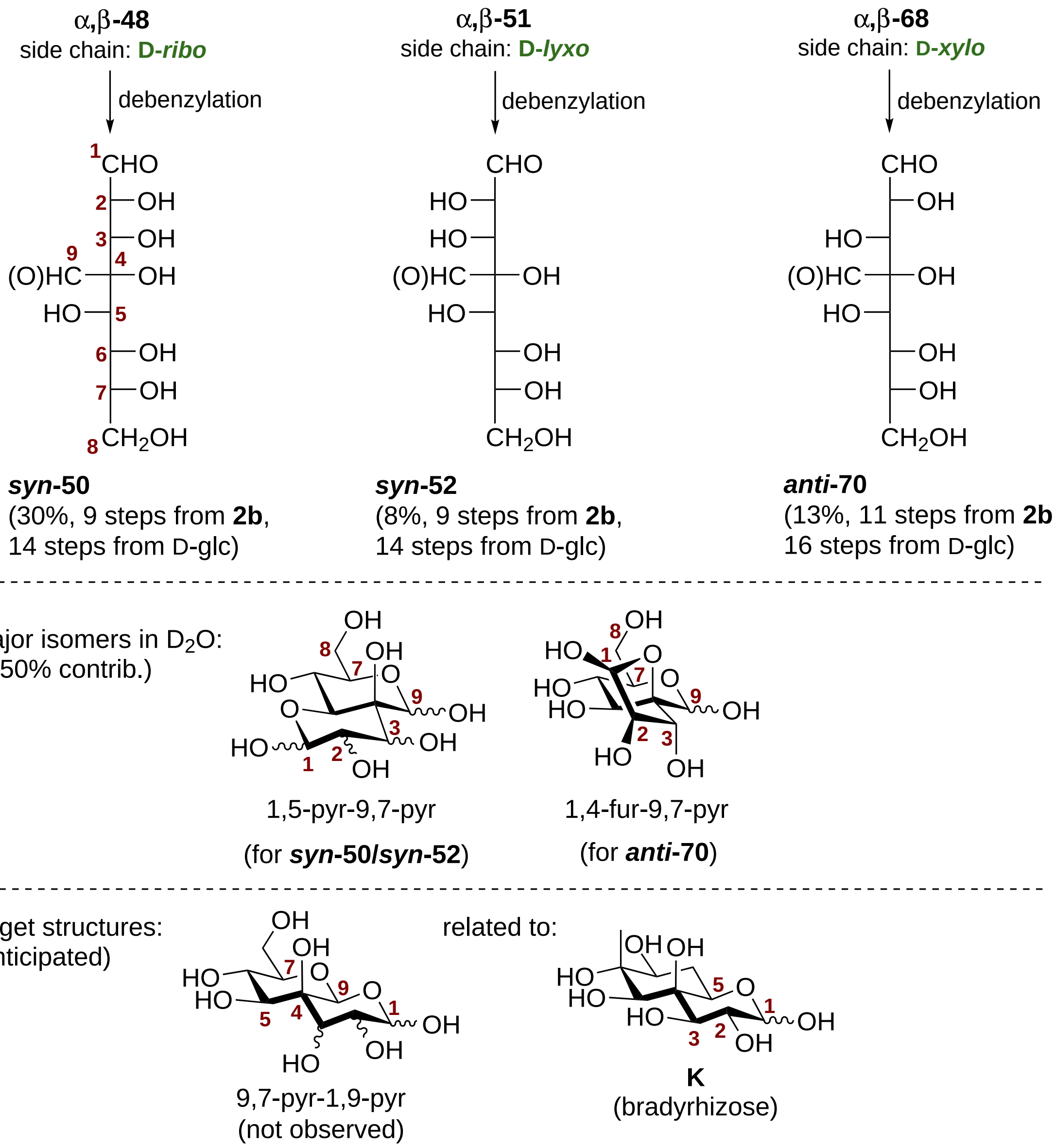
α,β-48
side chain: D-ribo
debenzylation
α,β-51
side chain: D-lyxo
debenzylation
α,β-68
side chain: D-xylo
debenzylation
1 CHO
2 OH
3 OH
9 (O)HC
4 OH
HO 5
6 OH
7 OH
8 CH2OH
syn-50
(30%, 9 steps from 2b,
14 steps from D-glc)
syn-52
(8%, 9 steps from 2b,
14 steps from D-glc)
anti-70
(13%, 11 steps from 2b,
16 steps from D-glc)
major isomers in D2O:
(> 50% contrib.)
1,5-pyr-9,7-pyr
(for syn-50/syn-52)
1,4-fur-9,7-pyr
(for anti-70)
target structures:
(anticipated)
9,7-pyr-1,9-pyr
(not observed)
related to:
K
(bradyrhizose)

(1,5-pyranose-9,7-pyranoses or spiro-1,4-furanose-9,7-pyranoses) were identified to be the major species in solution. These results indicated a distinct alteration of the preferred hemiacetal isomeric forms upon changing the carbasugar motif of bradyrhizose into a conventional β-mannoside structure. Although this suggested that the obtained target structures were no suitable analogs for the natural bradyrhizose monosaccharide, the presented work is an addition to the chemistry of higher-carbon sugars, to selective oxidation reactions of polyhydroxylated substrates, and to the complex stereochemistry of carbohydrate structures in general.

In a concluding project, basic reactivities were explored starting from the 2-*keto*-sugars **2a,b,c**. Treatment of these substrates with basic reagents (K_2CO_3) invoked an elimination of benzyl alcohol and formation of the carbohydrate 3,2-enolones **3b/40/72**. Similar observations have been described in the literature as a universal degradation reaction of 2-*keto*-sugars which is particularly frequent for ester-protected substrates. Upon subjecting these α,β-unsaturated carbonyl compounds to basic conditions in polar aprotic solvents (e.g. KO*t*Bu in DMF), a novel rearrangement into racemic 2-benzyloxy-4-benzyloxymethyl-4-hydroxy-2-alkoxycyclopent-2-enones was initiated. Mechanistic considerations suggested a cascade involving electrocyclic ring-opening to an achiral open-chain enolate species, followed by electrocyclic or intramolecular aldol-type ring closure towards the products **(±)-73,74,75**. Additionally, under the conditions of the re-arrangement, 2-ulosides **2b,c** could be transformed into the respective cyclopent-2-enone products in an elimination-rearrangement cascade process. Comparable rearrangements have been reported previously, however, these reactions resulted in the formation of the regioisomeric 5-hydroxycyclopent-2-enones. Mechanistic explanations for this experimental difference could be established. Furthermore, close investigations into observable side products and isomerization processes of the rearrangement reaction

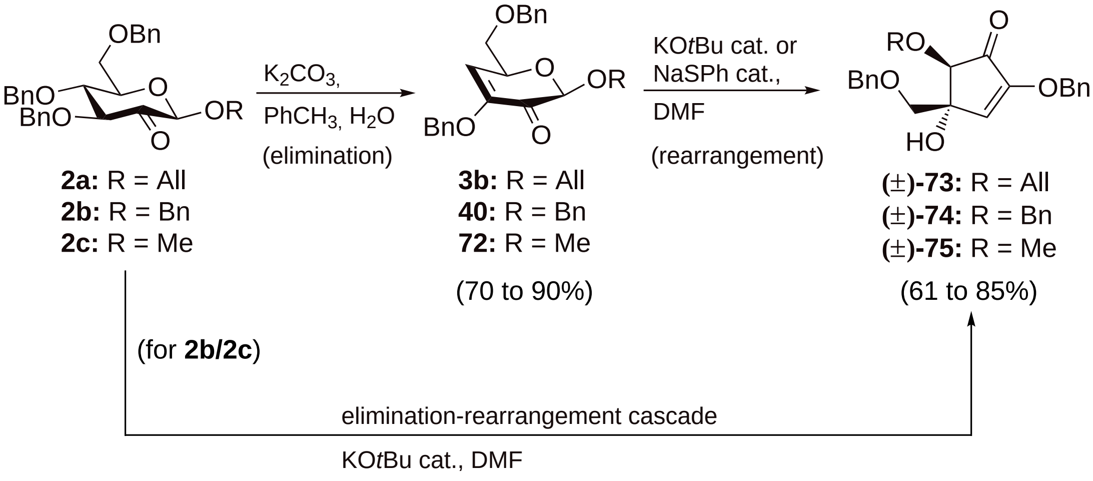
OBn
BnO
BnO
O
OR
O
2a: R = All
2b: R = Bn
2c: R = Me
K2CO3,
PhCH3, H2O
(elimination)
OBn
O
OR
BnO
O
3b: R = All
40: R = Bn
72: R = Me
(70 to 90%)
KOtBu cat. or
NaSPh cat.,
DMF
(rearrangement)
RO
O
BnO
OBn
HO
(±)-73: R = All
(±)-74: R = Bn
(±)-75: R = Me
(61 to 85%)
(for 2b/2c)
elimination-rearrangement cascade
KOtBu cat., DMF

provided an additional understanding of this interesting transformation in the context of the molecular diversity of unsaturated carbohydrates and the derived carbocyclic products.

List of Abbreviations and Symbols

1,2-DCE 1,2-dichloroethane

2,2-DMP 2,2-dimethoxypropane

α specific rotation

α anomeric descriptor in carbohydrate structures

β anomeric descriptor in carbohydrate structures

Å Angstrom; 0.1 nm

Ac acetyl

acac acetylacetonate

AD asymmetric dihydroxylation

AIBN azobisisobutyronitrile

Aliquat 336 *N*-methyl-*N*,*N*,*N*-trioctylammonium chloride

All allyl

Ar aryl

ATCC American Type Culture Collection

BINOL 1,1'-bi-2-naphthol

Bn benzyl

Boc *tert*-butyloxycarbonyl

BQ benzoquinone

Bz benzoyl

brsm based on recovered starting material

bs broad singlet (NMR)

C chair conformation

calcd. calculated

cl. cleavage

CLB *para*-chlorobenzoate

CM cytoplasmic membrane

COSY correlation spectroscopy (NMR)

CSA camphorsulfonic acid

δ chemical shift in NMR spectroscopy [ppm]

d doublet (NMR)

DABCO 1,4-diazabicyclo[2.2.2]octane

dd doublet of doublets (NMR)

DEPT distortionless enhancement by polarization transfer (NMR)

DHQ dihydroquinine

DHQD dihydroquinidine

DIBAL-H diisobutylaluminium hydride

DIC *N,N'*-diisopropylcarbodiimide

diglyme bis(2-methoxyethyl) ether

DMAP 4-dimethylaminopyridine

DMDO dimethyldioxirane

DMF dimethylformamide

DMP Dess-Martin periodinane

DMSO dimethyl sulfoxide

DNJ 1-deoxynojirimycin

d.r. diastereomeric ratio

ϵ molar attenuation coefficient

E envelope conformation

EC Enzyme Commission number

ee enantiomeric excess

EPR electron paramagnetic resonance

equiv. equivalents

ESI electrospray ionization

FAB fast atom bombardment

FTICR fourier-transform ion cyclotron resonance

Fuc L-fucose

FUR furanose

Gal D-galactose

GC gas chromatography

gem geminal

GH glycoside hydrolase, glycosidase

Glc D-glucose

GlcN D-glucosamine

GlcNAc *N*-acetyl-D-glucosamine

GlcOS D-glucosone

GT glycosyltransferase

H half-chair conformation

H.-G. Hoveyda-Grubbs catalyst

HMBC heteronuclear multiple bond correlation (NMR)

HMDS hexamethyldisilazide

HPLC high-performance liquid chromatography

HQ hydroquinone

HR high resolution

HSQC heteronuclear single quantum coherence (NMR)

***i*-Bu** isobutyl

IM intramolecular

IND indolinyl

***i*-Pr** isopropyl

IUPAC International Union for Pure and Applied Chemistry

J coupling constant in NMR spectroscopy [Hz]

Kdo 3-deoxy-α-D-*manno*-oct-2-ulosonic acid

LA Lewis acid

LDA lithium diisopropylamide

LDmanHep L-*glycero*-D-*manno*-heptose

LPS lipopolysaccharides

m multiplet (NMR)

***m*-CPBA** *meta*-chloroperoxybenzoic acid

Me methyl

MMPP magnesium monoperoxyphthalate

MOPS 3-(*N*-morpholino)propanesulfonic acid

M.p. melting point

MS mass spectrometry

MS molecular sieves

MTPA α-methoxy-α-(trifluoromethyl)phenylacetic acid

NBS *N*-bromosuccinimide

***n*-Bu** *n*-butyl

Neu neuraminic acid

NMO *N*-methylmorpholine *N*-oxide

NOE nuclear overhauser effect (NMR)

NOESY nuclear overhauser spectroscopy (NMR)

OM outer membrane

OMP outer membrane proteins

ox. oxidation

PBN *N*-*tert*-butyl-α-phenylnitrone

PDH pyranose 2-dehydrogenase

Pg protecting group

PHAL phthalazine

POx pyranose 2-oxidase

Py pyridine

PYR pyranose

q. quaternary

RCM ring-closing metathesis

RDS rate-determining step

red. reduction

R_f retention factor (TLC)

RP reversed phase

r.t. room temperature

s singlet (NMR)

sat. saturated

SET single electron transfer

sh shoulder (UV/Vis spectroscopy)

Sug sugar

t triplet (NMR)

TBAF tetra-*n*-butylammonium fluoride

TBDPS *tert*-butyldiphenylsilyl

TBS *tert*-butyldimethylsilyl

***t*-Bu** *tert*-butyl

TCICA trichloroisocyanuric acid

TEMPO 2,2,6,6-tetramethylpiperidin-*N*-oxyl

Tf trifluoromethanesulfonyl

TFA trifluoroacetic acid

TFAA trifluoroacetic acid anhydride

TFE 2,2,2-trifluoroethanol

THF tetrahydrofuran

THP tetrahydro-2*H*-pyran-2-yl

TIPS triisopropylsilyl

TLC thin-layer chromatography

TMS trimethylsilyl

TOCSY total correlation spectroscopy (NMR)

TOF time of flight ion separation

TS	transition state
Ts	toluenesulfonyl
UV	ultraviolet radiation
vic	vicinal
Vis	visible light

List of Compounds

Given below is a list of all numbered compounds, and cross-references to the corresponding reaction schemes are included. For compounds isolated multiple times from different reactions, the respective highest yield synthesis is referenced. Additionally, literature references are given for known compounds.

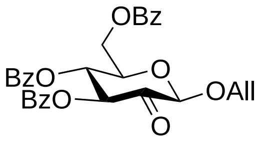

1a
(Scheme 2.10)

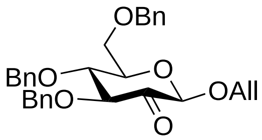

2a
(Scheme 2.13)

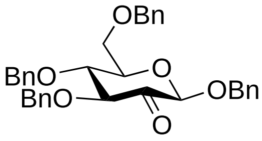

2b [37]
(Scheme 2.13)

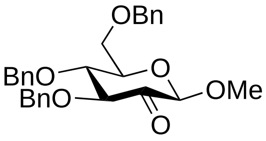

2c [69]
(Scheme 2.13)

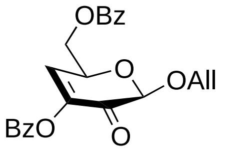

3a
(Scheme 2.10)

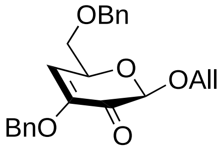

3b
(Scheme 5.7)

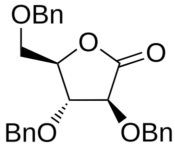

4 [59,60]
(Scheme 2.10)

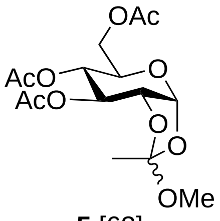

5 [63]
(Scheme 2.11)

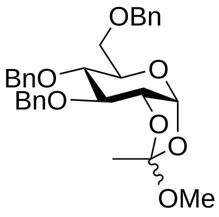

6 [282,283]
(Scheme 2.11)

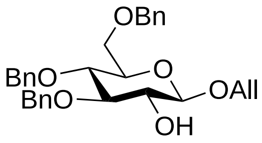

7 [61,284]
(Scheme 2.11)

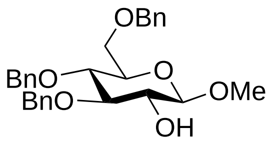

8 [67,69]
(Scheme 2.11)

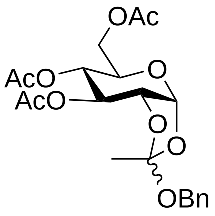

9 [62]
(Scheme 2.12)

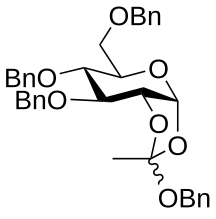

10 [62]
(Scheme 2.12)

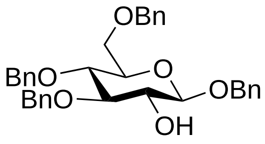

11 [62]
(Scheme 2.12)

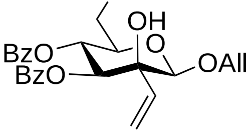

12
(Scheme 3.9)

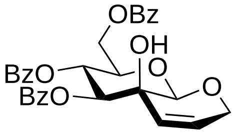

13
(Scheme 3.9)

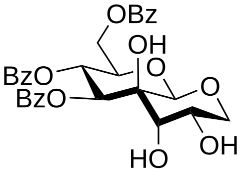
OBz
OH
O
O
BzO
BzO
HO
OH

14
(Scheme 3.9)

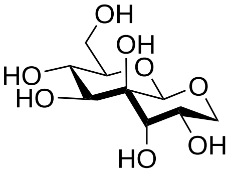
OH
OH
O
O
HO
HO
HO
OH

***syn*-15**
(Scheme 3.11)

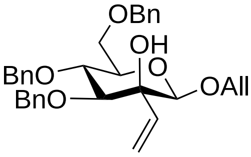
OBn
OH
O
BnO
BnO
OAll

16
(Scheme 3.10)

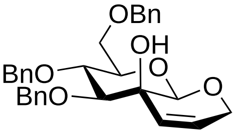
OBn
OH
O
O
BnO
BnO

17
(Scheme 3.11)

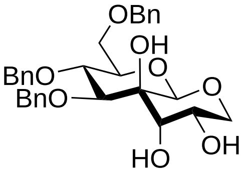
OBn
OH
O
O
BnO
BnO
HO
OH

18
(Scheme 3.11)

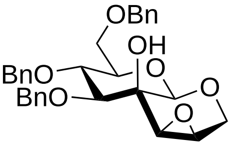
OBn
OH
O
O
BnO
BnO
O

19
(Scheme 3.11)

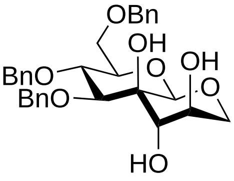
OBn
OH
O
OH
O
BnO
BnO
HO

20
(Scheme 3.11)

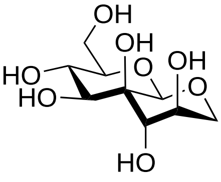
OH
OH
O
OH
O
HO
HO
HO

***anti*-21**
(Scheme 3.11)

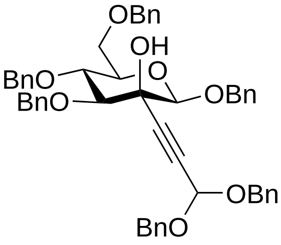
OBn
OH
O
BnO
BnO
OBn
OBn
BnO

22
(Scheme 4.16)

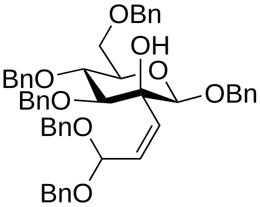
OBn
OH
O
BnO
BnO
OBn
BnO
BnO

23
(Scheme 4.16)

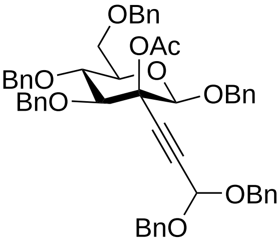
OBn
OAc
O
BnO
BnO
OBn
OBn
BnO

24
(Scheme 4.17)

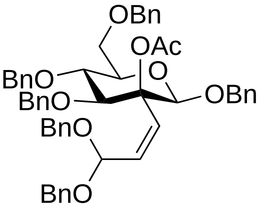
OBn
OAc
O
BnO
BnO
OBn
BnO
BnO

25
(Scheme 4.17)

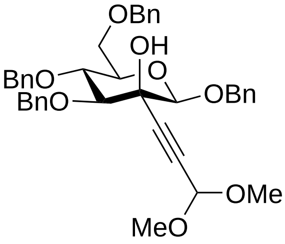
OBn
OH
O
BnO
BnO
OBn
OMe
MeO

26
(Scheme 4.17)

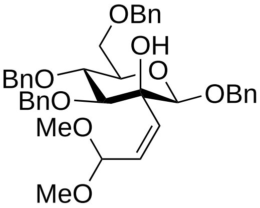
OBn
OH
O
BnO
BnO
OBn
MeO
MeO

27
(Scheme 4.17)

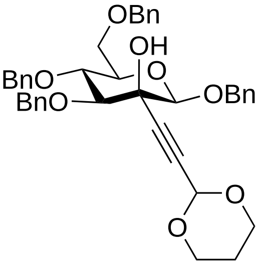
OBn
OH
O
BnO
BnO
OBn
O
O

28
(Scheme 4.17)

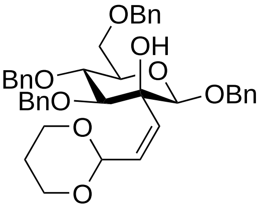
OBn
OH
O
BnO
BnO
OBn
O
O

29
(Scheme 4.17)

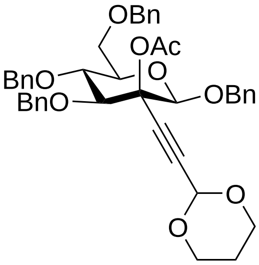
OBn
OAc
O
BnO
BnO
OBn
O
O

30
(Scheme 4.17)

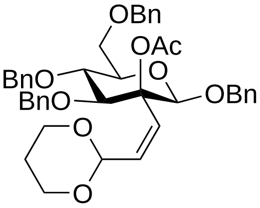
OBn
OAc
O
BnO
BnO
OBn
O
O

31
(Scheme 4.17)

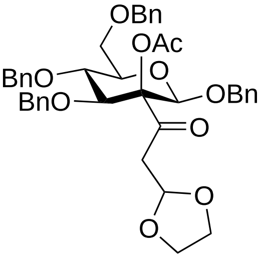
OBn
OAc
O
BnO
BnO
OBn
O
O
O

32
(Scheme 4.18)

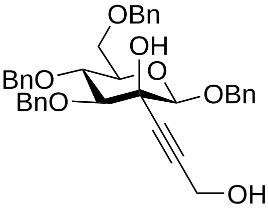
OBn
OH
O
BnO
BnO
OBn
OH

33
(Scheme 4.20)

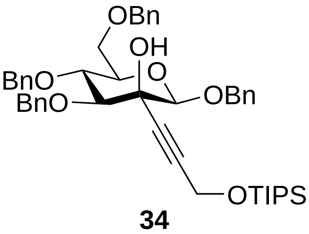
OBn
OH
O
BnO
BnO
OBn
OTIPS

34
(Scheme 4.20)

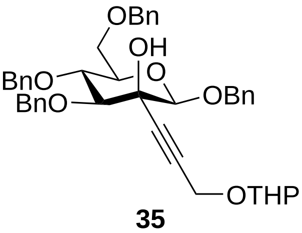
OBn
OH
O
BnO
BnO
OBn
OTHP

35
(Scheme 4.20)

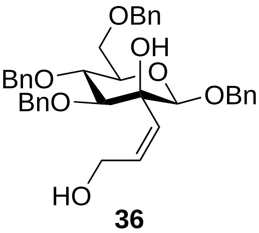
OBn
OH
O
BnO
BnO
OBn
HO

36
(Scheme 4.20)

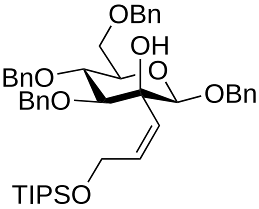
OBn
OH
O
BnO
BnO
OBn
TIPSO

37
(Scheme 4.20)

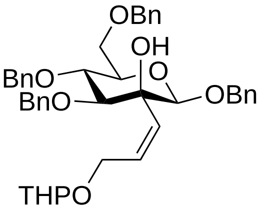

38
(Scheme 4.20)

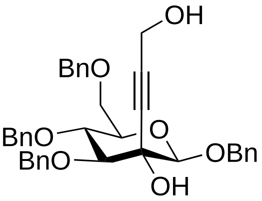

39
(Scheme 4.21)

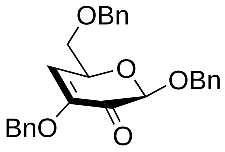

40
(Scheme 5.7)

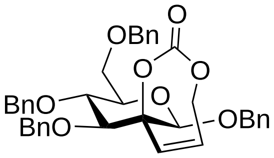

41
(Scheme 4.22)

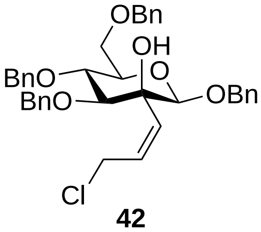

42
(Scheme 4.22)

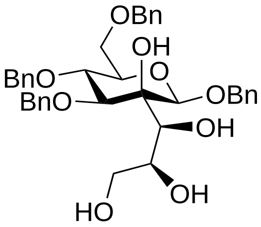

(7*S*,8*S*)-43
(Scheme 4.23)

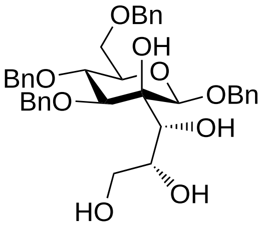

(7*R*,8*R*)-44
(Scheme 4.23)

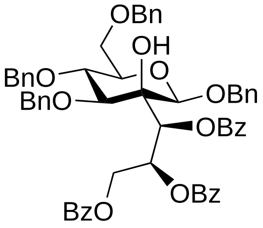

(7*S*,8*S*)-45
(Scheme 4.23)

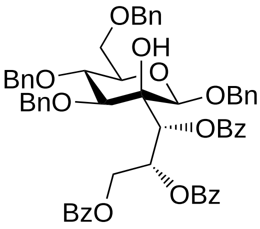

(7*R*,8*R*)-46
(Scheme 4.23)

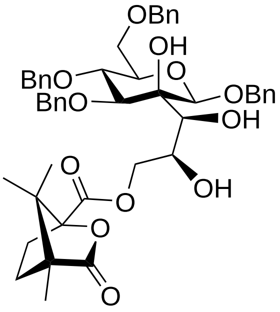

(7*S*,8*S*)-47
(Scheme 4.24)

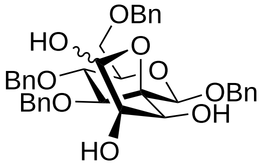

α,β-48
(Scheme 4.28)

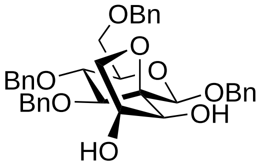

(7*S*,8*S*)-49
(Table 4.3)

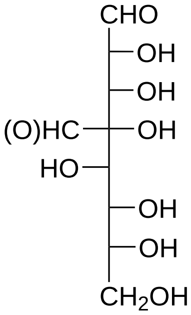

***syn*-50**
(Scheme 4.28)

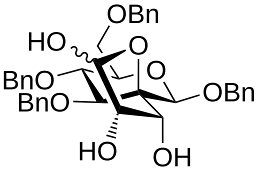

α,β-51
(Scheme 4.28)

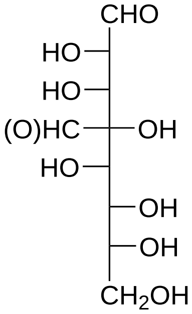

***syn*-52**
(Scheme 4.28)

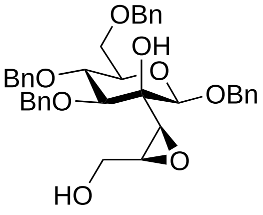

(7*S*,8*S*)-53
(Scheme 4.29)

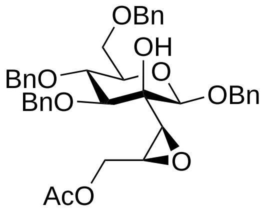

(7*S*,8*S*)-54
(Scheme 4.29)

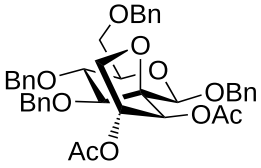

(7*S*,8*R*)-55
(Scheme 4.29)

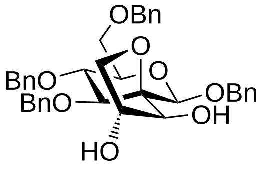

(7*S*,8*R*)-56
(Scheme 4.29)

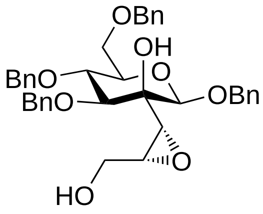

(7*R*,8*R*)-57
(Scheme 4.29)

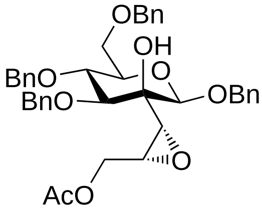

(7*R*,8*R*)-58
(Scheme 4.29)

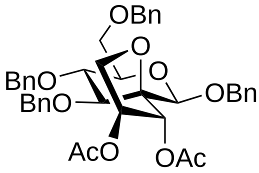

(7*R*,8*S*)-59
(Scheme 4.29)

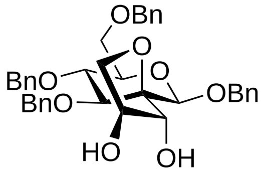

(7*R*,8*S*)-60
(Scheme 4.29)

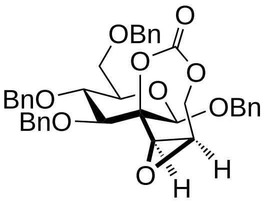

(7*R*,8*R*)-61
(Scheme 4.31)

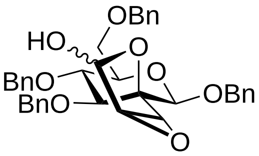

α,β-**62**
(Scheme 4.32)

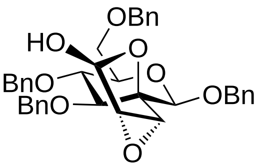

α,β-**63**
(Scheme 4.32)

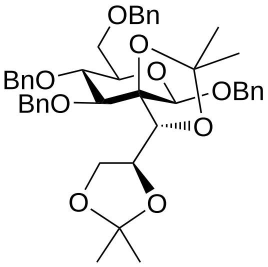

(7*R*,8*S*)-64
(Scheme 4.33)

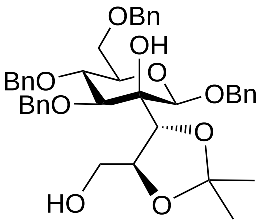

(7*R*,8*S*)-65
(Scheme 4.33)

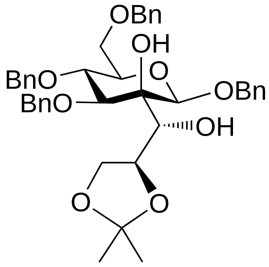

(7*R*,8*S*)-66
(Scheme 4.33)

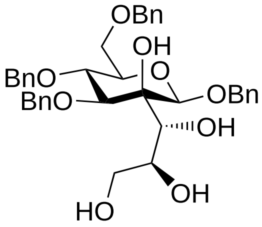

(7*R*,8*S*)-67
(Scheme 4.33)

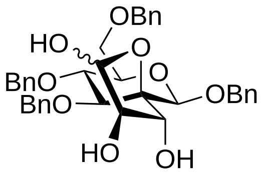

α,β-**68**
(Scheme 4.35)

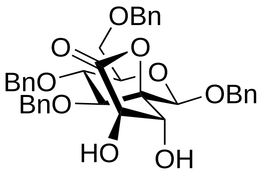

(7*R*,8*R*)-69
(Scheme 4.35)

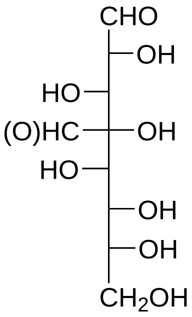

***anti*-70**
(Scheme 4.35)

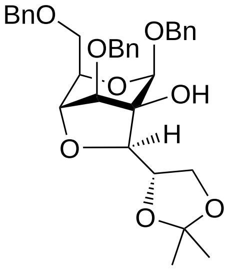

(7*R*,8*S*)-71
(Scheme 4.36)

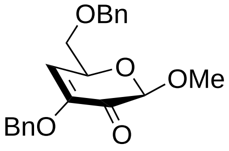

72
(Scheme 5.7)

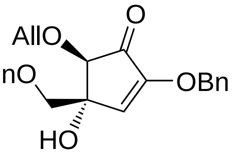

(±)-73
(Table 5.2)

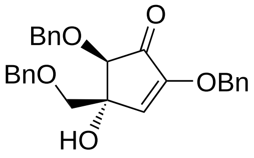

(±)-74
(Table 5.2)

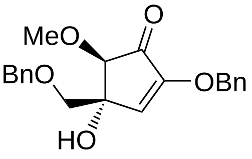

(±)-75
(Table 5.2)

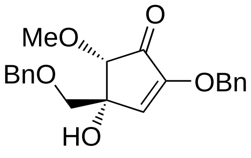

(±)-76
(Scheme 5.11)

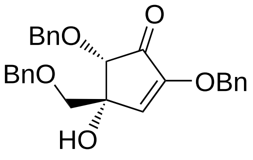

(±)-77
(Scheme 5.17)

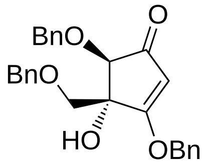

(±)-78
(Scheme 5.17)

A. X-Ray Crystallography

X-ray Data of Compound 2b

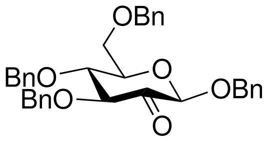

2b

Colorless needles of **2b** were grown by slow diffusion of *n*-pentane into a solution of the compound (20 mg) in ethyl acetate/chloroform (2:1, 750 µL) at r.t.

For structural data: **CCDC 1505647** *via* `https://www.ccdc.cam.ac.uk`.

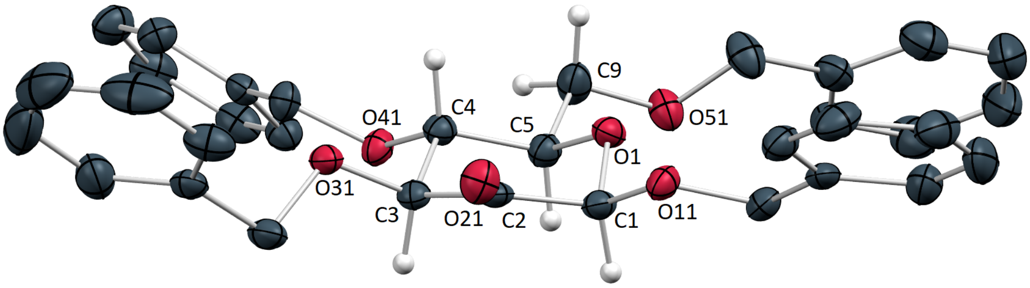

Figure A.1 X-ray structure of compound **2b**. Hydrogen atoms of the benzyl ethers and a disorder involving the O51 benzyl group are omitted for clarity. Ellipsoids are drawn at the 50% probability level. Red = oxygen, gray = carbon, white = hydrogen.

Table A.1 Crystal data and refinement parameters for compound **2b**. Estimated standard deviations are given in parentheses.

parameter	**2b**
Empirical formula	$C_{34}H_{34}O_6$
Formula weight (g/mol)	538.61
Temperature (K)	100(2)
Radiation type	CuKα
Wavelength (Å)	1.54178
Crystal system	Monoclinic
Space group	$P2_1$
a (Å)	12.5198(4)
b (Å)	7.6052(3)
c (Å)	15.2218(5)
α (°)	90
β (°)	102.2180(10)
γ (°)	90
Cell volume (Å^3)	1416.52(9)
Z	2
Density (calculated) (Mg/m^3)	1.263
Crystal size (mm^3)	0.430 × 0.066 × 0.052
θ range (°)	2.970 to 66.615
Reflections collected	12973
Independent reflections (R_{int})	4840 (0.0196)
Goodness-of-fit on F^2	1.057
Final R indices [$I>2\sigma(I)$]	$R_1 = 0.0295$, $wR_2 = 0.0754$
R indices (all data)	$R_1 = 0.0302$, $wR_2 = 0.0760$

X-ray Data of Compound 11

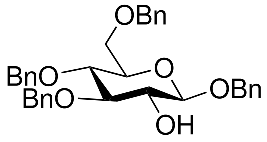

11

Crystals of **11** were obtained by evaporation of a solution of the compound in *n*-hexane/ethyl acetate. Upon drying, the residual oil crystallized to give colorless prisms.

For structural data: **CCDC 1909188** *via* `https://www.ccdc.cam.ac.uk`.

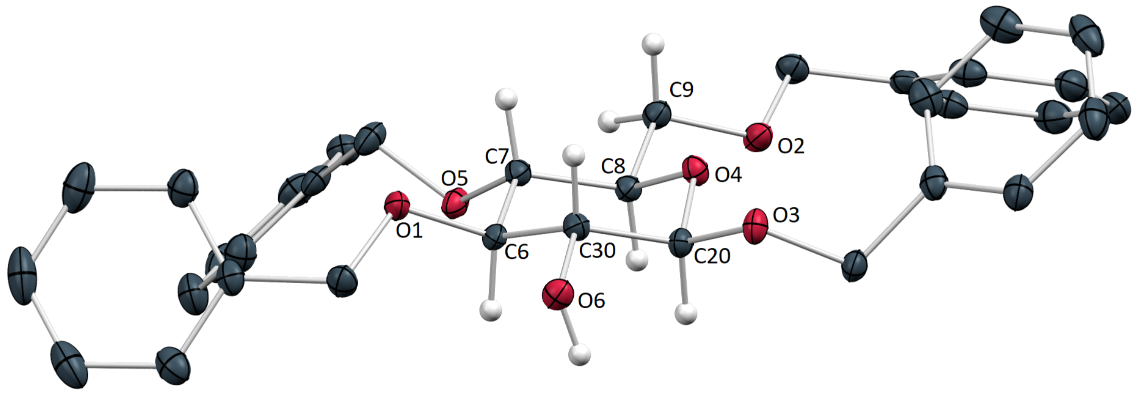

Figure A.2 X-ray structure of compound **11**. Hydrogen atoms of the benzyl ethers are omitted for clarity. Ellipsoids are drawn at the 50% probability level. Red = oxygen, gray = carbon, white = hydrogen.

Table A.2 Crystal data and refinement parameters for compound **11**. Estimated standard deviations are given in parentheses.

parameter	**11**
Empirical formula	$C_{34}H_{36}O_6$
Formula weight (g/mol)	540.63
Temperature (K)	110(2)
Radiation type	MoKα
Wavelength (Å)	0.71073
Crystal system	Orthorhombic
Space group	$P2_12_12_1$
a (Å)	8.0111(2)
b (Å)	10.8059(2)
c (Å)	32.7521(6)
α (°)	90
β (°)	90
γ (°)	90
Cell volume (Å^3)	2835.26(10)
Z	4
Density (calculated) (Mg/m^3)	1.267
Crystal size (mm^3)	0.14 × 0.12 × 0.10
θ range (°)	1.985 to 27.890
Reflections collected	31154
Independent reflections (R_{int})	6733 (0.0201)
Goodness-of-fit on F^2	1.008
Final R indices [$I>2\sigma(I)$]	$R_1 = 0.0322$, $wR_2 = 0.0771$
R indices (all data)	$R_1 = 0.0366$, $wR_2 = 0.0798$

X-ray Data of Compound *syn*-15

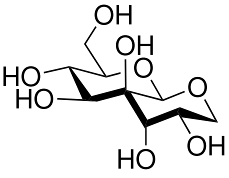

***syn*-15**

Colorless plates of ***syn*-15** were obtained by adding water dropwise to a suspension of the compound (36 mg) in boiling methanol (1 mL) to a clear solution. Subsequent cooling to 4 °C over several days resulted in crystallization.

For structural data: **CCDC 1427168** *via* `https://www.ccdc.cam.ac.uk`.

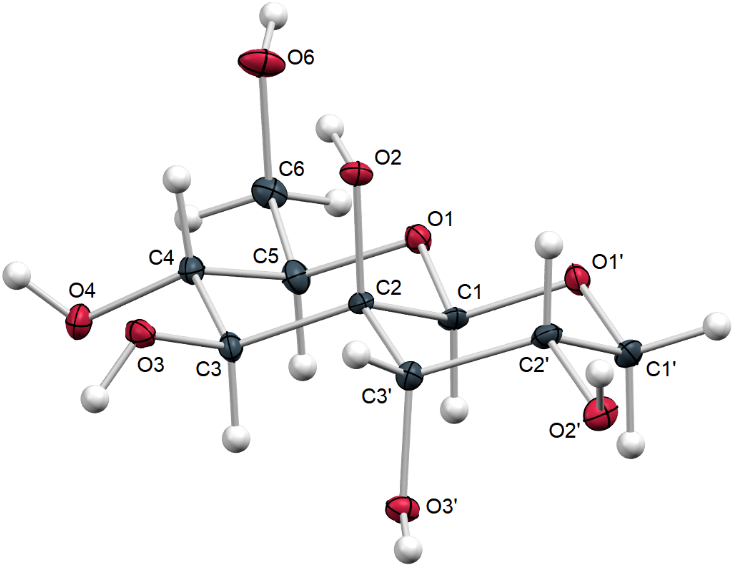

Figure A.3 X-ray structure of compound ***syn*-15**. A second molecule in the asymmetric unit is omitted. Ellipsoids are drawn at the 50% probability level. Red = oxygen, gray = carbon, white = hydrogen.

Table A.3 Crystal data and refinement parameters for compound ***syn*-15**. Estimated standard deviations are given in parentheses.

parameter	***syn*-15**
Empirical formula	$C_9H_{16}O_8$
Formula weight (g/mol)	252.22
Temperature (K)	100(2)
Radiation type	CuKα
Wavelength (Å)	1.54178
Crystal system	Monoclinic
Space group	$P2_1$
a (Å)	9.0765(3)
b (Å)	10.3405(3)
c (Å)	10.7638(3)
α (°)	90
β (°)	90.0570(10)
γ (°)	90
Cell volume (Å^3)	1010.24(5)
Z	4
Density (calculated) (Mg/m^3)	1.658
Crystal size (mm^3)	0.298 × 0.187 × 0.072
θ range (°)	4.107 to 66.664
Reflections collected	6541
Independent reflections (R_{int})	3016 (0.0149)
Goodness-of-fit on F^2	1.032
Final R indices [$I>2\sigma(I)$]	$R_1 = 0.0220$, $wR_2 = 0.0561$
R indices (all data)	$R_1 = 0.0220$, $wR_2 = 0.0561$

Table A.4 Selected bond lengths, angles and torsion angles for ***syn*-15**. Estimated standard deviations are given in parentheses.

bond	(Å)	bond	(Å)	bond	(Å)
C1-C2	1.535(5)	C3-C4	1.527(4)	C6-O6	1.429(4)
C1-O1	1.405(3)	C3-O3	1.421(4)	C1'-O1'	1.446(3)
C1-O1'	1.411(3)	C4-C5	1.534(4)	C1'-C2'	1.524(4)
C2-C3	1.535(4)	C4-O4	1.425(3)	C2'-C3'	1.526(4)
C2-C3'	1.533(4)	C5-C6	1.507(4)	C2'-O2'	1.438(3)
angle	(°)	angle	(°)	torsion	(°)
O1-C1-O1'	104.2(2)	C4-C5-C6	112.5(2)	O1'-C1-C2-O2	58.6(3)
C1-O1'-C1'	111.4(2)	C4-C5-O1	111.1(2)	O1-C1-C2-O2	-56.6(3)
C1-O1-C5	110.5(2)	C6-C5-O1	107.3(2)	O1-C1-O1'-C1'	-179.9(2)
C1-C2-C3	106.7(2)	C1'-C2'-C3'	111.4(2)	O2-C2-C3'-O3'	172.6(2)
C3'-C2-O2	104.8(2)	O2'-C2'-C3'	110.0(2)	O3'-C3'-C2'-O2'	-53.7(3)
C3-C2-C3'	113.7(2)	C2-C3'-C2'	108.3(2)	O1'-C1-O1-C5	174.2(2)
C2-C3-C4	109.7(2)	O3'-C3'-C2'	110.6(2)		
C3-C4-C5	109.7(2)				

Table A.5 Hydrogen-bonding interactions of ***syn*-15** for $d_{O\cdots H} < 3.0$ Å and $\theta_{O-H\cdots O} > 90°$. Type: 2c (two-centered classical, including type: H···O···H'), bif. (bifurcated, type: O···H(-O)···O').

contact	O···O (Å)	H···O (Å)	O-H···O (°)	type	symm. op.
O22'-H22A···O1	2.97	2.19	154.9	2c	x,y,1+z
O3'-H3B···O1	3.21	2.90	103.7	bif.	2-x,-1/2+y,-z
O3-H3C···O1'	2.73	1.90	172.8	2c	2-x,-1/2+y,-z
O2-H2C···O3'	2.82	2.08	145.8	2c	2-x,-1/2+y,-z
O2'-H2B···O21	2.89	2.06	166.6	bif.	x,y,z
O2'-H2B···O23	3.40	2.92	118.1	bif.	1-x,1/2+y,1-z
O4-H4A···O2'	2.84	2.03	161.7	2c	1+x,y,z
O3'-H3B···O6	2.74	1.91	169.5	bif.	2-x,-1/2+y,-z
O6-H6···O23	2.73	1.90	173.0	2c	1+x,y,-1+z

Table A.5 Continued: hydrogen-bonding interactions of ***syn*-15**.

contact	O···O (Å)	H···O (Å)	O-H···O (°)	type	symm. op.
O23-H23D···O21	3.01	2.24	152.1	bif.	1-x,-1/2+y,1-z
O22-H22C···O24	2.83	2.04	154.9	2c	1-x,-1/2+y,1-z
O23-H23D···O26	3.12	2.46	136.5	bif.	1-x,-1/2+y,1-z
O23’-H23B···O26	2.81	2.03	155.4	2c	1-x,-1/2+y,1-z

X-ray Data of Compound 17

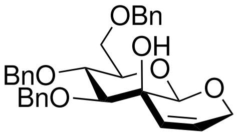
OBn
OH
O
O
BnO
BnO

17

Colorless needles of **17** were obtained by slow concentration of a solution of the compound in *n*-hexane/ethyl acetate at r.t.

For structural data: **CCDC 1497333** *via* `https://www.ccdc.cam.ac.uk`.

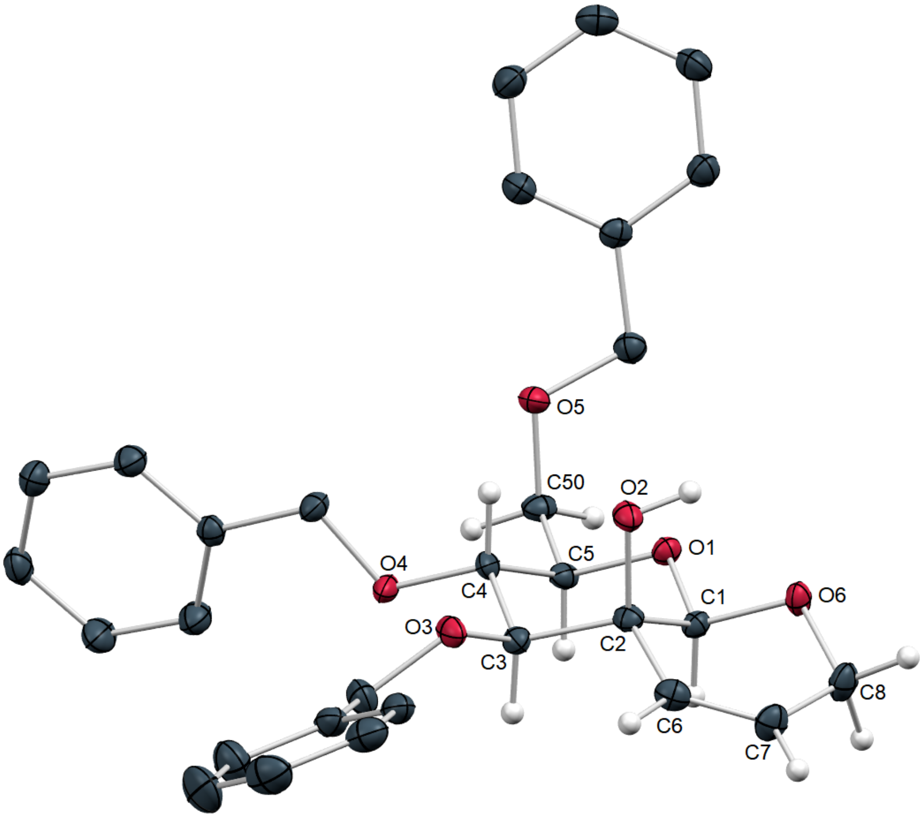
O5
C50
O2
O1
C5
O4
C4
C1
O6
O3
C3
C2
C8
C6
C7

Figure A.4 X-ray structure of compound **17**. Hydrogen atoms of the benzyl ethers are omitted for clarity. Ellipsoids are drawn at the 50% probability level. Red = oxygen, gray = carbon, white = hydrogen.

Table A.6 Crystal data and refinement parameters for compound **17**. Estimated standard deviations are given in parentheses.

parameter	**17**
Empirical formula	$C_{30}H_{32}O_6$
Formula weight (g/mol)	488.55
Temperature (K)	100(2)
Radiation type	MoKα
Wavelength (Å)	0.71073
Crystal system	Monoclinic
Space group	$P2_1$
a (Å)	13.4668(7)
b (Å)	5.4807(3)
c (Å)	17.8748(10)
α (°)	90
β (°)	107.555(3)
γ (°)	90
Cell volume (Å^3)	1257.85(12)
Z	2
Density (calculated) (Mg/m^3)	1.290
Crystal size (mm^3)	0.430 × 0.090 × 0.030
θ range (°)	1.586 to 26.683
Reflections collected	13024
Independent reflections (R_{int})	5731 (0.0534)
Goodness-of-fit on F^2	1.017
Final R indices [$I>2\sigma(I)$]	$R_1 = 0.0482$, $wR_2 = 0.0869$
R indices (all data)	$R_1 = 0.0720$, $wR_2 = 0.0981$

X-ray Data of Compound 23

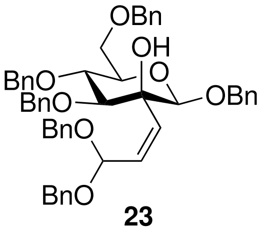
OBn
OH
O
BnO
BnO
OBn
BnO
BnO

23

Colorless needles of **23** were grown by vapor diffusion of *n*-pentane into a solution of the compound (20 mg) in ethyl acetate/chloroform (2:1, 750 µL) at r.t.

For structural data: **CCDC 1505648** *via* `https://www.ccdc.cam.ac.uk`.

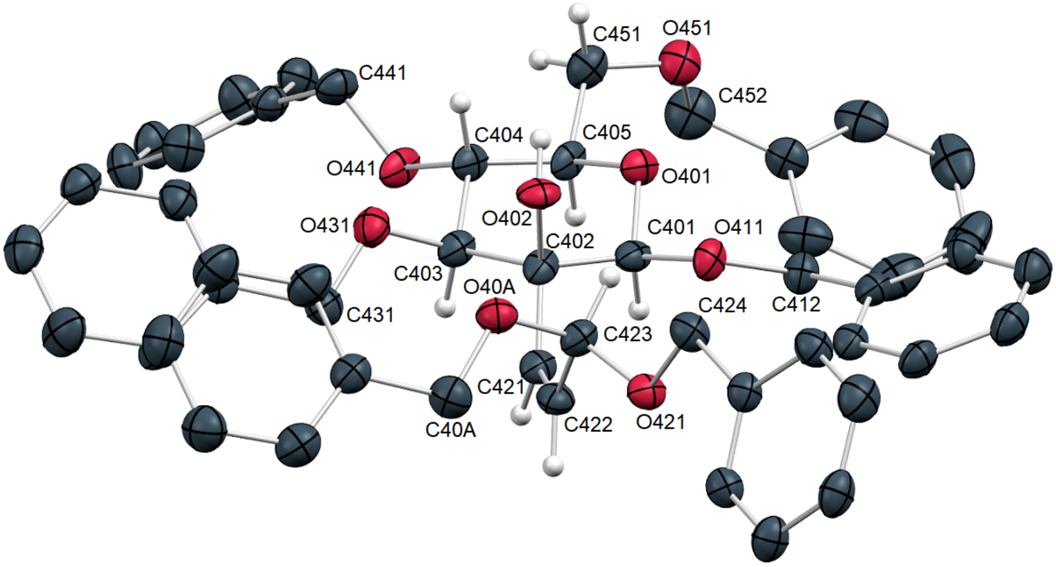
C451
O451
C441
C452
C404
C405
O441
O401
O402
O431
C402
C401
O411
C403
O40A
C424
C412
C431
C423
C421
C40A
C422
O421

Figure A.5 X-ray structure of compound **23**. One out of four molecules in the asymmetric unit is shown. Hydrogen atoms of the benzyl ethers are omitted for clarity. Ellipsoids are drawn at the 50% probability level. Red = oxygen, gray = carbon, white = hydrogen.

Table A.7 Crystal data and refinement parameters for compound **23**. Estimated standard deviations are given in parentheses.

parameter	**23**
Empirical formula	$C_{51}H_{52}O_8$
Formula weight (g/mol)	792.92
Temperature (K)	101(2)
Radiation type	MoKα
Wavelength (Å)	0.71073
Crystal system	Triclinic
Space group	$P1$
a (Å)	9.7674(7)
b (Å)	15.2213(10)
c (Å)	29.934(2)
α (°)	90.647(3)
β (°)	93.386(3)
γ (°)	108.083(3)
Cell volume ($Å^3$)	4221.1(5)
Z	4
Density (calculated) (Mg/m^3)	1.248
Crystal size (mm^3)	0.432 × 0.096 × 0.077
θ range (°)	1.364 to 27.300
Reflections collected	127433
Independent reflections (R_{int})	36514 (0.1116)
Goodness-of-fit on F^2	0.971
Final R indices [$I>2\sigma(I)$]	$R_1 = 0.0675$, $wR_2 = 0.1343$
R indices (all data)	$R_1 = 0.1392$, $wR_2 = 0.1693$

X-ray Data of Compound 41

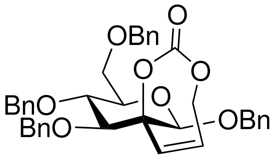
OBn
O
O
O
O
BnO
BnO
OBn

41

Colorless needles of **41** were grown by vapor diffusion of *n*-pentane into a solution of the compound (10 mg) in acetone-D_6 (500 µL) at r.t.

For structural data: **CCDC 1895600** *via* `https://www.ccdc.cam.ac.uk`.

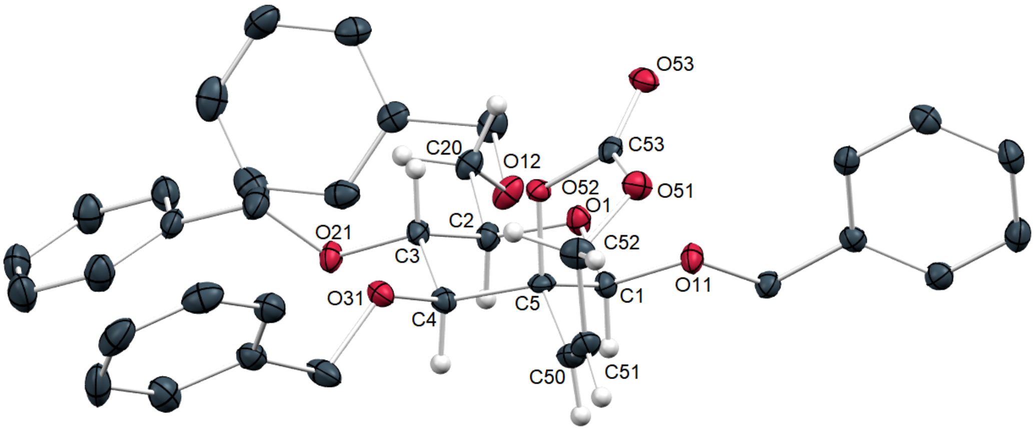
O53
C53
C20
O12
O52
O51
O1
C2
O21
C3
C52
O11
C1
O31
C5
C4
C50
C51

Figure A.6 X-ray structure of compound **41**. Hydrogen atoms of the benzyl ethers are omitted for clarity. Ellipsoids are drawn at the 50% probability level. Red = oxygen, gray = carbon, white = hydrogen.

Table A.8 Crystal data and refinement parameters for compound **41**. Estimated standard deviations are given in parentheses.

parameter	**41**
Empirical formula	$C_{38}H_{38}O_8$
Formula weight (g/mol)	622.68
Temperature (K)	100(2)
Radiation type	MoKα
Wavelength (Å)	0.71073
Crystal system	Monoclinic
Space group	$P2_1$
a (Å)	8.5680(4)
b (Å)	10.1981(5)
c (Å)	18.5348(9)
α (°)	90
β (°)	98.016(2)
γ (°)	90
Cell volume (Å^3)	1603.70(13)
Z	2
Density (calculated) (Mg/m^3)	1.290
Crystal size (mm^3)	0.272 × 0.062 × 0.047
θ range (°)	2.219 to 28.885
Reflections collected	31261
Independent reflections (R_{int})	8389 (0.0473)
Goodness-of-fit on F^2	1.017
Final R indices [$I>2\sigma(I)$]	$R_1 = 0.0405$, $wR_2 = 0.0776$
R indices (all data)	$R_1 = 0.0558$, $wR_2 = 0.0845$

X-ray Data of Compound (7*S*,8*S*)-47

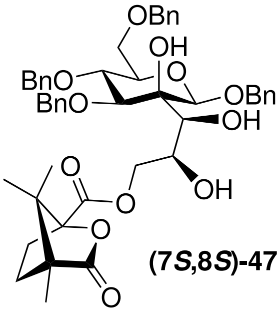
OBn
OH
O
BnO
BnO
OBn
OH
O
O
OH
O
O

(7*S*,8*S*)-47

Colorless needles of **(7*S*,8*S*)-47** were grown by vapor diffusion of diethyl ether into a solution of the compound (20 mg) in acetonitrile (450 µL) at r.t.

For structural data: **CCDC 1895601** *via* `https://www.ccdc.cam.ac.uk`.

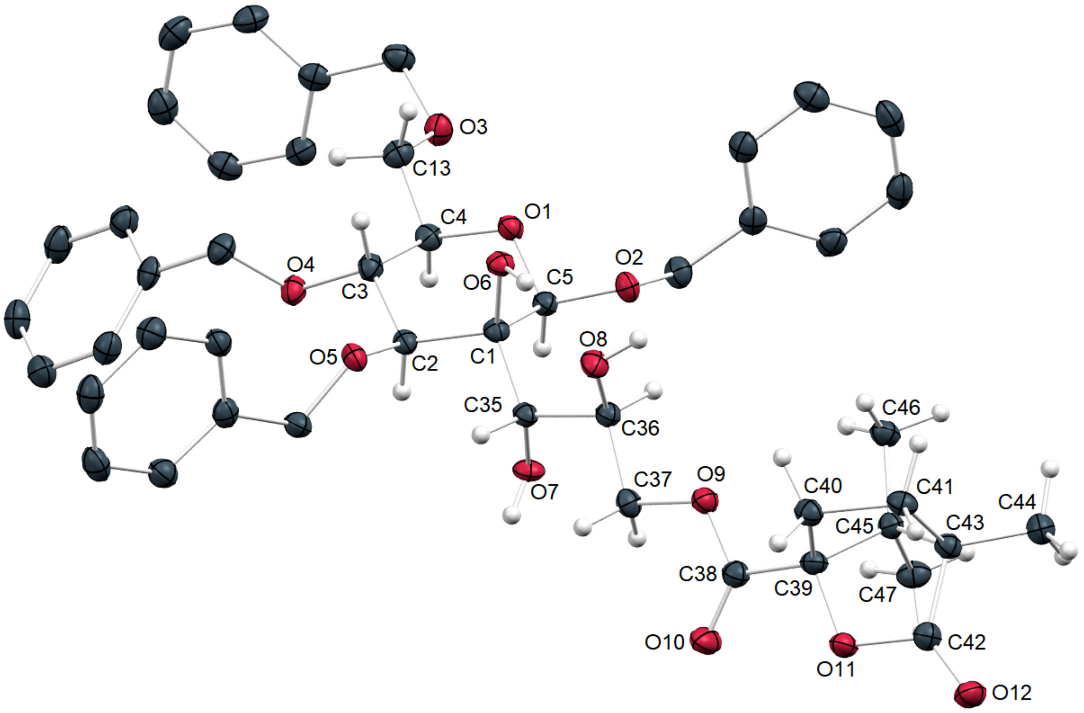
O3
C13
C4
O1
O4
C3
O6
C5
O2
O5
C2
C1
O8
C35
C36
C46
O7
C37
O9
C40
C41
C44
C45
C43
C38
C39
C47
O10
O11
C42
O12

Figure A.7 X-ray structure of compound **(7*S*,8*S*)-47**. Hydrogen atoms of the benzyl ethers are omitted for clarity. Ellipsoids are drawn at the 50% probability level. Red = oxygen, gray = carbon, white = hydrogen.

Table A.9 Crystal data and refinement parameters for compound **(7*S*,8*S*)-47**. Estimated standard deviations are given in parentheses.

parameter	**(7*S*,8*S*)-47**
Empirical formula	$C_{47}H_{54}O_{12}$
Formula weight (g/mol)	810.90
Temperature (K)	100(2)
Radiation type	CuKα
Wavelength (Å)	1.54178
Crystal system	Monoclinic
Space group	$P2_1$
a (Å)	11.0987(2)
b (Å)	6.02780(10)
c (Å)	30.6688(4)
α (°)	90
β (°)	91.6070(10)
γ (°)	90
Cell volume (Å^3)	2050.96(6)
Z	2
Density (calculated) (Mg/m^3)	1.313
Crystal size (mm^3)	0.474 × 0.106 × 0.070
θ range (°)	1.441 to 66.626
Reflections collected	32675
Independent reflections (R_{int})	7017 (0.0292)
Goodness-of-fit on F^2	1.060
Final R indices [$I>2\sigma(I)$]	$R_1 = 0.0266$, $wR_2 = 0.0658$
R indices (all data)	$R_1 = 0.0279$, $wR_2 = 0.0665$

X-ray Data of Compound (7*R*,8*R*)-61

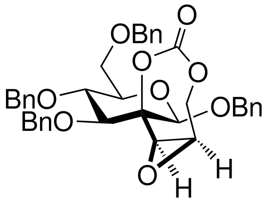
OBn
O
O
O
O
BnO
BnO
OBn
H
O
H

(7*R*,8*R*)-61

Colorless plates of **(7*R*,8*R*)-61** were obtained by vapor diffusion of diethyl ether into a solution of the compound (12 mg) in acetone-D_6 (600 µL) at r.t.

For structural data: **CCDC 1895599** *via* `https://www.ccdc.cam.ac.uk`.

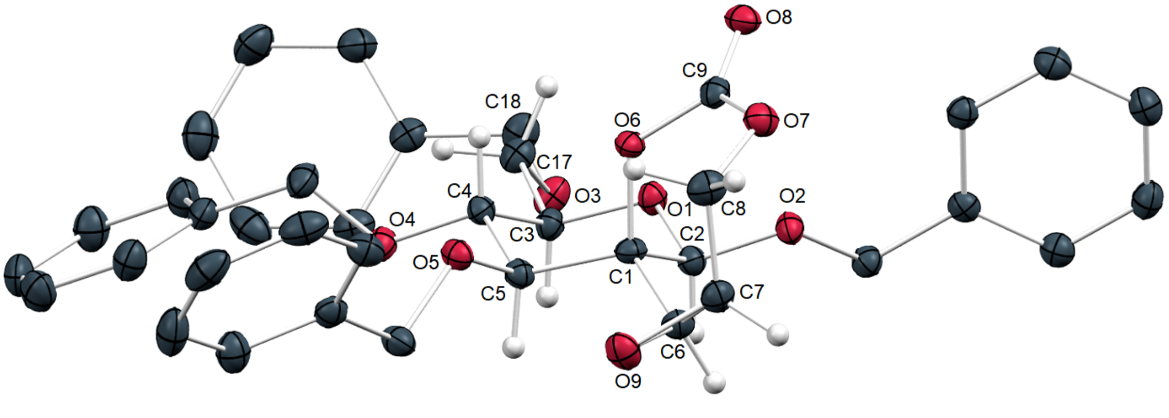
O8
C9
C18
O7
O6
C17
C4
O3
O1
C8
O2
O4
C3
C2
O5
C1
C5
C7
C6
O9

Figure A.8 X-ray structure of compound **(7*R*,8*R*)-61**. Hydrogen atoms of the benzyl ethers are omitted for clarity. Ellipsoids are drawn at the 50% probability level. Red = oxygen, gray = carbon, white = hydrogen.

Table A.10 Crystal data and refinement parameters for compound **(7*R*,8*R*)-61**. Estimated standard deviations are given in parentheses.

parameter	**(7*R*,8*R*)-61**
Empirical formula	$C_{38}H_{38}O_9$
Formula weight (g/mol)	638.68
Temperature (K)	100(2)
Radiation type	MoKα
Wavelength (Å)	0.71073
Crystal system	Monoclinic
Space group	$P2_1$
a (Å)	8.5337(3)
b (Å)	10.1228(4)
c (Å)	18.6351(7)
α (°)	90
β (°)	99.1070(10)
γ (°)	90
Cell volume (Å^3)	1589.50(10)
Z	2
Density (calculated) (Mg/m^3)	1.3340
Crystal size (mm^3)	0.273 × 0.176 × 0.140
θ range (°)	1.107 to 29.074
Reflections collected	30538
Independent reflections (R_{int})	8504 (0.0502)
Goodness-of-fit on F^2	1.042
Final R indices [$I>2\sigma(I)$]	$R_1 = 0.0392$, $wR_2 = 0.0849$
R indices (all data)	$R_1 = 0.0468$, $wR_2 = 0.0896$

X-ray Data of Compound α-63

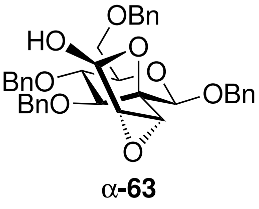
OBn
HO
O
O
BnO
BnO
OBn
O

α-63

side chain: α-D-*lyxo*

Colorless needles of **α-63** were obtained by slow concentration of a solution of **α,β-63** (16 mg) in toluene/CH_2Cl_2 (3:2; 1 mL) at r.t.

For structural data: **CCDC 1895602** *via* `https://www.ccdc.cam.ac.uk`.

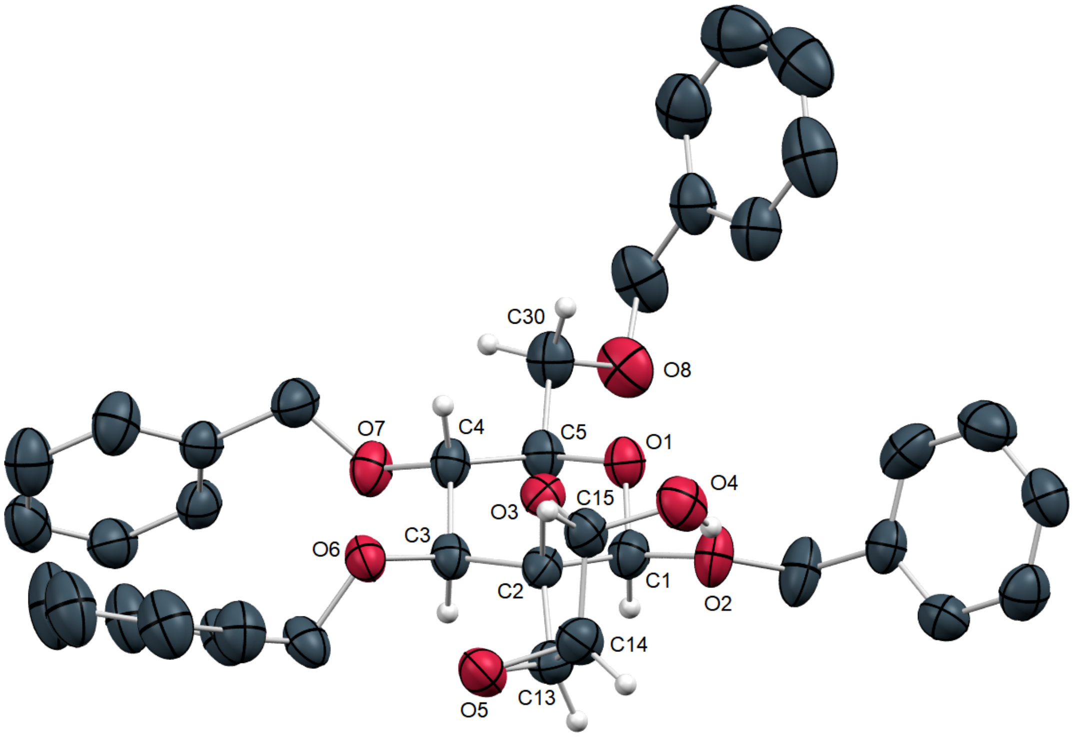
C30
O8
O7
C4
C5
O1
O3
C15
O4
O6
C3
C2
C1
O2
C14
O5
C13

Figure A.9 X-ray structure of compound **α-63**. Hydrogen atoms of the benzyl ethers and a disorder involving the O6 benzyl group are omitted for clarity. Ellipsoids are drawn at the 50% probability level. Red = oxygen, gray = carbon, white = hydrogen.

Table A.11 Crystal data and refinement parameters for compound **α-63**. Estimated standard deviations are given in parentheses.

parameter	**α-63**
Empirical formula	$C_{37}H_{38}O_8$
Formula weight (g/mol)	610.67
Temperature (K)	173(2)
Radiation type	MoKα
Wavelength (Å)	0.71073
Crystal system	Monoclinic
Space group	$P2_1$
a (Å)	12.082(2)
b (Å)	9.8858(17)
c (Å)	13.502(2)
α (°)	90
β (°)	93.491(2)
γ (°)	90
Cell volume ($Å^3$)	1609.7(5)
Z	2
Density (calculated) (Mg/m^3)	1.260
Crystal size (mm^3)	0.720 × 0.110 × 0.069
θ range (°)	2.197 to 28.925
Reflections collected	16500
Independent reflections (R_{int})	8045 (0.0533)
Goodness-of-fit on F^2	1.026
Final R indices [$I>2\sigma(I)$]	$R_1 = 0.0533$, $wR_2 = 0.1182$
R indices (all data)	$R_1 = 0.1003$, $wR_2 = 0.1440$

X-ray Data of Compound (±)-75

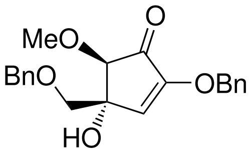

(±)-**75**

Colorless needles of (±)-**75** were obtained by vapor diffusion of *n*-pentane into a solution of the compound (25 mg) in toluene (200 µL) at r.t.

For structural data: **CCDC 1553837** *via* `https://www.ccdc.cam.ac.uk`.

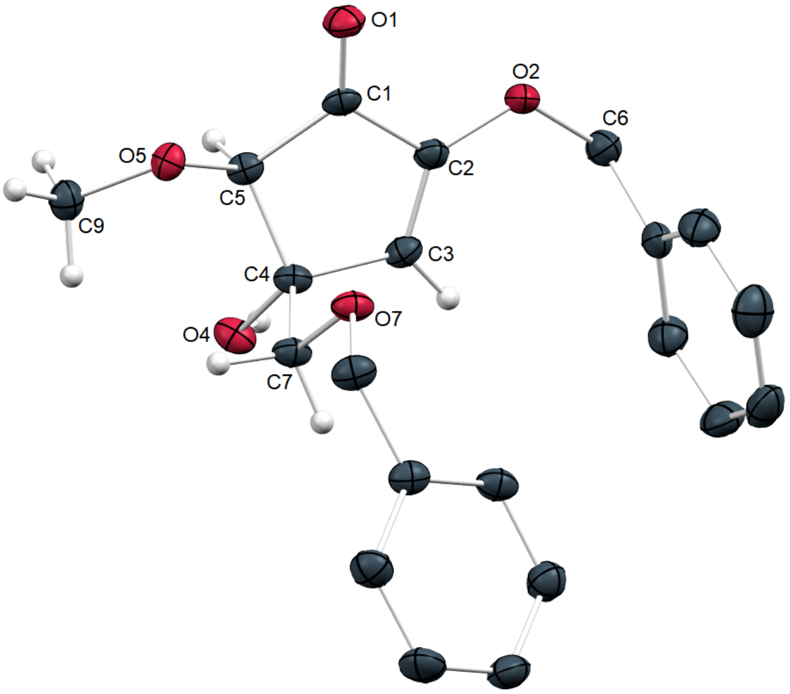

Figure A.10 X-ray structure of compound (±)-**75**. Hydrogen atoms of the benzyl ethers are omitted for clarity. Ellipsoids are drawn at the 50% probability level. Red = oxygen, gray = carbon, white = hydrogen.

Table A.12 Crystal data and refinement parameters for compound **(±)-75**. Estimated standard deviations are given in parentheses.

parameter	**(±)-75**
Empirical formula	$C_{21}H_{22}O_5$
Formula weight (g/mol)	354.38
Temperature (K)	100(2)
Radiation type	CuKα
Wavelength (Å)	1.54178
Crystal system	Orthorhombic
Space group	$Pna2_1$
a (Å)	22.3577(5)
b (Å)	14.3796(3)
c (Å)	5.53140(10)
α (°)	90
β (°)	90
γ (°)	90
Cell volume (Å^3)	1778.32(6)
Z	4
Density (calculated) (Mg/m^3)	1.324
Crystal size (mm^3)	1.161 × 0.081 × 0.036
θ range (°)	3.655 to 72.392
Reflections collected	17136
Independent reflections (R_{int})	3200 (0.0492)
Goodness-of-fit on F^2	1.016
Final R indices [$I>2\sigma(I)$]	$R_1 = 0.0320$, $wR_2 = 0.0778$
R indices (all data)	$R_1 = 0.0356$, $wR_2 = 0.0796$

B. HPLC Chromatograms

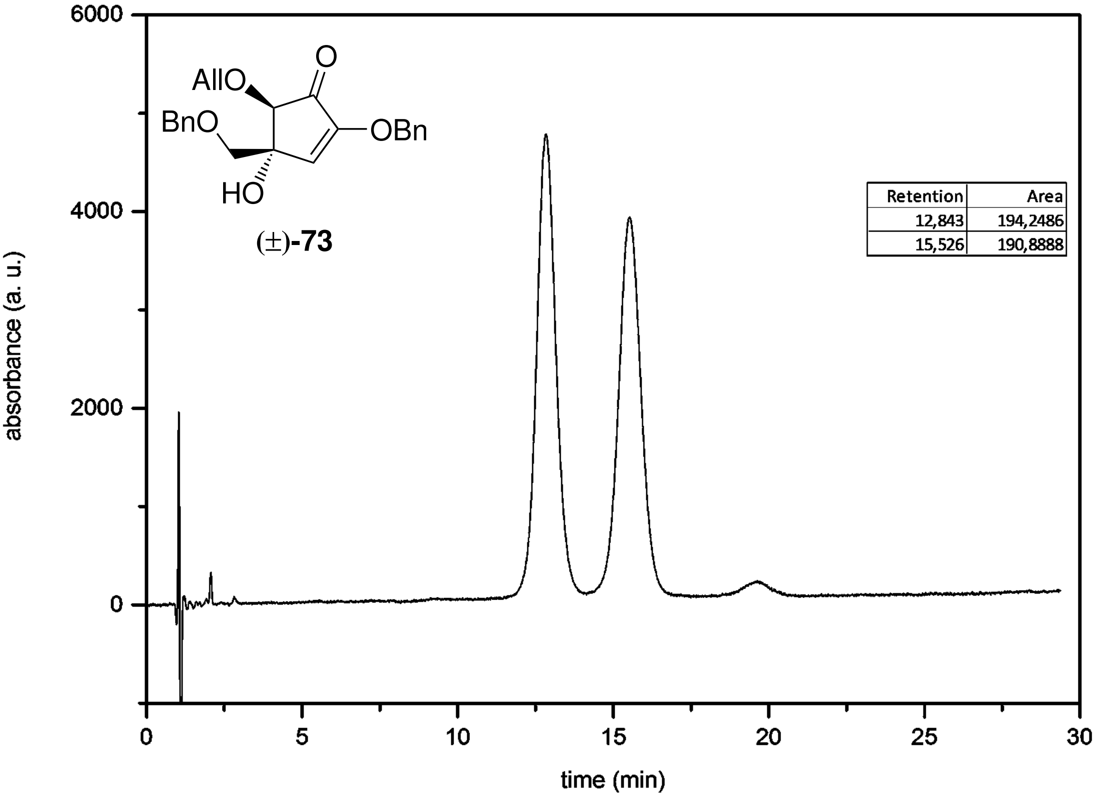

(±)-**73**

Retention	Area
12,843	194,2486
15,526	190,8888

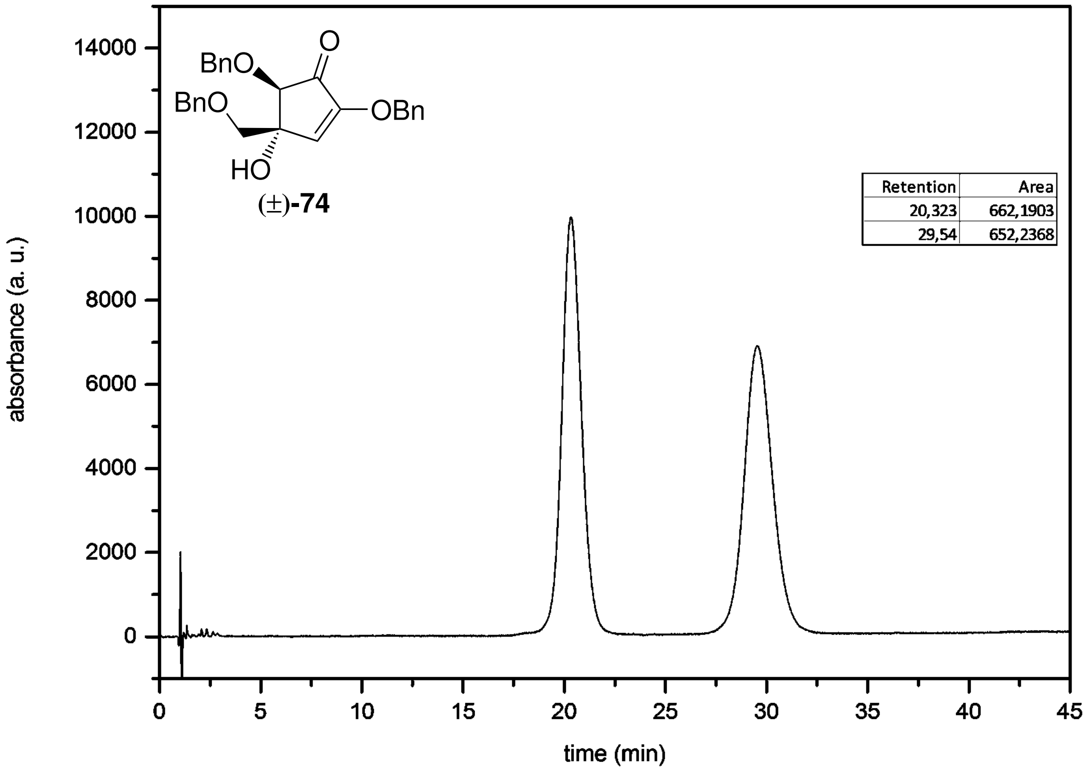

(±)-**74**

Retention	Area
20,323	662,1903
29,54	652,2368

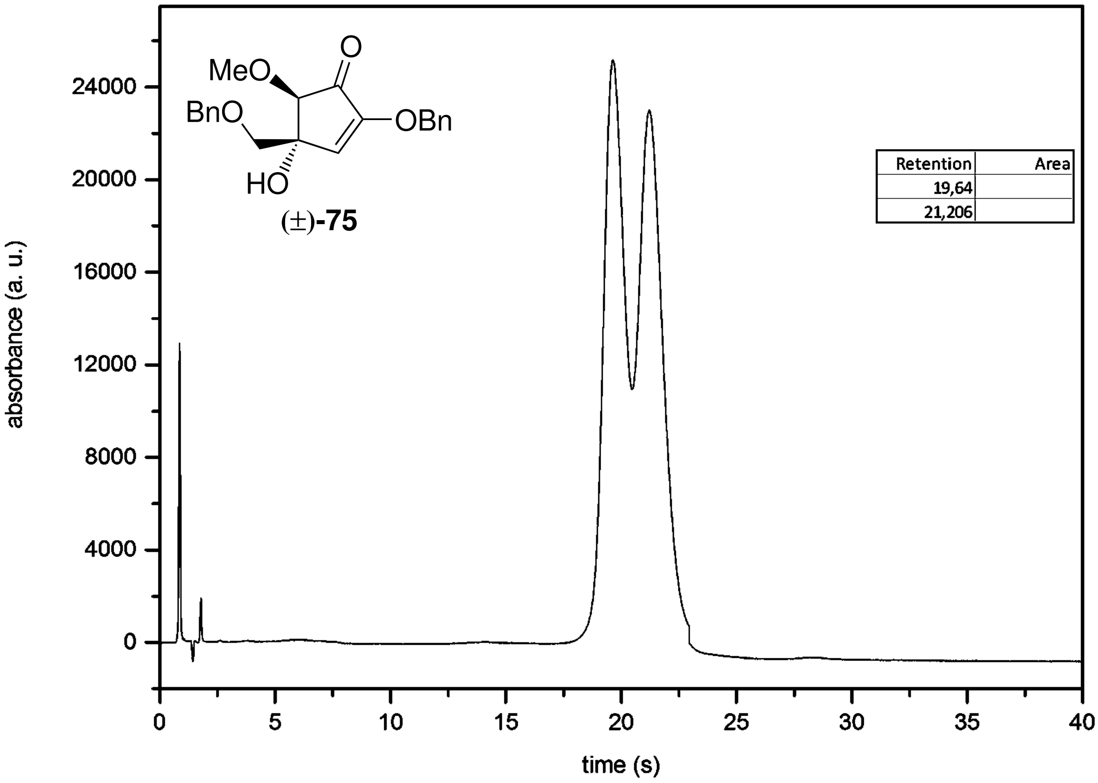

Retention	Area
19,64	
21,206	

C. Antimicrobial Screenings

Antimicrobial screenings were performed by the CO-ADD initiative (The Community for Open Antimicrobial Drug Discovery), located at the University of Queensland, 306 Carmody Rd, St. Lucia, QLD, 4072, Australia. Screenings involved the compounds **3b**, **40**, **72**, **(±)-73**, **(±)-74**, **(±)-75** and **(±)-76**. Given below is the employed standard protocol as described by CO-ADD:

> Inhibition of bacterial growth (against *Staphylococcus aureus* (Sa; ATCC 43300), *Escherichia coli* (Ec; ATCC 25922), *Klebsiella pneumoniae* (Kp; ATCC 700603), *Acinetobacter baumannii* (Ab; ATCC 19606) and *Pseudomonas aeruginosa* (Pa; ATCC 27853)) was determined by measuring the absorbance at 600 nm (OD_{600}), using a Tecan M1000 Pro monochromator plate reader. The percentage of growth inhibition was calculated for each well, using the negative control (media only) and positive control (bacteria without inhibitors) on the same plate as references. Growth inhibition of *Candida albicans* (Ca; ATCC 90028) was determined by measuring absorbance at 530 nm (OD_{530}), while the growth inhibition of *Cryptococcus neoformans var. grubii* (Cn; H99, ATCC 208821) was determined by measuring the difference in absorbance between 600 and 570 nm ($OD_{600\text{-}570}$), after the addition of resazurin (0.001% final concentration) and incubation at 35 °C for an additional 2 h. The absorbance was measured using a Biotek Synergy HTX plate reader. The percentage of growth inhibition was calculated for each well, using the negative control (media only) and positive control (fungi without inhibitors) on the same plate as references.
>
> Negative inhibition values indicate that the growth rate is higher compared to the negative control (bacteria/fungi only, set to 0% inhibition). The growth rates for all bacteria and fungi has a variation of ± 10%. Any significant variation (or outliers/hits) is identified by the modified Z-Score, and actives are selected by a combination of inhibition value and Z-Score. The Z-Score is calculated based on the sample population using a modified Z-Score method which accounts for possible skewed sample population. The modified method uses median and MAD (median average derivation) instead of average and sd, and a scaling factor[285]:
> $M(i) = 0.6745 \cdot (x(i) - \text{median}(x)\,\text{MAD})$. $M(i)$ values of > 2.5 label outliers or hits. Active samples: equal or above 80% and Z-score above 2.5 for either replicate (n = 2 on different plates). Partial active samples: inhibition values between 50.9% and 79.9% or abs(Z-score) below 2.5. Inactive samples: inhibition values below 50% and/or abs(Z-score) below 2.5.

Table C.1 Results of the antimicrobial screening of compounds **3b**, **40**, **72**, (±)-**73**, (±)-**74**, (±)-**75** and (±)-**76**.

	3b	**40**	**72**	**(±)-73**	**(±)-74**	**(±)-75**	**(±)-76**
Sa inhib. 1	18.72	16.01	12.53	12.37	10.95	12.97	1.10
Sa Z-score 1	0.12	0.31	0.56	0.57	0.67	0.53	1.36
Sa inhib. 2	10.86	15.27	15.47	13.04	10.85	16.37	15.79
Sa Z-score 2	0.80	0.46	0.45	0.63	0.80	0.38	0.43
Ec inhib. 1	10.72	10.04	7.57	8.20	8.43	7.35	–0.95
Ec Z-score 1	0.27	0.38	0.76	0.67	0.63	0.80	2.08
Ec inhib. 2	4.57	6.60	4.31	7.25	7.42	8.69	9.47
Ec Z-score 2	1.37	1.02	1.41	0.90	0.87	0.65	0.52
Kp inhib. 1	14.06	12.26	11.07	10.53	13.63	16.20	17.26
Kp Z-score 1	0.18	0.38	0.51	0.56	0.23	–0.04	–0.15
Kp inhib. 2	8.00	6.68	9.74	8.88	7.53	13.79	8.44
Kp Z-score 2	0.11	0.28	–0.11	0.00	0.17	–0.63	0.05
Pa inhib. 1	1.28	9.78	4.26	8.47	6.83	8.78	4.73
Pa Z-score 1	1.49	0.24	1.05	0.43	0.67	0.39	0.98
Pa inhib. 2	9.88	6.85	7.35	7.17	5.46	13.90	0.72
Pa Z-score 2	–0.66	–0.21	–0.28	–0.25	0.00	–1.26	0.70
Ab inhib. 1	5.07	13.45	3.25	4.03	11.02	6.61	–0.99
Ab Z-score 1	0.72	–0.62	1.02	0.89	–0.23	0.47	1.70
Ab inhib. 2	1.69	8.94	4.75	–0.43	15.36	6.59	0.51
Ab Z-score 2	0.91	–0.43	0.34	1.31	–1.63	0.00	1.13
Ca inhib. 1	14.01	4.56	15.35	7.12	14.78	6.67	2.90
Ca Z-score 1	–1.22	0.04	–1.40	–0.30	–1.33	–0.24	0.26
Ca inhib. 2	12.44	6.99	15.28	10.35	2.31	4.77	4.14
Ca Z-score 2	–1.11	–0.21	–1.57	–0.76	0.54	0.14	0.24
Cn inhib. 1	–48.81	–37.46	–59.63	–45.11	–51.71	–60.42	–33.77
Cn Z-score 1	0.27	0.02	0.51	0.18	0.33	0.52	–0.06
Cn inhib. 2[a]	–	–	–	–	–	–	–
Cn Z-score 2[a]	–	–	–	–	–	–	–

[a] For Cn sample 2: quality test not passed.

D. Selected 2D NMR Spectra

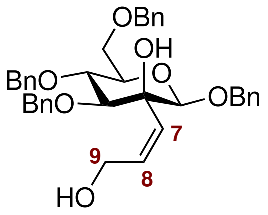

36
(acetone-D_6)

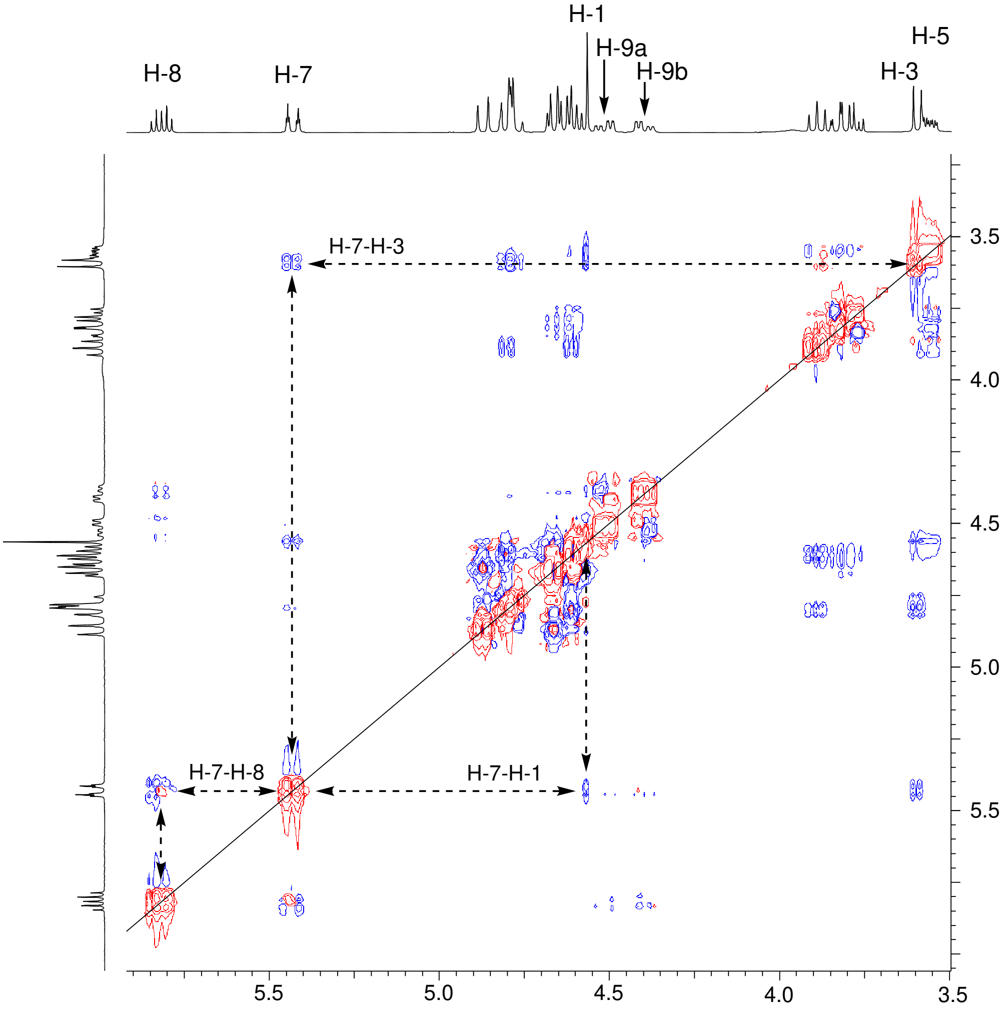

Figure D.1 Section of the H,H-NOESY spectrum of **36** at 400.2 MHz in acetone-D_6. Significant signals are labeled, and dashed arrows indicate NOE contacts between the axial H-1/H-3 and the alkene H-7. The shown spectrum is symmetrized.

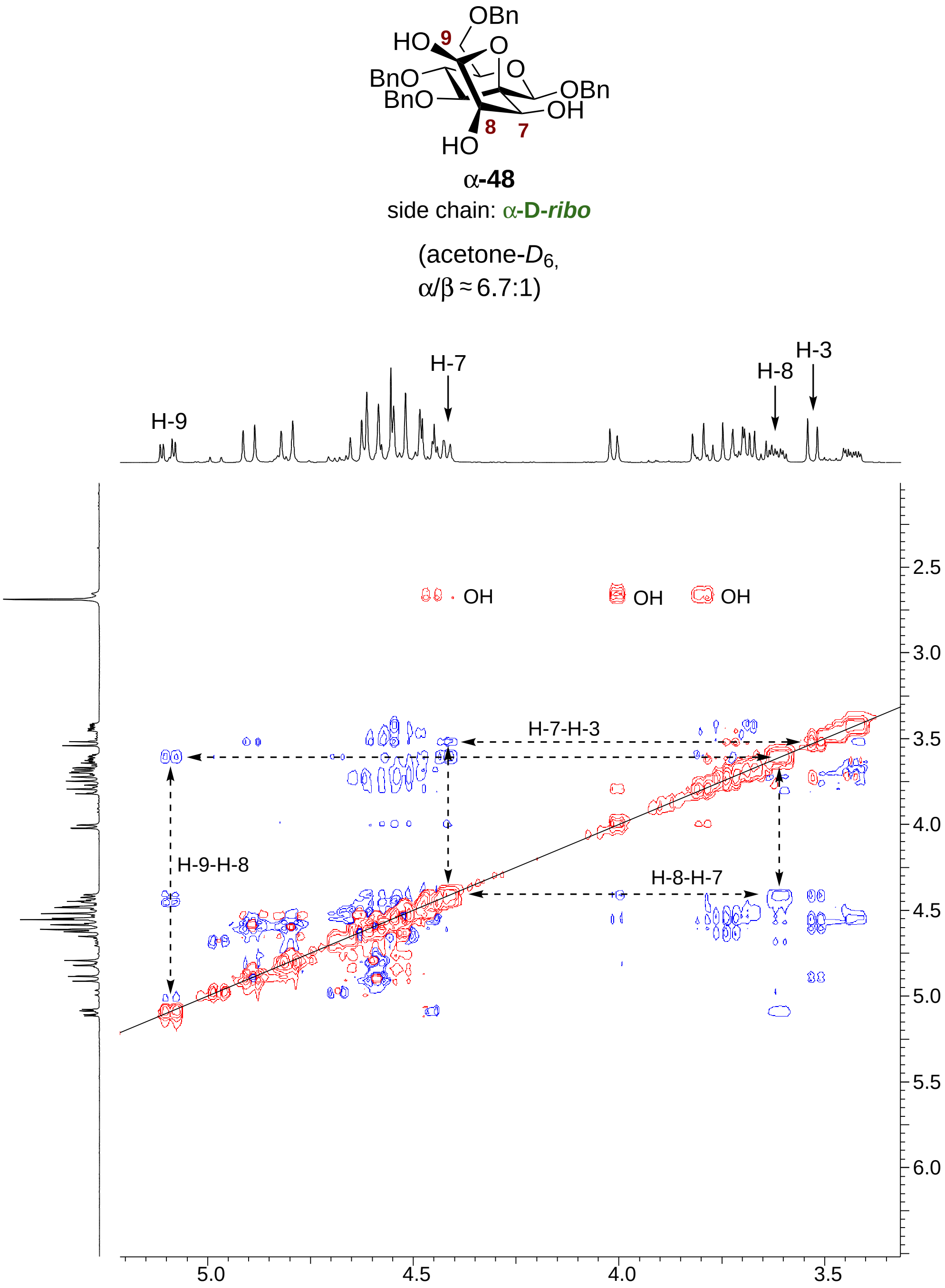

Figure D.2 Section of the H,H-NOESY spectrum of **α,β-48** (α/β ≈ 6.7:1) at 400.2 MHz in acetone-D_6. Significant signals of the α-isomer are labeled, and dashed arrows refer to NOE contacts between the side chain H-7/H-8/H-9 and the axial carbohydrate H-3. The shown spectrum is symmetrized.

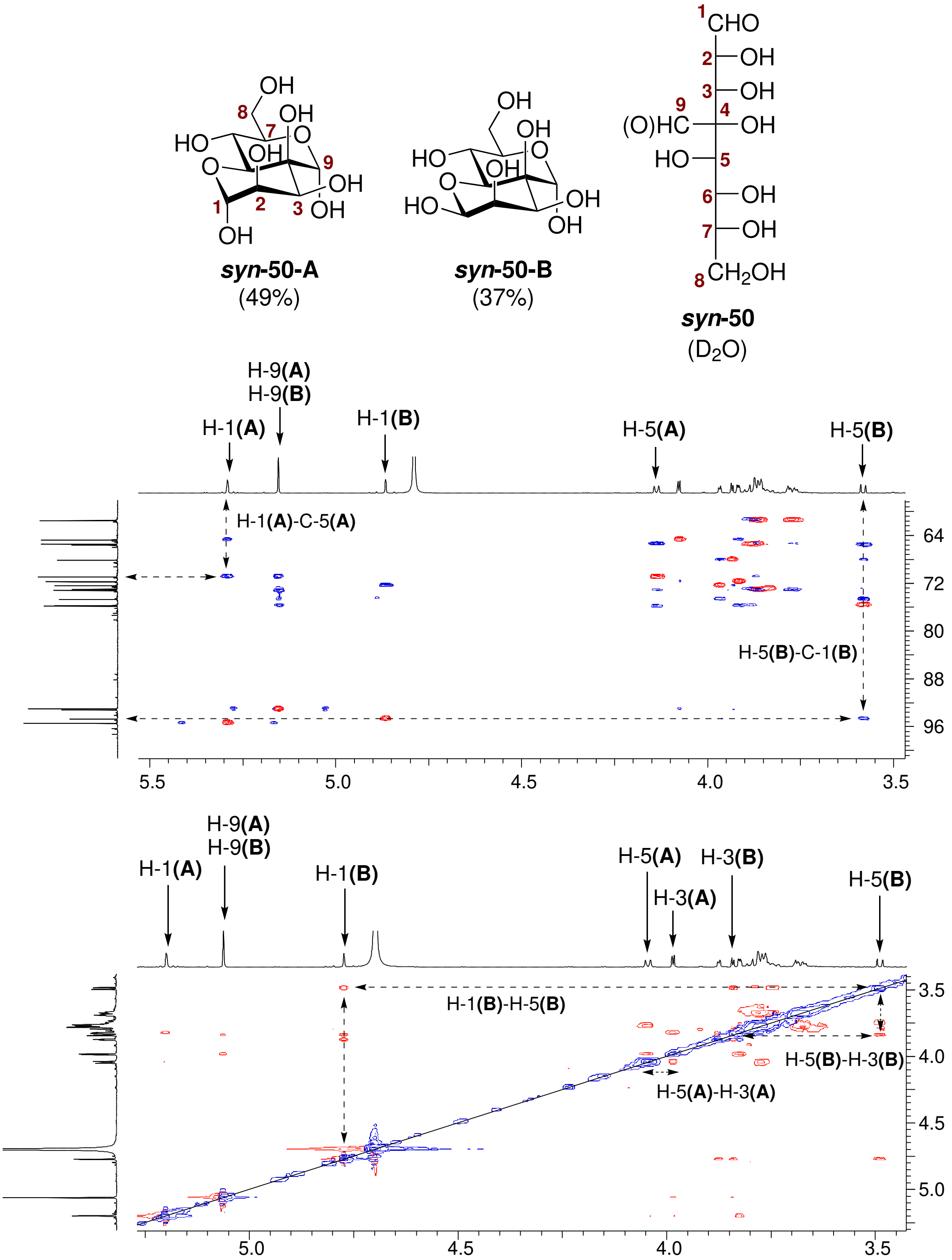

Figure D.3 Top: combined C,H-HSQC (red) and C,H-HMBC (blue) spectrum of ***syn*-50** at 700.3 MHz/176.1 MHz in D_2O. Significant signals of both isomers ***syn*-50-A** and ***syn*-50-B** are labeled. Dashed arrows refer to key couplings indicating the *C*-1–*O*-5 ring closure. Bottom: H,H-NOESY spectrum of ***syn*-50** at 700.3 MHz in D_2O. Dashed arrows refer to correlations indicating spatial proximity in a *syn*-relationship in the respective isomer. The shown spectrum is symmetrized.

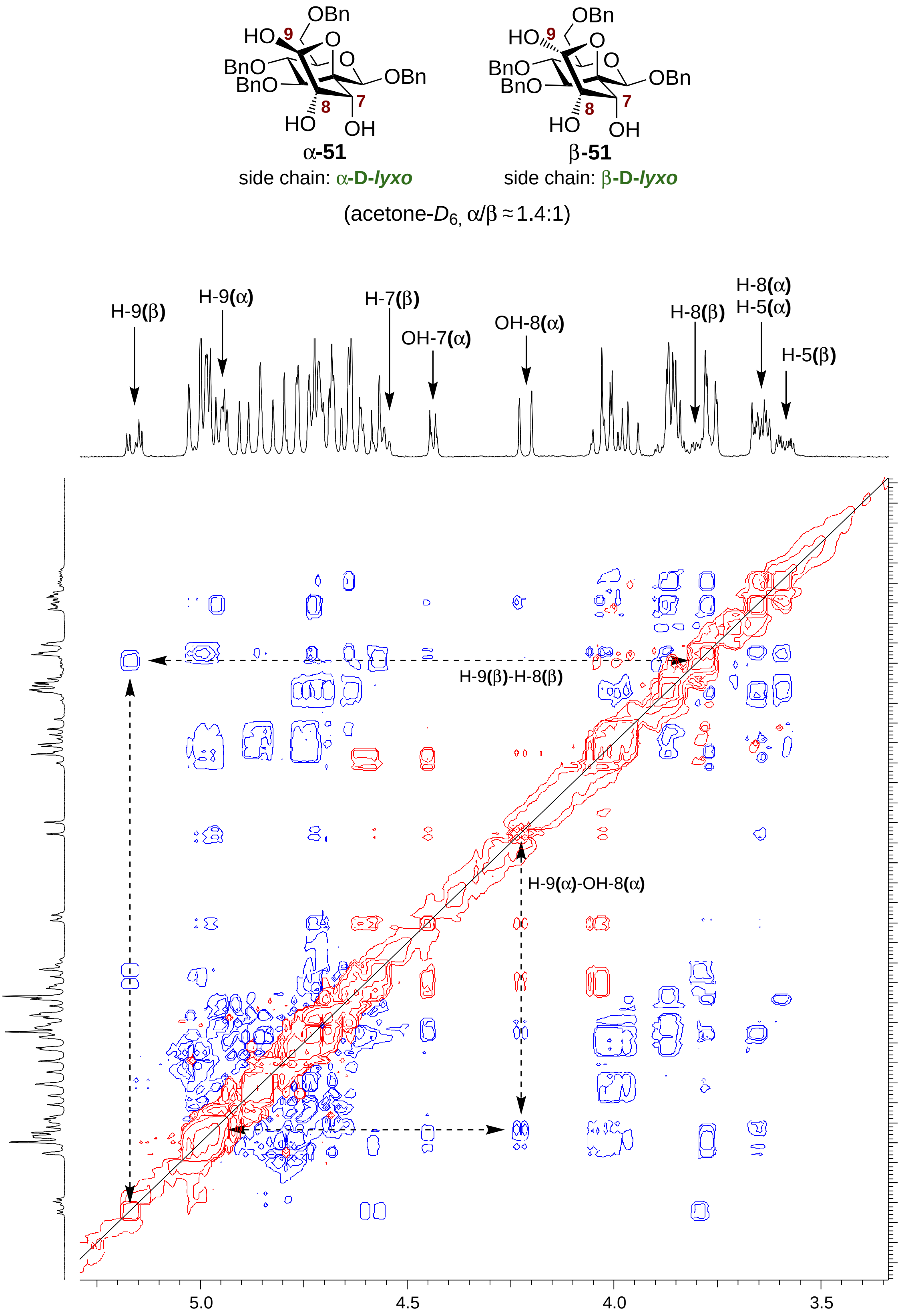

Figure D.4 Section of the H,H-NOESY spectrum of **α,β-51** (α/β ≈ 1.4:1) at 600.1 MHz in acetone-D_6. Significant signals are labeled, and dashed arrows refer to NOE contacts between the side chain H-9(**β**) and H-8(**β**), and between H-9(**α**) and OH-8(**α**). The shown spectrum is symmetrized.

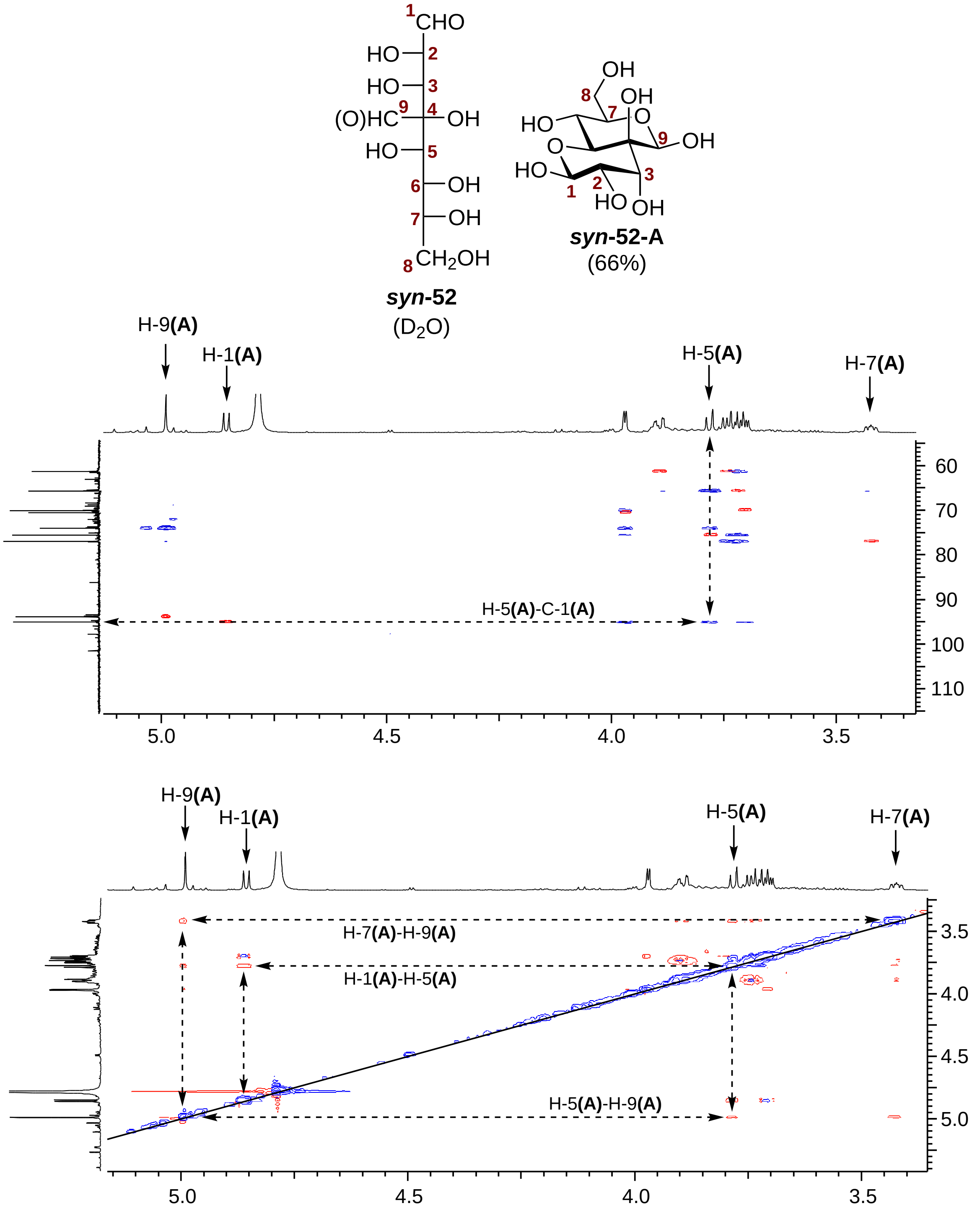

Figure D.5 Top: combined C,H-HSQC (red) and C,H-HMBC (blue) spectrum of ***syn*-52** at 700.3 MHz/176.1 MHz in D_2O. Significant signals of isomer ***syn*-52-A** are labeled. Dashed arrows refer to key couplings indicating the *C*-1–*O*-5 ring closure. Bottom: H,H-NOESY spectrum of ***syn*-52** at 700.3 MHz in D_2O. Dashed arrows refer to correlations indicating spatial proximity in a *syn*-relationship in the respective isomer. The shown spectrum is symmetrized.

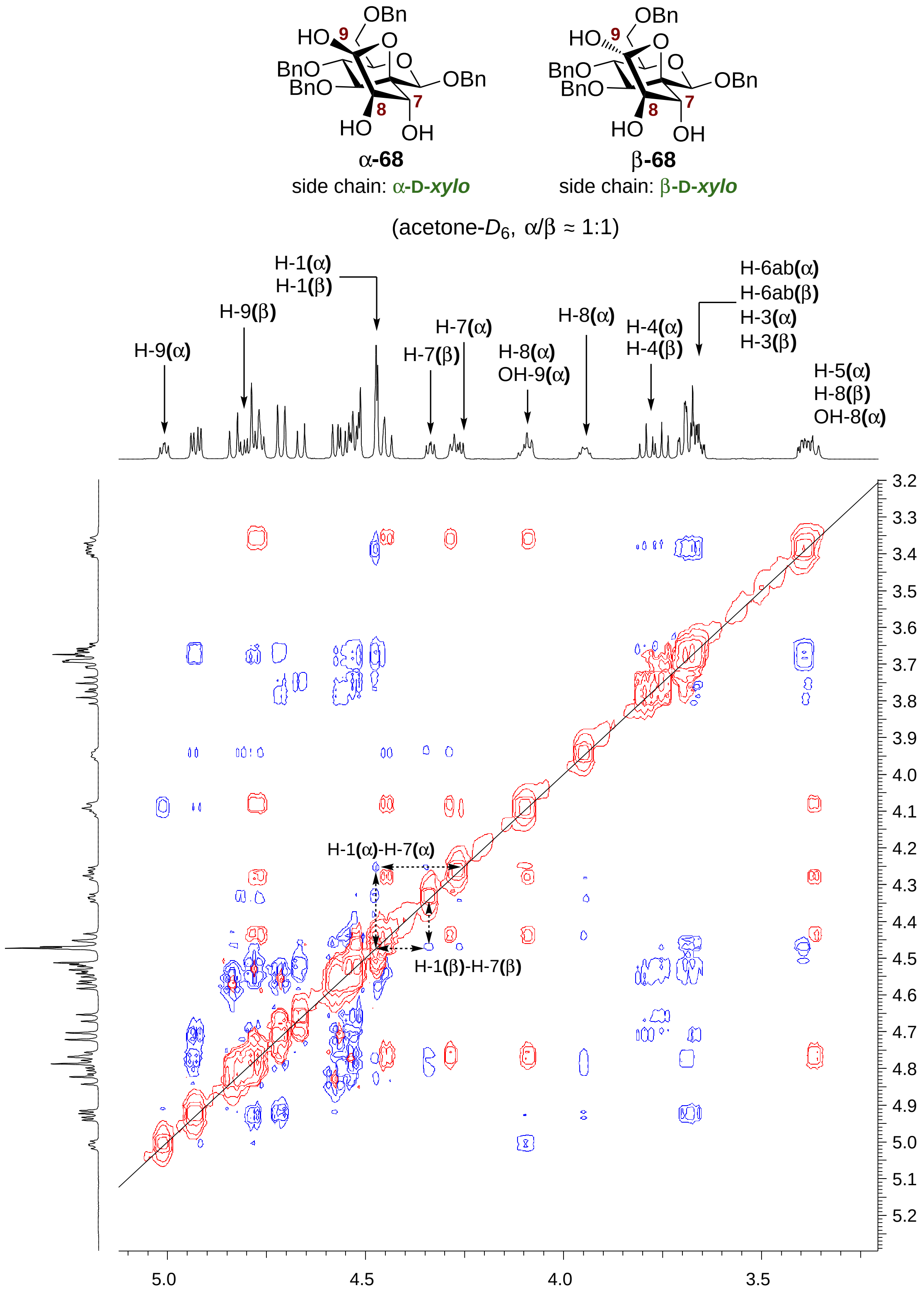

Figure D.6 Section of the H,H-NOESY spectrum of **α,β-68** (α/β ≈ 1:1) at 600.1 MHz in acetone-D_6. Significant signals are labeled, and dashed arrows refer to NOE contacts between the side chain H-7 and the carbohydrate H-1. The shown spectrum is symmetrized.

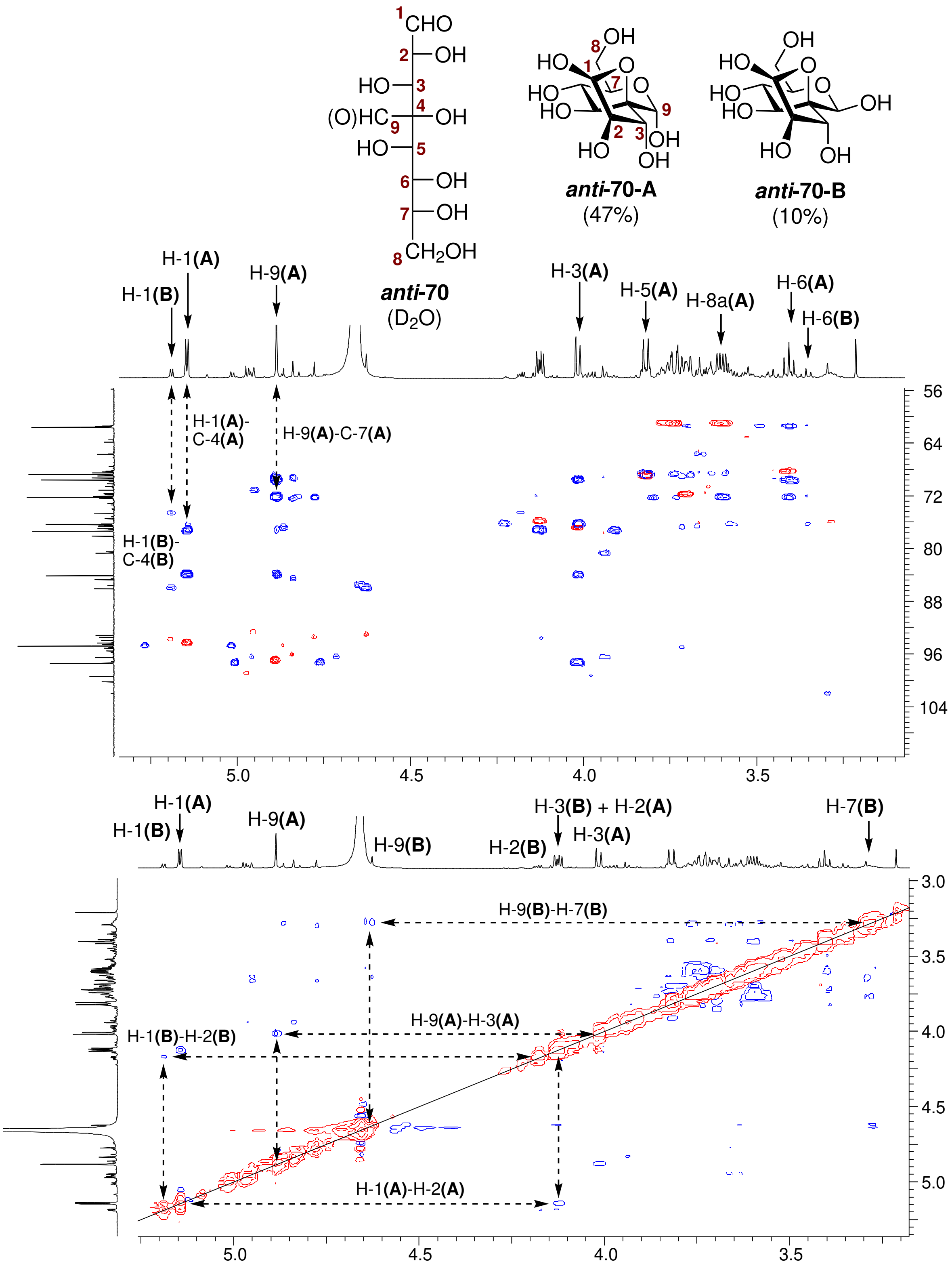

Figure D.7 Top: combined C,H-HSQC (red) and C,H-HMBC (blue) spectrum of ***anti*-70** at 700.3 MHz/176.1 MHz in D_2O. Significant signals of isomers ***anti*-70-A** and ***anti*-70-B** are labeled. Dashed arrows refer to key couplings indicating the *C*-1–*O*-4 and *C*-9–*O*-7 ring closures. Bottom: H,H-NOESY spectrum of ***anti*-70** at 700.3 MHz in D_2O. Dashed arrows refer to correlations indicating spatial proximity in a *syn*-relationship in the respective isomer. The shown spectrum is symmetrized.

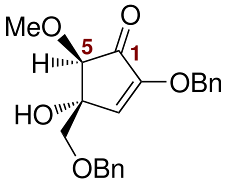

(±)-75
(acetone-D_6)

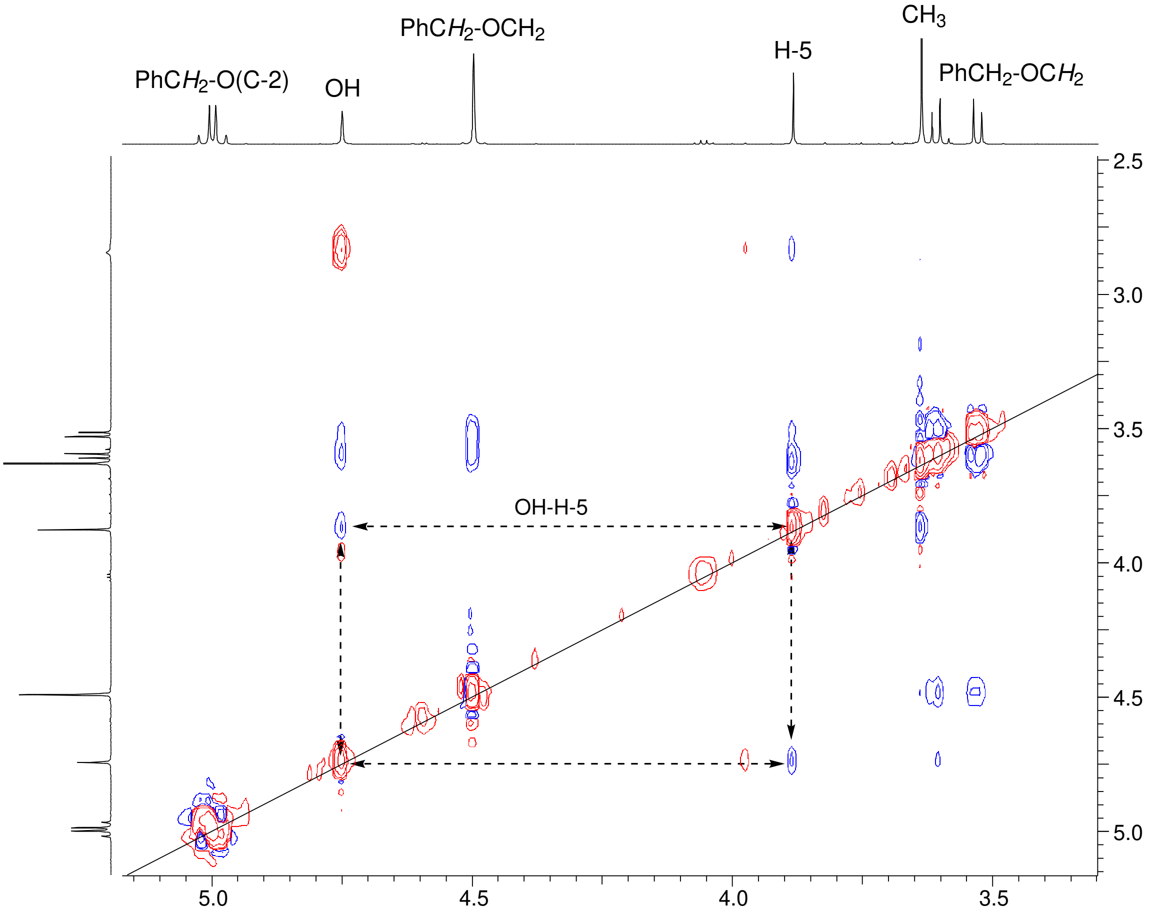

Figure D.8 Section of the H,H-NOESY spectrum of **(±)-75** at 600.1 MHz in acetone-D_6. Significant signals are labeled, and dashed arrows refer to NOE contacts between the *H*-5 and the *C*-4-OH. The shown spectrum is unprocessed.

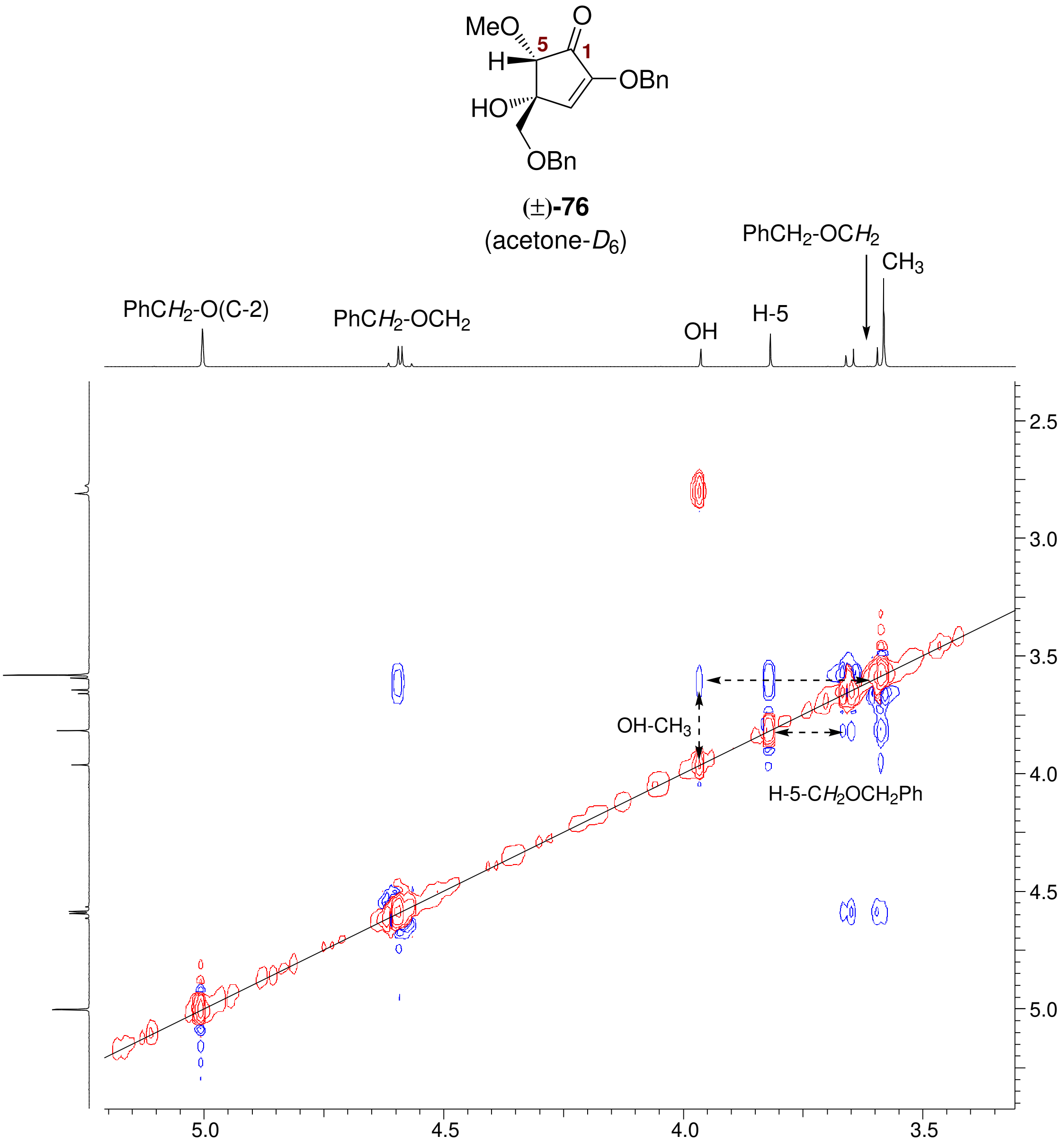

Figure D.9 Section of the H,H-NOESY spectrum of **(±)-76** at 600.1 MHz in acetone-D_6. Significant signals are labeled, and dashed arrows refer to NOE contacts between the C-4-OH and the CH$_3$, and between the H-5 and the PhCH$_2$OCH_2, respectively. The shown spectrum is unprocessed.

E. NMR Spectra

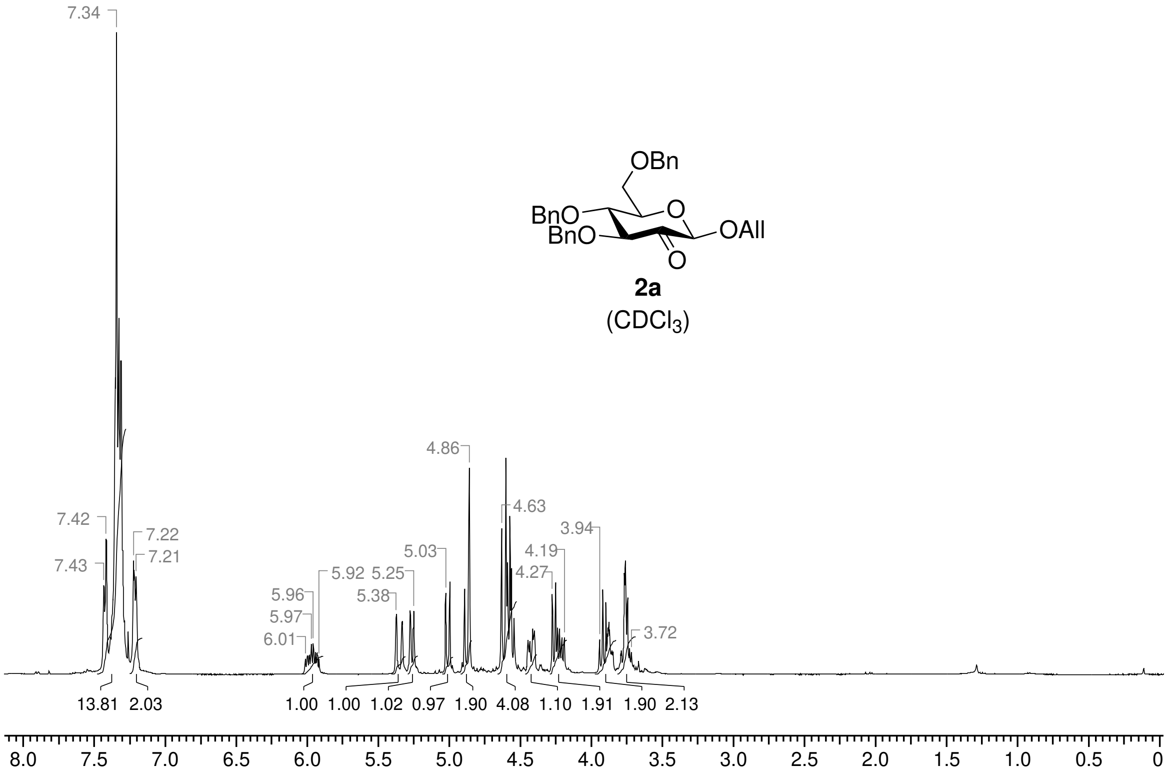
7.34
7.42
7.43
7.22
7.21
5.96
5.97
6.01
5.92
5.25
5.38
5.03
4.86
4.63
4.19
4.27
3.94
3.72
OBn
BnO
BnO
O
OAll
O
2a
(CDCl$_3$)
13.81
2.03
1.00
1.00
1.02
0.97
1.90
4.08
1.10
1.91
1.90
2.13
8.0
7.5
7.0
6.5
6.0
5.5
5.0
4.5
4.0
3.5
3.0
2.5
2.0
1.5
1.0
0.5
0

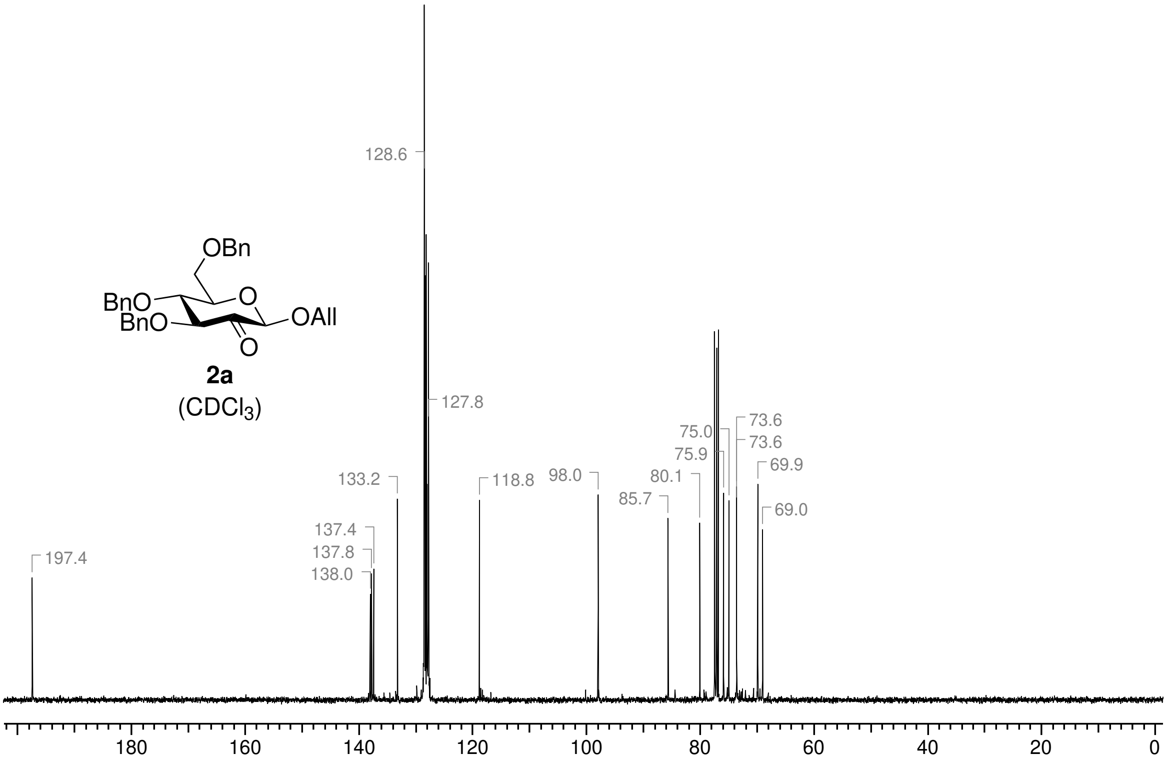
128.6
OBn
BnO
BnO
O
OAll
O
2a
(CDCl$_3$)
127.8
73.6
73.6
75.0
75.9
69.9
133.2
118.8
98.0
80.1
85.7
69.0
137.4
137.8
138.0
197.4
180
160
140
120
100
80
60
40
20
0

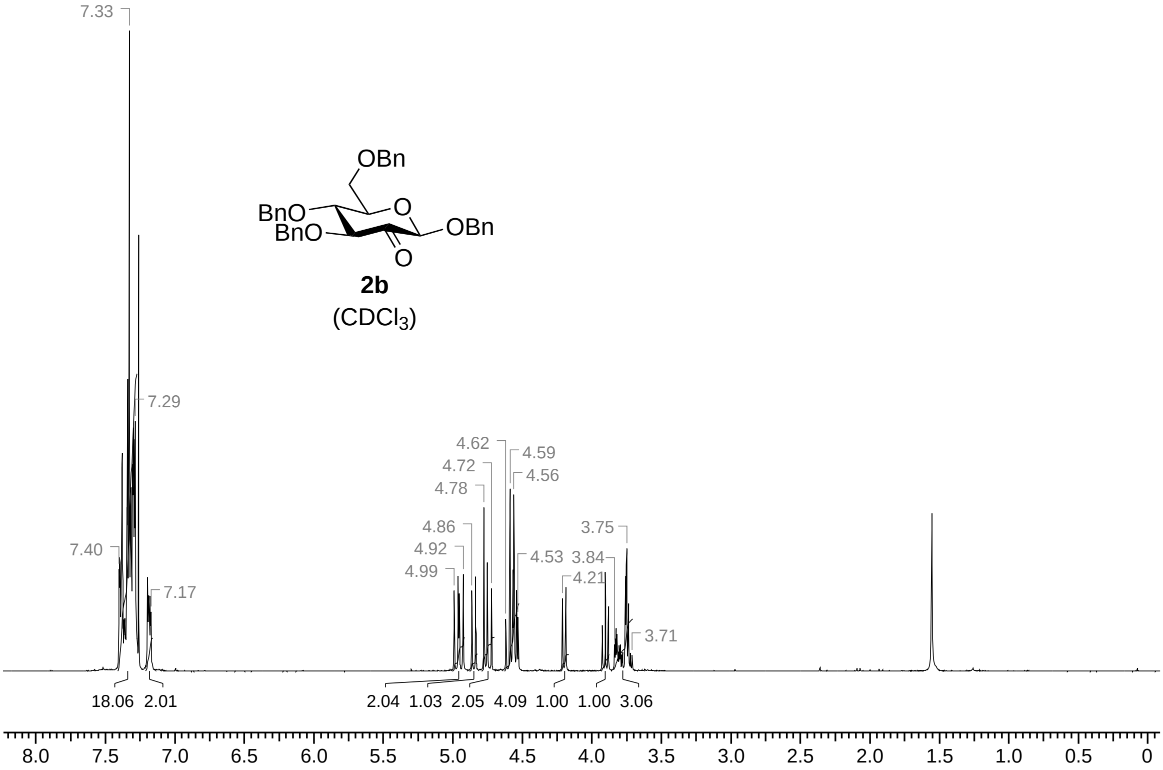

7.33
7.29
7.40
7.17
4.62
4.72
4.78
4.59
4.56
4.86
4.92
4.99
4.53
3.75
3.84
4.21
3.71
OBn
BnO
BnO
O
OBn
O
2b
(CDCl$_3$)
18.06
2.01
2.04
1.03
2.05
4.09
1.00
1.00
3.06
8.0
7.5
7.0
6.5
6.0
5.5
5.0
4.5
4.0
3.5
3.0
2.5
2.0
1.5
1.0
0.5
0

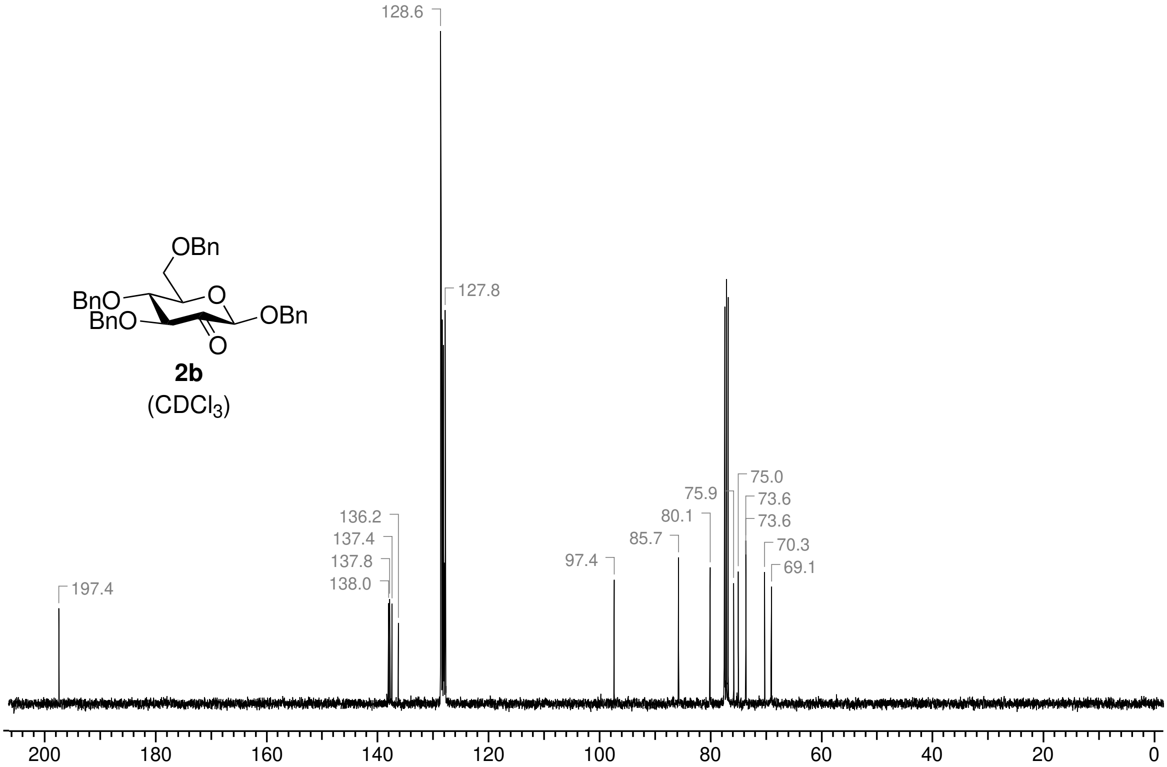

128.6
127.8
OBn
BnO
BnO
O
OBn
O
2b
(CDCl$_3$)
197.4
136.2
137.4
137.8
138.0
97.4
85.7
80.1
75.9
75.0
73.6
73.6
70.3
69.1
200
180
160
140
120
100
80
60
40
20
0

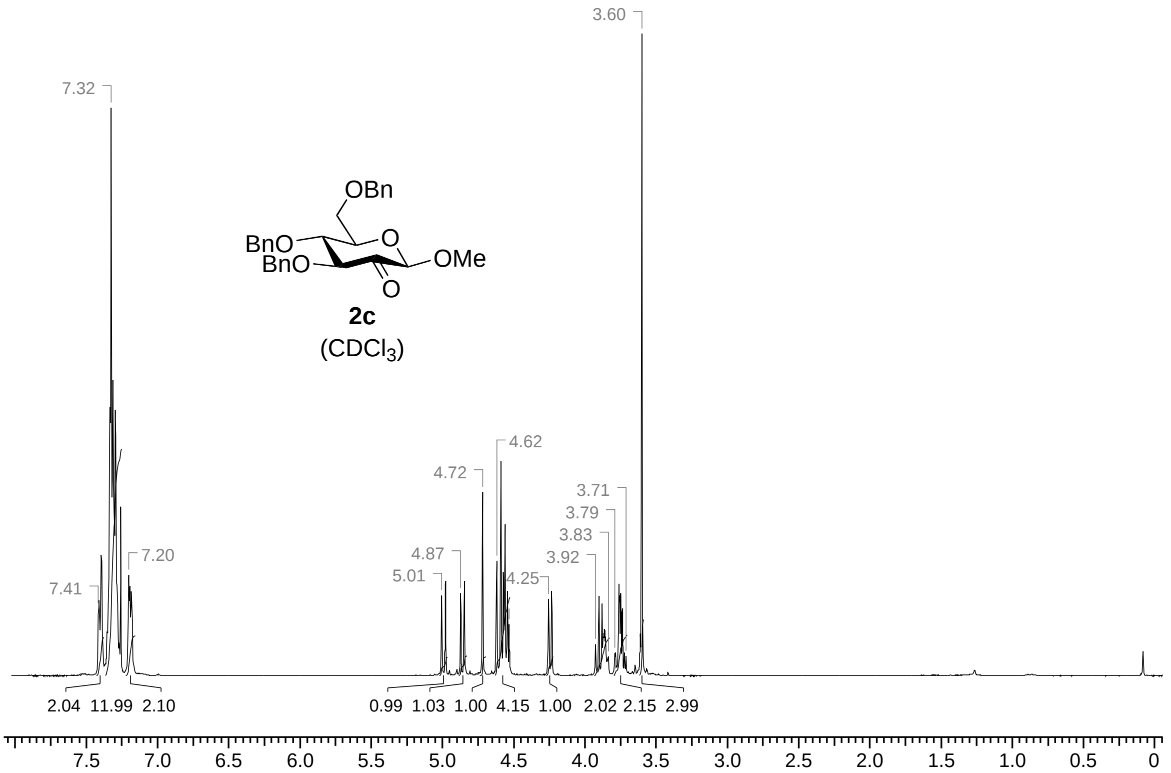
OBn
BnO
BnO
O
OMe
O
2c
(CDCl3)
3.60
7.32
7.41
7.20
5.01
4.87
4.72
4.62
4.25
3.92
3.83
3.79
3.71
2.04 11.99 2.10
0.99 1.03 1.00 4.15 1.00 2.02 2.15 2.99
7.5 7.0 6.5 6.0 5.5 5.0 4.5 4.0 3.5 3.0 2.5 2.0 1.5 1.0 0.5 0

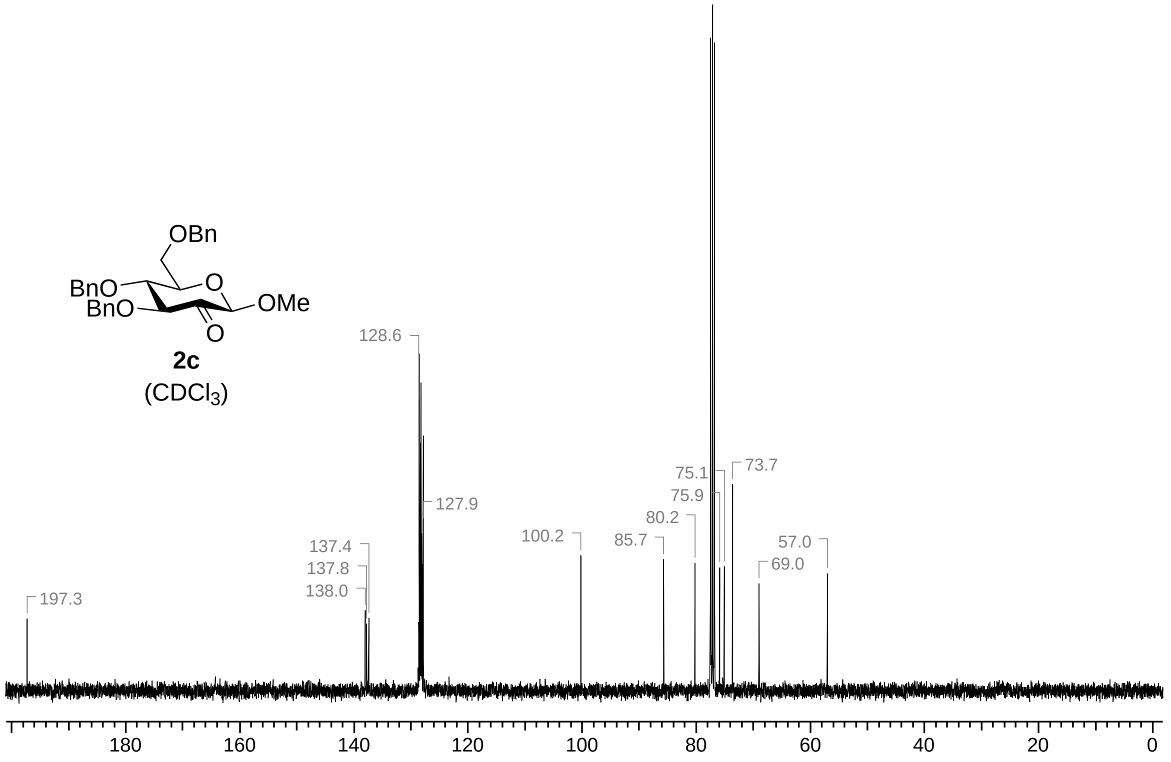
OBn
BnO
BnO
O
OMe
O
2c
(CDCl3)
197.3
138.0
137.8
137.4
128.6
127.9
100.2
85.7
80.2
75.9
75.1
73.7
69.0
57.0
180 160 140 120 100 80 60 40 20 0

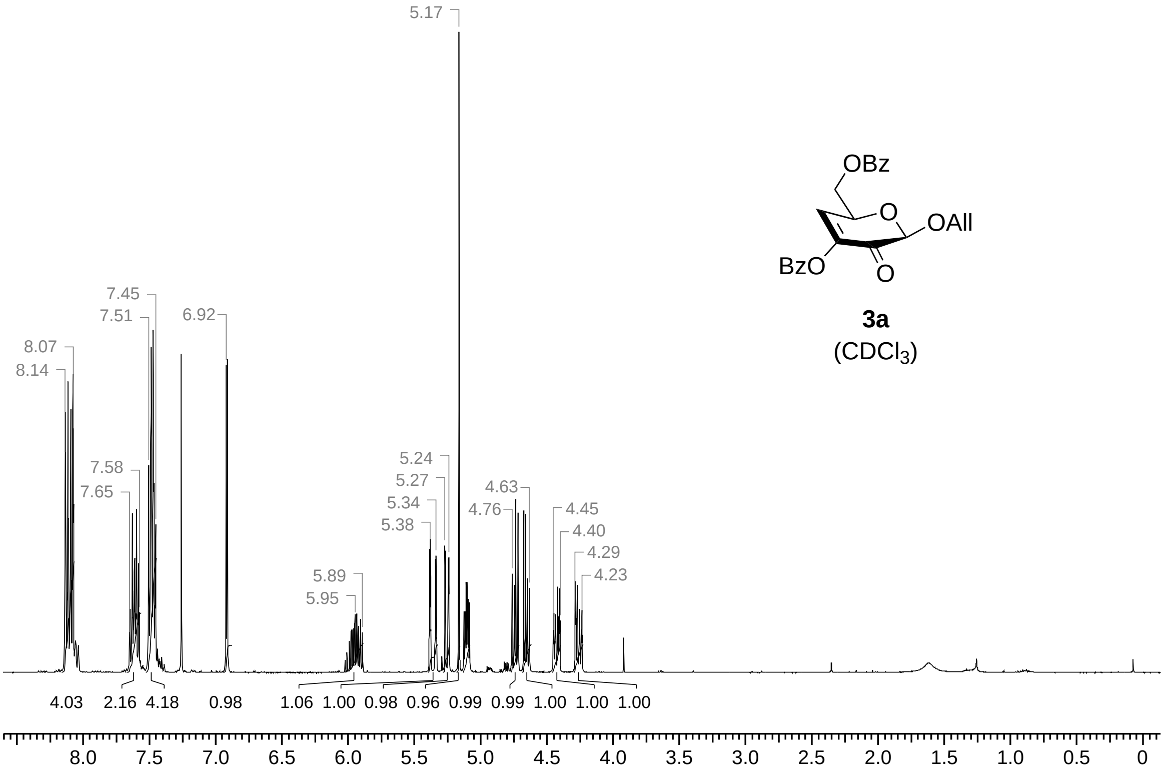
5.17
7.45
7.51
6.92
8.07
8.14
7.58
7.65
5.24
5.27
5.34
5.38
4.63
4.76
4.45
4.40
4.29
4.23
5.89
5.95
4.03 2.16 4.18 0.98 1.06 1.00 0.98 0.96 0.99 0.99 1.00 1.00 1.00
8.0 7.5 7.0 6.5 6.0 5.5 5.0 4.5 4.0 3.5 3.0 2.5 2.0 1.5 1.0 0.5 0
OBz
O
OAll
BzO
O
3a
($CDCl_3$)

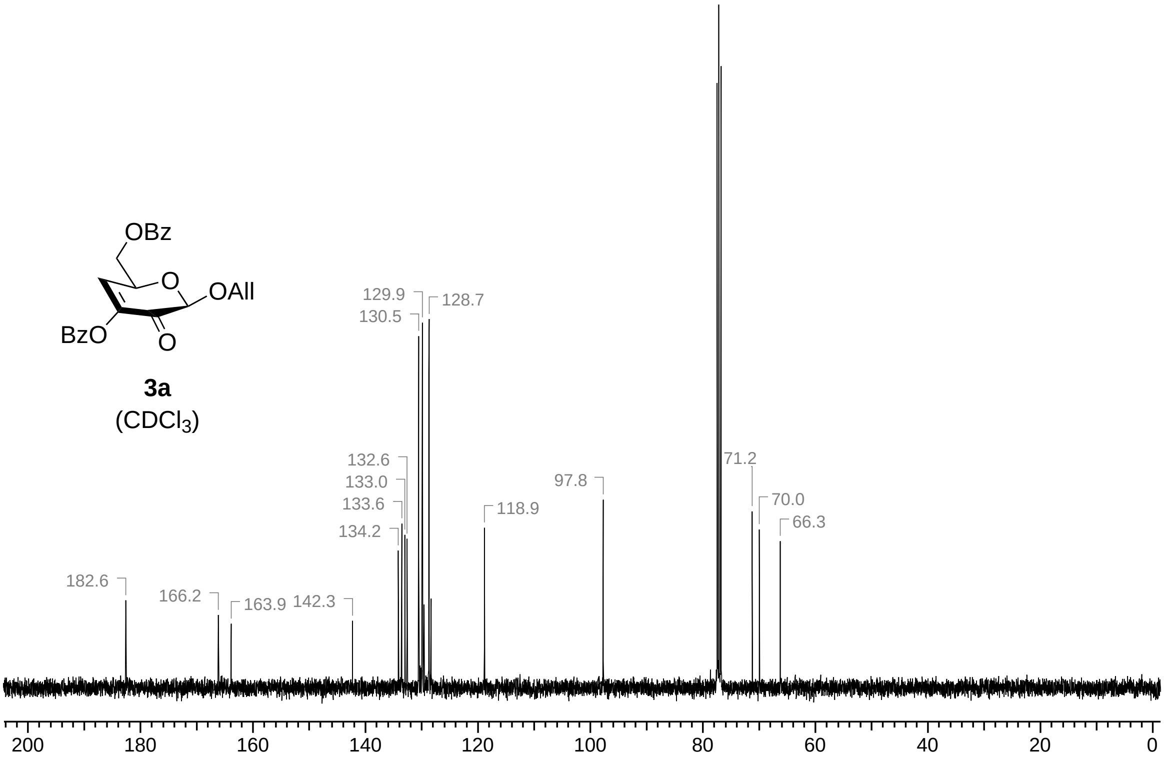
OBz
O
OAll
BzO
O
3a
($CDCl_3$)
129.9
130.5
128.7
132.6
133.0
133.6
134.2
118.9
97.8
71.2
70.0
66.3
182.6
166.2
163.9
142.3
200 180 160 140 120 100 80 60 40 20 0

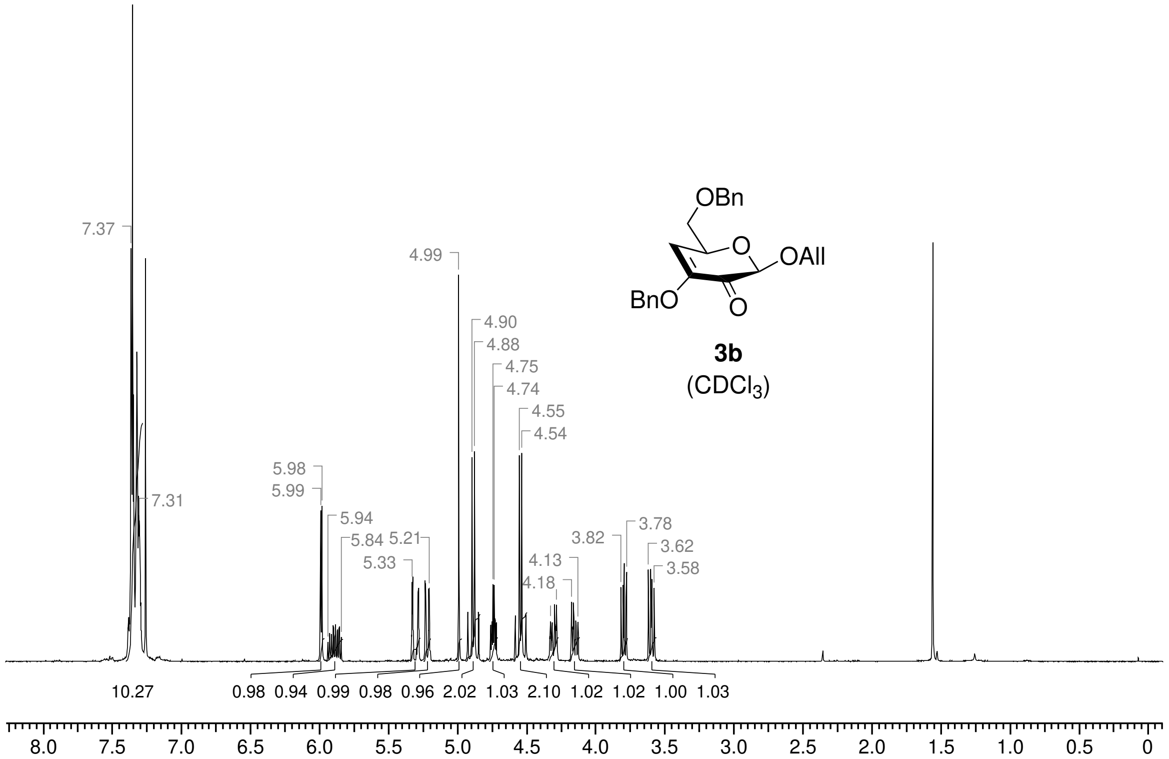
OBn
O
OAll
BnO
O
3b
(CDCl$_3$)
7.37
7.31
5.98
5.99
5.94
5.84
5.21
5.33
4.99
4.90
4.88
4.75
4.74
4.55
4.54
4.13
4.18
3.82
3.78
3.62
3.58
10.27
0.98
0.94
0.99
0.98
0.96
2.02
1.03
2.10
1.02
1.02
1.00
1.03
8.0
7.5
7.0
6.5
6.0
5.5
5.0
4.5
4.0
3.5
3.0
2.5
2.0
1.5
1.0
0.5
0

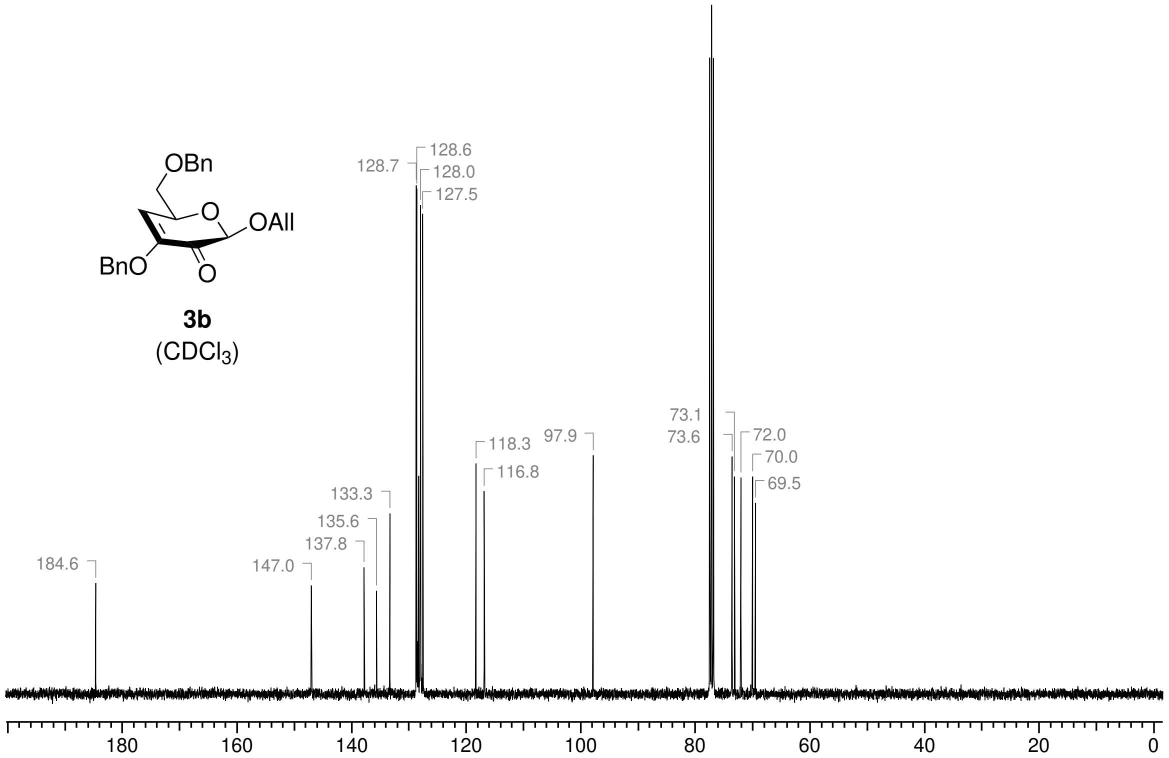
OBn
O
OAll
BnO
O
3b
(CDCl$_3$)
184.6
147.0
137.8
135.6
133.3
128.7
128.6
128.0
127.5
118.3
116.8
97.9
73.1
73.6
72.0
70.0
69.5
180
160
140
120
100
80
60
40
20
0

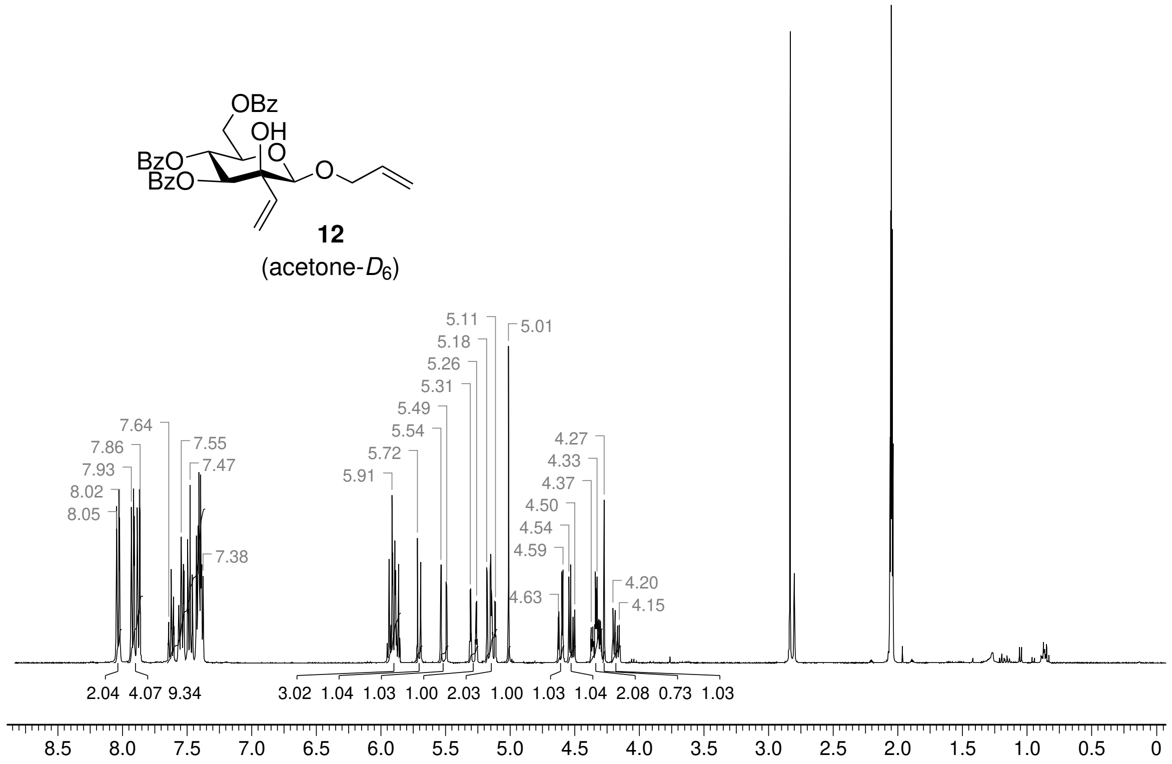
OBz
OH
O
BzO
BzO
O
12
(acetone-D_6)
5.11
5.01
5.18
5.26
5.31
5.49
5.54
5.72
5.91
7.64
7.86
7.93
8.02
8.05
7.55
7.47
7.38
4.27
4.33
4.37
4.50
4.54
4.59
4.63
4.20
4.15
2.04
4.07
9.34
3.02
1.04
1.03
1.00
2.03
1.00
1.03
1.04
2.08
0.73
1.03
8.5
8.0
7.5
7.0
6.5
6.0
5.5
5.0
4.5
4.0
3.5
3.0
2.5
2.0
1.5
1.0
0.5
0

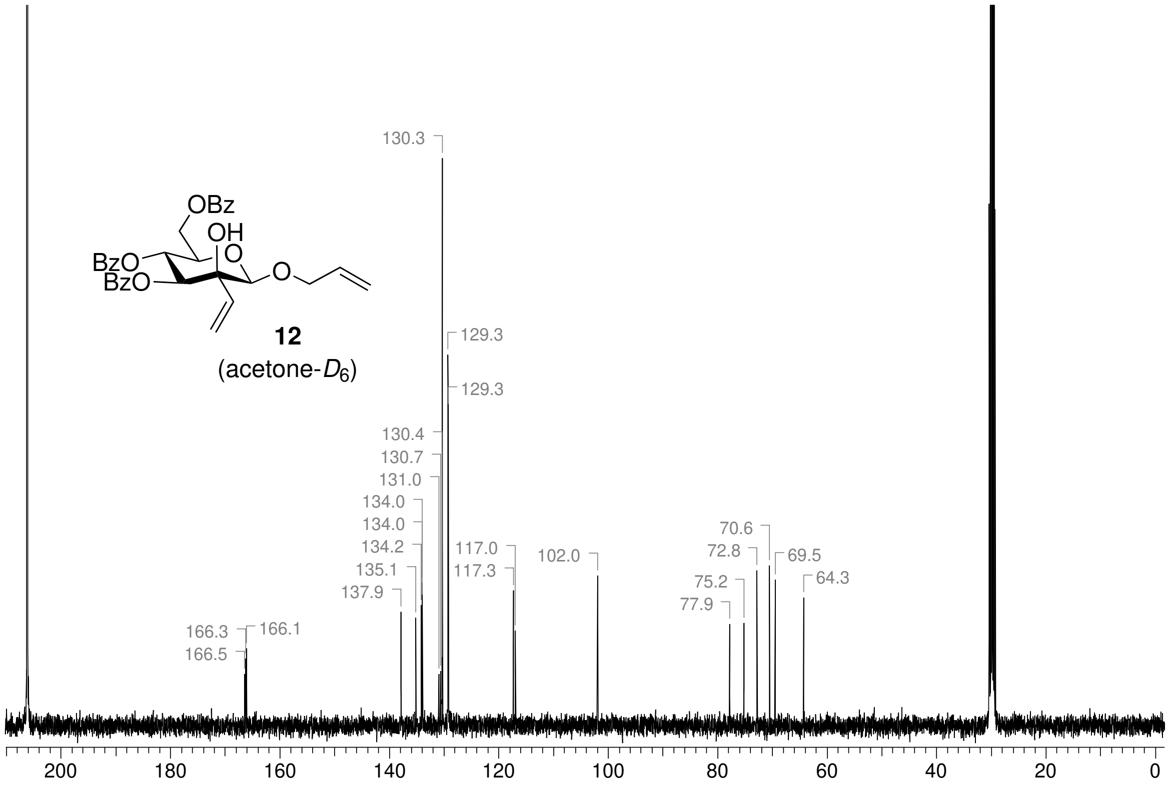
130.3
OBz
OH
O
BzO
BzO
O
12
(acetone-D_6)
129.3
129.3
130.4
130.7
131.0
134.0
134.0
134.2
135.1
137.9
117.0
117.3
102.0
70.6
72.8
69.5
75.2
64.3
77.9
166.3
166.1
166.5
200
180
160
140
120
100
80
60
40
20
0

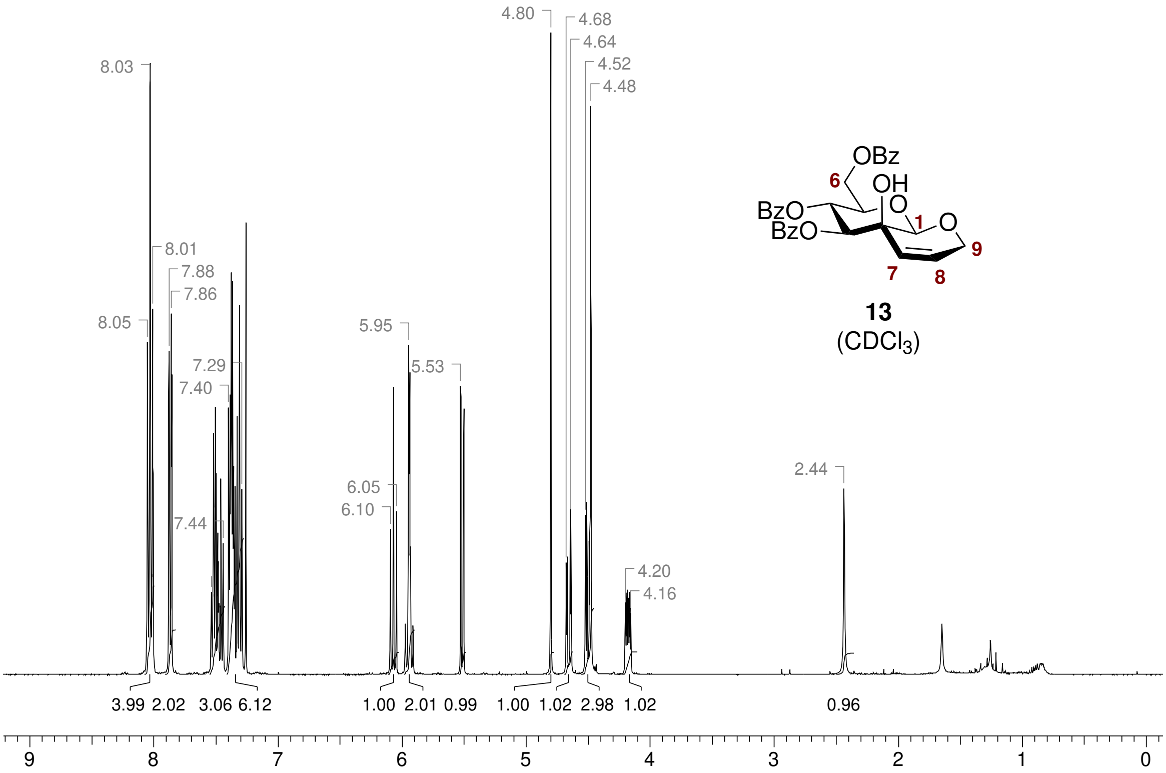
8.03
8.05
8.01
7.88
7.86
7.29
7.40
7.44
5.95
5.53
6.05
6.10
4.80
4.68
4.64
4.52
4.48
4.20
4.16
2.44
3.99 2.02 3.06 6.12
1.00 2.01 0.99
1.00 1.02 2.98 1.02
0.96
9 8 7 6 5 4 3 2 1 0
OBz
OH
BzO
BzO
O
O
1 6 7 8 9
13
(CDCl$_3$)

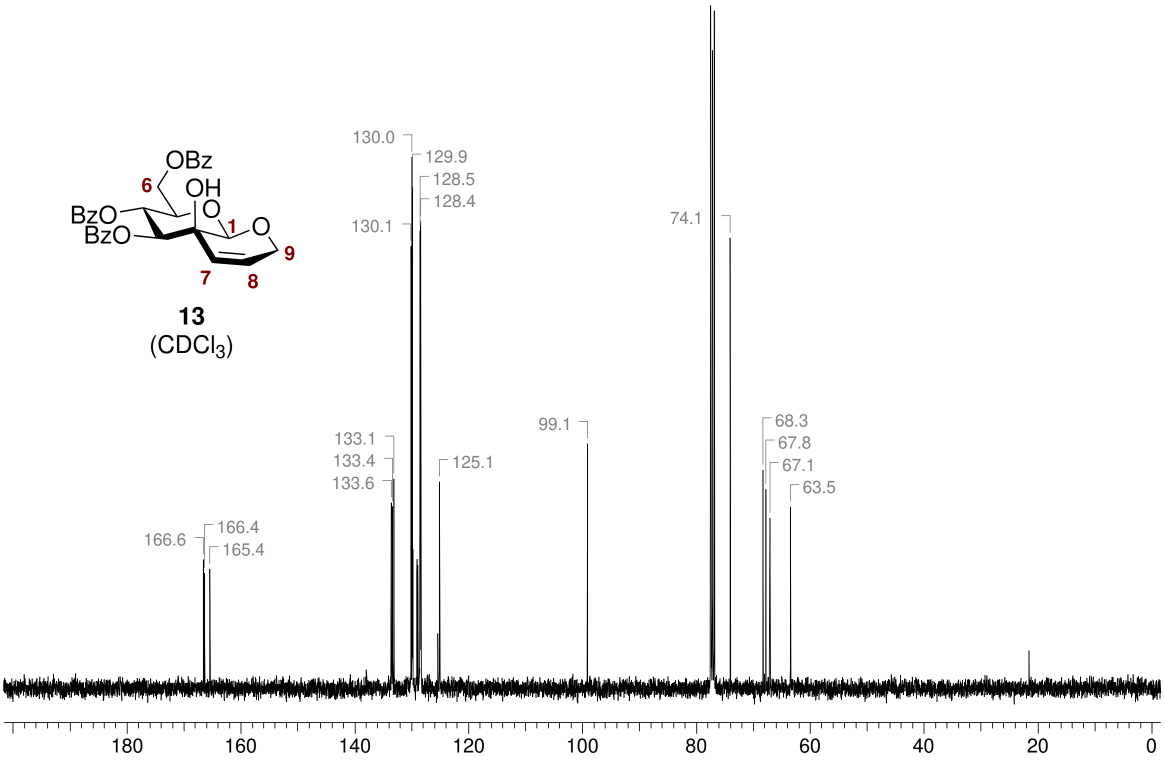
130.0
129.9
128.5
128.4
130.1
74.1
133.1
133.4
133.6
125.1
99.1
68.3
67.8
67.1
63.5
166.6
166.4
165.4
180 160 140 120 100 80 60 40 20 0
OBz
OH
BzO
BzO
O
O
1 6 7 8 9
13
(CDCl$_3$)

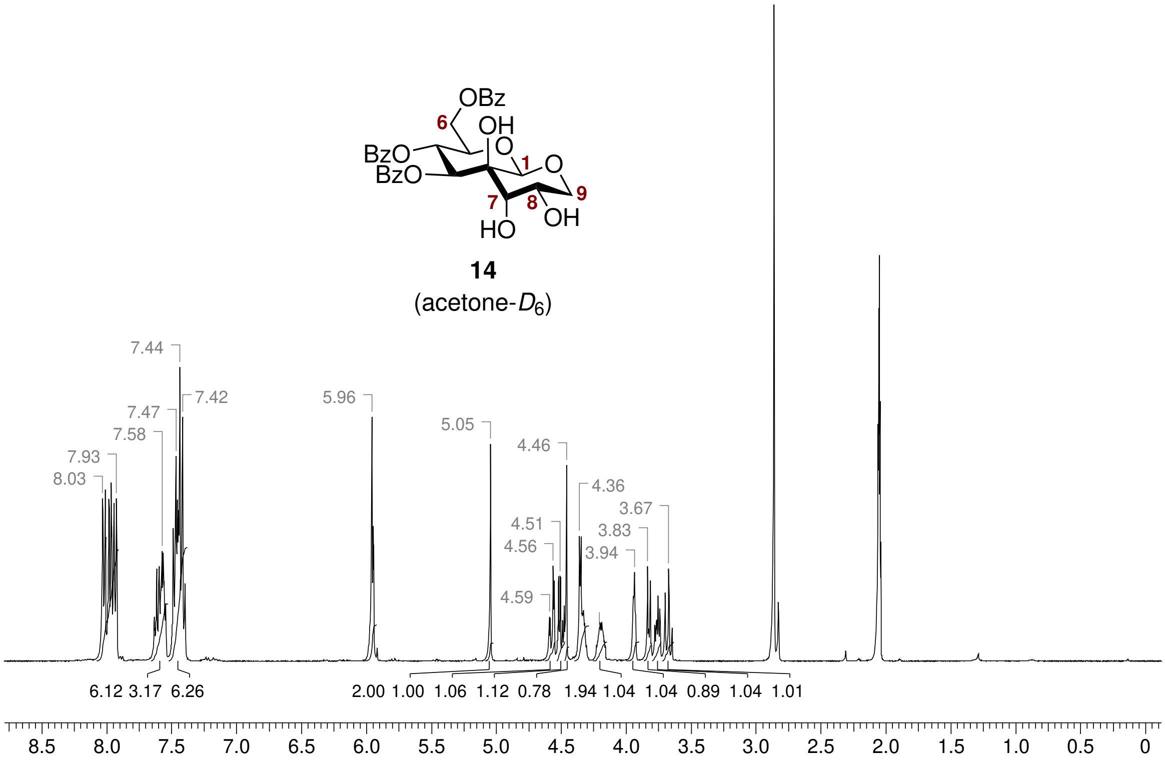
OBz
6
OH
O
1
O
BzO
BzO
7
8
9
HO
OH
14
(acetone-D_6)
7.44
7.42
7.47
7.58
7.93
8.03
5.96
5.05
4.46
4.36
3.67
4.51
3.83
4.56
3.94
4.59
6.12 3.17 6.26
2.00 1.00 1.06 1.12 0.78 1.94 1.04 1.04 0.89 1.04 1.01
8.5
8.0
7.5
7.0
6.5
6.0
5.5
5.0
4.5
4.0
3.5
3.0
2.5
2.0
1.5
1.0
0.5
0

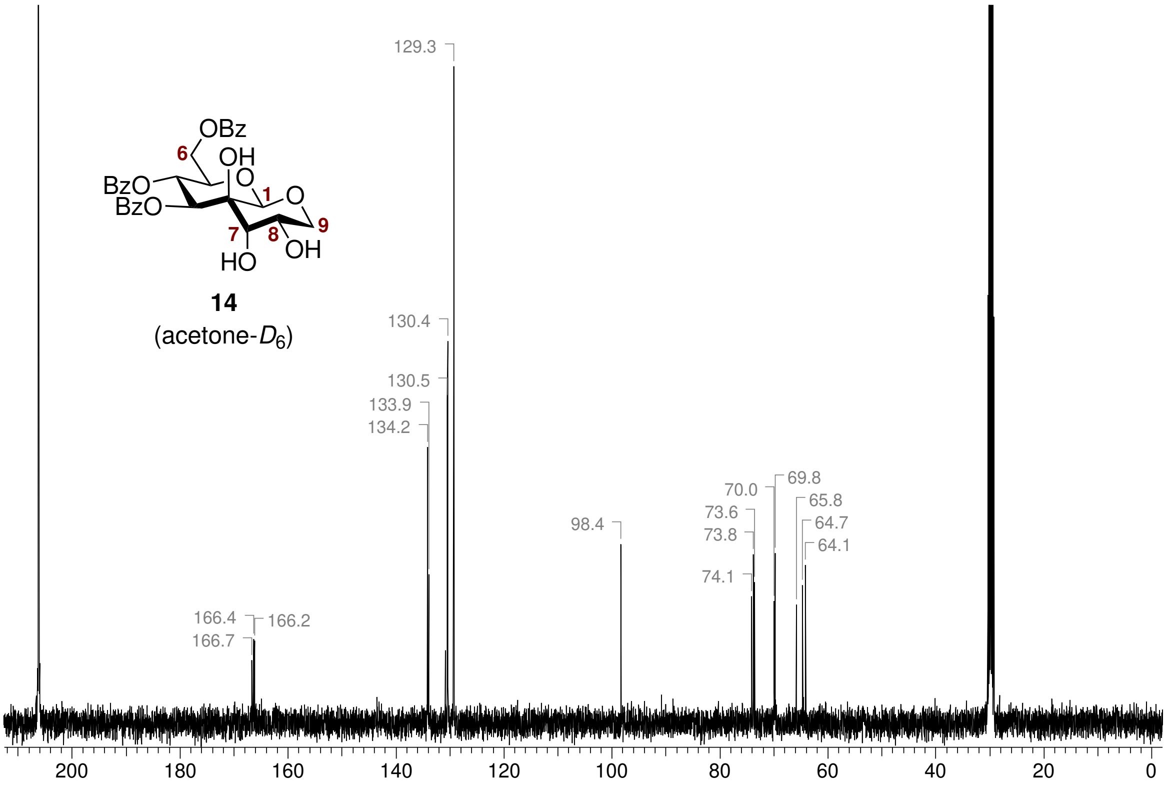
129.3
OBz
6
OH
O
1
O
BzO
BzO
7
8
9
HO
OH
14
(acetone-D_6)
130.4
130.5
133.9
134.2
70.0
69.8
65.8
73.6
64.7
98.4
73.8
64.1
74.1
166.4
166.2
166.7
200
180
160
140
120
100
80
60
40
20
0

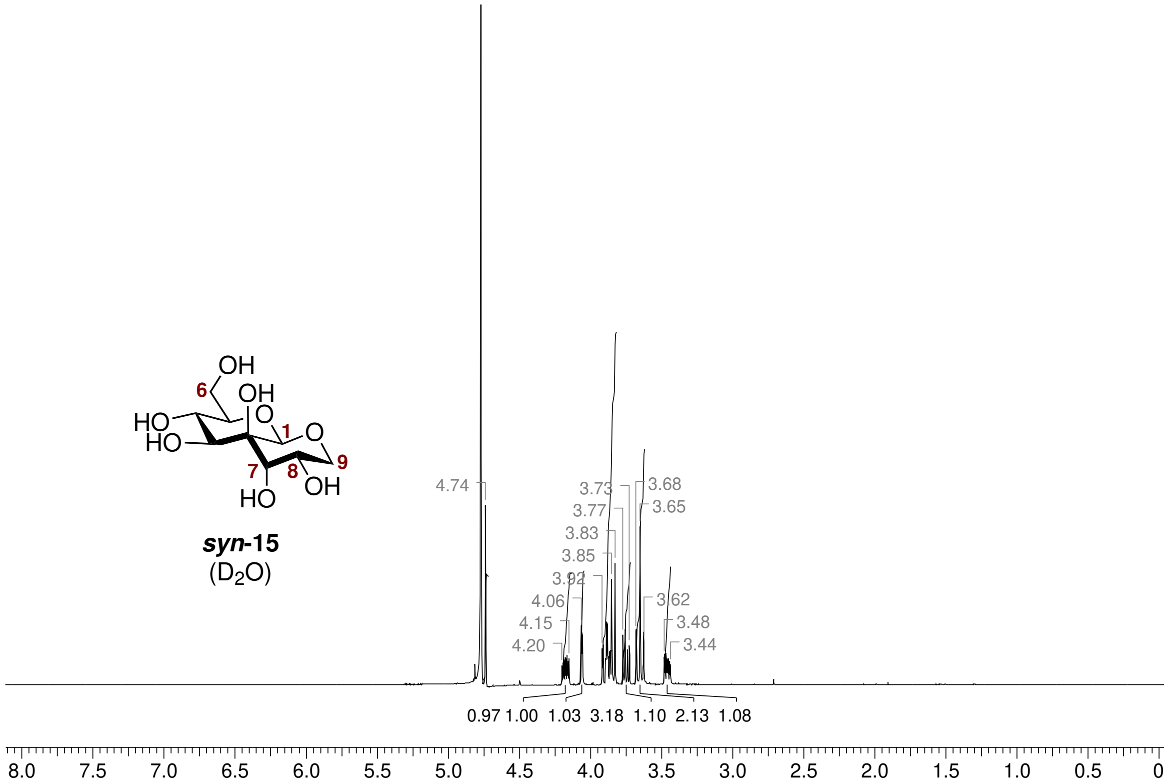
OH
6
OH
HO
HO
O
1
O
9
7
8
HO
OH
syn-15
(D2O)
4.74
3.73
3.77
3.83
3.85
3.92
4.06
4.15
4.20
3.68
3.65
3.62
3.48
3.44
0.97 1.00 1.03 3.18 1.10 2.13 1.08
8.0 7.5 7.0 6.5 6.0 5.5 5.0 4.5 4.0 3.5 3.0 2.5 2.0 1.5 1.0 0.5 0

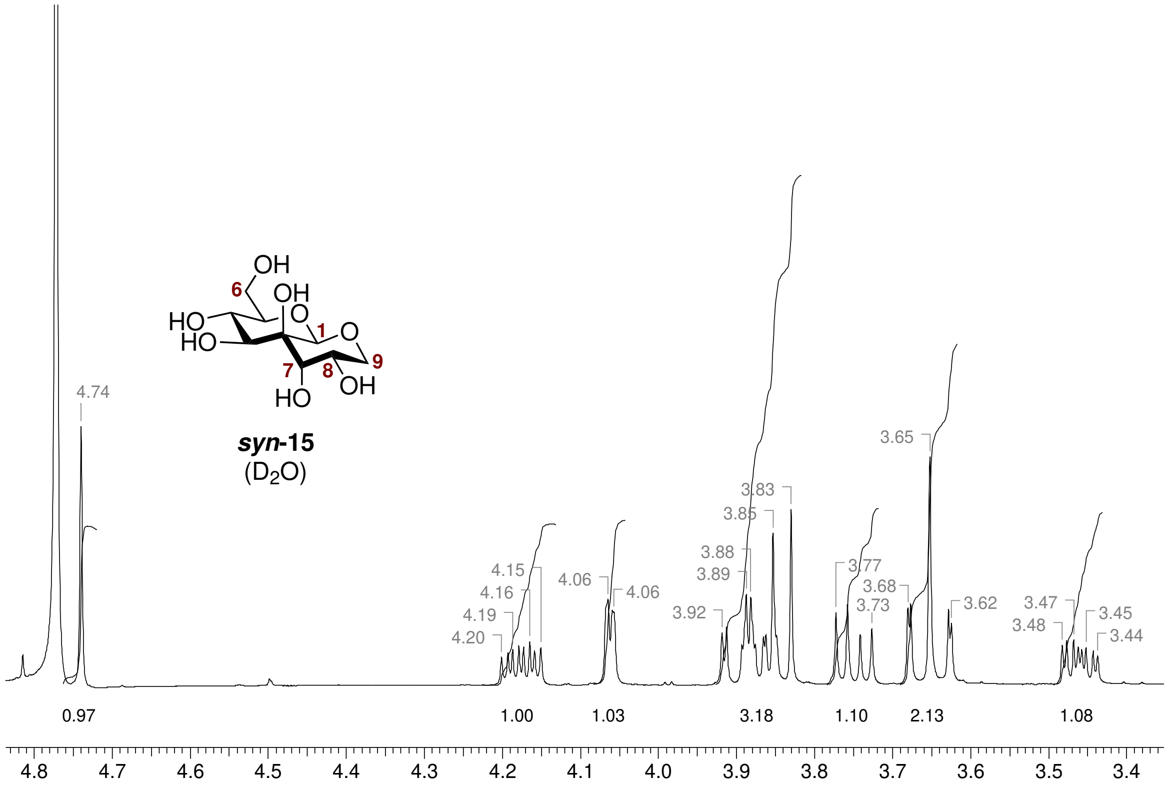
OH
6
OH
HO
HO
O
1
O
9
7
8
HO
OH
syn-15
(D2O)
4.74
4.15
4.16
4.19
4.20
4.06
4.06
3.92
3.88
3.89
3.83
3.85
3.77
3.68
3.73
3.65
3.62
3.47
3.48
3.45
3.44
0.97
1.00
1.03
3.18
1.10
2.13
1.08
4.8 4.7 4.6 4.5 4.4 4.3 4.2 4.1 4.0 3.9 3.8 3.7 3.6 3.5 3.4

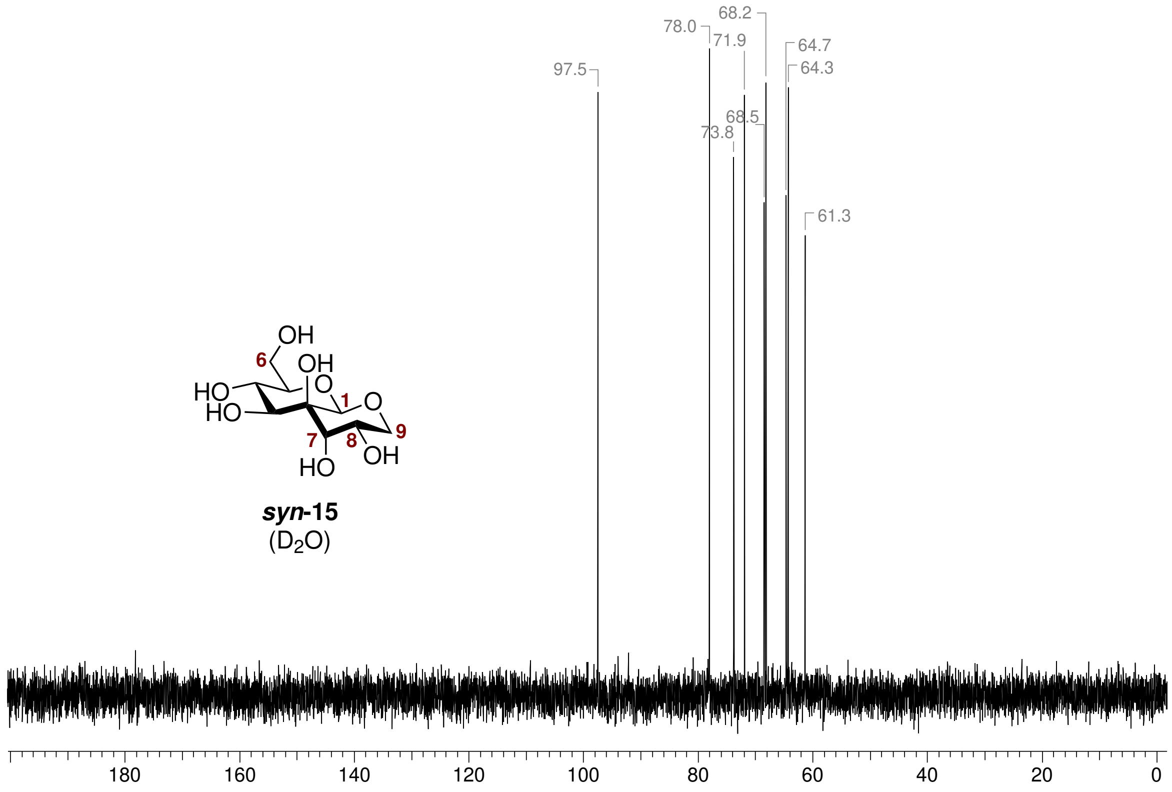
97.5
78.0
71.9
73.8
68.5
68.2
64.7
64.3
61.3
OH
6
OH
HO
O
1
O
HO
7
8
9
HO
OH
syn-15
(D_2O)
180
160
140
120
100
80
60
40
20
0

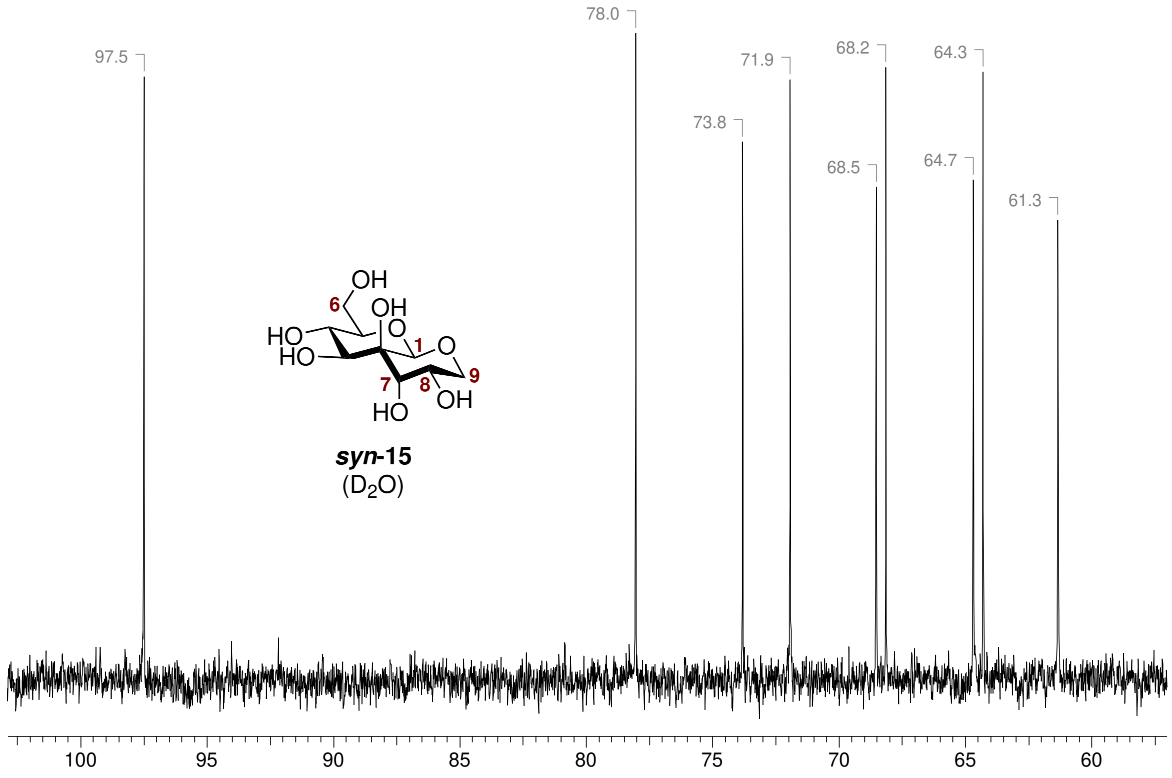
97.5
78.0
73.8
71.9
68.5
68.2
64.7
64.3
61.3
OH
6
OH
HO
O
1
O
HO
7
8
9
HO
OH
syn-15
(D_2O)
100
95
90
85
80
75
70
65
60

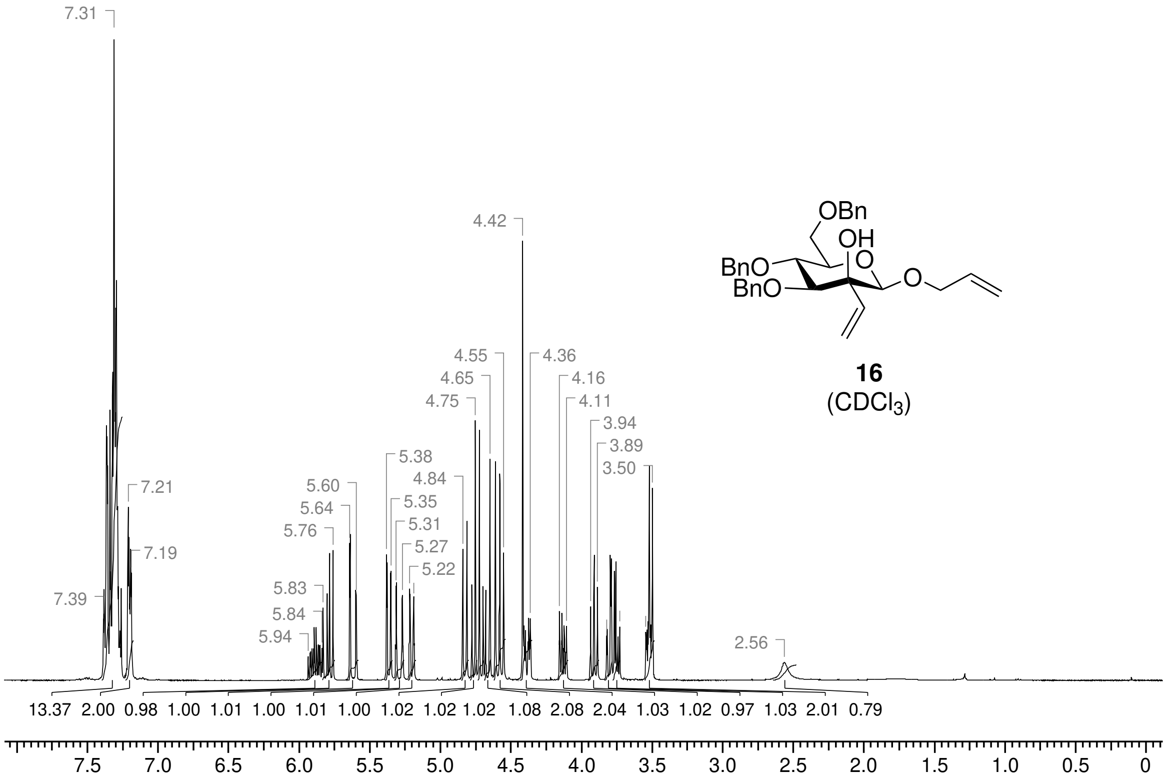
7.31
7.21
7.19
7.39
5.60
5.64
5.76
5.83
5.84
5.94
5.38
4.84
5.35
5.31
5.27
5.22
4.55
4.65
4.75
4.42
4.36
4.16
4.11
3.94
3.89
3.50
2.56
13.37 2.00 0.98 1.00 1.01 1.00 1.01 1.00 1.02 1.02 1.02 1.08 2.08 2.04 1.03 1.02 0.97 1.03 2.01 0.79
7.5 7.0 6.5 6.0 5.5 5.0 4.5 4.0 3.5 3.0 2.5 2.0 1.5 1.0 0.5 0
OBn
OH
O
BnO
BnO
O
16
(CDCl$_3$)

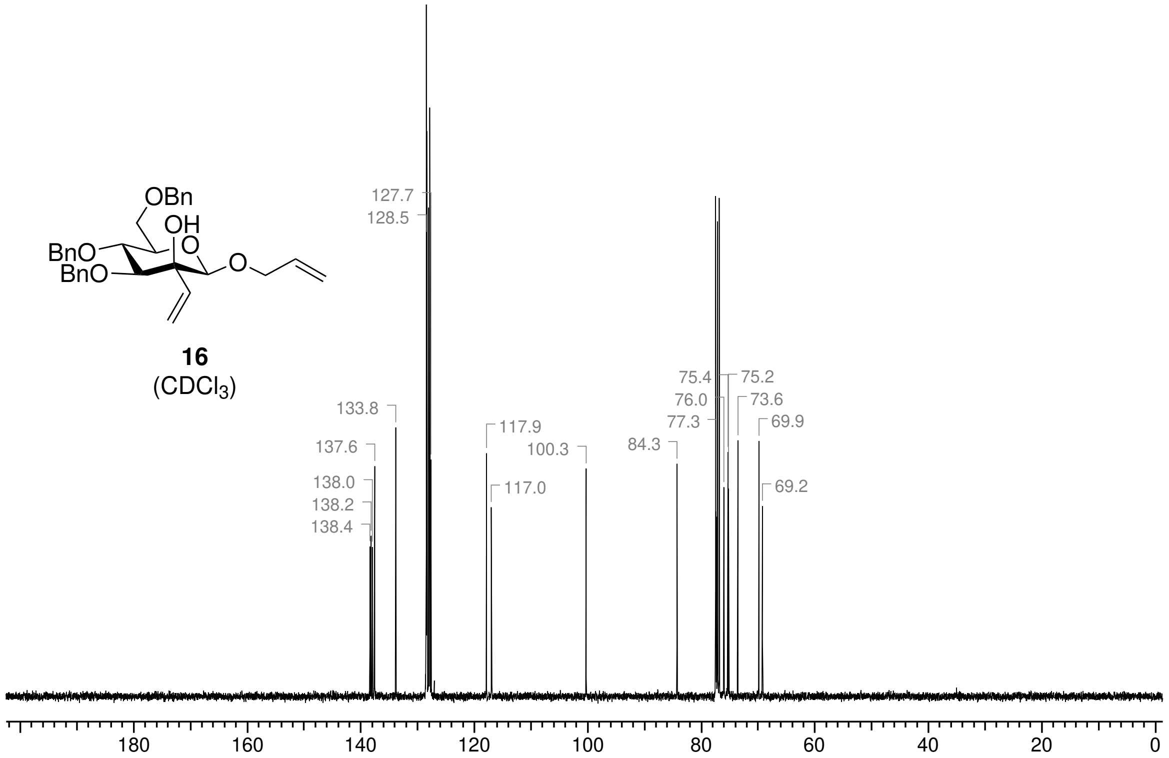
OBn
OH
O
BnO
BnO
O
16
(CDCl$_3$)
127.7
128.5
133.8
137.6
138.0
138.2
138.4
117.9
117.0
100.3
84.3
75.4
76.0
77.3
75.2
73.6
69.9
69.2
180 160 140 120 100 80 60 40 20 0

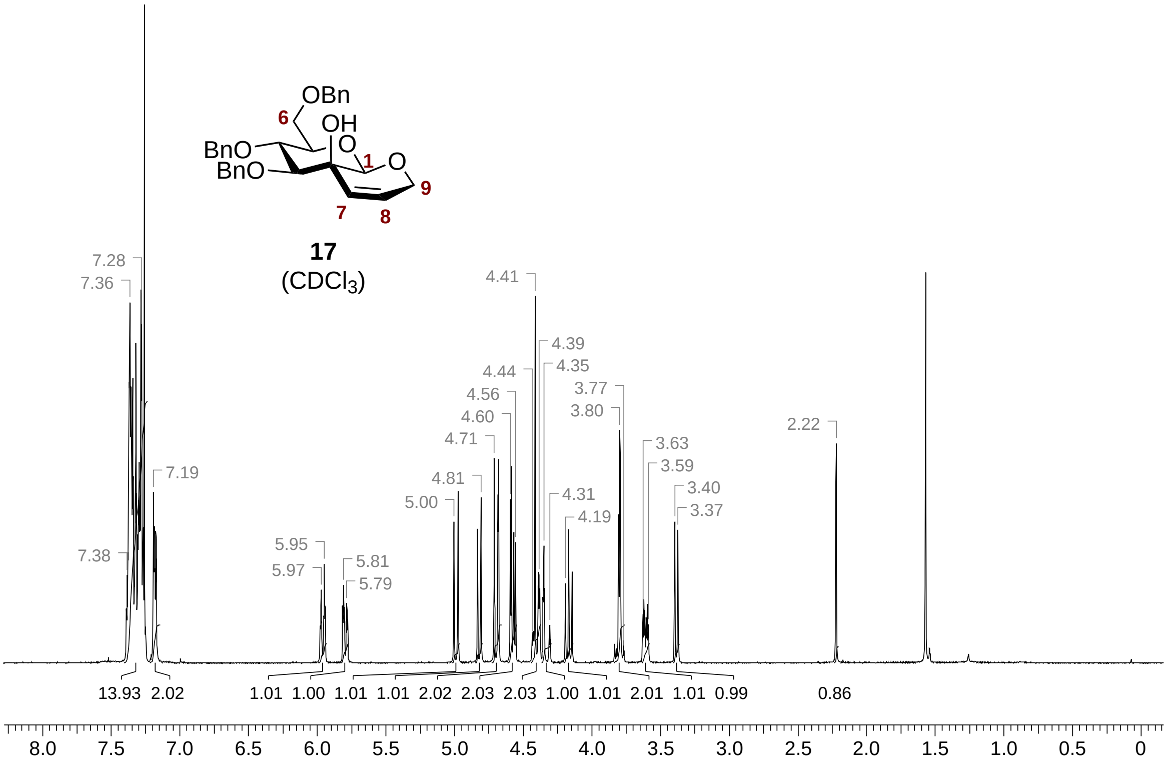

17
($CDCl_3$)

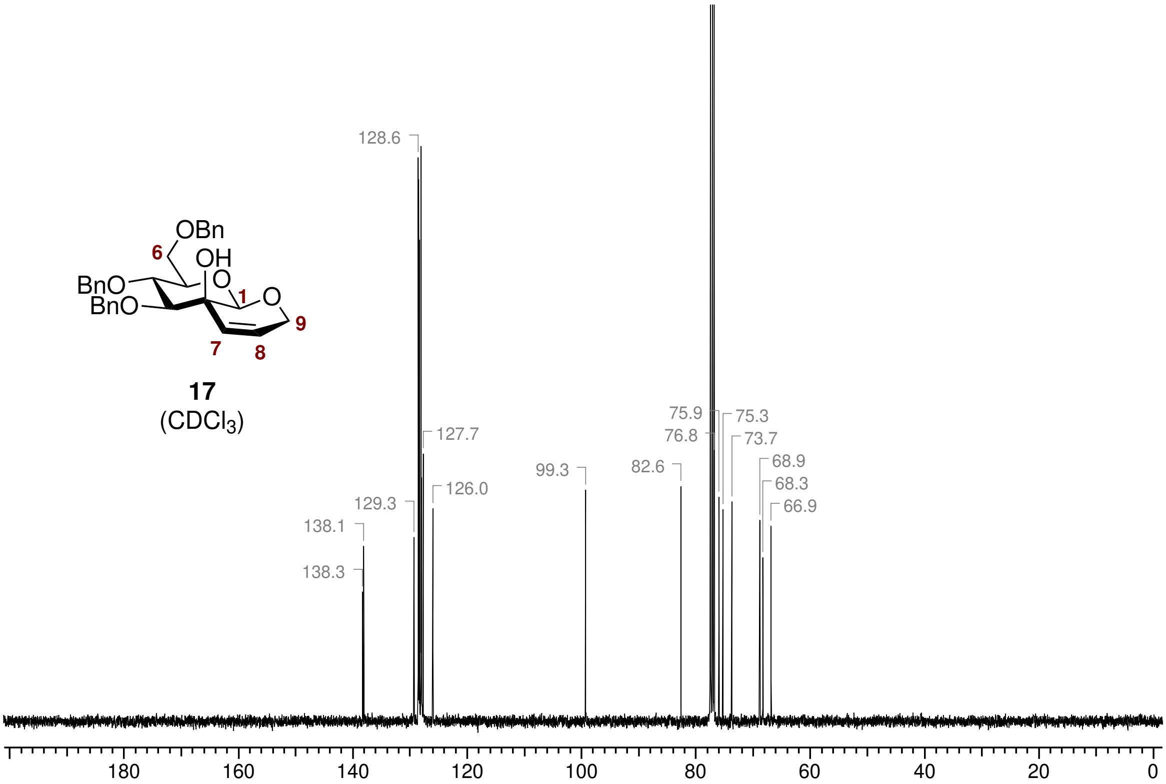

17
($CDCl_3$)

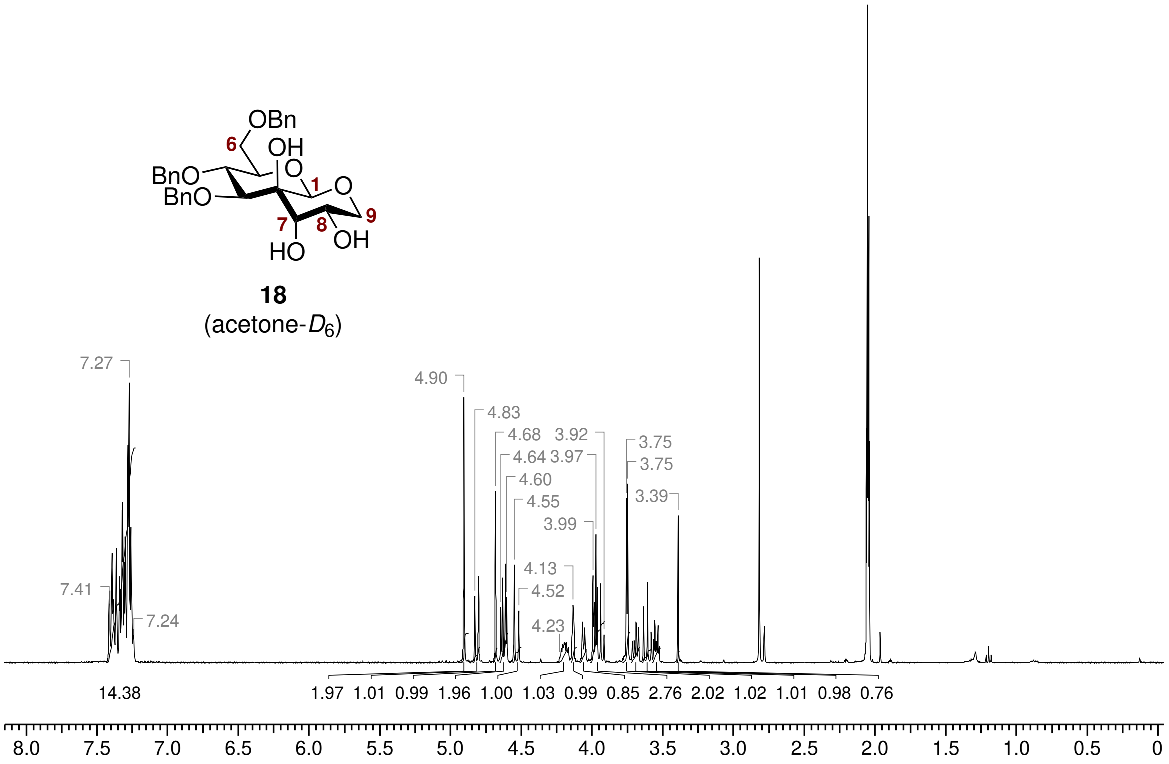
OBn
6
OH
BnO
BnO
O
1
O
9
7
8
HO
OH
18
(acetone-D_6)
7.27
7.41
7.24
4.90
4.83
4.68
4.64
4.60
4.55
3.92
3.97
3.99
4.13
4.52
4.23
3.75
3.75
3.39
14.38
1.97
1.01
0.99
1.96
1.00
1.03
0.99
0.85
2.76
2.02
1.02
1.01
0.98
0.76
8.0
7.5
7.0
6.5
6.0
5.5
5.0
4.5
4.0
3.5
3.0
2.5
2.0
1.5
1.0
0.5
0

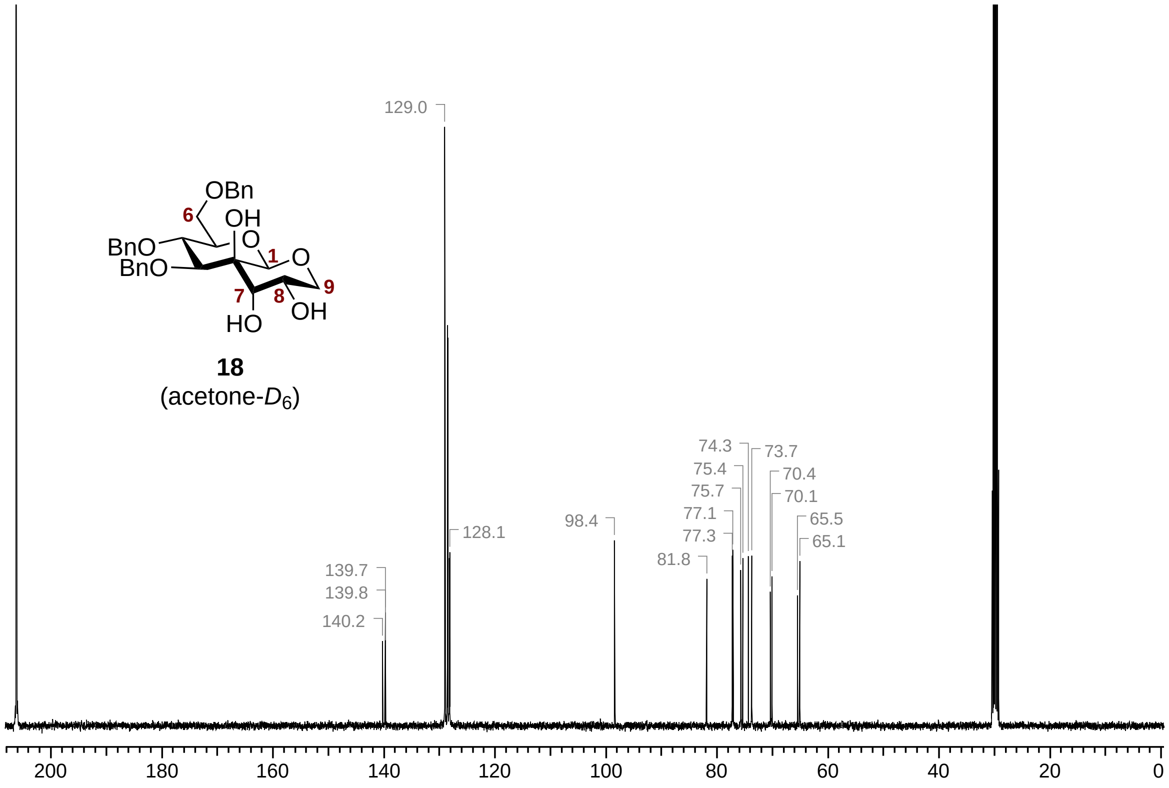
OBn
6
OH
BnO
BnO
O
1
O
9
7
8
HO
OH
18
(acetone-D_6)
129.0
128.1
139.7
139.8
140.2
98.4
74.3
75.4
75.7
77.1
77.3
81.8
73.7
70.4
70.1
65.5
65.1
200
180
160
140
120
100
80
60
40
20
0

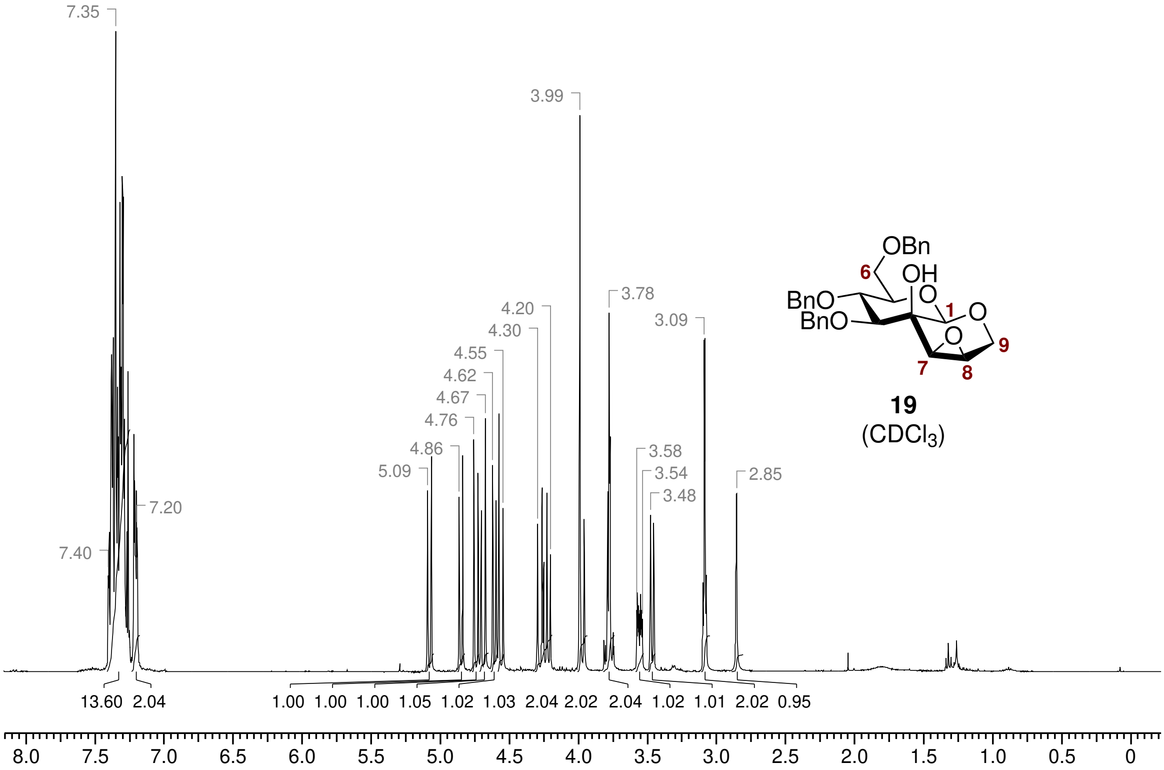
7.35
7.40
7.20
5.09
4.86
4.76
4.67
4.62
4.55
4.30
4.20
3.99
3.78
3.58
3.54
3.48
3.09
2.85
13.60 2.04
1.00 1.00 1.00 1.05 1.02 1.03 2.04 2.02 2.04 1.02 1.01 2.02 0.95
8.0 7.5 7.0 6.5 6.0 5.5 5.0 4.5 4.0 3.5 3.0 2.5 2.0 1.5 1.0 0.5 0
OBn
6
OH
BnO
BnO
O
1
O
O
9
7
8
19
(CDCl3)

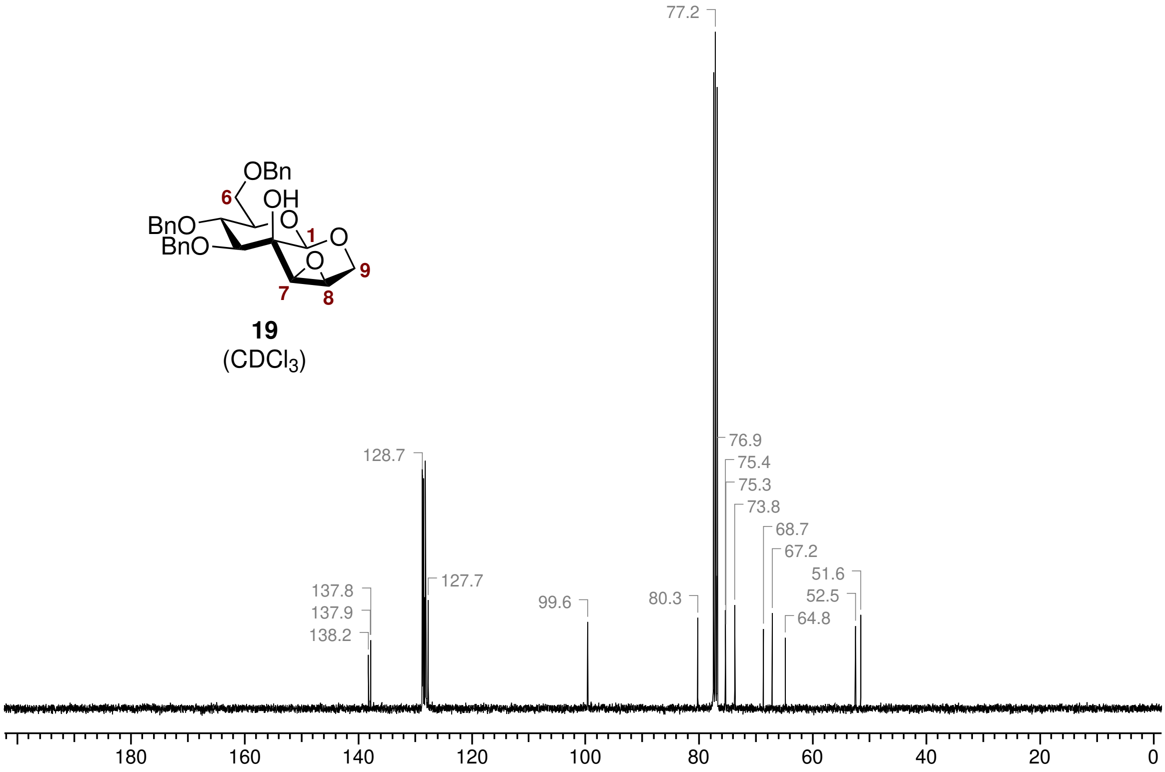
77.2
76.9
75.4
75.3
73.8
68.7
67.2
51.6
52.5
64.8
128.7
127.7
137.8
137.9
138.2
99.6
80.3
180 160 140 120 100 80 60 40 20 0
OBn
6
OH
BnO
BnO
O
1
O
O
9
7
8
19
(CDCl3)

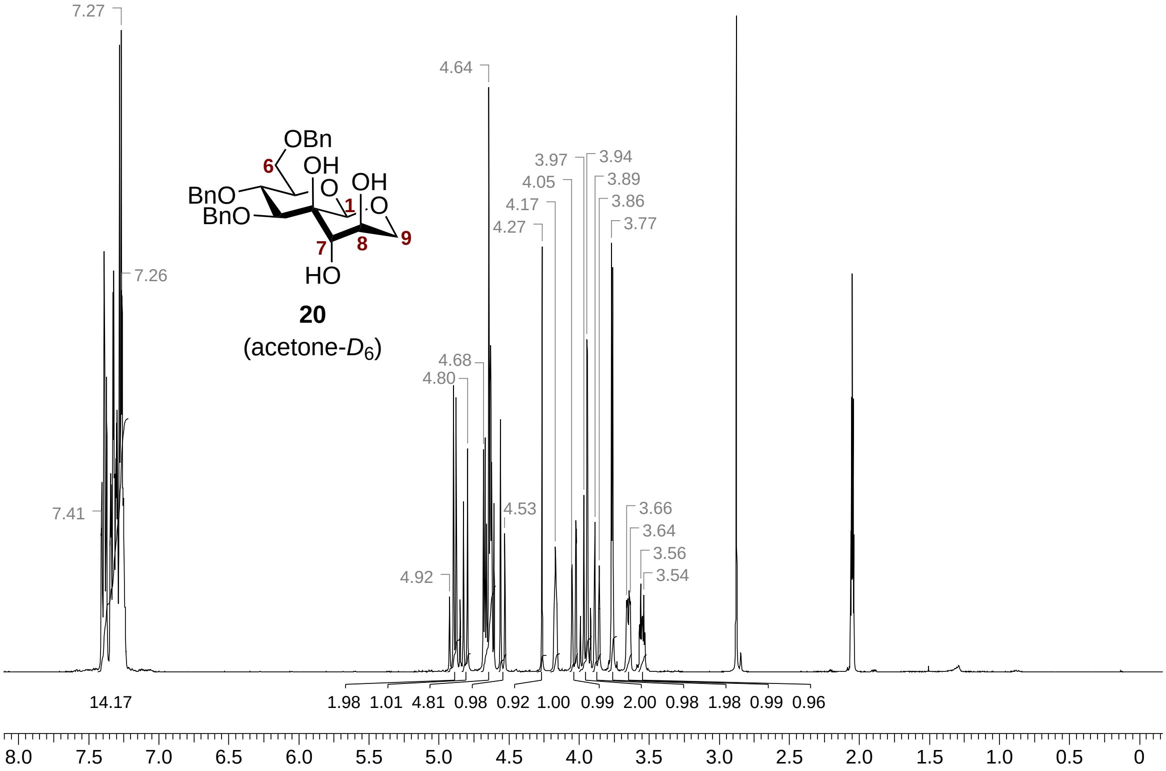
7.27
7.26
7.41
4.64
OBn
6
OH
O
OH
BnO
1
O
BnO
9
7
8
HO
20
(acetone-D_6)
3.97
3.94
4.05
3.89
4.17
3.86
4.27
3.77
4.68
4.80
4.53
4.92
3.66
3.64
3.56
3.54
14.17
1.98 1.01 4.81 0.98 0.92 1.00 0.99 2.00 0.98 1.98 0.99 0.96
8.0
7.5
7.0
6.5
6.0
5.5
5.0
4.5
4.0
3.5
3.0
2.5
2.0
1.5
1.0
0.5
0

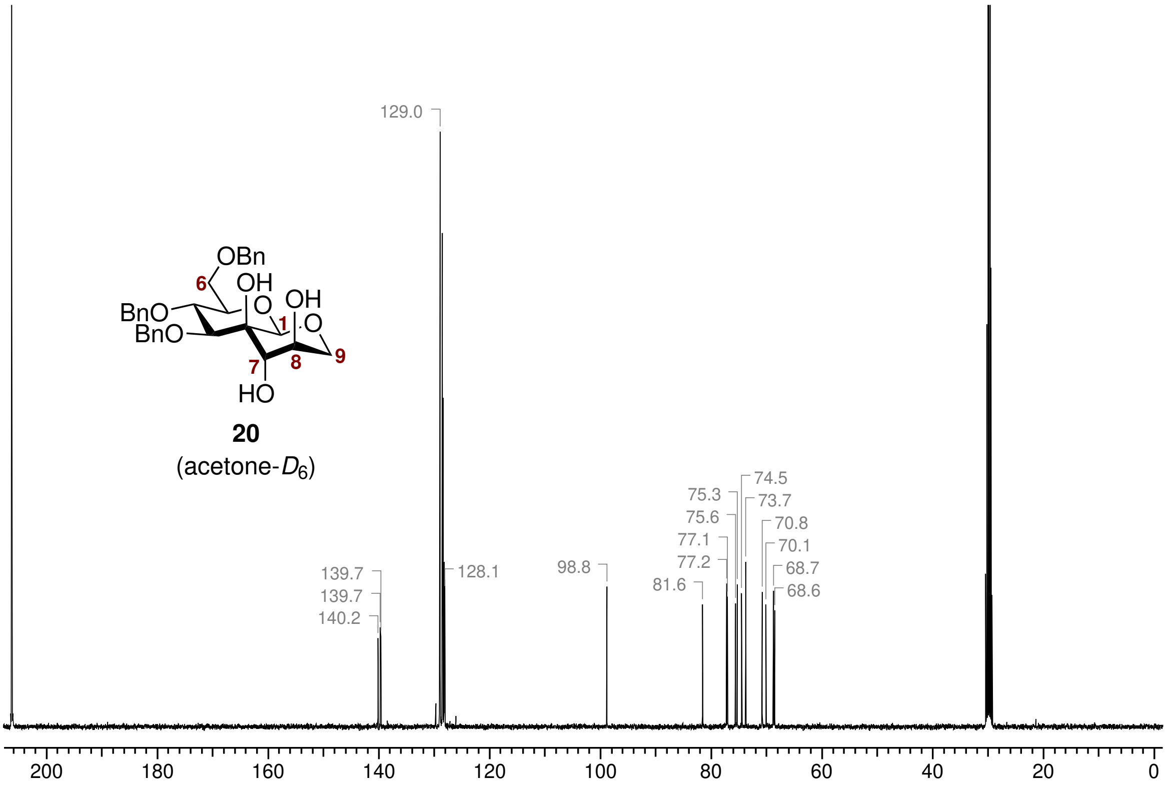
129.0
OBn
6
OH
O
OH
BnO
1
O
BnO
9
7
8
HO
20
(acetone-D_6)
75.3
74.5
73.7
75.6
70.8
77.1
70.1
77.2
68.7
81.6
68.6
98.8
128.1
139.7
139.7
140.2
200
180
160
140
120
100
80
60
40
20
0

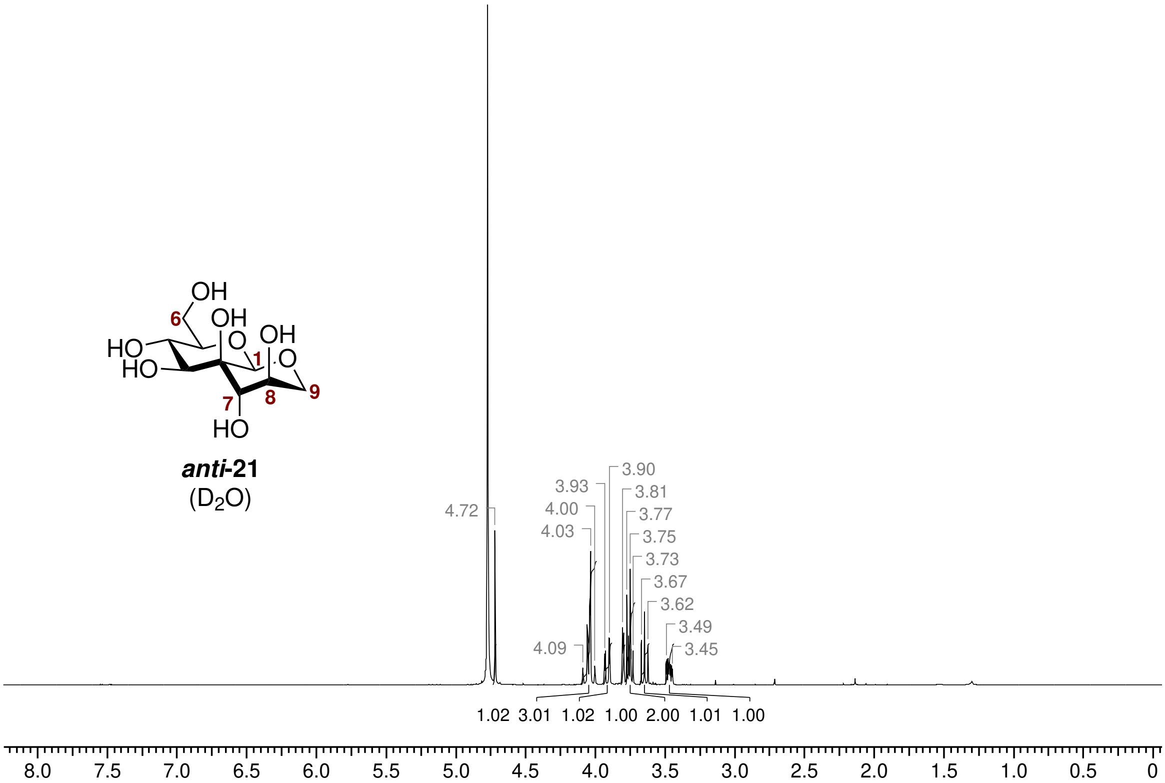
OH
6
OH
O
OH
HO
HO
1
O
9
7
8
HO
anti-**21**
(D_2O)
4.72
3.93
4.00
4.03
4.09
3.90
3.81
3.77
3.75
3.73
3.67
3.62
3.49
3.45
1.02 3.01 1.02 1.00 2.00 1.01 1.00
8.0
7.5
7.0
6.5
6.0
5.5
5.0
4.5
4.0
3.5
3.0
2.5
2.0
1.5
1.0
0.5
0

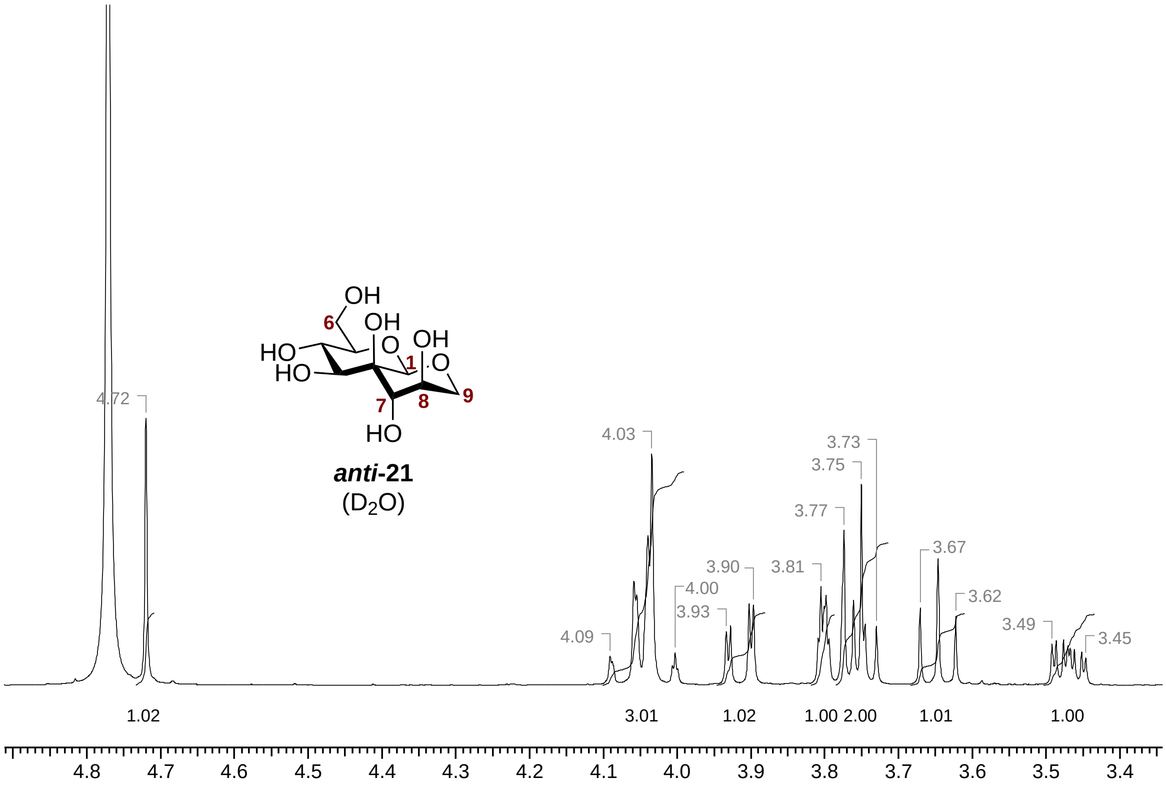
OH
6
OH
O
OH
HO
HO
1
O
9
7
8
HO
anti-**21**
(D_2O)
4.72
4.03
4.09
3.90
4.00
3.93
3.81
3.73
3.75
3.77
3.67
3.62
3.49
3.45
1.02
3.01
1.02
1.00 2.00
1.01
1.00
4.8
4.7
4.6
4.5
4.4
4.3
4.2
4.1
4.0
3.9
3.8
3.7
3.6
3.5
3.4

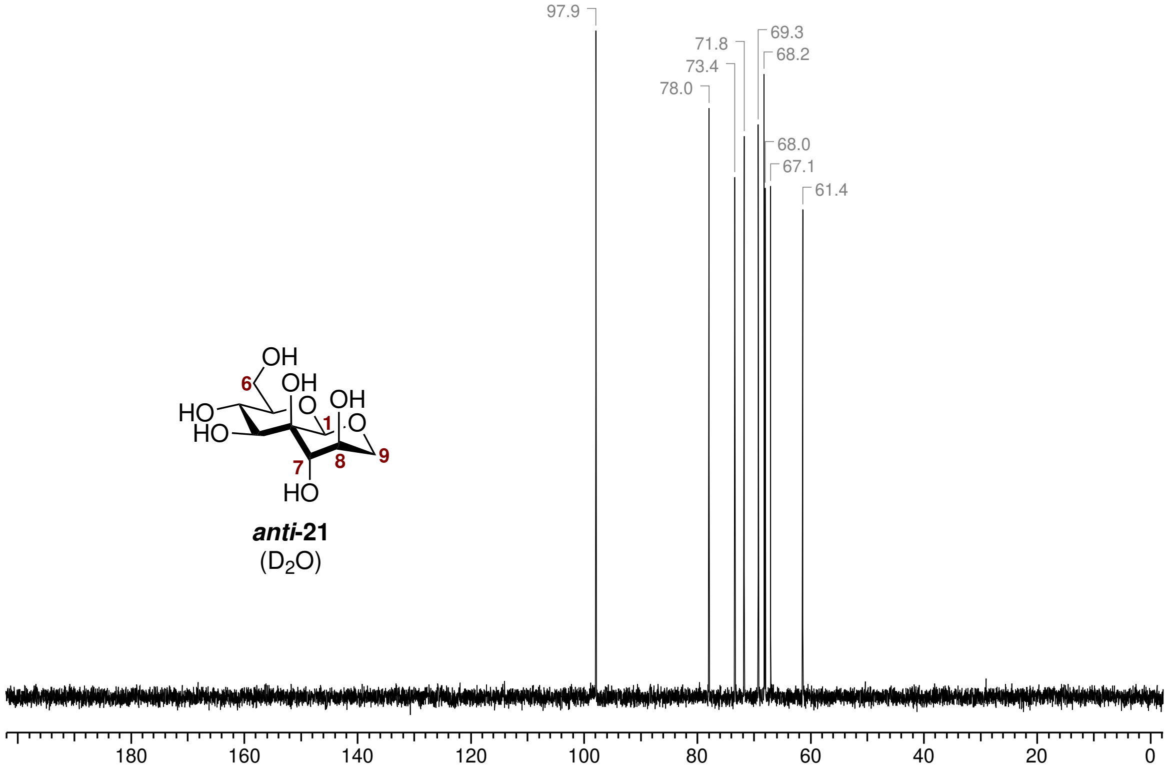
97.9
71.8
73.4
78.0
69.3
68.2
68.0
67.1
61.4
OH
6
OH
HO
O
OH
HO
1
O
9
7
8
HO
***anti*-21**
(D_2O)
180
160
140
120
100
80
60
40
20
0

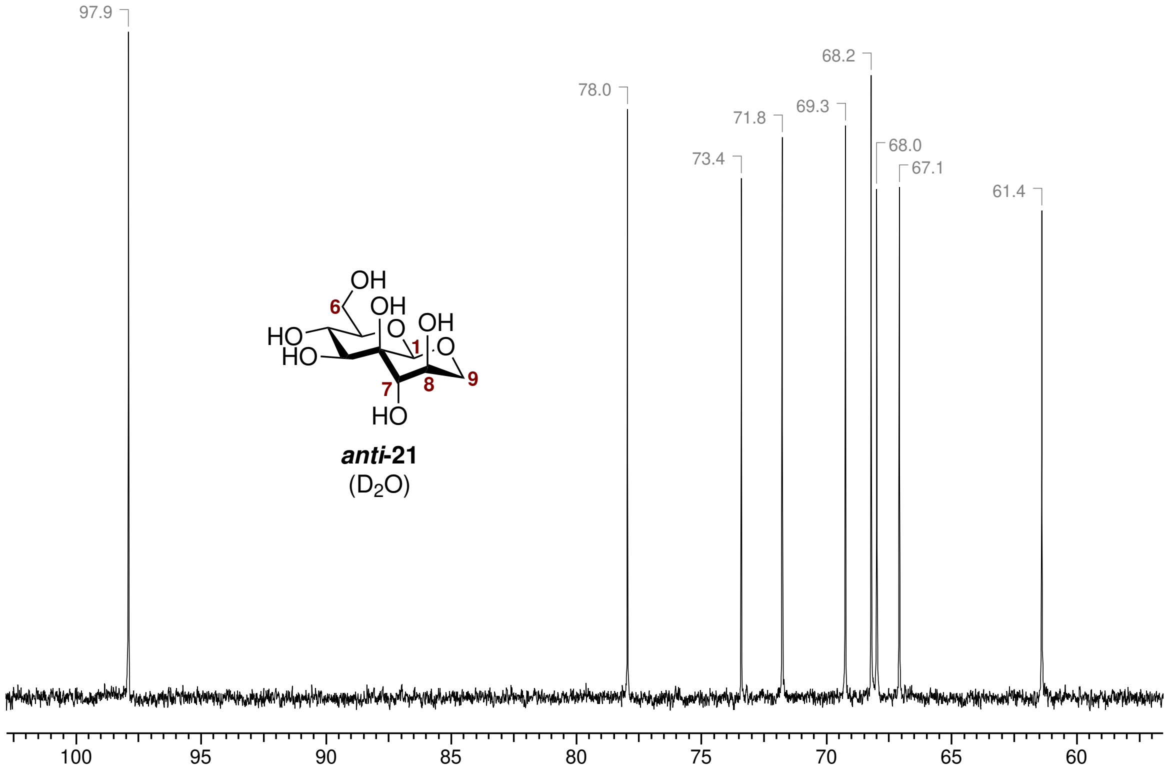
97.9
78.0
73.4
71.8
69.3
68.2
68.0
67.1
61.4
OH
6
OH
HO
O
OH
HO
1
O
9
7
8
HO
***anti*-21**
(D_2O)
100
95
90
85
80
75
70
65
60

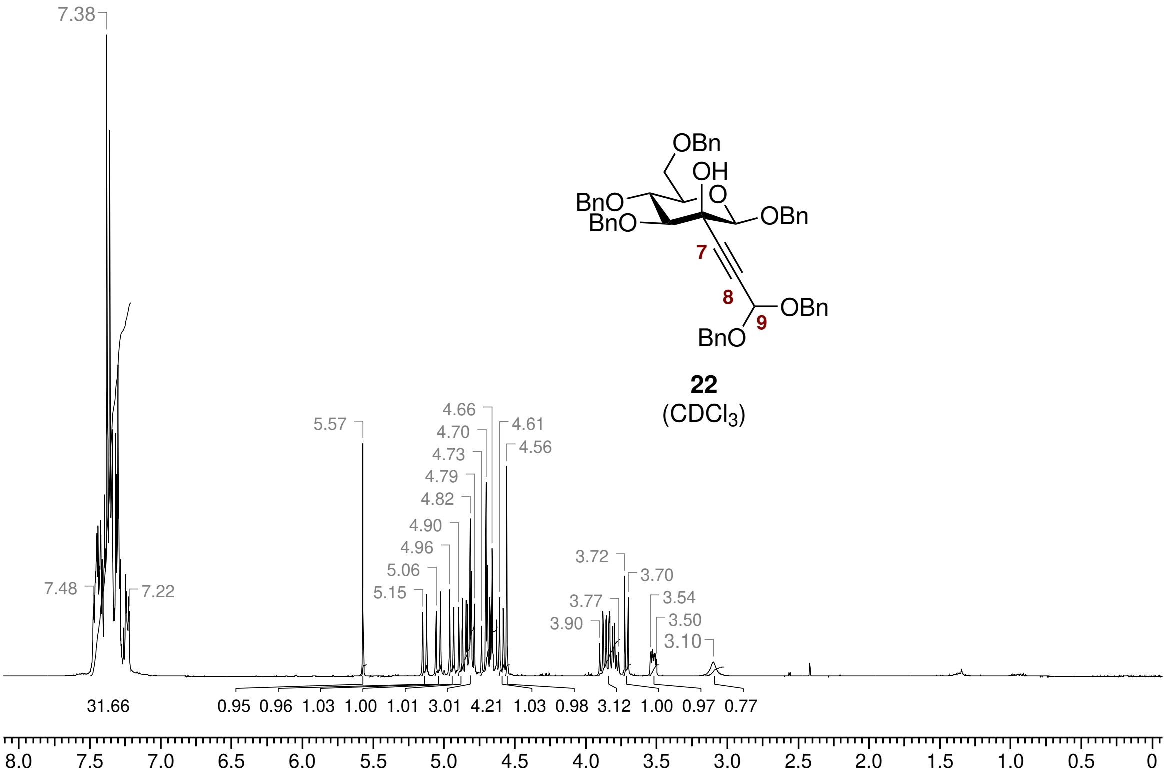
7.38
7.48
7.22
5.57
4.66
4.70
4.73
4.79
4.82
4.90
4.96
5.06
5.15
4.61
4.56
3.72
3.70
3.77
3.90
3.54
3.50
3.10
31.66
0.95 0.96 1.03 1.00 1.01 3.01 4.21 1.03 0.98 3.12 1.00 0.97 0.77
8.0 7.5 7.0 6.5 6.0 5.5 5.0 4.5 4.0 3.5 3.0 2.5 2.0 1.5 1.0 0.5 0
OBn
OH
BnO
BnO
O
OBn
7
8
OBn
9
BnO
22
(CDCl3)

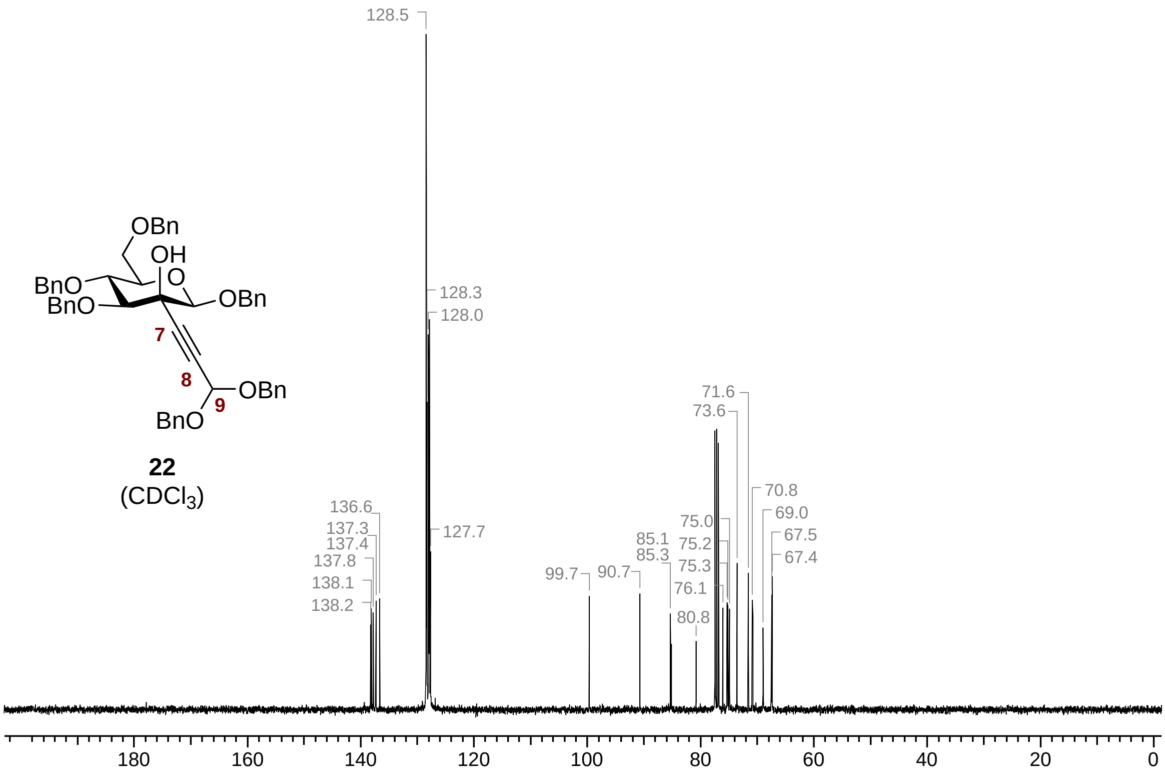
128.5
128.3
128.0
127.7
136.6
137.3
137.4
137.8
138.1
138.2
99.7
90.7
85.1
85.3
71.6
73.6
75.0
75.2
75.3
76.1
80.8
70.8
69.0
67.5
67.4
180 160 140 120 100 80 60 40 20 0
OBn
OH
BnO
BnO
O
OBn
7
8
OBn
9
BnO
22
(CDCl3)

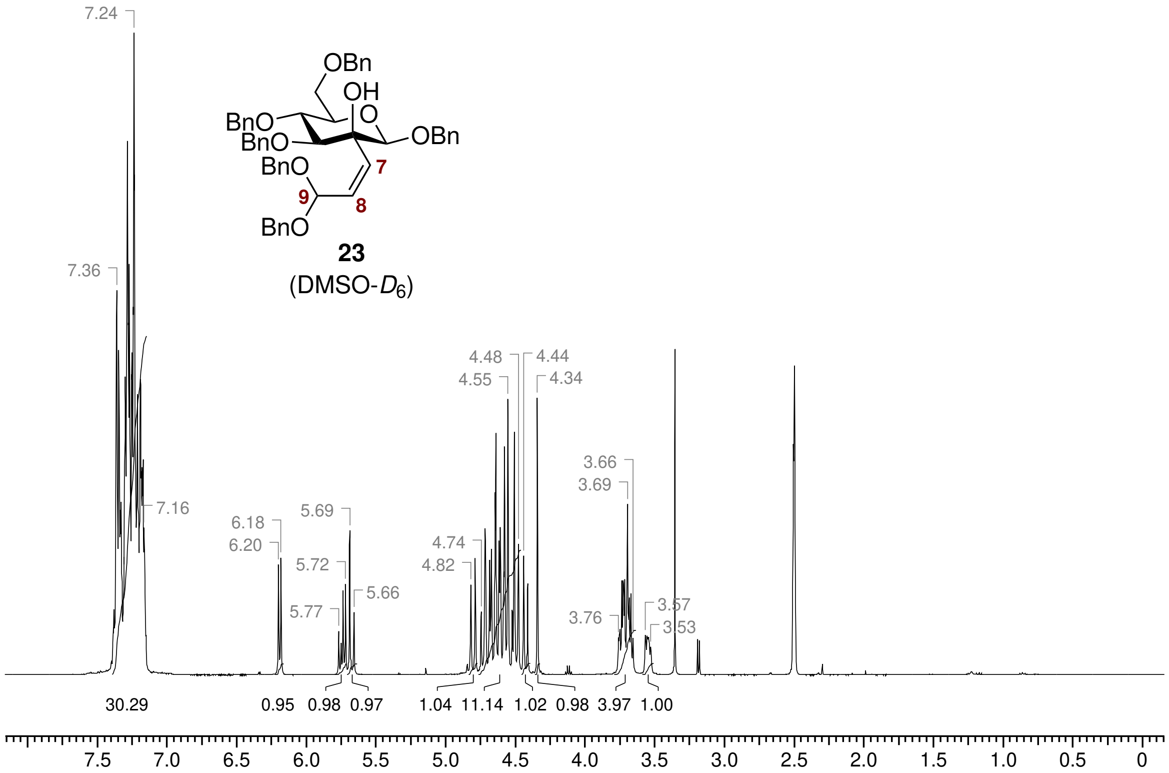
23
(DMSO-D_6)

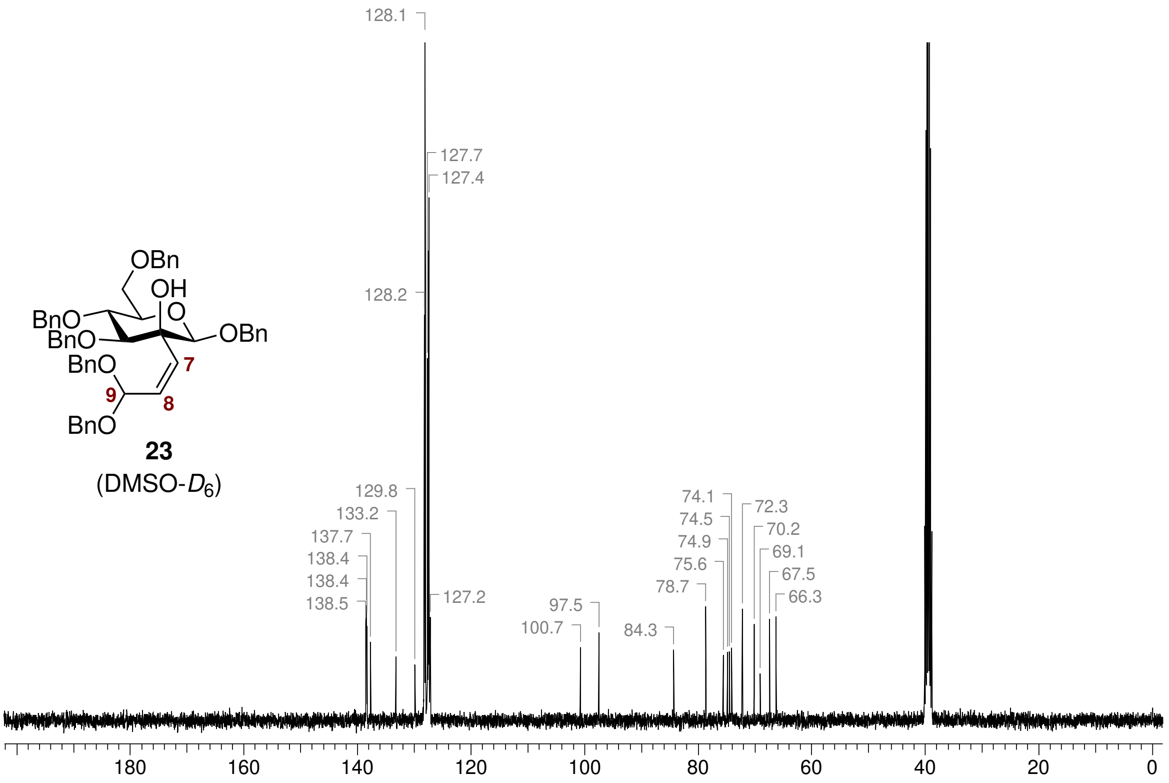
23
(DMSO-D_6)

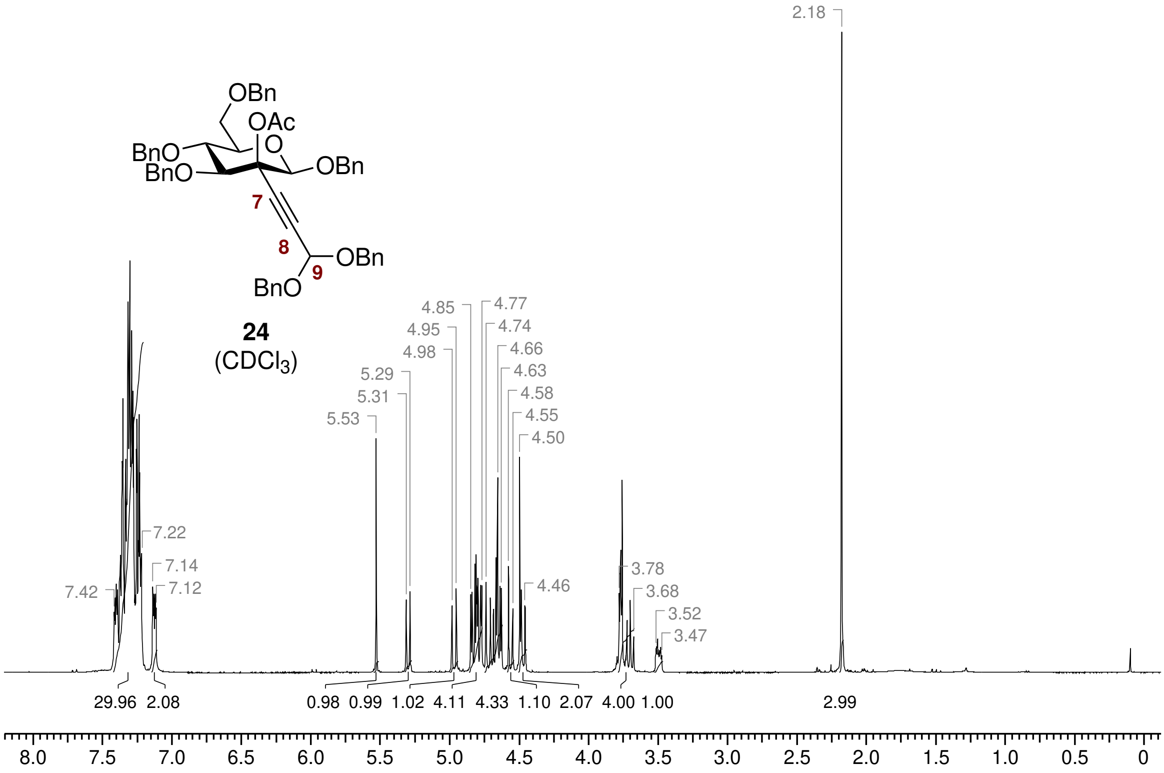
OBn
OAc
O
BnO
BnO
OBn
7
8
OBn
9
BnO
24
(CDCl$_3$)
2.18
4.85
4.95
4.98
5.29
5.31
5.53
4.77
4.74
4.66
4.63
4.58
4.55
4.50
7.22
7.14
7.12
7.42
4.46
3.78
3.68
3.52
3.47
29.96
2.08
0.98
0.99
1.02
4.11
4.33
1.10
2.07
4.00
1.00
2.99
8.0
7.5
7.0
6.5
6.0
5.5
5.0
4.5
4.0
3.5
3.0
2.5
2.0
1.5
1.0
0.5
0

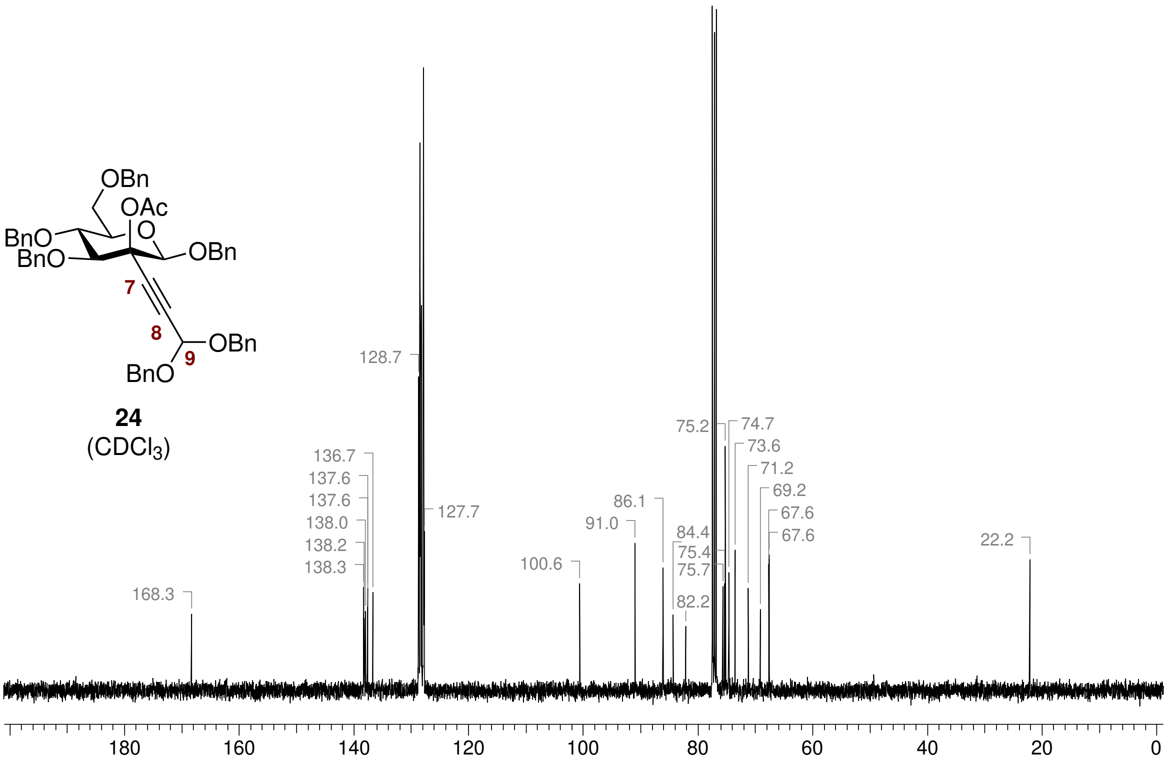
OBn
OAc
O
BnO
BnO
OBn
7
8
OBn
9
BnO
24
(CDCl$_3$)
128.7
136.7
137.6
137.6
138.0
138.2
138.3
127.7
168.3
100.6
91.0
86.1
84.4
75.4
75.7
82.2
75.2
74.7
73.6
71.2
69.2
67.6
67.6
22.2
180
160
140
120
100
80
60
40
20
0

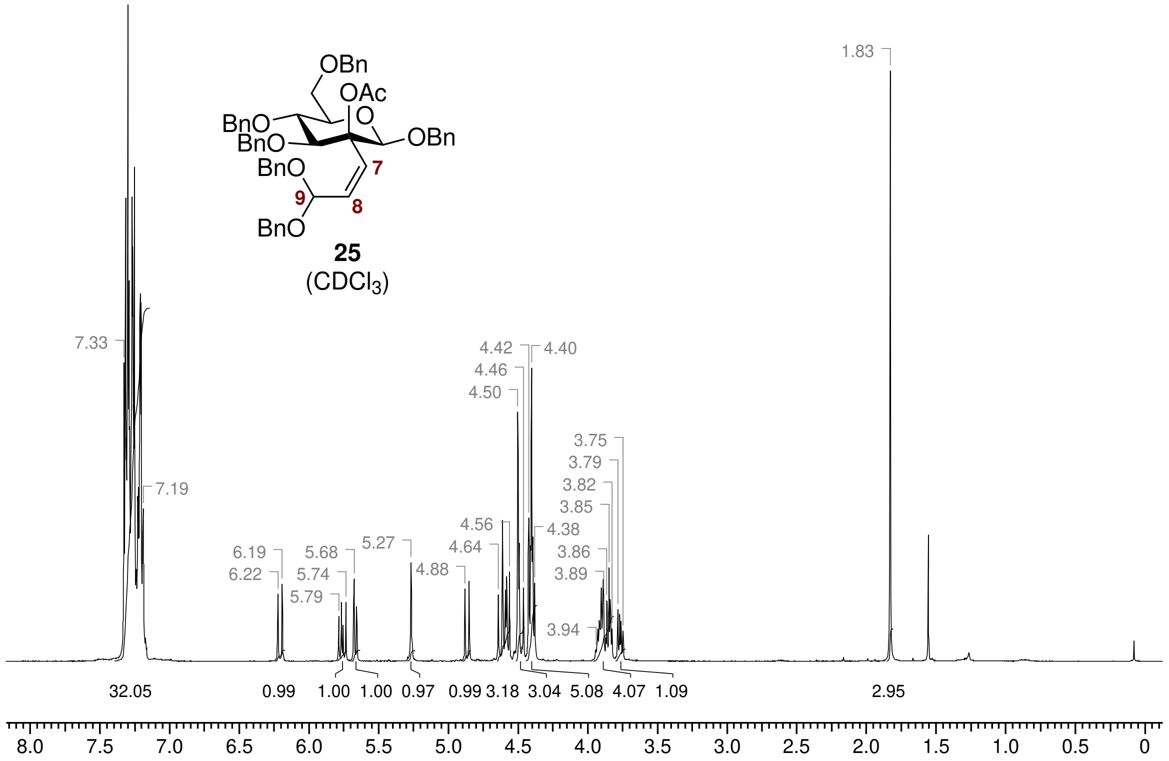
OBn
OAc
O
BnO
BnO
OBn
BnO
7
9
8
BnO
25
(CDCl$_3$)
1.83
7.33
7.19
6.19
6.22
5.68
5.74
5.79
5.27
4.88
4.56
4.64
4.42
4.40
4.46
4.50
4.38
3.75
3.79
3.82
3.85
3.86
3.89
3.94
32.05
0.99
1.00
1.00
0.97
0.99
3.18
3.04
5.08
4.07
1.09
2.95
8.0
7.5
7.0
6.5
6.0
5.5
5.0
4.5
4.0
3.5
3.0
2.5
2.0
1.5
1.0
0.5
0

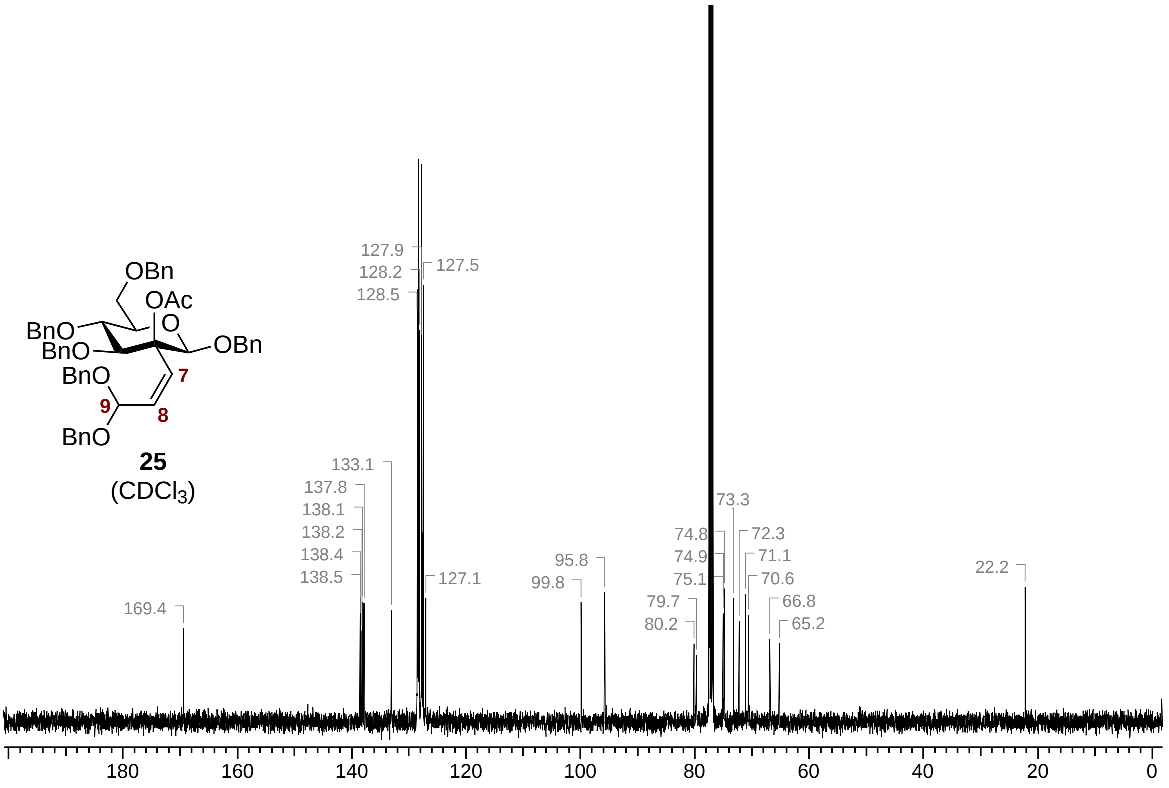
OBn
OAc
O
BnO
BnO
OBn
BnO
7
9
8
BnO
25
(CDCl$_3$)
127.9
128.2
128.5
127.5
133.1
137.8
138.1
138.2
138.4
138.5
127.1
169.4
95.8
99.8
73.3
74.8
74.9
75.1
79.7
80.2
72.3
71.1
70.6
66.8
65.2
22.2
180
160
140
120
100
80
60
40
20
0

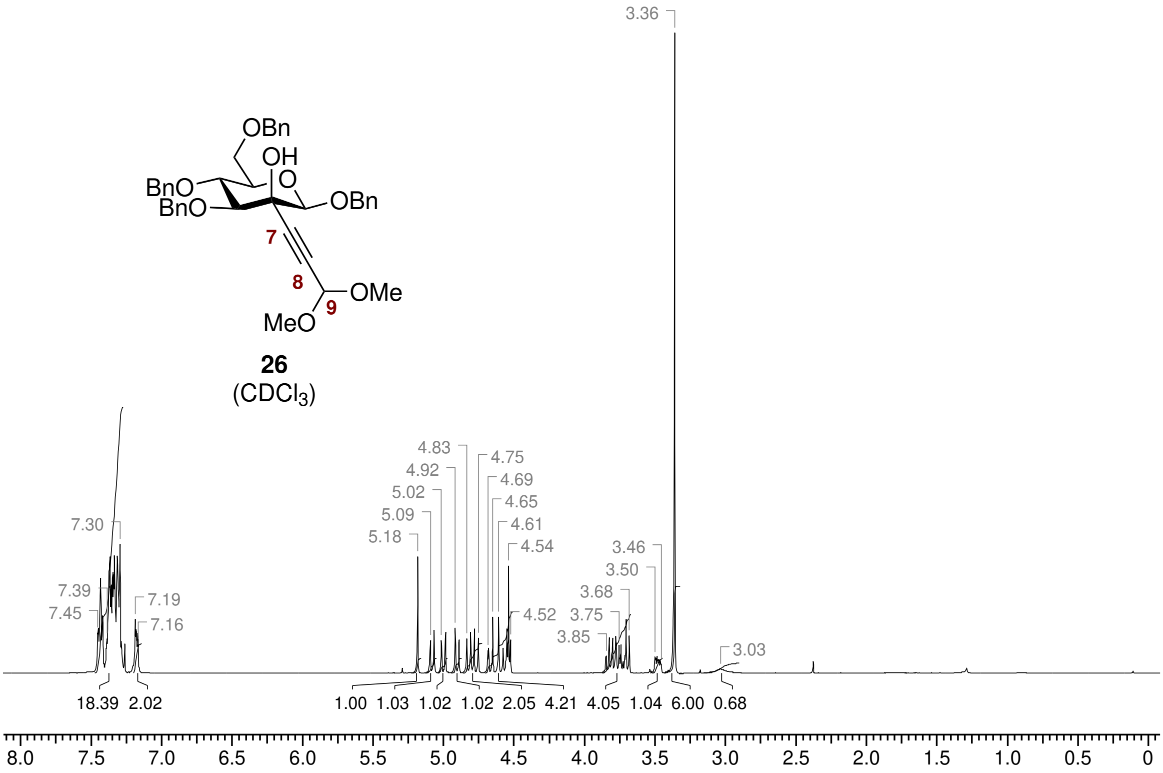
OBn
OH
O
BnO
BnO
OBn
7
8
9
OMe
MeO
26
(CDCl3)
3.36
4.83
4.92
5.02
5.09
5.18
4.75
4.69
4.65
4.61
4.54
4.52
7.30
7.39
7.45
7.19
7.16
3.46
3.50
3.68
3.75
3.85
3.03
18.39
2.02
1.00
1.03
1.02
1.02
2.05
4.21
4.05
1.04
6.00
0.68
8.0
7.5
7.0
6.5
6.0
5.5
5.0
4.5
4.0
3.5
3.0
2.5
2.0
1.5
1.0
0.5
0

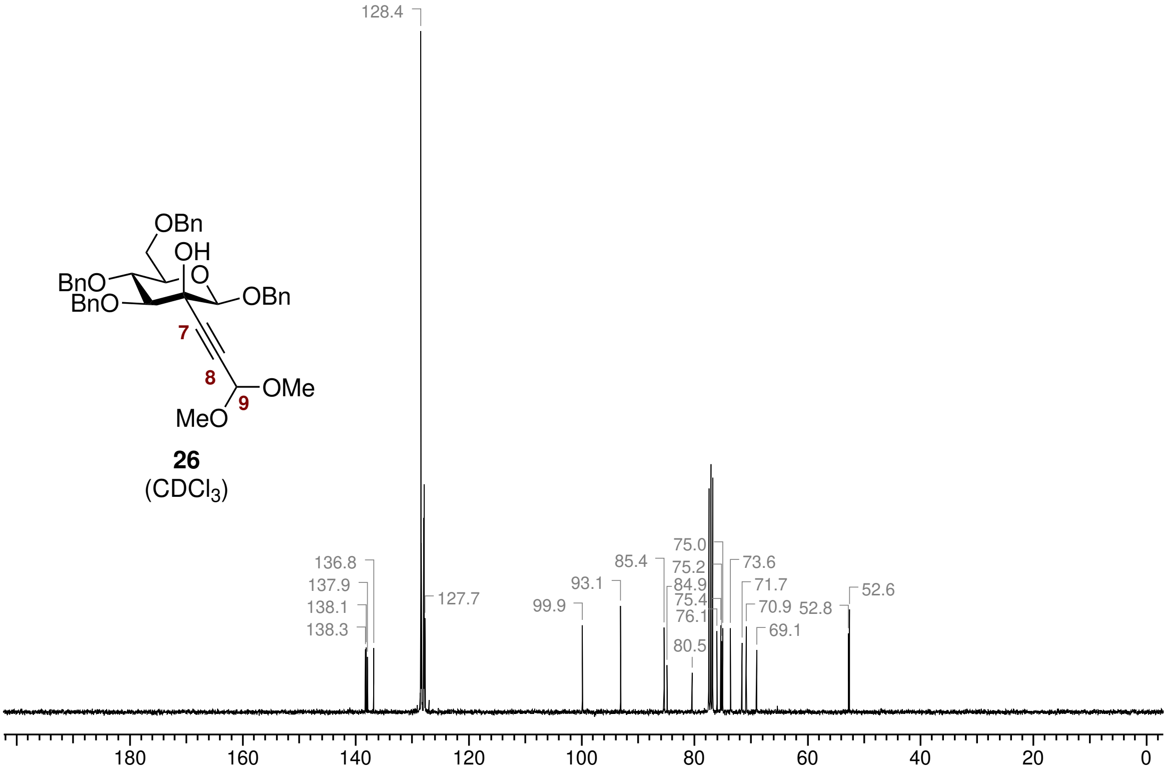
128.4
OBn
OH
O
BnO
BnO
OBn
7
8
9
OMe
MeO
26
(CDCl3)
136.8
137.9
138.1
138.3
127.7
99.9
93.1
85.4
84.9
80.5
75.0
75.2
75.4
76.1
73.6
71.7
70.9
69.1
52.8
52.6
180
160
140
120
100
80
60
40
20
0

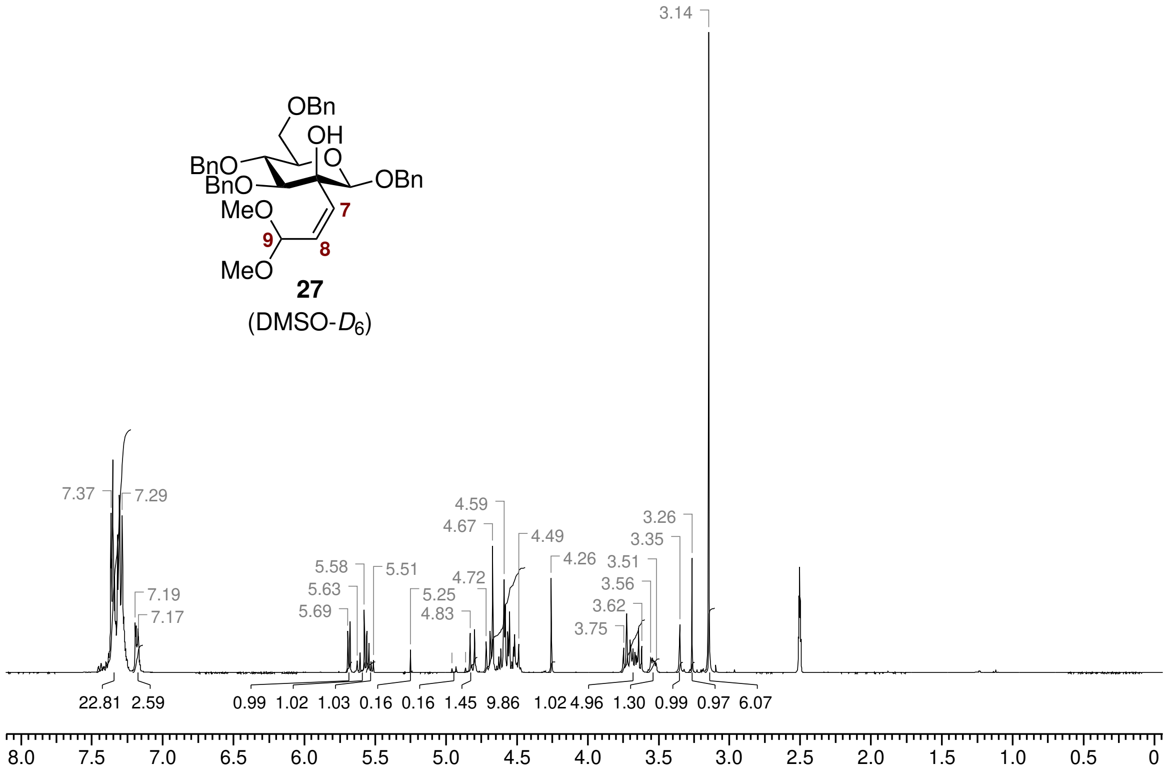
OBn
OH
O
BnO
BnO
OBn
MeO
7
9
8
MeO
27
(DMSO-D_6)
3.14
7.37
7.29
7.19
7.17
5.58
5.63
5.69
5.51
5.25
4.83
4.72
4.59
4.67
4.49
4.26
3.26
3.35
3.51
3.56
3.62
3.75
22.81
2.59
0.99
1.02
1.03
0.16
0.16
1.45
9.86
1.02
4.96
1.30
0.99
0.97
6.07
8.0
7.5
7.0
6.5
6.0
5.5
5.0
4.5
4.0
3.5
3.0
2.5
2.0
1.5
1.0
0.5
0

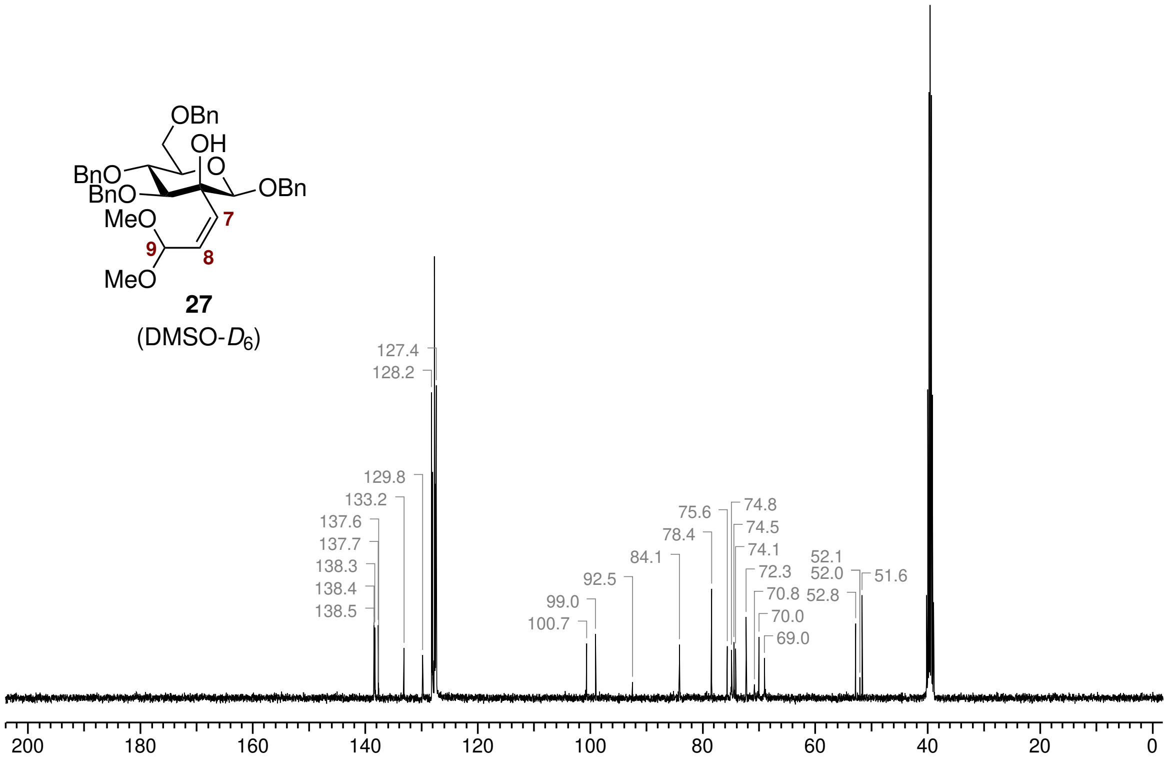
OBn
OH
O
BnO
BnO
OBn
MeO
7
9
8
MeO
27
(DMSO-D_6)
127.4
128.2
129.8
133.2
137.6
137.7
138.3
138.4
138.5
100.7
99.0
92.5
84.1
78.4
75.6
74.8
74.5
74.1
72.3
70.8
70.0
69.0
52.1
52.0
52.8
51.6
200
180
160
140
120
100
80
60
40
20
0

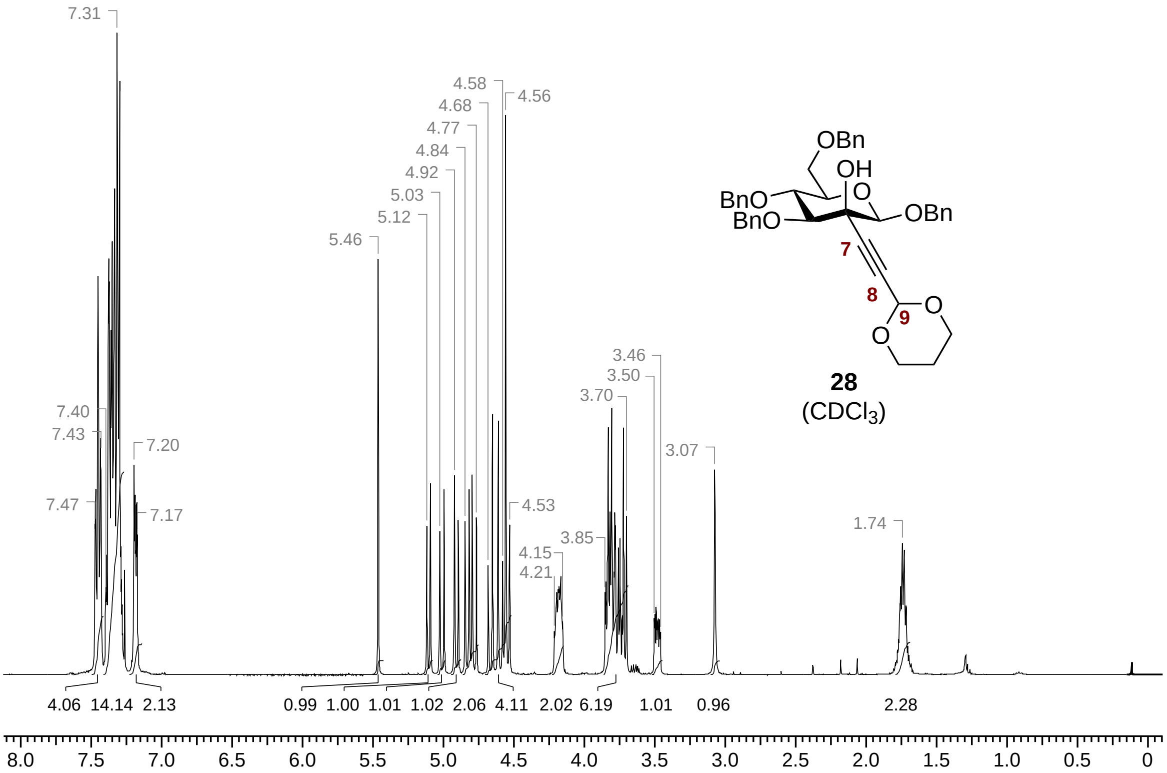
7.31
7.40
7.43
7.47
7.20
7.17
5.46
5.12
5.03
4.92
4.84
4.77
4.68
4.58
4.56
4.53
4.15
4.21
3.85
3.70
3.50
3.46
3.07
1.74
4.06 14.14 2.13
0.99 1.00 1.01 1.02 2.06 4.11 2.02 6.19 1.01 0.96
2.28
8.0 7.5 7.0 6.5 6.0 5.5 5.0 4.5 4.0 3.5 3.0 2.5 2.0 1.5 1.0 0.5 0
OBn
OH
BnO
BnO
O
OBn
7
8
9
O
O
28
(CDCl3)

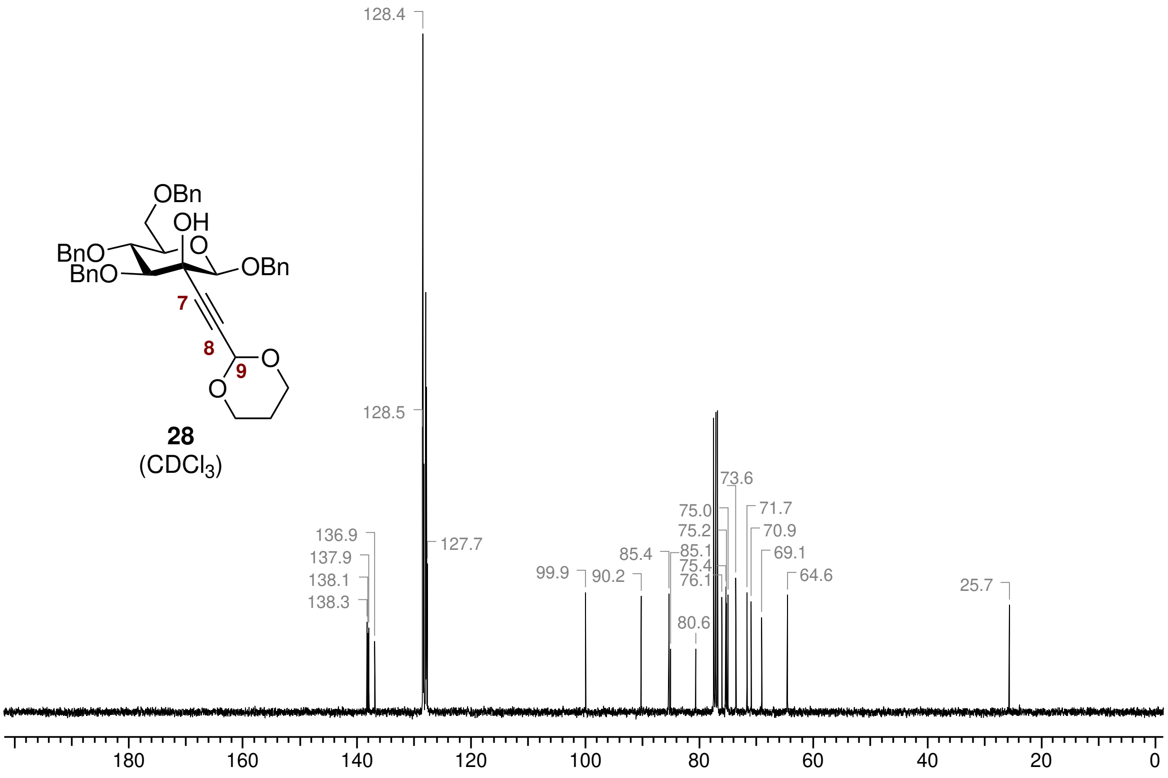
128.4
128.5
127.7
136.9
137.9
138.1
138.3
99.9
90.2
85.4
85.1
75.4
76.1
75.0
75.2
73.6
71.7
70.9
69.1
64.6
80.6
25.7
180 160 140 120 100 80 60 40 20 0
OBn
OH
BnO
BnO
O
OBn
7
8
9
O
O
28
(CDCl3)

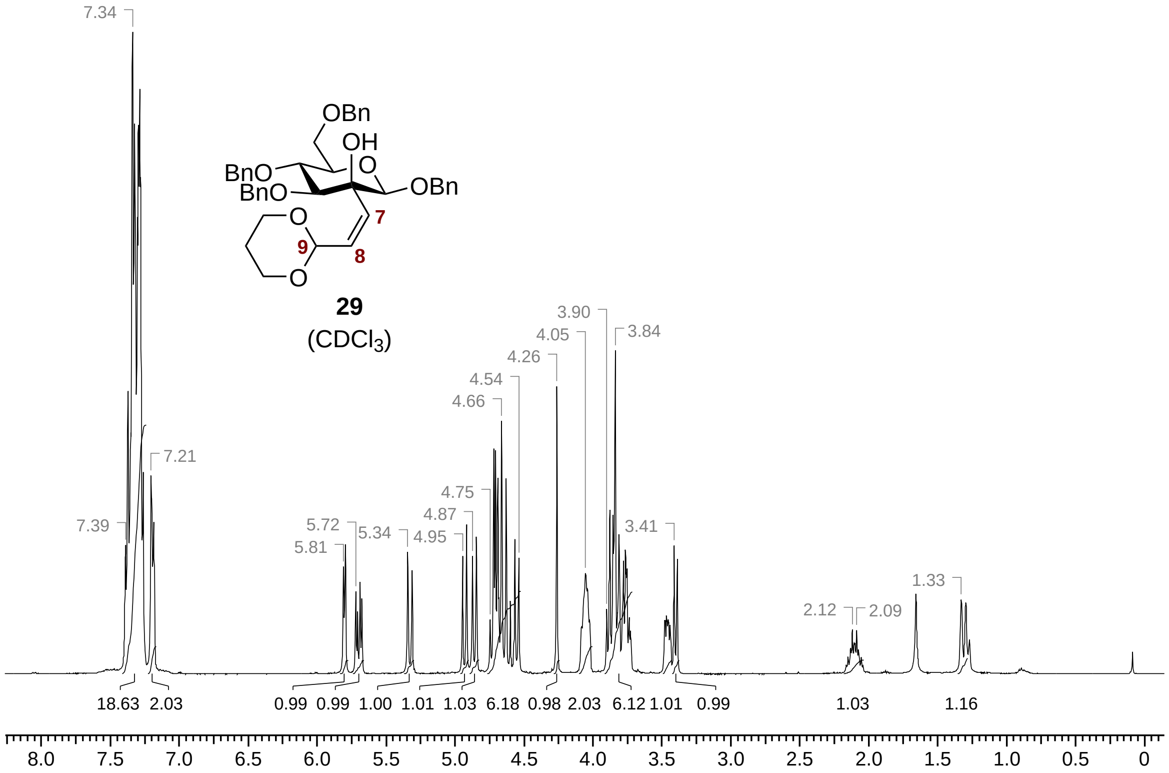
OBn
OH
BnO
BnO
O
OBn
O
7
9
8
O
29
(CDCl$_3$)
7.34
7.39
7.21
5.81
5.72
5.34
4.95
4.87
4.75
4.66
4.54
4.26
4.05
3.90
3.84
3.41
2.12
2.09
1.33
18.63
2.03
0.99
0.99
1.00
1.01
1.03
6.18
0.98
2.03
6.12
1.01
0.99
1.03
1.16
8.0
7.5
7.0
6.5
6.0
5.5
5.0
4.5
4.0
3.5
3.0
2.5
2.0
1.5
1.0
0.5
0

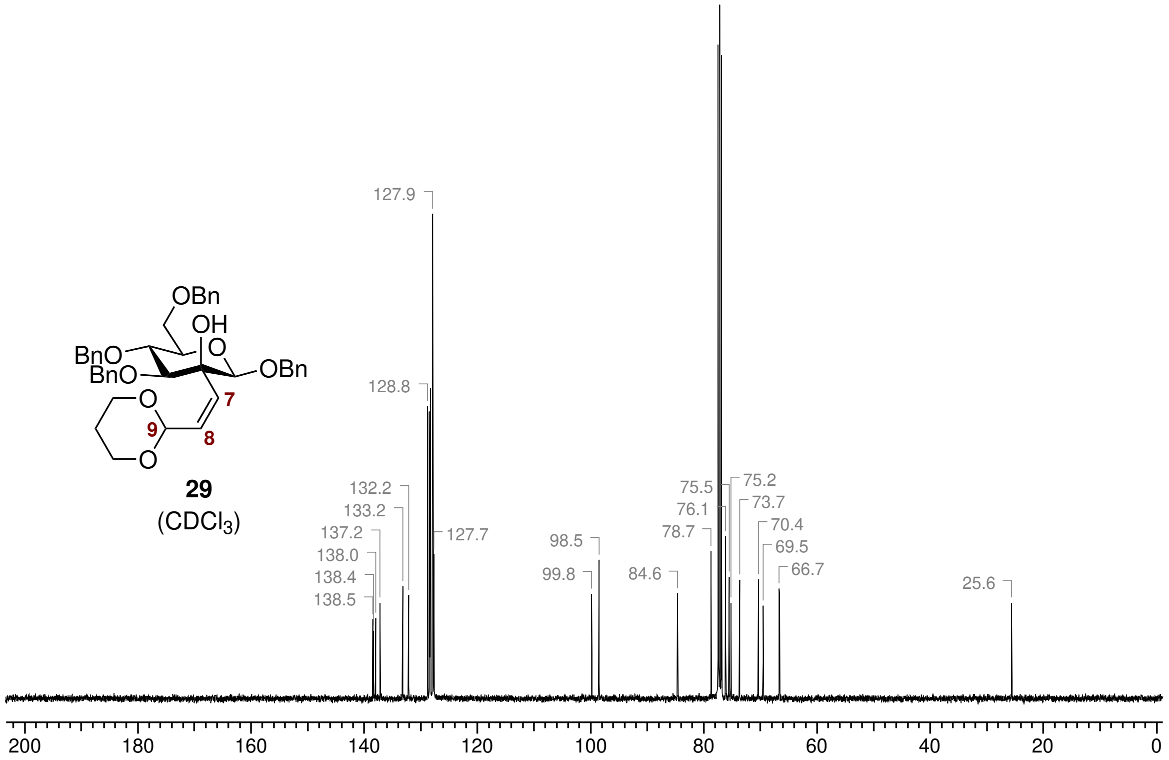
OBn
OH
BnO
BnO
O
OBn
O
7
9
8
O
29
(CDCl$_3$)
127.9
128.8
132.2
133.2
137.2
138.0
138.4
138.5
127.7
98.5
99.8
84.6
75.5
76.1
78.7
75.2
73.7
70.4
69.5
66.7
25.6
200
180
160
140
120
100
80
60
40
20
0

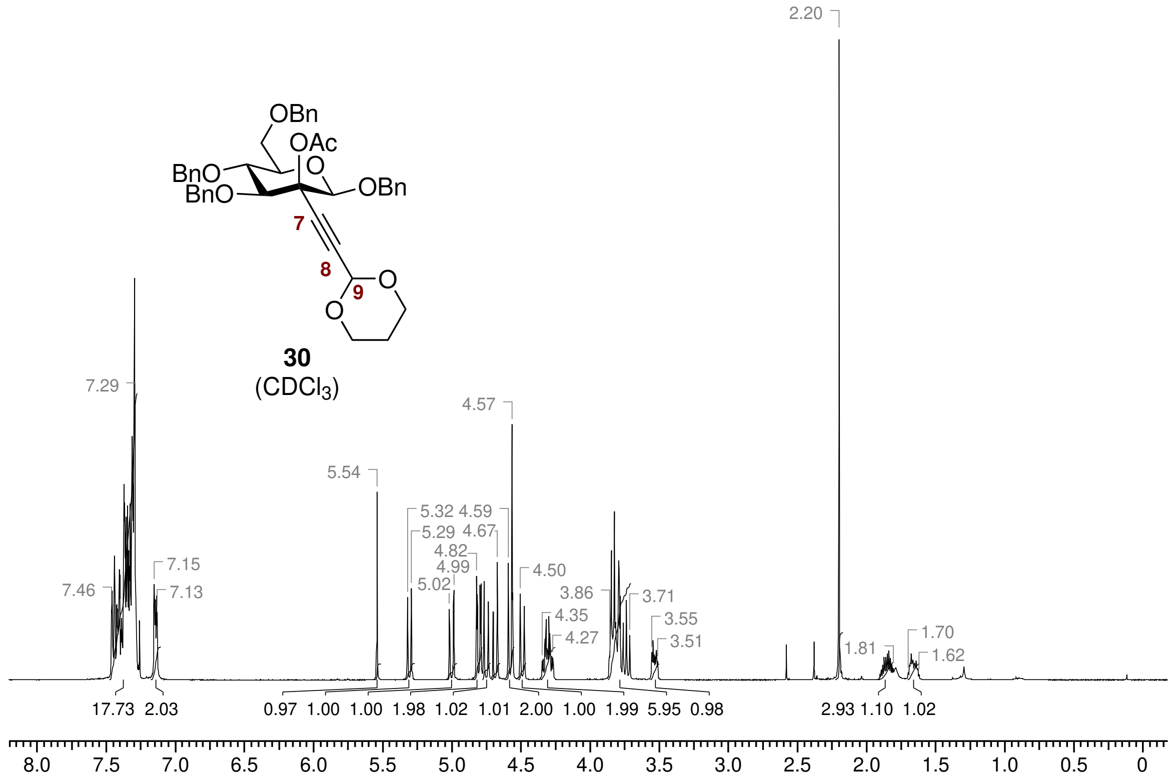

30

($CDCl_3$)

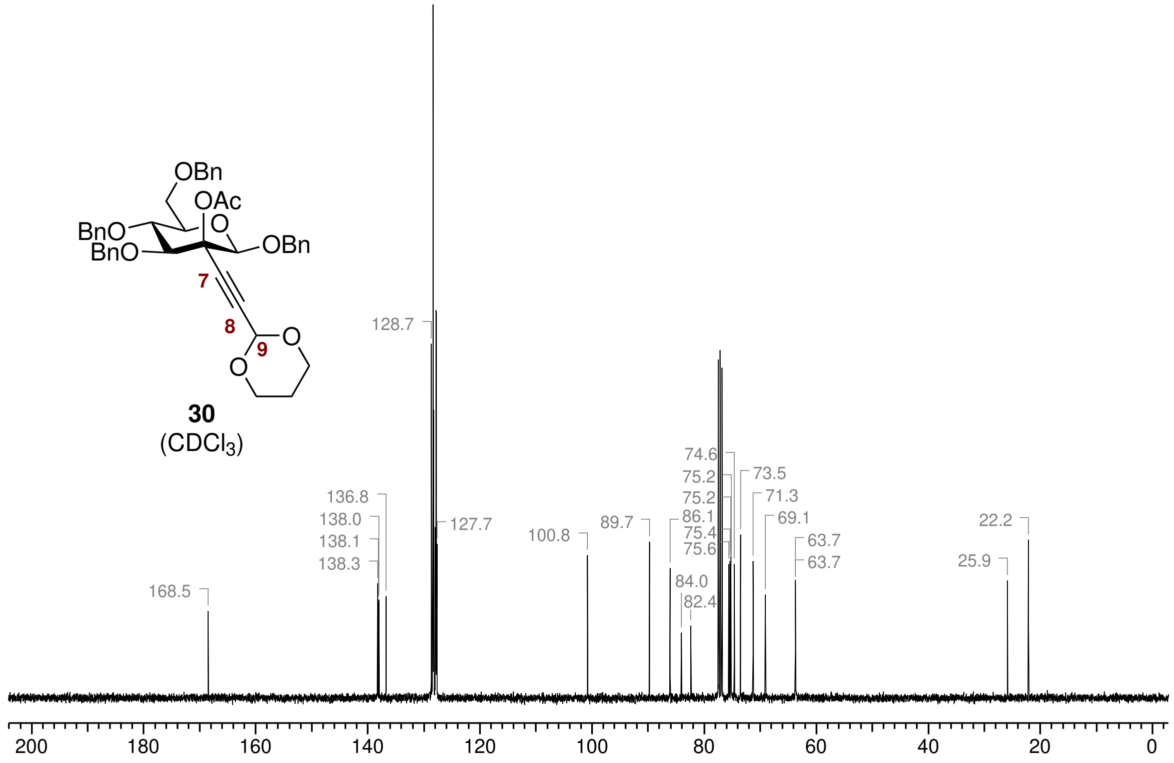

30

($CDCl_3$)

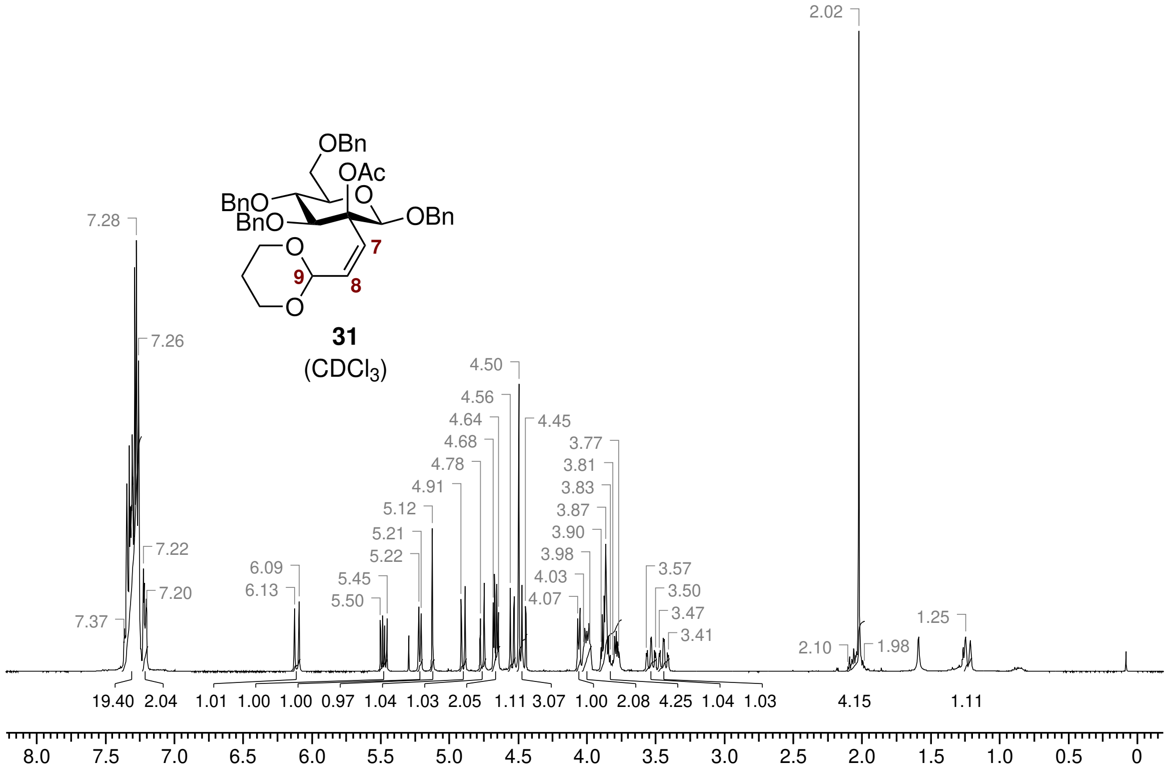
OBn
OAc
O
BnO
BnO
OBn
7
O
9
8
O
31
(CDCl$_3$)
7.28
7.26
7.22
7.20
7.37
6.09
6.13
5.45
5.50
5.12
5.21
5.22
4.91
4.78
4.68
4.64
4.56
4.50
4.45
3.77
3.81
3.83
3.87
3.90
3.98
4.03
4.07
3.57
3.50
3.47
3.41
2.10
2.02
1.98
1.25
19.40 2.04 1.01 1.00 1.00 0.97 1.04 1.03 2.05 1.11 3.07 1.00 2.08 4.25 1.04 1.03 4.15 1.11
8.0 7.5 7.0 6.5 6.0 5.5 5.0 4.5 4.0 3.5 3.0 2.5 2.0 1.5 1.0 0.5 0

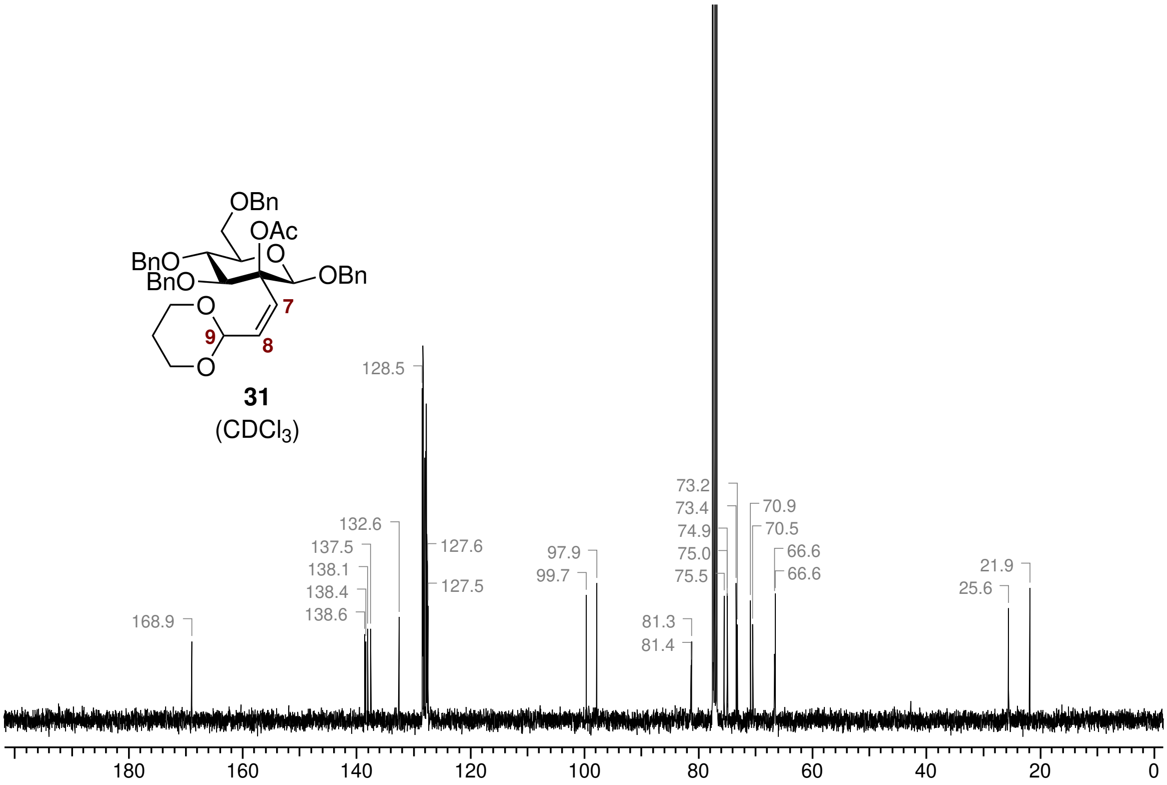
OBn
OAc
O
BnO
BnO
OBn
7
O
9
8
O
31
(CDCl$_3$)
128.5
132.6
137.5
138.1
138.4
138.6
127.6
127.5
168.9
97.9
99.7
81.3
81.4
73.2
73.4
74.9
75.0
75.5
70.9
70.5
66.6
66.6
21.9
25.6
180 160 140 120 100 80 60 40 20 0

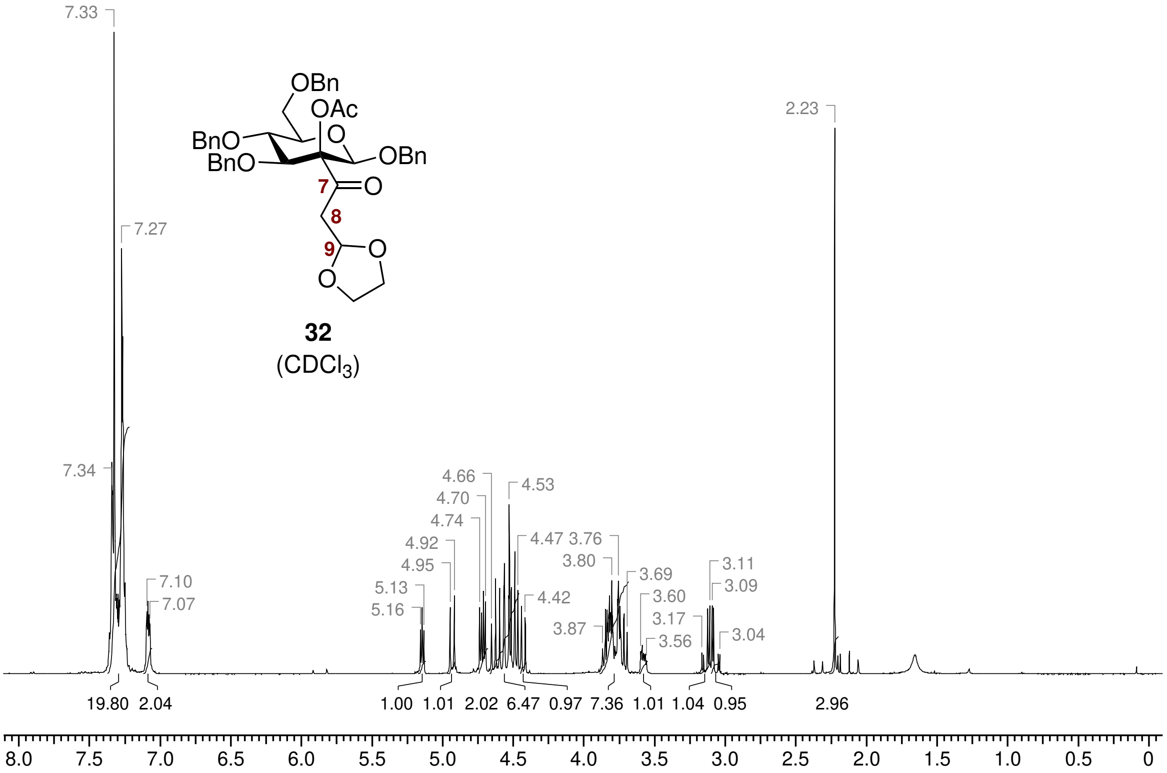
7.33
7.27
7.34
7.10
7.07
5.13
5.16
4.92
4.95
4.74
4.70
4.66
4.53
4.47
4.42
3.76
3.80
3.87
3.69
3.60
3.17
3.56
3.11
3.09
3.04
2.23
19.80
2.04
1.00
1.01
2.02
6.47
0.97
7.36
1.01
1.04
0.95
2.96
8.0
7.5
7.0
6.5
6.0
5.5
5.0
4.5
4.0
3.5
3.0
2.5
2.0
1.5
1.0
0.5
0
OBn
OAc
BnO
BnO
O
OBn
7
O
8
9
O
O
32
(CDCl3)

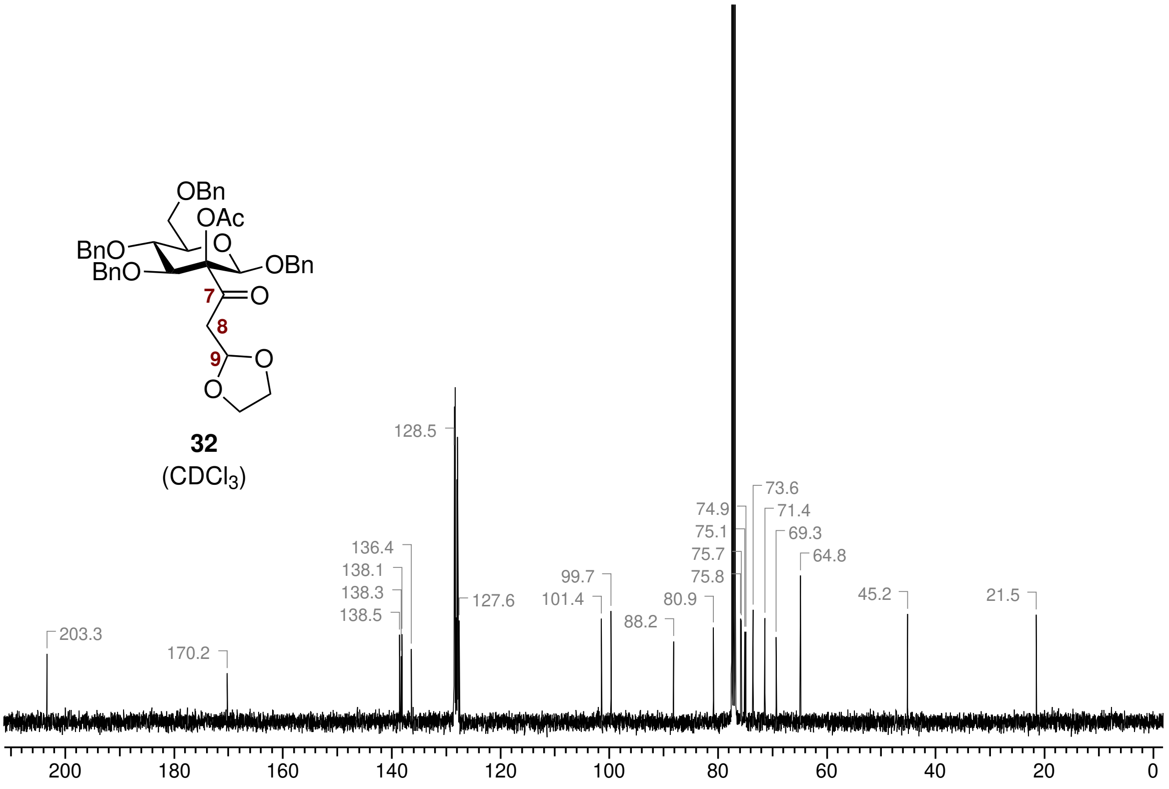
203.3
170.2
136.4
138.1
138.3
138.5
128.5
127.6
99.7
101.4
88.2
80.9
74.9
75.1
75.7
75.8
73.6
71.4
69.3
64.8
45.2
21.5
200
180
160
140
120
100
80
60
40
20
0
OBn
OAc
BnO
BnO
O
OBn
7
O
8
9
O
O
32
(CDCl3)

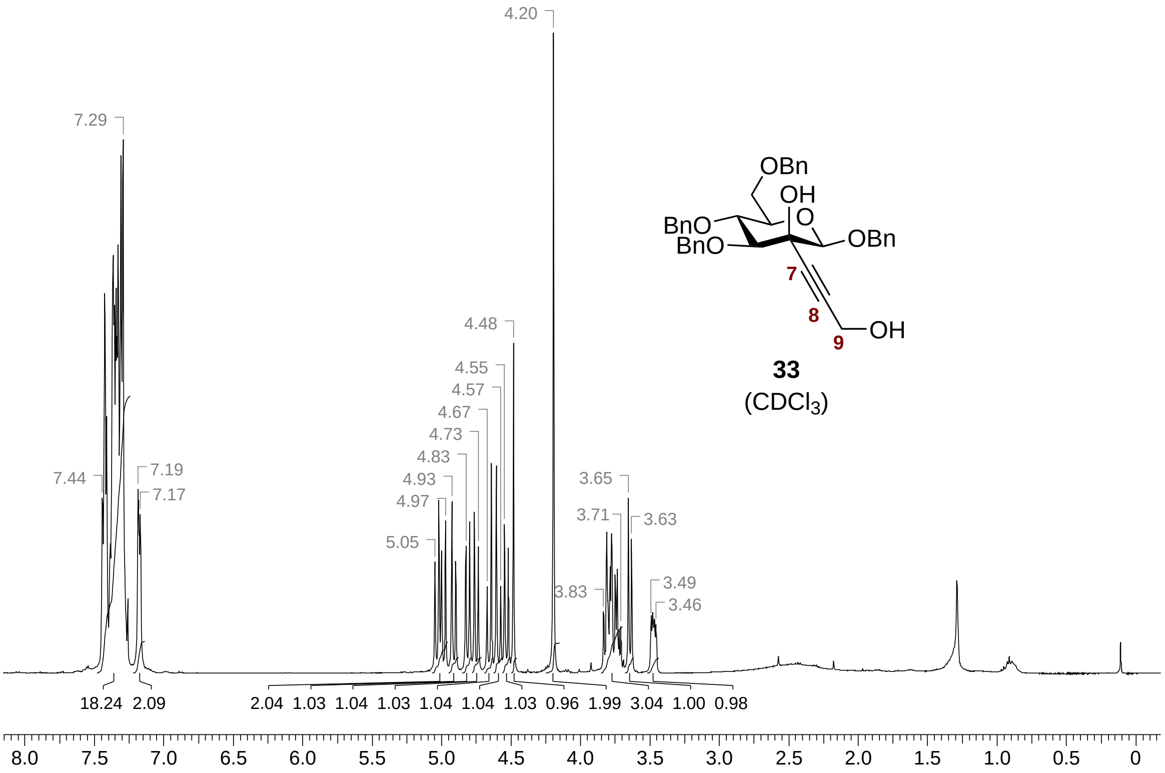
4.20
7.29
7.44
7.19
7.17
4.48
4.55
4.57
4.67
4.73
4.83
4.93
4.97
5.05
3.65
3.71
3.63
3.83
3.49
3.46
18.24 2.09
2.04 1.03 1.04 1.03 1.04 1.04 1.03 0.96 1.99 3.04 1.00 0.98
8.0 7.5 7.0 6.5 6.0 5.5 5.0 4.5 4.0 3.5 3.0 2.5 2.0 1.5 1.0 0.5 0
OBn
OH
O
BnO
BnO
OBn
7
8
9
OH
33
(CDCl3)

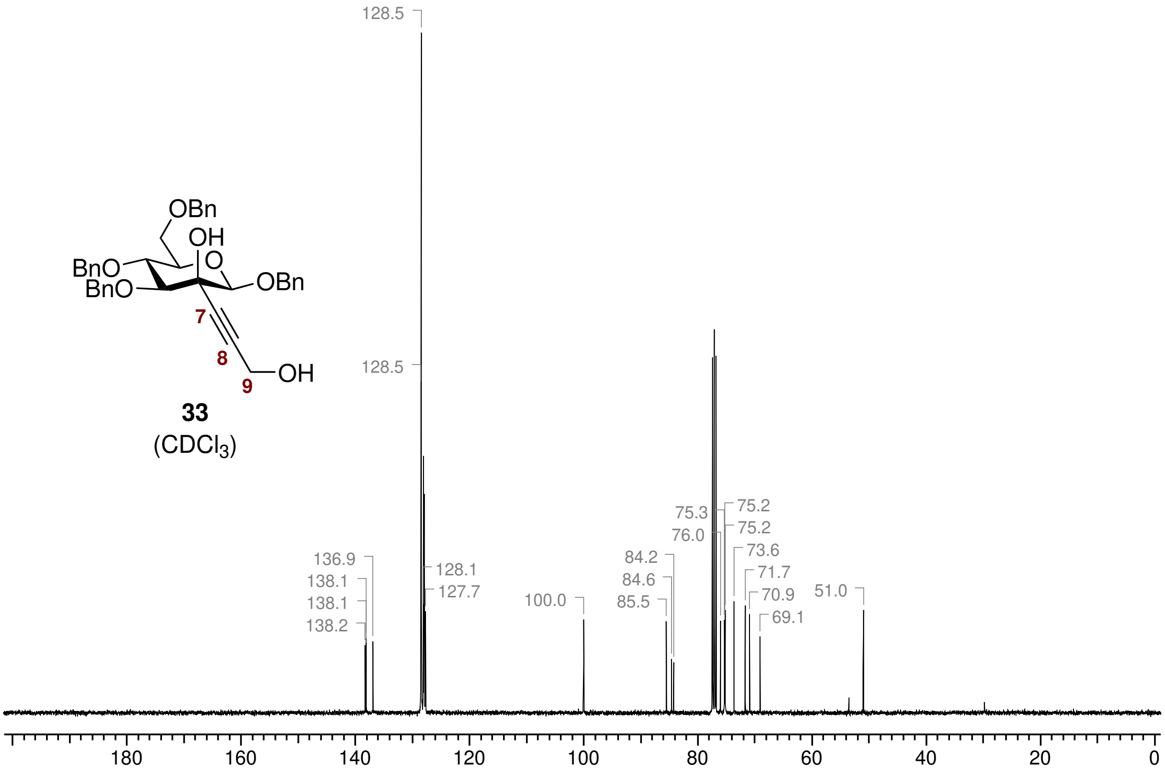
128.5
128.5
OBn
OH
O
BnO
BnO
OBn
7
8
9
OH
33
(CDCl3)
136.9
138.1
138.1
138.2
128.1
127.7
100.0
84.2
84.6
85.5
75.3
76.0
75.2
75.2
73.6
71.7
70.9
69.1
51.0
180 160 140 120 100 80 60 40 20 0

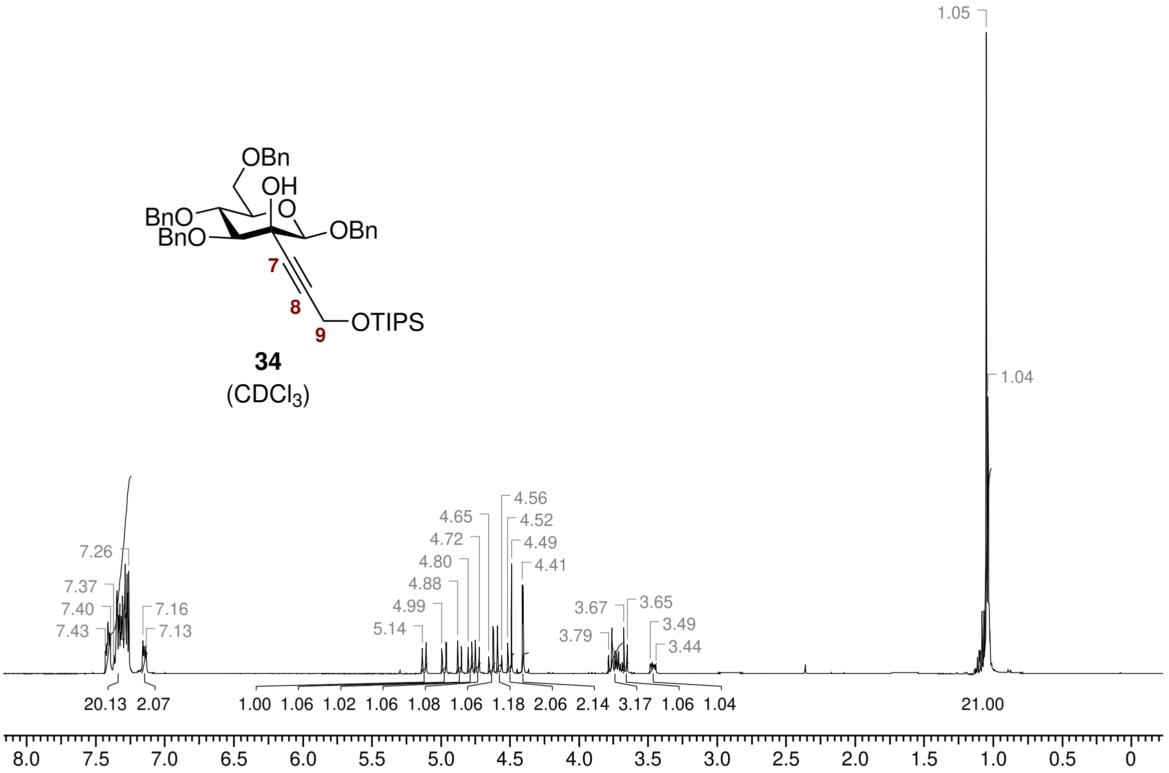
OBn
OH
O
BnO
BnO
OBn
7
8
9
OTIPS
34
(CDCl3)
1.05
1.04
7.26
7.37
7.40
7.43
7.16
7.13
4.65
4.72
4.80
4.88
4.99
5.14
4.56
4.52
4.49
4.41
3.67
3.79
3.65
3.49
3.44
20.13 2.07
1.00 1.06 1.02 1.06 1.08 1.06 1.18 2.06 2.14 3.17 1.06 1.04
21.00
8.0 7.5 7.0 6.5 6.0 5.5 5.0 4.5 4.0 3.5 3.0 2.5 2.0 1.5 1.0 0.5 0

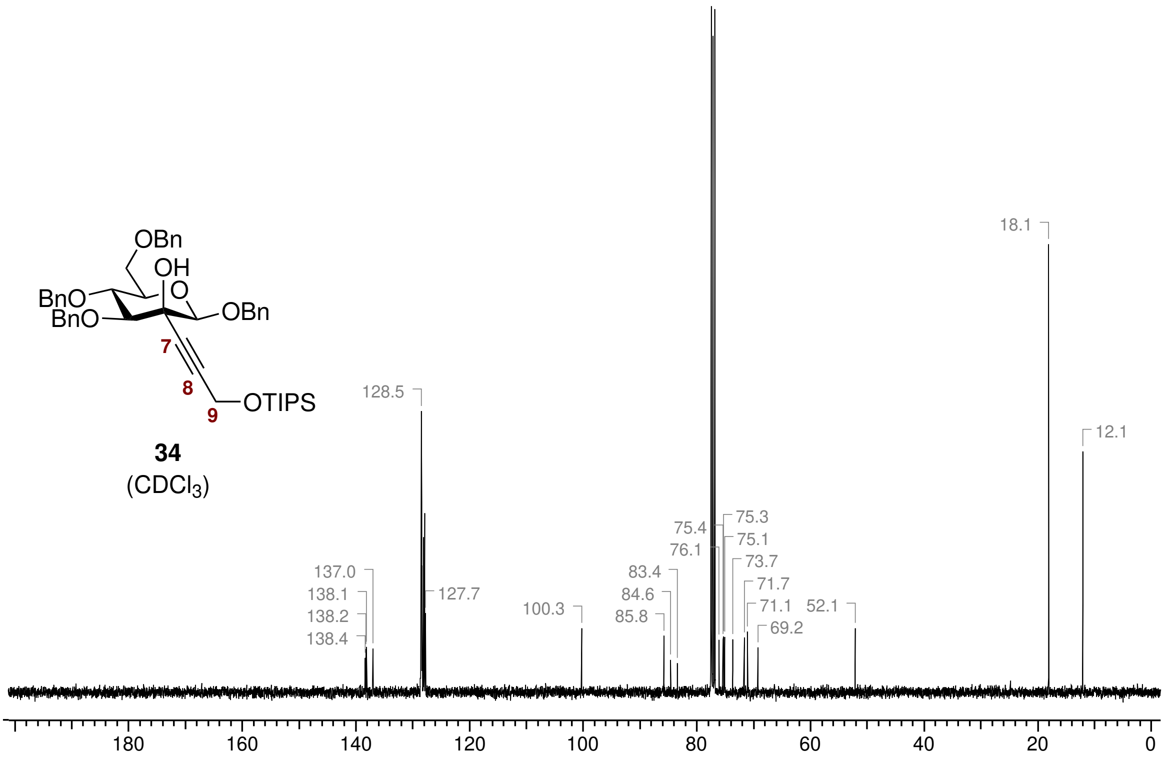
OBn
OH
O
BnO
BnO
OBn
7
8
9
OTIPS
34
(CDCl3)
18.1
12.1
128.5
127.7
137.0
138.1
138.2
138.4
100.3
83.4
84.6
85.8
75.4
76.1
75.3
75.1
73.7
71.7
71.1
52.1
69.2
180 160 140 120 100 80 60 40 20 0

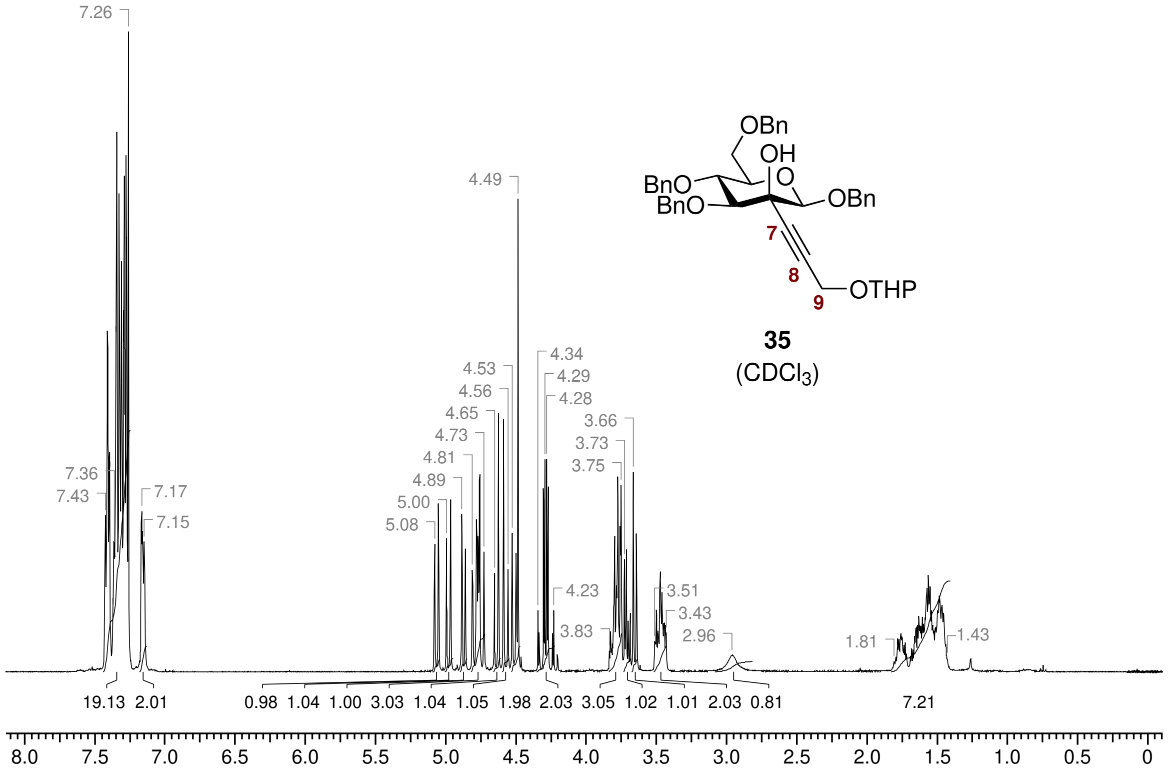
7.26
7.36
7.43
7.17
7.15
4.49
4.53
4.56
4.65
4.73
4.81
4.89
5.00
5.08
4.34
4.29
4.28
3.66
3.73
3.75
4.23
3.83
3.51
3.43
2.96
1.81
1.43
19.13 2.01 0.98 1.04 1.00 3.03 1.04 1.05 1.98 2.03 3.05 1.02 1.01 2.03 0.81 7.21
8.0 7.5 7.0 6.5 6.0 5.5 5.0 4.5 4.0 3.5 3.0 2.5 2.0 1.5 1.0 0.5 0
OBn
OH
BnO
BnO
O
OBn
7
8
9
OTHP
35
(CDCl$_3$)

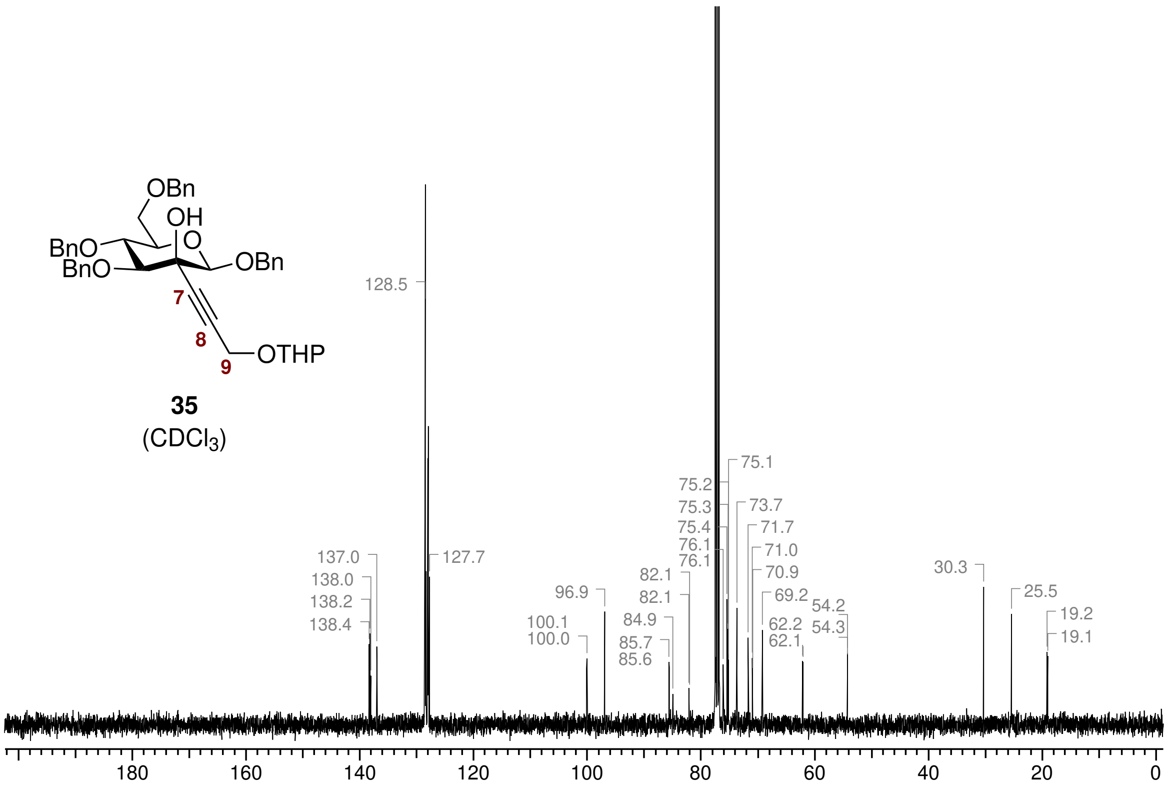
OBn
OH
BnO
BnO
O
OBn
7
8
9
OTHP
35
(CDCl$_3$)
128.5
127.7
137.0
138.0
138.2
138.4
100.1
100.0
96.9
84.9
85.7
85.6
82.1
82.1
75.2
75.3
75.4
76.1
76.1
75.1
73.7
71.7
71.0
70.9
69.2
62.2
62.1
54.2
54.3
30.3
25.5
19.2
19.1
180 160 140 120 100 80 60 40 20 0

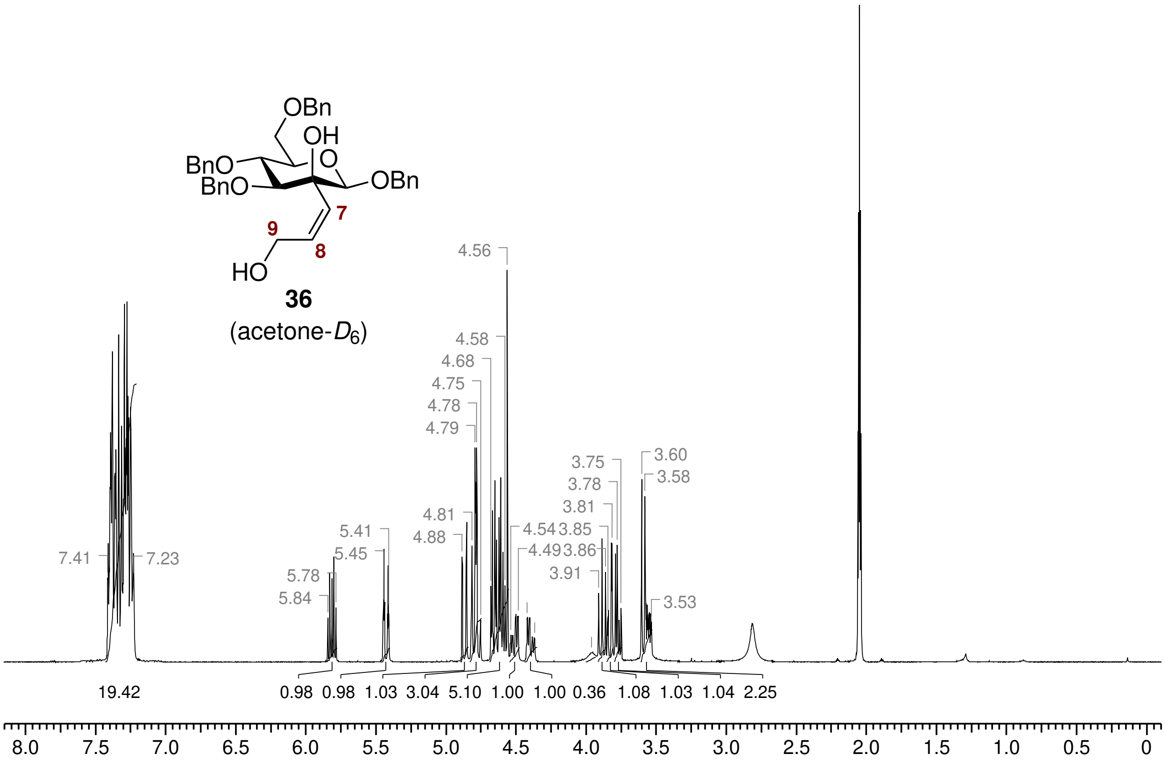
OBn
OH
O
BnO
BnO
OBn
7
9
8
HO
36
(acetone-D_6)
7.41
7.23
5.78
5.84
5.41
5.45
4.81
4.88
4.56
4.58
4.68
4.75
4.78
4.79
4.54
4.49
3.75
3.78
3.81
3.85
3.86
3.91
3.60
3.58
3.53
19.42
0.98 0.98 1.03 3.04 5.10 1.00 1.00 0.36 1.08 1.03 1.04 2.25
8.0 7.5 7.0 6.5 6.0 5.5 5.0 4.5 4.0 3.5 3.0 2.5 2.0 1.5 1.0 0.5 0

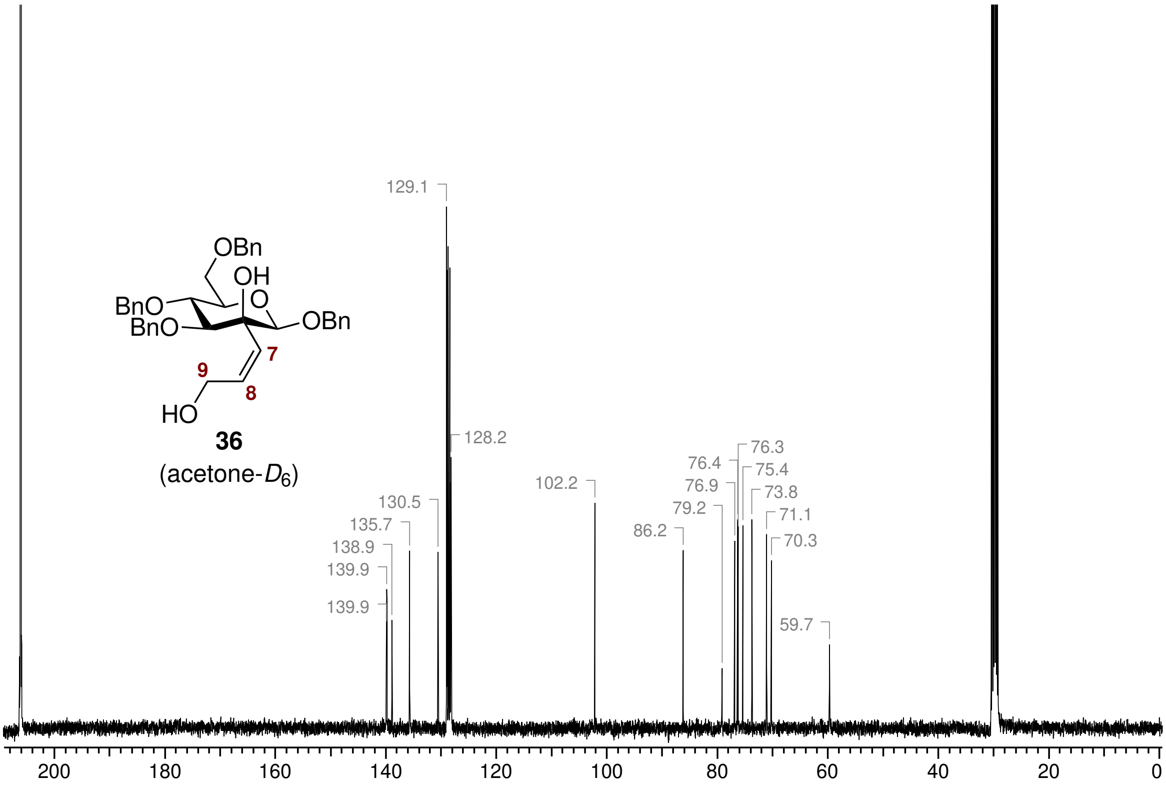
OBn
OH
O
BnO
BnO
OBn
7
9
8
HO
36
(acetone-D_6)
129.1
128.2
130.5
135.7
138.9
139.9
139.9
102.2
86.2
79.2
76.9
76.4
76.3
75.4
73.8
71.1
70.3
59.7
200 180 160 140 120 100 80 60 40 20 0

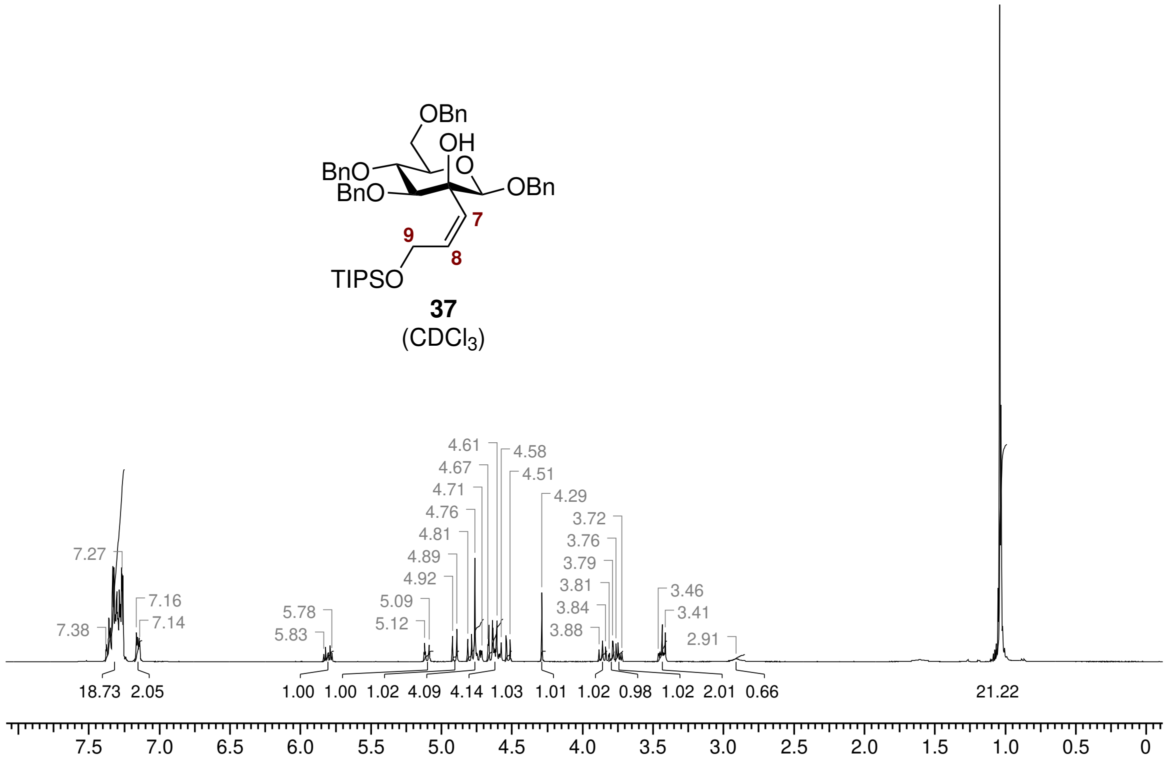
OBn
OH
O
BnO
BnO
OBn
7
9
8
TIPSO
37
(CDCl3)
4.61
4.58
4.67
4.51
4.71
4.29
4.76
3.72
4.81
3.76
4.89
3.79
4.92
3.81
3.46
5.09
3.84
3.41
5.12
3.88
2.91
7.27
7.16
7.14
7.38
5.78
5.83
18.73
2.05
1.00
1.00
1.02
4.09
4.14
1.03
1.01
1.02
0.98
1.02
2.01
0.66
21.22
7.5
7.0
6.5
6.0
5.5
5.0
4.5
4.0
3.5
3.0
2.5
2.0
1.5
1.0
0.5
0

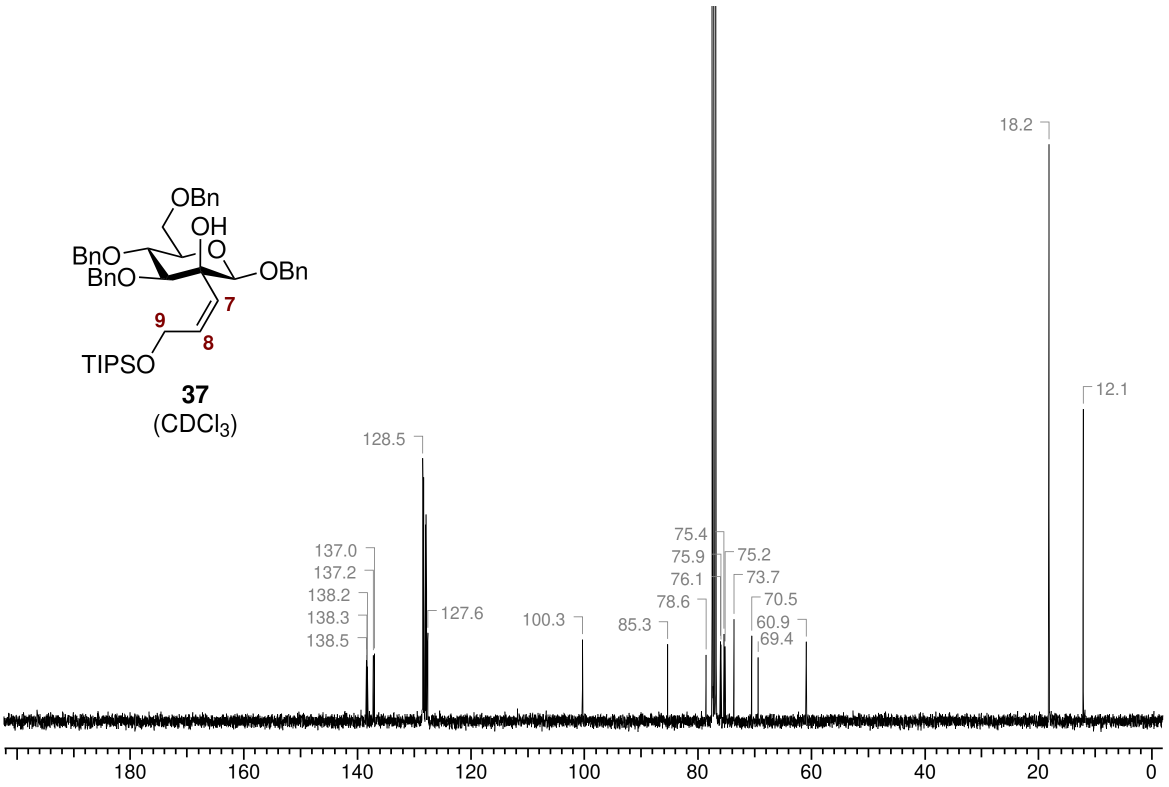
OBn
OH
O
BnO
BnO
OBn
7
9
8
TIPSO
37
(CDCl3)
18.2
12.1
128.5
75.4
75.9
75.2
76.1
73.7
78.6
70.5
137.0
137.2
138.2
138.3
138.5
127.6
100.3
85.3
60.9
69.4
180
160
140
120
100
80
60
40
20
0

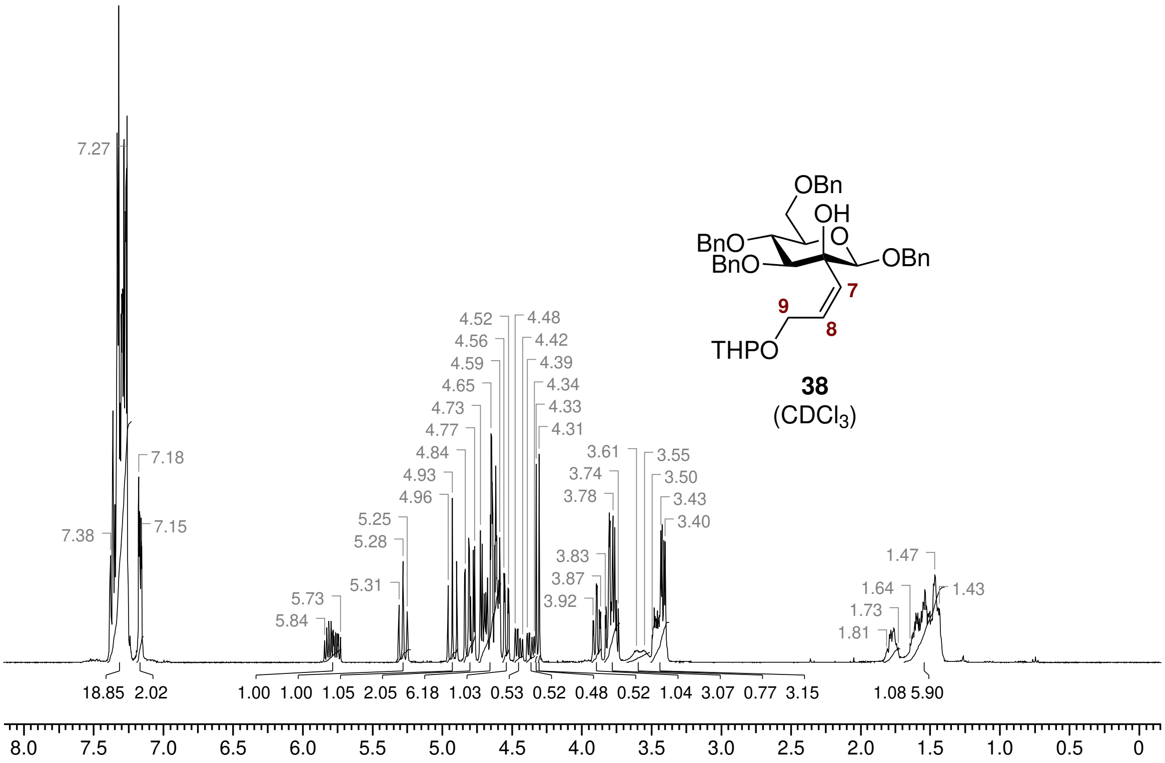
7.27
7.38
7.18
7.15
5.73
5.84
5.31
5.25
5.28
4.52
4.56
4.59
4.65
4.73
4.77
4.84
4.93
4.96
4.48
4.42
4.39
4.34
4.33
4.31
3.61
3.74
3.78
3.83
3.87
3.92
3.55
3.50
3.43
3.40
1.47
1.64
1.73
1.81
1.43
18.85 2.02
1.00 1.00 1.05 2.05 6.18 1.03 0.53 0.52 0.48 0.52 1.04 3.07 0.77 3.15
1.08 5.90
8.0 7.5 7.0 6.5 6.0 5.5 5.0 4.5 4.0 3.5 3.0 2.5 2.0 1.5 1.0 0.5 0
OBn
OH
O
BnO
BnO
OBn
7
9
8
THPO
38
(CDCl3)

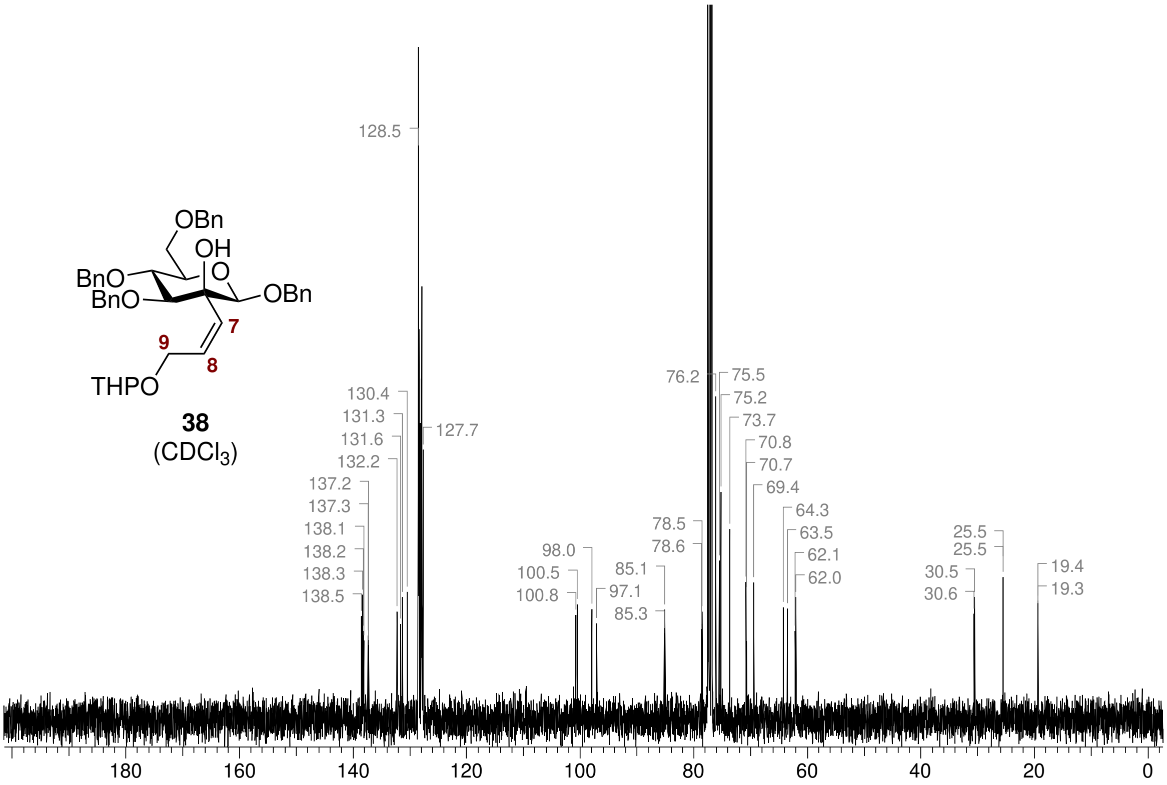
128.5
OBn
OH
O
BnO
BnO
OBn
7
9
8
THPO
38
(CDCl3)
130.4
131.3
131.6
132.2
127.7
137.2
137.3
138.1
138.2
138.3
138.5
98.0
100.5
100.8
85.1
97.1
85.3
78.5
78.6
76.2
75.5
75.2
73.7
70.8
70.7
69.4
64.3
63.5
62.1
62.0
25.5
25.5
30.5
30.6
19.4
19.3
180 160 140 120 100 80 60 40 20 0

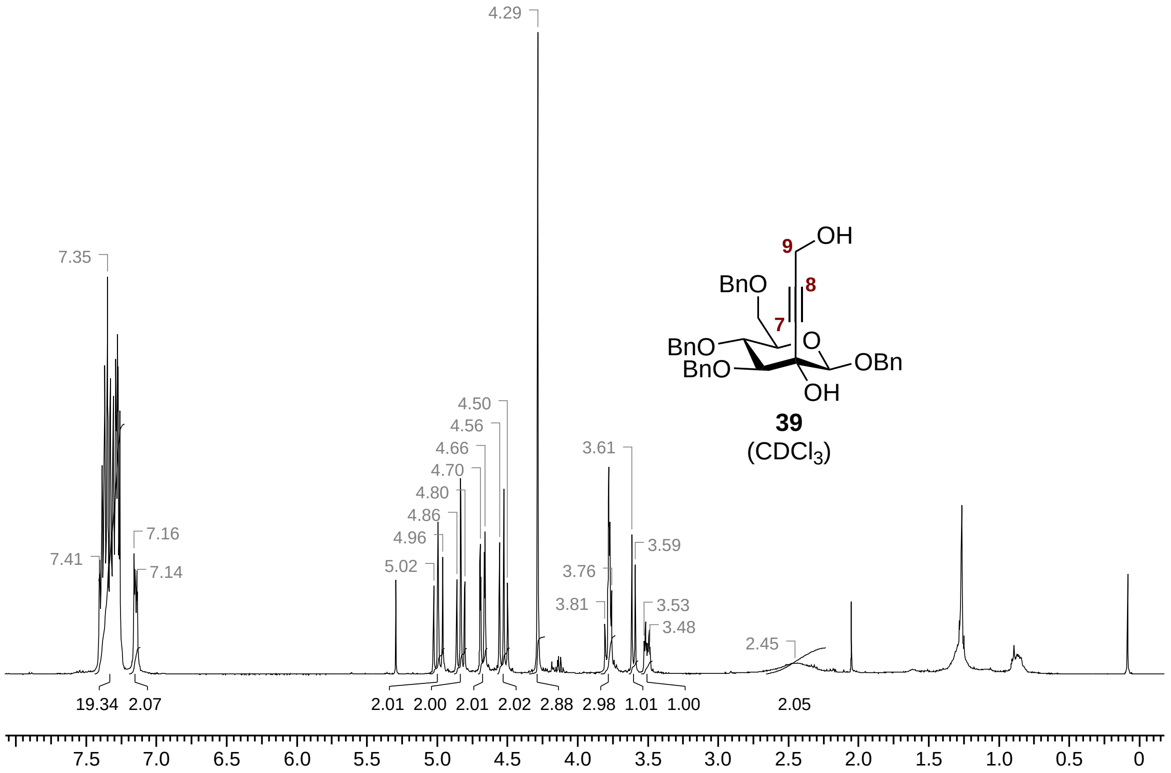

39
($CDCl_3$)

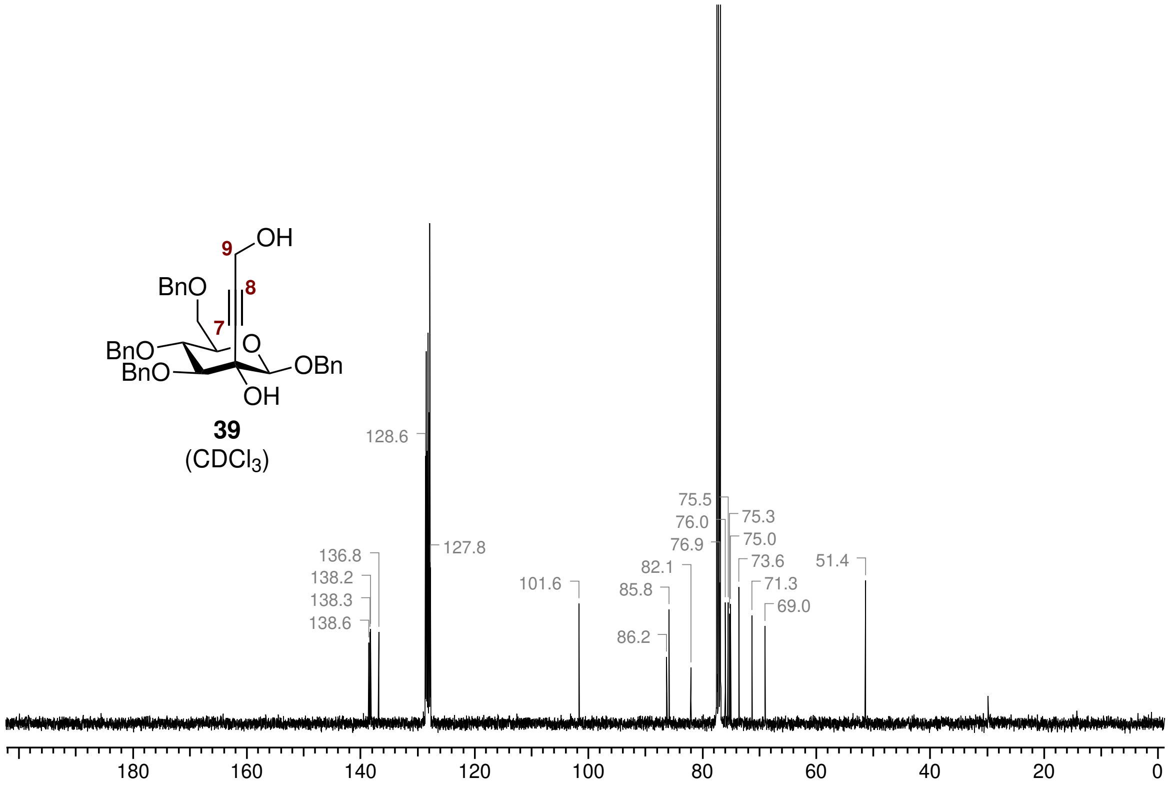

39
($CDCl_3$)

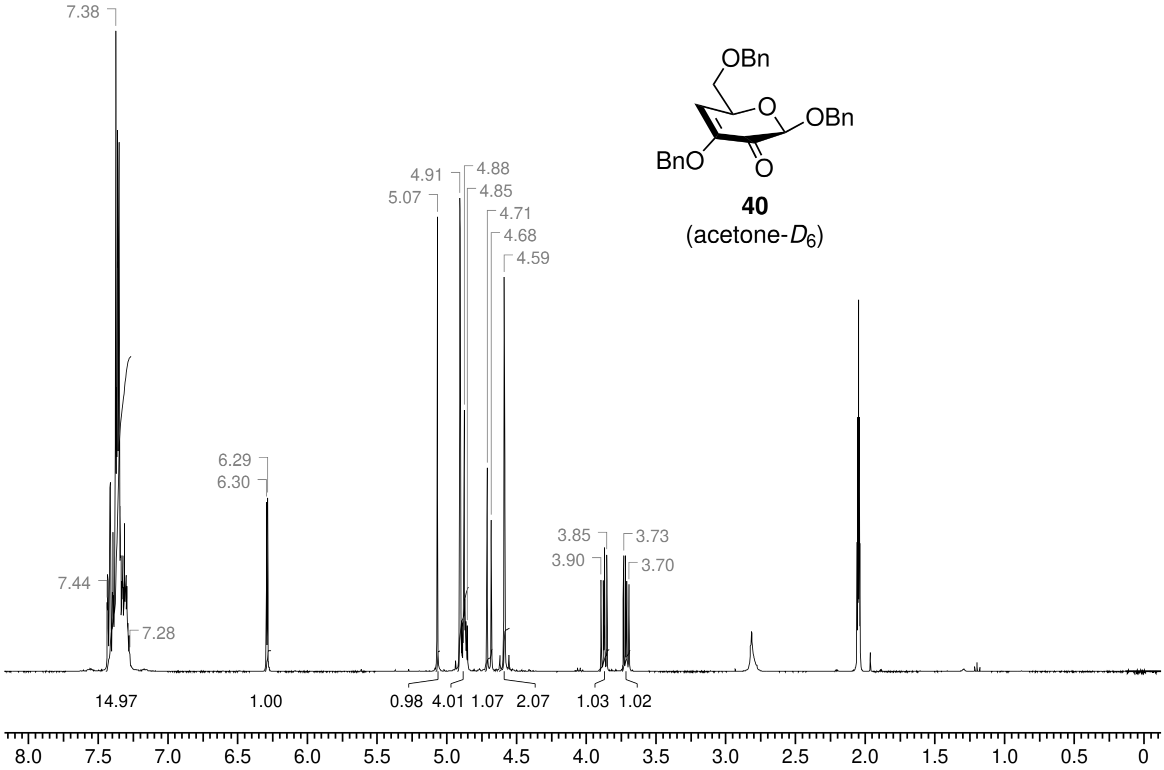

40
(acetone-D_6)

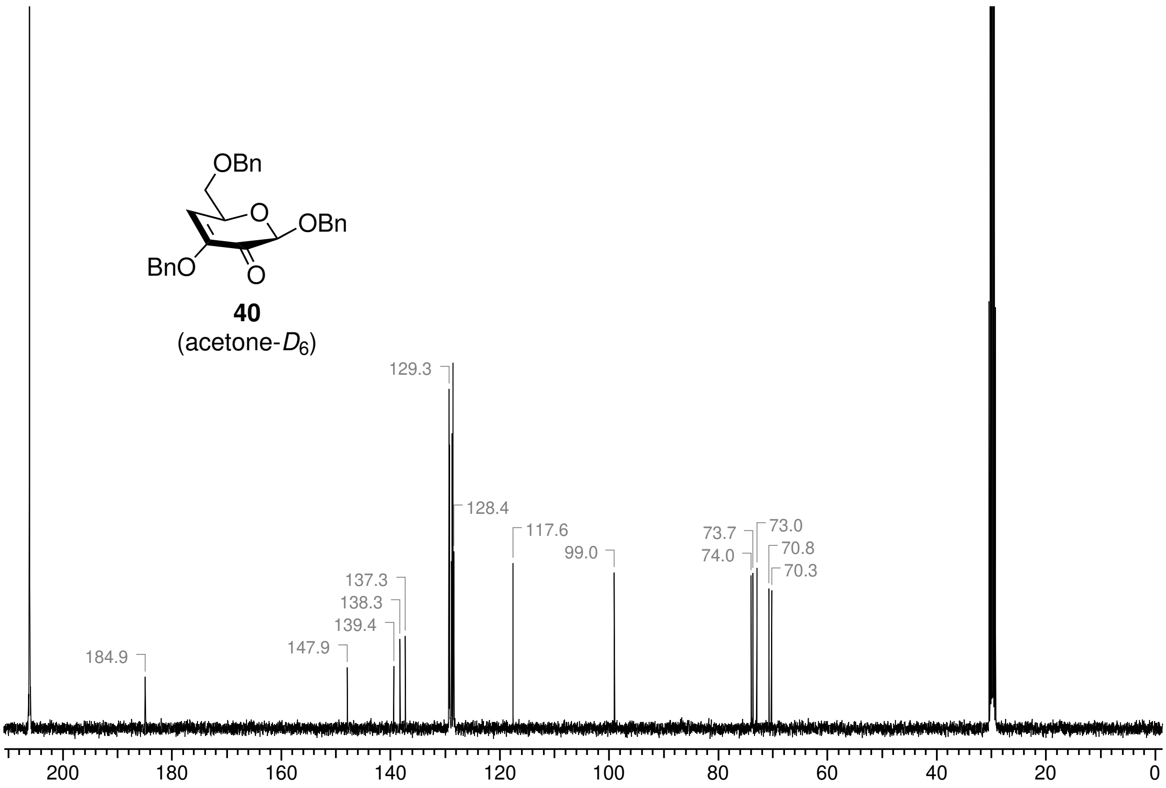

40
(acetone-D_6)

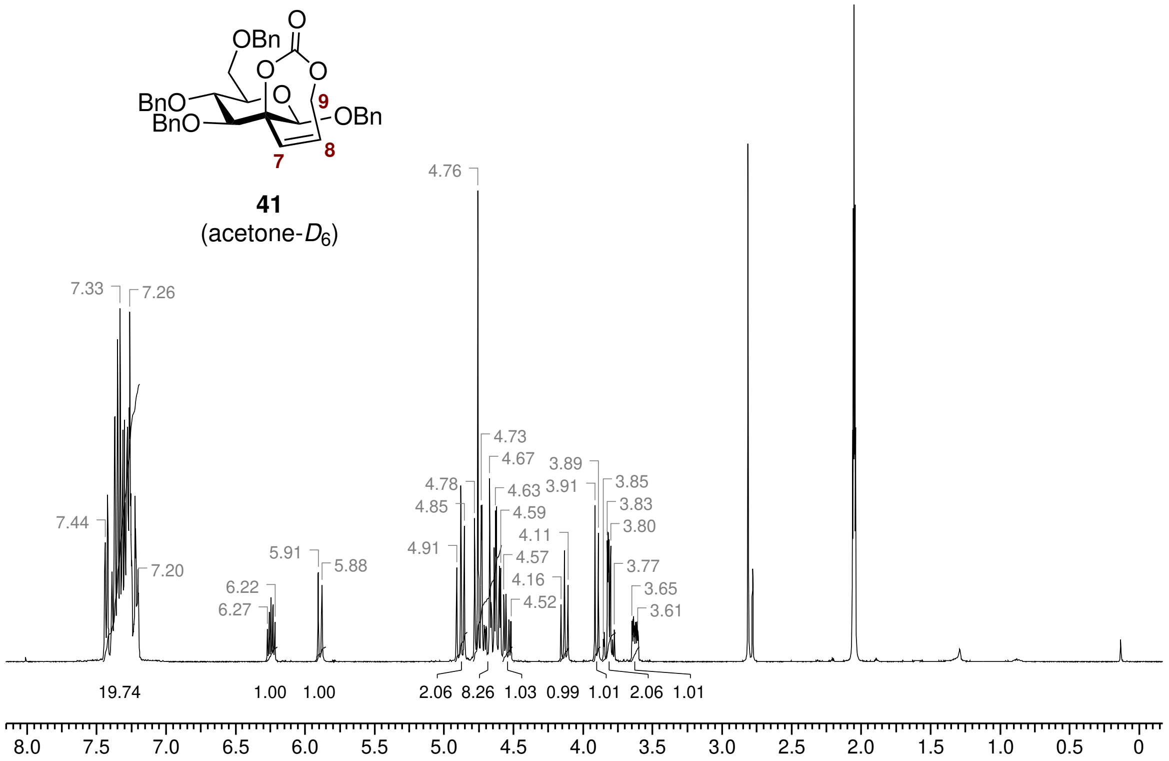
OBn
O
O
O
O
BnO
BnO
9
OBn
7
8
41
(acetone-D_6)
7.33
7.26
7.44
7.20
6.22
6.27
5.91
5.88
4.76
4.73
4.67
4.78
4.85
4.91
4.63
4.59
4.11
4.57
4.16
4.52
3.89
3.91
3.85
3.83
3.80
3.77
3.65
3.61
19.74
1.00
1.00
2.06
8.26
1.03
0.99
1.01
2.06
1.01
8.0
7.5
7.0
6.5
6.0
5.5
5.0
4.5
4.0
3.5
3.0
2.5
2.0
1.5
1.0
0.5
0

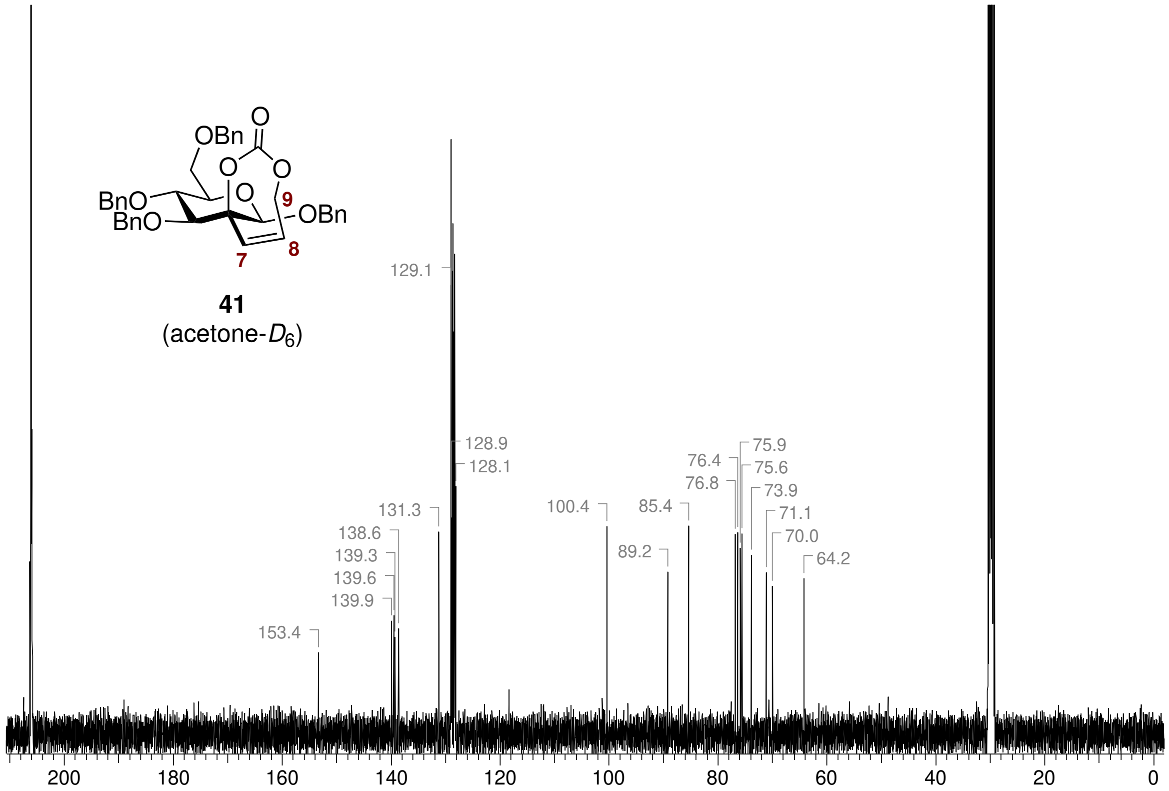
OBn
O
O
O
O
BnO
BnO
9
OBn
7
8
41
(acetone-D_6)
129.1
128.9
128.1
131.3
138.6
139.3
139.6
139.9
153.4
100.4
85.4
89.2
76.4
76.8
75.9
75.6
73.9
71.1
70.0
64.2
200
180
160
140
120
100
80
60
40
20
0

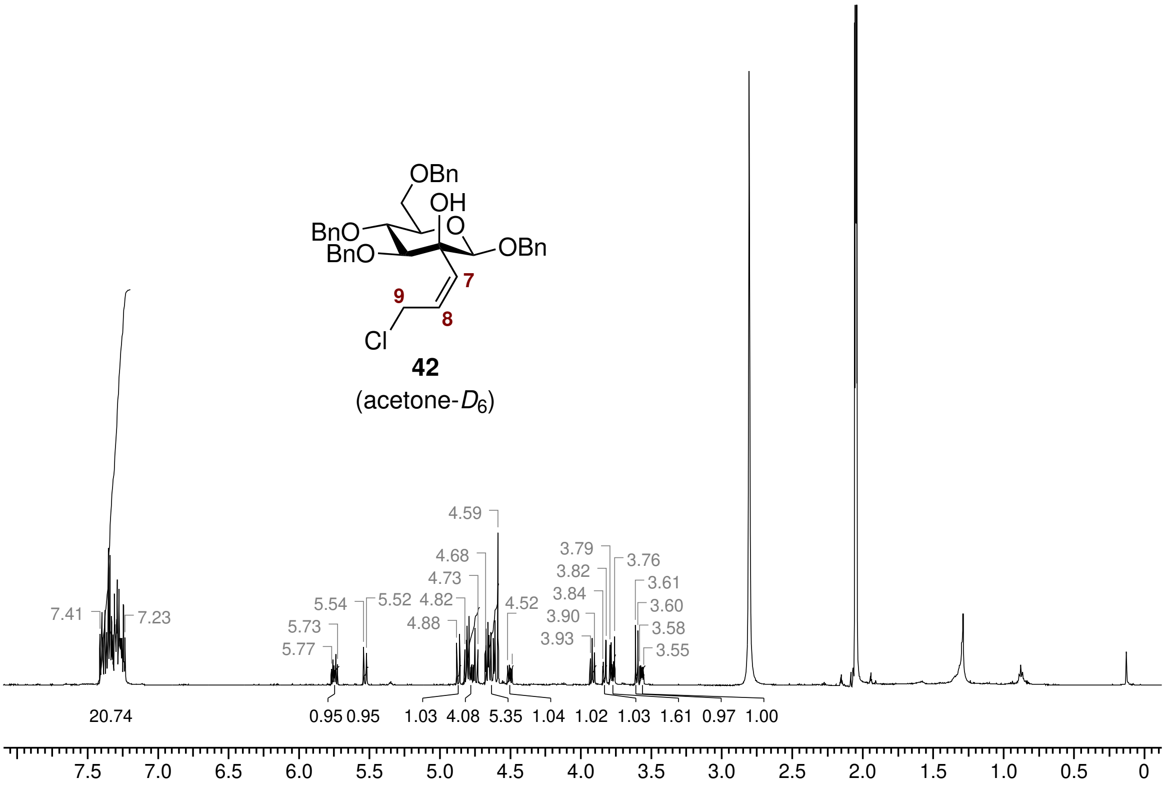
OBn
OH
BnO
BnO
O
OBn
7
8
9
Cl
42
(acetone-D_6)
7.41
7.23
5.77
5.73
5.54
5.52
4.88
4.82
4.73
4.68
4.59
4.52
3.93
3.90
3.84
3.82
3.79
3.76
3.61
3.60
3.58
3.55
20.74
0.95 0.95 1.03 4.08 5.35 1.04 1.02 1.03 1.61 0.97 1.00
7.5 7.0 6.5 6.0 5.5 5.0 4.5 4.0 3.5 3.0 2.5 2.0 1.5 1.0 0.5 0

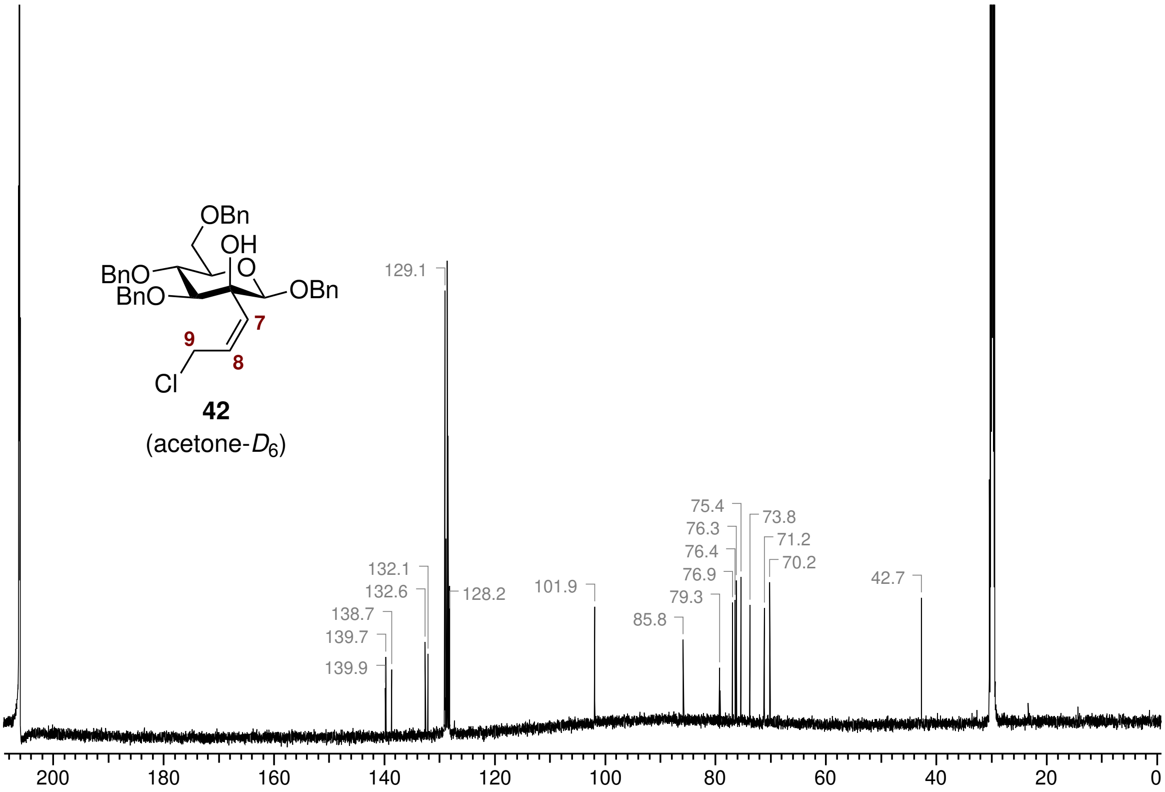
OBn
OH
BnO
BnO
O
OBn
7
8
9
Cl
42
(acetone-D_6)
129.1
128.2
132.1
132.6
138.7
139.7
139.9
101.9
85.8
79.3
76.9
76.4
76.3
75.4
73.8
71.2
70.2
42.7
200 180 160 140 120 100 80 60 40 20 0

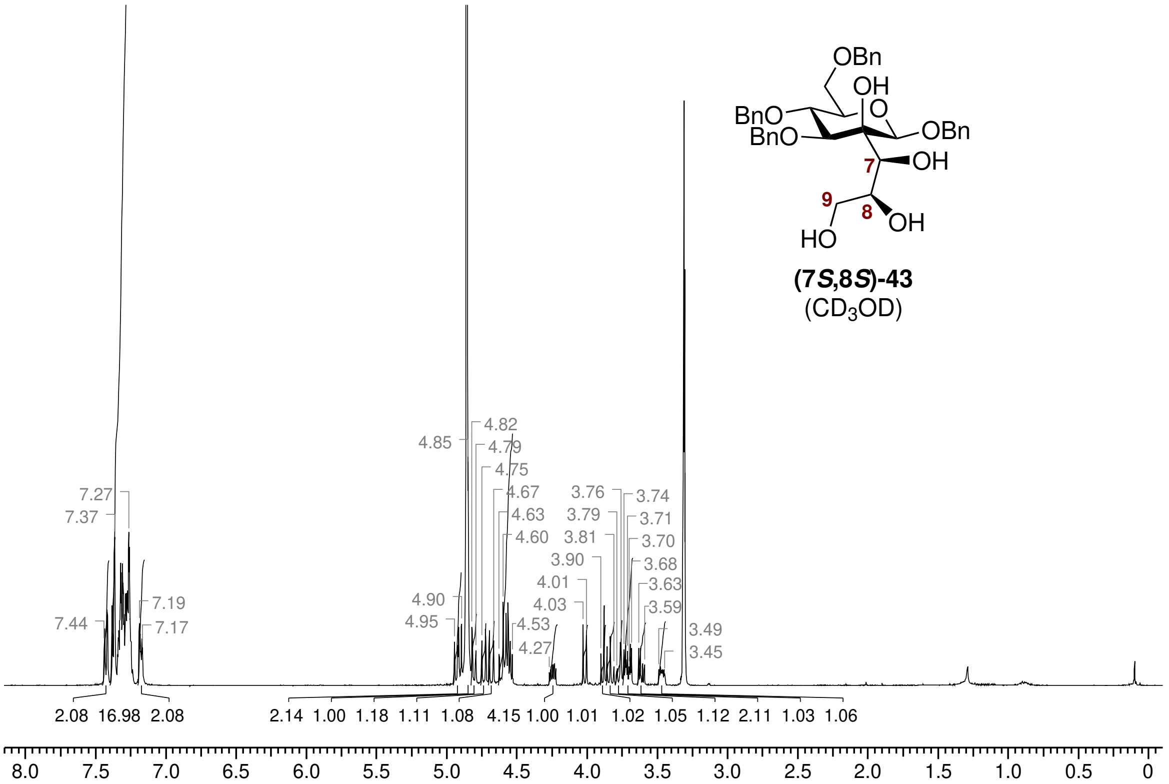
(7*S*,8*S*)-43
(CD$_3$OD)

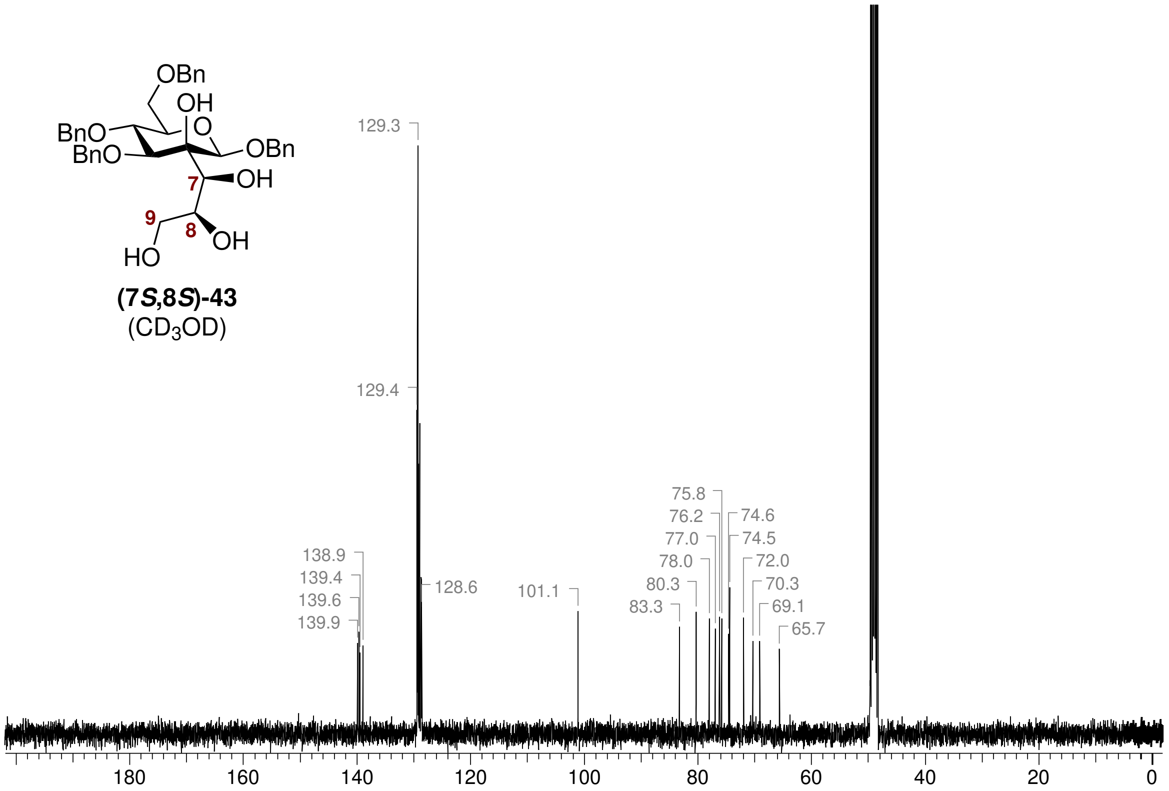
(7*S*,8*S*)-43
(CD$_3$OD)

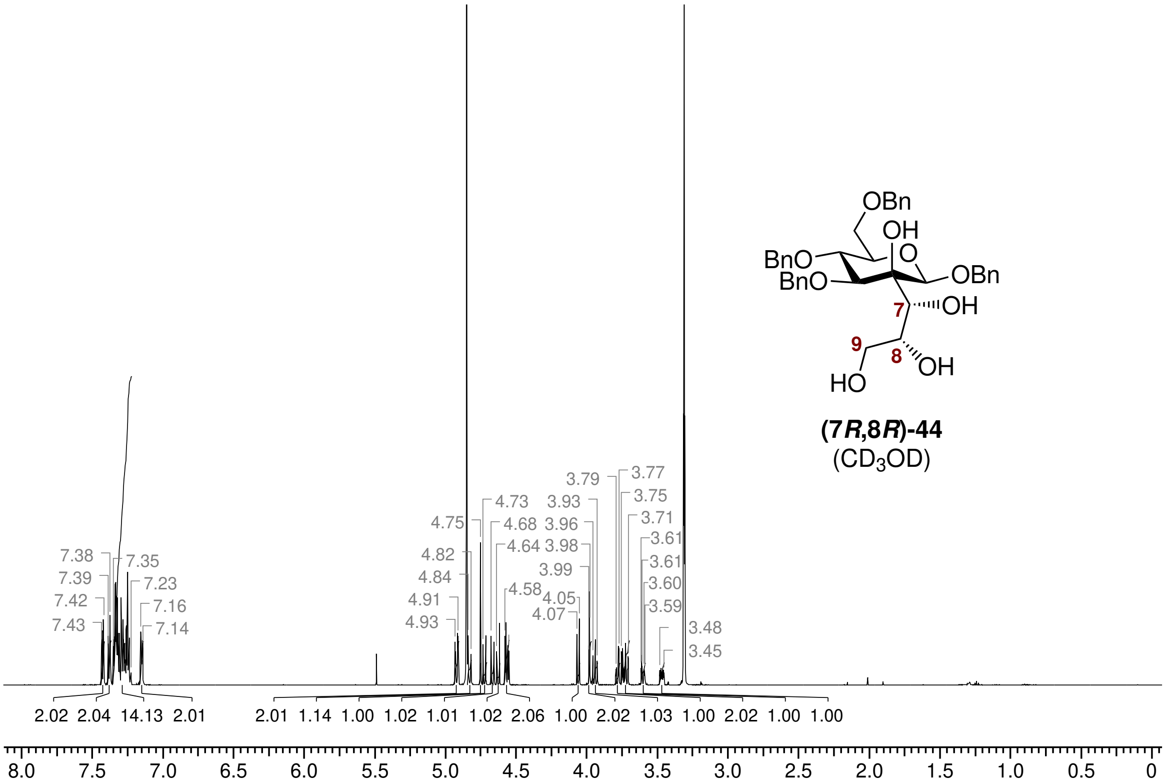

(7*R*,8*R*)-44
(CD_3OD)

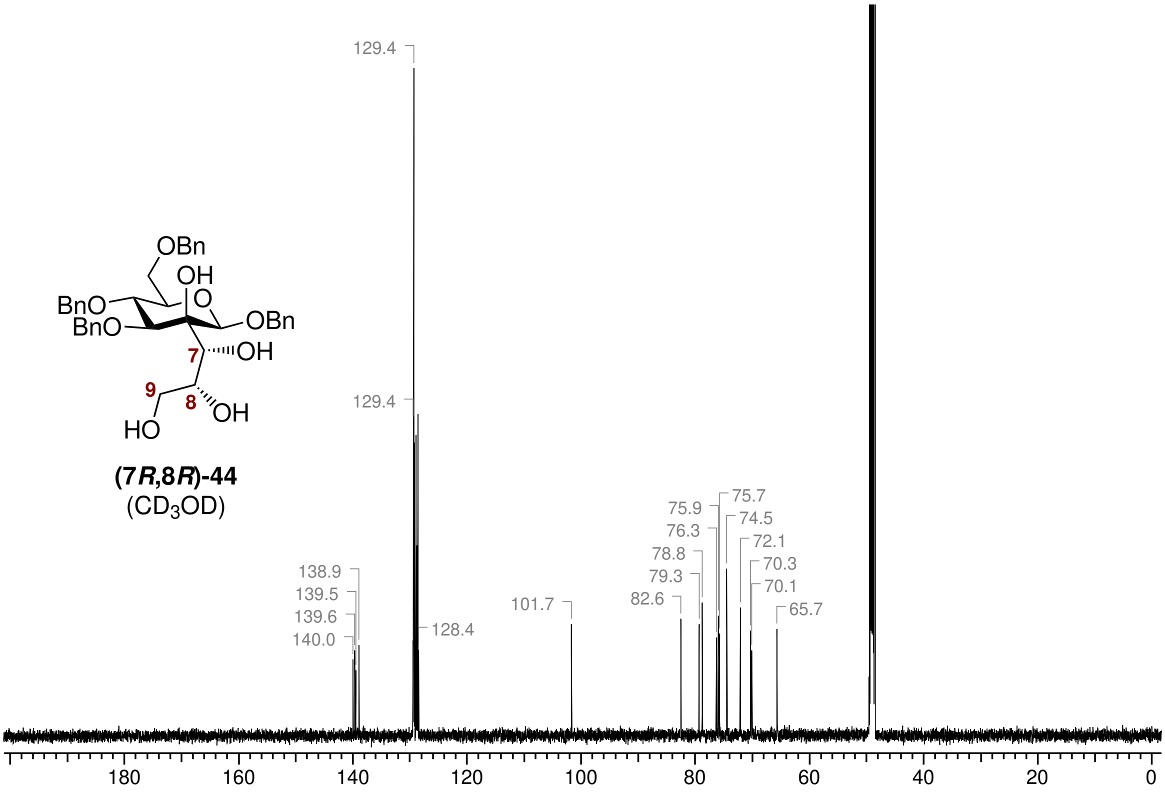

(7*R*,8*R*)-44
(CD_3OD)

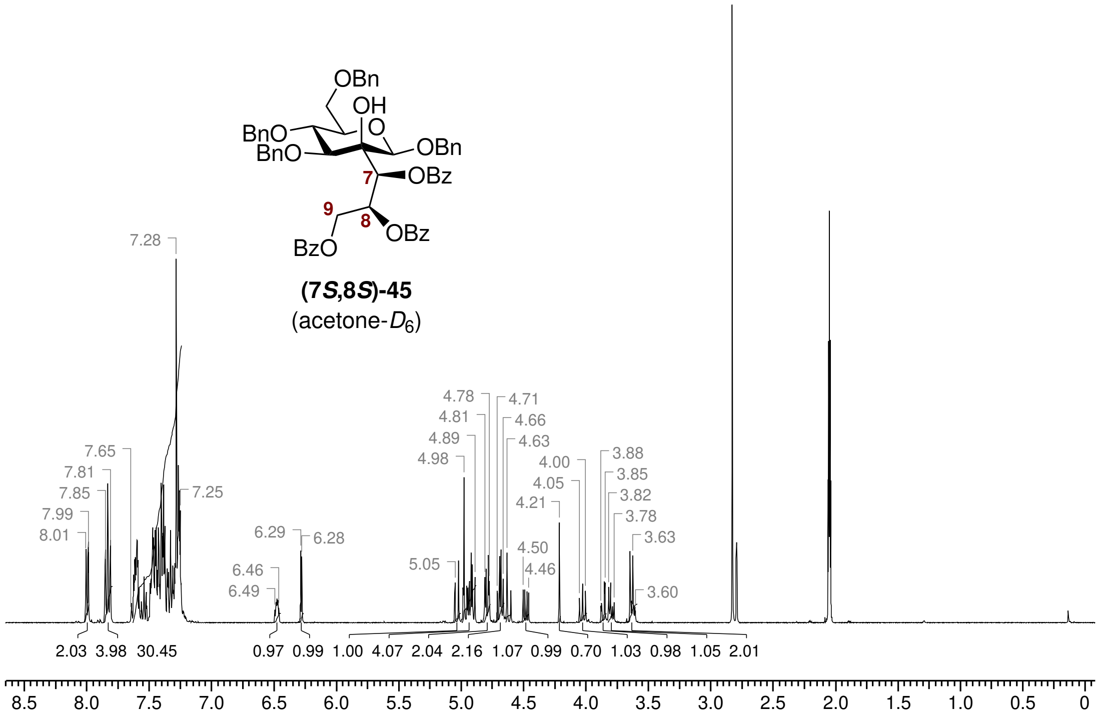
OBn
OH
O
BnO
BnO
OBn
7
OBz
9
8
OBz
BzO
(7S,8S)-45
(acetone-D6)
7.28
7.25
7.65
7.81
7.85
7.99
8.01
6.29
6.28
6.46
6.49
4.78
4.81
4.89
4.98
5.05
4.71
4.66
4.63
4.00
4.05
4.21
4.50
4.46
3.88
3.85
3.82
3.78
3.63
3.60
2.03 3.98 30.45 0.97 0.99 1.00 4.07 2.04 2.16 1.07 0.99 0.70 1.03 0.98 1.05 2.01
8.5 8.0 7.5 7.0 6.5 6.0 5.5 5.0 4.5 4.0 3.5 3.0 2.5 2.0 1.5 1.0 0.5 0

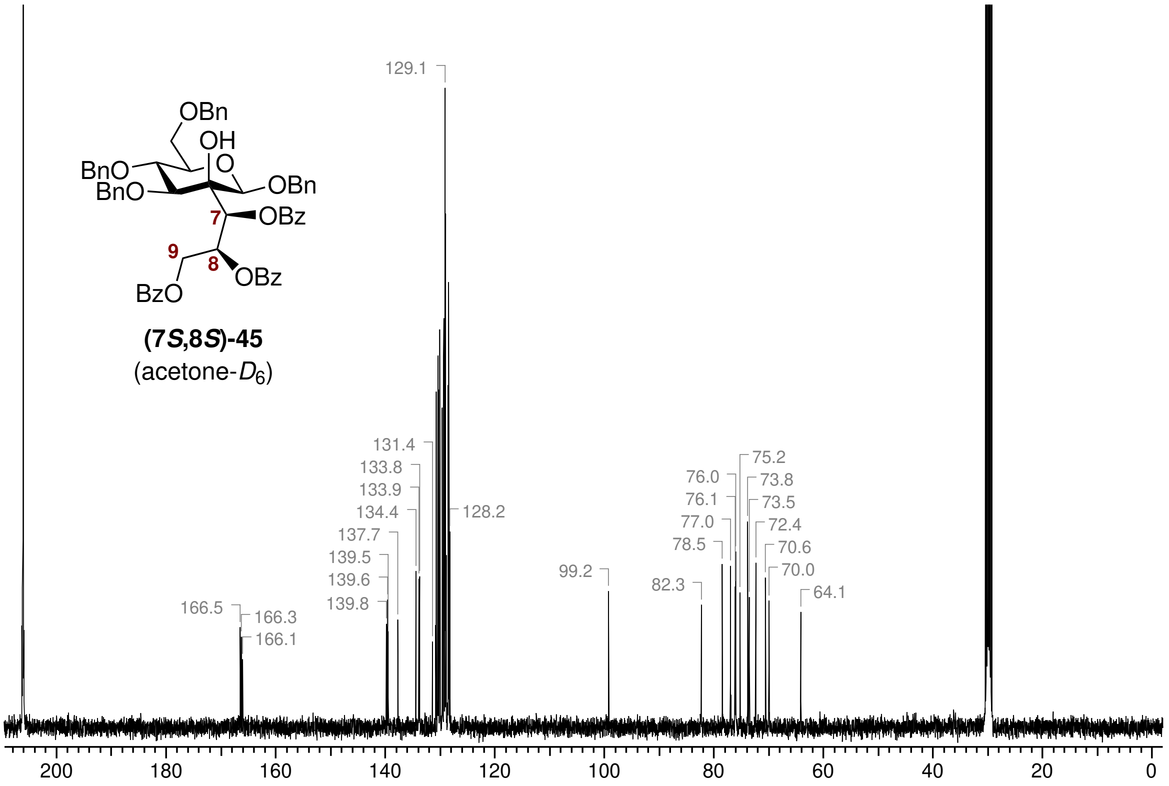
OBn
OH
O
BnO
BnO
OBn
7
OBz
9
8
OBz
BzO
(7S,8S)-45
(acetone-D6)
129.1
131.4
133.8
133.9
134.4
137.7
139.5
139.6
139.8
128.2
166.5
166.3
166.1
99.2
82.3
76.0
76.1
77.0
78.5
75.2
73.8
73.5
72.4
70.6
70.0
64.1
200 180 160 140 120 100 80 60 40 20 0

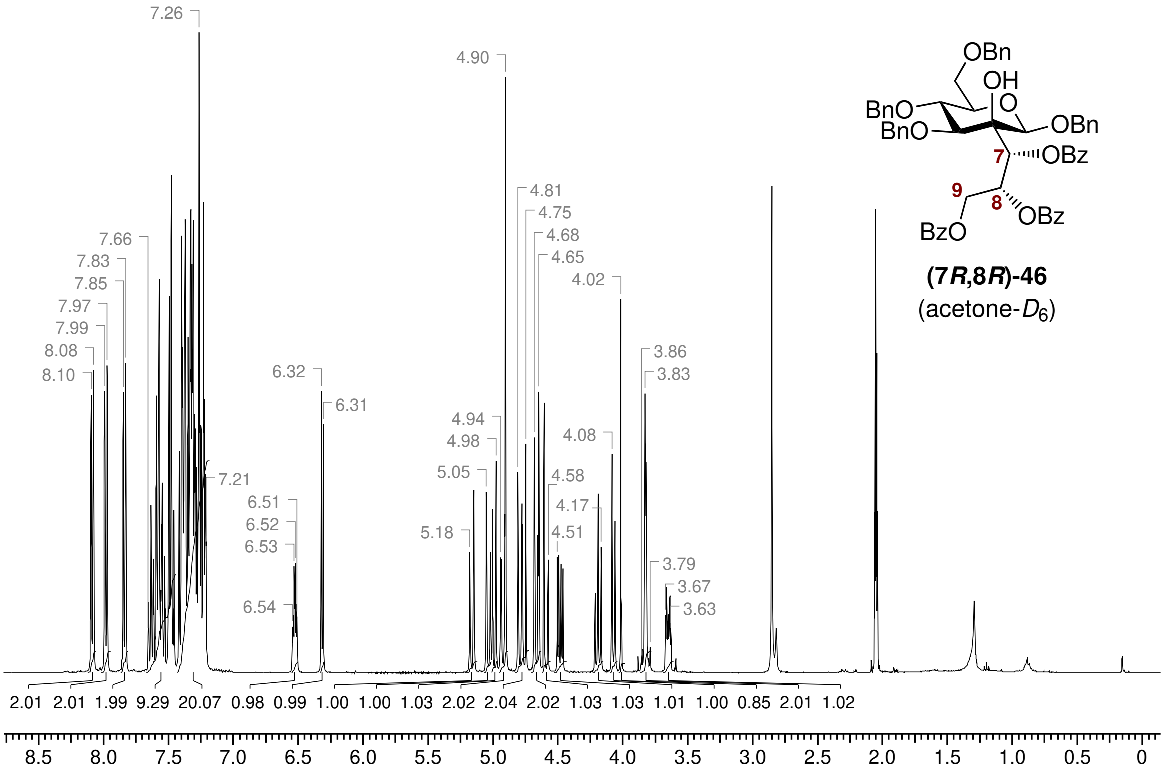
7.26
4.90
7.66
7.83
7.85
7.97
7.99
8.08
8.10
6.32
6.31
7.21
6.51
6.52
6.53
6.54
4.94
4.98
5.05
5.18
4.81
4.75
4.68
4.65
4.02
4.08
4.58
4.17
4.51
3.86
3.83
3.79
3.67
3.63
2.01 2.01 1.99 9.29 20.07 0.98 0.99 1.00 1.00 1.03 2.02 2.04 2.02 1.03 1.03 1.01 1.00 0.85 2.01 1.02
8.5 8.0 7.5 7.0 6.5 6.0 5.5 5.0 4.5 4.0 3.5 3.0 2.5 2.0 1.5 1.0 0.5 0
OBn
OH
O
BnO
BnO
OBn
7
OBz
9
8
OBz
BzO
(7*R*,8*R*)-46
(acetone-D_6)

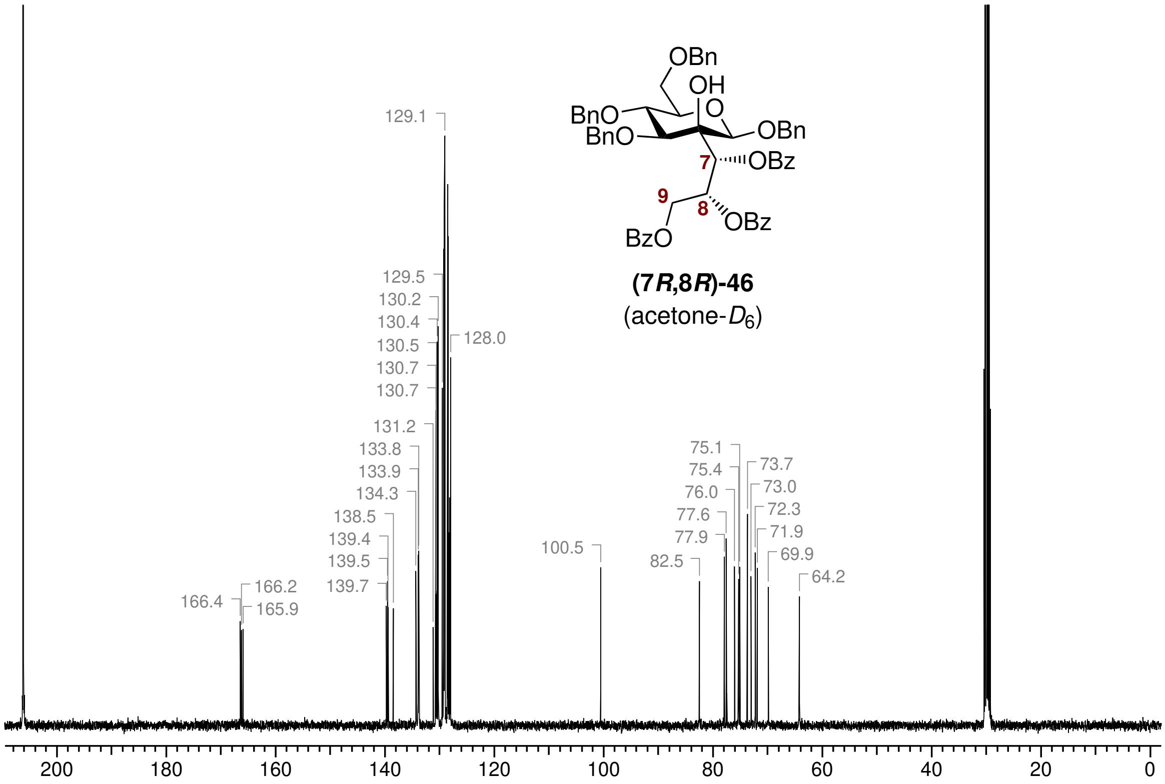
129.1
129.5
130.2
130.4
130.5
130.7
130.7
128.0
131.2
133.8
133.9
134.3
138.5
139.4
139.5
139.7
166.4
166.2
165.9
100.5
75.1
75.4
76.0
77.6
77.9
82.5
73.7
73.0
72.3
71.9
69.9
64.2
200 180 160 140 120 100 80 60 40 20 0
OBn
OH
O
BnO
BnO
OBn
7
OBz
9
8
OBz
BzO
(7*R*,8*R*)-46
(acetone-D_6)

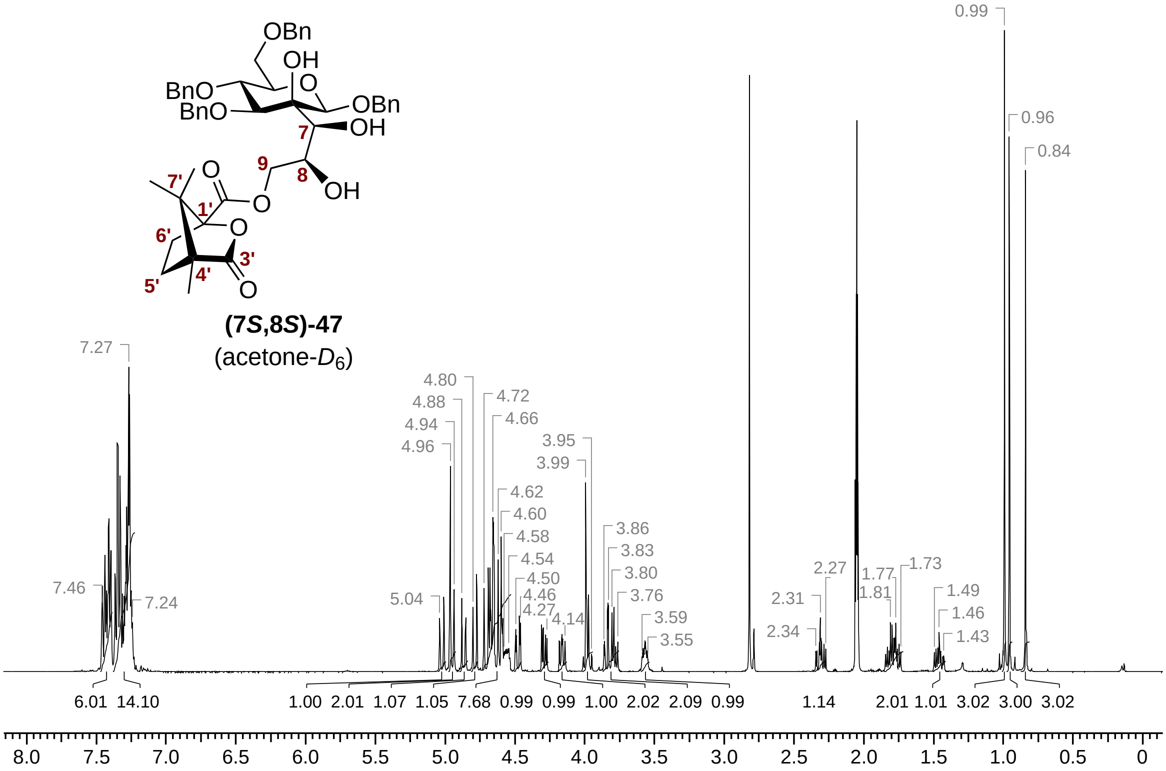

(7*S*,8*S*)-47
(acetone-D_6)

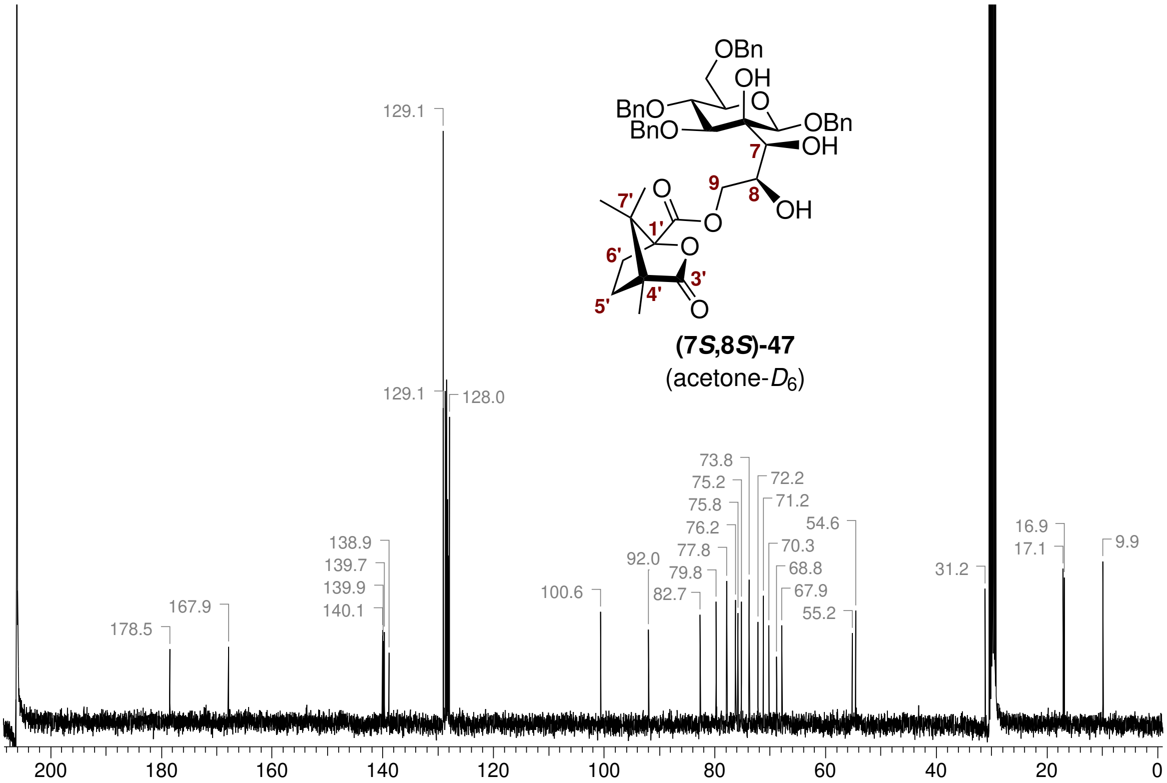

(7*S*,8*S*)-47
(acetone-D_6)

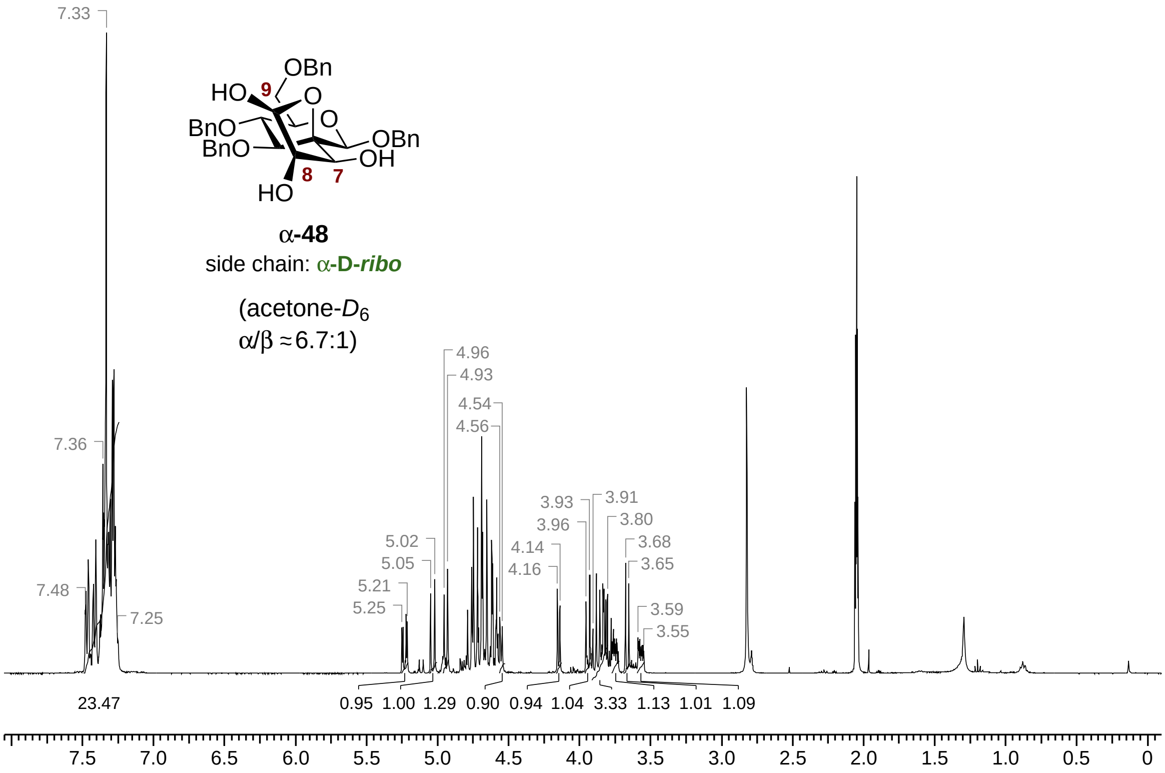
OBn
HO
9
O
O
BnO
BnO
OBn
OH
8
7
HO
α-48
side chain: α-D-ribo
(acetone-D6
α/β ≈ 6.7:1)
7.33
7.36
7.48
7.25
5.02
5.05
5.21
5.25
4.96
4.93
4.54
4.56
3.93
3.96
4.14
4.16
3.91
3.80
3.68
3.65
3.59
3.55
23.47
0.95
1.00
1.29
0.90
0.94
1.04
3.33
1.13
1.01
1.09
7.5
7.0
6.5
6.0
5.5
5.0
4.5
4.0
3.5
3.0
2.5
2.0
1.5
1.0
0.5
0

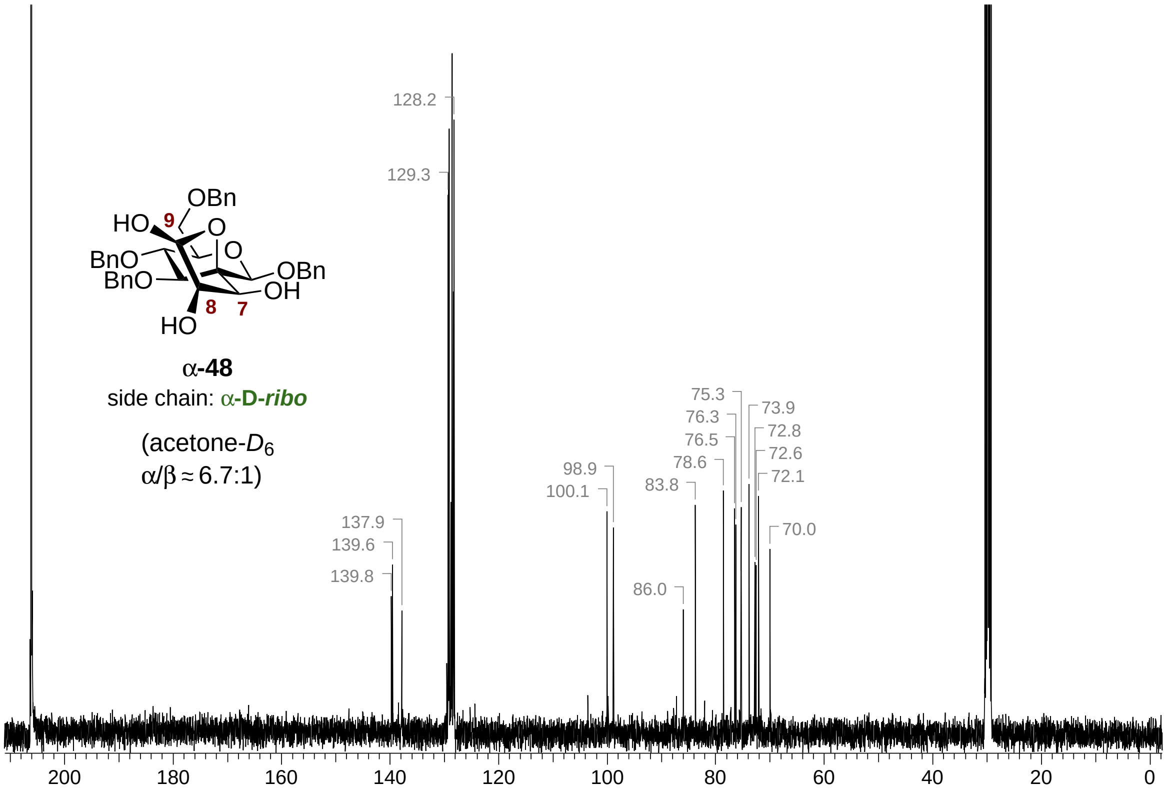
OBn
HO
9
O
O
BnO
BnO
OBn
OH
8
7
HO
α-48
side chain: α-D-ribo
(acetone-D6
α/β ≈ 6.7:1)
128.2
129.3
137.9
139.6
139.8
98.9
100.1
83.8
86.0
75.3
76.3
76.5
78.6
73.9
72.8
72.6
72.1
70.0
200
180
160
140
120
100
80
60
40
20
0

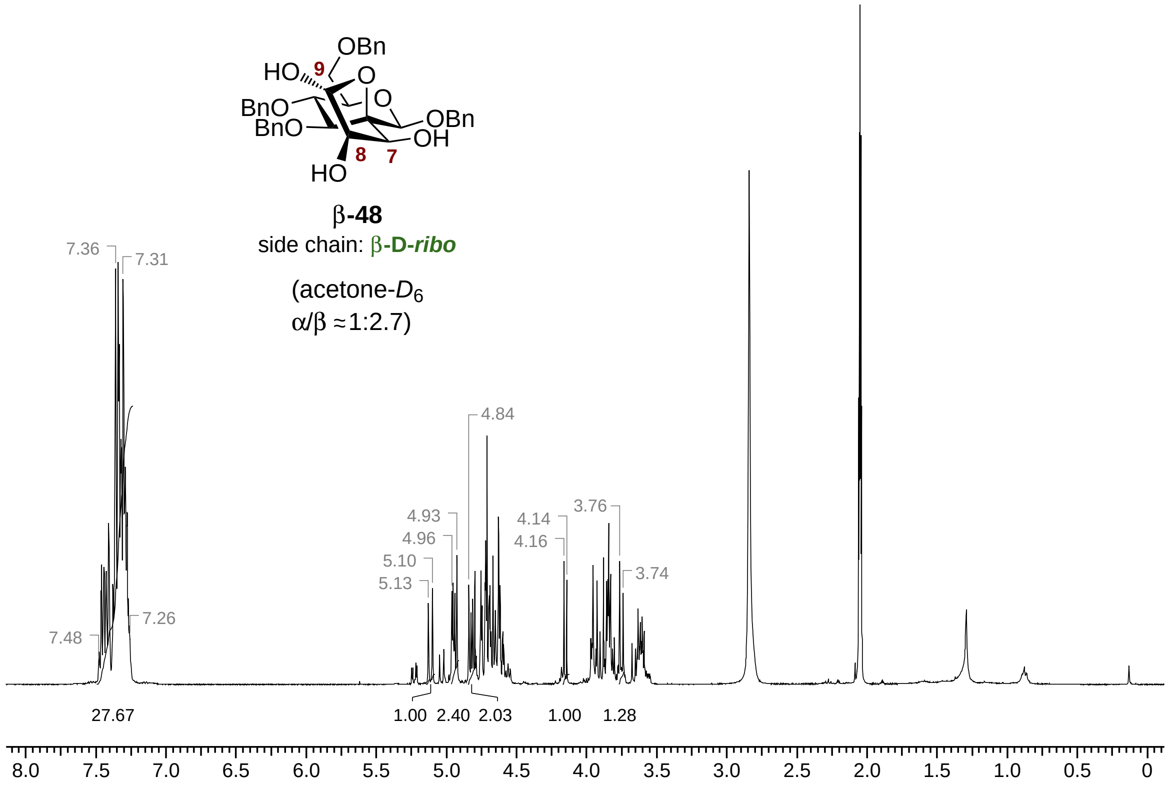
OBn
HO
9
O
O
BnO
BnO
OBn
OH
8
7
HO
β-48
side chain: β-D-ribo
(acetone-D6
α/β ≈1:2.7)
7.36
7.31
7.48
7.26
4.84
4.93
4.96
5.10
5.13
4.14
4.16
3.76
3.74
27.67
1.00
2.40
2.03
1.00
1.28
8.0
7.5
7.0
6.5
6.0
5.5
5.0
4.5
4.0
3.5
3.0
2.5
2.0
1.5
1.0
0.5
0

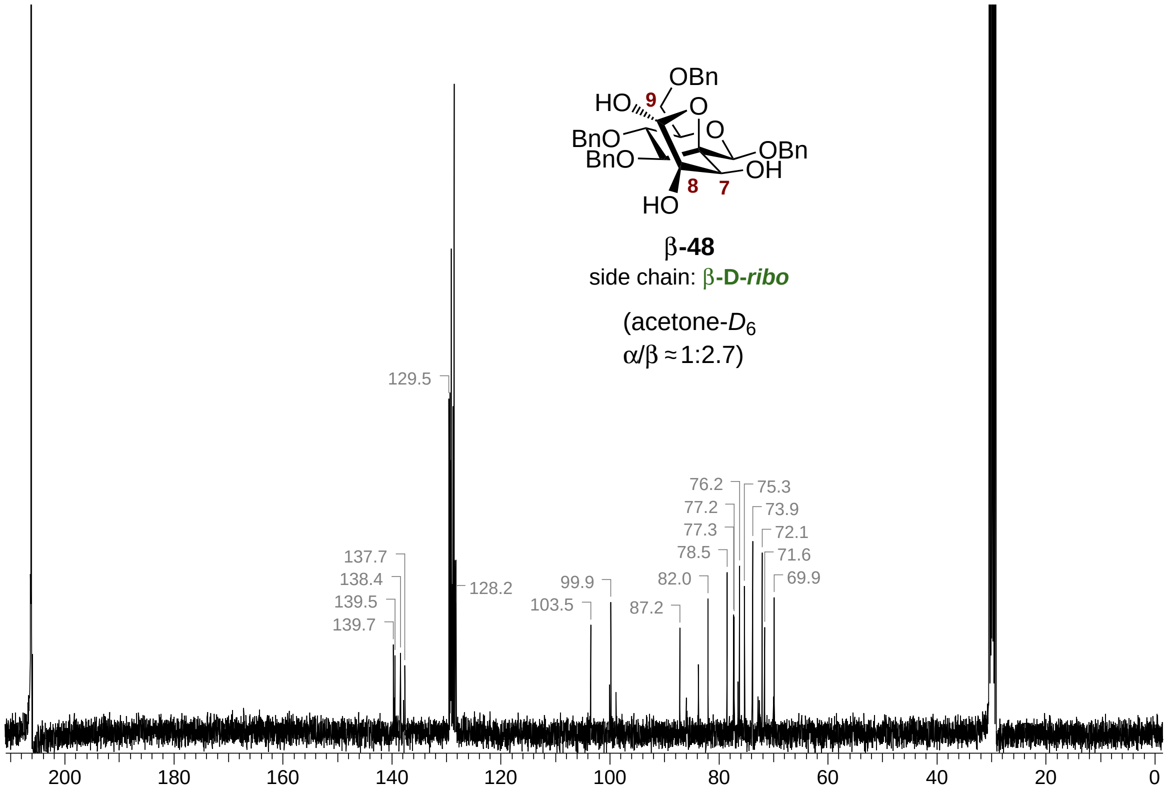
OBn
HO
9
O
O
BnO
BnO
OBn
OH
8
7
HO
β-48
side chain: β-D-ribo
(acetone-D6
α/β ≈1:2.7)
129.5
128.2
137.7
138.4
139.5
139.7
99.9
103.5
87.2
82.0
78.5
77.3
77.2
76.2
75.3
73.9
72.1
71.6
69.9
200
180
160
140
120
100
80
60
40
20
0

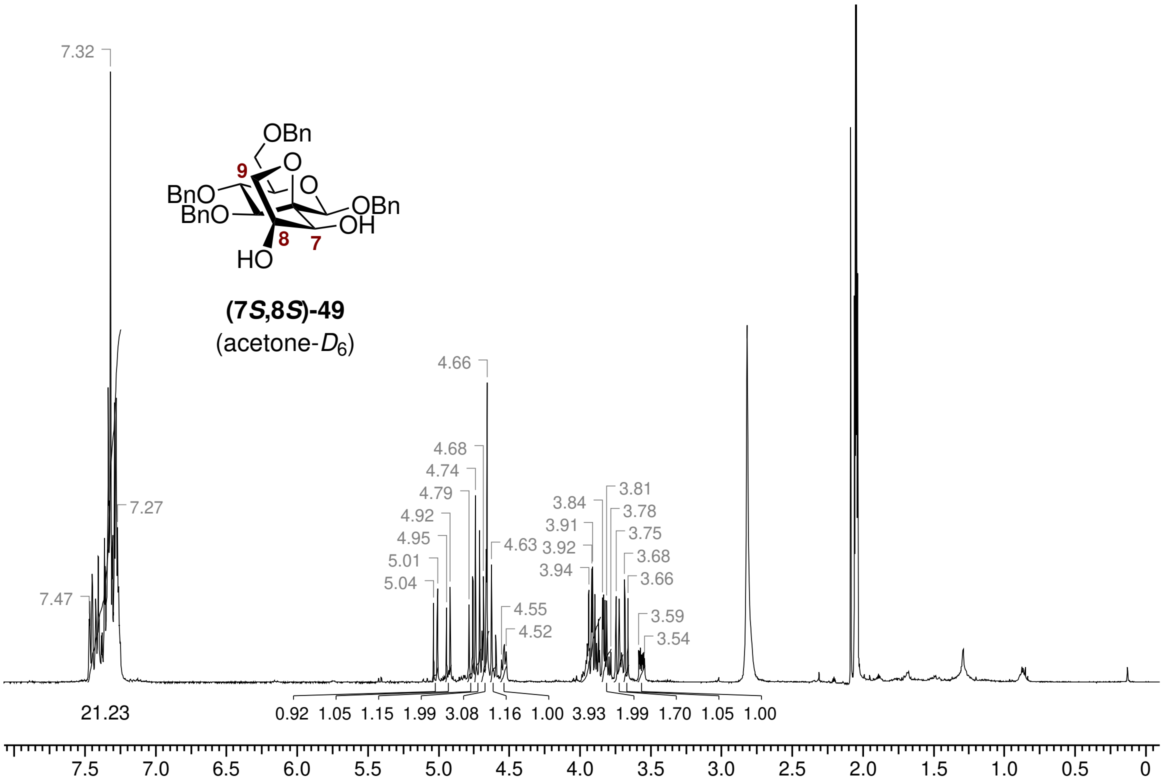
OBn
9
BnO
BnO
O
O
OBn
OH
8
7
HO
(7S,8S)-49
(acetone-D6)
7.32
7.27
7.47
4.66
4.68
4.74
4.79
4.92
4.95
5.01
5.04
4.63
4.55
4.52
3.84
3.91
3.92
3.94
3.81
3.78
3.75
3.68
3.66
3.59
3.54
21.23
0.92 1.05 1.15 1.99 3.08 1.16 1.00 3.93 1.99 1.70 1.05 1.00
7.5 7.0 6.5 6.0 5.5 5.0 4.5 4.0 3.5 3.0 2.5 2.0 1.5 1.0 0.5 0

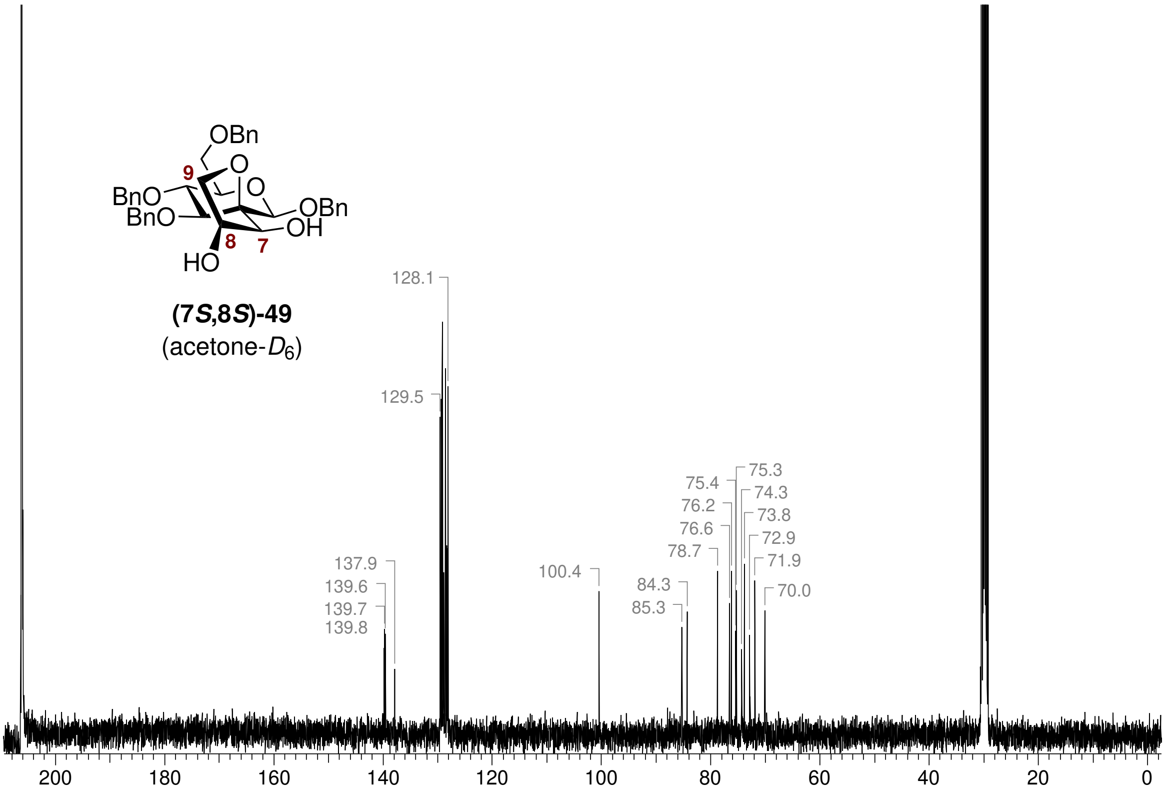
OBn
9
BnO
BnO
O
O
OBn
OH
8
7
HO
(7S,8S)-49
(acetone-D6)
128.1
129.5
137.9
139.6
139.7
139.8
100.4
84.3
85.3
78.7
76.6
76.2
75.4
75.3
74.3
73.8
72.9
71.9
70.0
200 180 160 140 120 100 80 60 40 20 0

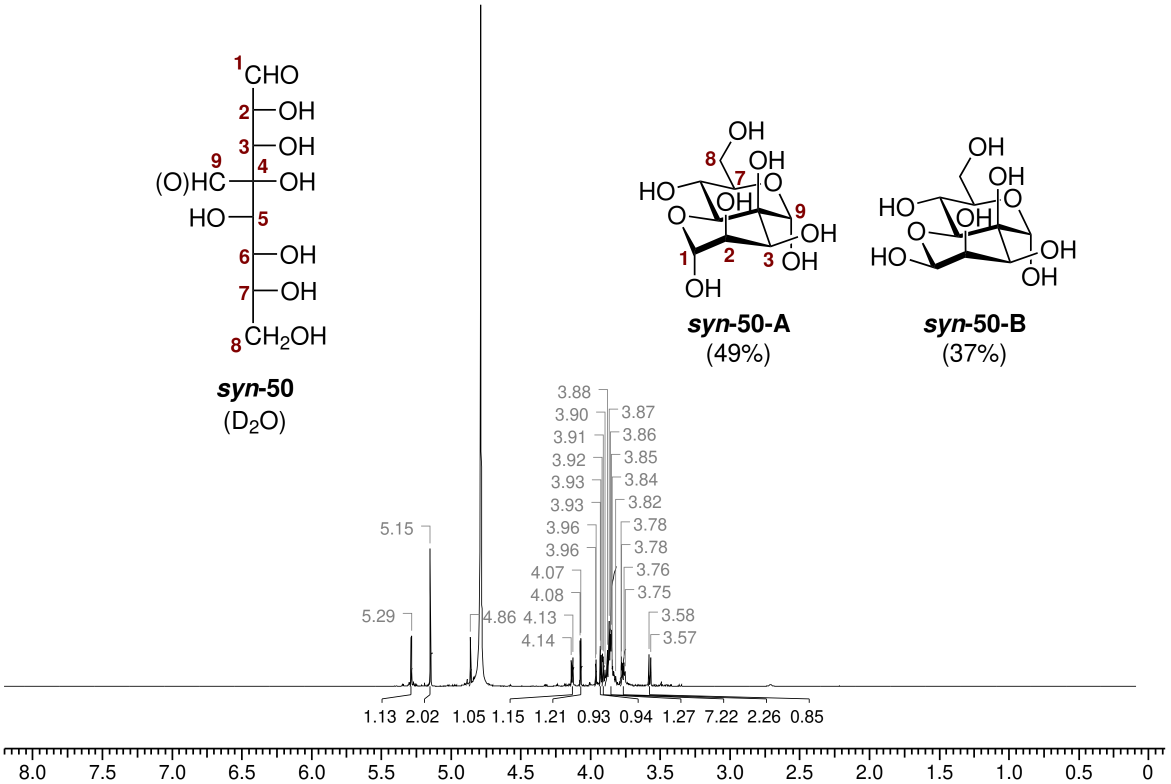
1 CHO
2 OH
3 OH
9 (O)HC 4 OH
HO 5
6 OH
7 OH
8 CH2OH
syn-50
(D2O)
syn-50-A
(49%)
syn-50-B
(37%)
5.29
5.15
4.86
4.13
4.14
4.07
4.08
3.96
3.96
3.93
3.93
3.92
3.91
3.90
3.88
3.87
3.86
3.85
3.84
3.82
3.78
3.78
3.76
3.75
3.58
3.57
1.13 2.02 1.05 1.15 1.21 0.93 0.94 1.27 7.22 2.26 0.85
8.0 7.5 7.0 6.5 6.0 5.5 5.0 4.5 4.0 3.5 3.0 2.5 2.0 1.5 1.0 0.5 0

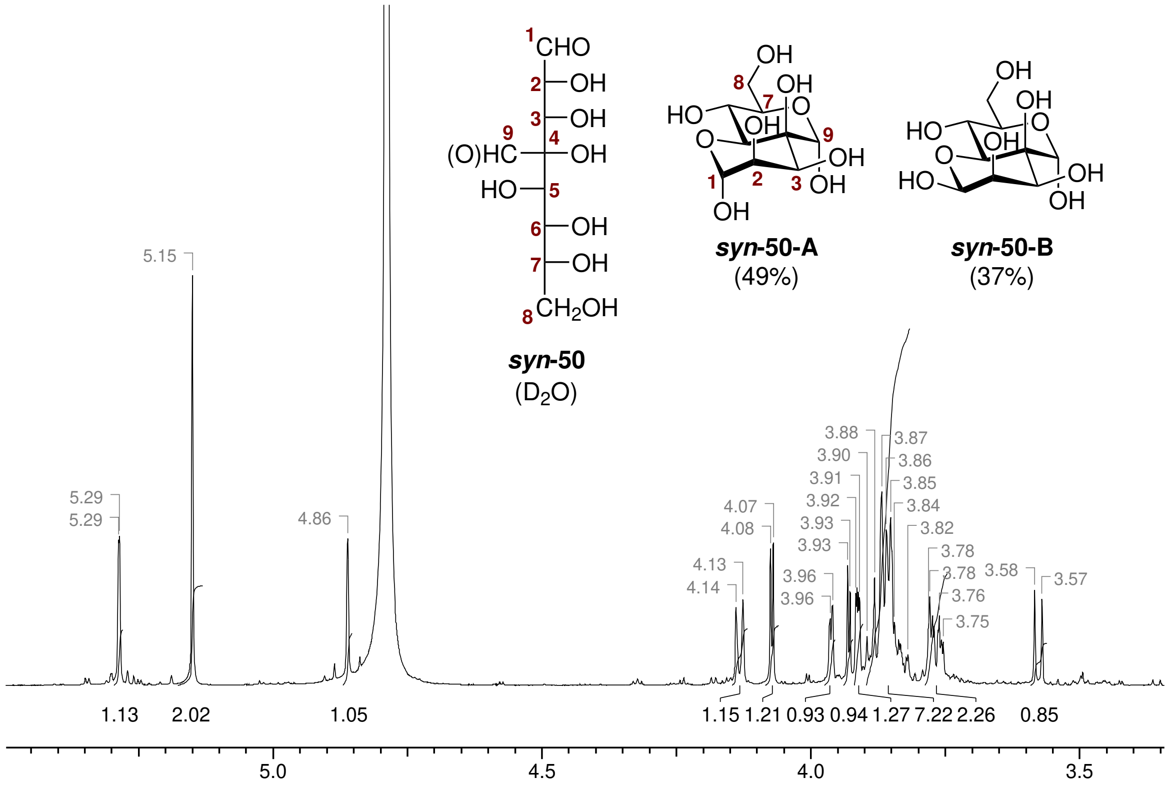
1 CHO
2 OH
3 OH
9 (O)HC 4 OH
HO 5
6 OH
7 OH
8 CH2OH
syn-50
(D2O)
syn-50-A
(49%)
syn-50-B
(37%)
5.29
5.29
5.15
4.86
4.13
4.14
4.07
4.08
3.96
3.96
3.93
3.93
3.92
3.91
3.90
3.88
3.87
3.86
3.85
3.84
3.82
3.78
3.78
3.76
3.75
3.58
3.57
1.13 2.02 1.05 1.15 1.21 0.93 0.94 1.27 7.22 2.26 0.85
5.0 4.5 4.0 3.5

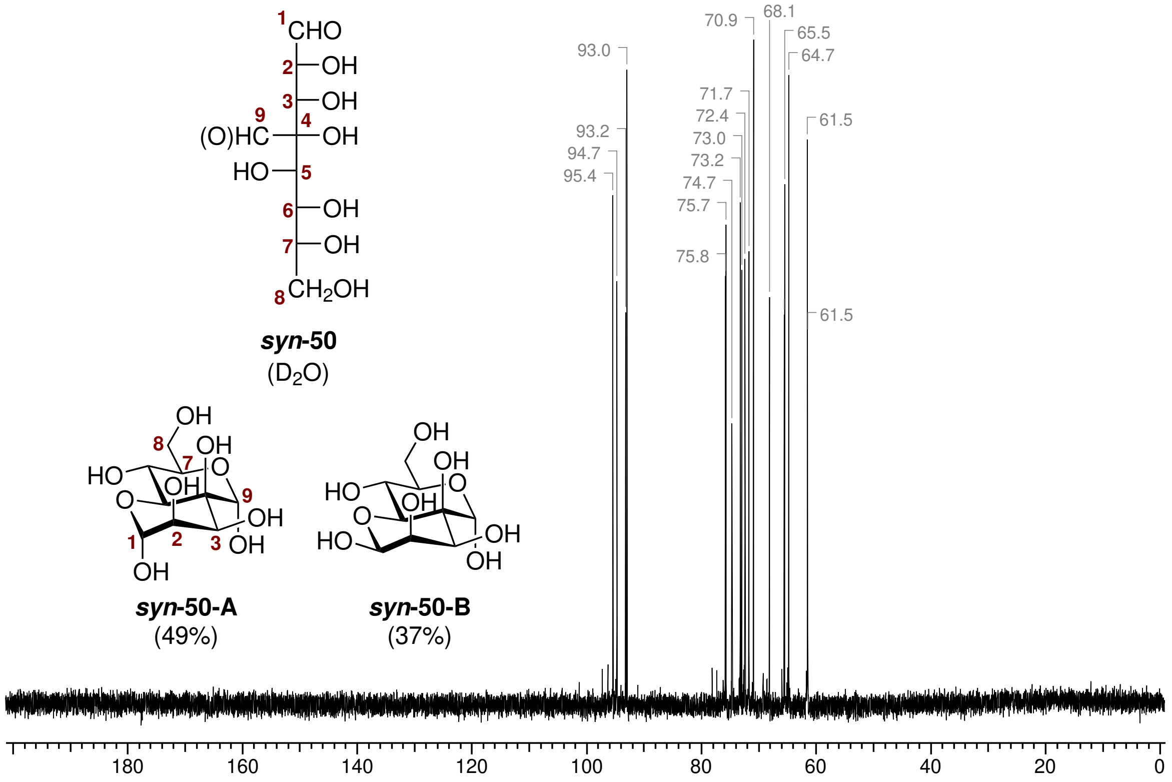
1 CHO
2 OH
3 OH
9 (O)HC
4 OH
HO 5
6 OH
7 OH
8 CH2OH
syn-50
(D2O)
syn-50-A
(49%)
syn-50-B
(37%)
93.0
93.2
94.7
95.4
70.9
68.1
65.5
64.7
71.7
72.4
73.0
73.2
74.7
75.7
75.8
61.5
61.5
180
160
140
120
100
80
60
40
20
0

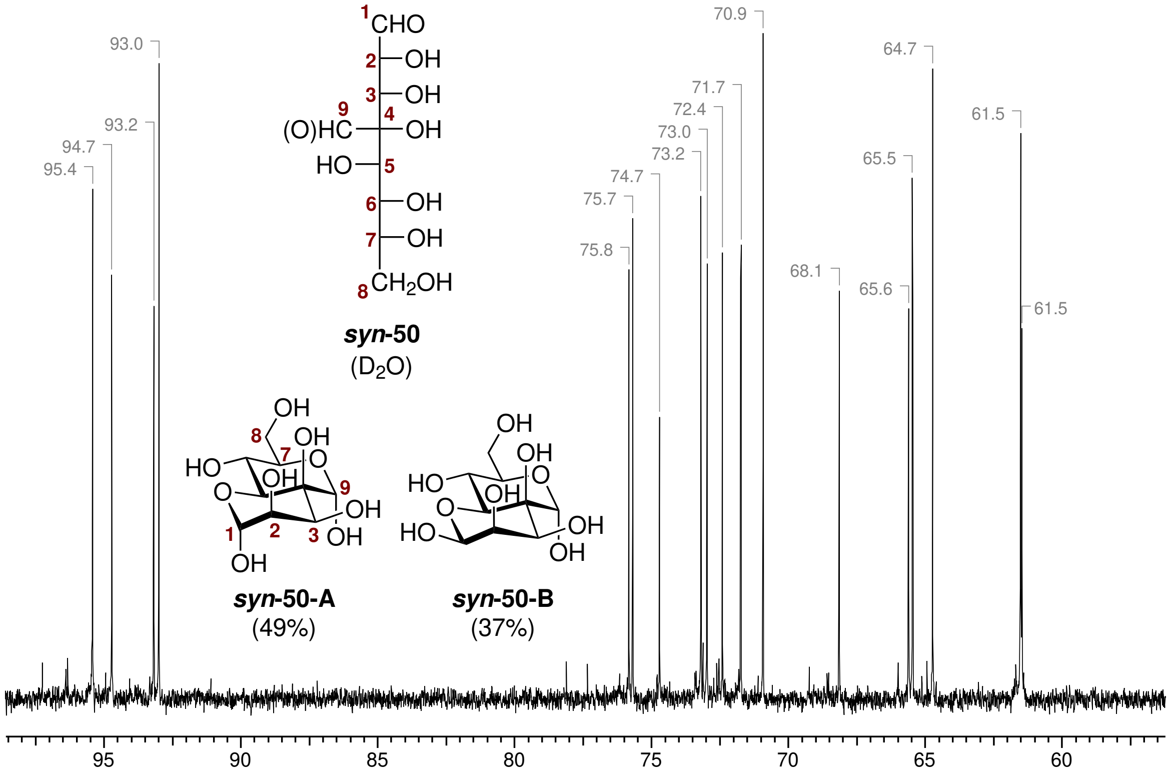
1 CHO
2 OH
3 OH
9 (O)HC
4 OH
HO 5
6 OH
7 OH
8 CH2OH
syn-50
(D2O)
syn-50-A
(49%)
syn-50-B
(37%)
93.0
93.2
94.7
95.4
70.9
64.7
61.5
71.7
72.4
73.0
73.2
74.7
75.7
75.8
65.5
68.1
65.6
61.5
95
90
85
80
75
70
65
60

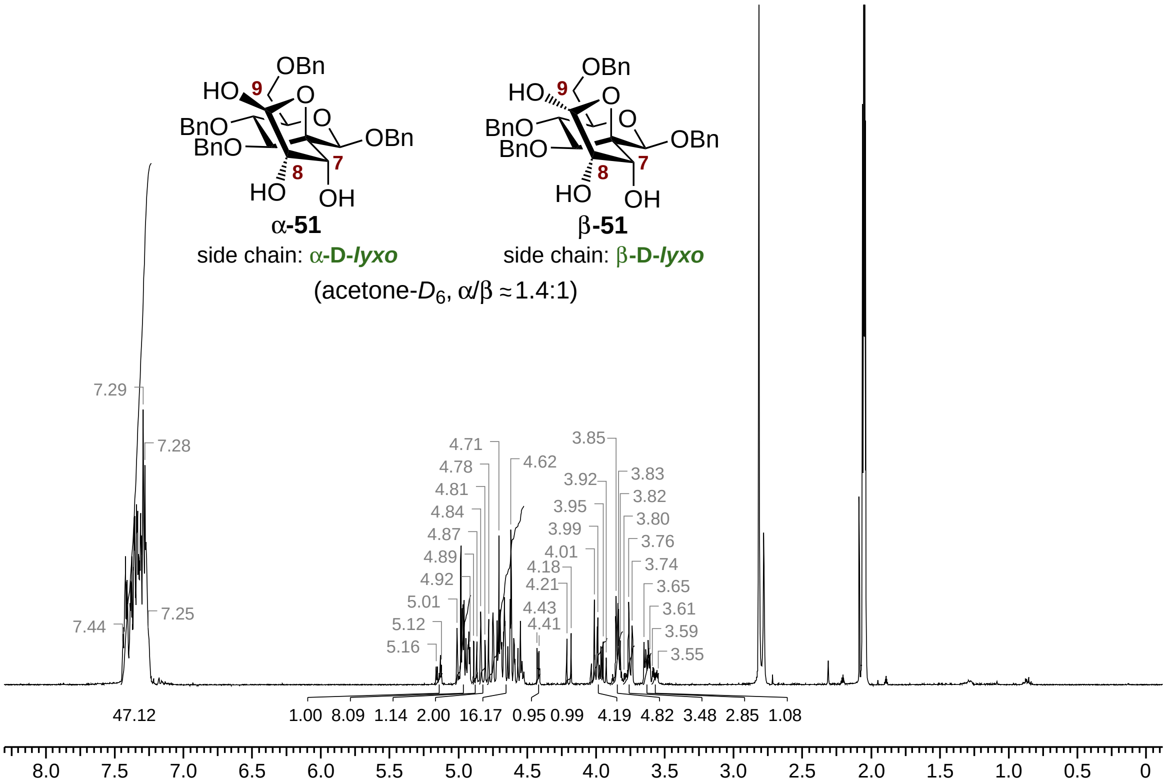
OBn
HO
9
O
O
BnO
BnO
OBn
8
7
HO
OH
α-51
side chain: α-D-*lyxo*
β-51
side chain: β-D-*lyxo*
(acetone-D_6, α/β ≈1.4:1)
7.29
7.28
7.25
7.44
4.71
4.78
4.81
4.84
4.87
4.89
4.92
5.01
5.12
5.16
4.62
4.18
4.21
4.43
4.41
3.85
3.92
3.95
3.99
4.01
3.83
3.82
3.80
3.76
3.74
3.65
3.61
3.59
3.55
47.12
1.00 8.09 1.14 2.00 16.17 0.95 0.99 4.19 4.82 3.48 2.85 1.08
8.0 7.5 7.0 6.5 6.0 5.5 5.0 4.5 4.0 3.5 3.0 2.5 2.0 1.5 1.0 0.5 0

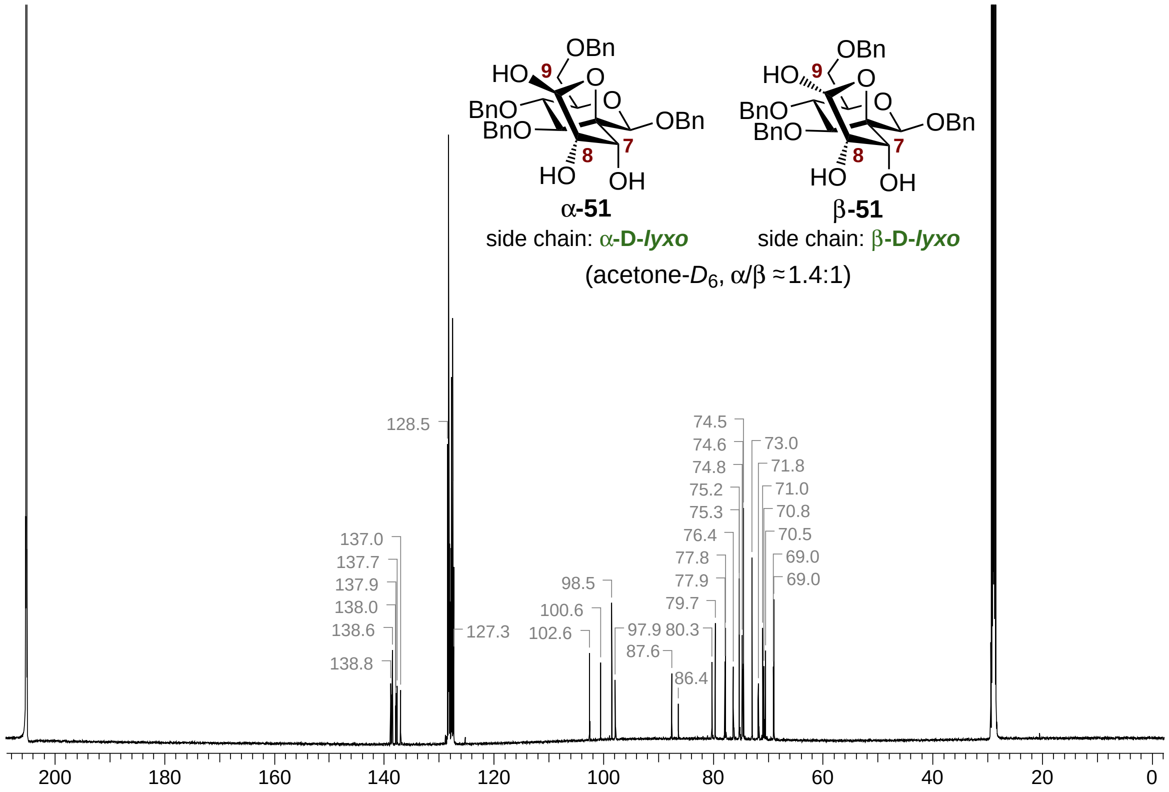
OBn
HO
9
O
O
BnO
BnO
OBn
8
7
HO
OH
α-51
side chain: α-D-*lyxo*
β-51
side chain: β-D-*lyxo*
(acetone-D_6, α/β ≈1.4:1)
128.5
137.0
137.7
137.9
138.0
138.6
138.8
127.3
98.5
100.6
102.6
97.9
80.3
87.6
86.4
79.7
77.9
77.8
76.4
75.3
75.2
74.8
74.6
74.5
73.0
71.8
71.0
70.8
70.5
69.0
69.0
200 180 160 140 120 100 80 60 40 20 0

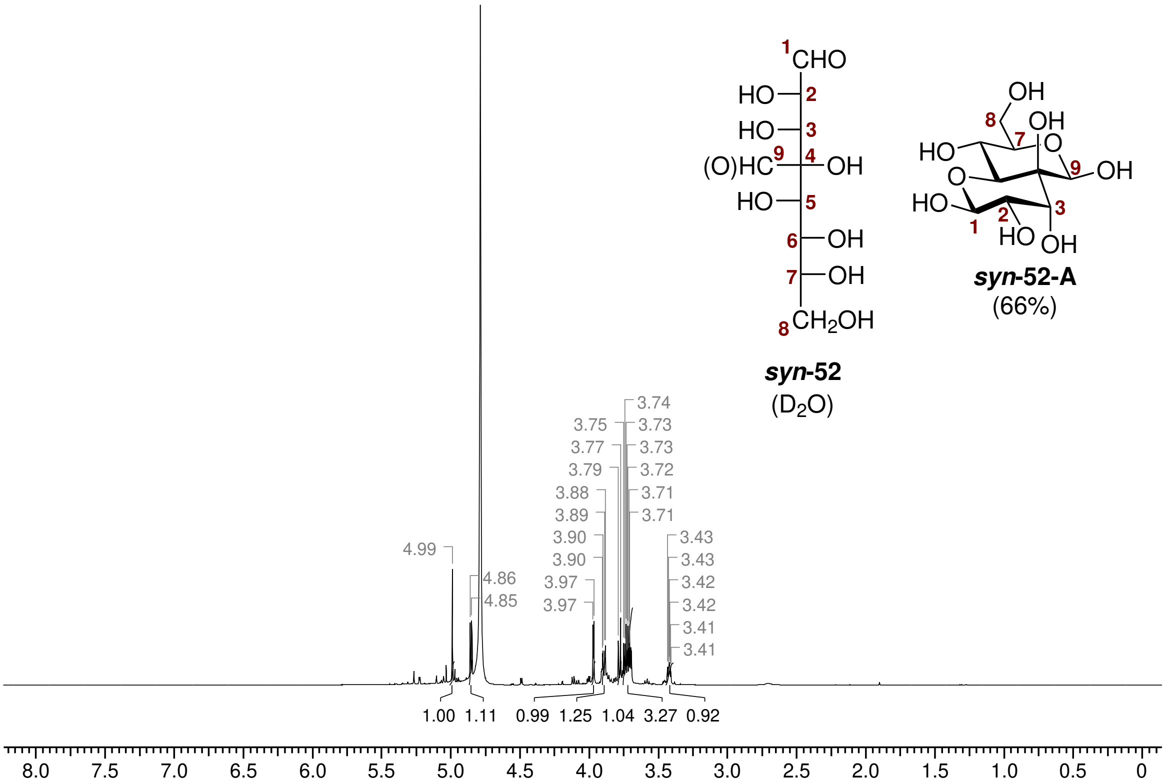

1 CHO
HO 2
HO 3
(O)HC 9 4 OH
HO 5
6 OH
7 OH
8 CH2OH
syn-52
(D2O)
syn-52-A
(66%)
4.99
4.86
4.85
3.97
3.97
3.90
3.90
3.89
3.88
3.79
3.77
3.75
3.74
3.73
3.73
3.72
3.71
3.71
3.43
3.43
3.42
3.42
3.41
3.41
1.00 1.11 0.99 1.25 1.04 3.27 0.92
8.0 7.5 7.0 6.5 6.0 5.5 5.0 4.5 4.0 3.5 3.0 2.5 2.0 1.5 1.0 0.5 0

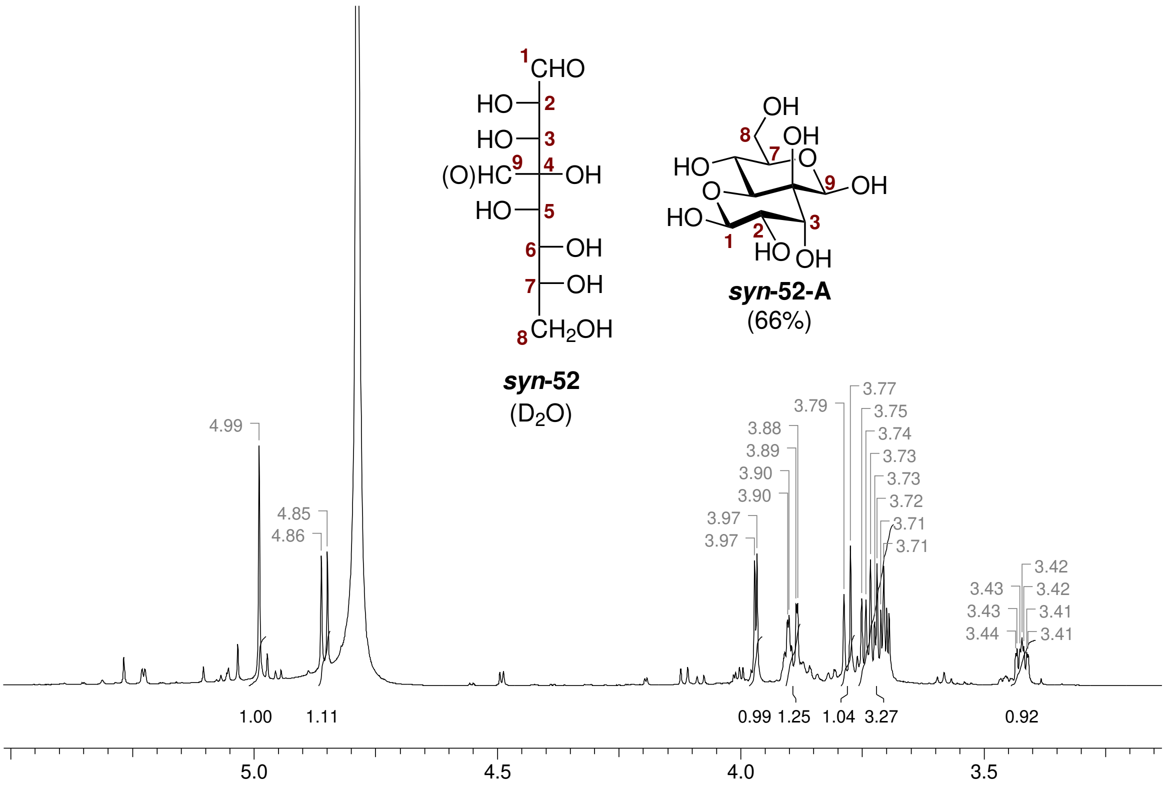

1 CHO
HO 2
HO 3
(O)HC 9 4 OH
HO 5
6 OH
7 OH
8 CH2OH
syn-52
(D2O)
syn-52-A
(66%)
4.99
4.85
4.86
3.88
3.89
3.90
3.90
3.97
3.97
3.79
3.77
3.75
3.74
3.73
3.73
3.72
3.71
3.71
3.43
3.43
3.44
3.42
3.42
3.41
3.41
1.00 1.11 0.99 1.25 1.04 3.27 0.92
5.0 4.5 4.0 3.5

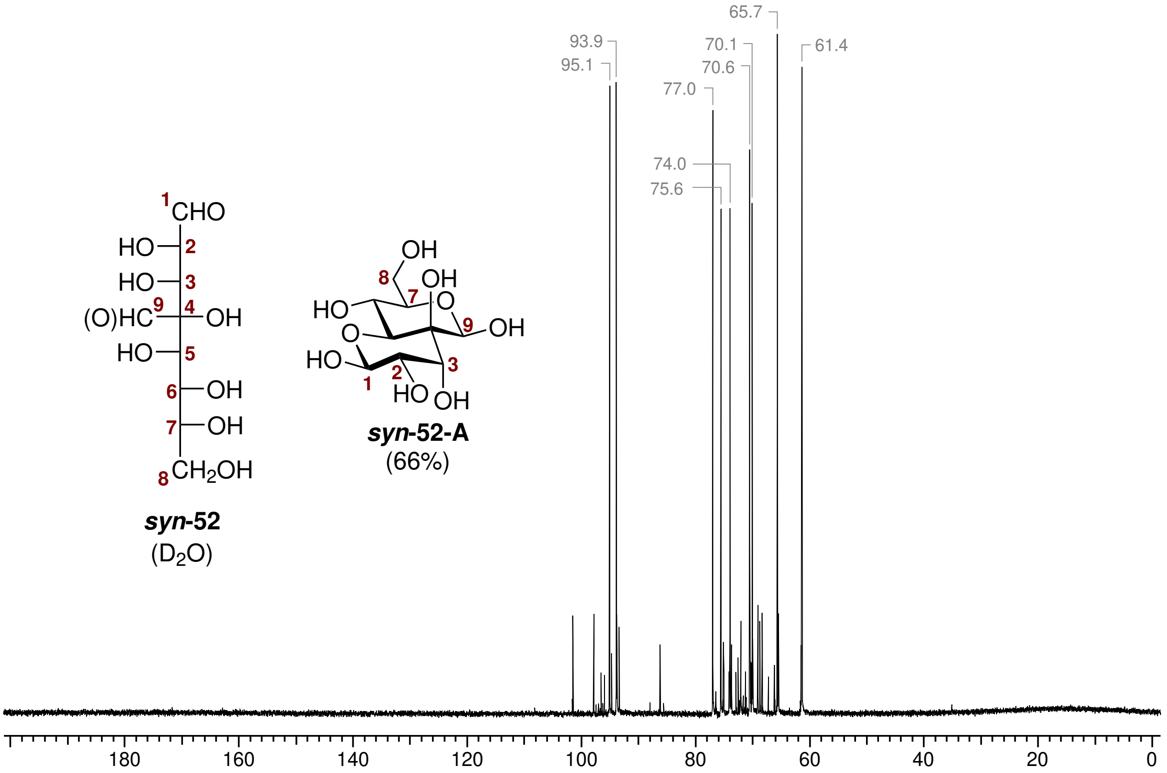
93.9
95.1
65.7
70.1
70.6
77.0
61.4
74.0
75.6
1 CHO
HO 2
HO 3
(O)HC 9 4 OH
HO 5
6 OH
7 OH
8 CH2OH
syn-52
(D2O)
OH
8
7
OH
O
HO
9
OH
O
HO
1
2
3
HO
OH
syn-52-A
(66%)
180
160
140
120
100
80
60
40
20
0

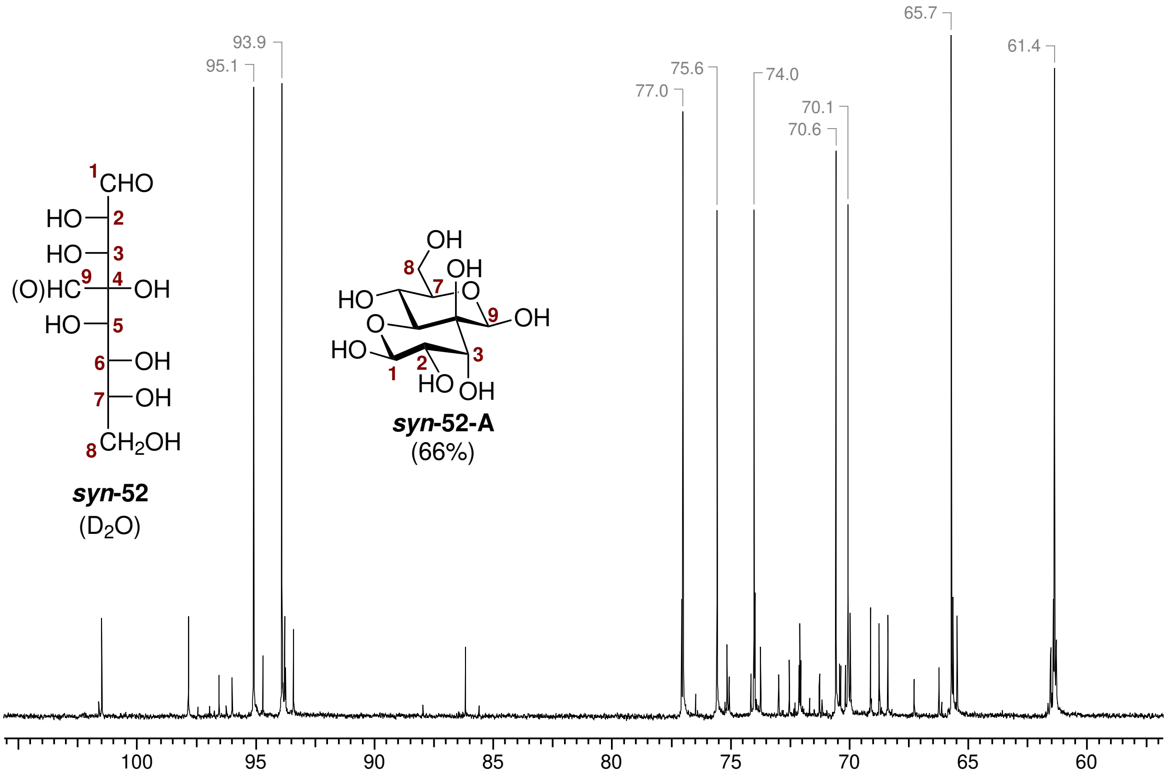
93.9
95.1
75.6
77.0
74.0
65.7
61.4
70.1
70.6
1 CHO
HO 2
HO 3
(O)HC 9 4 OH
HO 5
6 OH
7 OH
8 CH2OH
syn-52
(D2O)
OH
8
7
OH
O
HO
9
OH
O
HO
1
2
3
HO
OH
syn-52-A
(66%)
100
95
90
85
80
75
70
65
60

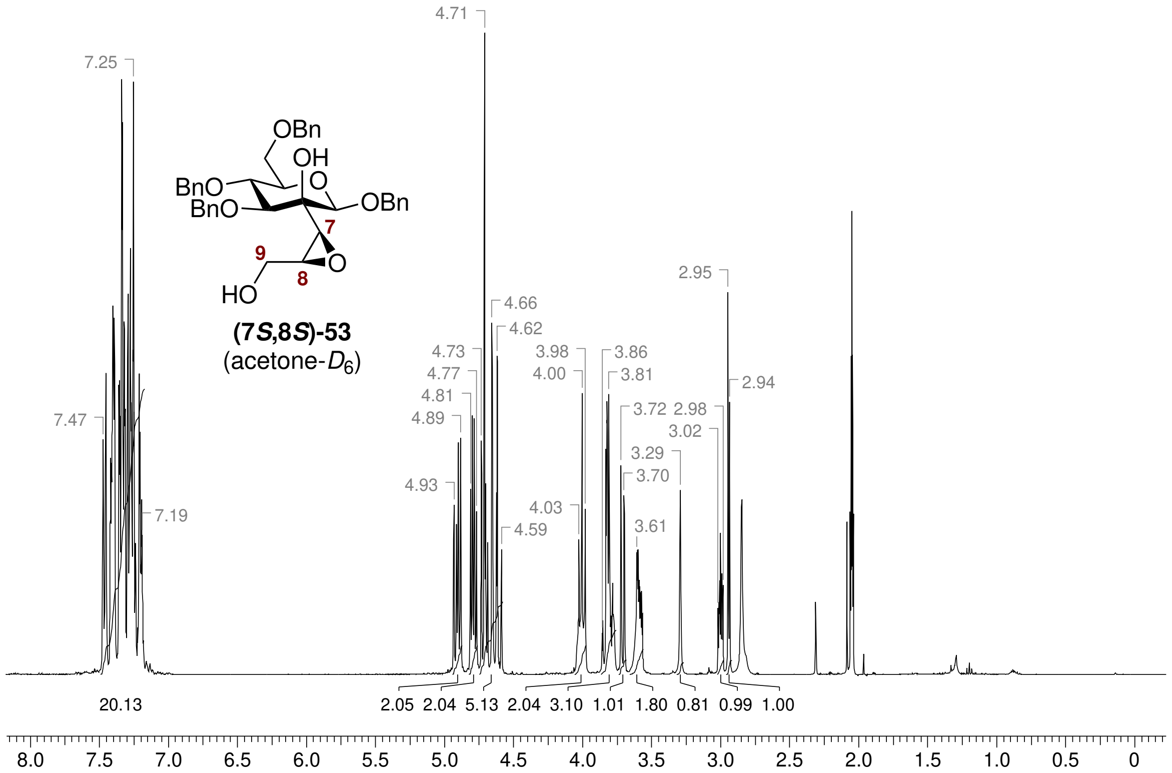
OBn
OH
O
BnO
BnO
OBn
7
9
8
O
HO
(7S,8S)-53
(acetone-D6)
7.25
7.47
7.19
4.71
4.66
4.62
4.73
4.77
4.81
4.89
4.93
4.59
3.98
4.00
4.03
3.86
3.81
3.72
3.70
3.61
3.29
2.98
3.02
2.95
2.94
20.13
2.05
2.04
5.13
2.04
3.10
1.01
1.80
0.81
0.99
1.00
8.0
7.5
7.0
6.5
6.0
5.5
5.0
4.5
4.0
3.5
3.0
2.5
2.0
1.5
1.0
0.5
0

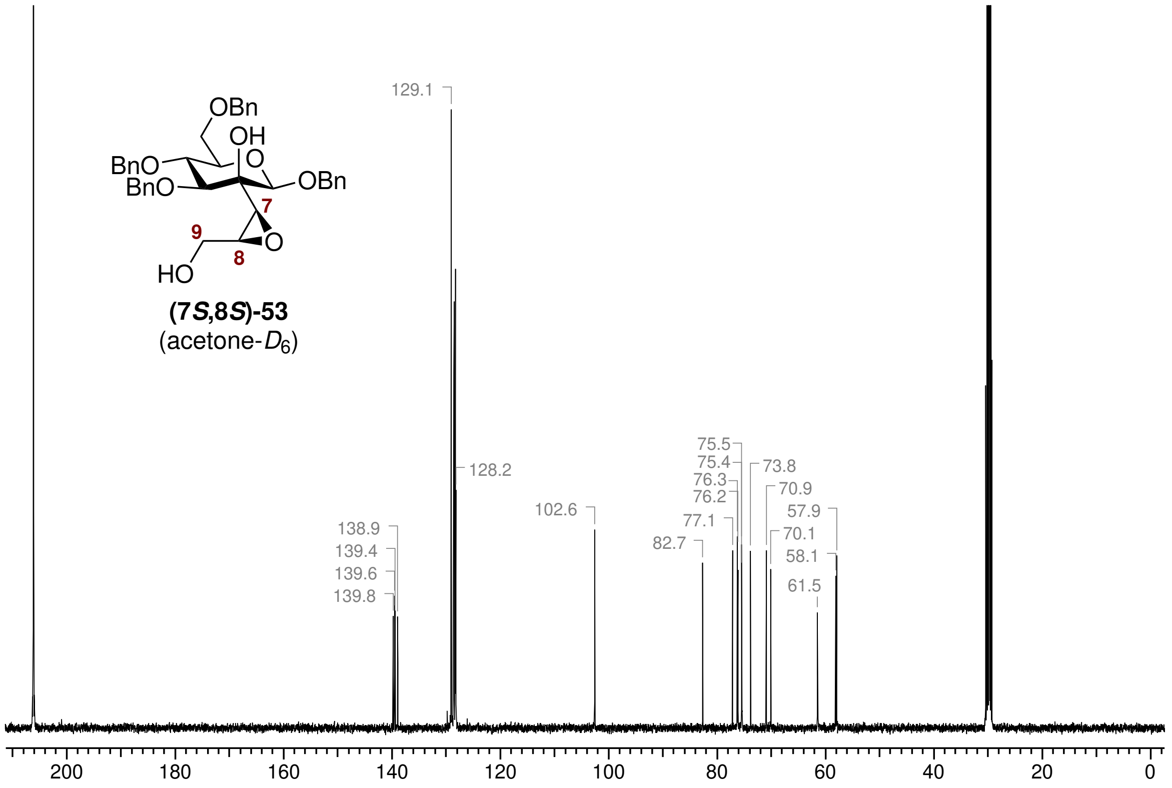
OBn
OH
O
BnO
BnO
OBn
7
9
8
O
HO
(7S,8S)-53
(acetone-D6)
129.1
128.2
138.9
139.4
139.6
139.8
102.6
82.7
77.1
76.2
76.3
75.4
75.5
73.8
70.9
70.1
57.9
58.1
61.5
200
180
160
140
120
100
80
60
40
20
0

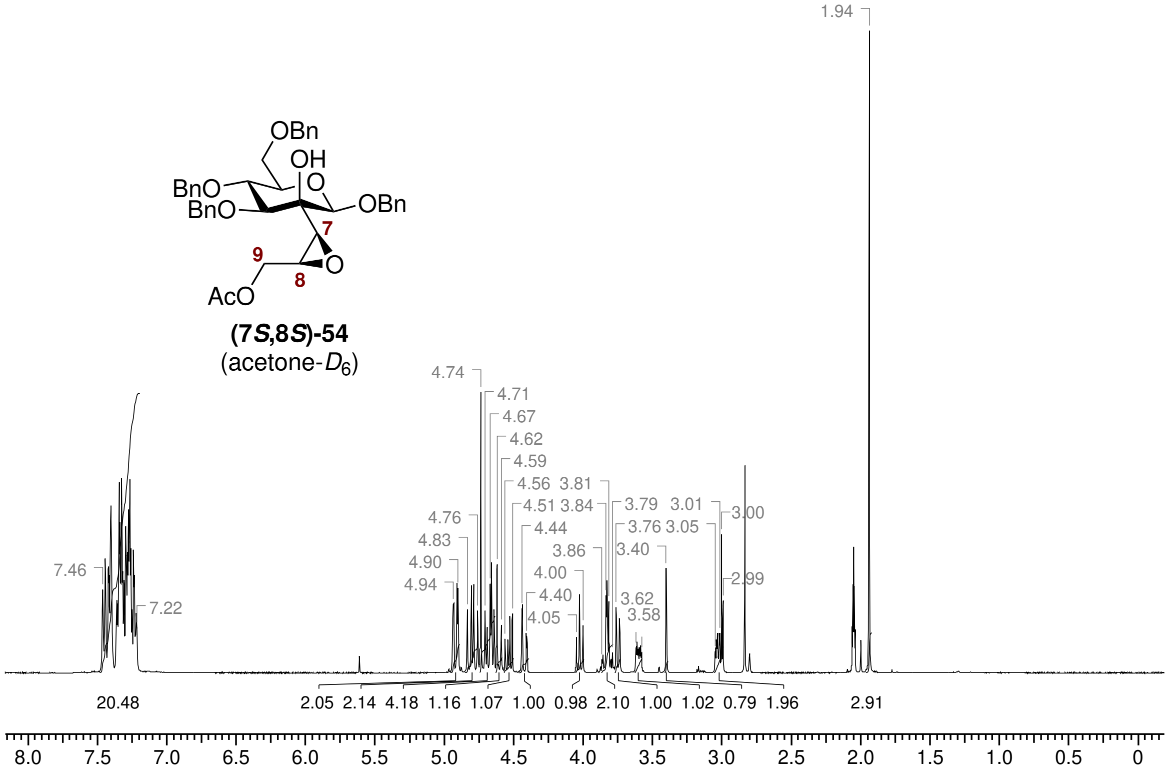
OBn
OH
O
BnO
BnO
OBn
7
9
8
O
AcO
(7S,8S)-54
(acetone-D6)
1.94
4.74
4.71
4.67
4.62
4.59
4.56
4.51
4.44
4.76
4.83
4.90
4.94
4.00
4.40
4.05
3.81
3.84
3.86
3.79
3.76
3.40
3.62
3.58
3.01
3.05
3.00
2.99
7.46
7.22
20.48
2.05 2.14 4.18 1.16 1.07 1.00 0.98 2.10 1.00 1.02 0.79 1.96
2.91
8.0 7.5 7.0 6.5 6.0 5.5 5.0 4.5 4.0 3.5 3.0 2.5 2.0 1.5 1.0 0.5 0

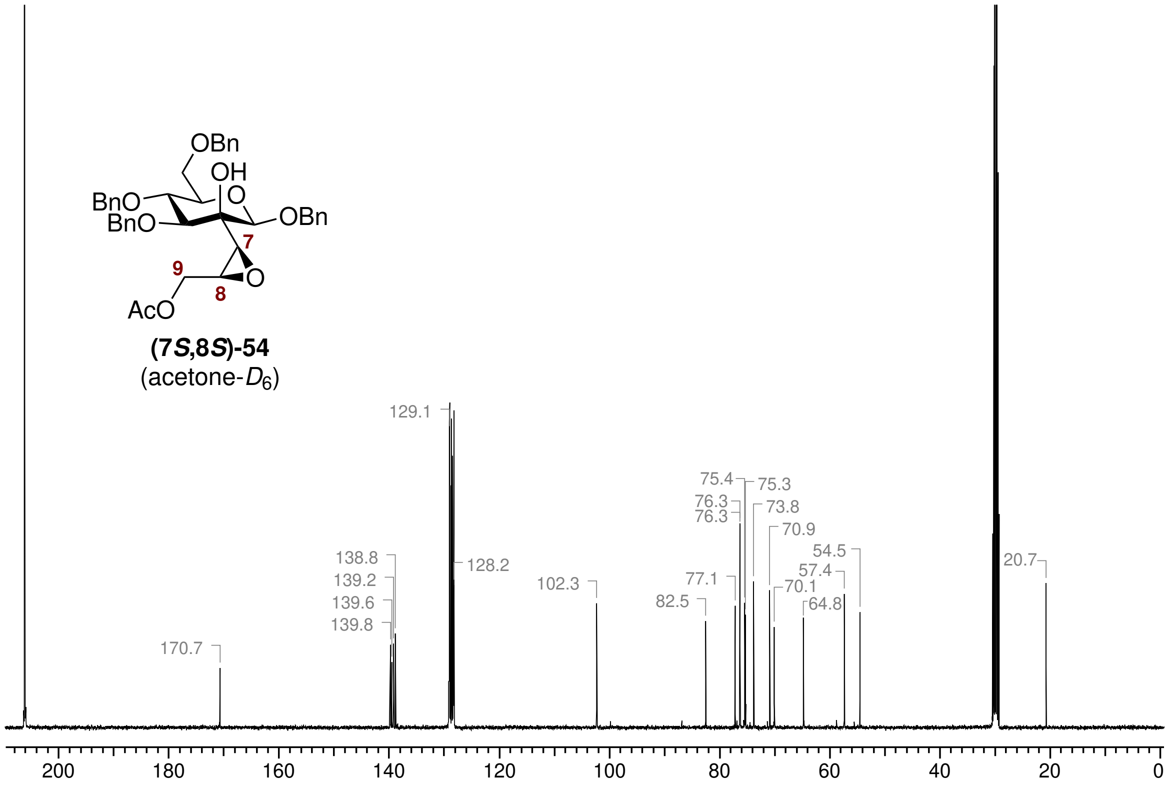
OBn
OH
O
BnO
BnO
OBn
7
9
8
O
AcO
(7S,8S)-54
(acetone-D6)
129.1
128.2
138.8
139.2
139.6
139.8
170.7
102.3
82.5
77.1
75.4
75.3
76.3
76.3
73.8
70.9
70.1
64.8
54.5
57.4
20.7
200 180 160 140 120 100 80 60 40 20 0

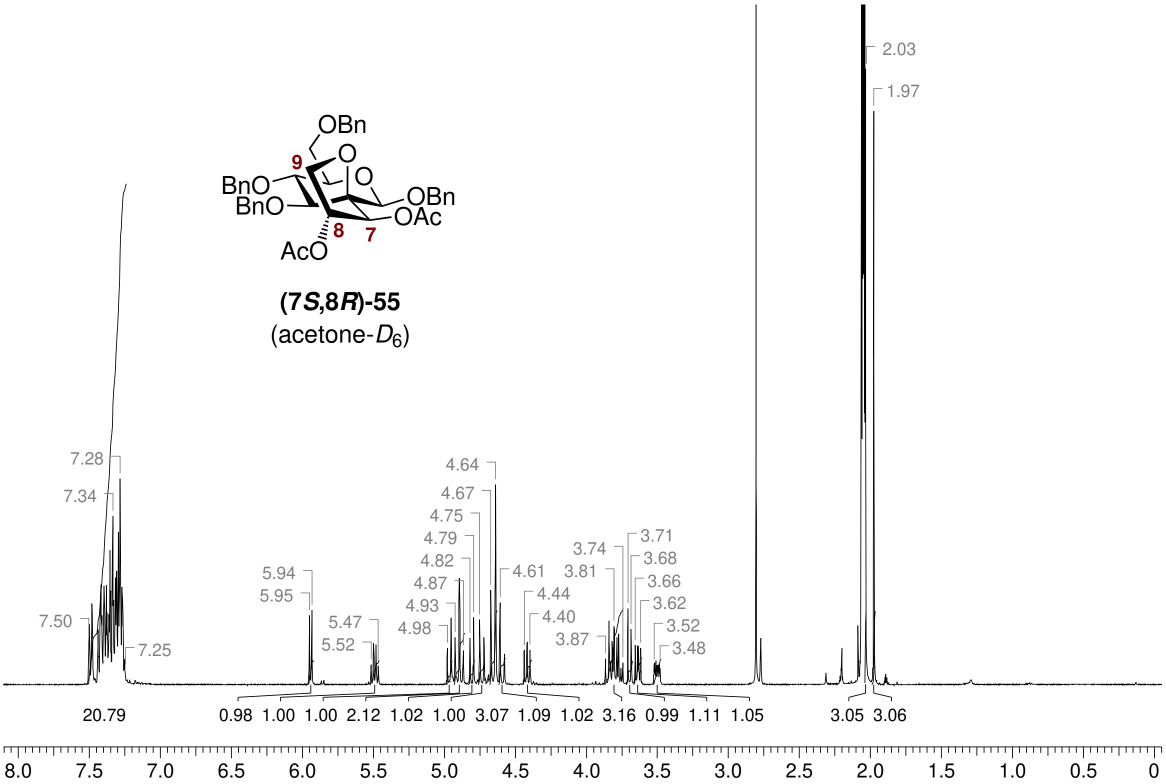
OBn
9
BnO
BnO
O
O
OBn
OAc
8
7
AcO
(7S,8R)-55
(acetone-D6)
2.03
1.97
7.28
7.34
7.50
7.25
5.94
5.95
5.47
5.52
4.64
4.67
4.75
4.79
4.82
4.87
4.93
4.98
4.61
4.44
4.40
3.74
3.81
3.87
3.71
3.68
3.66
3.62
3.52
3.48
20.79
0.98 1.00 1.00 2.12 1.02 1.00 3.07 1.09 1.02 3.16 0.99 1.11 1.05
3.05 3.06
8.0 7.5 7.0 6.5 6.0 5.5 5.0 4.5 4.0 3.5 3.0 2.5 2.0 1.5 1.0 0.5 0

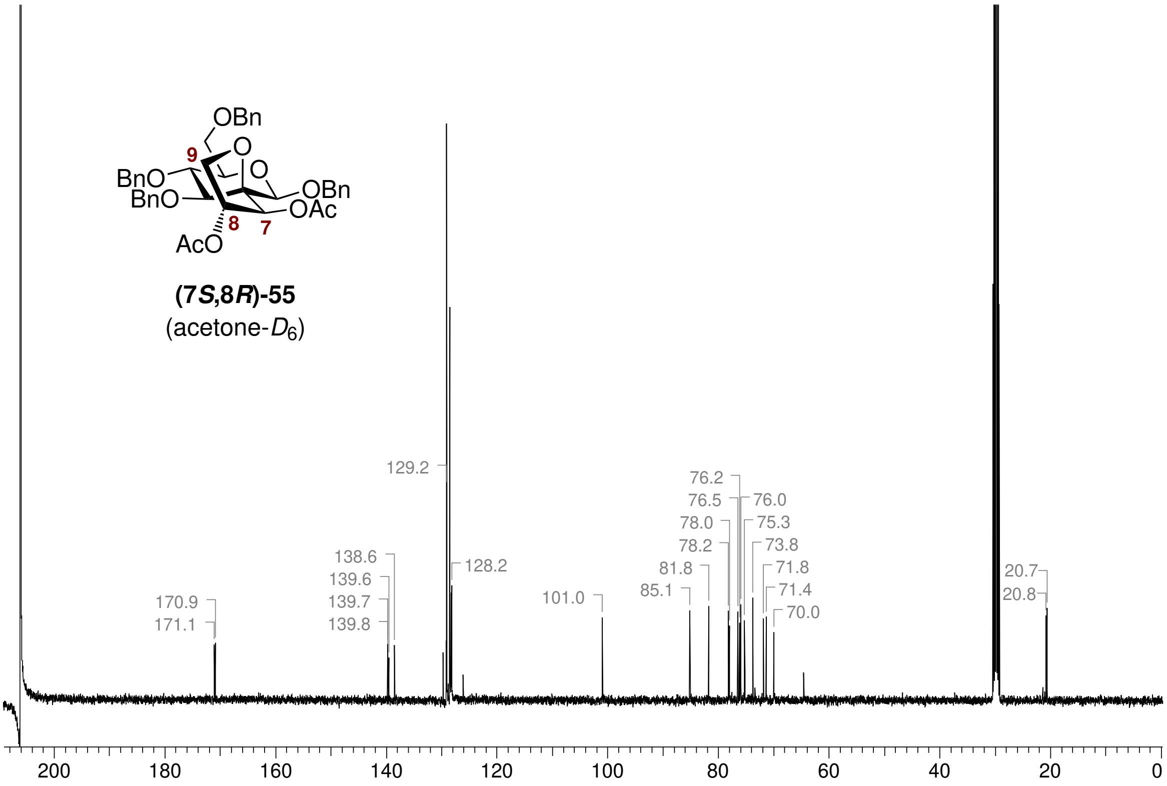
OBn
9
BnO
BnO
O
O
OBn
OAc
8
7
AcO
(7S,8R)-55
(acetone-D6)
129.2
138.6
139.6
139.7
139.8
128.2
170.9
171.1
101.0
76.2
76.5
78.0
78.2
81.8
85.1
76.0
75.3
73.8
71.8
71.4
70.0
20.7
20.8
200 180 160 140 120 100 80 60 40 20 0

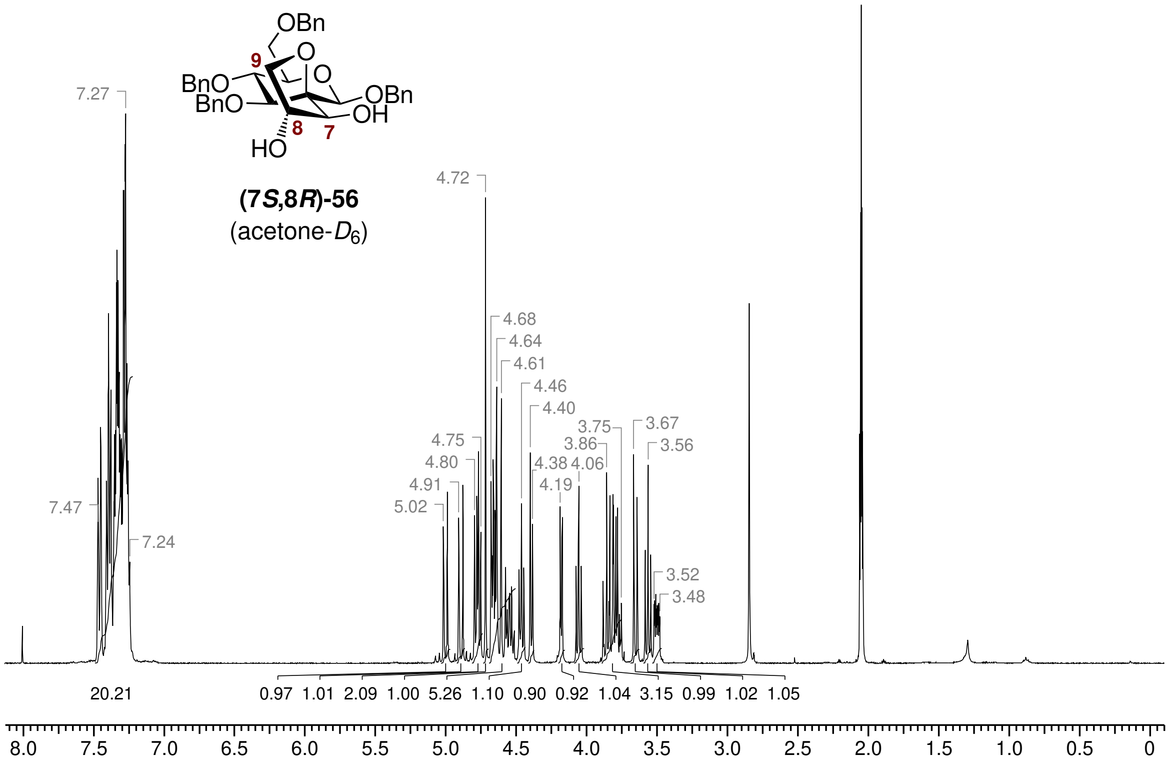
OBn
9
BnO
BnO
O
O
OBn
OH
8
7
HO
(7S,8R)-56
(acetone-D6)
7.27
7.47
7.24
4.72
4.68
4.64
4.61
4.46
4.40
4.75
4.80
4.91
5.02
3.75
3.86
4.38
4.06
4.19
3.67
3.56
3.52
3.48
20.21
0.97 1.01 2.09 1.00 5.26 1.10 0.90 0.92 1.04 3.15 0.99 1.02 1.05
8.0 7.5 7.0 6.5 6.0 5.5 5.0 4.5 4.0 3.5 3.0 2.5 2.0 1.5 1.0 0.5 0

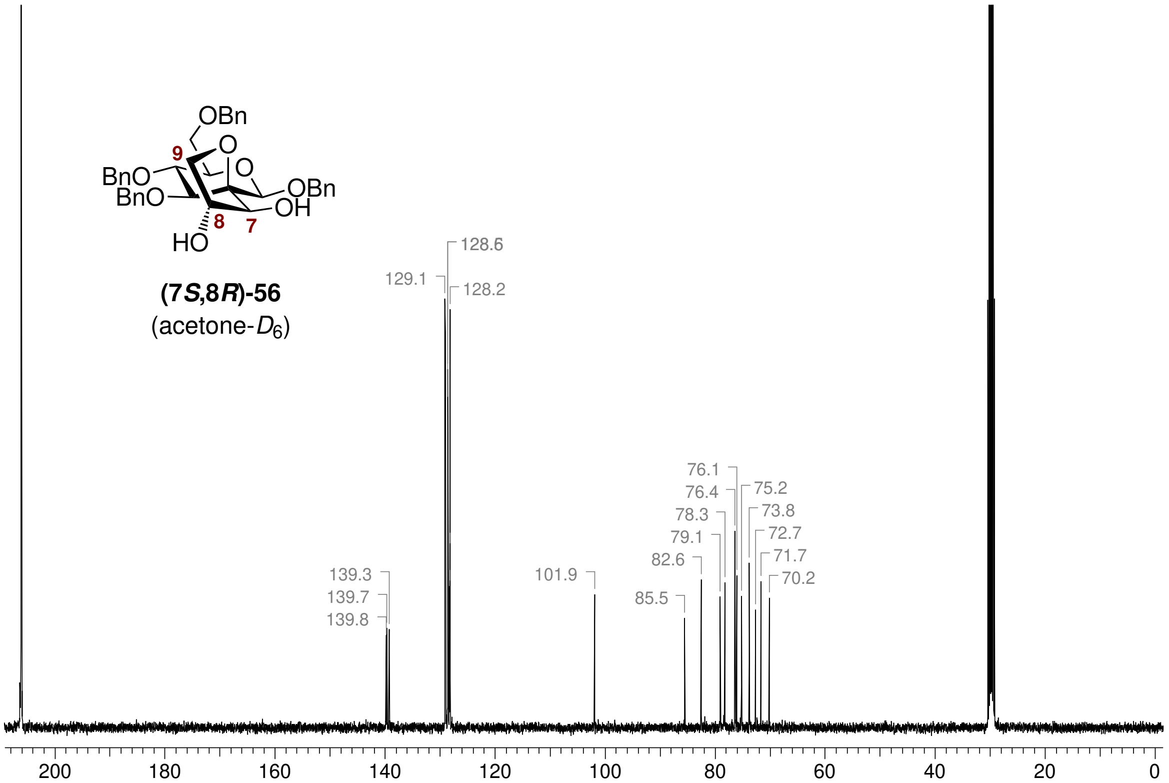
OBn
9
BnO
BnO
O
O
OBn
OH
8
7
HO
(7S,8R)-56
(acetone-D6)
128.6
129.1
128.2
76.1
76.4
75.2
78.3
73.8
79.1
72.7
82.6
71.7
70.2
139.3
139.7
139.8
101.9
85.5
200 180 160 140 120 100 80 60 40 20 0

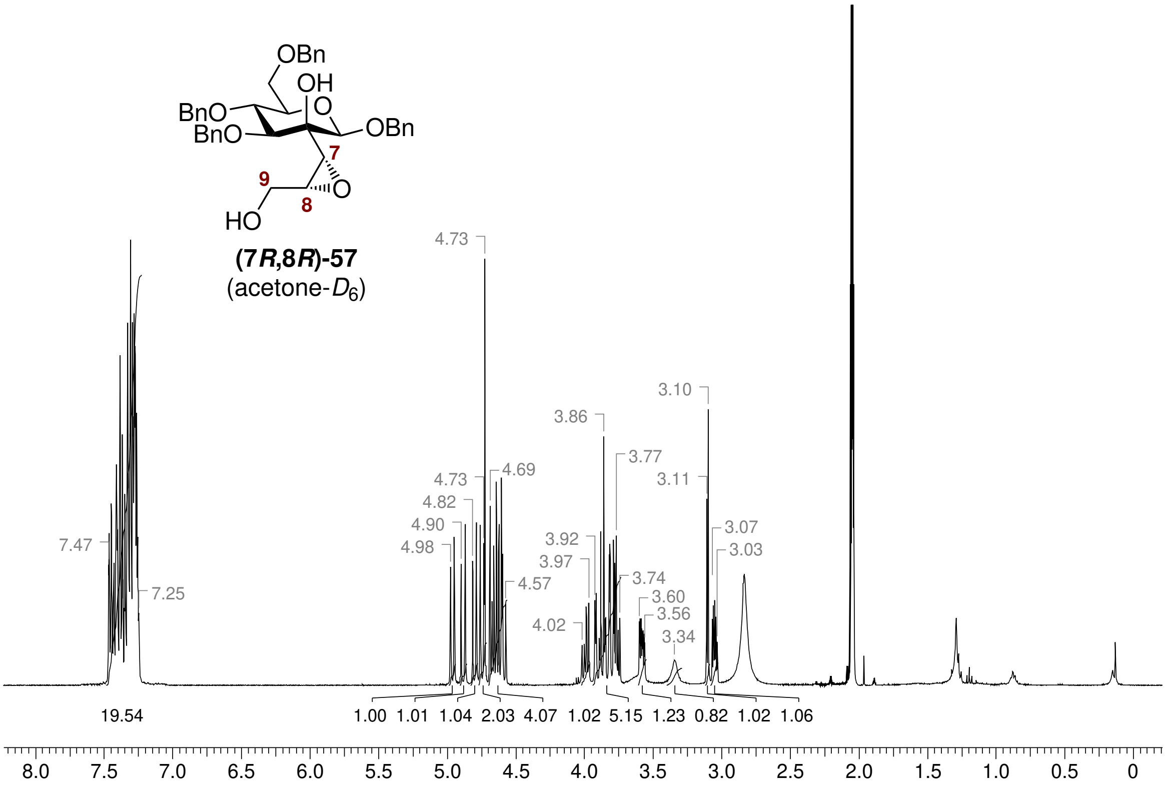

(7*R*,8*R*)-57
(acetone-D_6)

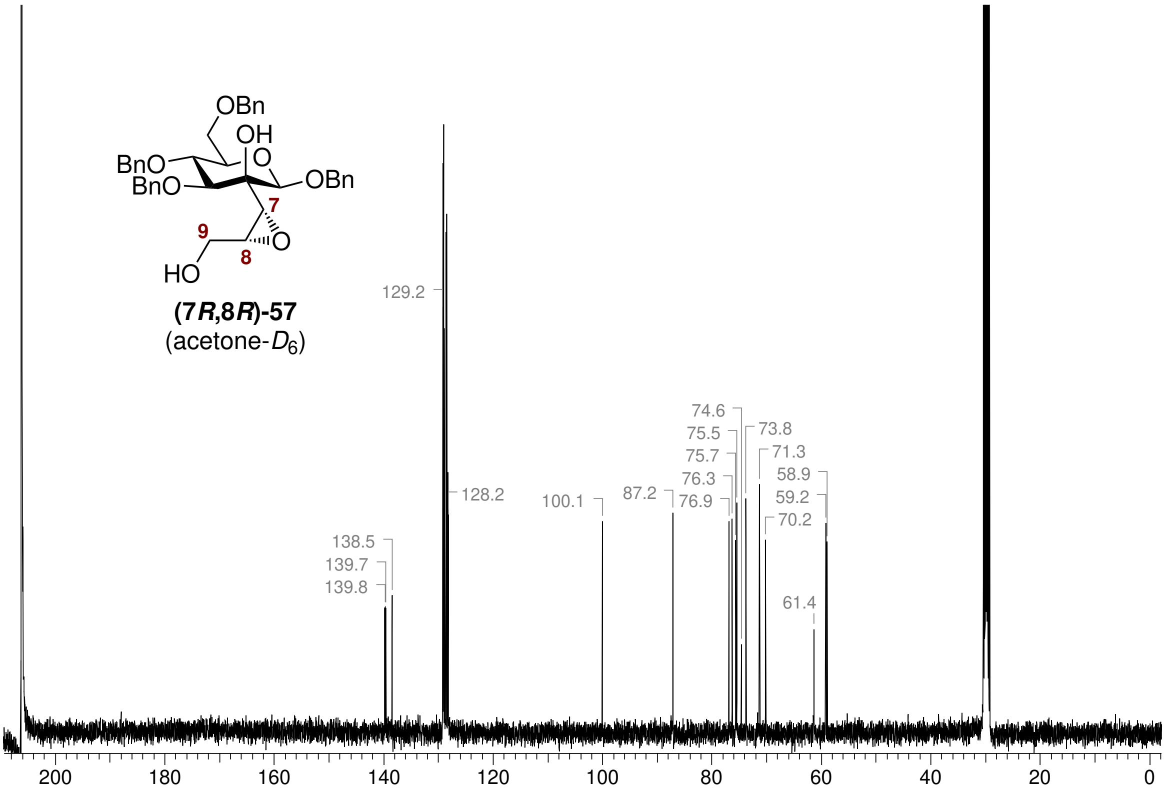

(7*R*,8*R*)-57
(acetone-D_6)

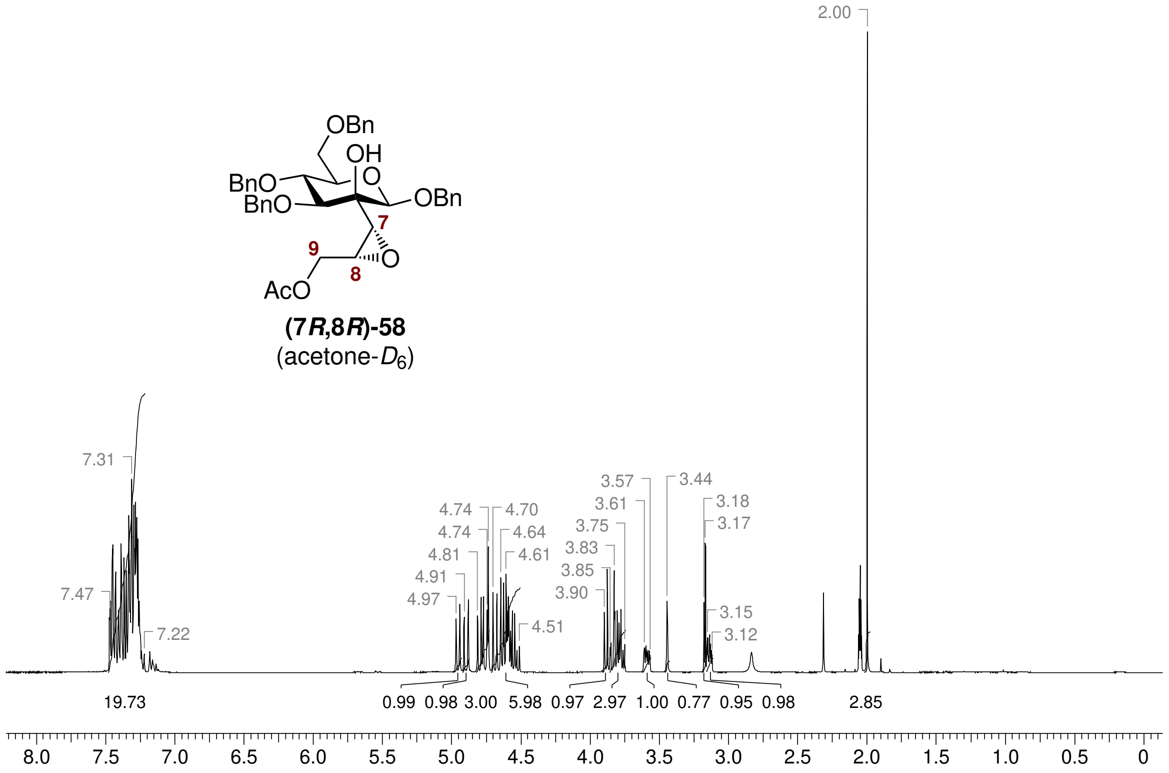

(7*R*,8*R*)-58
(acetone-D_6)

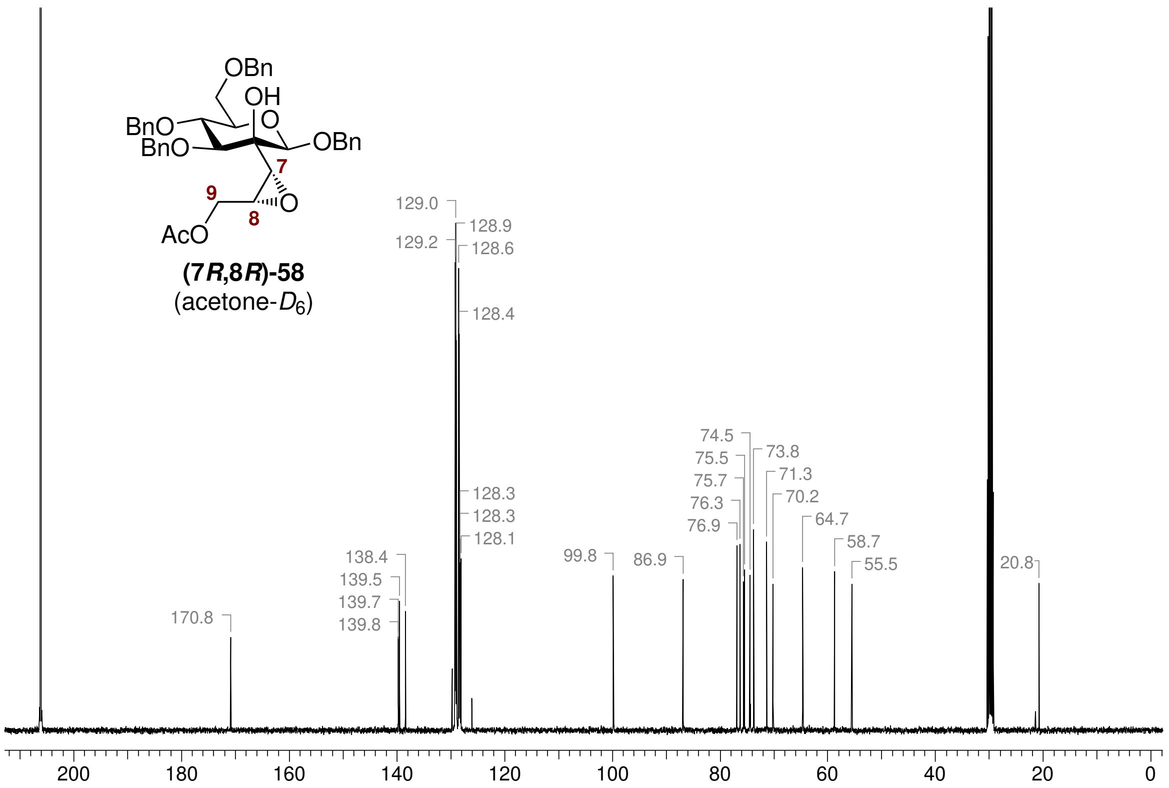

(7*R*,8*R*)-58
(acetone-D_6)

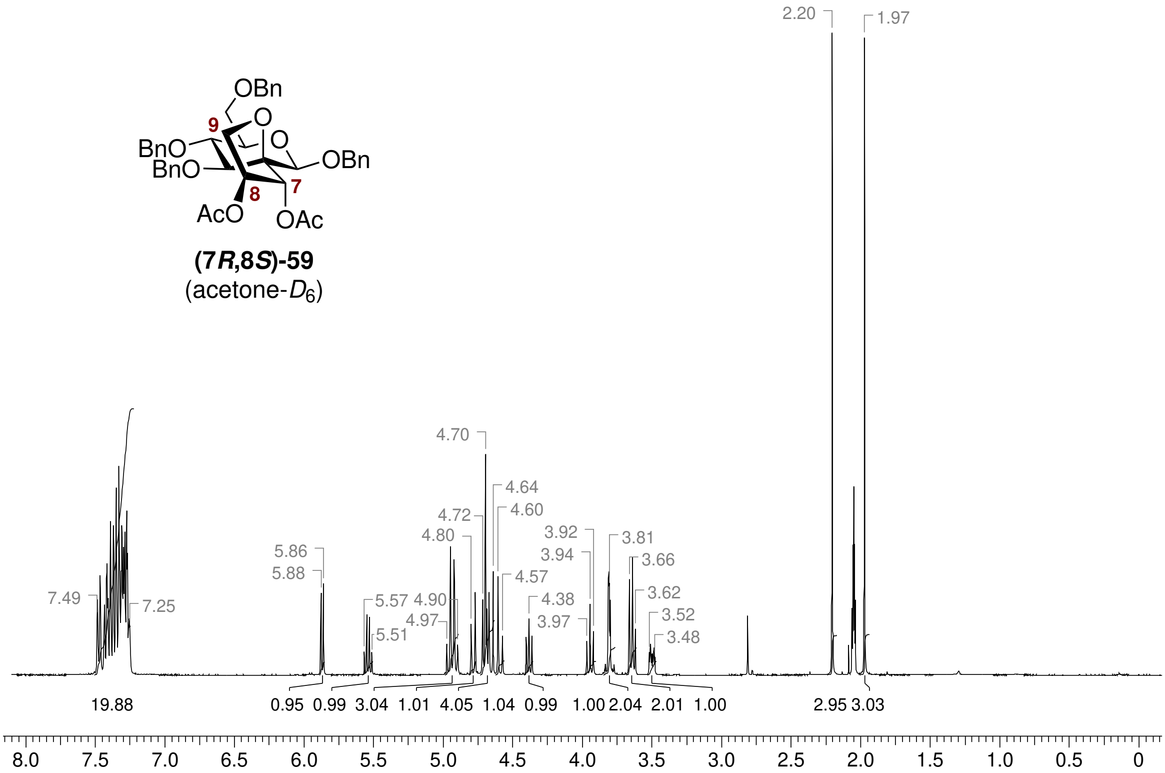
OBn
O
9
O
BnO
BnO
OBn
8
7
AcO
OAc
(7R,8S)-59
(acetone-D6)
2.20
1.97
4.70
4.64
4.60
4.72
4.80
3.92
3.81
3.66
3.94
5.86
5.88
4.57
7.49
7.25
5.57
4.90
4.97
5.51
4.38
3.97
3.62
3.52
3.48
19.88
0.95
0.99
3.04
1.01
4.05
1.04
0.99
1.00
2.04
2.01
1.00
2.95
3.03
8.0
7.5
7.0
6.5
6.0
5.5
5.0
4.5
4.0
3.5
3.0
2.5
2.0
1.5
1.0
0.5
0

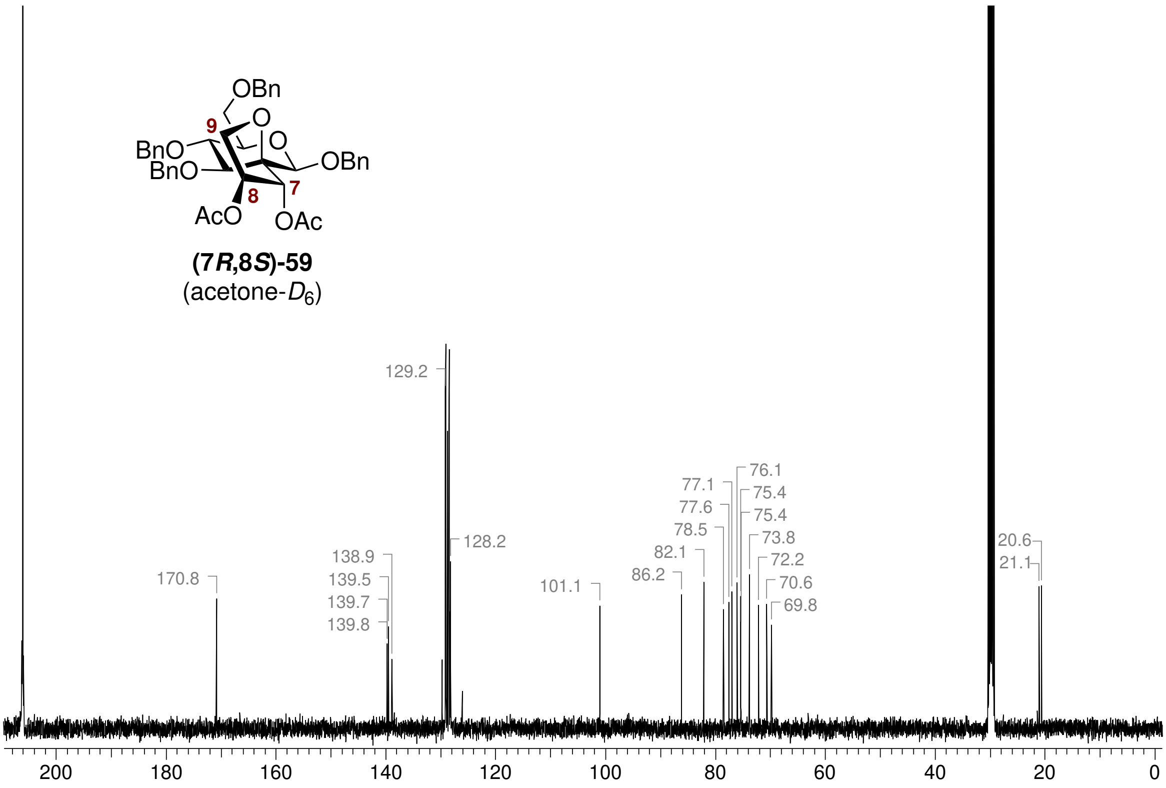
OBn
O
9
O
BnO
BnO
OBn
8
7
AcO
OAc
(7R,8S)-59
(acetone-D6)
129.2
128.2
170.8
138.9
139.5
139.7
139.8
101.1
86.2
82.1
78.5
77.6
77.1
76.1
75.4
75.4
73.8
72.2
70.6
69.8
20.6
21.1
200
180
160
140
120
100
80
60
40
20
0

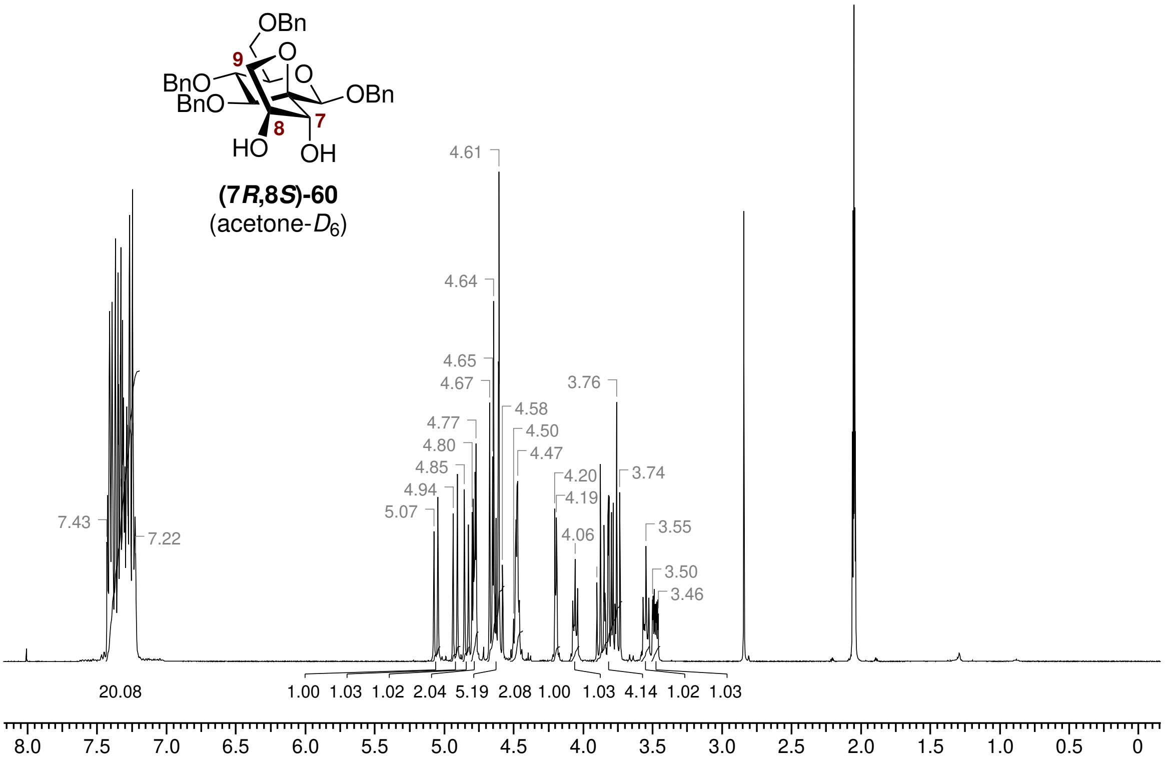
OBn
9
O
BnO
BnO
O
OBn
8
7
HO
OH
(7R,8S)-60
(acetone-D6)
7.43
7.22
5.07
4.94
4.85
4.80
4.77
4.67
4.65
4.64
4.61
4.58
4.50
4.47
4.20
4.19
4.06
3.76
3.74
3.55
3.50
3.46
20.08
1.00
1.03
1.02
2.04
5.19
2.08
1.00
1.03
4.14
1.02
1.03
8.0
7.5
7.0
6.5
6.0
5.5
5.0
4.5
4.0
3.5
3.0
2.5
2.0
1.5
1.0
0.5
0

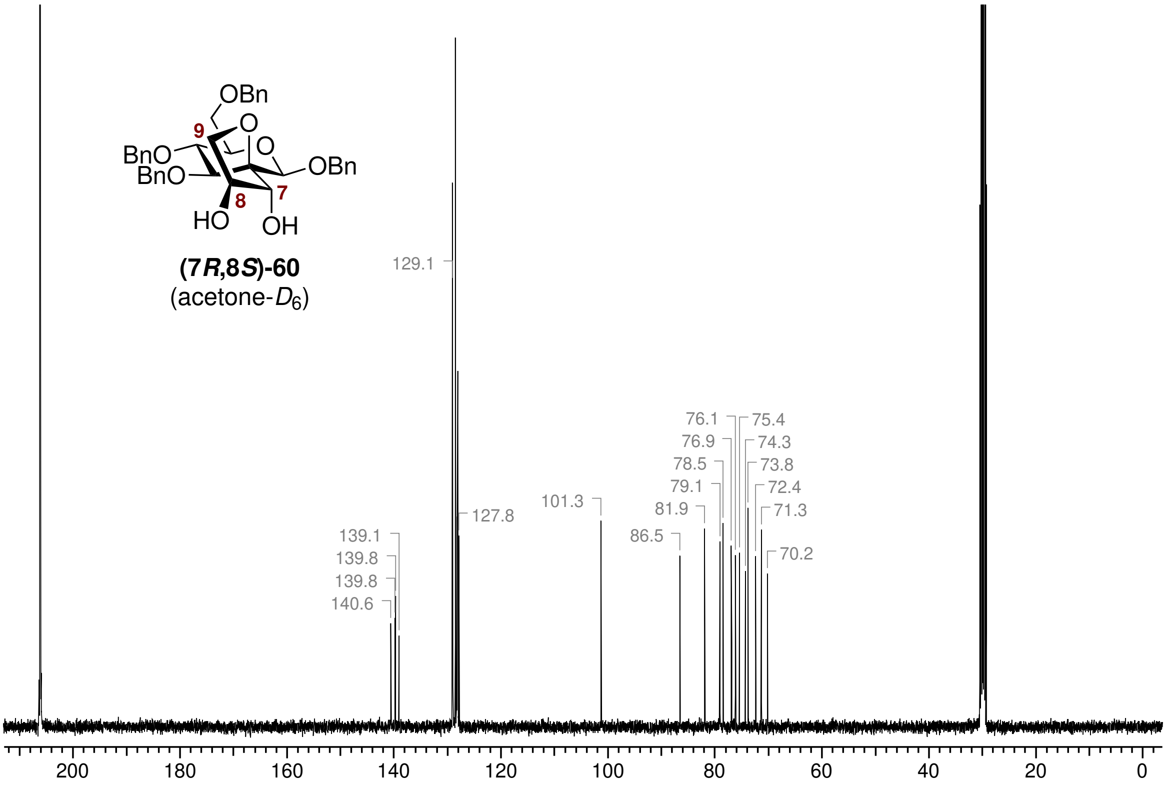
OBn
9
O
BnO
BnO
O
OBn
8
7
HO
OH
(7R,8S)-60
(acetone-D6)
129.1
127.8
139.1
139.8
139.8
140.6
101.3
86.5
81.9
79.1
78.5
76.9
76.1
75.4
74.3
73.8
72.4
71.3
70.2
200
180
160
140
120
100
80
60
40
20
0

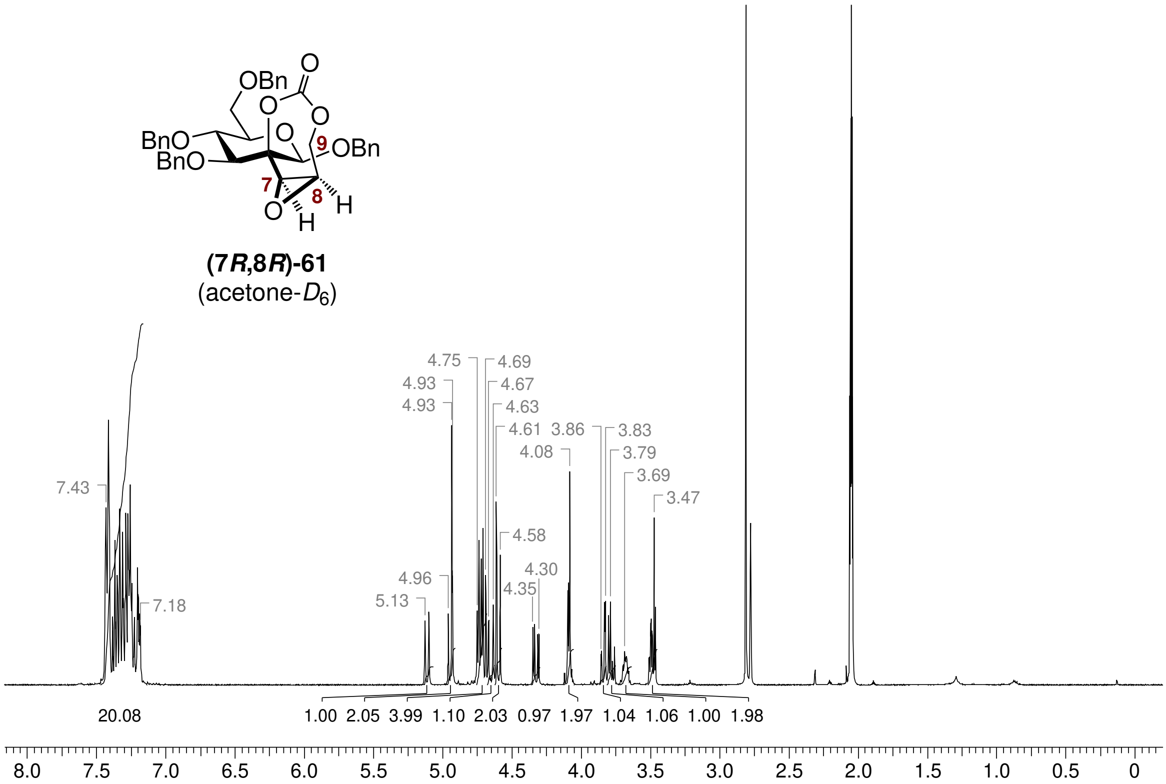
(7*R*,8*R*)-61
(acetone-D_6)

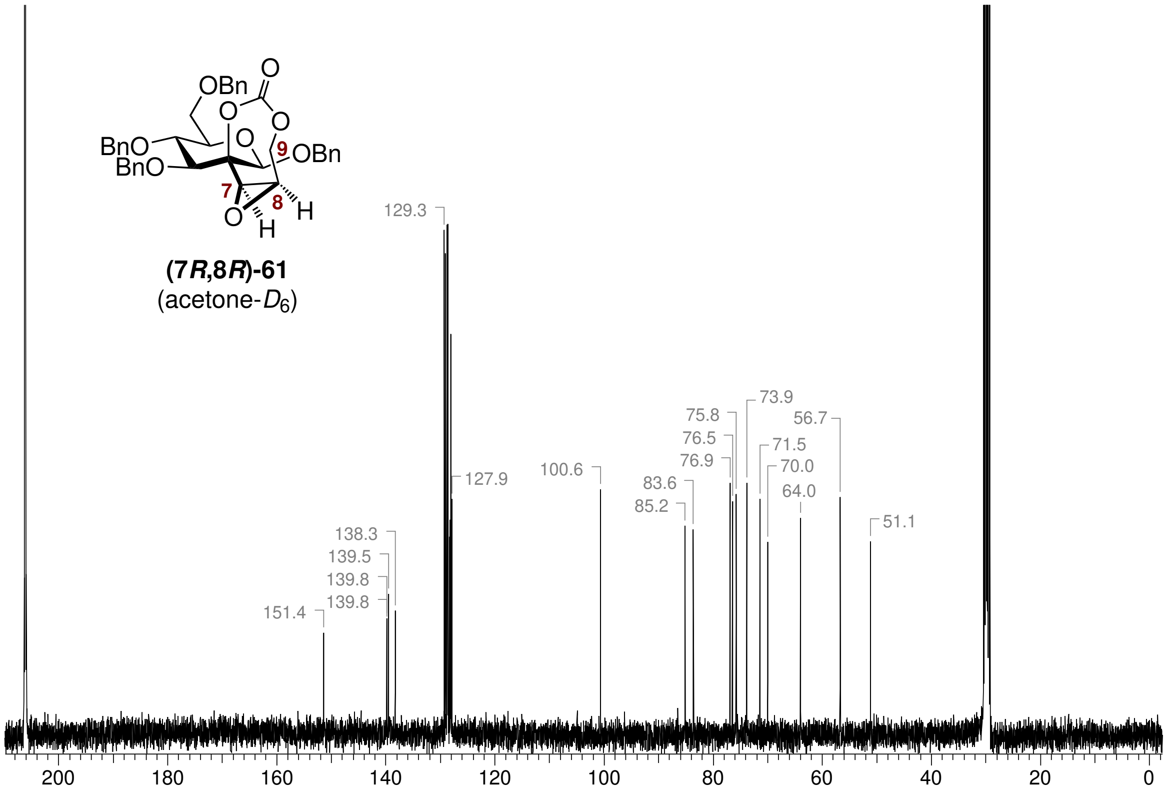
(7*R*,8*R*)-61
(acetone-D_6)

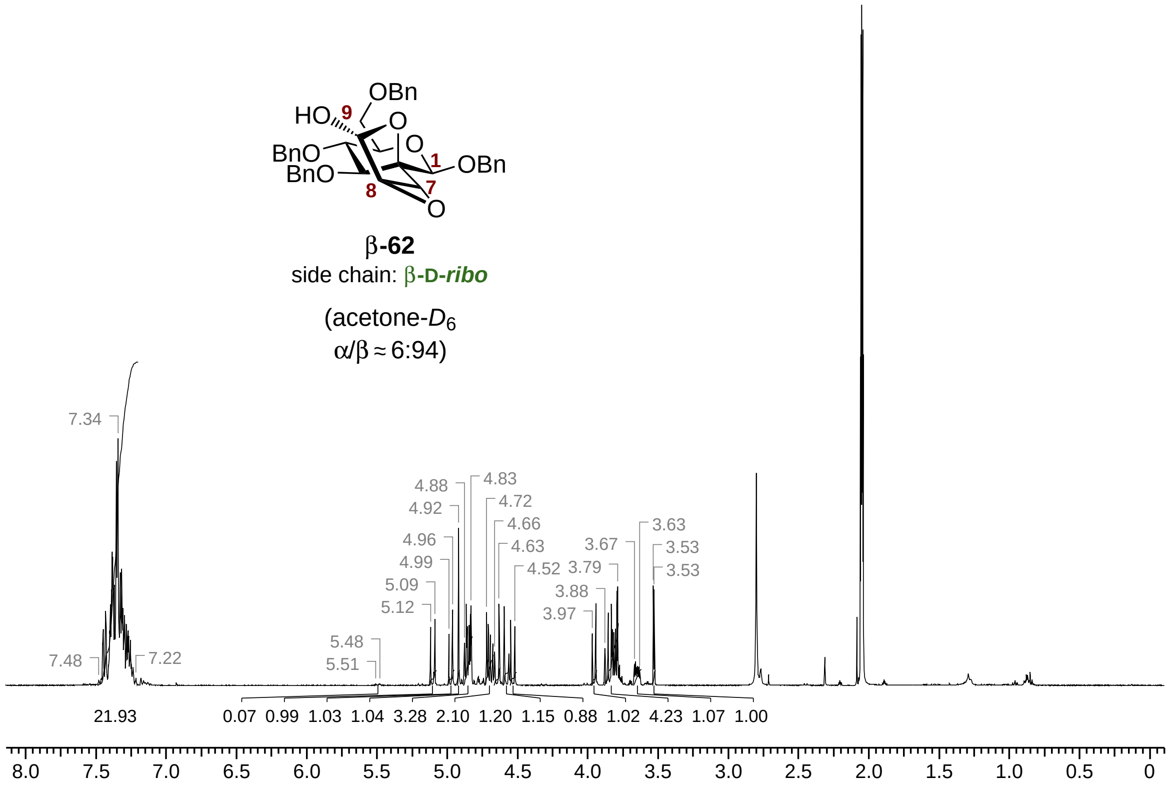
OBn
HO
9
O
O
1
OBn
BnO
BnO
8
7
O
β-62
side chain: β-D-ribo
(acetone-D6
α/β ≈ 6:94)
7.34
7.48
7.22
5.48
5.51
5.09
5.12
4.96
4.99
4.88
4.92
4.83
4.72
4.66
4.63
4.52
3.67
3.79
3.88
3.97
3.63
3.53
3.53
21.93
0.07 0.99 1.03 1.04 3.28 2.10 1.20 1.15 0.88 1.02 4.23 1.07 1.00
8.0 7.5 7.0 6.5 6.0 5.5 5.0 4.5 4.0 3.5 3.0 2.5 2.0 1.5 1.0 0.5 0

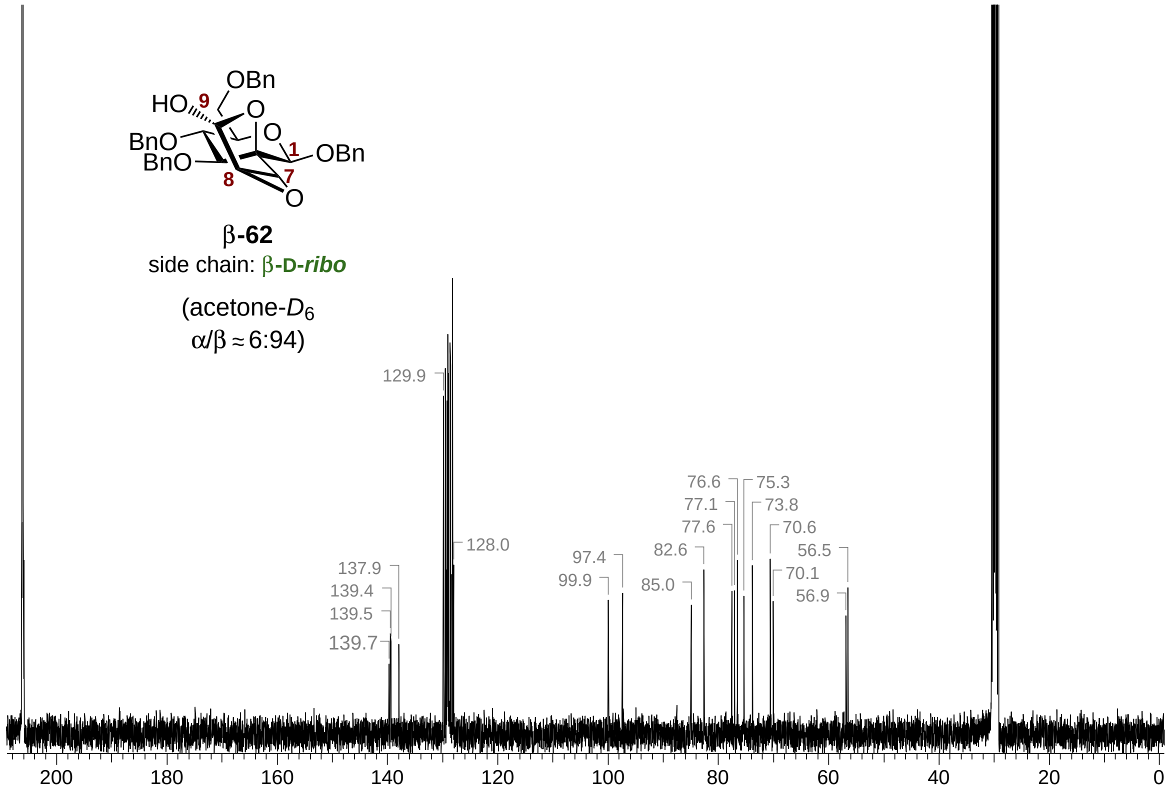
OBn
HO
9
O
O
1
OBn
BnO
BnO
8
7
O
β-62
side chain: β-D-ribo
(acetone-D6
α/β ≈ 6:94)
129.9
128.0
137.9
139.4
139.5
139.7
97.4
99.9
82.6
85.0
76.6
77.1
77.6
75.3
73.8
70.6
70.1
56.5
56.9
200 180 160 140 120 100 80 60 40 20 0

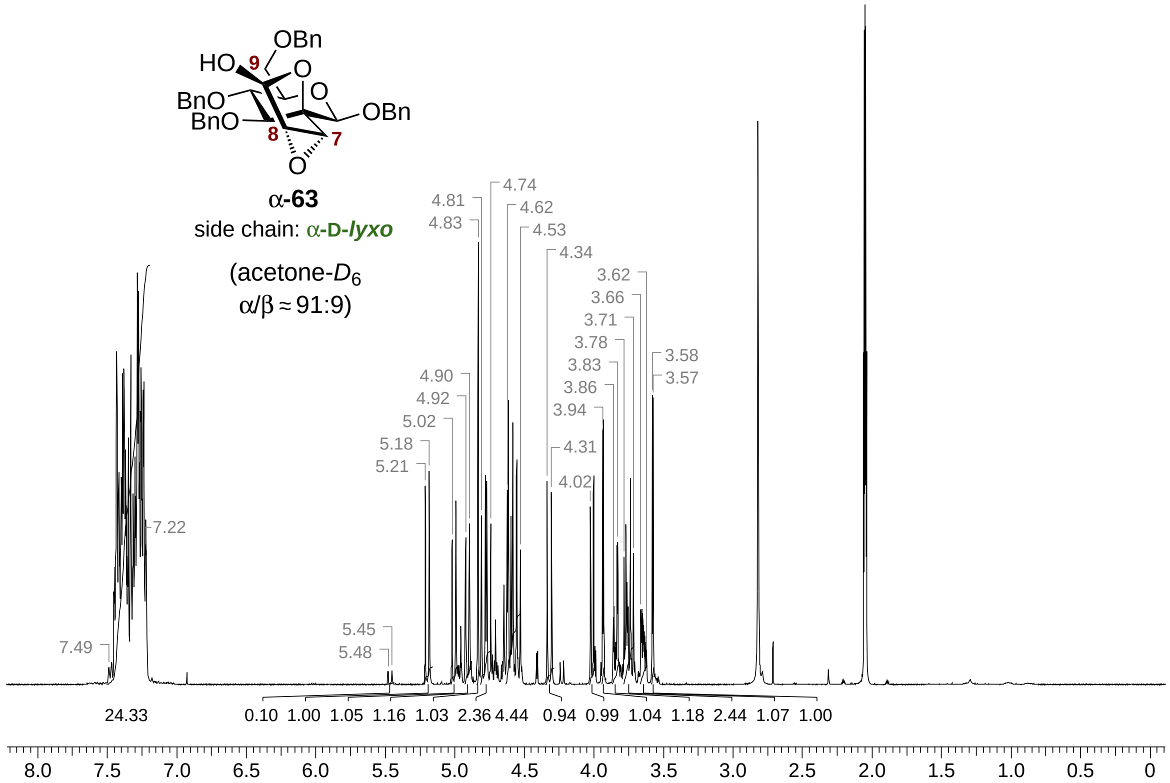
OBn
HO
9
O
O
BnO
BnO
OBn
8
7
O
α-63
side chain: α-D-lyxo
(acetone-D6
α/β ≈ 91:9)
4.74
4.81
4.62
4.83
4.53
4.34
3.62
3.66
3.71
3.78
3.58
3.83
3.57
4.90
3.86
4.92
3.94
5.02
5.18
4.31
5.21
4.02
7.22
5.45
7.49
5.48
24.33
0.10
1.00
1.05
1.16
1.03
2.36
4.44
0.94
0.99
1.04
1.18
2.44
1.07
1.00
8.0
7.5
7.0
6.5
6.0
5.5
5.0
4.5
4.0
3.5
3.0
2.5
2.0
1.5
1.0
0.5
0

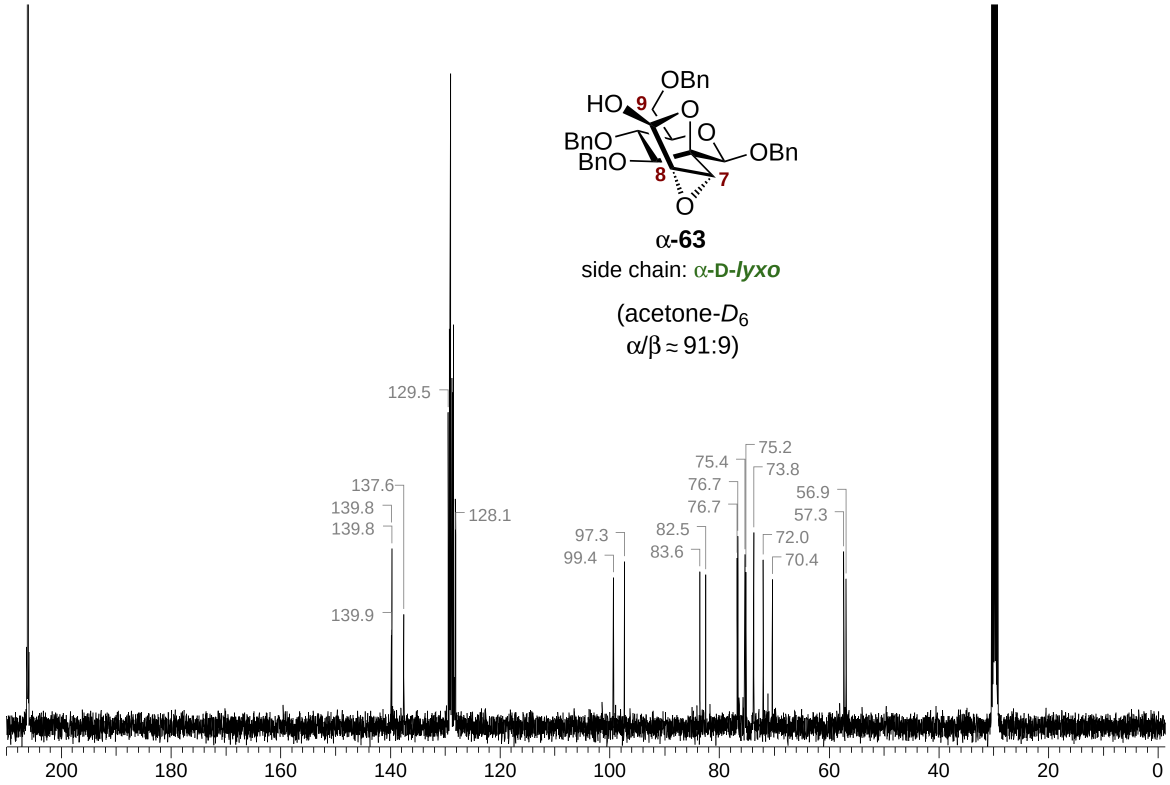
OBn
HO
9
O
O
BnO
BnO
OBn
8
7
O
α-63
side chain: α-D-lyxo
(acetone-D6
α/β ≈ 91:9)
129.5
75.2
75.4
73.8
137.6
76.7
56.9
139.8
128.1
76.7
57.3
139.8
97.3
82.5
72.0
99.4
83.6
70.4
139.9
200
180
160
140
120
100
80
60
40
20
0

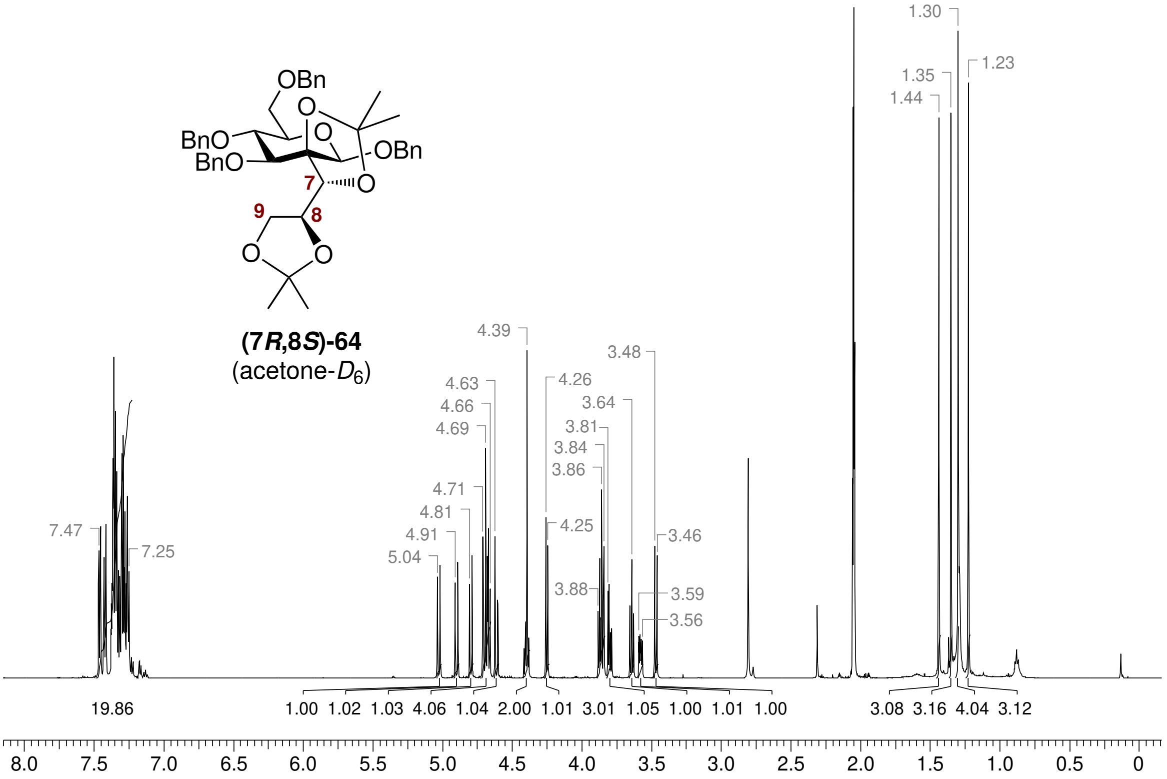

OBn
O
BnO
BnO
O
OBn
7
O
9
8
O
O
(7R,8S)-64
(acetone-D6)
7.47
7.25
5.04
4.91
4.81
4.71
4.69
4.66
4.63
4.39
4.26
4.25
3.48
3.64
3.81
3.84
3.86
3.88
3.46
3.59
3.56
1.30
1.35
1.44
1.23
19.86
1.00 1.02 1.03 4.06 1.04 2.00 1.01 3.01 1.05 1.00 1.01 1.00
3.08 3.16 4.04 3.12
8.0 7.5 7.0 6.5 6.0 5.5 5.0 4.5 4.0 3.5 3.0 2.5 2.0 1.5 1.0 0.5 0

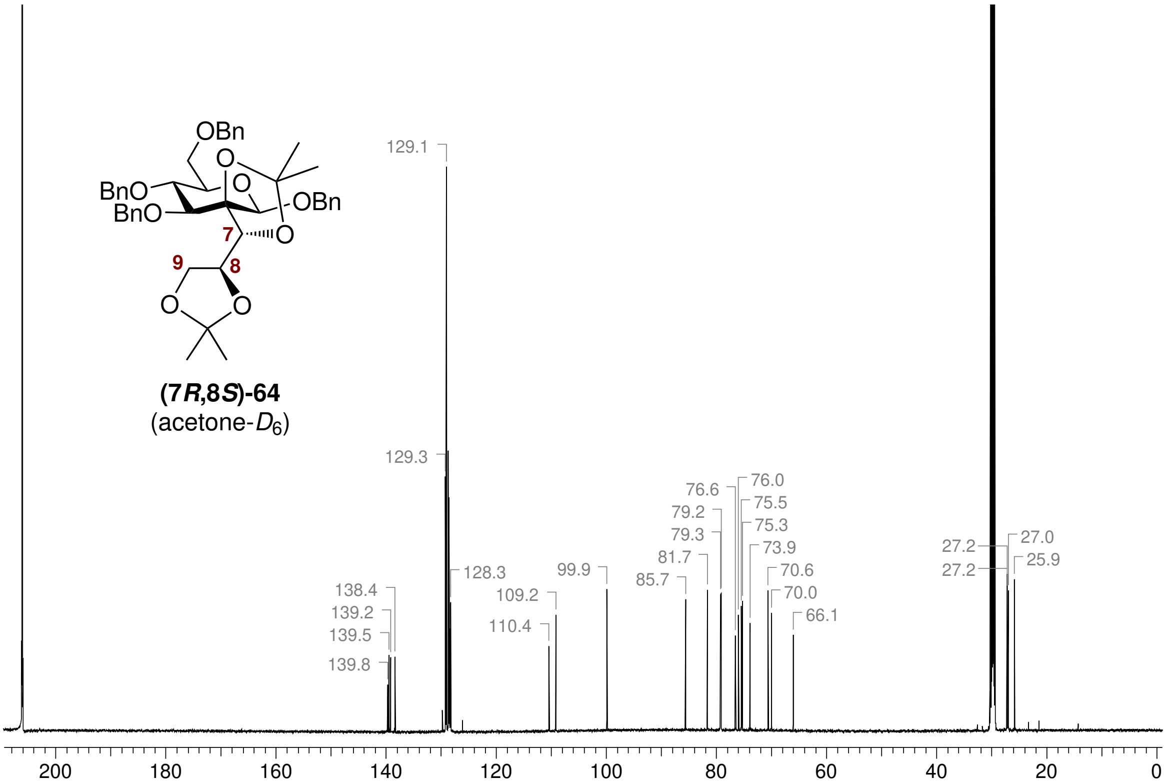

OBn
O
BnO
BnO
O
OBn
7
O
9
8
O
O
(7R,8S)-64
(acetone-D6)
129.1
129.3
128.3
138.4
139.2
139.5
139.8
109.2
110.4
99.9
85.7
81.7
79.3
79.2
76.6
76.0
75.5
75.3
73.9
70.6
70.0
66.1
27.2
27.2
27.0
25.9
200 180 160 140 120 100 80 60 40 20 0

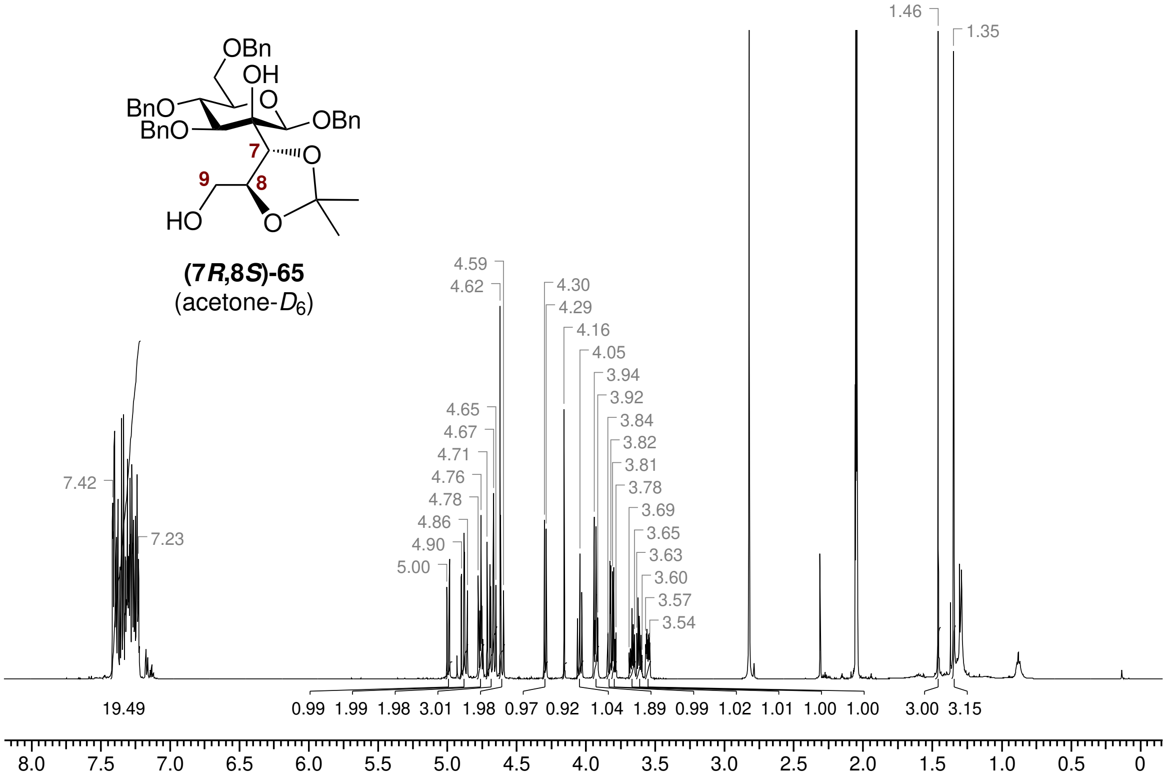
OBn
OH
O
BnO
BnO
OBn
7
8
9
O
HO
O
(7R,8S)-65
(acetone-D6)
1.46
1.35
7.42
7.23
4.59
4.62
4.65
4.67
4.71
4.76
4.78
4.86
4.90
5.00
4.30
4.29
4.16
4.05
3.94
3.92
3.84
3.82
3.81
3.78
3.69
3.65
3.63
3.60
3.57
3.54
19.49
0.99 1.99 1.98 3.01 1.98 0.97 0.92 1.04 1.89 0.99 1.02 1.01 1.00 1.00
3.00 3.15
8.0 7.5 7.0 6.5 6.0 5.5 5.0 4.5 4.0 3.5 3.0 2.5 2.0 1.5 1.0 0.5 0

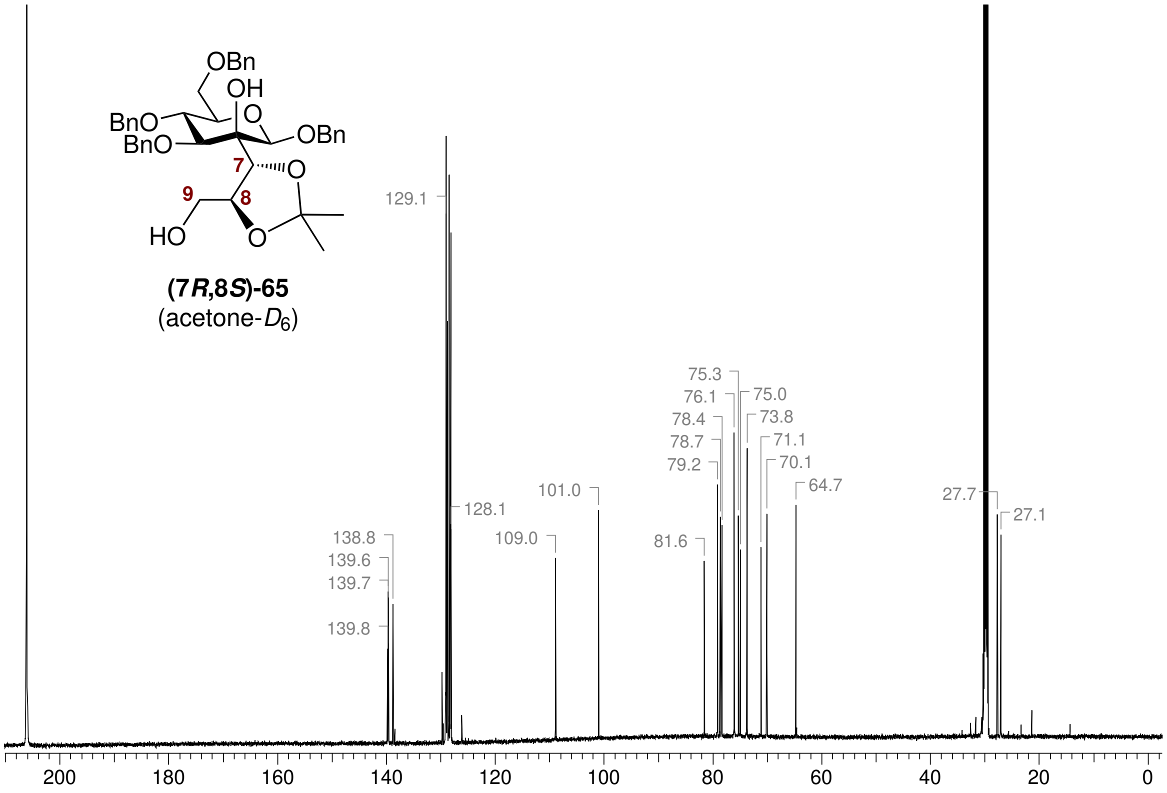
OBn
OH
O
BnO
BnO
OBn
7
8
9
O
HO
O
(7R,8S)-65
(acetone-D6)
129.1
128.1
138.8
139.6
139.7
139.8
109.0
101.0
81.6
75.3
76.1
78.4
78.7
79.2
75.0
73.8
71.1
70.1
64.7
27.7
27.1
200 180 160 140 120 100 80 60 40 20 0

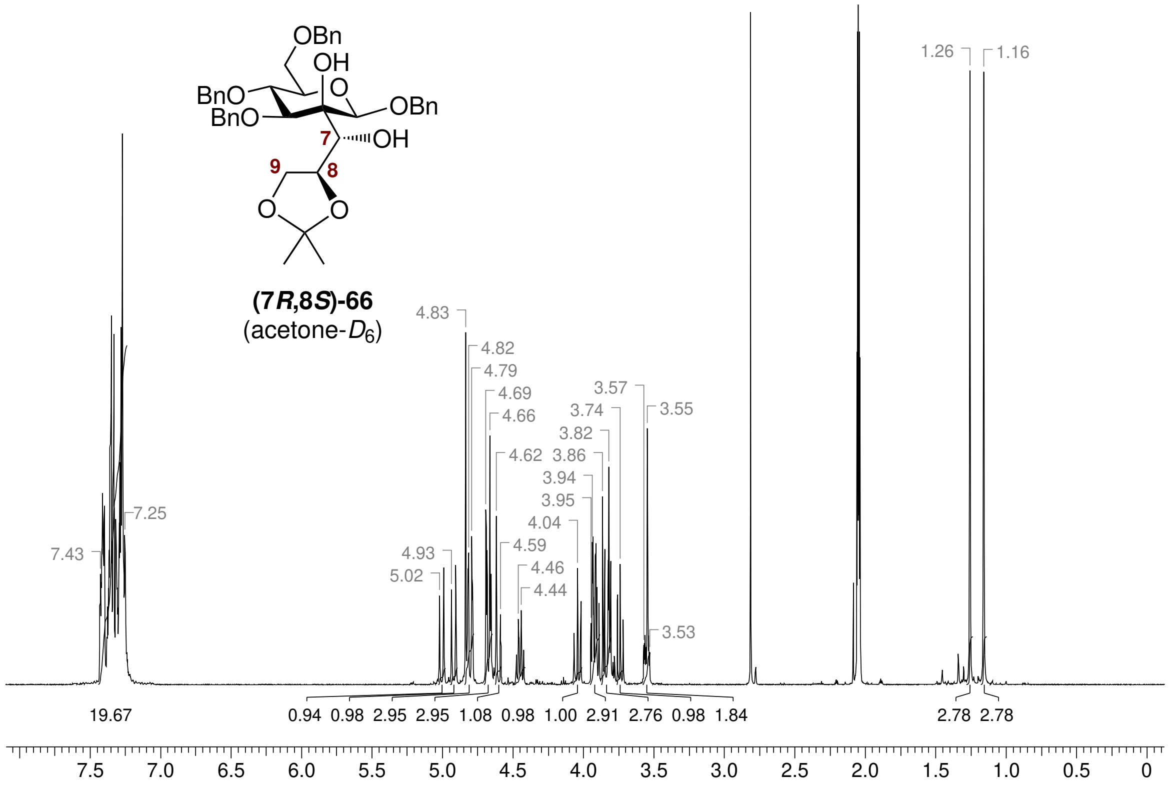
OBn
OH
O
BnO
BnO
OBn
7
OH
9
8
O
O
(7R,8S)-66
(acetone-D_6)
7.43
7.25
5.02
4.93
4.83
4.82
4.79
4.69
4.66
4.62
4.59
4.46
4.44
4.04
3.95
3.94
3.86
3.82
3.74
3.57
3.55
3.53
1.26
1.16
19.67
0.94 0.98 2.95 2.95 1.08 0.98 1.00 2.91 2.76 0.98 1.84
2.78 2.78
7.5 7.0 6.5 6.0 5.5 5.0 4.5 4.0 3.5 3.0 2.5 2.0 1.5 1.0 0.5 0

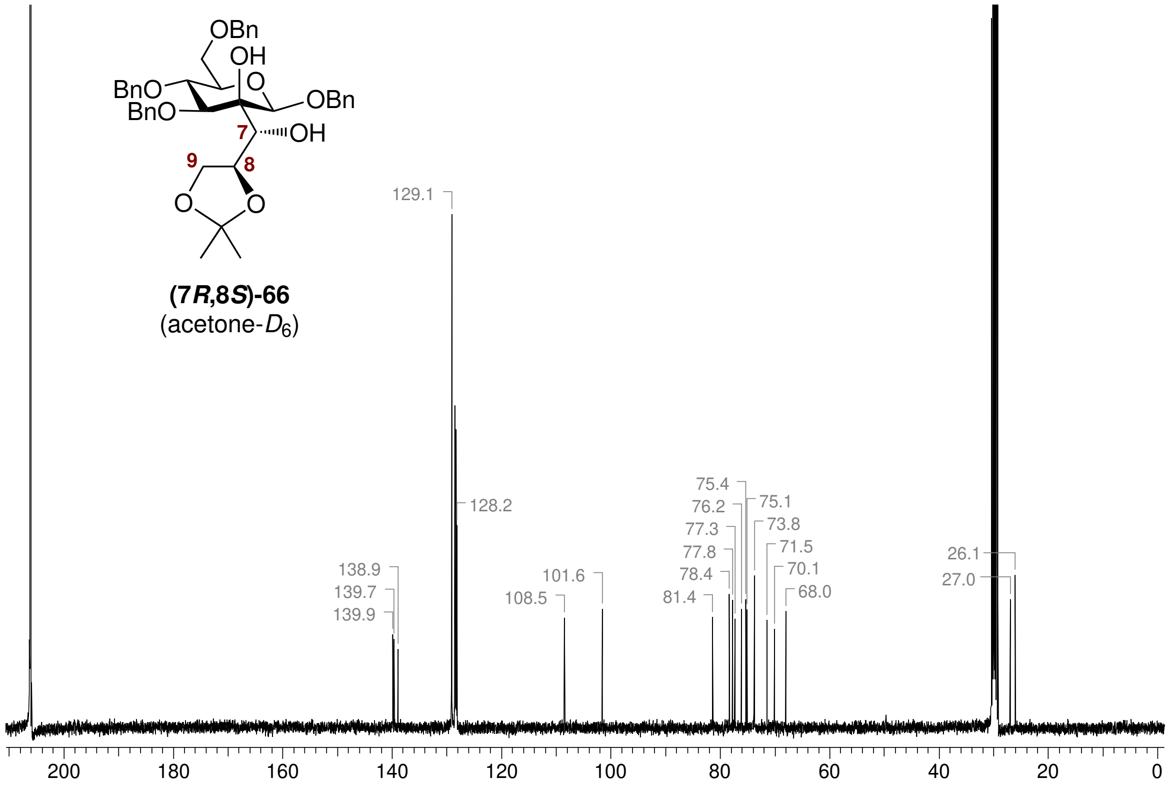
OBn
OH
O
BnO
BnO
OBn
7
OH
9
8
O
O
(7R,8S)-66
(acetone-D_6)
129.1
128.2
138.9
139.7
139.9
101.6
108.5
75.4
76.2
77.3
77.8
78.4
81.4
75.1
73.8
71.5
70.1
68.0
26.1
27.0
200 180 160 140 120 100 80 60 40 20 0

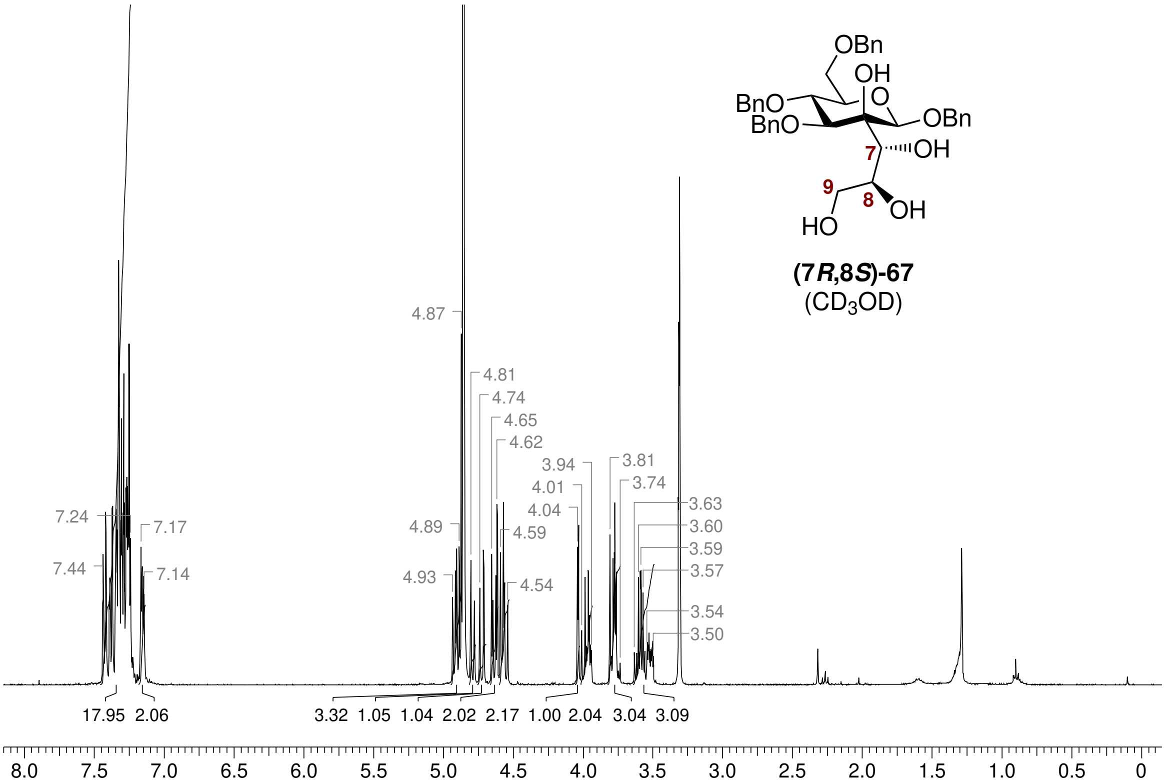

(7*R*,8*S*)-67
(CD_3OD)

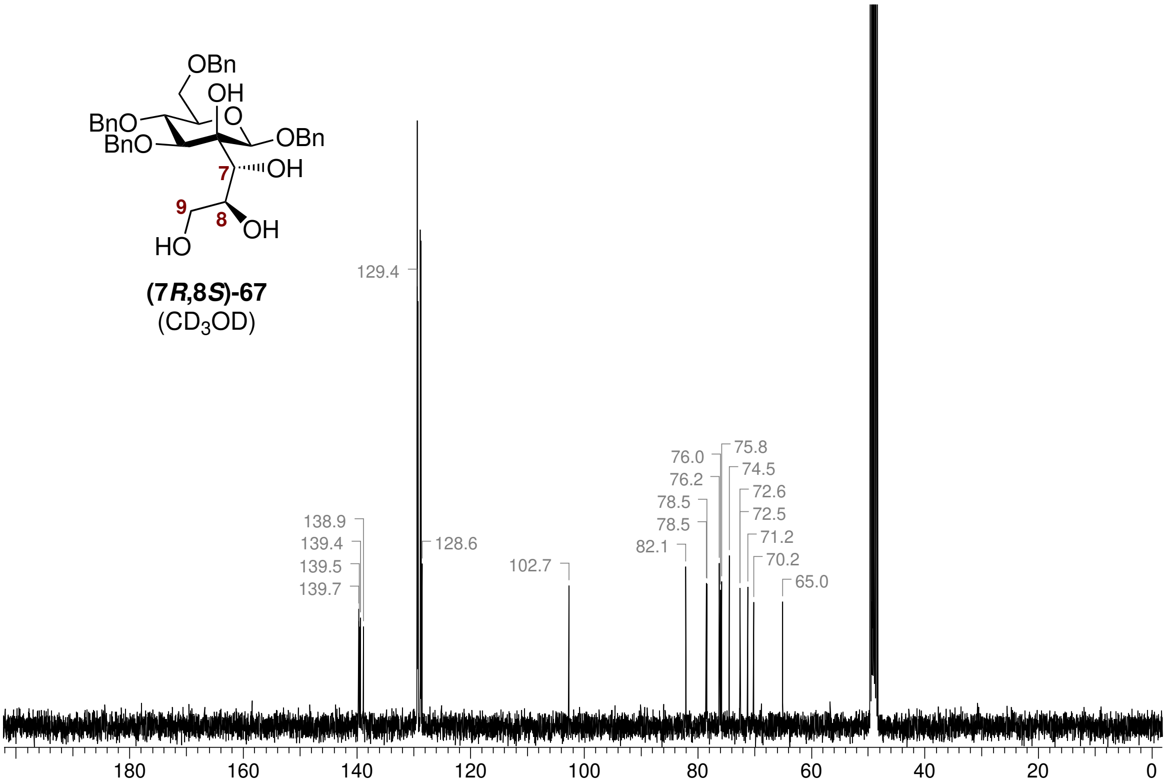

(7*R*,8*S*)-67
(CD_3OD)

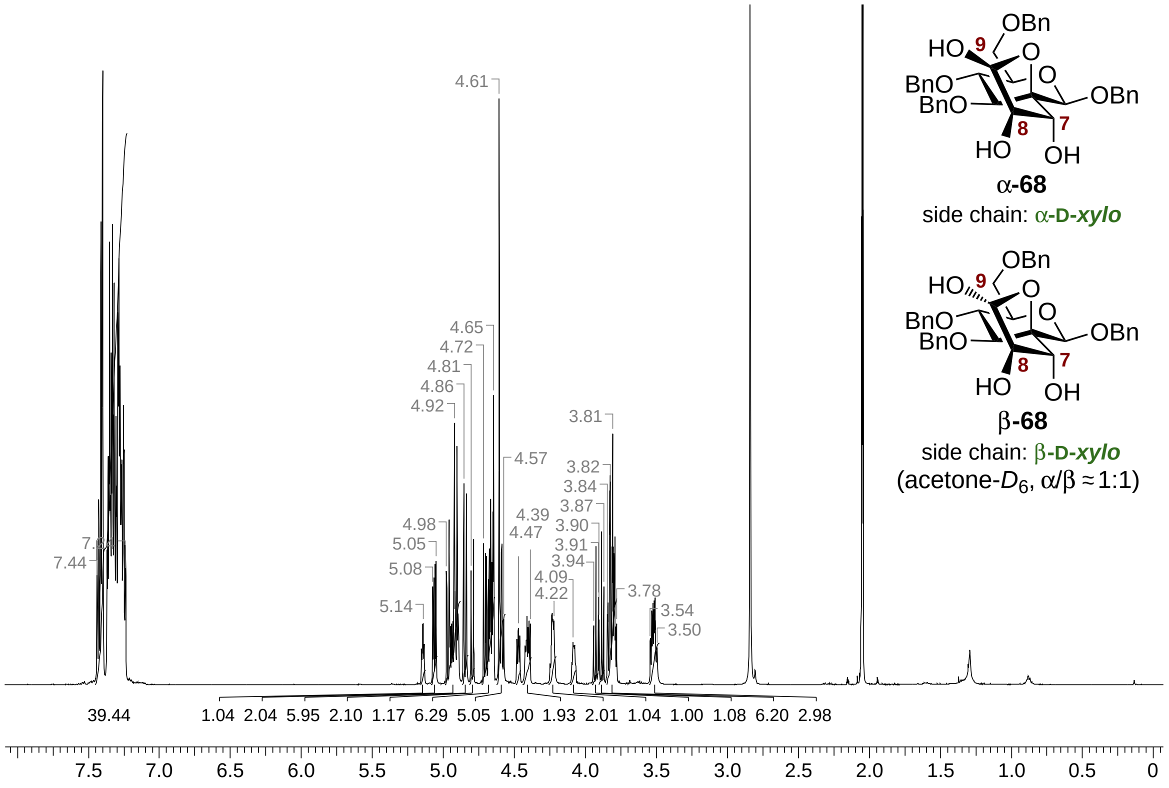

α-68
side chain: α-D-*xylo*

β-68
side chain: β-D-*xylo*
(acetone-D_6, α/β ≈ 1:1)

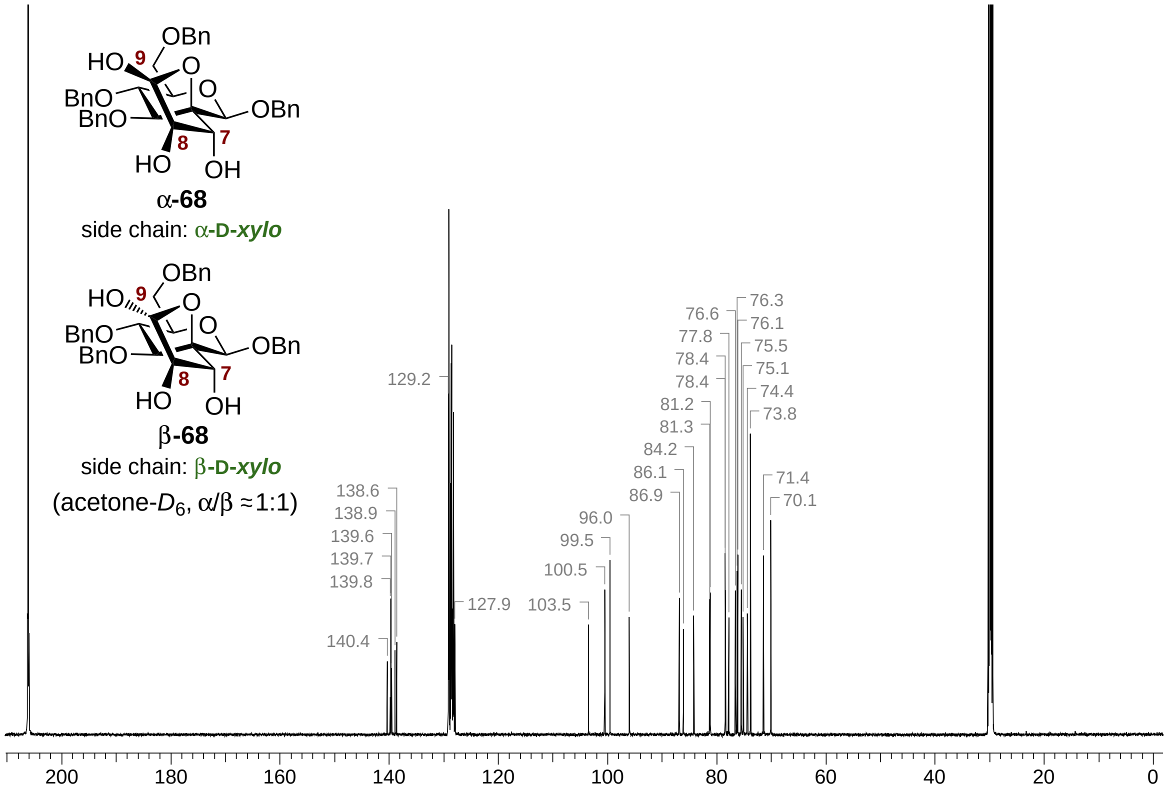

α-68
side chain: α-D-*xylo*

β-68
side chain: β-D-*xylo*
(acetone-D_6, α/β ≈ 1:1)

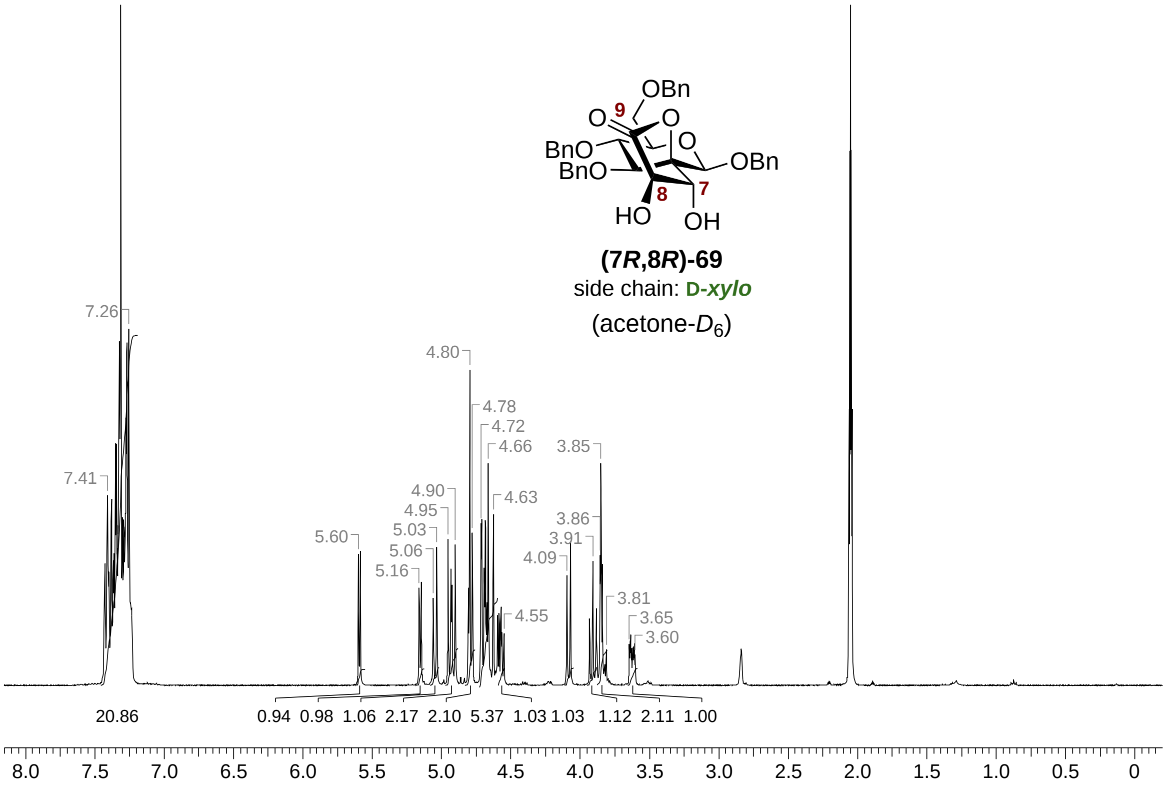
OBn
O
9
O
O
BnO
BnO
OBn
8
7
HO
OH
(7R,8R)-69
side chain: D-xylo
(acetone-D6)
7.26
7.41
5.60
5.16
5.06
5.03
4.95
4.90
4.80
4.78
4.72
4.66
4.63
4.55
4.09
3.91
3.86
3.85
3.81
3.65
3.60
20.86
0.94
0.98
1.06
2.17
2.10
5.37
1.03
1.03
1.12
2.11
1.00
8.0
7.5
7.0
6.5
6.0
5.5
5.0
4.5
4.0
3.5
3.0
2.5
2.0
1.5
1.0
0.5
0

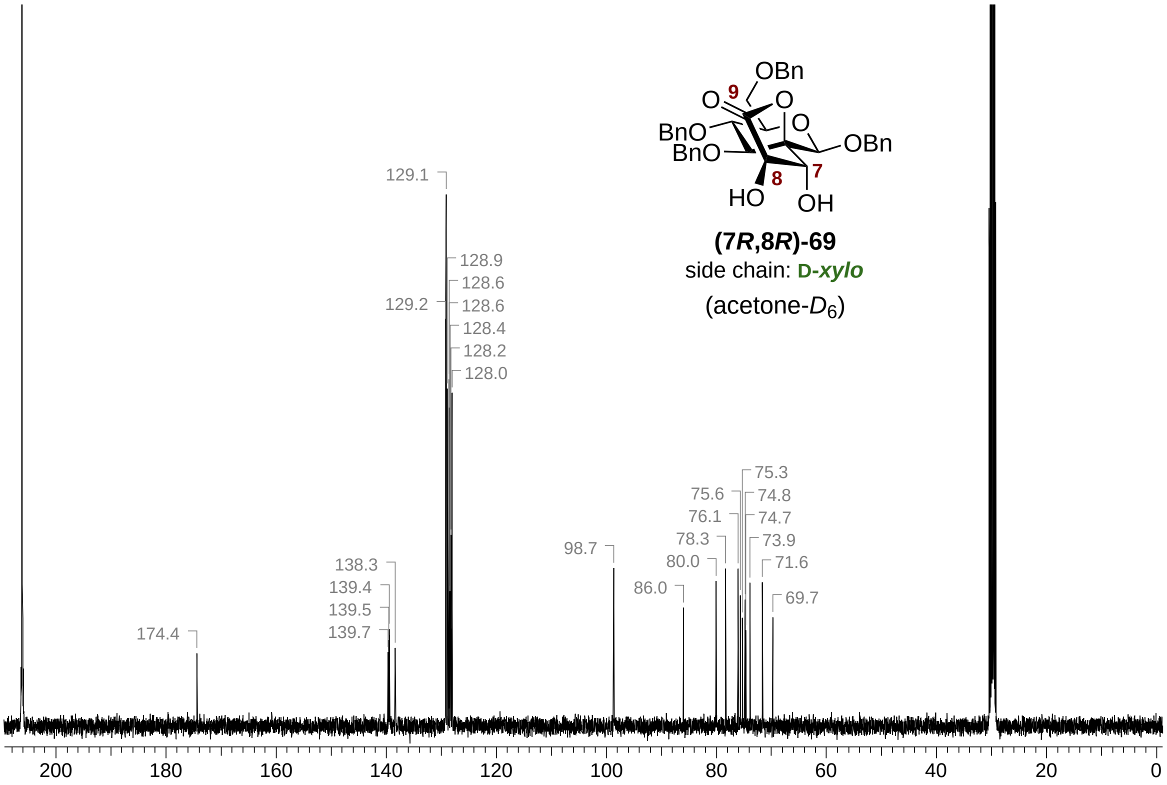
OBn
O
9
O
O
BnO
BnO
OBn
8
7
HO
OH
(7R,8R)-69
side chain: D-xylo
(acetone-D6)
129.1
129.2
128.9
128.6
128.6
128.4
128.2
128.0
138.3
139.4
139.5
139.7
174.4
98.7
86.0
80.0
78.3
76.1
75.6
75.3
74.8
74.7
73.9
71.6
69.7
200
180
160
140
120
100
80
60
40
20
0

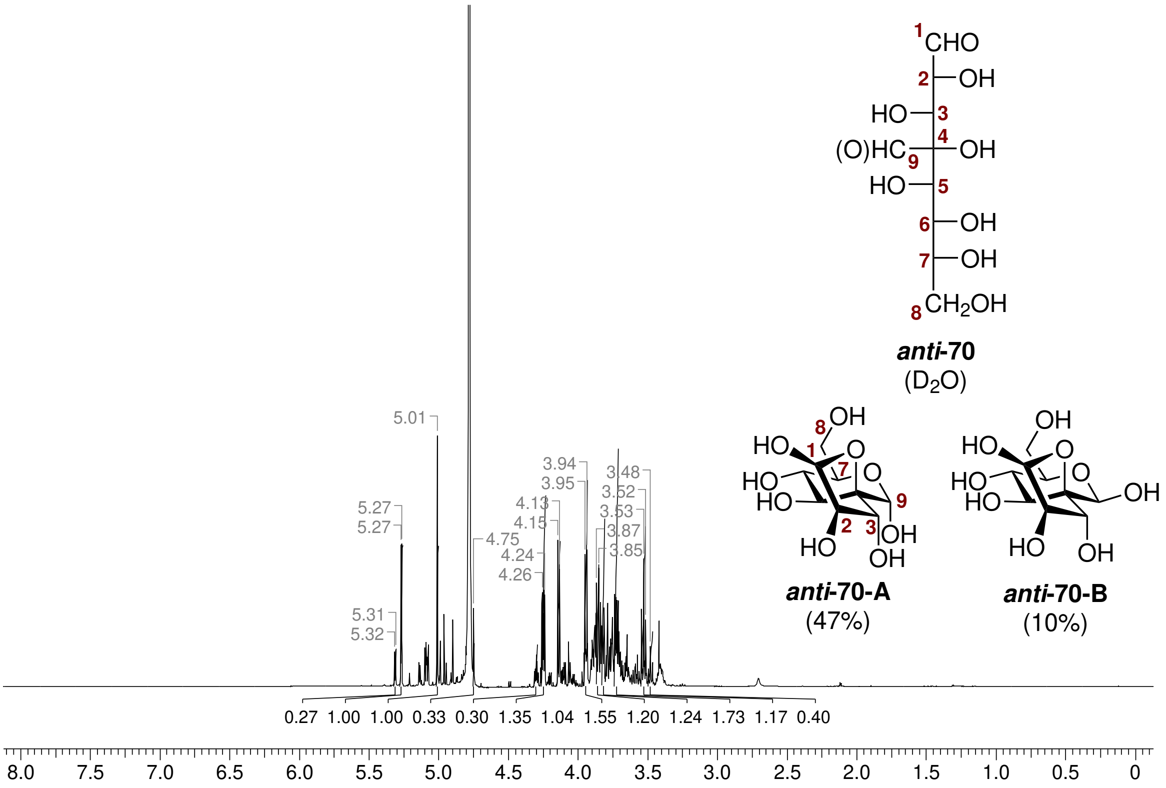
1 CHO
2 OH
HO 3
4 OH
(O)HC 9
HO 5
6 OH
7 OH
8 CH2OH
anti-70
(D2O)
anti-70-A
(47%)
anti-70-B
(10%)
5.01
5.27
5.27
5.31
5.32
4.75
4.13
4.15
4.24
4.26
3.94
3.95
3.48
3.52
3.53
3.87
3.85
0.27 1.00 1.00 0.33 0.30 1.35 1.04 1.55 1.20 1.24 1.73 1.17 0.40
8.0 7.5 7.0 6.5 6.0 5.5 5.0 4.5 4.0 3.5 3.0 2.5 2.0 1.5 1.0 0.5 0

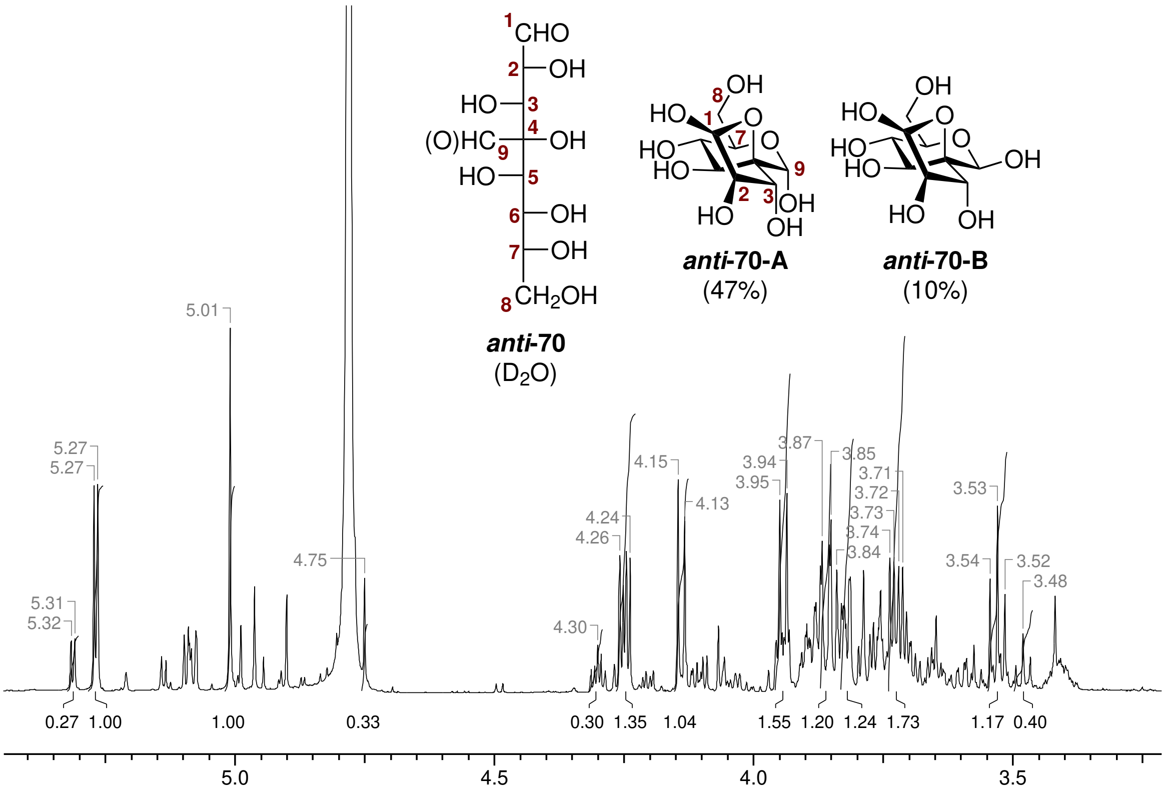
1 CHO
2 OH
HO 3
4 OH
(O)HC 9
HO 5
6 OH
7 OH
8 CH2OH
anti-70
(D2O)
anti-70-A
(47%)
anti-70-B
(10%)
5.01
5.27
5.27
5.31
5.32
4.75
4.30
4.24
4.26
4.15
4.13
3.94
3.95
3.87
3.85
3.71
3.72
3.73
3.74
3.84
3.53
3.54
3.52
3.48
0.27 1.00 1.00 0.33 0.30 1.35 1.04 1.55 1.20 1.24 1.73 1.17 0.40
5.0 4.5 4.0 3.5

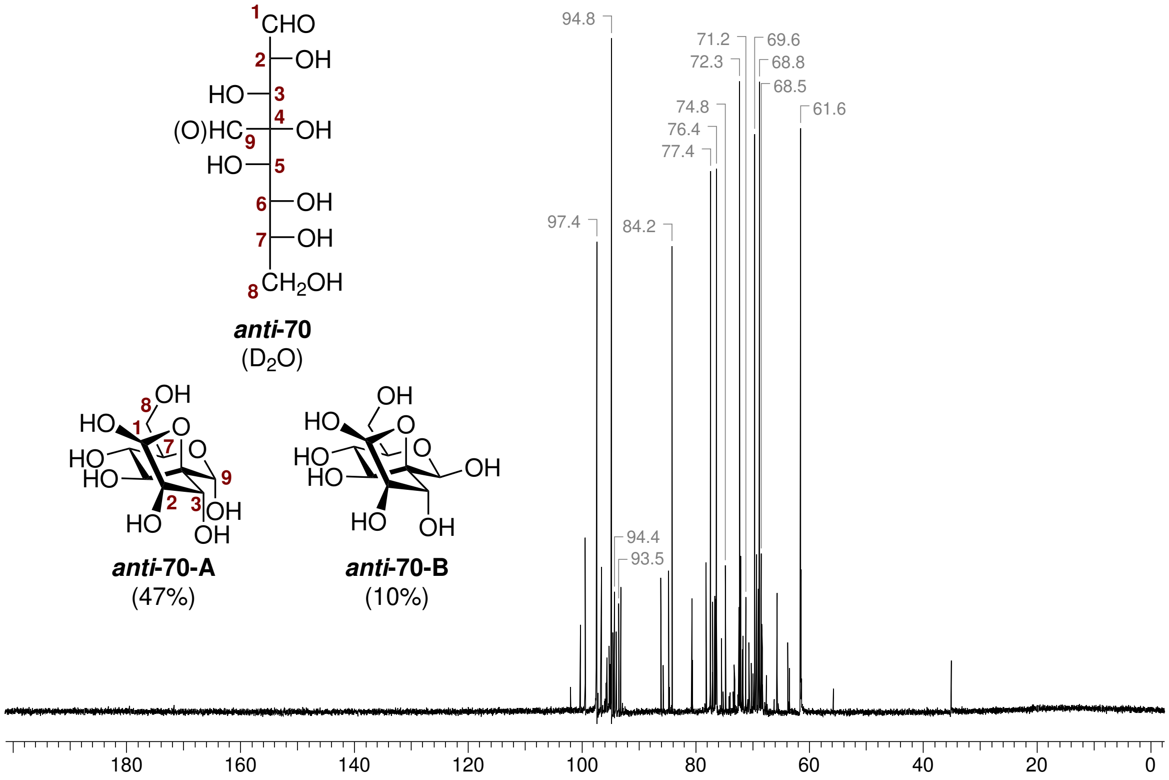
1 CHO
2 OH
HO 3
(O)HC 9 4 OH
HO 5
6 OH
7 OH
8 CH2OH
anti-70
(D2O)
8 OH
HO 1 O
7 O
HO
HO 9
2 3 OH
HO OH
anti-70-A
(47%)
OH
HO O
O
HO OH
HO
HO OH
anti-70-B
(10%)
94.8
71.2
72.3
69.6
68.8
68.5
74.8
76.4
77.4
61.6
97.4
84.2
94.4
93.5
180
160
140
120
100
80
60
40
20
0

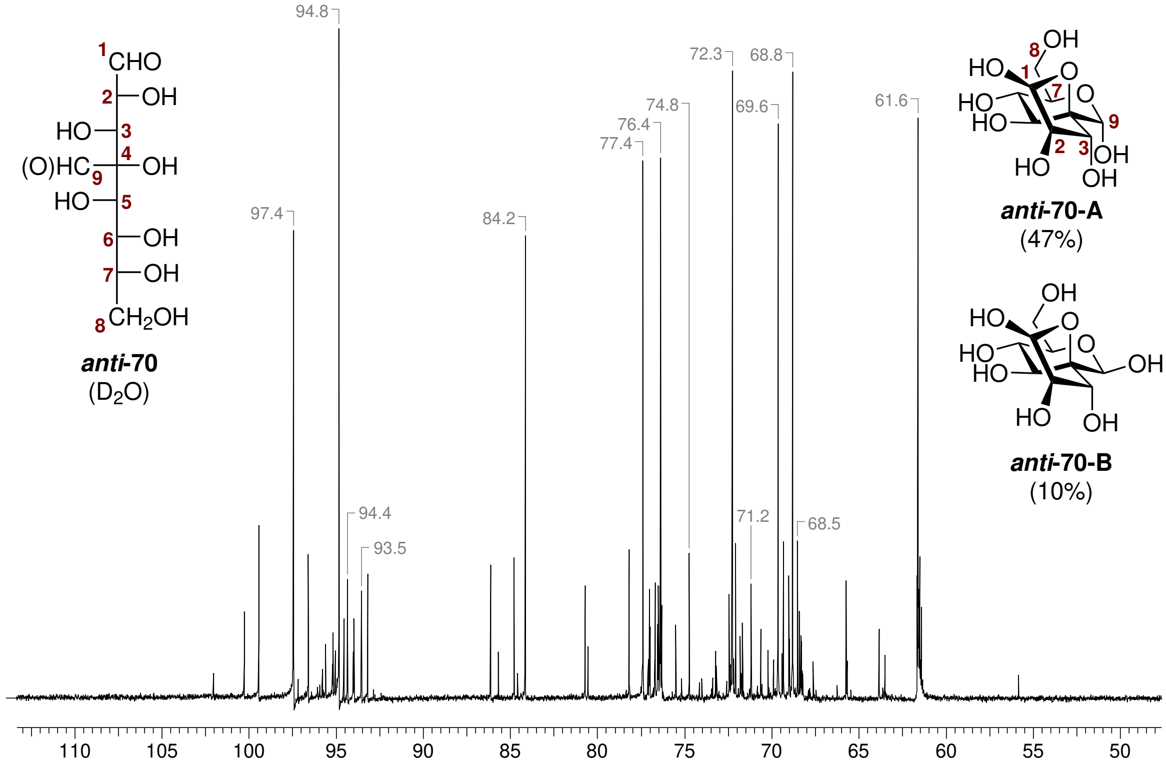
1 CHO
2 OH
HO 3
(O)HC 9 4 OH
HO 5
6 OH
7 OH
8 CH2OH
anti-70
(D2O)
94.8
72.3
68.8
74.8
69.6
61.6
76.4
77.4
97.4
84.2
94.4
93.5
71.2
68.5
8 OH
HO 1 O
7 O
HO
HO 9
2 3 OH
HO OH
anti-70-A
(47%)
OH
HO O
O
HO OH
HO
HO OH
anti-70-B
(10%)
110
105
100
95
90
85
80
75
70
65
60
55
50

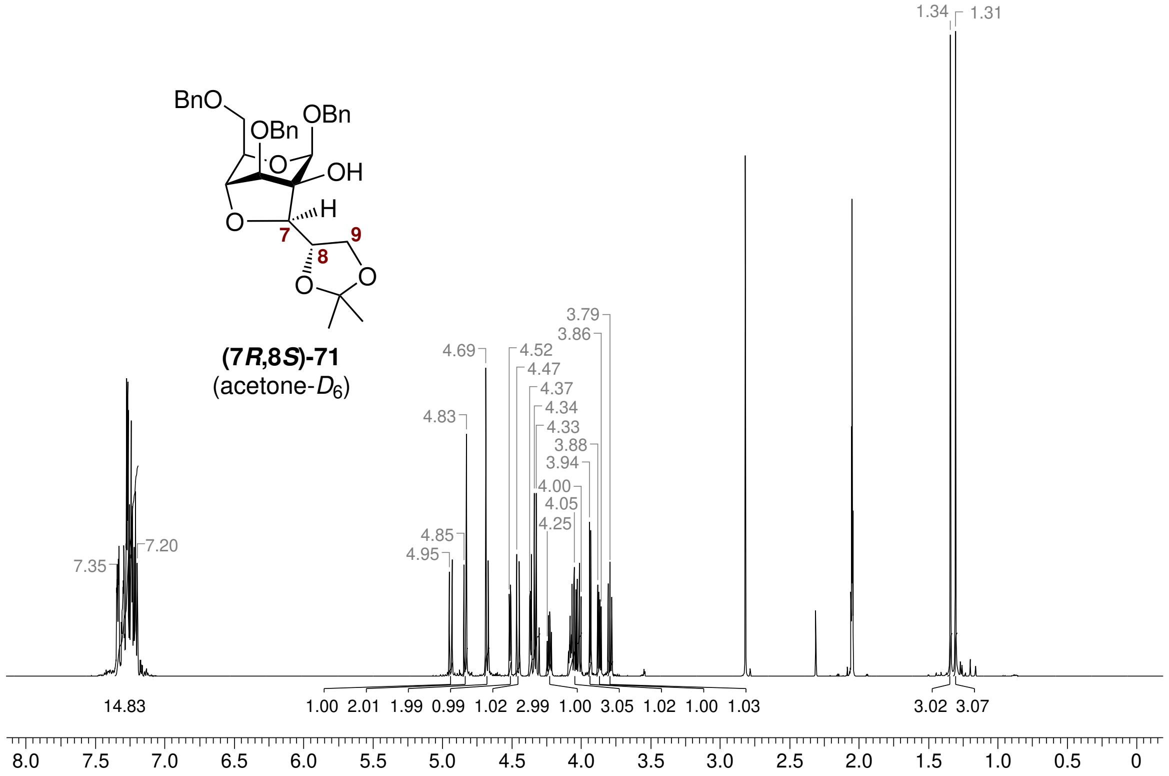
BnO
OBn
OBn
O
OH
H
O
7
8
9
O
O
(7R,8S)-71
(acetone-D6)
1.34
1.31
4.69
4.52
4.47
4.37
4.34
4.33
3.79
3.86
3.88
3.94
4.00
4.05
4.25
4.83
4.85
4.95
7.35
7.20
14.83
1.00 2.01 1.99 0.99 1.02 2.99 1.00 3.05 1.02 1.00 1.03
3.02 3.07
8.0 7.5 7.0 6.5 6.0 5.5 5.0 4.5 4.0 3.5 3.0 2.5 2.0 1.5 1.0 0.5 0

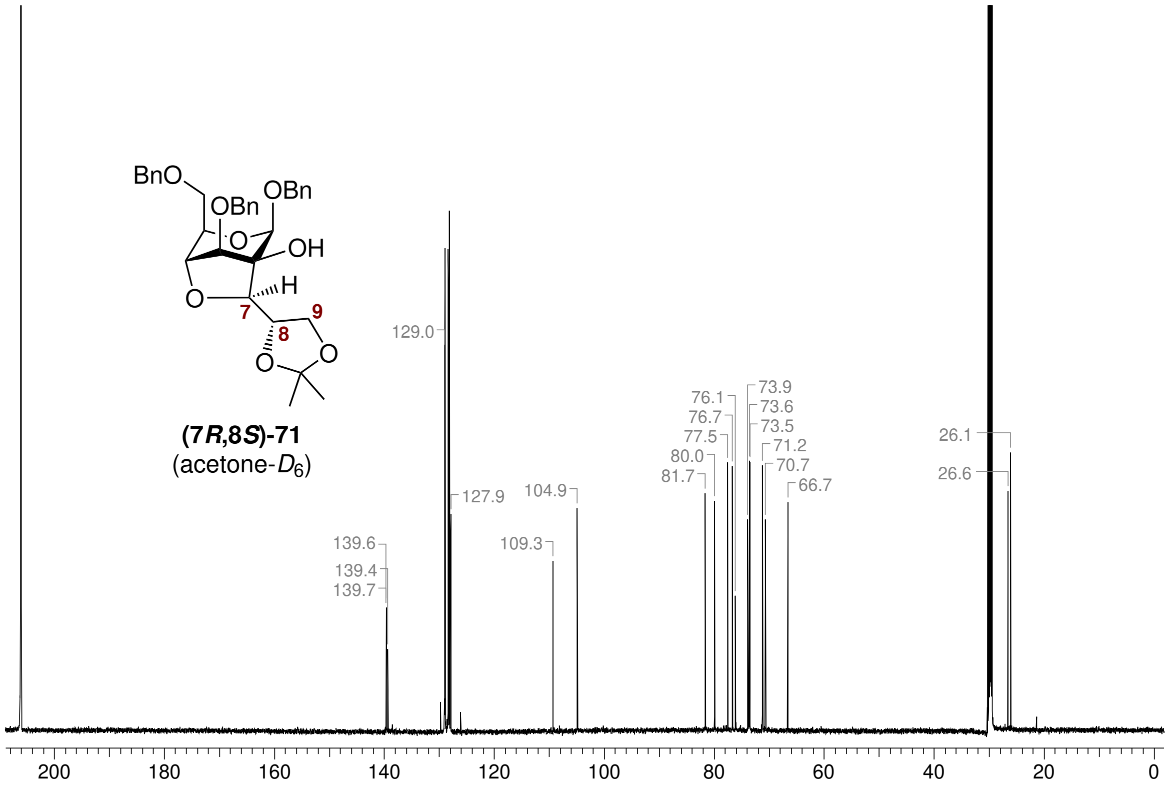
BnO
OBn
OBn
O
OH
H
O
7
8
9
O
O
(7R,8S)-71
(acetone-D6)
129.0
127.9
139.6
139.4
139.7
104.9
109.3
76.1
76.7
77.5
80.0
81.7
73.9
73.6
73.5
71.2
70.7
66.7
26.1
26.6
200 180 160 140 120 100 80 60 40 20 0

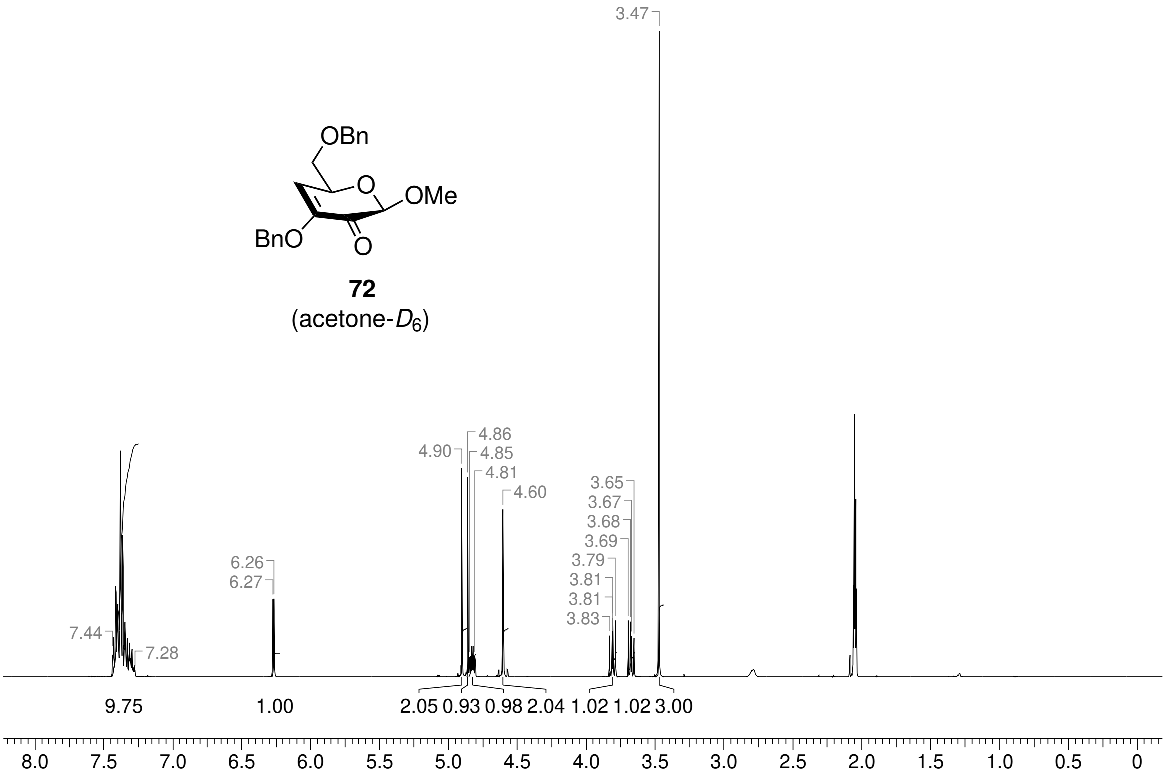
OBn
OMe
BnO
O
O
72
(acetone-D_6)
3.47
4.86
4.85
4.81
4.90
4.60
3.65
3.67
3.68
3.69
3.79
3.81
3.81
3.83
6.26
6.27
7.44
7.28
9.75
1.00
2.05
0.93
0.98
2.04
1.02
1.02
3.00
8.0
7.5
7.0
6.5
6.0
5.5
5.0
4.5
4.0
3.5
3.0
2.5
2.0
1.5
1.0
0.5
0

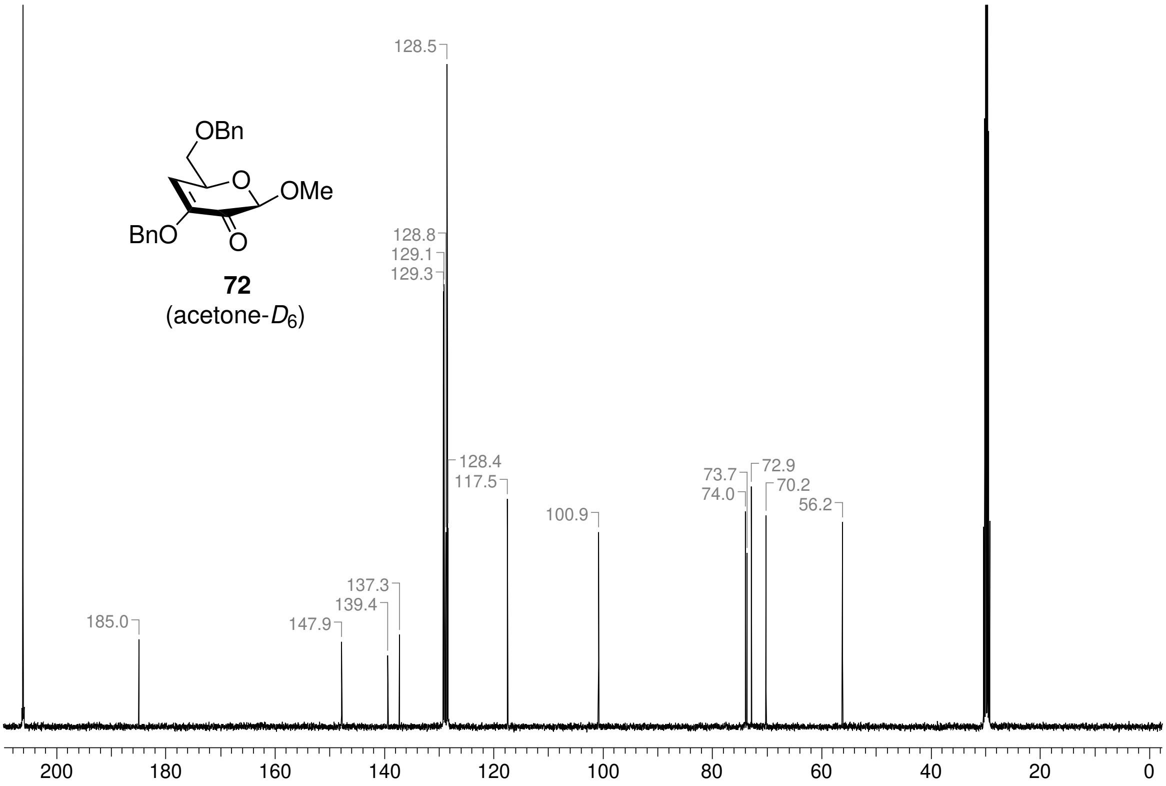
128.5
OBn
OMe
BnO
O
O
72
(acetone-D_6)
128.8
129.1
129.3
128.4
117.5
100.9
73.7
74.0
72.9
70.2
56.2
137.3
139.4
147.9
185.0
200
180
160
140
120
100
80
60
40
20
0

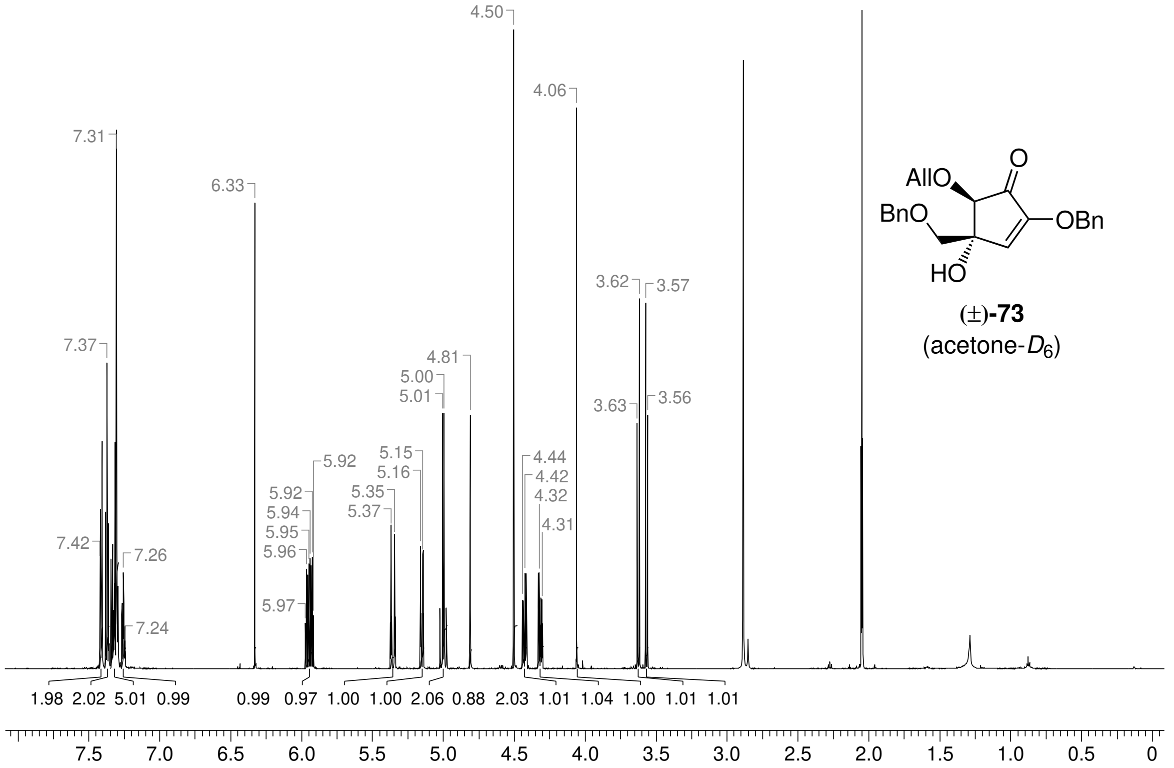

(±)-**73**
(acetone-D_6)

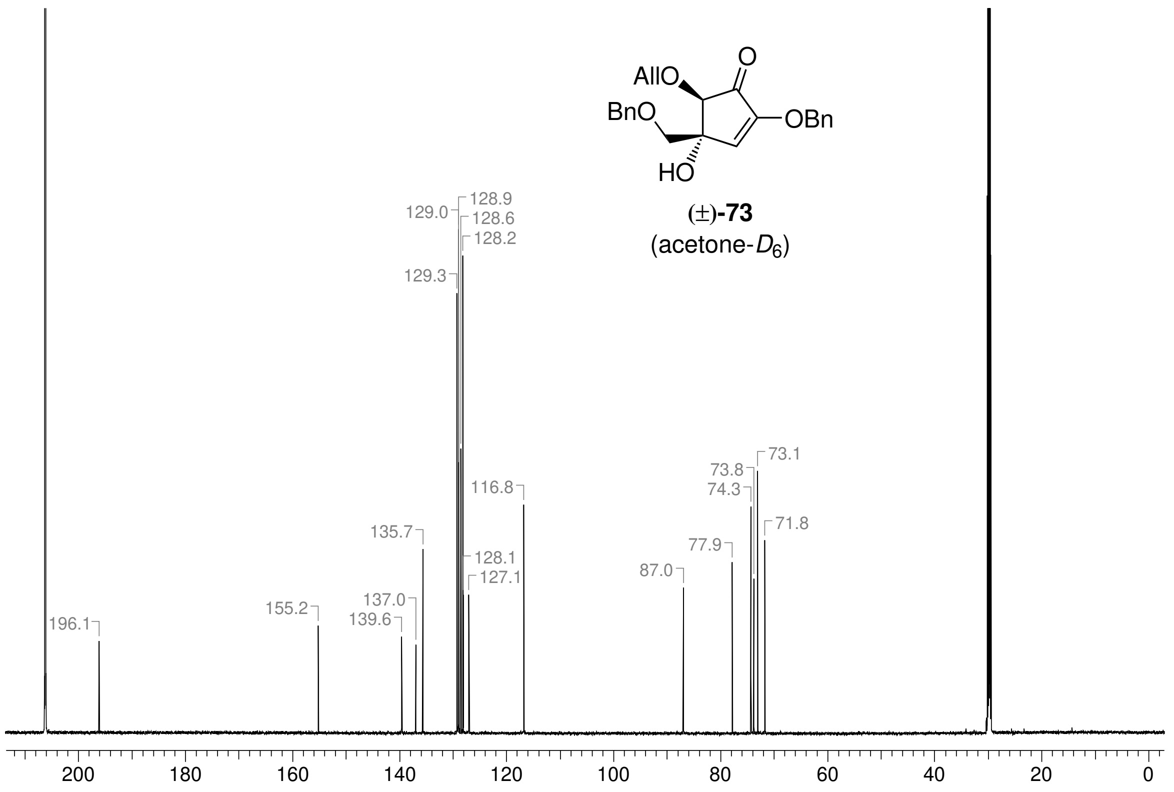

(±)-**73**
(acetone-D_6)

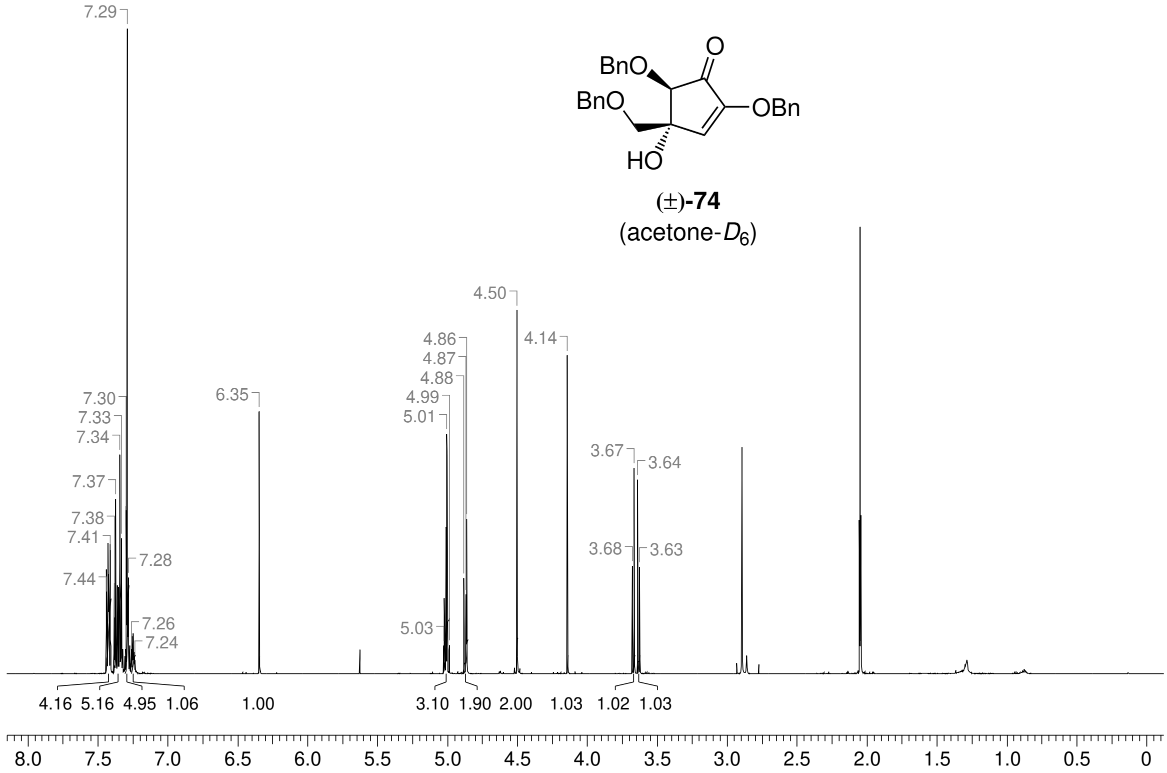

(±)-**74**
(acetone-D_6)

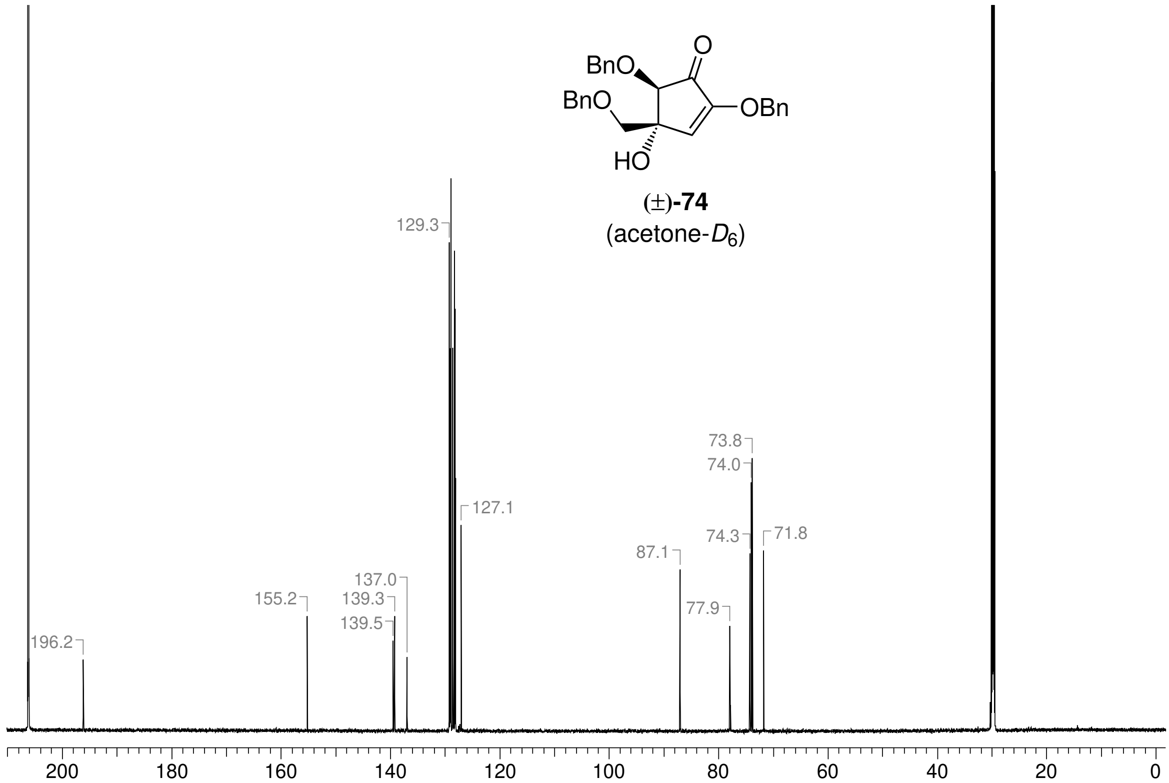

(±)-**74**
(acetone-D_6)

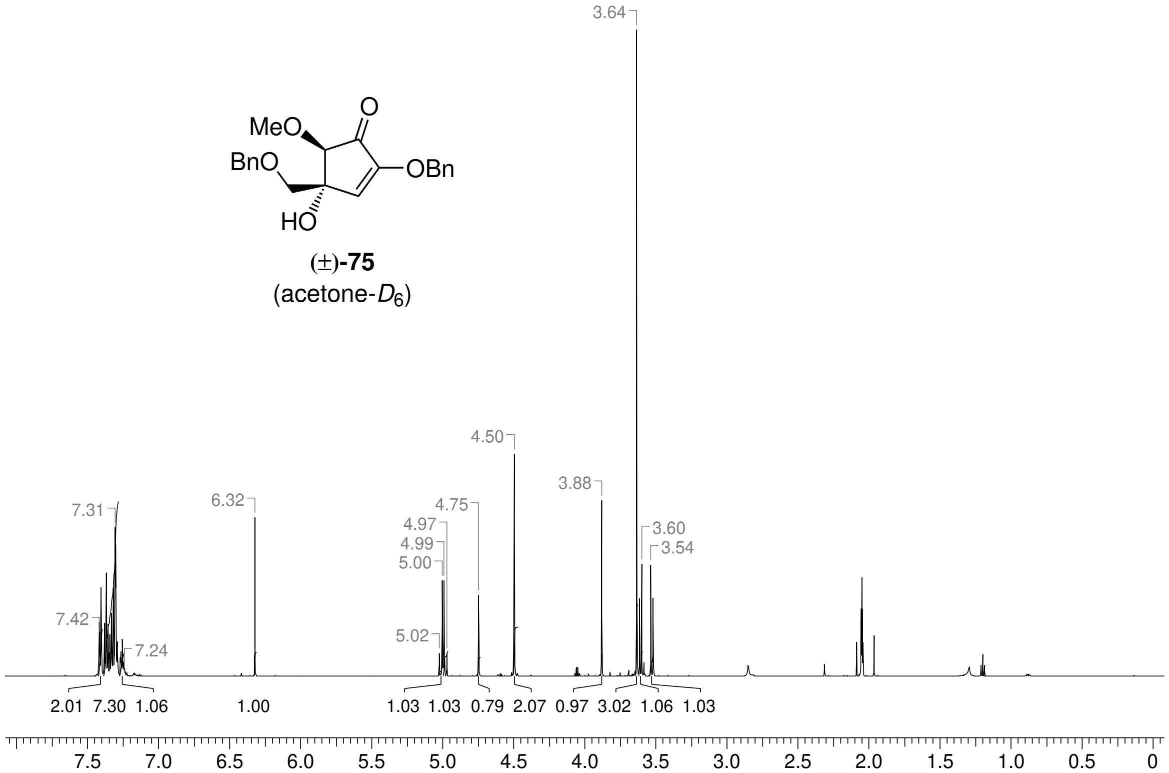
(±)-**75**
(acetone-D_6)

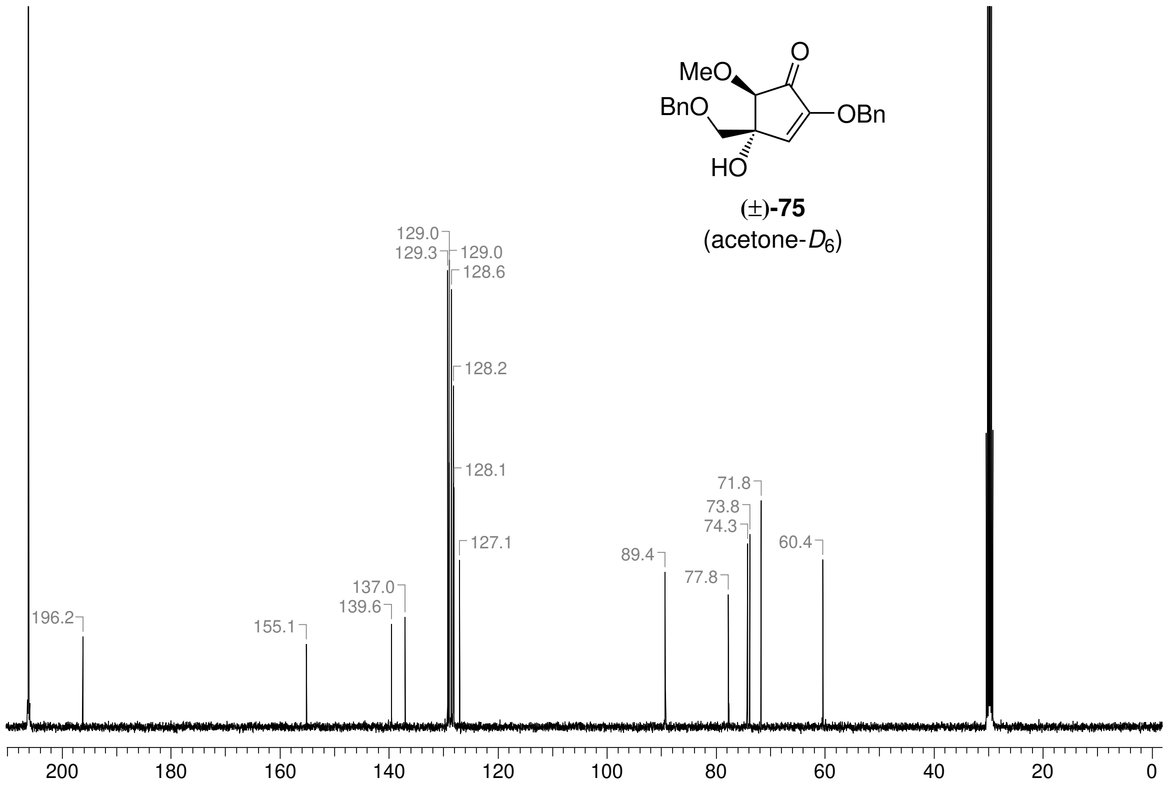
(±)-**75**
(acetone-D_6)

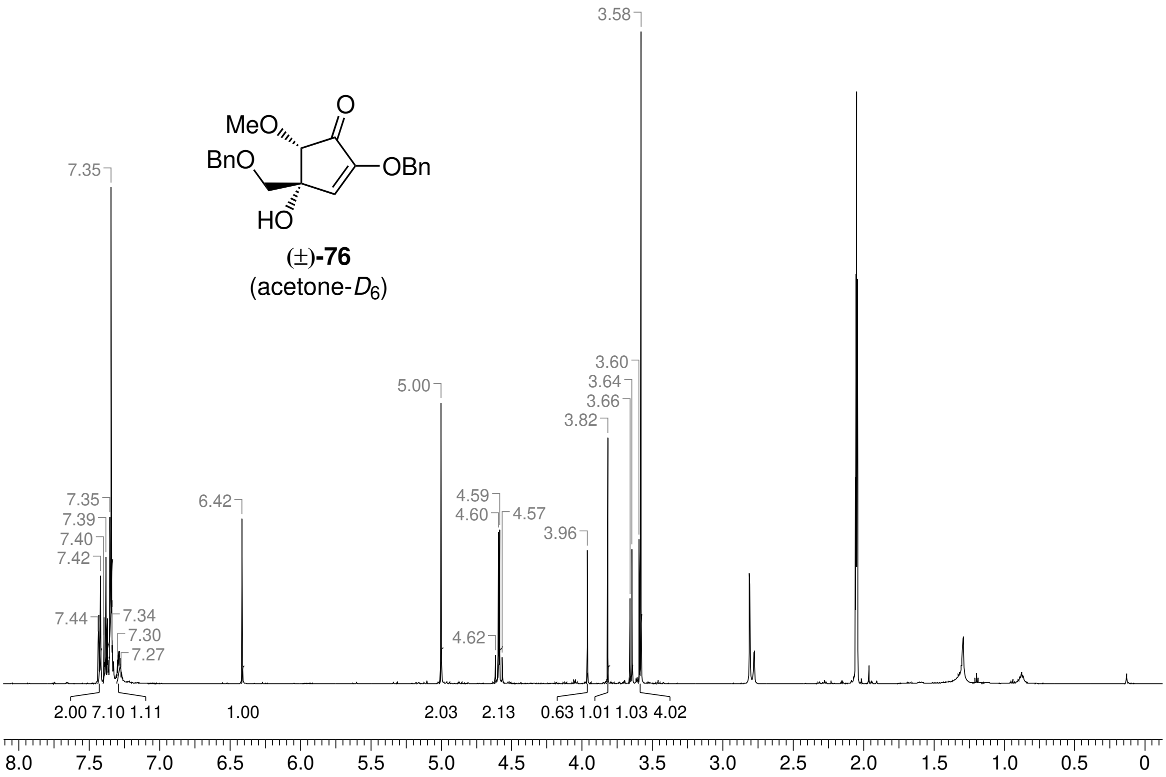
MeO
BnO
O
OBn
HO
(±)-76
(acetone-D_6)
3.58
7.35
3.60
3.64
3.66
3.82
5.00
7.35
7.39
7.40
7.42
6.42
4.59
4.60
4.57
3.96
7.44
7.34
7.30
7.27
4.62
2.00 7.10 1.11
1.00
2.03
2.13
0.63 1.01 1.03 4.02
8.0 7.5 7.0 6.5 6.0 5.5 5.0 4.5 4.0 3.5 3.0 2.5 2.0 1.5 1.0 0.5 0

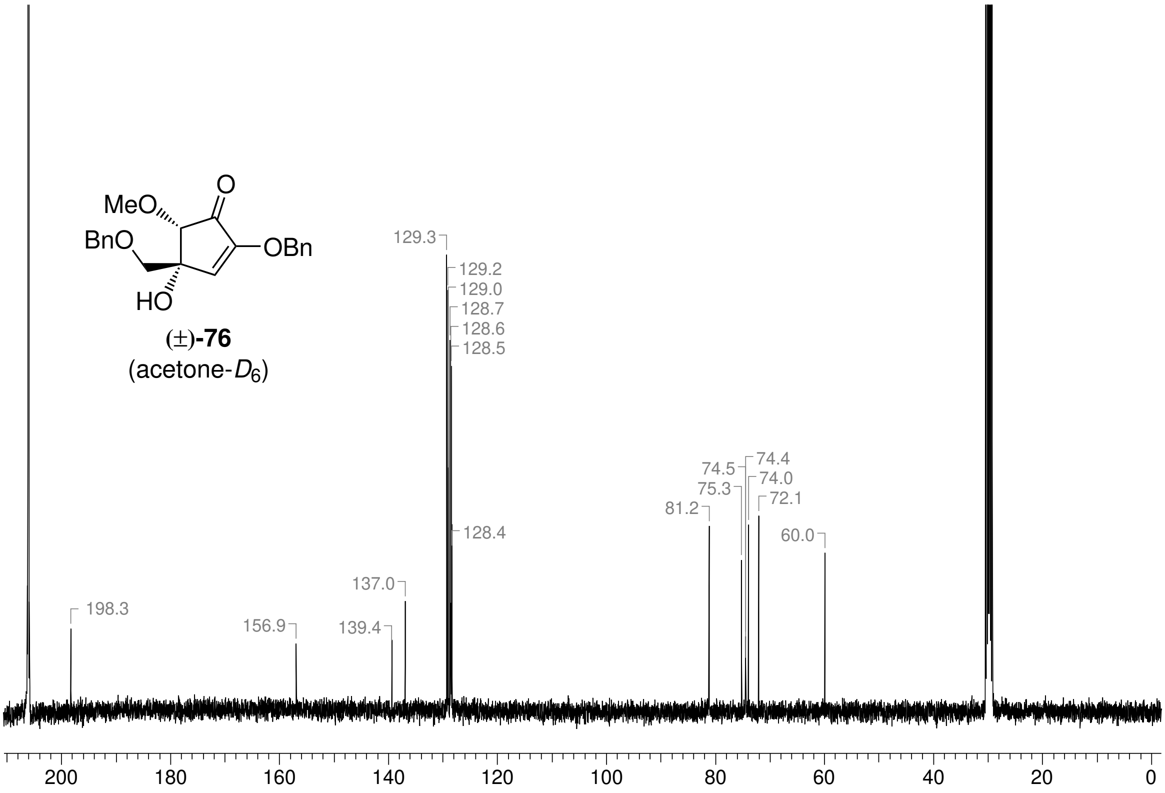
MeO
BnO
O
OBn
HO
(±)-76
(acetone-D_6)
129.3
129.2
129.0
128.7
128.6
128.5
74.5
74.4
74.0
75.3
72.1
81.2
60.0
128.4
137.0
198.3
156.9
139.4
200 180 160 140 120 100 80 60 40 20 0

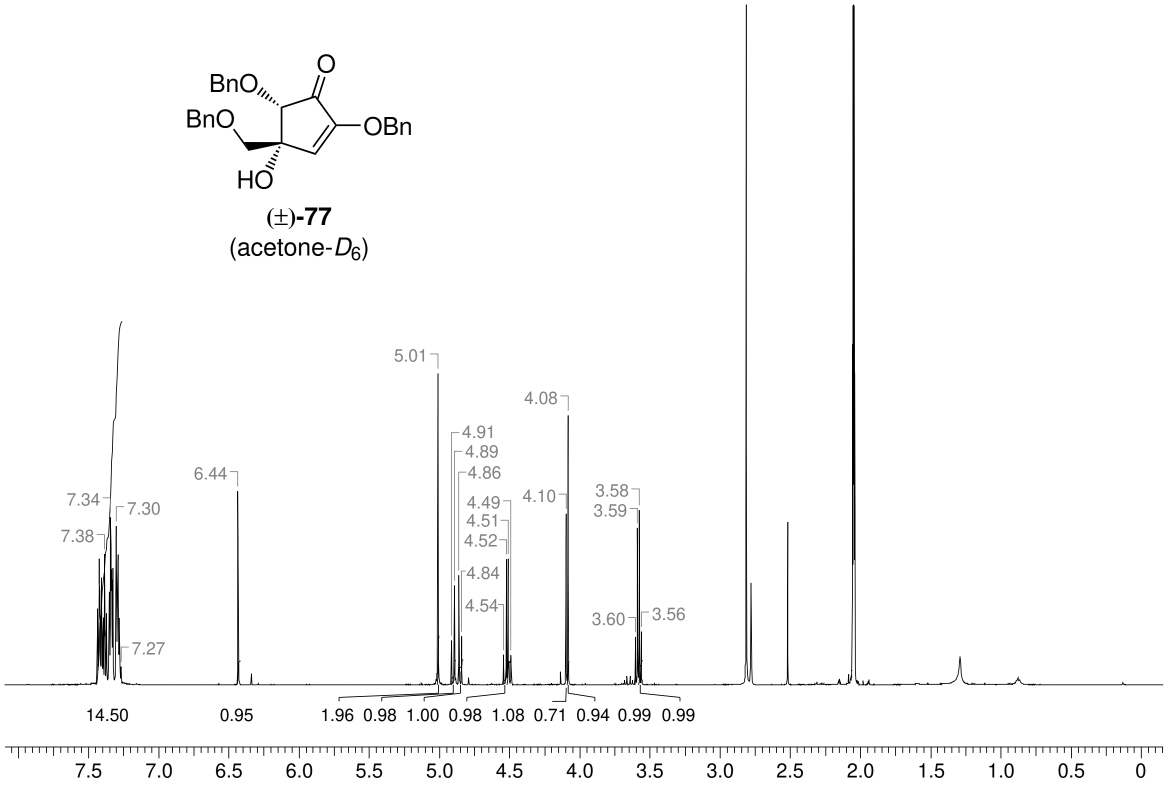
BnO
O
BnO
OBn
HO
(±)-77
(acetone-D_6)
7.34
7.30
7.38
7.27
6.44
5.01
4.91
4.89
4.86
4.49
4.51
4.52
4.84
4.54
4.08
4.10
3.58
3.59
3.60
3.56
14.50
0.95
1.96
0.98
1.00
0.98
1.08
0.71
0.94
0.99
0.99
7.5
7.0
6.5
6.0
5.5
5.0
4.5
4.0
3.5
3.0
2.5
2.0
1.5
1.0
0.5
0

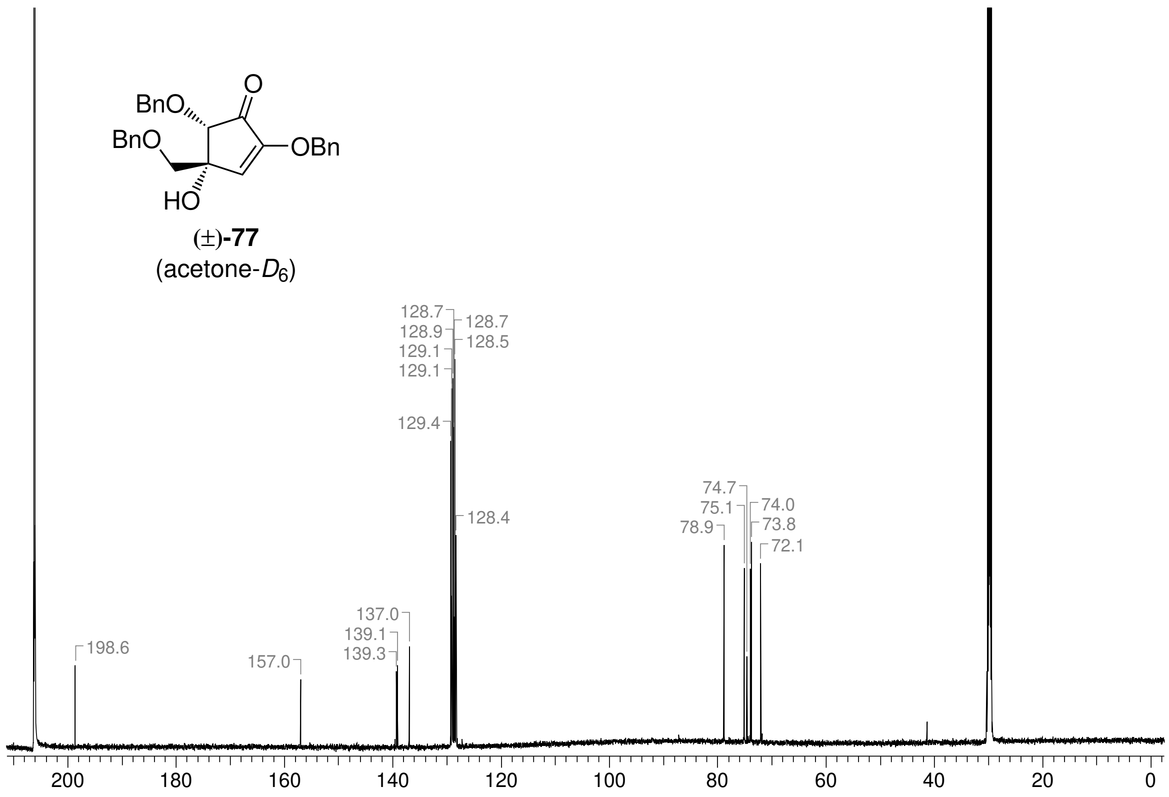
BnO
O
BnO
OBn
HO
(±)-77
(acetone-D_6)
128.7
128.9
129.1
129.1
129.4
128.7
128.5
128.4
74.7
75.1
78.9
74.0
73.8
72.1
198.6
157.0
137.0
139.1
139.3
200
180
160
140
120
100
80
60
40
20
0

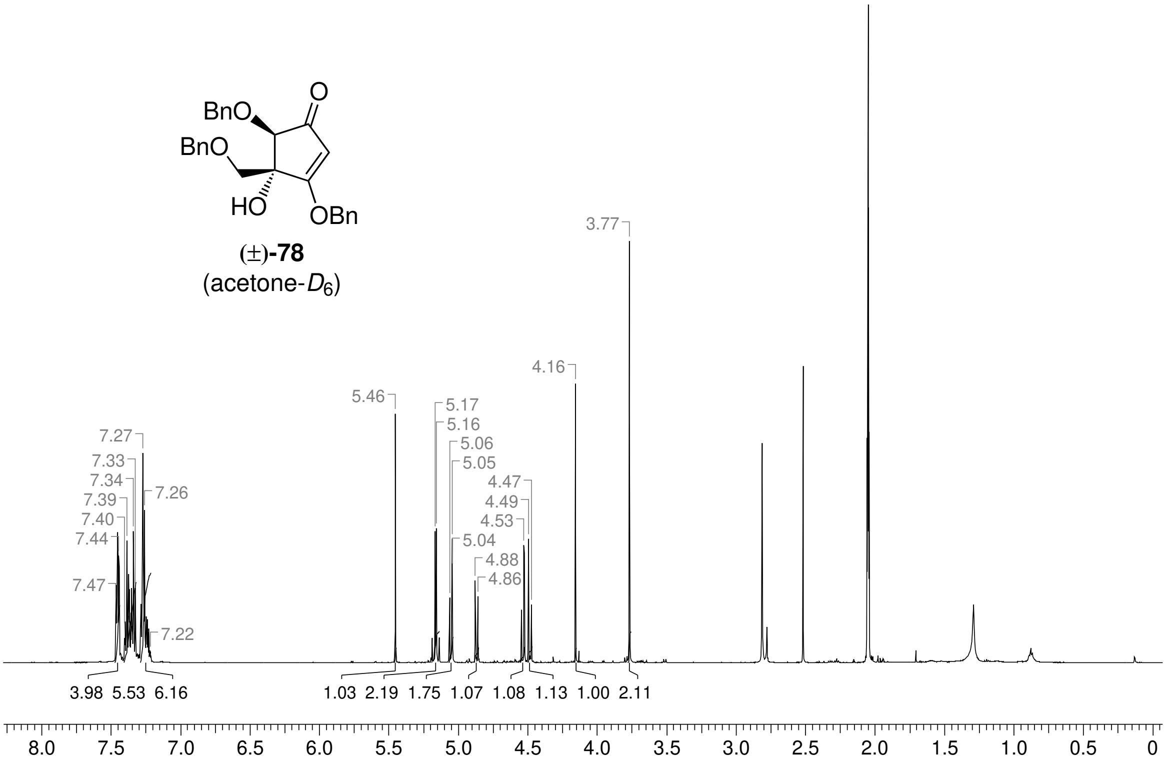
BnO
BnO
O
HO
OBn
(±)-78
(acetone-D6)
7.27
7.33
7.34
7.39
7.40
7.44
7.47
7.26
7.22
5.46
5.17
5.16
5.06
5.05
5.04
4.47
4.49
4.53
4.88
4.86
4.16
3.77
3.98 5.53 6.16
1.03 2.19 1.75 1.07 1.08 1.13 1.00 2.11
8.0 7.5 7.0 6.5 6.0 5.5 5.0 4.5 4.0 3.5 3.0 2.5 2.0 1.5 1.0 0.5 0

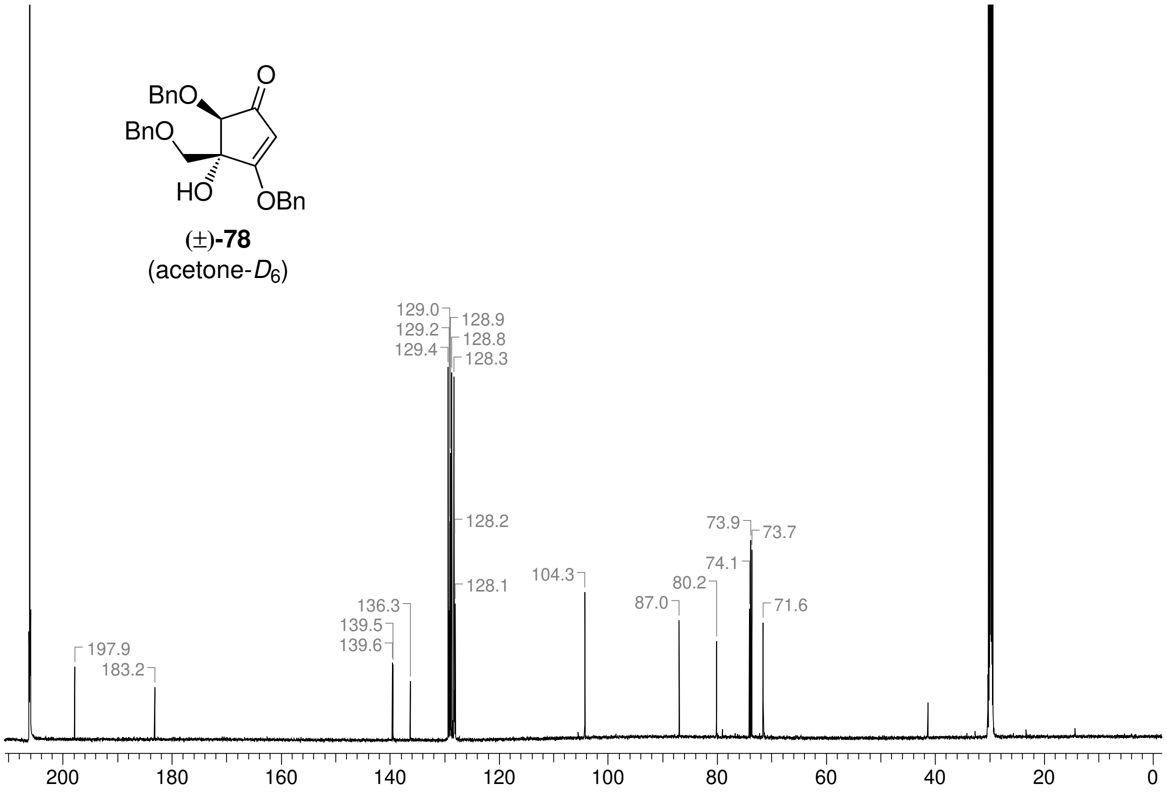
BnO
BnO
O
HO
OBn
(±)-78
(acetone-D6)
197.9
183.2
136.3
139.5
139.6
129.0
129.2
129.4
128.9
128.8
128.3
128.2
128.1
104.3
87.0
80.2
74.1
73.9
73.7
71.6
200 180 160 140 120 100 80 60 40 20 0

References

[1] J. Kost, R. Goldbart in *Handbook of Biodegradable Polymers*, (Eds.: A. J. Domb, J. Kost, D. M. Wiseman), CRC Press, Boca Raton, FL, **1997**, Chapter 14.

[2] J. M. Berg, J. L. Tymoczko, L. Stryer, *Biochemistry*, 7th ed., W. H. Freeman and Company, New York, **2011**.

[3] D. Klemm, B. Heublein, H. P. Fink, A. Bohn, *Angew. Chem. Int. Ed.* **2005**, *44*, 3358–3393, see also: *Angew. Chem.* **2005**, *117*, 3422–3458.

[4] *LMC International Ltd. for the European Commission*, Evaluation of the Community Policy for Starch and Starch Products, Final Report 2002, Brussels, **2002**.

[5] H. Ghazarian, B. Idoni, S. B. Oppenheimer, *Acta Histochem.* **2011**, *113*, 236–247.

[6] T. K. Lindhorst, *Essentials of Carbohydrate Chemistry and Biochemistry*, 3rd ed., Wiley-VCH, Weinheim, **2007**.

[7] A. Varki, *Glycobiology* **2017**, *27*, 3–49.

[8] Y. A. Knirel in *Bacterial Lipopolysaccharides*, (Eds.: Y. A. Knirel, M. A. Valvano), Springer-Verlag, Vienna, **2011**, Chapter 3, pp. 41–115.

[9] R. F. Maldonado, I. Sá-Correia, M. A. Valvano, *FEMS Microbiol. Rev.* **2016**, *40*, 480–493.

[10] J. Hansson, S. Oscarson, *Curr. Org. Chem.* **2000**, *4*, 535–564.

[11] S. N. Senchenkova, A. S. Shashkov, Y. A. Knirel, M. Ahmed, A. Mavridis, K. Rudolph, *Russ. Chem. Bull.* **2005**, *54*, 1276–1281.

[12] M. Adinolfi, M. M. Corsaro, C. De Castro, A. Evidente, R. Lanzetta, A. Molinaro, M. Parrilli, *Carbohydr. Res.* **1996**, *284*, 111–118.

[13] A. Silipo, M. R. Leone, G. Erbs, R. Lanzetta, M. Parrilli, W. S. Chang, M. A. Newman, A. Molinaro, *Angew. Chem. Int. Ed.* **2011**, *50*, 12610–12612, see also: *Angew. Chem.* **2011**, *123*, 12818–12820.

[14] W. Li, A. Silipo, A. Molinaro, B. Yu, *Chem. Commun.* **2015**, *51*, 6964–6967.

[15] K. C. Nicolaou, H. J. Mitchell, *Angew. Chem. Int. Ed.* **2001**, *40*, 1576–1624, see also: *Angew. Chem.* **2001**, *113*, 1624–1672.

[16] A. D. Mcnaught, *Pure Appl. Chem.* **1996**, *68*, 1919–2008.

[17] R. M. de Lederkremer, C. Marino, *Adv. Carbohydr. Chem. Biochem.* **2003**, *58*, 199–306.

[18] J. Gobert, M. A. Glomb, *J. Agric. Food Chem.* **2009**, *57*, 8591–8597.

[19] M. Hellwig, S. Gensberger-Reigl, T. Henle, M. Pischetsrieder, *Sem. Cancer Biol.* **2018**, *49*, 1–8.

[20] W. Zhang, A. S. Serianni, *J. Am. Chem. Soc.* **2012**, *134*, 11511–11524.

[21] K. Maurer, R. Böhme, *Ber. Dtsch. Chem. Ges. A/B* **1936**, *69*, 1399–1409.

[22] H. J. Haas, P. Schlimmer, *Liebigs Ann. Chem.* **1972**, *759*, 208–210.

[23] F. Abe, T. Yamauchi, *Chem. Pharm. Bull.* **1982**, *30*, 1183–1193.

[24] H. W. Ruelius, R. M. Kerwin, F. W. Janssen, *Biochim. Biophys. Acta* **1968**, *167*, 493–500.

[25] F. W. Janssen, H. W. Ruelius, *Biochim. Biophys. Acta* **1968**, *167*, 501–510.

[26] T. H. de Koker, M. D. Mozuch, D. Cullen, J. Gaskell, P. J. Kersten, *Appl. Environ. Microbiol.* **2004**, *70*, 5794–5800.

[27] J. Volc, E. Kubátová, D. A. Wood, G. Daniel, *Arch. Microbiol.* **1997**, *167*, 119–125.

[28] J. Volc, P. Sedmera, P. Halada, V. Přikrylová, G. Daniel, *Carbohydr. Res.* **1998**, *310*, 151–156.

[29] P. Staudigl, I. Krondorfer, D. Haltrich, C. K. Peterbauer, *Biomolecules* **2013**, *3*, 535–552.

[30] S. Köpper, S. Freimund, *Helv. Chim. Acta* **2003**, *86*, 827–843.

[31] H.-M. Liu, Y. Tsuda, *Chem. Pharm. Bull.* **1996**, *44*, 80–87.

[32] R. F. Butterworth, S. Hanessian, *Synthesis* **1971**, 70–88.

[33] O. Theander, *Acta Chem. Scand.* **1957**, *11*, 1557–1564.

[34] A. Assarsson, O. Theander, *Acta Chem. Scand.* **1958**, *12*, 1507–1511.

[35] N. A. Hughes, *Carbohydr. Res.* **1968**, *7*, 474–479.

[36] T. Nakamura, M. Shiozaki, *Tetrahedron* **2002**, *58*, 8779–8791.

[37] I. Fokt, S. Skora, C. Conrad, T. Madden, M. Emmett, W. Priebe, *Carbohydr. Res.* **2013**, *368*, 111–119.

[38] F. W. Lichtenthaler, T. Sakakibara, E. Oeser, *Carbohydr. Res.* **1977**, *59*, 47–61.

[39] F. W. Lichtenthaler, P. Jarglis, *Tetrahedron Lett.* **1980**, *21*, 1425–1428.

[40] F. W. Lichtenthaler, E. S. . El Ashry, V. H. Göckel, *Tetrahedron Lett.* **1980**, *21*, 1429–1432.

[41] F. W. Lichtenthaler, P. Jarglis, W. Hempe, *Liebigs Ann. Chem.* **1983**, 1959–1972.

[42] F. W. Lichtenthaler, U. Kläres, M. Lergenmüller, S. Schwidetzky, *Synthesis* **1992**, 179–184.

[43] F. W. Lichtenthaler, T. Schneider-Adams, *J. Org. Chem.* **1994**, *59*, 6728–6734.

[44] F. W. Lichtenthaler, *Chem. Rev.* **2011**, *111*, 5569–5609.

[45] W. Koenigs, E. Knorr, *Ber. Dtsch. Chem. Ges.* **1901**, *34*, 957–981.

[46] K. K. Liu, S. J. Danishefsky, *J. Org. Chem.* **1994**, *59*, 1892–1894.

[47] K. Sasaki, K. Tohda, *Tetrahedron Lett.* **2018**, *59*, 496–503.

[48] F. W. Lichtenthaler, *Pure Appl. Chem.* **1978**, *50*, 1343–1362.

[49] F. W. Lichtenthaler, P. Heidel, *Angew. Chem. Int. Ed.* **1969**, *8*, 978–979, see also: *Angew. Chem.* **1969**, *81*, 998–999.

[50] P. M. Collins, W. G. Overend, B. A. Rayner, *Carbohydr. Res.* **1973**, *31*, 1–16.

[51] I. Lundt, C. Pedersen, *Carbohydr. Res.* **1974**, *35*, 187–194.

[52] M. Miljković, D. Glišin, *J. Org. Chem.* **1975**, *40*, 3357–3359.

[53] M. Brehm, V. H. Göckel, P. Jarglis, F. W. Lichtenthaler, *Tetrahedron: Asymmetry* **2008**, *19*, 358–373.

[54] F. W. Lichtenthaler, K. Strobel, G. Reidel, *Carbohydr. Res.* **1976**, *49*, 57–67.

[55] S. Murao, Y. Hinode, E. Matsumura, A. Numata, K. Kawai, H. Ohishi, H. Jin, H. Oyama, T. Shin, *Biosci. Biotech. Biochem.* **1992**, *56*, 987–988.

[56] F. W. Lichtenthaler, U. Kraska, *Carbohydr. Res.* **1977**, *58*, 363–377.

[57] K. Maurer, *Ber. Dtsch. Chem. Ges. A/B* **1930**, *63*, 25–34.

[58] P. J. Beynon, P. M. Collins, P. T. Doganges, W. G. Overend, *J. Chem. Soc. C: Organic* **1966**, 1131–1136.

[59] Q. Meng, M. Hesse, *Helv. Chim. Acta* **1991**, *74*, 445–450.

[60] A. Bessmertnykh, F. Hénin, J. Muzart, *Carbohydr. Res.* **2004**, *339*, 1377–1380.

[61] V. Draghetti, L. Poletti, D. Prosperi, L. Lay, *J. Carb. Chem.* **2001**, *20*, 813–819.

[62] S. A. Nepogodiev, Z. Pakulski, A. Zamojski, O. Holst, H. Brade, *Carbohydr. Res.* **1992**, *232*, 33–45.

[63] N. K. Kochetkov, A. J. Khorlin, A. F. Bochkov, *Tetrahedron* **1967**, *23*, 693–707.

[64] Z. Yang, W. Lin, B. Yu, *Carbohydr. Res.* **2000**, *329*, 879–884.

[65] R. U. Lemieux, K. B. Hendriks, R. V. Stick, K. James, *J. Am. Chem. Soc.* **1975**, *97*, 4056–4062.

[66] G. Zemplén, A. Gerecs, I. Hadácsy, *Ber. Dtsch. Chem. Ges. A/B* **1936**, *69*, 1827–1828.

[67] C. Mayato, R. L. Dorta, J. T. Vázquez, *Tetrahedron: Asymmetry* **2004**, *15*, 2385–2397.

[68] D. B. Dess, J. C. Martin, *J. Org. Chem.* **1983**, *48*, 4155–4156.

[69] G. Ekborg, B. Lindberg, J. Lönngren, *Acta Chem. Scand.* **1972**, *26*, 3287–3292.

[70] X. Wu, T. Lipinski, E. Paszkiewicz, D. R. Bundle, *Chem. Eur. J.* **2008**, *14*, 6474–6482.

[71] L. Cipolla, L. Lay, F. Nicotra, *J. Org. Chem.* **2002**, *62*, 6678–6681.

[72] I. Adorjan, T. Rosenau, A. Potthast, P. Kosma, K. Mereiter, J. Pauli, C. Jäger, *Carbohydr. Res.* **2004**, *339*, 795–799.

[73] S. I. Awan, D. B. Werz, *Bioorg. Med. Chem.* **2012**, *20*, 1846–1856.

[74] R. Giuliano, *Curr. Org. Chem.* **2014**, *18*, 1686–1700.

[75] Y. D. Vankar, T. Linker, *Eur. J. Org. Chem.* **2015**, 7633–7642.

[76] I. Vilotijevic, T. F. Jamison, *Mar. Drugs* **2010**, *8*, 763–809.

[77] S. Hanessian, R. Roy, *Can. J. Chem.* **1985**, *63*, 163–172.

[78] F. W. Lichtenthaler, E. Cuny, O. Sakanaka, *Angew. Chem.* **2005**, *117*, 5024–5028, see also: *Angew. Chem. Int. Ed.* **2005**, *44*, 4944–4948.

[79] D. Hager, C. Paulitz, J. Tiebes, P. Mayer, D. Trauner, *J. Org. Chem.* **2013**, *78*, 10784–10801.

[80] P. M. Vadhadiya, C. V. Ramana, *Org. Lett.* **2015**, *17*, 1724–1727.

[81] B. Fraser-Reid, L. Magdzinski, B. F. Molino, D. R. Mootoo, *J. Org. Chem.* **1987**, *52*, 4495–4504.

[82] B. Fraser-Reid, B. F. Molino, L. Magdzinski, D. R. Mootoo, *J. Org. Chem.* **1987**, *52*, 4505–4511.

[83] S. J. Pérez, P. O. Miranda, D. A. Cruz, I. Fernández, V. S. Martín, J. I. Padrón, *Synthesis* **2015**, *47*, 1791–1798.

[84] G. Horne, F. X. Wilson, J. Tinsley, D. H. Williams, R. Storer, *Drug Discovery Today* **2011**, *16*, 107–118.

[85] B. G. Reddy, Y. D. Vankar, *Angew. Chem. Int. Ed.* **2005**, *44*, 2001–2004, see also: *Angew. Chem.* **2005**, *117*, 2037–2040.

[86] K. Ohtsubo, J. D. Marth, *Cell* **2006**, *126*, 855–867.

[87] T. M. Gloster, *Biochem. Soc. Trans.* **2012**, *40*, 913–928.

[88] A. Mallick, Y. D. Vankar, *Eur. J. Org. Chem.* **2014**, 4155–4161.

[89] R. Lahiri, A. A. Ansari, Y. D. Vankar, *Chem. Soc. Rev.* **2013**, *42*, 5102–5118.

[90] R. H. Grubbs, S. J. Miller, G. C. Fu, *Acc. Chem. Res.* **1995**, *28*, 446–452.

[91] D. D. Dhavale, M. M. Matin, *Tetrahedron* **2004**, *60*, 4275–4281.

[92] M. Malik, G. Witkowski, M. Ceborska, S. Jarosz, *Org. Lett.* **2013**, *15*, 6214–6217.

[93] A. A. Ansari, P. Rajasekaran, M. M. Khan, Y. D. Vankar, *J. Org. Chem.* **2014**, *79*, 1690–1699.

[94] M. Malinowski, T. Rowicki, P. Guzik, M. Wielechowska, W. Sas, *Eur. J. Org. Chem.* **2018**, 763–771.

[95] V. R. Doddi, P. K. Kancharla, Y. S. Reddy, A. Kumar, Y. D. Vankar, *Carbohydr. Res.* **2009**, *344*, 606–612.

[96] R. J. Ferrier, W. G. Overend, A. E. Ryan, *J. Chem. Soc.* **1962**, 3667–3670.

[97] M. Scholl, S. Ding, C. W. Lee, R. H. Grubbs, *Org. Lett.* **1999**, *1*, 953–956.

[98] V. Sharma, M. Ichikawa, H. H. Freeze, *Biochem. Biophys. Res. Commun.* **2014**, *453*, 220–228.

[99] K. Bock, C. Pedersen, *J. Chem. Soc. Perkin Trans. 2* **1974**, 293–297.

[100] K. Bock, C. Pedersen, *Acta Chem. Scand. B* **1975**, *29*, 258–264.

[101] E. Cleator, C. F. McCusker, F. Steltzer, S. V. Ley, *Tetrahedron Lett.* **2004**, *45*, 3077–3080.

[102] S. B. Garber, J. S. Kingsbury, B. L. Gray, A. H. Hoveyda, *J. Am. Chem. Soc.* **2000**, *122*, 8168–8179.

[103] S. Gessler, S. Randl, S. Blechert, *Tetrahedron Lett.* **2000**, *41*, 9973–9976.

[104] V. VanRheenen, R. C. Kelly, D. Cha, *Tetrahedron Lett.* **1976**, *17*, 1973–1976.

[105] J. K. Cha, W. J. Christ, Y. Kishi, *Tetrahedron Lett.* **1983**, *24*, 3943–3946.

[106] J. K. Cha, W. J. Christ, Y. Kishi, *Tetrahedron* **1984**, *40*, 2247–2255.

[107] R. C. Fuson, M. T. Mon, *J. Org. Chem.* **1961**, *26*, 756–758.

[108] D. B. Ushakov, V. Navickas, M. Ströbele, C. Maichle-Mössmer, F. Sasse, M. E. Maier, *Org. Lett.* **2011**, *13*, 2090–2093.

[109] H. Zong, H. Huang, J. Liu, G. Bian, L. Song, *J. Org. Chem.* **2012**, *77*, 4645–4652.

[110] T. Imamoto, N. Takiyama, K. Nakamura, *Tetrahedron Lett.* **1985**, *26*, 4763–4766.

[111] A. Metzger, A. Gavryushin, P. Knochel, *Synlett* **2009**, 1433–1436.

[112] O. Achmatowicz Jr., J. Jurczak, A. Konowal, A. Zamojski, *Org. Magn. Reson.* **1970**, *2*, 55–62.

[113] N. L. Holder, *Chem. Rev.* **1982**, *82*, 287–332.

[114] H. Abe, Y. Horii, M. Hagiwara, T. Kobayashi, H. Ito, *Chem. Commun.* **2015**, *51*, 6108–6110.

[115] A. E. DeCamp, S. G. Mills, A. T. Kawaguchi, R. Desmond, R. A. Reamer, L. Dimichele, R. P. Volante, *J. Org. Chem.* **1991**, *56*, 3564–3571.

[116] M. Malik, S. Jarosz, *Beilstein J. Org. Chem.* **2016**, *12*, 2602–2608.

[117] S. Dubbu, Y. D. Vankar, *Eur. J. Org. Chem.* **2017**, 5986–6002.

[118] E. J. Corey, R. Noyori, *Tetrahedron Lett.* **1970**, *4*, 311–313.

[119] M. S. Cooper, H. Heaney, A. J. Newbold, W. R. Sanderson, *Synlett* **1990**, 533–535.

[120] B.-L. Wang, H.-T. Gao, W. D. Z. Li, *J. Org. Chem.* **2015**, *80*, 5296–5301.

[121] W. Adam, J. Bialas, L. Hadjiarapoglou, *Chem. Ber.* **1991**, *124*, 2377.

[122] K. B. Sharpless, T. R. Verhoeven, *Aldrichimica Acta* **1979**, *12*, 63–73.

[123] A. H. Hoveyda, D. A. Evans, G. C. Fu, *Chem. Rev.* **1993**, *93*, 1307–1370.

[124] K. B. Sharpless, R. C. Michaelson, *J. Am. Chem. Soc.* **1973**, *95*, 6136–6137.

[125] L. Barriault, D. H. Deon, *Org. Lett.* **2001**, *3*, 1925–1927.

[126] W. Liu, P. J. Nichols, N. Smith, *Tetrahedron Lett.* **2009**, *50*, 6103–6105.

[127] A. Fürst, P. A. Plattner, *Helv. Chim. Acta* **1949**, *32*, 275–283.

[128] W. A. Bubb, *Concepts Magn. Reson. A* **2003**, *19*, 1–19.

[129] G. A. Jeffrey, W. Saenger, *Hydrogen Bonding in Biological Structures*, Springer-Verlag, Berlin Heidelberg, Germany, **1991**.

[130] T. Steiner, *Angew. Chem. Int Ed.* **2002**, *41*, 48–76, see also: *Angew. Chem.* **2002**, *114*, 50–80.

[131] C. Ceccarelli, G. A. Jeffrey, R. Taylor, *J. Mol. Struct.* **1981**, *70*, 255–271.

[132] G. A. Jeffrey, J. Mitra, *Acta Cryst. B.* **1983**, *B39*, 469–480.

[133] G. A. Jeffrey, *Crystallogr. Rev.* **2003**, *9*, 135–176.

[134] I. Y. Ponedel'kina, E. A. Khaibrakhmanova, V. N. Odinokov, *Russ. Chem. Rev.* **2010**, *79*, 63–75.

[135] S. D. Rychnovsky, R. Vaidyanathan, T. Beauchamp, R. Lin, P. J. Farmer, *J. Org. Chem.* **1999**, *64*, 6745–6749.

[136] L. Tebben, A. Studer, *Angew. Chem. Int. Ed.* **2011**, *50*, 5034–5068, see also: *Angew. Chem.* **2011**, *123*, 5138–5174.

[137] J. A. Cella, J. A. Kelley, E. F. Kenehan, *J. Chem. Soc. Chem. Commun.* **1974**, 943.

[138] W. F. Bailey, J. M. Bobbitt, K. B. Wiberg, *J. Org. Chem.* **2007**, *72*, 4504–4509.

[139] W. Adam, C. R. Saha-Möller, P. A. Ganeshpure, *Chem. Rev.* **2001**, *101*, 3499–3548.

[140] G. Tojo, M. Fernández, *Oxidation of Alcohols to Aldehydes and Ketones*, (Ed.: G. Tojo), Springer Science+Business Media, Inc., New York, **2006**.

[141] P. L. Anelli, C. Biffi, F. Montanari, S. Quici, *J. Org. Chem.* **1987**, *52*, 2559–2562.

[142] K. E. Henegar, S. W. Ashford, T. A. Baughman, J. C. Sih, R.-L. Gu, *J. Org. Chem.* **1997**, *62*, 6588–6597.

[143] S. Hanessian, V. Mascitti, P.-P. Lu, H. Ishida, *Synthesis* **2002**, 1959–1968.

[144] R. Siedlecka, J. Skarzewski, J. Młochowski, *Tetrahedron Lett.* **1990**, *31*, 2177–2180.

[145] A. De Mico, R. Margarita, L. Parlanti, A. Vescovi, G. Piancatelli, *J. Org. Chem.* **1997**, *62*, 6974–6977.

[146] M. Shibuya, M. Tomizawa, I. Suzuki, Y. Iwabuchi, *J. Am. Chem. Soc.* **2006**, *128*, 8412–8413.

[147] K. Murakami, Y. Sasano, M. Tomizawa, M. Shibuya, E. Kwon, Y. Iwabuchi, *J. Am. Chem. Soc.* **2014**, *136*, 17591–17600.

[148] L. H. B. Baptistella, G. Cerchiaro, *Carbohydr. Res.* **2004**, *339*, 665–671.

[149] T. Angata, A. Varki, *Chem. Rev.* **2002**, *102*, 439–469.

[150] M. J. Kiefel, M. von Itzstein, *Chem. Rev.* **2002**, *102*, 471–490.

[151] P. Kosma, *Curr. Org. Chem.* **2008**, *12*, 1021–1039.

[152] P. K. Jana, S. B. Mandal, A. Bhattacharjya, *Tetrahedron Lett.* **2011**, *52*, 6767–6771.

[153] R. Schaffer, H. S. Isbell, *J. Am. Chem. Soc.* **1959**, *81*, 2178–2183.

[154] R. Schaffer, *J. Am. Chem. Soc.* **1959**, *81*, 2838–2842.

[155] H. Paulsen, V. Sinnwell, *Chem. Ber.* **1978**, *111*, 869–878.

[156] T. Magauer, A. G. Myers, *Org. Lett.* **2011**, *13*, 5584–5587.

[157] M. Dischmann, Dissertation, Philipps-Universität Marburg, Marburg/Lahn, **2014**.

[158] S. Danishefsky, C. Maring, *J. Am. Chem. Soc.* **1985**, *107*, 7762–7764.

[159] N. Ikemoto, S. L. Schreiber, *J. Am. Chem. Soc.* **1992**, *114*, 2524–2536.

[160] A. Fürstner, M. Wuchrer, *Chem. Eur. J.* **2006**, *12*, 76–89.

[161] C. Contreras, R. Román, C. Pérez, F. Alarcón, M. Zavala, S. Pérez, *Chem. Pharm. Bull.* **2005**, *53*, 1408–1410.

[162] M. Menzel, T. Ziegler, *Eur. J. Org. Chem.* **2014**, 7658–7663.

[163] S. Jarosz, *Carbohydr. Res.* **1988**, *183*, 209–215.

[164] S. Jarosz, *Carbohydr. Res.* **1988**, *183*, 217–225.

[165] B. E. Rossiter, T. R. Verhoeven, K. B. Sharpless, *Tetrahedron Lett.* **1979**, *49*, 4733–4736.

[166] S. Okazaki, P. Tittabutr, A. Teulet, J. Thouin, J. Fardoux, C. Chaintreuil, D. Gully, J. F. Arrighi, N. Furuta, H. Miwa, M. Yasuda, N. Nouwen, N. Teaumroong, E. Giraud, *ISME J.* **2016**, *10*, 64–74.

[167] C. Masson-Boivin, J. L. Sachs, *Curr. Opin. Plant Biol.* **2018**, *44*, 7–15.

[168] J. Raymond, J. L. Siefert, C. R. Staples, R. E. Blankenship, *Mol. Biol. Evol.* **2004**, *21*, 541–554.

[169] Nathan Mueller, *Making Data-Driven Decisions on Soybean Inoculation*, University of Nebraska-Lincoln, Nebraska Extension CropWatch.unl.edu. **2017**, `https://cropwatch.unl.edu/2017/making-data-driven-decisions-soybean-inoculation`, online, accessed May 23, 2019.

[170] V. Oke, S. R. Long, *Curr. Opin. Microbiol.* **1999**, *2*, 641–646.

[171] E. Giraud, L. Moulin, D. Vallenet, V. Barbe, E. Cytryn, J.-C. Avarre, M. Jaubert, D. Simon, F. Cartieaux, Y. Prin, G. Bena, L. Hannibal, J. Fardoux, M. Kojadinovic, L. Vuillet, A. Lajus, S. Cruveiller, Z. Rouy, S. Mangenot, B. Segurens, C. Dossat, W. L. Franck, W.-S. Chang, E. Saunders, D. Bruce, P. Richardson, P. Normand, B. Dreyfus, D. Pignol, G. Stacey, D. Emerich, A. Verméglio, C. Médigue, M. Sadowsky, *Science* **2007**, *316*, 1307–1312.

[172] C. L. Aboussafy, L. B. A. Gersby, A. Molinaro, M.-A. Newman, T. L. Lowary, *J. Org. Chem.* **2019**, *84*, 14–41.

[173] W. Li, A. Silipo, L. B. A. Gersby, M.-A. Newman, A. Molinaro, B. Yu, *Angew. Chem. Int. Ed.* **2017**, *56*, 2092–2096, see also: *Angew. Chem.* **2017**, *129*, 2124–2128.

[174] M. Menzel, Diploma Thesis, University of Tübingen, **2010**.

[175] F. Fliegel, I. Beaudet, S. Watrelot-Bourdeau, N. Cornet, J.-P. Quintard, *J. Organomet. Chem.* **2005**, *690*, 659–673.

[176] H. Lindlar, R. Dubuis, *Org. Synth.* **1966**, *46*, 89–92.

[177] K. R. Campos, D. Cai, M. Journet, J. J. Kowal, R. D. Larsen, P. J. Reider, *J. Org. Chem.* **2001**, *66*, 3634–3635.

[178] L. K. Sydnes, B. Holmelid, O. H. Kvernenes, S. Valdersnes, M. Hodne, K. Boman, *Arkivoc* **2008**, *2008*, 242–268.

[179] M. García-Mota, J. Gómez-Díaz, G. Novell-Leruth, C. Vargas-Fuentes, L. Bellarosa, B. Bridier, J. Pérez-Ramírez, N. López, *Theor. Chem. Acc.* **2011**, *128*, 663–673.

[180] W.-Y. Siau, Y. Zhang, Y. Zhao, *Top. Curr. Chem.* **2012**, *327*, 33–58.

[181] K. B. Sharpless, W. Amberg, Y. L. Bennani, G. A. Crispino, J. Hartung, K.-S. Jeong, H.-L. Kwong, K. Morikawa, Z.-M. Wang, D. Xu, X.-L. Zhang, *J. Org. Chem.* **1992**, *57*, 2768–2771.

[182] R. Ray, D. S. Matteson, *Tetrahedron Lett.* **1980**, *21*, 449–450.

[183] E. Erdik, D. Kâhya, T. Daşkapan, *Synth. Commun.* **1998**, *28*, 1–7.

[184] F. He, Y. Bo, J. D. Altom, E. J. Corey, *J. Am. Chem. Soc.* **1999**, *121*, 6771–6772.

[185] T. K. M. Shing, E. K. W. Tam, V. W.-F. Tai, I. H. F. Chung, Q. Jiang, *Chem. Eur. J.* **1996**, *2*, 50–57.

[186] G. Höfle, W. Steglich, *Synthesis* **1972**, 619–621.

[187] G. Höfle, W. Steglich, H. Vorbrüggen, *Angew. Chem. Int. Ed.* **1978**, *17*, 569–583, see also: *Angew. Chem.* **1978**, *90*, 602–615.

[188] W. A. Szarek, A. Zamojski, K. N. Tiwari, E. R. Ison, *Tetrahedron Lett.* **1986**, *27*, 3827–3830.

[189] S. Yu, S. Ma, *Chem. Commun.* **2011**, *47*, 5384–5418.

[190] P. Dupau, R. Epple, A. A. Thomas, V. V. Fokin, K. B. Sharpless, *Adv. Synth. Catal.* **2002**, *344*, 421–433.

[191] K.-G. Ji, H.-T. Zhu, F. Yang, X.-Z. Shu, S.-C. Zhao, X.-Y. Liu, A. Shaukat, Y.-M. Liang, *Chem. Eur. J.* **2010**, *16*, 6151–6154.

[192] A. W. Burgstahler, G. N. Widiger, *J. Org. Chem.* **1973**, *38*, 3652–3653.

[193] C. Jeuck, Bachelor Thesis, University of Tübingen, **2017**.

[194] H. C. Kolb, M. S. Vannieuwenhze, K. B. Sharpless, *Chem. Rev.* **1994**, *94*, 2483–2547.

[195] C. Reik, Bachelor Thesis, University of Tübingen, **2017**.

[196] S. D. Rychnovsky, B. N. Rogers, T. I. Richardson, *Acc. Chem. Res.* **1998**, *31*, 9–17.

[197] T. R. Hoye, C. S. Jeffrey, F. Shao, *Nat. Protoc.* **2007**, *2*, 2451–2458.

[198] B. S. Hwang, E. Y. Yoon, E. J. Jeong, J. Park, E.-H. Kim, J.-R. Rho, *J. Org. Chem.* **2018**, *83*, 194–202.

[199] L. Maier, P. Khirsariya, O. Hylse, S. K. Adla, L. Černová, M. Poljak, S. Krajčovičová, E. Weis, S. Drápela, K. Souček, K. Paruch, *J. Org. Chem.* **2017**, *82*, 3382–3402.

[200] A. B. Charette in *Handbook of Reagents for Organic Synthesis. Chiral Reagents for Asymmetric Synthesis*, (Ed.: L. A. Paquette), John Wiley & Sons Ltd, Chichester, West Sussex, England, **2003**, Chapter 5, pp. 171–172, and references cited therein.

[201] M. Adinolfi, G. Barone, A. Iadonisi, L. Mangoni, R. Manna, *Tetrahedron* **1997**, *53*, 11767–11780.

[202] M. Angelin, M. Hermansson, H. Dong, O. Ramström, *Eur. J. Org. Chem.* **2006**, 4323–4326.

[203] A. W. Mazur, G. D. Hiler, *J. Org. Chem.* **1997**, *62*, 4471–4475.

[204] R. G. S. Ritchie, N. Cyr, B. Korsch, H. J. Koch, A. S. Perlin, *Can. J. Chem.* **1975**, *53*, 1424–1433.

[205] P. Mukerjee, M. Abid, F. C. Schroeder, *Org. Lett.* **2010**, *12*, 3986–3989.

[206] G. B. Payne, *J. Org. Chem.* **1962**, *27*, 3819–3822.

[207] C. S. Callam, R. R. Gadikota, T. L. Lowary, *J. Org. Chem.* **2001**, *66*, 4549–4558.

[208] K. S. Kim, D. M. Vyas, W. A. Szarek, *Carbohydr. Res.* **1979**, *72*, 25–33.

[209] J. R. Vyvyan, J. A. Meyer, K. D. Meyer, *J. Org. Chem.* **2003**, *68*, 9144–9147.

[210] A. Procopio, R. Dalpozzo, A. De Nino, L. Maiuolo, M. Nardi, B. Russo, *Adv. Synth. Catal.* **2005**, *347*, 1447–1450.

[211] K. Jeyakumar, D. K. Chand, *Synthesis* **2008**, 807–819.

[212] R. P. Hanzlik, M. Leinwetter, *J. Org. Chem.* **1978**, *43*, 438–440.

[213] R. Balamurugan, R. B. Kothapalli, G. K. Thota, *Eur. J. Org. Chem.* **2011**, 1557–1569.

[214] Y. Kim, P. L. Fuchs, *Org. Lett.* **2007**, *9*, 2445–2448.

[215] C. Weber, J. A. Czaplewska, A. Baumgaertel, E. Altuntas, M. Gottschaldt, R. Hoogenboom, U. S. Schubert, *Macromolecules* **2012**, *45*, 46–55.

[216] M. Pröhl, T. Bus, J. A. Czaplewska, A. Traeger, M. Deicke, H. Weiss, W. Weigand, U. S. Schubert, M. Gottschaldt, *Eur. J. Inorg. Chem.* **2016**, 5197–5204.

[217] J. R. Snyder, A. S. Serianni, *Carbohydr. Res.* **1987**, *163*, 169–188.

[218] W. Mackie, A. S. Perlin, *Can. J. Chem.* **1966**, *44*, 2039–2049.

[219] S. J. Angyal, *Adv. Carbohydr. Chem. Biochem.* **1984**, *42*, 15–68.

[220] G. A. Jeffrey, M. E. Gress, S. Takagi, *J. Am. Chem. Soc.* **1977**, *99*, 609–611.

[221] Y.-C. Tse, M. D. Newton, *J. Am. Chem. Soc.* **1977**, *99*, 611–613.

[222] F. A. Momany, M. Appell, G. Strati, J. L. Willett, *Carbohydr. Res.* **2004**, *339*, 553–567.

[223] N. M. Xavier, A. P. Rauter, *Carbohydr. Res.* **2008**, *343*, 1523–1539.

[224] M. B. Yunker, D. E. Plaumann, B. Fraser-Reid, *Can. J. Chem.* **1977**, *55*, 4002–4009.

[225] K. Tatsuta, K. Akimoto, M. Annaka, Y. Ohno, M. Kinoshita, *Bull. Chem. Soc. Jpn.* **1985**, *58*, 1699–1706.

[226] M. L. Uhrig, O. Varela, *Aust. J. Chem.* **2002**, *55*, 155–160.

[227] M. L. Uhrig, O. Varela, *Carbohydr. Res.* **2002**, *337*, 2069–2076.

[228] C. A. Iriarte Capaccio, O. Varela, *Tetrahedron: Asymmetry* **2004**, *15*, 3023–3028.

[229] W. G. Dauben, B. A. Kowalczyk, F. W. Lichtenthaler, *J. Org. Chem.* **1990**, *55*, 2391–2398.

[230] W. Zou, Z. Wang, E. Lacroix, S.-h. Wu, J. H. Jennings, *Carbohydr. Res.* **2001**, *334*, 223–231.

[231] S. Caddick, S. Khan, *J. Chem. Soc. Chem. Commun.* **1995**, 1971–1972.

[232] H. C. Kolb, H. M. R. Hoffmann, *Tetrahedron* **1990**, *46*, 5127–5144.

[233] S. Caddick, S. Khan, L. M. Frost, N. J. Smith, S. Cheung, G. Pairaudeau, *Tetrahedron* **2000**, *56*, 8953–8958.

[234] S. Caddick, S. Cheung, L. M. Frost, S. Khan, G. Pairaudeau, *Tetrahedron Lett.* **2000**, *41*, 6879–6882.

[235] S. Caddick, S. Cheung, V. E. Doyle, L. M. Frost, M. G. Soscia, V. M. Delisser, M. R. V. Williams, Z. C. Etheridge, S. Khan, P. B. Hitchcock, G. Pairaudeau, S. Vile, *Tetrahedron* **2001**, *57*, 6295–6303.

[236] M. D. Urbaniak, L. M. Frost, J. P. Bingham, L. R. Kelland, J. A. Hartley, D. N. Woolfson, S. Caddick, *Bioorg. Med. Chem. Lett.* **2003**, *13*, 2025–2027.

[237] J. P. M. Nunes, C. A. M. Afonso, S. Caddick, *Tetrahedron Lett.* **2009**, *50*, 3706–3708.

[238] J. P. M. Nunes, L. F. Veiros, P. D. Vaz, C. A. M. Afonso, S. Caddick, *Tetrahedron* **2011**, *67*, 2779–2787.

[239] R. M. Oechsner, Bachelor Thesis, University of Tübingen, **2016**.

[240] R. C. Pettersen, G. Ferguson, L. Crombie, M. L. Games, D. J. Pointer, *Chem. Commun.* **1967**, 716–717.

[241] K. Umino, N. Takeda, Y. Ito, T. Okuda, *Chem. Pharm. Bull.* **1974**, *22*, 1233–1238.

[242] A. W. Dunn, I. D. Entwistle, R. A. W. Johnstone, *Phytochemistry* **1975**, *14*, 2081–2082.

[243] K. Iguchi, M. Iwashima, K. Watanabe, *J. Nat. Prod.* **1995**, *58*, 790–793.

[244] T. Amagata, Y. Usami, K. Minoura, T. Ito, A. Numata, *J. Antibiot.* **1998**, *51*, 33–40.

[245] G. Le Goff, E. Adelin, G. Arcile, J. Ouazzani, *Tetrahedron Lett.* **2017**, *58*, 2337–2339.

[246] M. Conti, *Anti-Cancer Drugs* **2006**, *17*, 1017–1022.

[247] M. Conti, *Expert Opin. Drug Discov.* **2007**, *2*, 1153–1159.

[248] S. P. Roche, D. J. Aitken, *Eur. J. Org. Chem.* **2010**, 5339–5358.

[249] D. J. Aitken, H. Eijsberg, A. Frongia, J. Ollivier, P. P. Piras, *Synthesis* **2014**, *46*, 1–24.

[250] S. P. Simeonov, J. P. M. Nunes, K. Guerra, V. B. Kurteva, C. A. M. Afonso, *Chem. Rev.* **2016**, *116*, 5744–5893.

[251] Y. Wan, M. Alterman, M. Larhed, A. Hallberg, *J. Org. Chem.* **2002**, *67*, 6232–6235.

[252] I. Reile, S. Kalle, F. Werner, I. Järving, M. Kudrjashova, A. Paju, M. Lopp, *Tetrahedron* **2014**, *70*, 3608–3613.

[253] S. E. Steinhardt, J. S. Silverston, C. D. Vanderwal, *J. Am. Chem. Soc.* **2008**, *130*, 7560–7561.

[254] S. D. Jacob, J. L. Brooks, A. J. Frontier, *J. Org. Chem.* **2014**, *79*, 10296–10302.

[255] G. Piancatelli, A. Scettri, G. David, M. D'Auria, *Tetrahedron* **1978**, *34*, 2775–2778.

[256] O. Nieto Faza, C. S. López, R. Álvarez, Á. R. De Lera, *Chem. Eur. J.* **2004**, *10*, 4324–4333.

[257] S.-W. Li, R. A. Batey, *Chem. Commun.* **2007**, 3759–3761.

[258] P. J. Wright, A. M. English, *J. Am. Chem. Soc.* **2003**, *125*, 8655–8665.

[259] C. Galli, P. Gentili, O. Lanzalunga, *Angew. Chem. Int. Ed.* **2008**, *47*, 4790–4796, see also: *Angew. Chem.* **2008**, *120*, 4868–4874.

[260] Z. Xiang, *J. Mol. Struct.* **2012**, *1029*, 15–21.

[261] G. Damian, D. Petrisor, V. Miclaus, *J. Optoelectron. Adv. M.* **2007**, *9*, 1010–1013.

[262] D. N. Polovyanenko, V. F. Plyusnin, V. A. Reznikov, V. V. Khramtsov, E. G. Bagryanskaya, *J. Phys. Chem. B* **2008**, *112*, 4841–4847.

[263] K. G. Lewis, C. E. Mulquiney, *Tetrahedron* **1977**, *33*, 463–475.

[264] R. F. A. Gomes, J. A. S. Coelho, C. A. M. Afonso, *Chem. Eur. J.* **2018**, *24*, 9170–9186.

[265] Y. Cai, Y. Tang, I. Atodiresei, M. Rueping, *Angew. Chem. Int. Ed.* **2016**, *55*, 14126–14130, see also: *Angew. Chem.* **2016**, *128*, 14332–14336.

[266] C. Verrier, S. Moebs-Sanchez, Y. Queneau, F. Popowycz, *Org. Biomol. Chem.* **2018**, *16*, 676–687.

[267] O. J. Achmatowicz, P. Bukowski, B. Szechner, Z. Zwierzchowska, A. Zamojski, *Tetrahedron* **1971**, *27*, 1973–1996.

[268] A. K. Ghosh, M. Brindisi, *RSC Advances* **2016**, *6*, 111564–111598.

[269] E. J. Corey, *Experentia* **1983**, *39*, 1084–1085.

[270] M. Rosetti, M. Frasnelli, F. Fabbri, C. Arienti, I. Vannini, A. Tesei, W. Zoli, M. Conti, *Anticancer Res.* **2008**, *28*, 315–320.

[271] A. D. Argoudelis, J. F. Zieserl, *Tetrahedron Lett.* **1966**, *18*, 1969–1973.

[272] R. Laliberté, G. Médawar, Y. Lefebvre, *J. Med. Chem.* **1973**, *16*, 1084–1089.

[273] M. P. Georgiadis, *J. Med. Chem.* **1976**, *19*, 346–349.

[274] H. Ikeda, E. Kaneko, S. Okuzawa, D. Takahashi, K. Toshima, *Org. Biomol. Chem.* **2014**, *12*, 8832–8835.

[275] G. R. Fulmer, A. J. M. Miller, N. H. Sherden, H. E. Gottlieb, A. Nudelman, B. M. Stoltz, J. E. Bercaw, K. I. Goldberg, *Organometallics* **2010**, *29*, 2176–2179.

[276] L. Krause, R. Herbst-Irmer, G. M. Sheldrick, D. Stalke, *J. Appl. Cryst.* **2015**, *48*, 3–10.

[277] G. M. Sheldrick, *Acta Cryst. A* **2008**, *64*, 112–122.

[278] C. B. Hübschle, G. M. Sheldrick, B. Dittrich, *J. Appl. Cryst.* **2011**, *44*, 1281–1284.

[279] R. K. Boeckmann Jr., P. Shao, J. J. Mullins, *Org. Synth.* **2000**, *77*, 141.

[280] C. D. McCune, M. L. Beio, J. A. Friest, S. Ginotra, D. B. Berkowitz, *Tetrahedron Lett.* **2015**, *56*, 3575–3579.

[281] M. E. S. B. Barros, J. C. R. Freitas, J. M. Oliveira, C. H. B. Da Cruz, P. B. N. Da Silva, L. C. C. De Araújo, G. C. G. Militão, T. G. Da Silva, R. A. Oliveira, P. H. Menezes, *Eur. J. Med. Chem.* **2014**, *76*, 291–300.

[282] H. B. Boren, G. Ekborg, K. Eklind, P. J. Garegg, A. Pilotti, C.-G. Swahn, *Acta Chem. Scand.* **1973**, *27*, 2639–2644.

[283] N. K. Kochetkov, B. A. Dmitriev, O. S. Chizhov, E. M. Klimov, N. N. Malysheva, A. Y. Chernyak, N. E. Bayramova, V. I. Torgov, *Carbohydr. Res.* **1974**, *33*, C5–C7.

[284] G. Bellucci, G. Catelani, C. Chiappe, F. D' Andrea, G. Grigò, *Tetrahedron: Asymmetry* **1997**, *8*, 765–773.

[285] B. Iglewicz, D. C. Hoaglin, *The ASQC Basic Reference in Quality Control: Statistical Techniques. Volume 16: How to Detect and Handle Outliers*, ASQC Quality Press, Milwaukee, Wisconsin, United States, **1993**.